



University
of Glasgow

Wado, May Saleh (2020) *Characterisation of the cold acclimation process in spring and winter cereals*. PhD thesis.

<http://theses.gla.ac.uk/81623/>

Copyright and moral rights for this work are retained by the author

A copy can be downloaded for personal non-commercial research or study, without prior permission or charge

This work cannot be reproduced or quoted extensively from without first obtaining permission in writing from the author

The content must not be changed in any way or sold commercially in any format or medium without the formal permission of the author

When referring to this work, full bibliographic details including the author, title, awarding institution and date of the thesis must be given

Enlighten: Theses

<https://theses.gla.ac.uk/>
research-enlighten@glasgow.ac.uk



Characterisation of the Cold Acclimation Process in Spring and Winter Cereals

May Saleh Wado

**Thesis submitted in fulfilment of the requirements for the
degree of Doctor of Philosophy**

**Institute of Molecular, Cell and Systems Biology School of Life
Sciences**

**College of Medical, Veterinary and Life Sciences University
of Glasgow**

August, 2020

ABSTRACT

Vast tracts of viable agricultural land are located in the northern latitudes of Eurasia and North America. They experience very high seasonal productivity due to long warm days and plentiful rainfall remain, but are largely uncultivated due to late spring or early autumn frosts. Wild grasses survive these frost events and this has prompted intensive investigation into how to improve the cold tolerance of domesticated small grained cereals. This thesis presents work to investigate the relative importance of two environmental factors (i.e. non-freezing low night temperatures and night length (or photoperiod)) on cold acclimation in two diploid species from economically important crops; i.e. rye (*Secale cereal*, L.) and barley (*Hordeum vulgare*, L.).

A winter (California) and spring (Belgravia) cultivar of barley, and two cold-tolerant cultivars of rye (Forage and Kapitan), were grown to the three week stage over short warm nights (8hr at 16°C), and then exposed to long nights alone (15hr at 16°C), cool nights alone (8hr at 4°C), or both. The controls were raised under conditions of 8hr 16°C nights. The degree of cold tolerance conferred by these treatments was subsequently assessed 1, 2, 3, and 4 weeks post acclimation. Cold hardiness was assessed by measuring electrolyte leakage (cell lysis) from the leaf tissues, after exposure to a range of freezing temperatures, using modification of the Lethal Temperature 50 (LT₅₀) method (temperature that produces 50% cell lysis). These experiments reported a major difference in the cold acclimation processes of rye and barley. Consistent with reports in the literature; in both rye cultivars, cool night temperatures alone (34-38% improvement) and long night periods alone (<11% improvement) triggered a significant cold acclimation response. However, when applied together the response was strongly synergistic, i.e. more-than-additive (up to 16.2°C improvement, 100%). In contrast, with barley long nights alone (12-18% improvement) and cool night temperatures alone (80-88% improvement) there was conferred frost resistance, but when applied together (up to 11.2°C improvement, 100%) there was limited evidence of synergism, as the effect of temperature and night length appeared to be additive.

The transcriptional events that underpin the cold acclimation process in Arabidopsis are well characterised, and detailed temperature-sensing and photoperiod-sensing pathways have been proposed along with the crosstalk between two networks. In addition, it is well established that parts of these Arabidopsis pathways involve the action of the phytohormone Abscisic acid (ABA), whilst others do not. In particular, the process of *Vernalization*, as

triggered by *AtVRN1*, and the *ICE-CBF-COR* regulon has been implicated in conferring at least 30% of full cold tolerance on Arabidopsis. Homologues of several *VRN* and *ICE-CBF-COR* have been identified in the Triticeae, and so semi-quantitative (sq) RT-PCR was used with acclimated and non-acclimated leaf tissue to establish whether similar transcriptional events accompany the cold acclimation processes in Arabidopsis and barley. This approach provided inconclusive results, partly due to the scale of the experiments (over 800 samples). The experiments on *HvVRN1*, however, demonstrated that transcription occurred at a similar level in non-acclimated and cold acclimated leaves; thereby casting doubt on the universality of the Arabidopsis model in higher plants.

A transcriptome-wide approach, RNA-Seq, was selected to establish the pattern of transcriptional changes that accompanies cold acclimation in barley across three separate experiments. Winter barley *cv.* California plants were grown in non-acclimating conditions for three weeks, and then cold acclimated for up to four weeks. Leaf tissue was harvested two hours post-dawn and mRNA extracted, cDNA synthesised and between 30 and 50 million 75bp reads made for each replicate sample, using paired end Illumina NextSeq 500 technology. A novel analysis 'pipeline' was then written and the University of Glasgow Galaxy server used to process the reads and align them with the barley *cv.* Morex cDNA genome (63.7 Mb; IBSC, v2 2017) using the Kallisto package (Bray et al. 2016). Alignment with a cDNA genome dramatically reduced computational overheads; these are much greater when alignment is made to a large genome such as barley (5.3 Gb haploid genome). After indexing each of the reads to a specific barley sequence, the Kallisto output was analysed using an R-Script routine, incorporating the statistical analysis package DESeq 2 (Anders and Huber, 2010). Filtering was then applied to the DESeq 2 output in a spreadsheet to identify those sequences whose expression differed from that of the controls using the following criteria: 1, significantly different using a Benjamini-Hochberg corrected t-test; 2, greater than a two-fold change; abundance (BaseMean) score of over 1.0. The resulting data files were then analysed using set theory and Euler (Venn) diagrams to identify the common sequences amongst the treatments. Where sequences appeared in multiple data sets, a novel statistical method, a Hypergeometric Mass Function (HMF) was calculated, to estimate the probability that the multiple observations were real and not the result of random transcriptional events.

The first 'Condition' experiment was designed to identify components of temperature-sensing and photoperiod-sensing pathways; non-acclimated three-week-old *cv.* California

plants were exposed to cold acclimating conditions for a further two weeks (low night temperature alone, long night periods alone, both together, and controls – neither; n=3 biological replicates, 12 samples in total). Set analysis was permitted for the groups of genes to be identified known to be responsive to cool night temperatures (T) alone, long nights alone (P) alone, and to a combination of both only (I). For the upregulated genes, 18 responded to T alone and could be placed in a temperature-sensing pathway, 8 appeared to be triggered through the P pathway, and 6 were tentatively placed at the intersections (I) between both pathways. For down regulated sequences, 16 appeared to respond to long nights alone (P), but none could be unambiguously attributed to cool night temperatures alone or interactions between both conditions. The HMFs could be estimated for the up regulated I and T sequences, and were found to be $p < 3.7 \cdot 10^{-11}$. It is almost certain that these 24 I and T sequences respond to cold acclimating conditions. Full lists of the genes were identified as ‘significant’ by the B-H and HMF methods provided.

The second RNA-Seq experiment compared the transcriptome of the *cv.* California leaves exposed to non-acclimating and fully acclimating conditions (long, cool nights) for up to four weeks (‘Time-series’ experiment). Forty-eight of the up regulated TPI sequences that were identified in the first (‘Condition’) experiment were also identified as up regulated TPI sequences in the ‘Time-series’ experiment, and a corresponding 22 were identified in both experiments as down regulated. Unsurprisingly, the greatest number of changes was recorded at the end of the first week of acclimation, and this declined over time, so that the fewest changes were observed by week 4. In total, 3,697 up regulated and 5,059 down regulated sequences were identified as significant ($p < 0.1$ in the Benjamini-Hochberg corrected t-test method incorporated into DESeq 2, whereas 48 up- and 22 down regulated sequences were calculated to have an HMF of $p < 9.8 \cdot 10^{-12}$. Lists of the genes identified as ‘significant’ by the B-H and the more rigorous HMF methods were also provided.

The third RNA-Seq experiment compared the transcriptome of *cv.* California leaves that were non-acclimated or cold acclimated by the application of exogenous ABA (10^{-4} M) for up to 4 weeks (‘ABA Time-series’ experiment). The plants were not exposed to long nights or cool night temperatures. Measurements of the cold hardiness of leaves (LT₅₀ measurements) showed ABA treated leaves developed a cold tolerance comparable to plants exposed to long, cool nights for the same period of time suggesting that, unlike Arabidopsis, ABA is involved in all the cold signalling pathways in barley. Transcript profiling of the control and ABA treated leaves showed 1,356 significant up regulated and 3,542 down

regulated sequences (Benjamini-Hochberg statistic of $p < 0.1$). Of these, 306 of the up regulated sequences were also found in the ‘Time-series’ experiment, and an HMF of $p < 8.18 \cdot 10^{-11}$ was calculated. Similarly, the down regulated 1,343 were also found in the ‘Time-series’ down regulated data set, and the corresponding HMF was $p < 5.74 \cdot 10^{-11}$. The lists of genes identified as ‘significant’ in the B-H and the more rigorous HMF methods are provided.

During the ‘corrections’ stage of the preparation of this thesis Gene Ontology (GO) analysis became available on-line for analysing barley sequences. This offers an independently cross-checked annotation for gene function and KEGG (Kyoto Encyclopaedia for Genes and Genomes) pathway analysis. It is beyond the scope of this thesis to provide a detailed GO analysis for the thousands of sequences that have been identified by RNA-Seq and reported here, but several of those confirmed by the HMF as highly significant changes are discussed in detail in the Discussion. These include a DNA helicase (HORVU1Hr1G019290), which is a homologue of a helicase involved in the animal Wnt signalling pathway. Another up regulated cold acclimation sequence encodes a long non-coding RNA (lncRNA; HORVU6Hr1G005050); the role of lncRNAs in the vernalisation pathway of Arabidopsis and small grained cereals is currently emerging, but the role of this lncRNA remains to be established.

TABLE OF CONTENTS

Abstract	i
Table of Contents.	v
List of Tables.	xii
List of Figures.	xiv
Acknowledgements.	xviii
List of Abbreviations.	xix
Declaration.	xxiii
Chapter 1 Introduction to Cold Stress and Cold Acclimation in Small-Grained Cereal Crops	1
1.1 Global Challenge of Food Security.	2
1.2 Impact of Abiotic Stress on Food Productivity.	2
1.3 Strategies for Increasing Food Production.	6
1.4 Low Temperature Stress in Plants.	7
1.4.1 General Morphological and Physiological Changes Associated with Chilling Stress.	8
1.4.2 General Physiological Changes Associated with Freezing Temperatures.	8
1.4.3 Plant Strategies for Avoiding Frost Damage.	13
1.5 Cold Acclimation in Plants.	14
1.5.1 Cold Acclimation-Induced Changes in Membrane Lipids.	16
1.5.2 Cold Acclimation-Induced Changes in Sugars.	17
1.5.3 Cold Acclimation-Induced Changes in Compatible Solutes.	18
1.5.4 Proteins Associated with Freezing Tolerance.	20
1.6 Regulation of Stress Response Gene Expression.	23
1.6.1 Transcription Factors.	
1.6.2 Regulation of Gene Expression in Response to Cold Acclimating Temperatures.	25
1.7 Role of CBF Signalling in Cold Acclimation.	29

1.7.1	Post-transcriptional Regulation of CBF Signalling.	31
1.7.2	Post-translational Modification (PTM) in Regulation of CBF Signalling Pathway.	32
1.8	Role of Calcium in Cold Signalling.	32
1.8.1	The Cell Membrane Fluidity Hypothesis.	32
1.8.2	The Roles of Reactive Oxygen Species (ROS) in Cold Stress.	32
1.8.3	Regulatory Protein Kinases.	33
1.8.4	MAPK Cascades Mediation of Cold Signal Transduction.	34
1.9.	Negative Regulators of Low Temperature Signal Transduction.	35
1.9.1	HOS1: a Negative Regulator of Freezing Tolerance.	35
1.9.2	ZAT12: a Negative Regulator of Cold Acclimation.	36
1.9.3	MYB15 (MYELOBLASTOSIS 15).	37
1.10.	The ESKIMO1 Freezing Tolerance Genes.	37
1.10.1	The Arabidopsis eskimo1 Mutant.	37
1.11	The Role of the Phytohormone Abscisic Acid (ABA) in Abiotic Stress.	40
1.12.	Origin and Domestication of Cereals.	42
1.12.1	The Origin and Domestication History of Barley (<i>Hordeum vulgare</i> L).	42
1.13	Cold Acclimation in the Cereal Tribe Triticeae.	43
1.14.	Genetic Mapping of Cold Tolerance Traits in Cereals.	45
1.14.1	The Vernalisation Pathway in Cereals.	47
1.14.2	The Role of <i>VRN1</i> in Cereal Flowering and Frost Tolerance.	48
1.14.3	The Role of Photoperiod in Cereal Frost Tolerance.	50
1.14.4	The Role of Low Temperature and the <i>FR2</i> Locus in Cereal Frost Tolerance.	52
1.14.5	Flowering Time: Model of the Regulatory Pathway Mediated by Vernalisation.	55
1.15	Control of Flowering in the <i>Triticeae</i> Tribe.	55

1.15.1	Flowering in Spring Genotypes.	55
1.15.2	Flowering in Winter Genotypes.	55
1.15.3	Model Proposed for Regulation of Flowering and Cold Tolerance in Cereals.	56
1.16.	Current Models for Cold Signalling Pathway in Plants.	59
1.17.	Outstanding Questions Relating to Cold Acclimation in Cereals.	61
1.18	Hypotheses and Assumptions.	62
1.19.	Difficulties and Advantages of Working with Barley as a Model Plant.	64
1.20	Project Aims.	64
	Chapter 2: Materials and Methods	68
2.1	Plant Material and Growth Conditions.	68
2.1.1	Growth in Soil.	68
2.1.2	Growth Conditions.	68
2.2	Application of Exogenous ABA to Leaf Tissue.	69
2.3	Measurement of Freezing Tolerance (LT ₅₀).	70
2.3.1	Estimation of Freezing Tolerance Using the LT ₅₀ Methods.	70
2.4	Molecular Method for Nucleic Acids.	70
2.4.1	Isolation of Genomic DNA.	70
2.4.2	RNA Extraction Using the TRI Reagent Method.	71
2.4.3	RNA Treatment with DNase.	72
2.4.4	cDNA Synthesis.	73
2.4.5	PCR Primers.	73
2.5	Cloning PCR Fragment for Sequence Analysis.	76
2.5.1	PCR Amplification.	76
2.5.2	Purification of PCR Amplicon with Qi A quick Gel Extraction kit.	76
2.5.3	Cloning of Amplicons into TOPO 2.1 vector.	77
2.5.4	Colony PCR.	77
2.5.5	Purification of Plasmid from <i>E coli</i> .	78

2.5.6	Quantification of DNA and RNA.	78
2.5.7	Agarose Gel Electrophoresis of gDNA and cDNA.	78
2.5.8	Agarose Gel Electrophoresis of RNA.	79
2.5.9	DNA Sequencing.	79
2.6	RNA Sequencing.	79
2.7	Statistical Analysis.	80
2.7.1	General Statistics.	80
2.7.2	Analysis of Transcriptome Data Sets.	80
2.7.2.1	Calculation of the Hypergeometric Probability Mass Function.	81
2.7.2.2	Calculation of Probabilities from Set Theory.	82
2.7.2.3	Set Theory Manipulations.	83
	Chapter 3: The Effect of Photoperiod and Temperature on the Induction of Cold Acclimation in Cereals	85
3.1	Introduction.	85
3.2	Research Objective.	87
3.3	Methods for Measurement of Freezing Tolerance in Plants.	87
3.4	Assessment of Frost Tolerance (LT ₅₀) in Rye and Barley to Establish Conditions for Cold Acclimation Experiments.	88
3.5	Development of a Reproducible Method for Assessing Frost Damage.	94
3.6	Quantitative Determination of Lethal Temperatures (LT ₅₀).	95
3.6.1	Measurement of Freezing Tolerance (LT ₅₀) in Rye cv Forage.	95
3.6.2	Measurement of Freezing Tolerance (LT ₅₀) in Rye cv Kapitan.	97
3.6.3	Measurement of Freezing Tolerance (LT ₅₀) in Spring Barley cv Belgravia Leaves.	99
3.6.4	Measurement of Freezing Tolerance (LT ₅₀) of Winter Barley cv California Leaves.	102
3.7	Summary of the Effect of Photoperiod and Night Temperatures on Barley and Rye Cold Acclimation.	105
3.8	Comparison of the Effects of Photoperiod and Temperature on Mild and Severe Damage to Spring and Winter Barley.	107

3.9	Discussion.	110
3.9.1	Summary and Conclusions.	117
Chapter 4: Analysis of Key Cold Acclimation Sequences in Cold Acclimated Spring and Winter Barley		
4.1	Introduction.	118
4.2	Protocols for Quantifying Transcriptional Changes of Cold Acclimation Genes.	119
4.3	Primer Design and Amplification of Sequences Involved in Cold Acclimation.	119
4.3.1	PCR Primer Design for <i>HvVRN1</i> , <i>HvVRN1</i> , & <i>HvVRN3</i> .	119
4.3.2	PCR Primer Design for <i>HvActin</i> , <i>HvDHN5</i> , <i>HvCO1</i> , & <i>HvCOR14b</i> .	158
4.3.3	PCR Primer Design to the <i>CBF</i> Sequences in the Barley <i>FR2</i> Locus.	165
4.4	Semi-Quantitative RT-PCR.	170
4.5	Evidence that <i>cv</i> California is not a cold-tolerant winter barley.	171
4.6	Discussion and Conclusion.	172
Chapter 5: Changes in Leaf Transcript Abundance Accompanying Barley Cold Acclimation		
5.1	Introduction.	175
5.2	Acclimation Condition Experiment.	175
5.2.1	Plant Treatment and RNA Preparation.	176
5.2.2	Development of RNASeq Analysis Protocols for Barley.	176
5.2.3	cDNA synthesis.	179
5.2.4	Analyses of Data Quality from RNAseq Data Sets.	179
5.2.5	Alignment of RNAseq Data sets with Barley cDNA Library: Kallisto Pseudo-Alignment of Reads.	182
5.2.5.1	Statistical Analysis of Experimental Treatments.	185
5.2.5.2	Upregulated Sequences.	195
5.2.5.3	Downregulated Sequences.	204
5.2.5.4	Hypergeometric Probability.	212

5.3.	Full Cold Acclimation Time Series Experiment.	217
5.3.1	Quality Control and Statistical Analysis of RNASeq Data Sets.	217
5.3.2.	An RNA-Seq Validity Check; Comparison of Two Independent [TPI] Data Sets.	224
5.3.3	Time-Dependent Changes Compared With Non-Acclimated Controls.	227
5.4	Role of ABA in Barley Cold Acclimation.	234
5.4.1	Assessment of Cold Tolerance in Barley Plants Sprayed with ABA.	234
5.4.2	Transcriptome Profile of Barley <i>cv</i> California Leaves Treated with Exogenous ABA Applications.	238
5.4.3	An RNA-Seq Validity Check; Comparison of Transcriptome of Cold Acclimation Time Series and ABA Time Series.	251
5.5	Discussion.	231
5.5.1	Identification of Cold Tolerance Genes.	232
5.5.2	Time-dependent Expression of Cold Tolerance Genes.	235
5.5.3	Role of ABA in the Cold Acclimation Process in Barley.	236
	Chapter 6: General Discussion	238
6.1	Genomic Studies of Economically Important Plants.	238
6.2	Rationale for Studying Cold Acclimation in Barley.	239
6.3	The Role of Night Duration and Temperature on Freezing Tolerance.	240
6.4	Identification of Sequences Involved in Frost Tolerance in Barley.	241
6.5	Genome-wide Transcriptome Analysis of Cold Acclimation in Barley.	243
6.6	Time Series Transcriptome Analyses of Cold Acclimated Barley.	246
6.7	Transcriptome Analysis ABA-Treated Barley Leaves.	247
6.8	Limitations of Current Study.	248
6.9	Conclusion and Future Perspectives.	248
6.10	Addendum.	251
6.10.1	GO Analyses of TPI Sequences Responsive to Full Cold Acclimation Conditions for Two Weeks.	252

6.10.2	GO Analyses of Sequences Responsive to up to Four Weeks of Full Cold Acclimation Conditions and Foliar ABA Application.	254
6.10.3	Confirmation of Identified Cold Acclimation Sequences Using CRISPR.	258
	References.	
	Appendices.	

LIST OF TABLES

Table 1.1	Some TFs that are induced during the early phase of cold acclimation in <i>Arabidopsis</i>	30
Table 2.1	Details of PCR for Barley sequences studied	73
Table 3.1	Freezing Tolerance in Rye (<i>Secale cereal</i>) cv. Forrage	97
Table 3.2	Freezing Tolerance in Rye (<i>Secale cereale</i>) cv. Kapitan	99
Table 3.3	Freezing Tolerance of Spring Barley (<i>Hordeum vulgare</i>) cv. Belgravia Leaves.	102
Table 3.4	Freezing Tolerance of Winter Barley (<i>Hordeum vulgare</i>) cv. California Leaves.	105
Table 3.5	Effect of Cold Acclimation on the Freezing Tolerance (LT ₅₀) Severe Damage and (LT ₂₀) Mild Damage to Winter and Spring Barley Cultivars.	108
Table 3.6	The Contribution of Night Length (Photoperiod) to Full Cold Acclimation in Rye and Barley Cultivars	114
Table 4.1	Summary of PCR Results for Cold Acclimation Sequences in Barley	126
Table 4.2	Morex Genome Location for Individual GenBank <i>HvCBF</i> Genes	167
Table 5.1	Summary of Sample RNA Quality (RIN Number).	178
Table 5.2	FastQC Basic Statistics of High Throughput Sequencing Data Sets from Barley Leaves Cold Adapted for 2 Weeks.	184
Table 5.3	Summary of DESeq2 Pair-wise Treatment Comparisons for Expressed Genes in <i>Hordeum vulgare</i> (cv. California) Leaves Exposed for 2 Weeks to Different Cold Acclimation Conditions.	186
Table 5.4	Identification of Sequences regulated by Temperature Alone, Photoperiod Alone, or by an Interaction of Both Using Set Manipulations.	194

Table 5.5	Identification of Upregulated Cold Acclimation Sequences in Barley Induced by Photoperiod Alone, Low Night Temperatures Alone, and a Combination of Both Factors	198
Table 5.6	Identification of Down Regulated Cold Acclimation Sequences in Barley Suppressed by Photoperiod Alone, Low Night Temperatures Alone, and a Combination of Both Factors	206
Table 5.7	Hypergeometric Probabilities for Sequences Transcriptionally Regulated by Cold Acclimation.	215
Table 5.8	FastQC Basic Statistics of High Throughput Sequencing Data Sets from Barley Leaves Fully Cold Adapted for Up To 4 Weeks.	218
Table 5.9	Summary of DESeq2 Pair-wise Time Dependent Comparisons for Expressed Genes in <i>Hordeum vulgare</i> (cv. California) Leaves Exposed to Short Days and Low Temperatures.	221
Table 5.10.	Hypergeometric Probabilities for TPI Sequences Derived from Two Independent Cold Acclimation Experiments.	227
Table 5.11	Comparisons of Common Genes Regulated by Transition to Short Days and Low Temperatures: Time Series <i>cf.</i> Non-Acclimated Controls.	232
Table 5.12	Freezing Tolerance in Barley Cultivar California Leaves Induced by ABA Application.	238
Table 5.13	FastQC Basic Statistics of High Throughput Sequencing Data Sets from Barley Leaves Cold Adapted by 10-4 M ABA Application.	239
Table 5.14	Summary of Winter Barley (cv. California) Leaf Sequences	242
Table 5.15	Hypergeometric Probabilities for Common Genes Regulated by ABA Application.	247
Table 5.16	Hypergeometric Probabilities for Common Genes Regulated by ABA Application and Cold Acclimation	254

LIST OF FIGURES

Figure 1.1	Barley Field (Fiorenzuola, Northern Italy) Trial After a Cold Winter with a Long Snow Cover Period.	5
Figure 1.2	The plasma membrane is the primary site of the freezing injury and physical damage.	12
Figure 1.3	Cellular, biochemical and molecular changes involved in response to cold stress and cold acclimation	15
Figure 1.4	Transcription factors reported to have a major role in cold acclimation in <i>Arabidopsis</i> .	25
Figure 1.5	Schematic Illustration Summarizing the Regulation of CBF Expression in <i>Arabidopsis</i> .	39
Figure 1.6	Regulatory Network of Gene Expression in Response to Cold Acclimation.	41
Figure 1.7	Diagram of the Relative Positions of the Mapped Frost Resistance (<i>FR</i>) and Vernalisation (<i>VRN</i>) Genes on Chromosome 5H of Barley and Diploid Wheat.	46
Figure 1.8	Hypothetical model proposed for regulation of flowering and cold tolerance in cereals	58
Figure 1.9	The ICE/CBF/COR regulon cold signalling pathway in <i>Arabidopsis</i>	61
Figure 2.1	Cold Acclimation Regimes (Photoperiod and Cool Night Temperature)	69
Figure 2.2	The Observed and Expected Number of Sequences Calculated from Set Theory.	84
Figure 2.3	Explanation of Set Theory Manipulations Used in This Study	84
Figure 3.1	Survival of Non-Acclimated Rye (<i>Secale cereale</i>) cv. Kapitan Exposed to One Night of Freezing Temperatures.	91
Figure 3.2	Cold Acclimation Regimes for Barley and Rye	92
Figure 3.3	Calculated GDD for Cold-Acclimated Barley Plants.	93

Figure 3.4	Effect of Cold Acclimation on Freezing Tolerance (LT ₅₀) of Rye Forage Leaves.	96
Figure 3.5	Effect of Cold Acclimation on The Freezing Tolerance (LT ₅₀) of Rye (<i>Secale cereale</i>) cv. Kapitan Leaves.	98
Figure 3.6	Effect of Cold Acclimation on The Freezing Tolerance (LT ₅₀) of Spring Barley cv. Belgravia Leaves.	100
Figure 3.7	Effect of Cold Acclimation on the Freezing Tolerance (LT ₅₀) of Winter Barley Lines cv. California Leaves.	104
Figure 3.8	The Effects of Photoperiod and Night Temperatures on Cold Acclimation in Rye (<i>Secale cereale</i>) and Barley (<i>Hordeum vulgare</i>).	106
Figure 3.9	Comparing the Effects of Photoperiod and Temperature on Mild and Severe Damage to Spring and Winter Barley.	109
Figure 4.1	Gene Structure of <i>HvVRN1</i> from Six Barley Cultivars	122
Figure 4.2	Gene Structure of Barley <i>HvVRN2</i> from Three Barley Cultivars.	123
Figure 4.3	Gene Structure of <i>HvVRN3</i> Sequences from Eleven Barley Cultivars.	125
Figure 4.4	Agarose Gel Electrophoresis Images of the PCR Amplicons Generated for Barley <i>HvVRN1</i> , <i>HvVRN2</i> and <i>HvVRN3</i> .	158
Figure 4.5	Agarose Gel Electrophoresis Images of the PCR Amplicons for Barley <i>HvActin</i> , <i>HvCBF10A</i> , <i>HvCBF15A</i> , and <i>HvCBF6A</i>	161
Figure 4.6	Agarose Gel Electrophoresis Images of PCR Amplicons of Barley <i>HvCBF4B</i> , <i>HvCOR14b</i> , and <i>HvCBF16</i>	162
Figure 4.7	Agarose Gel Electrophoresis Images of the PCR Amplicons of Barley <i>HvCOR14b</i> and <i>HvCO1</i>	163
Figure 4.8	Agarose Gel Electrophoresis Images of the PCR Amplicons of Barley <i>HvCBF6B</i> and <i>HvDHN5</i>	165
Figure 4.9	Agarose Gel Electrophoresis Images of the PCR Amplicons of Barley <i>HvCBF2C</i> , <i>HvCBF9</i> , <i>HvCBF3</i> , and <i>HvCBF12C</i>	168

Figure 4.10	Semi-quantitative RT-PCR of <i>HvVRN1</i> , <i>HvVRN2</i> , and <i>HvVRN3</i> expression in Non-Acclimated and Cold-acclimated Leaves of Barley <i>cv.</i> California	169
Figure 5.1	Barley Total RNA Electrophoretogram from Agilent 2100 Bioanalyser.	177
Figure 5.2	Workflow for Automated Quality Control and Kallisto Alignment of Barley (<i>cv.</i> California) RNASeq Reads to the Barley (<i>cv.</i> Morex) cDNA Library.	180
Figure 5.3	Two-Dimensional Principal Component Analysis of Transcript Profiles in Cold Acclimated <i>Hordeum vulgare</i> (<i>cv.</i> California) Leaves.	188
Figure 5.4	DESeq2 Barley Gene Expression Heat Maps: Comparison of Cold Acclimation Treatments.	192
Figure 5.5	Venn Diagram Identifying Cold Acclimation Barley Sequences Up Regulated by Temperature Alone, Photoperiod Alone, and a Combination of Both Factors.	196
Figure 5.6	Venn Diagram Identifying Cold Acclimation Barley Sequences Down Regulated by Temperature Alone, Photoperiod Alone, and a Combination of Both Factors.	205
Figure 5.7	Hypergeometric Distribution for Intersection of Sequences in Independent RNA-Seq Experiments.	214
Figure 5.8	Two-Dimensional Principal Component Analysis of a Time Series Transcript Profile in Cold Acclimated <i>Hordeum vulgare</i> (<i>cv.</i> California) Leaves.	220
Figure 5.9	DESeq2 Barley Gene Expression Heat Maps: Comparison of Time Series Samples for Cold Acclimation Treatment.	224
Figure 5.10	Venn Diagram Comparing TPI Responsive Sequences Derived from Two Independent Experiments.	225
Figure 5.11	Hypergeometric distribution for Intersection of sequences in two independent RNA-Seq experiments.	226

Figure 5.12	Venn Diagram of Time Series Changes in Barley Genes ‘Upregulated’ by Transition to Both Short Days and Low Temperatures.	229
Figure 5.13	Venn Diagram of Time Series Changes in Barley Genes ‘Downregulated’ by Transition to Both Short Days and Low Temperatures.	230
Figure 5.14	Transient Changes in Gene Expression Accompanying Exposure to Cold Acclimation Conditions.	231
Figure 5.15	The Effect of ABA Applications of Barley Leaf Cold Tolerance (LT ₅₀).	237
Figure 5.16	Two-Dimensional Principal Component Analysis of Transcript Profiles in Cold Acclimated <i>Hordeum vulgare</i> (cv. California) Leaves Treated with ABA.	241
Figure 5.17	Time Series Heat Maps for Barley Sequences Responsive to Exogenous Foliar ABA Application.	244
Figure 5.18	Venn Diagram of Time-Dependent Increases in Barley Leaf Genes Abundance Induced by ABA Application.	245
Figure 5.19	Venn Diagram of Time-Dependent Decreases in Barley Leaf Genes Abundance Induced by ABA Application.	246
Figure 5.20	Transient Changes in Gene Expression Resulting from Exogenous Foliar ABA Application.	250
Figure 5.21	Venn Diagram Comparing of All Sequences Induced by up to 4 Weeks of Foliar ABA Application and Cold Acclimation	252
Figure 5.22	Venn Diagram Comparing of All Sequences Suppressed by up to 4 Weeks of Foliar ABA Application and Cold Acclimation	253
Figure 6.1	Overview of Wnt Signalling Pathway in Plants	256
Figure 6.2	CRISPR-Cas9 is a method that is used to target and alter specific sequences with the ability to replace removed sequence with new sequences.	259



وَفَوْقَ كُلِّ ذِي عِلْمٍ عَلِيمٌ

In the name of God, the Most Gracious, the Most Merciful.

“Over every possessor of knowledge is one [more] knowing” (Quran, 12:76)

ACKNOWLEDGEMENTS

Countless thanks and praise to Allah for helping me to achieve this thesis and assisting me in this short life. Also I am indebted to my supervisor, Doctor Peter Dominy, for the spiritual support, the guidance, the kindness, the opportunity, and his help in the preparation of this thesis ‘no award can describe his assistance’. Many thanks to him for giving me advice throughout the course of this undertaking. I highly appreciated all the valuable discussions we had throughout the Ph.D. period about my experimental designs and outcomes. I don’t think I have enough words to thank him for his assistance.

I would also like to thank all people of the Dominy group especially: Dr Mohammad Alamosa, Janet Liard and all other students and colleagues who worked together with me. For all the assistance and even the little favours and support they provided me with during the four years of my project. I am especially thankful for everyone in the Bower Building. Many thanks to all my friends who have supported me. In particular the Ministry of Higher Education of Saudi Arabia for the financial support from Saudi Arabia and staff in Taibah University, Al Madinah al Munawwarah, Saudi Arabia.

Last, but by no means least, massive thanks to my parents. The unlimited support and encouragement from my father and mother from the beginning and for their particular cares and prayers and wishes. I think no words can express my thanks to them, what they have done has been so fruitful for me.

I express thanks to my sons Almutasim and Muntasir and my daughter Hanin, for the warm environment they provided for with and their patience during my study period. I would like to thank my brothers and sisters and all the members of my family. Unquestionably, I would not have completed this work without the support from them, and without the help of Allah and the help of all people mentioned above.

LIST OF ABBREVIATIONS

ABA	Abscisic Acid
AP2/ERF	PETALA 2/ERE binding Factor
ABRE	ABA-Responsive Element
Ac	Acclimatization
Bp	Base pair
Bhlh	Basic helix-loop-helix
CA	Cold acclimation
cDNA	Complementary Deoxyribonucleic Acid
<i>CO</i>	Cold Regulated genes
CRT/DRE	C-repeat /Dehydration Responsive Element
<i>cv, cvs</i>	Cultivar / cultivars
CAMTA	Calmodulin-binding Transcription Activator
CBF	C-repeat Binding Factor
CE	Coupling Element
DHA	Dihydrogen Adenosine Phosphate
DHN	Dehydrin
DNA	Deoxyribonucleic acid
DRE	Drought Responsive Element
DREB	Dehydration-Responsive Element Binding
DRE/CRT	Dehydration-Responsive Element/C-repeat
EAR motif	ERF-associated amphiphilic repression motif
EE	Evening element
ERE	Ethylene-Responsive Element

EIN3	Ethylene insensitive 3
ETH	Ethylene
EST	Expressed Sequence Tag
EREBP	Ethylene-Responsive Element-Binding Protein
FAO	Food and Agricultural Organization of the United
<i>FR1</i>	Frost resistance 1
<i>FR2</i>	Frost resistance 2
Fr-A1	Frost resistance hexaploid wheat
Fr-H1	Frost resistance <i>Hordeum</i> (barley)
FT	Freezing Tolerance
FLC1	Flowering Locus C gene
FP	Forward primer
gDNA	genomic Deoxyribonucleic acid
GA	Gibberellin
HOS1	responsive genes1
HSF	Heat shock transcription factor
I	Interaction
ICE1	inducer of CBF expression 1
ICEr	Induction of CBF expression region
LT	Low Temperature

LEA	Late embryogenesis abundant
ICEr	Induction of CBF expression region
LD/LT	Long Day / Low Temperature
LD/WT	Long Day / Warm Temperature
LT ₅₀	Lethal temperate 50
MAPKs	Mitogen Activated Protein Kinases
MS medium	Murashige and Skoog medium
NA	Non acclimation
P	Photoperiod
PCR	Polymerase Chain Reaction
pH	Hydrogen Ion Concentration Unit
Ppm	Part Per Million
QPCR	Quantitative real-time polymerase chain reaction
QTL	Quantitative trait locus
ROS	Reactive Oxygen Species
RP	Reverse primer
Rpm	Revolution per Minute
RT	Room Temperature
RT-PCR	Reverse Transcriptase Polymérase Chain Rection
SDS	Sodium Dodecyl Sulphate

SD/WT	Short Day/ Warm (night) Temperature
SD/LT	Short Day Low Temperature
T	Temperature
TmCBF	<i>Triticum monococcum</i> CBF
TFs	Transcription Factors
TR	Transpiration Rate
t/ha	Ton/ Hectare
TAE	Tris-acetate EDTA
<i>TmCBF</i>	<i>Triticum monococcum</i> CBF
Tris	Tris (hydroxyethyl) amino methane
UV	Ultra violet
V/v	volume/volume
VRN	Vernalization
<i>VRN1</i>	Vernalization 1
W/v	Weight/volume

Declaration

I declare that this thesis for the degree of Doctor of Philosophy has been edited entirely by me and the work presented herein was performed by me unless stated otherwise.

Signature: Date:

Chapter 1 Introduction to Cold Stress and Cold Acclimation in Small-Grained Cereal Crops

1.1 Global Challenges for Food Security

Over the past 150 years, there has been an enormous global increase in food production (Kishore & Shewmaker, 1999). This is due to the use of chemical and organic fertilisers, pesticide chemicals that eradicate insects and weeds, the employment of better agronomic methods, the availability of water for agricultural purposes, and, more recently, the utilisation of genetic manipulation technologies to produce better strains and breeds (Huang et al., 2002). For example, since the start of the Green Revolution 50 years ago, there has been an approximately twofold increase in the production of cereal foods (Kishore & Shewmaker, 1999), and in the 1960s, the programme led to a reduction of approximately 20% in universal food shortages in Asia (Toenniessen et al., 2003). However, in order to meet the demand for food in the 21st century, it has become necessary to use new lands for agricultural purposes to increase food production.

One of the challenges facing the food production industry is that the rate of food production is not consistent around the world. This is due to differences in climate and terrain, and the unequal distribution of resources and experienced workforce (Barrett, 2010). In addition, food production has reached the limit of highest possible yield (yield potential) of any given crop (Barrett, 2010). Across the five continents, an estimated 183 countries import food from other countries that are known to be sparsely populated and strictly agricultural. For example, 80% of cereal supplies come from the USA, Canada, Australia, and Argentina (Census Bureau & Press of USA, 2004).

Nonetheless, this situation may change over the next seven decades, particularly given that the population of the USA is continually increasing, and predicted to double to 540 million people (Census et al., 2004). The total world population is also increasing and is projected to rise by more than one billion by 2030, and by over 2.4 billion by 2050 (Bruinsma, 2017; UN, 2016). To feed this increasing population, agricultural food production must be increased by 70% by 2050 (Timan et al., 2011; Wani et al., 2014). Considering these trends

in population growth, it is possible that, by 2050, these countries will have ceased to export food to enable them to meet the needs of their growing populations (Lester Russell Brown & Kane, 1995).

The world's population has increased by about three and a half times since 1900 (Pimentel et al., 1997). According to statistical data from the World Bank and the United Nations FAO, between 1 and 2 billion people suffer from malnutrition as a result of inadequate provision of food, low income, and unbalanced food allocation (Pimentel et al., 1997). Most of these people live in developing countries; the statistic mentioned above includes one third of the population of sub-Saharan Africa (I. FAO, 2016). Population growth leads to environmental crises, frequent human conflict, and social disturbances (Brown, 2011; Carpenter & Watson, 1994). It also leads to an increased demand for agricultural land, meaning that, as farming extends into tropical arid lands, new technologies for irrigation are needed, and the application of fertilisers becomes critical to increasing the yields of these dry lands. Moreover, the growth in the world's population has resulted in the increased occupation and urbanisation of lands that could have been used for crop production.

An important goal for researchers in this context is to increase the production yield of crops in general. In barley and all cereal crops, this aim must be achieved by increasing the quality and amounts of the grain harvested while cultivating the smallest possible area of agricultural land – that is, increasing crop production by increasing yields (T/Ha) – due to the low availability of suitable new agricultural lands.

The current strategy of clearing more lands to grow crops and use of chemical fertilisers could have serious impacts on the environment and long-term climate change. It is clear that more sustainable strategies are required to address the global challenge of ensuring food security.

1.2 Impact of Abiotic Stress on Food Productivity

Environmental stresses play a crucial role in the productivity, survival, and reproductive biology of plants and crops. Plants are subjected to many forms of environmental stress, (drought, salinity, temperature (high/low), chilling and freezing, radiation-UVB, heavy metal toxicity, and irradiance (length of photoperiod). Temperature and light (length of

photoperiod) are two of the most important factors, significantly affecting the life processes of all organisms. Temperature stresses experienced by plants are usually classified into three types: (a) chilling stress (occurring at low temperatures above freezing); (b) freezing stress (occurring at low temperatures below freezing); and (c) high temperature stress. All plants can suffer from chilling and freezing damage caused by a drop in the temperature of the surrounding environment. However, the nature of the damage, and the ways in which the damage can occur, differ significantly (Burchett et al., 2006). Chilling damage takes place when the temperature remains above freezing point (i.e., 32°F or 0°C). Thus, plants that grow in tropical and subtropical climates are more vulnerable to chilling damage (Xin & Browse, 2000). However, plants that live in temperate forests are also vulnerable to chilling injuries. The factors that determine the sensitivity of plants to such damage include the degree and the duration of the drop in temperature, the age of the plant, its hydration state, and the season during which the temperature falls (Burchett et al., 2006; Xin & Browse, 2000).

Low temperatures cause changes in the different physiological and biochemical processes that control normal metabolic pathways (Lantican, 2001). As a result, the characteristic signs of chilling damage will appear; these include colour changes, failure to grow, flaccidity, and even genetic changes (Bagdonas, Georg & Gerber, 1978). Previous studies have assumed that the physical nature of the cell membrane in plants suffering chilling damage changes from the usual elastic liquid-crystalline to a rigid gel structure. However, this assumption has not yet been proved (Burchett, Niven & Fuller, 2006; Bakht et al., 2006). In addition, low but non-freezing temperatures can cause a range of damage symptoms in susceptible plants (Burchett, Niven & Fuller, 2006), such as interference with germination, delay in flowering and harvest production, and changes to the storage times of the plant.

Low temperatures have a negative impact on the growth and distribution of plants. Each plant has its own cold temperature limit which cannot be exceeded, and unique responses are required in order to avoid injury to the plant. When temperature is lowered, every plant has a unique ability to respond to temperature changes that occur in minutes or over hours in an open field or a greenhouse. During this time, the biosynthetic activities of the plant are reduced and normal physiological processes may be inhibited, leading to permanent injuries and/or death as a result of chilling. The rapidity of the temperature change, as well as the

length of time the plant is exposed to lower temperatures, matters greatly (Tantau et al., 2004).

As previously mentioned, damage due to freezing temperatures is a worldwide issue, and frost damage to crops has been a problem for humans since cereal crops were first cultivated. Just one night of freezing temperatures can lead to complete loss of a cereal crop. The exception to this is in tropical latitudes, where temperatures rarely fall below freezing point (32 F/0 °C), at least at low altitudes. Generally, frost damage in subtropical climates is associated with slow-moving cold air masses that may bring between one to three nights of between 7 and 10 hours of sub-zero temperatures (Tantau et al., 2004).

Farmers often use the terms ‘freezing’ and ‘frosting’, however, technically, the word ‘frosting’ is used to refer to the formation of ice crystals on surfaces and ‘freezing’ is a phase change from vapour to ice (Alonso-Blanco et al., 2005). Despite this, the word freezing is widely used to describe a meteorological event when crops and plants face freezing injury.

A frost occurs when the air temperature drops to 0°C or lower, but a freeze takes place when extracellular water within the plant freezes (i.e., changes from liquid to ice). This damages the plant tissue, depending on tolerance factors (such as the solute content of the cells). Frost damage to crops often results not from low temperatures but from this extracellular (i.e., not inside the cells) ice formation inside the plant tissue, which draws the water out, causing dehydration and injury to the cells. Following cold periods, plants tend to harden against freeze injury and soften following a warm period (Tantau et al., 2004).

Temperature is a critical factor in the plant environment and plays a significant role in growth and development of plants. Low temperatures due to seasonal variations and geographical distribution on the Earth inhibit plant growth and survival. Approximately two thirds of the world’s land mass is annually subjected to temperatures below 0°C, and approximately half suffers from freezing temperatures below -20°C (Erwin, 2004). Agriculture is affected by frequent extreme temperature changes, which impacts grain productivity. Thus, improving cereal productivity is not only a matter of increasing the yield potential of the germplasm, but also of improving yield stability by ensuring enhanced tolerance to abiotic stresses such as cold.

Most crops of economic importance are sensitive to temperatures below 10°C (Jean-Benoit, 2013). Rye (*Secale cereale*) and winter barley (*Hordeum vulgare*) are two such crops that belong to the wheat tribe (*Triticeae*). They are commonly used for food production, such as beer and bread, and for animal fodder. Freezing temperatures in the winter or spring can result in significant losses in the yields of these economically important crops (Figure 1.1).



Figure 1.1: Barley Field (Fiorenzuola, Northern Italy) Trial After a Cold Winter with a Long Snow Cover Period.

A barley genotype (centre) showing a high level of winter damage; only a few plants remain alive after winter, and some cultivars are completely devastated by winter conditions. Reproduced from Thalhammer et al. (2014).

1.3 Strategies for Increasing Food Production

Abiotic stress is a primary threat to agricultural production. Stress conditions cause a reduction in growth and development, which ultimately affect the yield of crops. Under stress conditions, plants develop and express various mechanisms to adapt or deal with the associated challenges. While these natural defence mechanisms are usually sufficient to allow the survival of the plants, the responses are often inadequate to prevent a decrease in crop yield due to stress factors. Therefore, many strategies have been employed to produce abiotic stress-tolerant crop plants. Cold stress is an example of abiotic stress that constitutes a major environmental factor seriously affecting plant growth and development (Körner, 2016), and thus influencing crop productivity. Temperate region cereals such as wheat, barley, and rye commonly encounter freezing temperatures when overwintering as well as during their active growth season. For example, winterkill or frost damage during the formation of reproductive organs or seeds for both spring and winter cultivars can eliminate plant productivity. Hence, cold stress is a major factor that limits food productivity from cereal crop plants.

Since the latter part of the 19th century, botanists and plant scientists have been examining how plants respond and adapt to wide temperature changes, in particular, low temperature stress or cold shock (Gusta & Wisniewski, 2013). Some studies have focused on the challenge of maintaining or increasing crop yield under conditions in which the plants are exposed to frost. It has been found that shortening the time period between sowing and harvesting could avoid periods of frosts and allow multiple harvests per year.

Research on frost tolerance raises several questions, such as, 'How do plants adapt to freezing temperatures and acclimate to survive the formation of ice within their tissues?' Higher latitudes often have occasional sporadic frosts in winter, which crops may not survive, thus decreasing production (Sanghera et al., 2011). In contrast to cereal crops, many wild grasses can survive both chilling and freezing temperatures at high latitudes (Tondelli et al., 2011). Many of the major cereal crops, including wheat, barley, and temperate cereals, do not survive freezing conditions well. This raises the need to improve cereal crop freezing tolerance to increase production at high latitudes. Previous efforts to improve plant stress tolerance have typically used classical breeding methods; however, these methods are slow in practice. Genetic engineering offers a viable alternative, but using this technology to

manipulate plant defence systems is only as powerful as our comprehension of the systems themselves. A better understanding of plant stress signal perception, and transduction and activation of defence responses at the cellular and molecular level, is therefore imperative.

One area of active current research is focused on understanding the biological mechanisms underlying plant tolerance to frost. More recently, an increased understanding has emerged of the regulation of the genes involved in cold adaptation, freezing responses, and response to environmental stress in general. Recent studies have made progress in understanding the various genetic protective responses to stress stimuli, using the model plant *Arabidopsis thaliana*.

1.4 Low Temperature Stress in Plants

As a result of global warming, alterations in seasonal patterns are often accompanied with changes in temperature and occurrence of freezing stress that can appear without any previous chilling period (Warren, 1998). Natural tolerance to low temperatures varies widely between plant species. Some plant species can survive the ravages of extreme cold (Nilsson-Leissner, 1929), with some capable of enduring temperatures as low as -196°C (Sakai & Larcher, 1987). On the other hand, mild chilling temperatures between 0 and 5°C are lethal to other species, for example, tomato. Plants growing in tropical countries are generally unable to withstand even mild chilling (Zhu & Zhu, 2007), while some cultivated crops, such as winter wheat, can tolerate temperatures below -25°C (Atıcı & Nalbantoğlu, 2003). Temperate plants are often tolerant of chilling temperatures, and it is known that these plants have developed mechanisms to increase their ability to withstand freezing temperatures following a period of low but non-freezing temperatures (Janská et al., 2010; Kume et al., 2005; Levitt, 1980b; Monroy et al., 2007). This process, called cold acclimation, is a multigenic and quantitative trait that is associated with complex physiological and biochemical changes (Monroy et al., 2007; Stitt & Hurry, 2002; Winfield et al., 2010). Significantly, cold stress, which includes both chilling and freezing injuries, modifies gene expression and plant metabolism with consequent effects on many biological functions (Chang et al., 2010; Chinnusamy et al., 2007; Goulas et al., 2006; Stitt & Hurry, 2002).

1.4.1 General Morphological and Physiological Changes Associated with Chilling Stress

When the temperature remains above freezing (0°C), plants that grow in tropical and subtropical climates are often vulnerable to chilling damage (Xin & Browse, 2000). Plants that live in temperate regions are also vulnerable to chilling damage, but frost damage is more significant. The factors that determine the sensitivity of plants to chilling damage include the degree and duration of the drop in temperature, the age of the plant, its hydration state, and the season during which the temperature falls (Xin & Browse, 2009; Burchett et al., 2006).

The wide range of physiological, biochemical, and molecular changes that occur in plants exposed to low temperatures require a robust global approach to studying the response. Exposure to low temperatures reduces the normal functioning of cellular processes, and water and nutrient uptake. Chilling injury is associated with a complex array of cellular dysfunctions; some of these can be visible, such as colour changes, when the plant becomes brown or yellow in colour (Fig. 1.1). The plant may also become flaccid and late flowering may occur (Lukatkin, Brazaityte, Bobinas & Duchovskis, 2012). Typical symptoms of chilling injury include loss of vitality, reduced leaf expansion, wilting, chlorosis, necrosis, and changes in root growth (Noh et al., 2009). Sterility is another phenotypic indicator of chilling stress (Mahajan & Tuteja, 2005). Changes at the physiological level include reduced growth caused by inhibition of photosynthesis (Ruelland & Zachowski, 2010), along with disruption in protein assembly, general metabolic reactions, production of free radicals (Mahajan & Tuteja, 2005), and even death (Levitt, 1980). Damage can be reduced in plants by acclimating them to chilling through gradual exposure to low temperatures.

1.4.2 General Physiological Changes Associated with Freezing Temperatures

At night, the temperature of the above-ground parts of plants is determined almost entirely by the ambient air temperature (Rada et al., 1985). When the air temperature falls and approaches 0°C, conditions start to become stressful for some plants (e.g., tomatoes). This can lead to a perturbation of metabolic activity and normal physiological processes may be

inhibited leading to permanent injury and/or death in chilling-sensitive plants. Chilling-tolerant but freezing-sensitive plants are generally able to survive temperatures slightly below zero but are severely damaged upon ice formation within tissues. Hence, to understand the effects of cold stress on plants, it is necessary to distinguish between positive temperatures chilling stress (chilling temperatures above freezing; 0–15°C) and negative temperatures freezing stress (freezing temperatures below 0°C) (Thomashow, 1999; Yadav, 2011). The extent of injury to the plant depends on its sensitivity to freezing at the time of the event and the length of time the temperature is below the ‘critical damage’ temperature. Exposure to freezing temperatures cause more severe damage to cells than chilling temperatures because freezing can trigger the rupture of the cell membrane and formation of intracellular ice, which leads to cell death.

The response of plants to sub-zero temperatures manifests mainly in two phenomena: super cooling and ice nucleation. Super cooling is a metastable state of water in which it remains liquid below 0°C. This is a freeze avoidance mechanism which, in some cases, is supported by the presence of antifreeze proteins (AFPs) and antifreeze agents (Davies, 2014). Super cooling is disrupted by ice nucleation (Duman & Wisniewski, 2014). Ice nucleation can be either homogeneous or heterogeneous (Lee et al., 1995). Freezing is heterogeneous in nature (Wilson et al., 2003) and is initiated by extrinsic or intrinsic ice nucleators. In plants, extrinsic ice nucleators are caused by bacteria and fungi, which often reside in the phyllosphere (Wisniewski et al., 2008). Freezing injury occurs when ice is formed in the extracellular spaces of plant tissues (Fig. 1.2). Ice formation is dependent on the presence of ice nucleators (organic or inorganic substances) and the rate at which the external temperature drops (Levitt, 1980a; Mazur, 1969; Palta & Weiss, 2018; Weiser, 1970). Ice formation in the apoplast reduces its water potential, which leads to withdrawal of water from the cells (Bredow & Walker, 2017). This loss of water causes cell shrinkage and, subsequently, cellular dehydration. It follows that freezing stress is accompanied by dehydration stress at the cellular level. If cooling proceeds at a slow or moderate pace, cellular dehydration will occur to the extent required to establish equilibrium between the intra and extracellular aqueous spaces. This will prevent intracellular freezing resulting in a non-lethal effect of the cooling process. If there are no ice nucleators present (no dust, bacteria, or any other particle), and the water is very clean, it remains in a super-cooled state above -38°C, the temperature at which water self-nucleates (Thomashow, 1998). Ice nucleating agents have been found in the extracellular liquid of a number of species,

including perennial trees such as prunus (Gross et al., 1988), citrus (Constantinidou & Menkissoglu, 1992), and the annual winter rye (Brush et al., 1994).

Plants are most vulnerable to freezing injury at their membranes, primarily through frost-induced cellular dehydration (Steponkus, 1984; Webb et al., 1994). Freezing stress causes the membrane to rigidify, destabilises protein complexes, and impairs photosynthesis (Zhu, 2016) when environmental temperatures fall below 0°C, and can cause more serious injury to the plant when extracellular ice crystals penetrate into the cells of plant tissues (Palta & Weiss, 2018; Pearce, 2001). The accumulation of intercellular ice physically disrupts the cell membrane (Palta & Weiss, 2018), causing lysis and cellular dehydration.

Because the chemical potential of ice is lower than that of liquid water at a given temperature, the water potential of extracellular fluid is lowered relative to the intracellular fluid (Thomashow, 1999). Liquid water always moves from a higher to a lower water potential. Under freezing conditions, the movement of water from the cytoplasm to the intercellular space continues until an equilibrium is reached between the liquid phases of the intracellular and the extracellular water. This results in cellular dehydration, cell shrinkage, and an increased endogenous solute concentration. Upon thawing, water moves rapidly back through the plasma membrane, causing the protoplast to burst before it regains its original size; this process is called expansion-induced lysis (Xin & Browse, 2000). As the cells burst, ions and solutes leak into the surrounding interstitial spaces, giving a water-soaked appearance to the plant tissues; the inability to regain turgor is a typical symptom of freezing injury in plants (Palta et al., 1977).

On the other hand, in cold-acclimated plant cells, freezing causes cells to dehydrate and shrink, while the plasma membrane forms exocytotic extrusions that are reincorporated into the plasma membrane during rehydration, and the cells are able to swell to their original size without lysis (Steponkus et al., 1988; Uemura & Yoshida, 1984). Thus, the major sources of freezing damage result from cellular dehydration, membrane damage, and changes in genes expression and protein function (Thomashow, 1998).

Plant membranes to undergo chilling and freezing through frost-cellular dehydration that occurs during freeze–thaw cycles or lacerations caused by ice crystals. Structural and functional changes can also occur through oxidative damage to membranes during freezing and thawing (Thomashow, 1999; Wolkers et al., 2007). Reactive oxygen species (ROS) are

usually present in cells at low levels under normal conditions. However, ROS can accumulate under freezing stress through suppression of the enzymatic scavenging system during freeze-induced dehydration (Wolkers et al., 2007).

At the molecular level, freezing affects membrane lipids, proteins, and nucleic acids (Wolkers et al., 2007). The fluidity of the cell membrane is determined by the structure and composition of its lipids and proteins. Cold exposure also causes changes in membrane lipid composition (Yoshida et al., 1998; Yoshida & Uemura, 1984). Induced cellular dehydration alters the organisation of the lipid bilayer by destabilising hydrophobic lipid–lipid and protein–lipid interactions within the membrane (Pearce, 1999). One form of freezing damage is caused by the formation of lipid hexagonal II phases in regions where the plasma membrane and the chloroplast envelope are closely apposed (Steponkus et al., 1988). Therefore, during freezing, cell membranes undergo a phase transition from a flexible crystalline state to a solid gel-like state. This results in damage at macroscopic structural level, and local aggregations of proteins and lipids, known as lateral phase separation (Wolkers et al., 2007).

One interesting observation of cold-acclimated leaf cells relates to behaviour of the plasma membrane during freeze-induced cell dehydration. As cells dehydrate during the freezing process, tension on the plasma membrane is maintained at a critical level by reducing the amount of membrane surrounding the cell. In non-acclimated leaf cells of oats, rye, and *Arabidopsis*, this is achieved by removal of small patches of membrane to make intracellular vesicles. By contrast, in cold-acclimated cells, tension is maintained not by the removal of patches of membrane, but by forming long, thin extracellular extensions (protrusions); hence, the surface area of the membrane is maintained despite the decreasing volume of the protoplast (Steponkus et al., 1988; Woolfe et al., 1983; Dowgert et al., 1984; Yamazaki et al., 2008). It is understood that this difference in the behaviour of plasma membrane in response to freeze-induced dehydration accounts for the expansion-induced lysis of non-acclimated cells that occurs during the thaw stage. Here, the sudden appearance of water in the cell wall space that occurs when extracellular ice melts at 0°C and quickly enters the dehydrated cell and the intracellular vesicles that formed during the slow freeze process cannot re-integrate plasma membrane quickly enough to accommodate the rapidly increasing cell volume; hence, lysis occurs. This is not understood to be the case for cold-acclimated cells, as the plasma membrane that forms the extracellular extensions are

contiguous and this allows rapid expansion without rupture. It is not clear what processes lead to the different properties of non-acclimated and cold-acclimated plasma membrane, but change in the lipid composition has been implicated. Another, perhaps more likely, explanation is a change in the structure of the cell cytoskeleton, as the extracellular extensions must have some internal support to maintain their shape.

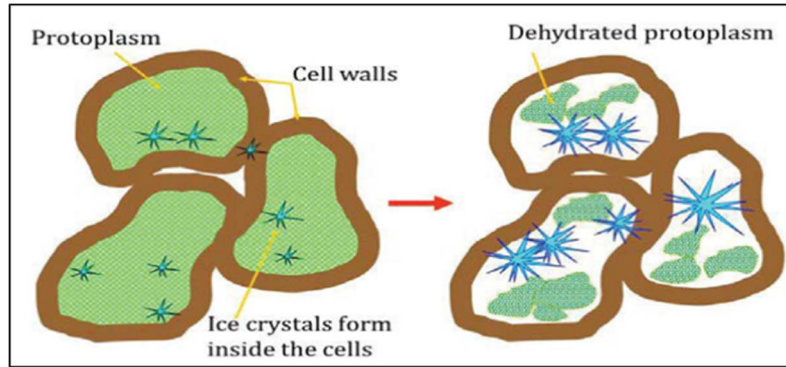


Figure 1.2: The Plasma Membrane is the Primary Site of Freezing Injury and Physical Damage.

Ice crystals form and grow in a plant's tissues, leading to dehydration of the plant's cells, rupturing its membranes and killing the living protoplasm (Source: UGA Cooperative Extension B1467; Effects of Low Temperature on Plants).

1.4.3 Plant Strategies for Avoiding Frost Damage

Plant tissues encountering low temperature have two general strategies to survive low temperature stress: avoidance or tolerance of freezing (Sakai & Larcher, 1987; 2012). Plants can avoid freezing mainly through super cooling of tissue water in xylem tissues (Ishikawa, 1984; Sakai & Larcher, 2012). However, this mechanism has limited value since it occurs only in special organs such as seeds, overwintering buds, or xylem ray parenchyma cells in many hardwood trees and shrubs (Sakai & Larcher, 1987). Therefore, tolerance is the main way by which plants can survive freezing stress and various such strategies have been adopted by plants.

‘Sweetening’ is one of these strategies that plants may use to avoid frost or freeze damage, and is often seen in cool-season vegetables. When exposed to freezing temperatures, the water in the cells of non-acclimated cool-season vegetables turns to ice and then bursts through the cell membrane. There are cold-hardy varieties of vegetables and fruit which produce extra sugars during cold acclimation; the increased concentration of sugars lowers the freezing point of water and stops the water in the cells from freezing, thereby avoiding membrane rupture. This explains why frost-tolerant vegetables tend to get sweeter under cool temperatures, because the sweetening process takes time to provide protection and the autumn cool-down takes place in a slow and consistent way.

There are other protective strategies that plants can deploy in order to reduce the effect of freezing injury and ice formation; one is the synthesis of AFP, where plants secrete AFPs into the apoplast. This strategy has been observed in several freezing-tolerant monocotyledons, such as winter barley, winter rye, and winter wheat. The synthesis of AFPs does not appear to be a general response of plants to low temperature; rather, it is specific to particular plants (Antikainen & Griffith, 1997). Many cold-tolerant species are able to prevent the accumulation of ice in their tissues using this strategy; however, the AFPs may not protect against the damaging effects of freezing on plant physiology.

Other tolerance mechanisms involve controlling the formation of ice crystals at certain sites within plant tissues (Sakai & Larcher, 1987; Single, 1964). Evergreen conifers undergo dormancy to survive low temperature (LT), whereas many other plant species can increase their degree of freeze tolerance in response to low, non-freezing temperatures through the phenomenon known as cold acclimation.

1.5 Cold Acclimation in Plants

Most temperate plant species become more frost tolerant when exposed to progressively lower temperatures (Sanghera et al., 2011), but the ability to survive winter is dependent on the rate of hardening and the ultimate level and stability of hardiness (Anower et al., 2016). Tolerance to freeze-induced dehydration is the major survival strategy in most cold-hardy plant species. The changes in water relations at the cellular level during freezing have been well documented. At one extreme are plants from tropical regions that have virtually no capacity to survive even the slightest freeze. In contrast, herbaceous plants from temperate regions can generally survive freezing temperatures ranging from -5°C to -30°C , depending on the species, whereas perennials in the boreal forests routinely survive winter temperatures below -30°C .

The process of cold acclimation can take hours, at best, and days or more for many plants. There are also limits as to how quickly cold acclimation can happen for the plant to adapt to temperature shifts. Some plants cannot respond quickly enough, and when such changes in temperature occur, parts of the plant become vulnerable. A plant's response to cold stress can be divided into four phases: the early cold exposure phase, the acclimation phase, the resistance phase, and the de-acclimation phase (Sakai & Larcher, 2012).

A cold-acclimation mechanism has been proposed by which the cold signal is transduced from the membrane to the nucleus (Kidokoro et al., 2017), leading to a series of biochemical and physiological changes in the cell and an interactive network of transcription factors (TFs) resulting in expression of cold-responsive genes that activate stress tolerance (Medina et al., 2011; Theocharis, Clément & Barka, 2012). Several cold-regulated genes, known as COR (cold-regulated), KIN (cold-induced), LTI (low temperature induced), and RD (responsive to dehydration) genes, are triggered in response to cold treatment (Zhu et al., 2007). In addition, it is known that TFs such as dehydration-responsive element (DRE) and abscisic acid induced protein (*abi3*) are involved as part of the response to low temperature stress conditions in *Arabidopsis* (Theocharis et al., 2012).

The changes brought about by cold acclimation has also been shown to protect the photosynthetic machinery mediated through the enhanced expression of CBFs (Savitch et al., 2005), possibly through sensitivity to feedback-limited photosynthesis (Dahal et al., 2012). The detailed nature and molecular mechanism of these freezing tolerance systems are

not yet well understood. Plants, like other organisms, accumulate low molecular weight water-soluble compounds known as ‘compatible solutes’ or ‘osmolytes’ in response to the osmotic stress caused by low temperature and other abiotic stresses (Giri, 2011). Examples of soluble osmolytes include carbohydrates, polyamines, amino acid (proline), glycine, betaine, and a variety of sugars (Gupta & Kaur, 2005; Yoshida et al., 1998; Tantau & Dörffling, 1991). These, in conjunction with dehydrin proteins (DHNs), hydrophilic proteins (LEA) proteins, and CORs, act to stabilise both membrane phospholipids and proteins and cytoplasmic proteins, maintain hydrophobic interactions, and scavenge ROS (Stockinger et al., 1997; Thomashow, 1999, Griffith & Yaish, 2004). The changes in gene expression during cold acclimation were first demonstrated by Guy et al. (1985). Since then, research has focused on identifying these genes and seeking to understand their function and regulation. These genes are discussed further in Section 1.5.4 of this chapter, and some of the most commonly observed changes during cold acclimation and cold stress are summarised in Figure 1.3 below.

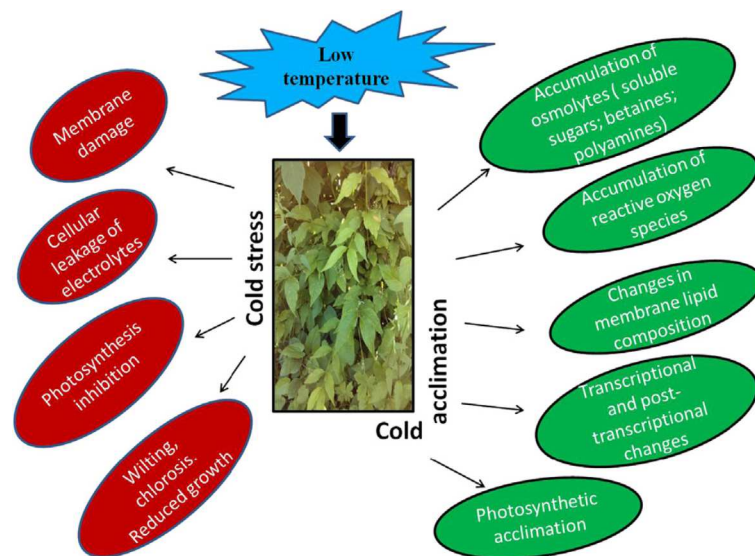


Figure 1.3: Cellular, Biochemical, and Molecular Changes Involved in Response to Cold Stress and Cold Acclimation.

Reproduced from Megha et al. (2014). See text for details.

1.5.1 Cold Acclimation-Induced Changes in Membrane Lipids

The plasma membrane is one of the primary sites at which the damaging effects of low temperatures are observed at the cellular level. A decrease in temperature causes plasma membranes to rigidify. In addition, cold acclimation results in changes in the lipid composition of the plasma membrane. The effect of low temperature on cellular membranes results in a slowdown of metabolism, solidification of cell membranes, and loss of membrane functions. It is known that the plasma membrane is the primary site of such injury and may be irreversibly damaged due to a consequence of extracellular freezing (Uemura et al., 2006).

The changes that occur in *Arabidopsis* plasma membranes at low temperature include an increase in phospholipids and a decrease in sphingolipid (for example, glucocerebroside) and free sterol content (Uemura et al., 1995). Such alterations change the cryo-behaviour of the plasma membrane and restore membrane fluidity at low temperatures (Steponkus et al., 1990). Similar increases in phospholipid content have been observed in many different plant species, from monocotyledonous to dicotyledonous, and from herbaceous to woody plants (Uemura et al., 2006).

Freezing stress usually results in ROS formation in plant cells, which damages membrane lipids, nucleic acids, and proteins, and disturbs the homeostasis of the organism (Ali et al., 2010). Changes in membrane lipid composition provide protection to the plasma membrane and chloroplast envelope from injury (Matteucci et al., 2011). The increased content of unsaturated fatty acids reduces the threshold temperature for membrane damage in acclimated plants relative to that of non-acclimated ones (Theocharis et al., 2012). For example, chilling-sensitive varieties of rice have been observed to have a greater proportion of saturated fatty acids in the phosphatidylglycerol (PG) of the chloroplast membrane (Yokoi et al., 1998). The increase in the proportion of unsaturated species of phosphatidylcholine and the degree of fatty acid unsaturation in the plasma membrane plays a vital role in chilling tolerance (Nishida & Murata, 1996; Zheng, Li & Li, 2016). Lipids with a high composition of unsaturated fatty acids prevent the formation of expansion-induced lysis during the freezing/thawing cycle (Uemura & Steponkus, 1989; Palta & Weiss, 2018; Zheng et al., 2016).

Cold-acclimation mechanisms help stabilise the membrane and prevent intracellular ice formation to help offset freezing injury (Lata et al., 2011; Ruelland et al., 2009; Zhue, 2016).

Steponkus et al. (1990) reported differences in lipid ratios between cold-acclimated and non-acclimated rye plasma membranes. These analyses suggest that changes in lipid composition may reduce ultra-structural changes in the membrane occurring, due to membrane fusion (Fujikawa et al., 1999). Uemura et al. (1995) analysed changes in the lipid composition of *Arabidopsis* membranes during cold acclimation, and found increases in the proportion of membrane phospholipid, from 46.8% to 57.1%, during cold acclimation. Alterations that can contribute to increased freezing tolerance include increased levels of fatty acid desaturation in membrane phospholipids and changes in the levels and types of membrane sterols and cerebrosides. Whereas plasma membranes from non-acclimated plants suffer expansion-induced lysis and formation of hexagonal II phase lipids upon freezing, membranes from cold-acclimated plants do not (Steponkus & Webb, 1992). The stabilisation of membranes against freeze-induced injury appears to involve multiple mechanisms in the protoplasm (Kaplan et al., 2007; Xin & Browse, 2000; Zhao et al., 2009).

1.5.2 Cold Acclimation-Induced Changes in Sugars

The role of accumulation of soluble sugar in the development of freezing tolerance in plants is well documented (e.g., Levitt, 1980; Siminovitch, 1981). Several studies suggest that sugar functions as an osmotic substance and membrane stabiliser, and might be an antioxidant in cold stress responses (Bolouri-Moghaddam et al., 2010; Keunen et al., 2013; Valluru et al., 2008). It has been shown that the content of soluble sugars in *Arabidopsis* leaves increases dramatically during cold acclimation (Klotke et al., 2004; Rohde et al., 2003), and a link has been established between the induced alteration of sucrose metabolism and cold tolerance (Strand et al., 2003). Similar studies in cereals such as winter wheat (Hurry et al., 2004; Sagisaka et al., 1991), winter rye (Koster & Lynch, 1992), and winter *B. napus* (Gusta et al., 1995) have all shown a significant increase in total soluble sugars during cold acclimation. In addition to the cryoprotective role played by sucrose in plants, the sugar also helps to stabilise membranes by replacing the lost water, thus preventing lipid phase transitions (Zuther et al., 2004). The water-replacement hypothesis suggests that, during dehydration, sugars can substitute for water molecules (in particular, by hydrogen bonding) around the polar and charged groups present at the surface of phospholipid membranes and

proteins, thereby stabilising their native structure in the absence of water (Crowe & Clegg, 1988).

1.5.3 Cold Acclimation-Induced Changes in Compatible Solutes

The accumulation of low molecular weight water-soluble compounds known as ‘compatible solutes’ or ‘osmolytes’ is the common strategy adopted by many organisms to combat environmental stresses (Giri, 2011). Certain low molecular weight organic metabolites act as osmolytes and help plants to survive extreme osmotic stress. There is a marked increase in the levels of these metabolites during exposure to abiotic stresses and they are understood to help the plant adapt its stress tolerance. When present in high concentrations, these solutes do not perturb cellular functions (Papageorgiou & Murata, 1995), making it possible for them to function under stress conditions. Compatible solutes balance differences in the water potential between the cytoplasm and other parts of the tissue and are believed to protect macromolecules from the destructive action of physical and chemical factors (Chen & Murata, 2011).

The accumulation of osmolytes like glycine betaine (GB) in cells is reported to protect plants against cold stresses. Chen and Murata (2008) suggested that these osmolytes could function via two additional roles: GB could be involved in inhibiting ROS accumulation, activation of some stress-related genes, membrane protection, and protection of photosynthetic machinery; in addition, GB could influence expression of several endogenous genes in transgenic plants. Not all plants can accumulate GB in response to various abiotic stresses. For instance, cereals like wheat, maize, and barley do not accumulate a significant amount of GB naturally. (Chen & Murata, 2011). *Arabidopsis*, tomato, potato, and rice do not accumulate GB (Luo et al., 2012; Niu et al., 2007). Identification of genes for GB biosynthetic pathways has made it easy to engineer GB biosynthesis into non-accumulators via a transgenic approach for improved stress tolerance, and low levels of GB applied exogenously have also been shown to induce expression of stress-responsive genes coding for enzymes that scavenge reactive oxygen species (Chen & Murata, 2011). This finding suggests that GB can successfully balance the negative stress responses induced by low temperature and, therefore, can be used to improve the freezing tolerance of cold-stressed plants (Chen & Murata, 2011).

Free proline accumulates in plants in response to a wide range of abiotic and biotic stresses. It is known to occur widely in higher plants and normally accumulates in large quantities in response to environmental stresses (Ali et al., 1999; Kishor et al., 2005; Öztürk & Demir, 2002; Rhodes & Hanson, 1993; Verslues & Sharp, 1998). Proline is a naturally occurring amino acid, but it is also a compatible osmolyte that accumulates in many organisms. It is well-established as a protective molecule and has been reported to impart protection against cold stress into many plants, including higher plants. In addition to its role as an osmolyte for osmotic adjustment, proline contributes to stabilising sub-cellular structures such as membranes, proteins, and scavenging free radicals, and buffering cellular redox potential under stress conditions. The role of proline in plant responses to oxidative stress has been demonstrated extensively in experiments in which exogenous proline was applied (Hoque et al., 2007; Ozden et al., 2009), or in which proline synthesis or degradation was genetically engineered (Hong et al., 2000; Kocsy et al., 2005; Molinari et al., 2007). Proline has been shown to protect proteins during freeze–thaw cycles by creating a hydration shell for the protein (Crowe et al., 1990) and also acting as a molecular chaperone, thereby stabilising the structure and hence the function of crucial proteins and enzymes (Diehl et al., 2013). Proline also protects the genomic integrity of plants by maintaining the double-stranded structure of DNA (Law & Jacobsen, 2010), and provides a source of carbon and nitrogen for growth after stress relief (Giberti et al., 2014; Sharma et al., 2011; Szabados & Savoure, 2010). It also protects the plant by up-regulating the anti-oxidative stress machinery (Rejeb et al., 2014). Proline metabolism is involved in the regulation of intracellular redox potential and the storage and transfer of energy (Giberti et al., 2014; Sharma et al., 2011; Szabados & Savoure, 2010). Proline has additionally been shown to mitigate the harmful effects of cold stress in cold-stressed chickpea plants (Kumar et al., 2011).

It is well documented that proline accumulates robustly under cold stress. The importance of proline in improvement of stress tolerance in plants was demonstrated by manipulation of the genes that encode key enzymes of the proline synthesis or degradation pathway (Nanjo et al., 1999). In *Arabidopsis*, a more than two-fold increase in proline occurs after 4-hour exposure to a temperature of 4°C, followed by a continuous and remarkable up to 130-fold increase compared to the control level after 96 hours (Kaplan et al., 2007). This accumulation of proline is sustained even after new leaves develop in the cold (Hurry et al., 2000). In cereal crops such as wheat, proline increases in all cultivars. However, the extent of proline accumulation differs depending on the cultivar studied (Kamata & Uemura, 2004). For

example, after the initial surge in proline accumulation one week after cold exposure, prolonged cold acclimation resulted in different profiles (Wang et al., 2016). Kamata and Uemura's (2004) research, no further increase occurred in cultivar Haruyutaka, the least freezing-tolerant cultivar assayed, while the increase continued in Chihokukomugi, and Norstar which are more freezing-tolerant cultivars. Thus, even though proline accumulates in response to cold exposure, its content is not the limiting factor explaining the differences in freezing tolerance capacity in a population of *Arabidopsis* cultivars (Korn et al., 2008).

1.5.4 Proteins Associated with Freezing Tolerance

Dehydrins (DHNs) are a group of proteins that are postulated to protect lipid membranes against peroxidation (Theocharis et al., 2012) and also possess cryoprotective/antifreeze properties (Bravo et al., 2003; Hanin et al., 2011; Puhakainen et al., 2004). As discussed in Section 1.6.2, the basic function of genes in the CBF regulon is to protect cells against freezing and other stresses involving dehydration. Many genes that are triggered by a drop in temperature have been recognised in plants during the cold-acclimation stage (Tsuda et al., 2000; Zhao et al., 2016b). One class of such genes are known as late embryogenesis-abundant (LEA) genes. LEA proteins were first identified as a group of proteins that accumulate in cotton seeds during the late stages of development, when the embryo becomes desiccation-tolerant (Dure III et al., 1981). In all reported cases, the occurrence of these proteins was related to environmental stress conditions and their accumulation was almost always induced by cellular dehydration triggered by drought, desiccation, cold, salt, or freezing stress (Hinch & Thalhammer, 2012; Tunnacliffe et al., 2010). Most LEA proteins in *Arabidopsis* have been independently described as COR proteins because they are highly induced upon cold treatment (Thomashow, 1999).

LEA proteins are intrinsically disordered proteins (IDPs) under fully hydrated conditions, in which they adopt a predominantly α -helical structure during dehydration or in the presence of membranes (Thalhammer et al., 2010). Hence, it is frequently identified in the literature that their "unfolded, unstructured, disordered, and denatured state is a native, natural, inherent, and intrinsic" property of these proteins (Dunker et al., 2013). Several LEA proteins have been shown to be largely unstructured in dilute solutions, but fold into a mainly α -helical structure during drying (Hand et al., 2011; Hinch & Thalhammer, 2012).

However, this is not the case for all LEA proteins. Only very few of these proteins have been investigated in detail, limiting the scope for making more general structural and functional comparisons.

Plants respond to cold stress by regulating metabolism through the induction of the late-response genes (Byun et al., 2014), known as COR/LEA, or simply COR genes. The latter are induced by early-response elements, whereas late-response elements function several hours after exposure to cold-acclimation conditions. Many of the proteins encoded by these genes were later found to be part of the larger group of LEA proteins (Byun et al., 2014). There appears to be a good correlation between the expression of COR proteins and improved frost tolerance.

A growing number of genes have been shown to be induced during cold acclimation; many of these encode proteins with known activities that could potentially contribute to freezing tolerance (Hughes & Dunn, 1996; Thomashow, 1998). One of the best studied *Arabidopsis* COR/LEA proteins is COR15A; the gene was first cloned and described as cold and drought induced (Hajela et al., 1990). The protein accumulates in the soluble chloroplast stroma fraction shortly after exposure to cold and during cold acclimation (Lin & Thomashow, 1992; Thalhammer et al., 2014; Bryant, et al., 2014). This accumulation is necessary for the plants to obtain their full, cold-acclimated freezing tolerance (Thalhammer et al., 2014). The closest homologue of COR15A is COR15B, with 82% nucleic acid sequence identity (Thalhammer et al., 2010). The genes are localised in the nuclear genome, and the encoded proteins are targeted to the chloroplast stroma via signal peptides (Candat et al., 2013; Takahashi et al., 2013; Thomashow, 1998). The mature protein has a molecular mass of 9 kDa. Both mature proteins are highly hydrophilic and predominantly unstructured in solution; COR15A is mainly unstructured in dilute solutions, but folds into amphipathic α -helices in a helix-loop-helix formation in the presence of high concentrations of glycerol or by complete desiccation (Thalhammer et al., 2014; Thalhammer et al., 2010; Bremer et al., 2017). Crowding by high glycerol concentrations induces partial folding of COR15 proteins; this structural change is believed to contribute to leaf-freezing tolerance by stabilising cellular membranes. Under these conditions, the (partially) folded protein binds peripherally to membranes.

Over-expression of COR15a increases the freezing tolerance of chloroplasts in non-acclimated *Arabidopsis* (Bremer et al., 2017; Thalhammer et al., 2014). The COR15a

polypeptide is targeted to the stromal compartment of the chloroplasts. Ice crystallisation occurs in the intercellular spaces, leading to dehydration of the cells; this freeze-induced dehydration leads to an increase in intracellular solute concentrations and to membrane destabilisation and the synthesis of cryoprotective polypeptides. The protein folds into amphipathic α -helices in response to increased crowding conditions, such as high concentrations of glycerol. The partial folding of the protein into amphipathic α -helices due to freeze-induced increase in crowding may generate a hydrophobic face on the protein surface that could be responsible for a protective protein–membrane interaction (Bremer et al., 2017; Thalhammer et al., 2010). Although there is evidence for direct COR15A–membrane interactions, it is not known if this protein exerts its influence at the surface of membranes or in the chloroplast stroma.

1.6 Regulation of Stress Response Gene Expression

1.6.1 Transcription Factors

Genes induced during stress conditions not only protect cells from stress through the production of important metabolic proteins (functional proteins), but also regulate the genes for signal transduction in the stress response (regulatory proteins), for example, TFs (Akhtar et al., 2012; Shi et al., 2018).

TFs are sequence-specific DNA-binding proteins able to activate and/or repress transcription. They are responsible for the selectivity in gene regulation which is either tissue-specific, development-stage-specific, or via a stimulus-dependent pathway. TFs play an important role in regulating gene expression in plants and are rightly referred to as the master regulators of the cell. These proteins also play a major role in plant development and their response to the environmental and response signals during the whole life cycle of an organism (Akhtar et al., 2012; Shi et al., 2018). Over-expression of key TF genes has been shown in several studies to impart stress-tolerant phenotypes (Akhtar et al., 2012). TFs are a highly diverse family of proteins and generally function in multi-subunit protein complexes. They may bind directly to special promoter regions of DNA, which lie upstream of the coding region of a gene, or directly to the RNA polymerase molecule. TFs can activate or repress the transcription of a gene, which is generally a key determinant in whether the gene functions at a given time.

The functions of TFs have been elucidated by several genetic tools, including gene knockout and gene over-expression strategies. As some TFs display unique properties, the over-expression strategy has been particularly effective in revealing TF function (Shi et al., 2014). A detailed understanding of the molecular mechanisms underlying the activation/repression of specific genes through the binding of TFs is of utmost importance, as TFs can trigger a unique array of physiological and metabolic responses by modifying the protein profiles of plant cells. These metabolic adjustments help plants to respond to challenging environmental conditions, since plants are sessile and cannot avoid or escape environmental stresses. Several TFs are important candidates for adapting plants to external stress, since they regulate the expression of various stress-responsive genes, the regulons, by binding to their specific cis-element promoters. Both TFs and cis elements function in the promoter region

of different stress-related genes (Khan et al., 2017), and the over-expression or suppression of these genes may improve the plant's tolerance of stress.

Many stress inducible genes have been identified in plants (Mehrotra et al., 2014) and the products of these genes not only confer stress tolerance directly but also regulate the expression of other genes and signal transduction pathways under stress conditions (Bartels & Sunkar, 2005; Molassiotis & Fotopoulos, 2011; Shi et al., 2018). Stress-inducible expression of TFs includes members of the AP2/EREBP (apetala2/ethylene-responsive element-binding proteins) family, the MYB (myeloblastosis) family, the WRKY family, the NAC family (Puranik et al., 2012; Shao et al., 2015), the zinc-finger (ZF) family, the basic helix-loop-helix (bHLH) family, the basic-domain leucine zipper (bZIP) family (Wang et al., 2015), and the homeodomain TF family (Khan et al., 2017).

Several of these transcription factors with a regulatory role include the AREB, AP2/ERF, NAC, bZIP, MYC, and MYB TFs (Samarah, 2016). The bZIP family of TFs also function to control stress-responsive gene expression. One type of bZIP family TF, the ABFs (ABA-responsive factor), bind ABREs (abscisic acid responsive elements). These cis elements regulate the expression of cold-, drought-, and salt-induced genes via ABA-dependent signal transduction (Lee et al., 2010; Samarah, 2016).

One of the largest families of TF is the APETALA 2/ethylene-responsive element-binding protein (AP2/EREBP) (Figure 1.4). This family of TF genes is unique to plants and the encoded TFs are characterised by the presence of highly conserved AP2/ERF DNA-binding domains (Liu & Zhang, 2017; Shu et al., 2016). This family of TFs is known to be involved in abiotic stress response via the ABA biosynthetic pathway (Lee et al., 2010; Todaka et al., 2012). However, whole-genome expression analysis of stress inducible genes in *Arabidopsis* indicates the existence of interconnected regulatory networks between stress signal perception and the expression of stress-responsive genes (Todaka et al., 2012). Over-expression of the gene that regulates transcription of several downstream responsive genes seems to be a promising strategy for the development of new varieties with environmental stress tolerance attributes.

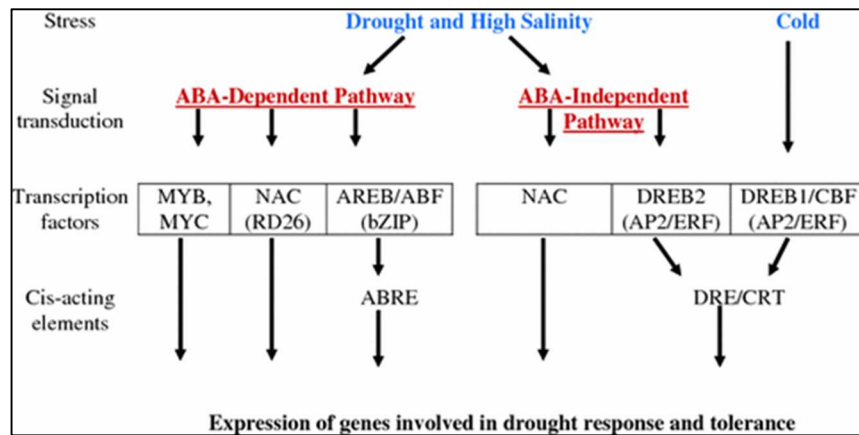


Figure 1.4: Transcription Factors Reported to have a Major Role in Cold Acclimation in *Arabidopsis*.

They primarily comprise of AREB, AP2/ERF, NAC, bZIP, MYC, and MYB transcription factors. Reproduced from Samarah (2016).

As discussed in Section 1.6.1, many TFs are involved in regulation of stress-responsive gene expression. Some stress genes are induced by several TFs, while the same TF may behave differently in response to different stress stimuli. The changes in gene expression during cold acclimation were first demonstrated by Guy et al. (1985). Since then, research has focused on identifying these genes and seeking to understand their function and regulation. The roles of these genes are discussed in detail in this chapter.

1.6.2 Regulation of Gene Expression in Response to Cold-Acclimating Temperatures

Several studies have shed light on how plants balance defence strategies with growth and development (Guo et al., 2018). Plants cannot move locations but rather must adapt to a stressful environment. During cold stress, a plant must be able to balance endogenous developmental cues and external signals to coordinate stress responses with developmental patterning to adapt to the environment throughout its life cycle (Guo et al., 2018).

Genes encoding TF in the model plant *Arabidopsis* constitute 6–10% of their genome. Studies on cold-regulated gene expression in *Arabidopsis* have resulted in the discovery of a family of transcriptional activators, the CBF/DREB1 (C-repeat binding factor/dehydration-responsive element binding 1) proteins, which have a key role in cold acclimation. The CBFs are a group of heterodimeric TFs; these genes were first studied in *Arabidopsis thaliana* (Fowler & Thomashow, 2002), and were later found in almost all the main cereal crops, such as barley, wheat, and rye (Sanghera et al., 2011). Subsequently, it has been shown that many transcriptional changes accompanying freezing tolerance – such as ERD (early responsive to dehydration), RD (responsive to dehydration), low temperature-induced (LTI), COR, and KIN (cold inducible) – are induced by both low temperature and drought stress (Ingram & Bartels, 1996; Nakashima et al., 2000; Pearce, 1999; Shinozaki & Yamaguchi-Shinozaki, 2000; Thomashow, 1999). Furthermore, a link between cold and drought stress responses can be inferred from experiments that demonstrate that mild drought stress confers an increase in freezing tolerance in plants (Nakashima et al., 2014; Webb et al., 1994). Some of these genes encode key enzymes for compatible solute biosynthesis that increases freezing tolerance via the accumulation of cryoprotective proteins and soluble sugars, thus repairing cold-rigidified membranes and stabilising cellular osmotic potential (Chinnusamy et al., 2007).

When *Arabidopsis* plants are exposed to low temperature (approximately 4°C), CBF genes are rapidly and transiently induced and generally reach their maximum level of expression after 1 to 2 hours of cold treatment (Gilmour et al., 1998; Zhao et al., 2016a). Within 15 minutes of plants being exposed to low temperatures, transcripts accumulate for the CBF1, CBF2, and CBF3 genes (Canella et al., 2010; Gilmour et al., 2000; Gilmour et al., 1998; Park et al., 2015), or DREB1B, DREB1C, and DREB1A (dehydration-responsive element binding 1A, B and C) (Liu et al., 1998; Mizoi et al., 2012; Thomashow et al., 1997). These encode transcriptional activators that are members of the AP2/EREBP (APETALA2/ethylene-responsive element-binding protein) family of DNA-binding proteins (Dietz et al., 2010; Liu et al., 1998; Mizoi et al., 2012; Shi et al., 2014; Thomashow et al., 1997). These TFs bind the cold- and dehydration-responsive DNA regulatory element, designated the C-repeat (CRT)/DRE (Kudo et al., 2018; Nakashima et al., 2014), that is present in the promoters of COR and many other cold-responsive genes and stimulate their transcription. Expression of the CBF regulon of target genes then leads to an increase in freezing tolerance (Gilmour et al., 1998; Medina et al., 2011). The mechanism whereby the

CBF3/DREB1A genes are activated by low temperature may involve the action of cold-responsive promoters (Maruyama et al., 2011; Shinwari et al., 1998) that are not subject to autoregulation (Jaglo-Ottosen et al., 1998). Thus, Gilmour et al. (1998) hypothesised the existence of a TF, designated ICE (inducer of CBF expression 1), that acts on the CBF3/DREB1A promoters (Fig. 1.5). Upon exposing plants to low temperature, ICE was proposed to become activated and stimulate transcription of the CBF/DREB1 genes, followed by induction of the CBF regulon. Thus, it has been concluded that the CBF regulon (CRT/DRE-containing genes that are induced by the CBF/DREB1 TFs) includes genes with a role in cold acclimation. These responses require expression of stress-responsive genes, which are regulated by a network of TFs. The AP2 domain of the CBF/DREB subfamily members binds CRT motif (5'-CCGAC-3') (Thomashow, 1998), present in one or several copies in the promoters of many COR genes, such as COR15a (Baker et al., 1994), where it is known as a low temperature responsive element (LTRE). Yamaguchi-Shinozaki and Shinozaki (1994) identified a 9-bp DNA element known as dehydration-responsive element (DRE) and showed that it was able to induce gene expression in response to dehydration and low temperature. Liu et al. (1998) identified that DREB1A, DREB2A, and DREB1B/CBF1 interact with DRE in response to cold and dehydration stresses. In *Arabidopsis*, the CBF proteins recognise the CRT/DRE cis element, which induces gene expression in response to LT and dehydration but not to ABA, whereas a five-base pair (5-bp) core DNA sequence from DRE, known as the C-repeat (CRT) motif (5'-CCGAC-3'), is sufficient to activate gene expression under cold stress (Magome et al., 2008; Sakuma et al., 2002; Thomashow, 1998). This motif is found in the promoters of a subset of COR genes. When plants are exposed to non-freezing low temperatures, CBF genes are rapidly induced, within 15 minutes, followed by the activation of downstream target COR genes (Liu et al., 1998; Park et al., 2015). Extensive studies have shown that three CRT binding factor/DRE binding factor 1 (CBF/DREB1) TFs that belong to the AP2/ERF (apetala2/ethylene-responsive factor) superfamily play critical roles in cold acclimation in *Arabidopsis* (Chinnusamy et al., 2007; Liu et al., 1998; Shi et al., 2014; Stockinger et al., 1997; Wang et al., 2017).

Another CBF TF gene, CBF4, has also been identified in *Arabidopsis* and induces COR genes in response to dehydration stress and ABA (Haake et al., 2002; Knight et al., 2004), in contrast to the three already identified CBF/DREB1 homologues, which are induced under cold stress (Haake et al., 2002). The CBF4 gene encodes a protein that is the closest homologue to the CBF1, 2, 3/DREB1abc transcriptional activators in *Arabidopsis*. Over-

expression of CBF4 in transgenic *Arabidopsis* increases downstream COR gene transcription by the activation of the C-repeat/dehydration-responsive element containing downstream genes that are involved in cold acclimation and drought adaptation. This leads to increased tolerance of both drought and low-temperature stresses because of the physiological similarity between freezing and drought stress, and the sequence and structural similarity of the CBF/DREB1 and the CBF4 proteins (Haake et al., 2002).

Since a major cause of freezing damage is freeze-induced dehydration (Steponkus & Webb, 1992; Thomashow, 1999), a plant's ability to survive freeze-induced dehydration is related to its adaptation to drought. Hence, it is not surprising that plants respond to low temperature and drought in very similar ways at the molecular level (Shinozaki & Yamaguchi-Shinozaki, 2000).

It has been noted that all CBF/DREB1 proteins share common signature motifs that bracket the AP2 domain; these motifs are found in CBF-like proteins that are conserved across species (Jaglo et al., 2001). It is proposed that a plant's response to cold and drought evolves from a common CBF-like TF, first through gene duplication and then through promoter evolution (Haake et al., 2002). DREB2A proteins are expressed in response to dehydration and salt stresses but not to low temperatures (Liu et al., 1998) (Fig. 1.5).

Aside from the AP2/EREBP DNA-binding domain, DREB1A and DREB2A proteins do not have strong sequence similarities (Liu et al., 1998). Therefore, it has been suggested that the DREB1A and DREB2A proteins function in separate signalling pathways under cold and dehydration stress conditions (Liu et al., 1998). Nakashima et al. (2000) identified and cloned the DREB2B protein and showed that it has the same function as DREB2A.

1.7 Role of CBF Signalling in Cold Acclimation

Molecular responses to abiotic stresses include stress perception, signal transduction to cellular components, gene expression, and metabolic changes (Agarwal et al., 2006; Zhao et al., 2015). The genes induced by stress not only function in protecting cells from stress through the production of important metabolic proteins, but also in regulating the downstream genes for signal transduction. Plants under low temperature (LT) stress exhibit a CBF-responsive pathway (Hu et al., 2013), which includes transcriptional, post-

transcriptional, translational, and post-translational regulators of LT-induced expression of the functional genes (Zhou et al., 2011).

This section describes the current understanding of the mechanism of CBF-dependent and independent LT responsive pathways and highlights aspects of the LT response pathways that are yet to be fully understood. In addition, the section discusses some other genes and proteins that are negative regulators of low temperature induced signal transduction. The role of ABA, an important plant hormone that plays a regulatory role in gene expression and many physiological processes in plants, is also described.

Research in the past two decades has gradually provided insight into how the CBF genes in *Arabidopsis* are up-regulated in response to LT. It has been established that the promoters of the CBF genes are responsive to LT (Shinwari et al., 1998). The *Arabidopsis* CBF genes are controlled by several TFs (Table 1.1), some of which are induced during the early phase of cold acclimation. Two ICE proteins, ICE1 and ICE2, have been identified in barley (Chinnusamy et al., 2003; Fursova et al., 2009). Both ICE1 and ICE2 are members of the basic helix-loop-helix (bHLH) family of transcriptional activators, and they both bind to the MYC binding sites of CBF promoters (Chinnusamy et al., 2003; Fursova et al., 2009; Chinnusamy et al., 2003) (see Fig. 1.5). Two potential binding sites for ICE1, ICEr1, and ICEr2 (inducer of CBF-expression regions 1 and 2) are also present in the *Arabidopsis* CBF2 promoter (Chinnusamy et al., 2003; Kim et al., 2015; Zarka et al., 2003). Several MYC binding sites, including the ICE1-like inducers (TaICE41 and TaICE87), are also present in the TaCBFIVd-B9 promoter of hexaploid wheat (Badawi et al., 2008). The ICE1 mutant exhibits impaired freezing tolerance and significant defects in the induction of CBF genes, whereas over-expression of ICE1 enhances the cold-induced up-regulation of CBF 1–3 (Chinnusamy et al., 2003; Ding et al., 2015). ICE2, a paralog of ICE1, is functionally redundant. However, a dominant-negative mutation of ICE1 (*ice1*) results in almost complete elimination of CBF3 transcript accumulation in response to LT. Significantly, however, the *ice-1* mutation has little effect on cold-induced accumulation of CBF2 transcripts, indicating that there are differences in the mechanisms of expression within the CBF/DREB1 gene family.

ICE1 is constitutively expressed in leaves, stems, and other tissues (Chinnusamy et al., 2003). Interestingly, ICE1/2 are specifically expressed in the stomatal cells of leaf tissues (Ding et al., 2015; Fursova et al., 2009) but induction of CBF3 expression occurs only upon

exposure to cold (Chinnusamy et al., 2003). Furthermore, enhanced expression of CBF2 was observed in the *ice1* mutant, suggesting a possible negative regulation of CBF2 by CBF3 (Chinnusamy et al., 2003). However, over-expression of wheat TaICE41 and TaICE87 in *Arabidopsis* increases CBF and COR gene expression, leading to enhanced freezing tolerance only upon cold acclimation, or only after exposure to LT (Badawi et al., 2008) (see Fig. 1.5).

Table 1.1: Some Transcription Factors Induced During the Early Phase of Cold Acclimation in *Arabidopsis*. Reproduced from Shi et al. (2018).

Factor	Protein characteristics	Direct target(s)	Effect on freezing tolerance (negative/positive)
ICE1	Transcription factor	CBF1, CBF2, CBF3	Positive
ICE2	Transcription factor	CBF1, CBF2, CBF3	Positive
CAMTA3	Transcription activator	CBF1, CBF2	Positive
CRLK1/2	Protein kinases	MEKK1-MKK2-MPK4	Positive
MPK3/6	Protein kinases	ICE1, MYB15	Negative/Positive
CRPK1	Protein kinase	14-3-3 proteins	Negative
OST1	Protein kinase	ICE1, BTF3, BTF3L	Positive
HOS1	E3 ubiquitin ligase	ICE1	Negative
EIN3	Transcription factor	CBF1, CBF2, CBF3	Negative

1.7.1 Post-transcriptional Regulation of CBF Signalling

Post-transcriptional regulation is an important mechanism for regulating CBF expression, one example of which is the regulation of mRNA export to the cytoplasm from the nucleus. A dead box RNA helicase encoding gene, LOS4 (low expression of osmotically responsive genes 4) (see Fig. 1.5) identified in *Arabidopsis* is localised in the nuclear rim and is required for RNA export. Plants with LOS4 deletions are chilling-sensitive and display reduced

induction of CBFs and their target genes, providing evidence that RNA export is involved in regulation of CBF expression (Gong et al., 2002). A recessive mutation *los4-1* impairs cold-induced transcript accumulation of CBF genes and renders plants more sensitive to chilling and freezing stresses. Thus, mRNA export seems to play a critical role in stress responses and regulation of plant growth and development.

In addition to the factors discussed above, it has also been reported that the expression of CBF genes is repressed by their own gene product, or by the products of their downstream genes (Guo et al., 2002; Huang et al., 2012). Other genes and proteins known to be negative regulators of low temperature induced signal transduction are discussed below in Section 1.7.2.

1.7.2 Post-translational Modification (PTM) in Regulation of the CBF Signalling Pathway

In *Arabidopsis*, three members of the CBF gene family exhibit high sequence similarity: CBF1, CBF2, and CBF3 (DREB1B, DREB1C, and DREB1A). The expression of CBF genes in *Arabidopsis* is positively and negatively regulated by several TFs. For example, the bHLH TFs ICE1 and ICE2 positively regulate the expression of CBFs (Ding et al., 2018; Jiang et al., 2017; Lee & Thomashow, 2012b). ICE1 is ubiquitinated by HOS1, leading to ICE1 degradation, thus inhibiting the ICE1-mediated activation of downstream CBF/COR genes under LT (Dong et al., 2006; Park et al., 2011; Park et al., 2015). However, the SUMOylation of ICE1 by SIZ1 and SIZ2 inhibits the degradation of ICE1, thus maintaining expression of CBF/COR genes (Liu & Zhou, 2018; Park et al., 2011).

1.8 Role of Calcium in Cold Signalling

1.8.1 The Cell Membrane Fluidity Hypothesis

The cell membrane fluidity hypothesis is a current model that proposes that the reduction in membrane fluidity caused by falling temperature triggers the activation of a protein receptor on the plasma membrane (Bajwa et al., 2014; Guo et al., 2017; Holmstrup et al., 2014). The

LT subsequently leads to many biochemical and physiological changes, any one of which could act as recognition point for temperature sensing. Some of these biochemical changes involve modifications in the membrane composition, leading to alteration in membrane fluidity (Örvar et al., 2000), increased calcium influx (Chinnusamy et al., 2006), production of reactive oxygen species (Ruelland et al., 2009), changes in the organisation of the cytoskeleton (Örvar et al., 2000), and chromatin remodelling (Stockinger et al., 2001).

Cold stress leads to a decrease in cell membrane fluidity, which is accompanied by an increase in Ca^{2+} channel activity in plants. (Gong et al., 1998; Knight et al., 1991a). One possible primary cold signal sensor is the Ca^{2+} channel itself, located on the plasma membrane (Aldon et al., 2018). Hence, the low-temperature response of a plant cell leads to an influx of Ca^{2+} into the cytoplasm through Ca^{2+} channels, resulting in an intracellular Ca^{2+} signalling cascade involving Ca^{2+} -binding proteins that induce downstream actions, such as the expression of CBF/COR genes in the cold-signalling pathway (Chinnusamy et al., 2010; Guo et al., 2018; Guo et al., 2017).

1.8.2 The Roles of Reactive Oxygen Species (ROS) in Cold Stress

In addition to Ca^{2+} , emerging evidence suggests that other messenger molecules such as ROS are produced by enzymes in plant cells and fine-tune the plant's control of growth and defence against both biotic and abiotic stresses, including cold stress. Chilling is known to induce the production of ROS, which causes damage to cellular components or hinders the repair of photosystem two, PSII (Nishiyama et al., 2001). Examples of such ROS include peroxides, superoxide, hydroxyl radical, singlet oxygen (Hayyan et al., 2016), alpha-oxygen, and hydrogen peroxide (H_2O_2) (Tyystjärvi, 2013).

ROS levels can increase dramatically during cold stress, resulting in significant damage to cell structures (Devasagayam et al., 2004). Cumulatively, this is known as oxidative stress. ROS play dual roles in plant cells; on the one hand, they induce gene expression and protein synthesis to protect cells from stress; on the other, they induce oxidative stress (Heidarvand & Maali-Amiri, 2013; Qi et al., 2018). ROS can damage lipid, DNA, RNA, and proteins, which, in theory, contributes to the physiology of ageing. ROS are produced as a normal product of cellular metabolism. In particular, hydrogen peroxide (H_2O_2) is a major

contributor to oxidative damage; upon cold stress, plants accumulate H₂O₂, and excessive H₂O₂ has a deleterious effect on plant cells. Some evidence suggests that there is a close linkage between Ca²⁺ and ROS; for instance, that low ROS levels promote Ca²⁺ influx into the cytoplasm (Rihan et al., 2017).

1.8.3 Regulatory Protein Kinases

As mentioned above (Section 1.8.1), one possible primary cold signal sensor is the plasma membrane Ca²⁺ channel. In response to cold stress, Ca²⁺ acts as a secondary messenger that is recognised by calcium-binding proteins, many of which function as Ca²⁺ sensors that rapidly transduce external signals from the plasma membrane to the nucleus (Kudla et al., 2018) (see Fig. 1.5).

Several calcium-decoding proteins, which function as sensors to rapidly transduce external signals to inside the cell, have been identified (Kudla et al., 2018). These include sets of plant-specific Ca²⁺ sensors, such as calmodulin (CaM)-like proteins (CMLs) (Zhu et al., 2015), Ca²⁺-dependent protein kinases (CDPKs), and calcineurin B-like proteins (CBLs), indicating that plants possess specific tools and machineries to convert Ca²⁺ signals into appropriate responses (DeFalco et al., 2010; McCormack et al., 2005; Reddy et al., 2011; Zhu et al., 2015). In addition, other CMLs and CDPKs are involved in plant immune responses mounted against viruses, bacteria, fungi, bacteria, and insects (Cheng et al., 2013; Do Heo et al., 1999). There are indications of a direct role of several protein kinases belonging to diverse families, including CaM, CBLs, CMLs, CDPKs, and mitogen-activated protein kinases (MAPKs) (DeFalco et al., 2010; McCormack et al., 2005; Reddy et al., 2011; Xiaoyang Zhu et al., 2015). However, their conversion into biological responses requires Ca²⁺ sensors for decoding and relaying (Aldon et al., 2018; Hashimoto & Kudla, 2011). Several protein kinases involved in CBF signalling have been successfully isolated. For instance, CDPKs play an important role as Ca²⁺ sensors in response to cold stress (Knight et al., 1996; Luan et al., 2002; Sanders et al., 2002), and cold-responsive protein kinase 1 (CRPK1) is a cold-activated plasma membrane-localised protein kinase. These findings support the hypothesis that cold signals are initially transmitted from the plasma membrane (Liu et al., 2017).

Direct evidence for the transduction of cold signals from the plasma membrane to the nucleus was obtained through the discovery of CRPK1. This cytoplasmic, receptor-like kinase is localised at the plasma membrane (Liu et al., 2017). After CRPK1 is activated by low temperature or cold, it phosphorylates 14-3-3 proteins, which causes their translocation from the cytosol to the nucleus, where they interact with CBF proteins and stimulate or promote their degradation (Liu et al., 2017). This plays a negative role, via the classical CBF pathway, in regulating the excessive cold response in *Arabidopsis* (Baumann, 2017; Guo et al., 2017; Liu et al., 2017). The 14-3-3 proteins, which are phosphorylated by CRPK1, shuttle from the cytosol to the nucleus to promote the degradation of CBFs (Baumann, 2017; Guo et al., 2017), and thus regulate the duration of the cold defence response. Other positive and negative regulators also regulate the expression of CBF genes.

1.8.4 MAPK Cascades Mediation of Cold Signal Transduction

Phosphorylation is the most common post-translational modification leading to signal transduction and amplification (Mann & Jensen, 2003). Several protein kinases are involved in regulating cold acclimation in *Arabidopsis* (Lehti-Shiu & Shiu, 2012; Yang et al., 2013). Functional analyses in plants revealed that CDPKs are important components of the plant defence system, acting alongside and in synergy with the MAPKs-dependent signalling cascade (Guo et al., 2018; Truman et al., 2013; Zhao et al., 2017). MAPK cascades have also been proposed to function in cold responses (Li et al., 2017). A typical MAPK cascade contains three protein kinases: MAP kinase kinase kinase (MAP3K), MAP kinase kinase (MAP2K), and MAP kinase (MAPK) (Guo et al., 2018; Truman et al., 2013; Zhao et al., 2017).

During cold acclimatisation, ICE1 can be phosphorylated by MAPK3/6 in the MAPK cascade (Li et al., 2017), leading to the degradation of ICE1 by an unknown E3 ligase (Jung et al., 2012). Meanwhile, 14-3-3 proteins, which are phosphorylated by CRPK1, transfer from the cytosol to the nucleus to promote the degradation of CBFs (Catalá et al., 2014; Guo et al., 2018; Lee & Thomashow, 2012a). However, it remains unclear how cold activates these protein kinases during the early stages of LT perception.

As described above, the transcription factor ICE1 activates CBF and COR gene expression (Chinnusamy et al., 2003; Lee, Henderson, & Zhu, 2005). However, ICE1 expression is not responsive to cold treatment (Miura et al., 2007), suggesting that post-translational modifications are important for the functioning of ICE1. Indeed, multiple post-translational modifications have been shown to control the turnover and duration of ICE1 under LT (Liu & Zhou, 2018).

It is known that LT-induced SUMOylation of ICE1 by the SIZ1 SUMO E3 ligase is important for the stabilisation and activation of ICE1, which is regulated primarily at the protein level (Miura et al., 2007). SUMOylation mediated by the SUMO E3 ligases usually protects proteins from degradation. In *Arabidopsis*, SIZ1 (SAP and Miz) encodes a SUMO E3 ligase that is required for freezing tolerance (Miura et al., 2007). CBF proteins were recently found to be degraded by the 26S proteasome pathway (Ding et al., 2018; Liu et al., 2017).

1.9 Negative Regulators of Low Temperature Signal Transduction

Besides positive transcriptional regulators, there are also several TFs that negatively regulate the expression of CBFs and their downstream genes (Agarwal et al., 2006; Ding et al., 2018; Shi et al., 2012; Vogel et al., 2005). These are required to reduce the levels of certain genes after cold acclimation and to facilitate subsequent freezing tolerance. Examples include the *Arabidopsis* genes HOS1, ZAT12, and MYB15 (Shi et al., 2012).

1.9.1 HOS1: a Negative Regulator of Freezing Tolerance

Some negative transcriptional regulation is required to reduce levels of certain transcripts after cold acclimation and to facilitate subsequent freezing tolerance. For instance, the *Arabidopsis* gene HOS1 (high expression of osmotically responsive 1) encodes a protein with modified RING (really interesting new gene) finger. Ubiquitination of ICE1 by an E3 ligase degrades ICE1 through the ubiquitin/26S proteasome pathway and thus acts as a cold signalling attenuator (Dong et al., 2006; Miura et al., 2007), but under cold stress polyubiquitination of ICE1 is prevented by SUMOylation by the SIZ1-SUMO E3 ligase.

ICE1 physically interacts with a R2R3 MYB transcriptional activator, MYB15, to induce expression of DREB1/CBF and provide cold tolerance in *Arabidopsis* (Agarwal et al., 2006). HOS1 physically interacts with and ubiquitinates ICE1, thus reducing its stability.

HOS1 was the first RING finger protein reported to function in LT signal transduction. It is localised in the cytosol at normal temperatures but accumulates in the nucleus in response to cold (Lee et al., 2001), where it negatively regulates expression of CBF and, therefore, COR transcription. Dong et al. (2006) suggested that HOS1-mediated ICE1 degradation is responsible, at least in part, for the transient nature of CBF induction during cold acclimation. The over-expression of HOS1 decreased freezing tolerance in *Arabidopsis* by repressing the expression of CBF3 (Dong et al., 2006; Ishitani et al., 1998; Lee et al., 2001). SIZ1-mediated SUMOylation of ICE1 results in decreased expression of MYB15 and promotes CBF3/DREB1A expression in *Arabidopsis* (Miura et al., 2007), indicating that SUMOylation might be stabilising the ICE1 protein and/or increasing its activity by activating expression of CBF and repression of MYB15. Potential SUMOylation sites have been reported in TaICE41 and TaICE87 (Sarhan et al., 2008), which are similar to AtICE1. This suggests that regulation of CBF expression in wheat might be similar to in *Arabidopsis* (see Fig. 1.5).

1.9.2 ZAT12: a Negative Regulator of Cold Acclimation

In *Arabidopsis*, a cold-induced C2H2 zinc-finger TF, ZAT12, is another protein that appears to function as a negative regulator of cold-induced genes (see Fig. 1.5). Transgenic over-expression of ZAT12 decreases the expression of CBFs under cold stress. Transcriptome analysis of ZAT12-over-expressing *Arabidopsis* revealed that the ZAT12 regulon consists of at least 24 COS (cold standard set) genes, of which nine are cold-induced and 15 are cold-repressed (Vogel et al., 2005). Over-expression of ZAT12 did not cause any alterations in freezing tolerance; however, transgenic plants over-expressing ZAT12 accumulated much lower levels of CBF1-3, suggesting a negative regulation of the CBF cold response pathway (Vogel et al., 2005). Another TF, the C2H2 zinc-finger protein ZAT10/STZ, possibly acts as a negative regulator of cold-induced gene expression (Lee et al., 2001). Transient expression assays showed that ZAT10 can negatively regulate RD29A expression under cold treatment, while LOS2 acts as a negative regulator of ZAT10 (Lee et al., 2001). Recently,

EIN3, one of the TFs in the ethylene (ETH) signalling pathway, has been identified as a repressor of CBFs during cold acclimation (Shi et al., 2012) (see Fig. 1.5). EIN3 directly binds to the promoters of CBFs and negatively regulates the expression of downstream cold-induced genes.

1.9.3 MYB15 (MYELOBLASTOSIS 15)

CBFs are negatively regulated by upstream TFs. MYB15 is a member of the R2R3-MYB family of TFs, which can bind to the MYB recognition elements in the promoters of CBF genes (GGTAGGT or TTGGTG) (Romero et al., 1998) to down-regulate CBF expression (Dong et al., 2006). MYB15 is induced by cold and the protein physically interacts with ICE1; over-expression of MYB15 leads to reduced CBF transcripts along with a reduction in freezing tolerance (Dong et al., 2006).

Transgenic *Arabidopsis* over-expressing MYB15 show less induction of CBFs under LT and thereby less LT tolerance (Dong et al., 2006), whereas *myb15* T-DNA knockout mutant plants show enhanced expression of CBFs during cold acclimation and enhanced freezing tolerance (Dong et al., 2006). An interaction of MYB15 with ICE1 has also been proposed, as an over-expression of MYB15 is observed in *ice1* mutants under cold stress conditions (Agarwal et al., 2006; Chinnusamy et al., 2003). However, the biological significance of this interaction remains unclear. Most of the currently known components of the cold response transcriptional network, as described in the above sections, are summarised in Figure 1.5.

1.10 The ESKIMO1 Freezing Tolerance Genes

1.10.1 The *Arabidopsis* eskimo1 Mutant

Investigating changes in gene expression during cold acclimation is one of the primary ways through which current understanding of freezing tolerance has been acquired (Thomashow, 1999). Mutations have also provided insight into which genes are involved when changes in freezing-tolerance phenotype are identified. The first mutation described, *eskimo1*, elevates the level of the compatible solute proline. The *Arabidopsis* *esk1* mutants display elevated

levels of freezing tolerance in the absence of cold acclimation, and the *esk1* mutant shows constitutive freezing tolerance that is independent of the CBF regulon (Xin, 1998; Xin et al., 2007), which is constitutively expressed, in freezing-tolerant plants in the absence of cold acclimation. This mutation does not affect the expression of well-known cold-regulated genes, and this finding led to a new hypothesis that plants need to activate different signalling pathways in order to fully acclimate to cold (Kurepin et al., 2013; Xin, 1998). ESK1 was suggested to be a negative regulator of freezing tolerance (Fursova et al., 2009; Xin et al., 2007). As *esk1* plants do not overexpress CRT/DRE-regulated cold-responsive genes, the *esk1* mutation does not affect the expression of four major DRE/CRT classes of COR genes – COR6.6, COR15A, COR47, and COR78 – which shows that ESK1 is not involved in the CBF-mediated pathway of cold acclimation (Xin & Browse, 2000). The mechanism of ESK1 action is not known, but the fact that the two available *esk1* alleles are recessive suggests that ESK1 may act as a negative regulator of cold acclimation (Fursova et al., 2009). Thus, the cold-acclimation process is complicated, with parallel or branched pathways (see Fig. 1.5). The ESK1 protein is believed to be an acetyl transferase located in the cell wall that maintains esterification of pectins, but how this relates to stress tolerance is uncertain (Yuan et al., 2013).

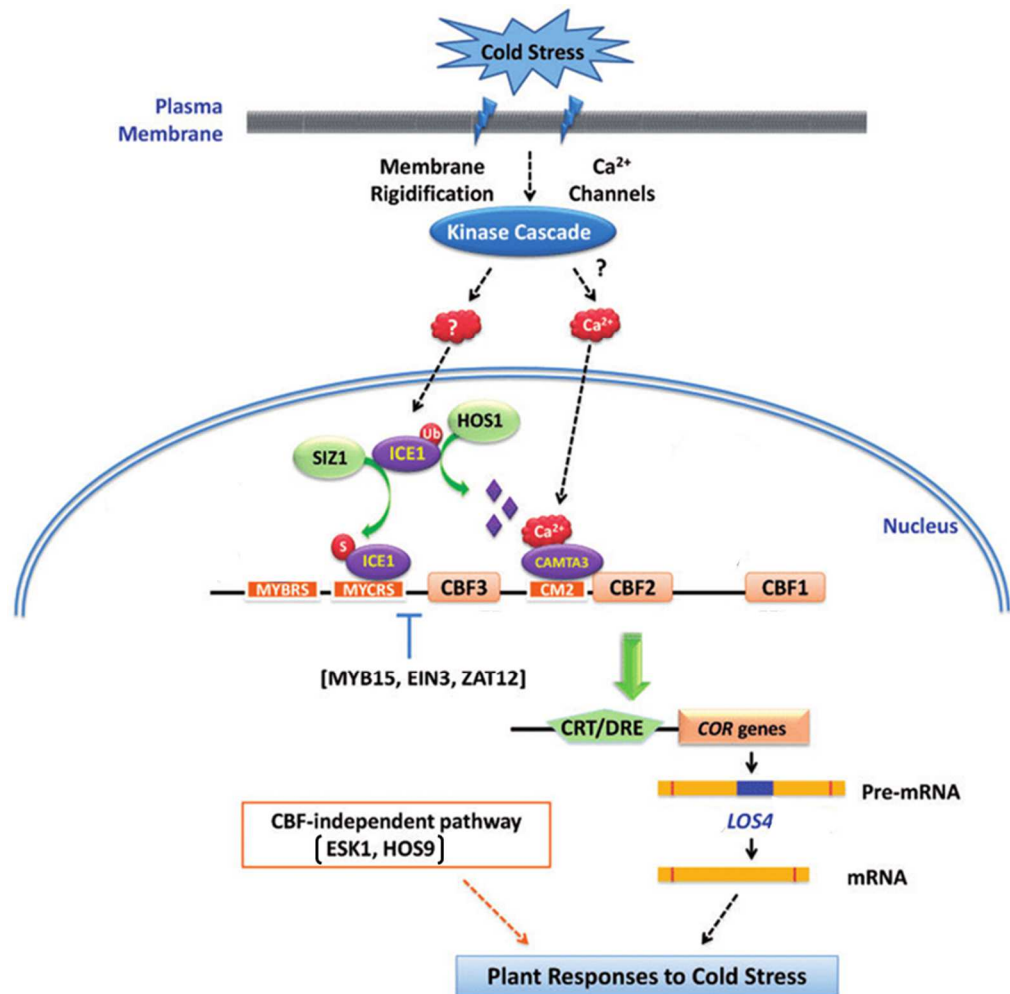


Figure 1.5: Schematic Illustration Summarising the Regulation of CBF Expression in *Arabidopsis*.

Regulation of the CBF signalling pathway during cold acclimation. Cold-signalling pathway involves multiple regulatory mechanisms, including transcriptional, post-transcriptional, and post-translational regulation, which are triggered by unknown temperature sensors. Some key components of the circadian clock also have effects on plant cold responses. The major components involved in the CBF-dependent signalling pathway are illustrated. Arrows indicate positive regulation, whereas lines ending with a bar indicate negative regulation. Question marks denote connections not yet determined. Abbreviations: Ca²⁺ dependent protein kinase; COR, cold-responsive; CRT, C-repeat element; DRE, dehydration Response element; HOS, high expression of osmotically responsive genes; ICE1, inducer of CBF expression 1; LOS, low expression of osmotically responsive genes; STZ, salt-tolerant zinc finger TF; ZAT, zinc cation diffusion transporter protein; CAMTA3, calmodulin-binding transcription activator 3; ESK1, eskimo 1; EIN3, ethylene insensitive 3; MYBRS, MYB transcription factor recognition sequence; MYCRS, MYC transcription factor recognition sequence; CM2, conserved DNA motif2; Ub, ubiquitin; S, SUMO. Reproduced from Shi et al. (2014).

1.11 The Role of the Phytohormone Abscisic Acid (ABA) in Abiotic Stress

Plants cannot escape or avoid environmental stresses, such as cold, salinity, and drought; thus, their ability to respond to environmental stimuli is essential to their survival, and they have evolved mechanisms to overcome the detrimental effects of stress. Plant growth regulators (phytohormones) are involved in every aspect of plant growth and development and play key roles in stress responses (Fujita et al., 2006; Vítámvás et al., 2012). ABA is a phytohormone with roles at various stages of plant development (Finkelstein, 2013; Wani & Kumar, 2015). It is also an important messenger that acts as the signalling mediator for regulating the adaptive response of plants to different environmental stress conditions, such as salt, osmotic, and cold stress (Dodd et al., 2008; Dodd et al., 2010; Puértolas et al., 2014), as such, ABA is also called a stress hormone (Mehrotra et al., 2014).

The literature review in this section will discuss the role of ABA in response to abiotic stress at the molecular level, ABA signalling, and the effect of ABA in respect to gene expression in cold stress. In plants, when environmental conditions are harsh, the level of ABA increases via ABA biosynthesis; this biosynthesis starts in plastids and is completed in the cytosol. In higher plants, ABA is synthesised via the mevalonic acid-independent pathways; this is known as the indirect pathway (Xiong & Yang, 2003). The increased level of ABA leads to its binding to receptors to initiate signal transduction, leading to cellular responses to stresses (Ng et al., 2014). It is therefore not surprising that phytohormone levels are affected when plants are exposed to LT (Vítámvás et al., 2012).

Plant responses to environmental stress have been widely studied in *Arabidopsis*, and the mechanisms of ABA signalling have been elucidated. In general, the adaptive responses of plants to various stress conditions can be either ABA-dependent or ABA-independent (Baker et al., 1995; Bray et al., 1996; Shinozaki & Yamaguchi-Shinozaki, 2007; Yoshida et al., 2014). ABA acts as an endogenous messenger and salt and drought stress signal transmission to initiate downstream gene expression occurs mainly via ABA signalling. Cold-induced signalling likely occurs via secondary messengers such as calcium, IP₃, or ROS, which subsequently induce changes to the phytohormone levels (Clapham, 2007; DeFalco et al., 2010). Through increased or decreased levels, the phytohormones amplify the 'cold signal' or lead to induction of a second set of signalling pathways (Ng et al., 2014). There is no clear boundary between these two pathways and there is significant interplay

between them and the components involved. Several studies have shown that cold acclimation activates multiple low temperature-responsive pathways (Fowler & Thomashow, 2002; Seki et al., 2003; Thomashow, 2001). Some of these studies suggest that common signal transduction pathways are activated by these different stress stimuli (Dubouzet et al., 2003; Thomashow, 1999). These observations suggest that elements of the ABA-dependent and ABA-independent pathways interact (Yoshida et al., 2014; Fujita et al., 2006; Rasool et al., 2018) (see Fig. 1.6). These aspects, and the recent advances in determining the nature and function of genes with roles in freezing tolerance, will be explored further in Chapter 5.

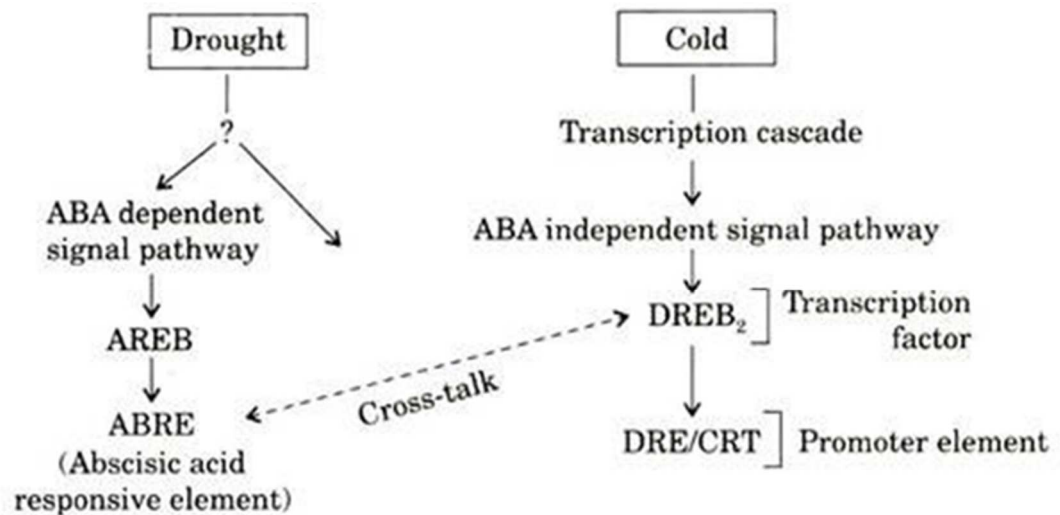


Figure 1.6: Regulatory Network of Gene Expression in Response to Cold Acclimation.

Both ABA-dependent and ABA-independent pathways affect plant responses to cold stress. External applications of ABA have been revealed to increase drought tolerance in some plant species, and ABA levels in plants is known to generally increase during abiotic stress conditions (e.g., drought, increased soil salinity, and both heat and cold stress), and ABA can increase plants' adaptation to various abiotic stresses (ABRE: ABA-responsive element). Reproduced from Tuteja (2007) and Xue and Loveridge (2004).

1.12 Origin and Domestication of Cereals

1.12.1 The Origin and Domestication History of Barley (*Hordeum vulgare* L.)

Cereals account for 50% of the total global calories provided by food products, with wheat and barley products contributing to one-fifth of the human diet (FAO, 2012). From 3,000 to 4,000 B.C., the rate at which wheat spread from the Fertile Crescent to Europe, Africa, and Asia was estimated to be 1 km per year. Thus, it took approximately 5,000 years to reach China (Feldman, 2000). The Fertile Crescent region is bordered by the Mediterranean coast and plains of the Tigris and Euphrates basins, and stretches throughout the Syrian Desert, extending to central Israel, and Jordan (Maeda et al., 2016). Hexaploid wheat was introduced to Mexico by the Spaniards in the 15th century and was taken to Australia at the end of 17th century (Feldman, 2000). Wheat production in Canada began in the early 18th century and the first recorded attempt at growing wheat in Saskatchewan took place between 1753 and 1756 in the Carrot River Valley. Red Fife is Canada's oldest wheat variety, the commercial production of which likely started in the 1880s in Peterborough, Ontario. Selkirk settlers from Scotland spread the wheat cultivation westward to reach Manitoba in the early 19th century, and subsequently wheat rapidly became the most important crop grown on the Prairies (DePauw et al., 2011). In 1919, wheat was grown on 4 million hectares in Saskatchewan.

Important food crops including wheat, rice, barley, and maize belong to the grass family *Poaceae*. The *Poaceae* family of flowering grass is the most important of all plant families to human economies because it provides the majority of mankind's food calories. Barley, wheat, and oat in the *Pooideae* subfamily, rice in *Ehrhartoideae*, and maize with sorghum and sugarcane in *Panicoideae* are just some examples of crops belonging to the *Poaceae* family, that together contribute to more than 75% of the world's food production (Vigeland et al., 2013). Other species from different genera are of great agricultural value for food production. For example, wheat and barley grain also contribute to animal feed and several bio-based industrial products. Bread, biscuits, cakes, breakfast cereals, and pasta are the main wheat products consumed by nearly 35% of the world population (Yaqoob et al., 2018). Most of the calories in wheat and barley grain are derived from the carbohydrate-rich seed endosperm (Yaqoob et al., 2018), which also contains proteins that confer good dough-

making qualities. The presence of valuable minerals, vitamins, and fibre add additional value to cereal-based food products (Balk et al., 2019).

Barley (*Hordeum vulgare* L.) is one of the founder crops of Old-World agriculture and was one of the first domesticated cereals (Zohary et al., 2012). In 2016, barley was ranked fourth among grains in quantity produced (141 million tonnes) globally, after maize, wheat, and rice, accounting for approximately 7% of the global cereal production (Food, 2016). The origin and domestication of barley from the archaeological remains of barley grains found at various sites in the Fertile Crescent indicate that the crop was domesticated in approximately 8000 B.C. (Diamond et al., 1993; Zohary & Hopf, 2000). The wild relative of the plant is known as *Hordeum spontaneum* C. Koch. In modern taxonomy, *Hordeum vulgare* L. and *Hordeum spontaneum* C. Koch, as well as *Hordeum agriocrithon* Åberg, are considered subspecies of *Hordeum vulgare* (von Bothmer & Jacobsen, 1985).

1.13 Cold Acclimation in the Cereal Tribe *Triticeae*

Environmental stresses play crucial roles in the productivity, survival, and reproductive biology of plants and crops. As discussed previously, plants are subjected to many forms of environmental stress, (drought, salinity, temperature (high/low), chilling and freezing, radiation, chemicals, heavy metals, and light (length of the photoperiod)). Temperature and light (length of the photoperiod) are two of the most important factors that significantly affect the life processes of all organisms. Low temperatures due to seasonal variations and geographical distribution on Earth inhibit plant growth and survival. Approximately two thirds of the world's land mass is annually subjected to temperatures below 0 °C and approximately half of that land experiences very low freezing temperatures below -20°C (Beck et al., 2004). Agriculture is affected by frequent extreme temperature changes, which impact grain productivity. Thus, improving cereal productivity is not only a matter of increasing the yield potential of the current germplasm, but also of improving yield stability by ensuring enhanced tolerance to abiotic stresses, such as cold. For example, large economic losses are regularly experienced in the agricultural sector in the USA, particularly in the state of Florida, where the citrus industry has been devastated by frost or freezing damage in fruit and trees, costing billions of dollars. A frost in California in December 1998 caused approximately \$700 million worth of damage (Tiefenbacher et al., 2000).

Cereals in the *Triticeae* tribe can be separated into three agronomic classes: winter, spring, and facultative. Freezing tolerance in plants is not normally a constitutive trait, but an acquired one. To acquire freezing tolerance, a plant must be exposed to gradually decreasing temperatures, a process called cold acclimation (Thomashow, 1998). Cold acclimation involves the activation of signalling pathways that increase freezing tolerance (Guy et al., 1985; Thomashow, 1998). In *Triticeae*, freezing tolerance in winter genotypes is greater than that of spring genotypes. Winter genotypes are sown in the autumn, overwinter, and flower in spring of the following year; by contrast, the spring genotypes are sown in the spring and are harvested in late summer to early autumn of the same year. This difference in growing seasons is primarily because winter genotypes require a vernalisation period of 1–8 weeks of cold temperature exposure (0–10°C) in order to transition from the vegetative to the reproductive stage of growth. Spring genotypes, on the other hand, are inherently reproductively competent and do not require vernalisation to flower. Development in winter genotypes is tightly regulated by changes in day length, whereas spring genotypes have a reduced sensitivity to photoperiod. Facultative genotypes can be as cold-tolerant as winter genotypes, but do not require vernalisation to flower, and can be photoperiod-sensitive or insensitive (Tondelli et al., 2006; von Zitzewitz et al., 2011; von Zitzewitz et al., 2005). Wheat and barley are cool-season annuals grown around the world but mostly between the latitudes 30°–60° N and 27°–40° S (Curtis, 2002). Whereas wheat can survive temperatures as low as -22°C, the lowest temperature that barley can survive is approximately -17 °C (Fowler et al., 1996; Fowler & Limin, 2004; Sutka, 1994; Taleei et al., 2010). Within each species, individual genotypes also differ significantly (Fowler et al., 1999). Certain cultivars can overwinter in temperate climates, while other cultivars cannot. The capacity to overwinter is often referred to as ‘winter hardiness’ and involves the activation of many component traits including tolerance of freezing, desiccation, anoxia, ice-encasement, and resistance to diseases (Fowler et al., 1999). In addition to the difference in freezing tolerance levels between species, differences also occur within species. For example, some wheat and barley cultivars will not survive below -6°C, while others survive below -14°C. In summary, growth habits mainly differ in their level of freezing tolerance, response to vernalisation, and sensitivity to photoperiod. These three factors together define the winter-hardiness of a plant, i.e., its ability to survive through the temperate climate winter (Jeknić et al., 2014; Levitt, 1980a; Sakai & Larcher, 1987; 2012). This difference in ability to tolerate freezing stress is

controlled by several signalling pathways that interact in a complex network, making winter-hardiness a particularly complex trait.

The following sections provide a literature review of topics relevant to the objectives of the present study. First, is a review of the vernalisation pathway and the regulation of a key protein, *VRNI*, in cereals. This is followed by a section on the role of photoperiod in cold acclimation in cereals and, finally, a section on the integration of the temperature sensing and photoperiod-sensing pathways. Specific emphasis is given to the role of the CBF/COR regulon on cold acclimation, as this pathway has been well studied in *Arabidopsis*.

1.14 Genetic Mapping of Cold Tolerance Traits in Cereals

Initial studies of cold acclimation in hexaploid wheat using monosomic and chromosome substitution lines associated at least 10 out of the 21 chromosome pairs with cold tolerance (Sutka, 1994). The combined effect of the cold-induced gene products influences the level of LT tolerance. At the genetic level, LT tolerance in wheat is controlled by two major QTLs on the long arm of chromosome 5A: frost resistance-A1 (formerly *FRI*) (Snape et al., 2001; Sutka & Snape, 1989; Tóth et al. 2003), and Fr-A2, which is located 30 cm distal to Fr-A1 (Galiba et al., 1995; Galiba et al., 2009; Vágújfalvi et al., 2003) (see Fig. 1.7). The Fr-A1 locus co-segregates with *VRNI*, a gene known to be involved in the initiation of flowering in winter cereals. A dominant allele at both loci confers the spring habit, whereas dominant Fr-A1 with a recessive *VRNI* allele confers the winter habit (Sutka & Snape, 1989). From studies on homozygous (*VRNI/VRNI*) and heterozygous (*VRNI/VRNI*) mutant lines of the diploid wheat *T. monococcum*, it was concluded that the *VRNI* protein promotes flowering in the crown meristem in long days, and initiates the suppression of the COR regulon in leaves in short days (Dhillon et al., 2010). The Fr-A2 QTL is associated with a cluster of CBF genes (Båga et al., 2009; Campoli et al., 2009; Francia et al., 2004; Knox et al., 2010; Miller et al., 2006; Vágújfalvi et al., 2005; Vágújfalvi et al., 2003). At least 11 of the *CBF* genes in the *FR2* interval function to regulate *COR/LEA* gene expression during cold acclimation (Stockinger et al., 2007; Sutton et al., 2009; Francia et al., 2004).

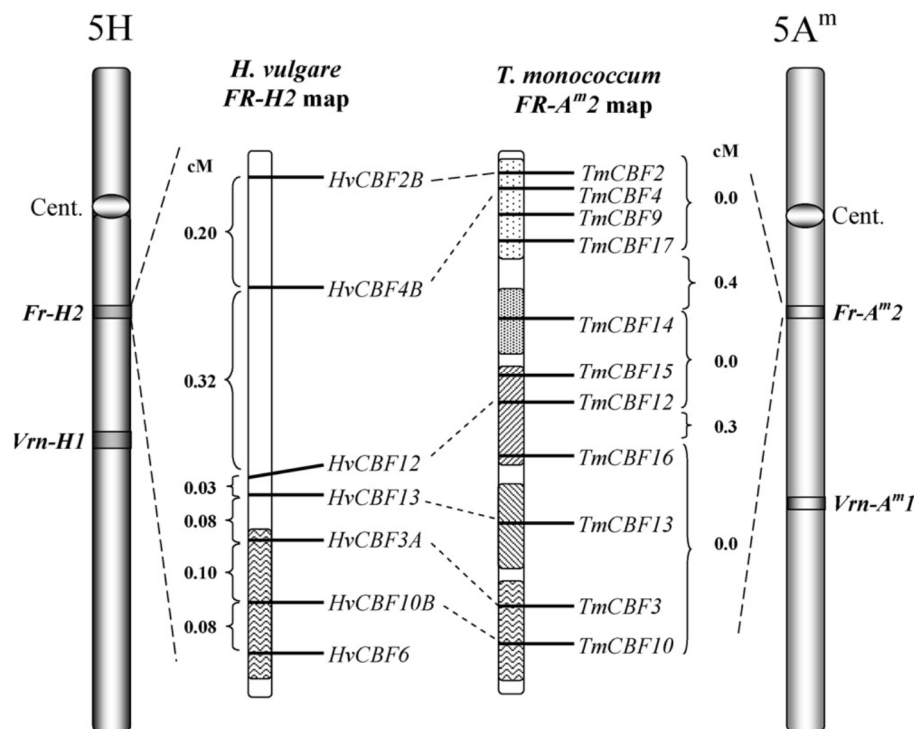


Figure 1.7: Diagram of the Relative Positions of the Mapped Frost Resistance (*FR*) and Vernalisation (*VRN*) Genes on Chromosome 5H of Barley and Diploid Wheat.

The *FR2* chromosome region is magnified. Genetic distances are in cM. Diagram reproduced from Galiba et al. (2009).

1.14.1 The Vernalisation Pathway in Cereals

In winter wheat and barley varieties, long exposures to non-freezing cold temperatures in winter accelerate flowering time in spring (vernalisation) and improve freezing tolerance (cold acclimation). However, when plants initiate their reproductive development, freezing tolerance decreases, suggesting a connection between the two processes. Differences in genes regulating the initiation of the reproductive phase by vernalisation (*VRN* genes) (Turner et al., 2005; Yan et al., 2003) and photoperiod (*PPD* genes) (Beales et al., 2007; Turner et al., 2005) are reported to have an impact on frost tolerance. The genetic basis of vernalisation responsiveness has been extensively studied in a few economically important core *Pooideae* species (Ream et al., 2014), revealing two key epistatic vernalisation genes – *VERNALIZATION1* (*VRN1*); *FRUITFULL1*, *FUL1*) and *VRN2* – and their downstream floral integrator *VRN3* (*FLOWERING LOCUS T*, or *FT*) (Amasino, 2004; Danyluk et al., 2003; Distelfeld et al., 2009; Greenup et al., 2009; Preston & Sandve, 2013; Ream et al., 2014). There is particular interest in *VRN* genes in this study, as they are regulated by long exposures to cold but non-freezing temperatures, the same conditions required for plant acclimation to freezing temperatures. The recent identification of the main genes responsible for the natural variation in vernalisation requirement and cold acclimation has provided new insights into the regulation of frost tolerance in temperate cereals. Hence, the roles of these genes and their possible interactions are discussed in this section. Three *VRN* loci affecting vernalisation requirement and two *PPD* loci affecting photoperiod sensitivity have been identified in wheat and barley (Díaz et al., 2012; Turner et al., 2005). These loci and their interactions are described in the sections below.

1.14.2 The Role of *VRN1* in Cereal Flowering and Frost Tolerance

Early genetic studies revealed a correlation between growth habit and freezing tolerance, where wheat genotypes having a spring growth habit were less freezing-tolerant than genotypes having a winter growth habit (Díaz et al., 2012). Thus, temperate cereals are usually classified into winter and spring classes based on their growth habit. Varieties with a winter growth habit require long exposures to cold temperatures to accelerate flowering in spring (vernalisation requirement), whereas those with a spring growth habit do not. It was mentioned in Section 1.14. That two major QTLs conferring frost tolerance in the *Triticeae* tribe map to the long arm of homologous group of chromosome 5. The first region (*FRI*) includes a gene, *VRN1*, involved with the initiation of cold-induced flowering and this has led to the speculation that *VRN1* is involved in both the cold-induced initiation of flowering in the crown meristem (vernalisation) and cold acclimation in leaves (Dubcovsky et al., 2006; Yan et al., 2004) (see Fig. 1.8).

The current model for controlling vernalisation in *Triticeae* involves the activity of three TFs in leaf tissues: *VRN1*, *VRN2*, and *VRN3* (see Fig. 1.8). Most studies on vernalisation in these cereals have focused on the role of *VRN1* in *Triticum aestivum*. In hexaploid wheat, the homeologous copies of *VRN1* are located on homeologous chromosomes 5A (*VRN-A1* on 5A, formerly *VRN1*), 5B (*VRN-B1* on 5B, formerly *VRN2*) and 5D (*VRN-D1* on 5D, formerly *VRN3*) (Flood & Halloran, 1986; Snape et al., 2001) and they map to equivalent positions to *VRN-H1* in *H. vulgare*, *VRN-R1* in *Secale* cereal, and *VRN-Am1* in diploid wheat *T. monococcum* (Cockram et al., 2007; Dubcovsky et al., 1998). Copies of the other two vernalisation genes that regulate flowering in *Triticeae*, *VRN2* and *VRN3*, are located close to the centromere on chromosome 5 and on chromosome 7S, respectively (Distelfeld et al., 2009; Yan et al., 2004; Yan et al., 2006).

Early studies (Law et al., 1976; Snape et al., 1976) indicated that the *VRN-A1* locus has the greatest effect in the elimination of the vernalisation requirement, with some alleles, such as *VRN-A1a*, conferring insensitivity to vernalisation (Appendino & Slafer, 2003; Liuling Yan et al., 2004). The variability in these loci is spread across the commercial germplasm but the allelic frequencies may vary depending on the region of the world in which they are cultivated (Stelmakh, 1990; Liuling Yan et al., 2004).

The second important locus that has been identified is *FR2* (frost resistance 2). This is a 0.8 cm chromosomal region that encompasses a cluster of genes encoding CBFs. CBF TFs are known regulators of the COR genes, which are induced by cold and confer tolerance to subsequent freezing temperatures (acclimation) (Francia et al., 2004; Kocsy et al., 2010; Miller et al., 2006; Skinner et al., 2005; Stockinger et al., 2007; Tondelli et al., 2014). *FRI* and *FR2* reside on homologous group 5 chromosomes, and are between 20–50 cm apart, depending on the mapping population (Stockinger et al., 2006) (see Fig. 1.6). In barley, *FRI* is identified as *FR-H1* (H denotes *Hordeum*), and the homoeologous *FRI* in wheat is *FR-A1* (A denotes the A genome of hexaploid wheat). *FRI* co-segregates with *VRN1* (see Fig. 1.7) (Stockinger et al., 2006).

A molecular isolation of *VRN1* revealed that this gene encodes a MADS-box protein similar to the *Arabidopsis* meristem identity gene *APETALA1* (*API*) (Danyluk et al., 2003; Trevaskis et al., 2003; Yan et al., 2003). The MADS-box binding protein is constitutively expressed in spring genotypes, and is induced during vernalisation in winter genotypes (Danyluk et al., 2003; Liuling Yan et al., 2004). The MADS-box meristem identity gene (*VRN1*) plays an essential role in the regulation of the transition between vegetative and reproductive phases, and its deletion results in *Arabidopsis* plants that fail to flower; gene duplications of the *VRN1* homologue that occurred after the monocot–dicot divergence resulted in three paralogous genes – *APETALA1* (*API*), *CAULIFLOWER* (*CAL*), and *FRUITFULL* (*FRU*) – that have retained partial ability to promote the transition of the vegetative shoot apical meristem (SAM) to the reproductive phase. Simultaneous deletions of all three genes are required to generate non-flowering *Arabidopsis* plants (Ferrándiz et al., 2000). However, *FRI* and *VRN1* co-segregate and, to date, these two traits have not been successfully segregated (Stockinger et al., 2007). Genetic studies have yet to show if *FRI* is an independent gene or merely a pleiotropic effect of *VRN1* (Francia et al., 2004; Hayes et al., 1993; Roberts, 1990; Vashegyi et al., 2010). This issue is of fundamental importance to understanding the regulatory processes affecting the capacity to survive freezing temperatures.

In winter genotypes, *VRN1* is epigenetically silenced in autumn by chromatin modifications. Specifically, histone protein H3K27 is trimethylated (histone 3 protein is trimethylated at Lysine 27 to give H3K27m3) and H3K4 is de-methylated; this keeps the chromosome in a ‘closed’ state, preventing transcription of *VRN1*. With the onset of cold conditions

(vernalisation) the methylation state is reversed and H3K27 and H3K4m3 accumulate, opening up the chromatin and allowing *VRN1* transcription (Oliver et al., 2009). In the leaf, the accumulation of *VRN1* protein, a MADS-box TF, acts in two ways: first, it initiates flowering by suppressing *VRN2* in leaves (an inhibitor of the translocatable flowering promoter *VRN3*) (see Section 1.14.5); second, it begins to reverse cold acclimation, which is achieved partly by shutting down the CBF regulon (which accounts for approximately 20% of the induced cold tolerance in cereals), though other pathways must also be shut down – how this is achieved remains unclear (Dhillon et al., 2009). Spring genotypes tend to carry deletions in the promoter region and first large intron of the *VRN1* gene; hence, the chromatin modifications described above are thought to be absent and, consequently, there is no requirement for vernalisation (Oliver et al., 2009).

1.14.3 The Role of Photoperiod in Cereal Frost Tolerance

Growth of plants depends on two factors: length of the day (or, more accurately, the length of the night period) and ambient temperature. Consequently, autumn/winter plants take longer to produce their yields than spring/summer plants (Uemura et al., 2006). Seeds that are planted in the autumn can produce crops in late autumn, early winter, or in the spring (Uemura et al., 2006). The latter is possible because some of the seeds that were planted in the autumn can stay alive in the ground throughout the winter, due to their ability to resist low temperatures, and then produce a useful harvest in the spring.

Plants possess circadian rhythms, which are entrained when plants encounter a ‘zeitgeber’, normally the onset of dawn (Song et al., 2015). This controls a number of functions in the plant, such as flowering, leaf motion, maturity, and germination. It also regulates gas exchange, aroma release, enzyme function, and photosynthesis. This circadian regulation is produced and self-maintained within the internal environment of the plant and remains somewhat stable over a range of temperatures (Song et al., 2015). This self-regulation system of the plant is characterised by the interplay of two transcription-translation feedback mechanisms; the first of these involves proteins that have Per-Amt-Sim (PAS) domains which mediate protein–protein interactions; the second consists of numerous photoreceptors that adjust the plant’s biological clock in response to changes in the light state (Fowler et al., 2014). A detailed understanding of this regulatory system in plants could be used to advise

farmers on how to avoid large losses resulting from LT and enable them to produce crops throughout the four seasons of the year (Fowler et al., 2014).

Photoperiod also plays an important role in determining winter hardiness (Hayes et al., 1993; Jackson, 2009). Wheat, barley, and rye are all long days (LD) plants. Long days and short night periods within a 24-hour day promote reproductive development, while short light and long dark periods are conducive to maintaining plants in a vegetative growth phase (Laurie, 1997). ‘Dicktoo’, a winter-hardy facultative barley, is significantly delayed in reproductive development when grown under short days (SD) conditions but can be completely switched to the reproductive growth phase by LD photoperiods (Fowler et al., 2014). This switch is paralleled by the appearance of *VRN1* transcripts (Danyluk et al., 2003), and a concomitant decrease in winter hardiness (Fowler et al., 2014). The leaves of barley contain the photoreceptor phytochrome C (*PHYC*) and the downstream regulators of photoperiod PPDI and CONSTANS (CO) (see Fig. 1.8). The photochromic receptors act as sensors for the long daylight hours during spring (Galiba et al., 2009), while PPDI and CO regulate the transition from a vegetative to a reproductive crown meristem (Fowler et al., 2014).

The photoperiod response locus (*Ppd-1*) protein is a pseudo response regulator which plays an important role in controlling circadian cycles and maintaining an appropriate level of expression of CONSTANS (CO) in LD regardless of the temperature. The CO proteins interact with *VRN3* (flowering locus T, FT), enhancing its expression and promoting flowering (Lazaro et al., 2012). In addition, in winter barley there are two major loci regulating the photoperiod response: *Ppd-H1* and *Ppd-H2*, located on chromosomes 2H and 1H, respectively. The main cause of differences in photoperiod arises from deletions in *Ppd-H1*, resulting in allelic differences in flowering time of 7 to 12 days (Laurie et al., 1994; Turner et al., 2005). There is a second photoperiod sensitivity gene (*Ppd-H2*) in winter barley, which has been characterised and mapped to chromosome 1 (HvFT3). Mutations in this allele confer photoperiod insensitivity, triggering early flowering under SD even if vernalisation requirements are not fulfilled (Acerete et al., 2011).

PPD-1 normally promotes flowering time under LD (16 h light/8 h dark) (Kiseleva et al., 2017; Laurie et al., 1994; Pérez-Gianmarco et al., 2018). A dominant allele of *PPD-1* (*Ppd-1*) promotes flowering under LD by up-regulating the expression of *VRN3* in leaves; the protein is then translocated to the crown meristem where it up-regulates *VRN1* expression (see Fig. 1.8) (Turner et al., 2005). In barley, a recessive allele of *PPD-H1*, resulting from a

loss-of-function mutation in its coding sequence, shows reduced or no sensitivity to photoperiod and results in delayed flowering under LD (Turner et al., 2005). Thus, facultative barley genotypes harbouring the LD-responsive *Ppd-H1* allele (*VRN1/VRN2/Ppd-1*) flower earlier than those harbouring the photoperiod-insensitive allele (*VRN1/VRN2/ppd-1*) (Hemming et al., 2008).

The photoperiod locus *PPD-2* affects flowering time under SD (8 h light/16 h dark; Laurie et al., 1995). Under SD, a dominant allele of *PPD-2* promotes flowering, whereas a recessive allele, resulting from deletions within the gene, delays flowering (Karsai et al., 2008; Kikuchi et al., 2009). Vernalisation of winter genotypes initiates a positive response, while up-regulation of *VRN1* downregulates *VRN2*, releasing *VRN3* from repression, which reinforces *VRN1* expression, ultimately causing flowering (Distelfeld, et al., 2009).

In conclusion, the light-sensing mechanisms in leaves that entrain photoperiodicity are well established with regard to the control of flowering (see Section 1.14.5). However, unlike the temperature-sensing pathway, it is unclear how the photoperiod-sensing pathway integrates into the regulation of cold tolerance in plants.

1.14.4 The Role of Low Temperature and the *FR2* Locus in Cereal Frost Tolerance

A set of tandemly duplicated *CBF* TFs are found at the *FR2* locus. *CBF* TFs are known regulators of the *COR* genes, which are induced by cold and confer tolerance to subsequent freezing temperatures (acclimation). Natural differences in frost tolerance in both wheat and barley have been mapped to the *FR2* locus and are associated with differences in threshold induction temperatures and/or transcript levels of several *CBF* genes. Following this logic, LT tolerance is regulated in part by the *CBF* genes. It is difficult to estimate the relative importance of the *CBF* regulon in cold acclimation in *Triticeae*; it has been suggested that approximately 20% of the cold-responsive genes in *Arabidopsis* are regulated through *CBF* TFs (Vogel et al., 2005), but estimates for cereals are not available. Regardless, the *CBF* pathway remains the best characterised cold-signalling pathway in plants and its relative importance in conferring cold tolerance on wheat and barley is currently unclear.

An understanding of the function of CBFs was first gained from their discovery in *Arabidopsis*; a more detailed account of the role of CBFs in *Arabidopsis* is given in Section 1.7.1. Members of the CBF gene family have now been identified in 54 genera: 23 monocotyledons and 31 dicotyledons including 13 woody plants. Among *Poaceae*, CBFs have been isolated and characterised in several frost-resistant species, such as wheat (*Triticum spp.*), barley (*Hordeum vulgare* L.), ryegrass (*Lolium tremulentum*), rye (*Secale cereale* L.), and also in LT-sensitive crops such as rice (*Oryza sativa*) and maize (*Zea mays*) (Jaglo et al., 2001; Vágújfalvi et al., 2005).

It is observed that in *Arabidopsis* and in some grasses, the expression level of some *CBF* genes showed a rapid induction in response to cold exposure, with transcript abundance peaking 4–12 hours after plants were subjected to a temperature decrease (Dubouzet et al., 2003; Vágújfalvi et al., 2005; Navarro et al., 2009). More recently, the expression pattern of CBFs in wheat has been shown to be much more complex. An ultradian (two or more periods per 24 hours) periodicity was found for *CBF14* and *CBF15*, the CBFs at the *FR2* locus that are the most responsive to cold acclimation, with peaks of transcript abundance occurring in the middle of the light and middle of the dark periods (Skinner et al., 2018). Clearly, the regulation of these TFs that control the expression of COR proteins is complex and poorly understood.

In *Arabidopsis*, six *AtCBF* genes have been described, with three of them – *AtCBF1*, *AtCBF2*, and *AtCBF3*, located within a region of less than 10kb on chromosome 4 – being rapidly and transiently induced after exposure to low temperatures (Gilmour et al., 1998; Shinwari et al., 1998). However, in monocots, the CBF gene family is much larger compared with *Arabidopsis*. Rice has five CBF members (Zhen & Ungerer, 2008), whereas at least 13 are present in *T. monococcum* (Knox et al., 2008b) and 17 in barley (Tang et al., 2005). Some CBF groups are found only in the *Poideae*, suggesting that this expansion represents an adaptation of this group of species in order to colonise diverse temperate habitats (Novillo et al., 2004). At least 11 different CBF genes have been mapped within a small 0.7–0.8 cm region encompassing the *FR2* locus in both *T. monococcum* and barley (Campoli et al., 2009; Fricano et al., 2009). Since the order of these genes is conserved between these two species, a common gene-numbering system was adopted (Fricano et al., 2009; Tang et al., 2005). A cluster of at least 13 CBF genes occurs on the long arm of the homologous group 5 chromosomes, spanning a physical distance of approximately 850 kb and a genetic distance

of about 0.8 cm (Knox et al., 2008a; Miller et al., 2006; Skinner et al., 2005). In these cereal crops, the CBFs on chromosome 5 are coincident with one of the two major QTLs, *FR2*, identified in wheat and barley populations derived from crosses between winter and spring genotypes (Båga et al., 2007; Francia et al., 2004; Galiba et al., 1995; Galiba et al., 2009; Stockinger et al., 2007). The *FR2* CBFs belong to two phylogenetic clades or subgroups – *HvCBFIII* and *HvCBFIV* (Badawi et al., 2007; Skinner et al., 2005). The *HvCBFIII*-subgroup consists of *CBF12*, *CBF15*, *CBF16*, *CBF3*, *CBF6*, *CBF10*, and *CBF13*. The *HvCBFIV*-subgroup genes consists of *CBF2*, *CBF4*, *CBF9*, and *CBF14*. Except for *CBF3*, *CBF6*, *CBF10*, and *CBF13*, all the *FR2* CBFs are cold-responsive. Additional CBFs are also present dispersed on other chromosomes, and consists of *CBF1*, *CBF5*, *CBF7*, and *CBF11* (Stockinger et al., 2006). These *CBFs* belong to *HvCBFI* subgroup and are non-responsive to cold (Badawi et al., 2007; Skinner et al., 2005).

1.14.5 Flowering Time: Model of the Regulatory Pathway Mediated by Vernalisation

Studies have revealed that the genes described above (Section 1.14) interact, suggesting that all of them are integrated in the same regulatory pathway of flowering initiation in cereals mediated by vernalisation. Based on the knowledge acquired from the isolation of *VRN1*, *VRN2*, and *VRN3* genes, a model of molecular regulation has been proposed which integrates the vernalisation and photoperiod pathways.

The vernalisation genes *VRN1*, *VRN2*, and *VRN3* have been cloned in order to explain the regulatory pathway of the spike initiation in response to seasonal cues. The goal was to understand how plants integrate the day-length (long nights in winter; short nights in summer) response to prevent or promote the reproductive stage (Distelfeld, et al., 2009; Trevaskis et al., 2007).

1.15 Control of Flowering in the *Triticeae* Tribe

1.15.1 Flowering in Spring Genotypes

In the United Kingdom, spring varieties of barley are planted in March and harvested in early September. In these lines, LD promotes the transcription of *CONSTANS*, a TF that positively regulates the transcription of *VRN3* in leaves (see Fig. 1.8). *VRN3* is then translocated via phloem to the meristems crown and then activates the MADS-box TF *VRN1*. *VRN1* encodes a TF that is highly similar to the meristem identity gene *APETELLA1* (*Ap1*) from *Arabidopsis thaliana*, which is essential for the transition of the main vegetative meristem of the crown from a vegetative to a reproductive form. Once this transition has occurred, the meristem elongates and forms double ridges, which become the florets on the flowering stem (Galiba et al., 2009).

1.15.2 Flowering in Winter Genotypes

The *VRN2* locus includes two tightly linked and related genes (*ZCCT1* and *ZCCT2*), which both repress flowering initiation under LD. In diploid species, like barley or *T. monococcum*, simultaneous deletion or non-functional mutations of both genes is associated with recessive alleles for spring growth habits.

VRN3 is a functional homologue to the *Flowering Time* (*FT*), formerly described as a flowering promoter in *A. thaliana*. The protein product moves from leaf to shoot apex through the phloem. *VRN3* (*FT*) is considered a central flowering integrator, since the vernalisation and photoperiod signals converge on it. The day-length (LD) response is mediated by *Ppd1*, which acts in conjunction with the homologues of the cereal photoperiod gene *CONSTANS* (*CO*). In barley, there are two forms of *CO* genes; the first (*HvCO1*) is expressed from the time of flower appearance until initiation, whereas the second (*HvCO2*) is produced during the late phases of terminal spike formation and heading (Song et al., 2015). In addition, *CO* and *PPD1* trigger the expression of *HvVRN3*, which is homologous to *FT1* in *Arabidopsis*. Moreover, the expression of *HvVRN3* can be antagonised by *HvVRN2* in a way that is similar to *FLC1* suppression of *FT1* in *Arabidopsis* (Fowler et al., 2014). LD results in the stabilisation of *CO* proteins, which up-regulate *FT* resulting in the acceleration of flowering. This *CO* function appears to be conserved in temperate cereals.

1.15.3 Model Proposed for Regulation of Flowering and Cold Tolerance in Cereals

Winter lines are normally sown in autumn and harvested in early summer. The promotion of flowering in LD presents a problem for winter cereals growing in the autumn, as flowering might occur in early winter. To prevent cold damage to the temperature-sensitive reproductive meristem, winter lines have evolved a mechanism to suppress flowering in autumn. LD also promotes the synthesis of *VRN2* in leaves, which suppresses the synthesis of *VRN3*. In this case, *VRN1* does not accumulate in the crown meristem in the LD of autumn (see Fig. 1.8). The cold conditions of winter, however, do lead to the accumulation of *VRN1* in leaves through a *CO/VRN3*-independent pathway known as vernalisation, but the details of how this occurs are unclear. In addition, to promoting flowering, *VRN1* is also a

transcriptional suppressor of *VRN2* and, by the end of winter, enough *VRN1* has accumulated through the vernalisation pathway to remove the block on *VRN3* transcription (see Fig. 1.8). This release from suppression, coupled with the increasing day length, leads to a large increase in *VRN1* in the crown meristem and flowering in spring.

Winter lines that overwinter face the challenge of very low freezing temperatures and are therefore required to adapt to cold in order to become cold-hardy. Several important QTLs have been identified in cereals that confer cold tolerance, but as mentioned earlier, the major one is *FRI*, which maps to the same locus as the major vernalisation QTL, *VRN1*.

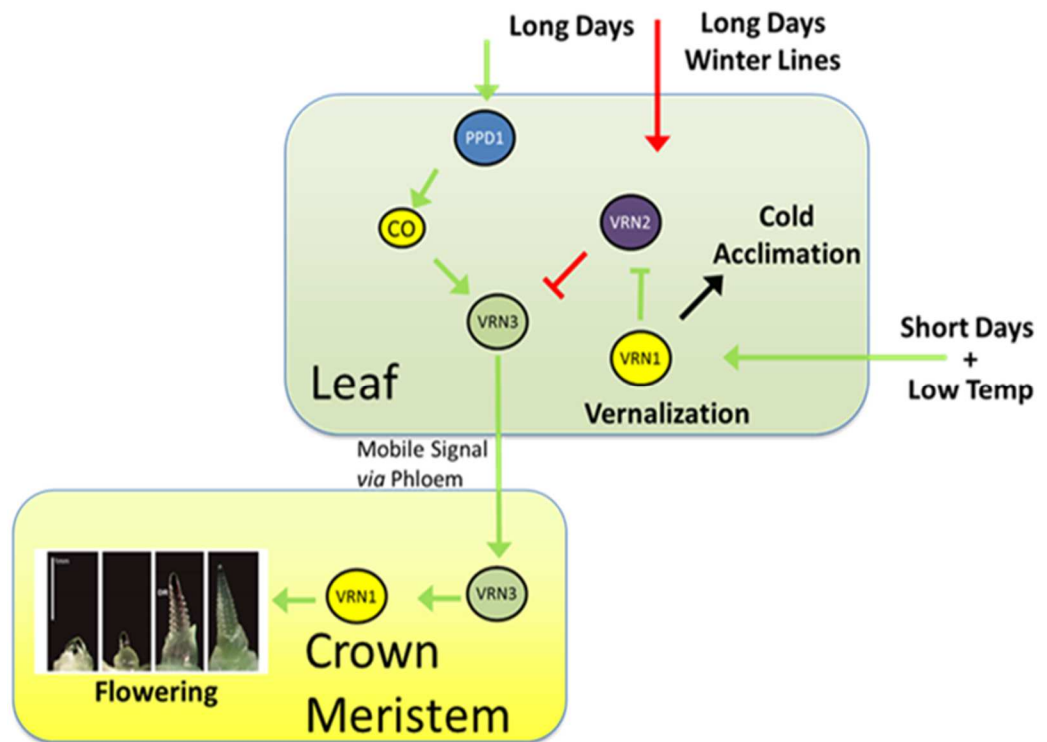


Figure 1.8: Hypothetical Model Proposed for Regulation of Flowering and Cold Tolerance in Cereals.

In both spring and winter varieties LD is sensed in leaves via the circadian clock. The pseudo response regulator (PPDH1) activates the TF CONSTANS (CO), leading to an accumulation of *VRN3* (a zinc-finger TF). *VRN3* is also known as FL, or florigen, a mobile signal that moves through the phloem to the crown meristem where it activates *VRN1*; this triggers the transition of the vegetative (left) to a reproductive (right) meristem and is required for flowering in cereals. In winter lines, precocious flowering in autumn is prevented by the (LD) activation of the suppressor of flowering *VRN2*. During winter, however, SD and LT epigenetically activates *VRN1* in leaves; this triggers the complex response of cold acclimation in leaves, leading to frost resistance. *VRN1* is also a suppressor of *VRN2* and, with the arrival of spring, flowering proceeds normally as *VRN3* is no longer suppressed; this requirement for cold-induced flowering in winter annuals and perennials is known as the vernalisation pathway. Abbreviations: PPD = photoperiod pseudo response regulator D; VRN = vernalisation.

1.16. Current Models for Cold-Signalling Pathway in Plants

This section summarises recent research achievements concerning cold perception and signal transduction in plants based on studies performed using the model *Arabidopsis* plants as discussed in Sections 1.7.1 and 1.7.2. using examples of economically important crops such as rice (Suh et al., 2010; Xu et al., 2008).

Figure 1.9 illustrates current models of cold stress signalling in plants, where changes in membrane fluidity (Örvar et al., 2000; Yamada et al., 2002) are directly proportional to variances in ambient temperature. It is also known that second-messenger molecules, such as calcium, IP3, and ROS act in signalling networks to transduce signals through protein kinases or TF cascades to activate complex signalling pathways (Chinnusamy et al., 2003; Chinnusamy et al., 2010; Chinnusamy et al., 2006; Viswanathan & Zhu, 2002). Protein kinases are responsible for the ability of plants to adapt to cold weather (Viswanathan & Zhu, 2002). Earlier studies revealed high activities of both the calcium-dependent protein kinase (CDPK) (Knight et al., 1996; Luan et al., 2002; Sanders et al., 2002) and the MAPK (Viswanathan & Zhu, 2002). During cold acclimation, however, the underlying mechanisms that plants use to perceive and transduce cold signals remain elusive.

Currently, the most thoroughly understood cold-signalling pathway is the ICE–CBF–COR transcriptional cascade, which plays a crucial role in the activation of multiple downstream COR genes (Thomashow, 1998, 2001, 2010). Since CBF transcripts begin accumulating within 15 minutes of plants' exposure to cold, it is proposed that a TF is already present in the cell at normal growth temperature that recognises the CBF promoters and induces CBF expression, but only after exposure to cool conditions (Winfield et al., 2010). This activator(s) is named ICE protein(s) and it is hypothesised that, upon exposing a plant to cold, modification of either ICE or an associated protein would allow ICE to bind to CBF promoters and activate CBF transcription (Chinnusamy et al., 2003).

The cold-signalling pathway activates the ICE1 protein, and AREB/ABFs are induced by ABA-mediated dehydration signalling pathway by both cold and dehydration stresses. ICE1 encodes a MYC transcriptional activator that in *Arabidopsis* binds to the CBF3 promoter. Thus, ICE1 plays a key role in regulating cold-responsive gene expression and cold tolerance in *Arabidopsis* (Liu & Zhang, 2017; Plieth et al., 1999; Zhao et al., 2017). *ICE1* is expressed constitutively, and its overexpression in wild-type plants

enhances the expression of the CBF regulon in the cold and improves the freezing tolerance of the transgenic plants (Chinnusamy et al., 2003).

CBFs are activated by ICE1 TFs (see Fig. 1.8) but repressed by HOS1 (Chinnusamy et al., 2003). Protein kinases (MAPKs), protein phosphatases (IP3) of type-2C/A protein phosphatase (PP2C/A), various classes of transcription factors including MYBs/MYCs, and several MYC and MYB family genes have been reported to be important regulators of ABA-responsive gene expression under cold stress. For instance, MYB96 is induced by ABA and drought, and enhances ABA-mediated drought and freezing tolerance (Guo et al., 2013; Seo et al., 2009). ICE1 is a MYC-type TF that binds to cis elements in the CBF/DREB1 promoter to induce the expression of *CBF3/DREB1A* (Liu et al., 1998; Stockinger et al., 1997; Thomashow, 1999). This is an AP2-type TF, used to regulate expression of COR genes. The cold-acclimation response is a very complex trait, involving multiple metabolic pathways, signalling networks, and several cell compartments. The affinity of some barley CBF TFs to bind to promoter elements becomes functional only when temperatures fall. However, the precise mechanisms for the activation of ICE1, and for transducing perceived signals and second messengers to ICE1 remain unknown (Thomashow, 2010). These genes control the biosynthesis of these transcription elements, which in turn attach to the preserved core sequence CCGAC (CRT/dehydration element (DRE)), in the promoters of a variety of dehydration-reactive genes, such as those responsible for timely reaction to frost.

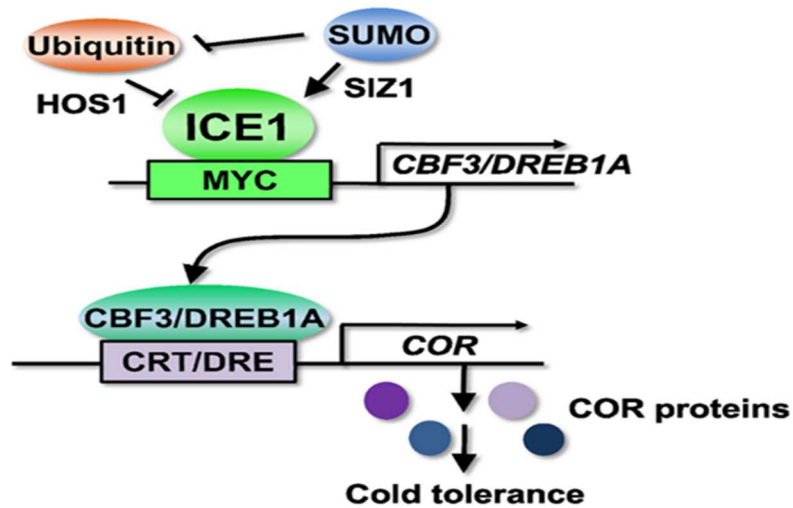


Figure 1.9: The ICE/CBF/COR Regulon Cold-signalling Pathway in *Arabidopsis*.

The cold-signalling pathway involves ICE1, a MYC transcriptional activator that binds to a MYC-type cis-promoter element controlling CBF3/DREB1A expression. CBF3/DREB1A encodes AP2-type transcription factors that transcriptionally regulate the expression of COR genes, which are believed to confer cold tolerance. The abundance of the ICE1 protein is regulated by ubiquitylation by HOS1, a ubiquitin E3 ligase, and targets ICE1 for proteasome-dependent degradation. SIZ1, a SUMO E3 ligase, mediates SUMOylation (SUMO conjugation) of ICE1, leading to blockage of ubiquitylation and stabilisation of the ICE1 protein. Figure reproduced from Miura and Furumoto (2013).

1.17 Outstanding Questions Relating to Cold Acclimation in Cereals

Despite the significant progress that has been made in understanding how plants adapt to cold temperature in the short term, there are still aspects of the biological systems that are not understood. Some of the outstanding questions in this research area include:

- How are cold temperatures sensed, and how is the signal transduced to the nucleus to regulate gene expression?
- What are the mechanisms of post-translational regulation of transcription factors under cold stress?
- To what extent are post-transcriptional processes involved in cold acclimation?
- What accounts for the differences in freezing tolerance among plant species?
- What accounts for the increase in freezing tolerance that occurs with cold acclimation?

- How does the CBF regulon bring about an increase in freezing tolerance?
- How is this information processed to activate the initial expression of cold-regulated genes?
- What is the regulatory logic that underlies the cascading pattern of the low-temperature gene network?
- What biological functions can be ascribed to the genes that constitute the various circuits of the network?

Determining the answers to these questions is not only of basic scientific interest, but also has potential practical applications in crop production. Freezing temperatures periodically cause significant losses in plant productivity and limit the geographical locations where crop and horticultural plant species can be grown. Despite considerable efforts, traditional breeding approaches have resulted in only modest improvements of freezing tolerance. Knowledge of the molecular basis of freezing tolerance and the cold-acclimation process could potentially lead to the development of new strategies to improve plants' freezing tolerance and result in increased plant productivity and expanded areas of agricultural production.

1.18 Hypotheses and Assumptions

Early research into cold tolerance has provided some insights into the mechanism through which plants survive cold stress. For instance, by the 1980s, it was known that freezing tolerance is a multigene trait, that freezing injury in most plants and tissues results largely from the severe cellular dehydration that occurs upon ice formation, and that the cellular membrane systems are the primary sites of freeze-induced injury and damage. However, at this point there was no consensus on the mechanistic basis of freezing tolerance and only limited knowledge of specific genes with functional roles in freezing tolerance and their modes of action. Hence, there remained critical deficiencies in our understanding of cold acclimation and practical efforts to improve the stress tolerance of agronomic plants.

Throughout the 1970s and early 1980s, increasing evidence suggested that gene expression was involved in cold acclimation. Weiser (1970) was one of the first researchers to hypothesise altered gene expression under low temperature in woody plants. Other studies

in herbaceous plants showed that there are changes in the levels of particular proteins after cold treatment, lending support to this idea (Guy & Haskell, 1987; Meza-Basso et al., 1986; Yoshida & Uemura, 1984). Guy et al. (1985) showed that there was synthesis of a population of new mRNAs in spinach leaves when plants were moved to 5 °C. Similar findings were seen in studies carried out in barley (Cattivelli & Bartels, 1989) and *Arabidopsis thaliana*, where in vitro translation of poly (A) RNA showed the synthesis of specific translatable mRNA populations under low temperatures (Gilmour et al., 1988; Mohapatra et al., 1987). Of those genes that are up-regulated in response to LT, the best studied are associated with regulating FT expression and encode proteins involved in protection against desiccation (Shinozaki & Yamaguchi-Shinozaki, 1996), chaperone functions (Sasaki et al., 2007; Zhang & Guy, 2006) and the accumulation of compatible solutes (Cook et al., 2004; Guy et al., 2008).

Several studies using the model plant *Arabidopsis* have increased our understanding of cold acclimation. These studies, which have been reviewed extensively, suggest that cold acclimation is a complex process accompanied by metabolic reprogramming and transcriptional responses (Chinnusamy et al., 2007; Janská et al., 2010). Cold acclimation involves the induction of many classes of proteins, such as CORs, which are reported to be cryoprotective proteins necessary for protection against LT stress (Marozsan-Toth et al., 2015). Another well-established component of the cold-acclimation system is the CBF-induced cold response pathway (Medina et al., 2011; Shi et al., 2018). CBFs are transcriptional activators known to induce COR transcription by binding to the C-repeat/dehydration-responsive element (CRT/DRE) in the regulatory regions of those genes (Shi et al., 2017). CBFs are major determinants of the freezing tolerance of plants (Gilmour et al., 2004; Park et al., 2015; Vogel et al., 2005). Cold acclimation involves the remodelling of cell and tissue structures and the reprogramming of metabolism and gene expression (Barrero-Gil & Salinas, 2018; Guy et al., 1985; Thomashow, 1999; Zhao et al., 2016b).

One major goal in cold acclimation research is identification of cold-responsive genes in economically important plants and the roles they play in freezing tolerance. It is assumed that many cold-responsive proteins likely mediate the biochemical and physiological changes required for growth and development at a low temperature. It is also possible that other proteins might have direct roles in freezing tolerance.

1.19 Difficulties and Advantages of Working with Barley as a Model Plant

This study will focus on two different cultivars of barley: California, which is reported to be a winter cultivar; and Belgravia, which is a spring cultivar (Galiba et al., 2009). Working with barley is challenging because the sequences that are deposited in the open access nucleic acid and protein databases come from more than 20 diverse cultivars of barley. Within each cultivar of barley, sequence divergence exists, which causes difficulties.

Barley was chosen for this study for several reasons. In addition to being an important crop in its own right, barley provides an excellent model for the *Triticeae*, in particular for the more complex hexaploid wheat. Barley is a diploid ($2n=14$) inbreeding crop and offers a number of advantages for biotechnology applications, and its genetics are relatively simple and easy to interpret. It is the world's fourth most economically important grain; unlike maize and rice, it is relatively cold-tolerant, growing in temperate latitudes up to 70° N. The genome of one cultivar, *Morex*, has been sequenced twice, in 2012 (IBSC, 2012) and in 2017 (IBSC, 2017). There are, however, several limitations when using barley. For instance, there are few open access bioinformatic tools available to exploit the plethora of molecular data that is now being generated. Experimental approaches to test hypotheses generated from sequencing are limited, as plant collections and methods to perform forward genetics are underdeveloped. In addition, there are many cultivars grown globally, but *cv Morex* has now been superseded, making the design of universal PCR primer pairs for sequences of interest problematic. Nevertheless, there are also good reasons to choose to investigate cold tolerance in this important crop. Food security is a major concern for humanity in the 21st century, and it is imperative to produce more food. This can be achieved by increasing the range of the major crops to higher latitudes, including barley, and also by increasing the yields.

1.20 Project Aims

The detailed information presented above illustrates the importance of cold acclimation for the survival of plants exposed to freezing temperatures. Modest advances in understanding why some plants are more tolerant of freezing conditions have arisen from molecular genetic studies on the model plant *Arabidopsis thaliana*.

Plant cold acclimation is an exciting area of research. Genes and proteins with roles in freezing tolerance are being identified, their mechanisms of action are being determined, and insights into how the cold-acclimation response is activated in response to low temperatures are emerging. In addition, novel strategies for improving plant freezing tolerance are being considered in light of the new results.

The original aims of this study were to build on earlier work carried out at the host laboratory. The long-term objective of the research group is to build a system biology model that helps to identify how adaptation to decreased temperatures is gained and preserved in barley. Achieving this objective will pave the way for the development of production methods that yield genotypes that are resistant to freezing injury caused by severe drops in temperature. It is hoped that findings in this research area will have a significant economic impact on global food production.

Both the cereal crop yield and the range of cultivation will need to be increased in the next few decades to ensure global food security. The range of cultivation of the elite cereal crop is constrained since all of the major cereals have their origins in the tropics or sub-tropics. In Central Asia and Central/Northern Canada, cereal grasses such as wheat are not grown extensively due to sporadic acute frosts which destroy juvenile plants in spring. However, many wild grasses grow in these habitats. Understanding the mechanisms by which these wild grasses tolerate low temperatures and why the elite cereal crops do not will provide a basis for developing arable crops that are tolerant of extreme cold conditions. It is expected that such understanding will enable the extension of the range of production.

In terms of the project aim, a great deal of the work in the current study will be devoted to investigating the roles of the *CBF* family of gene regulators in mediating the response of barley to frost tolerance. The focus will be on identifying which proteins are important in

conferring frost tolerance on barley. In terms of the target organism, the current study will investigate the cold acclimation process in spring and winter categories of barley and rye.

The objectives of the study are as follows:

1. Develop a robust and reliable quantitative assay for assessing the extent of freezing injury in cereal leaves. This will require resolving a given level of damage to $\pm 1.0^{\circ}\text{C}$.
2. Determine the role of low night temperatures and photoperiod (night length) on cold acclimation in small-grained cereals. Photoperiod (short nights/long days) promotes flowering in cereals, and in winter lines low night temperatures are also required (vernalisation). Both photoperiod (long nights/short days) and low night temperatures have been implicated in conferring cold tolerance but their relative importance and interaction is not well understood.
3. Assess the importance of ABA-dependent and ABA-independent signalling pathways in conferring cold tolerance on small-grained cereals. In *Arabidopsis* there is strong evidence for ABA-dependent and ABA-independent signalling pathways that interact and provide a measure of cold tolerance. It is not known whether these pathways also operate in small-grained cereal crops.
4. Investigate the importance of the ICE-CBF-COR regulon in spring and winter barley cultivars using quantitative and semi-quantitative RT-PCR. The genome of barley has been fully sequenced and it should be possible to study the expression levels of the barley homologues of the *Arabidopsis* ICE-CBF-COR regulon sequences to establish if this regulon is conserved in the *Triticeae* tribe.
5. Perform a full transcriptome analysis of the cold-acclimation process in a winter barley cultivar. These experiments may indicate the importance of signalling pathways other than ICE-CBF-COR. This will be conducted on barley plants exposed to cold-acclimating conditions for 7–28 days. Several transcriptome studies have been conducted on *Arabidopsis* during the cold-acclimation process and a great deal of detail has been gleaned on the changes that occur over the first two days. These studies, however, have not identified the mechanisms that accompany deep-cold acclimation in *Arabidopsis* or any other plant, which arise only after several weeks of exposure to appropriate conditions.

To achieve these objectives, leaves of the cold-hardy cereal crop rye (*Secale cereal* L.) and barley (*Hordeum vulgare* L.) lines will be exposed to a range of low temperatures and photoperiods of variable lengths to induce cold acclimation, and their freezing tolerance will be measured. Attached leaves will be probed using a range of techniques to monitor and measure solute leakage from leaves. This will help identify which processes are most cold sensitive. In addition, the transcript profiles of cold-acclimated leaves of barley will be analysed to identify which gene sequences are most associated with freezing tolerance.

It is also hoped that more information on the significance of *HvCBF* genes in providing frost tolerance to a spring (*cv* Belgravia) and winter (*cv* California) line will be acquired. To achieve this objective, techniques such as quantitative and semi-quantitative RT-PCR will be used to quantify which *HvCBF* genes respond to low temperatures and changes in photoperiod duration. The outline for expression of *HvCBF* genes in winter barley cultivars (California) will also be investigated using these techniques.

In the author's opinion, research about adaptation to falls in ambient temperatures has now reached its golden era. Over the past twenty years, significant progress has been made in our comprehension of plants' adaptation to changes in ambient temperatures, and there is every reason to believe that further significant and impressive achievements will be reached.

By integrating traditional genetic and biochemical approaches with robust novel proteomics and genomics, it is possible that, in the near future, an essential set of defining principles will emerge that will enable the creation of stress-resistant plants. This information will not only be an exciting academic success but could also be used for the production of important foods for the global population.

Chapter 2 Materials and Methods

2.1 Plant Material and Growth Conditions

2.1.1 Growth in Soil

Winter rye (*Secale cereal*, cv *Forage* and cv *Kapitan*) and winter barley cv *California* and spring barley cv *Belgravia* seeds were sown in trays containing damp filter paper and left in the dark at 20°C for four days to germinate. Seedlings were then transferred to pots (10% compost, 90% perlite) and placed in a controlled environment growth room (16/8 hour photoperiod, light intensity 300 $\mu\text{moles.m}^{-2} \text{ s}^{-1}$ at 20°C /16°C temperature day/night, humidity 60%) for 3 weeks.

2.1.2 Growth Conditions

Plants were grown in pots (10% compost, 90% perlite) for 3 weeks in a Long Day (LD) photoperiod (16/8 hr at 20°C/16°C) or Short Day (SD) photoperiod (9/15 hr at 20°C/16°C) and were subsequently acclimated for 1, 2, 3, and 4 weeks under one of four regimens (see Fig. 2.1)

1-Long Day Warm Night Temperature (LD/WT: 16hr light 20°C/8hr dark 16°C; non-acclimation).

2-Long Day Low Night Temperature (LD/LT: 16hr light 20°C/8hr dark 4°C; acclimation by low night temperature only).

3-Short Day Warm Night Temperature (SD/WT: 9hr light 20°C/15hr dark /16°C; acclimation by photoperiod only).

4-Short Days Low Night Temperature (SD/LT: 9hr light 20°C /15 hr dark/ 4°C; acclimation by photoperiod and night temperature).

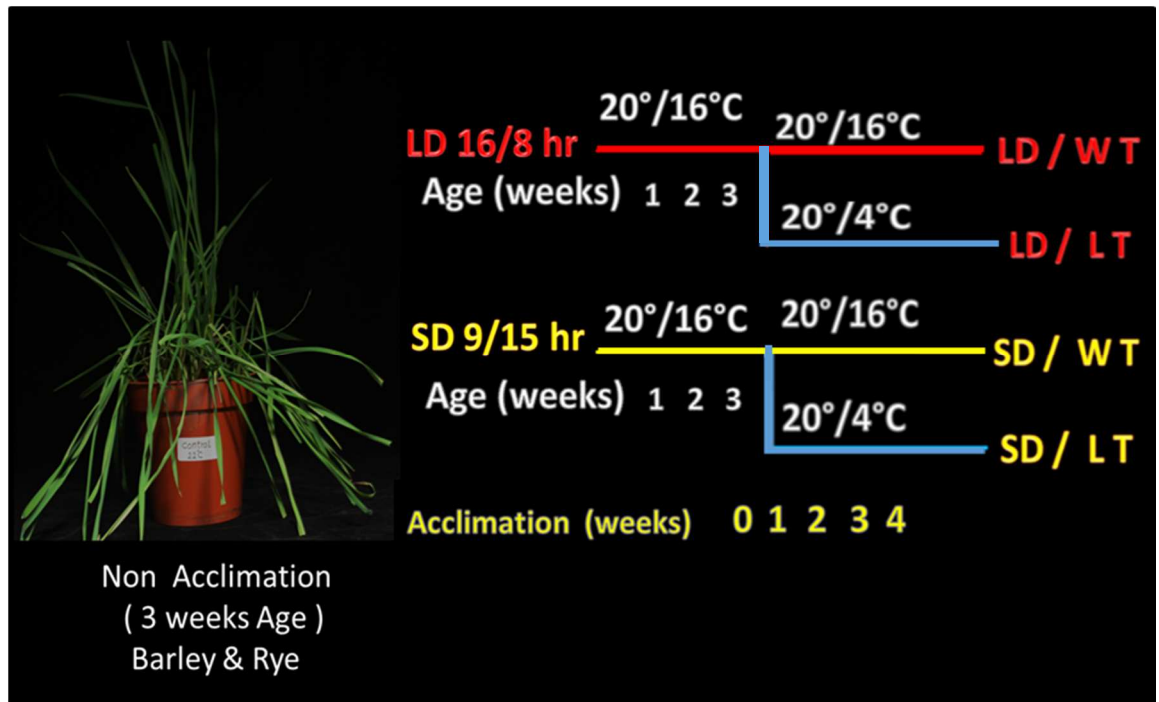


Figure 2.1: Cold-Acclimation Regimes (Photoperiod and Cool Night Temperature). This diagram presents the four regimes for cold acclimation using two photoperiods. 16 hours /8 (LD) or 9 hours (SD) of Light and two Night Temperature Regimes Warm Nights (+16°C) and Cool Nights (+4°C).

2.2 Application of Exogenous ABA to Leaf Tissue

ABA (sigma Aldrich Cat No 14375-45-2) was made up in deionised water substitute to concentrations of 10^{-5} M and 10^{-4} M, and 10ml of the solutions sprayed directly onto five plants every second day for up to 26 days. Leaves were harvested, washed in deionised water, and subsequently used for LT_{50} analysis (see Section 2.3) or RNA scan analysis (see Section 2.6).

2.3 Measurement of Freezing Tolerance (LT₅₀)

2.3.1 Estimation of Freezing Tolerance Using the LT₅₀ Methods

In the next step, leaf discs were taken from fully expanded third leaves and briefly washed in distilled water. Then, three discs were placed in disposable capped 1.5 ml tubes containing 1.0 ml deionised water with an electrical conductivity of less than 5 μ Siemens. These tubes were then placed in a controlled temperature cryo-bath and equilibrated for 60 minutes at each of the experimental temperatures (20°C, 10°C, 0°C, -4°C, -5°C, -6°C, -7°C, -8°C, -9°C, -10°C, -12°C, -14°C, -16°C, -18°C, -20°C, -22°C, and -24°C) unless stated otherwise. This is subsequently replicated three times. Tubes at each temperature were removed and placed immediately at 4°C to thaw overnight. The tubes were then shaken for 2 hours to extract electrolytes from the lysed cells. The electrical conductivity (μ Siemens) of the solution was measured using a conductivity meter. All the samples were subsequently re-frozen at -196°C for 15 minutes to induce 100% cell lysis, then thawed, and electrical conductivity re-assessed. The extent of damage was then assessed for each sample, as follows:

$$\frac{\mu\text{Siemens1 (before liquid nitrogen)}}{\mu\text{Siemens2 (after liquid nitrogen)}} \times 100\%$$

From these data, LT plots were constructed with percentage electrolyte leakage plotted on the y-axis (LT) and incubation temperature on the x-axis. Logistic curves for five parameters were fitted to the average values (n=3) but LT₅₀ values were estimated by interpolation between the local data points around the LT₅₀.

2.4 Molecular Method for Nucleic Acids

2.4.1 Isolation of Genomic DNA

In this stage, DNA was extracted from leaf tissue, either fresh or stored at -80°C, by grinding to a fine powder in a pre-chilled, clean pestle and mortar; care was taken to ensure the sample never thawed. The powdered plant samples were stored in liquid nitrogen until all the samples were processed. DNA was extracted by adding 500 μ l of the extraction buffer (200 mM Tris HCl pH 7.5, 250 mM NaCl, 25 mM EDTA, 0.5% SDS) to the frozen pulverised

samples in 1.5ml microfuge tubes, mixed gently by pipetting up and down, and then allowed to stand at room temperature until all the samples were processed. The samples were then centrifuged at 13,000 rpm for 7 minutes at room temperature. Then, 400 μ l of the supernatant was transferred to a fresh 1.5ml microfuge tube, mixed with 400 μ l of isopropanol, and centrifuged at 13,000 rpm for 2 minutes to pellet DNA. The isopropanol was removed, and DNA pellets washed in 95% ethanol taking care not to disturb the pellet. After the last ethanol wash, the samples were air dried by inverting microfuge tubes on a clean paper towel for at least 5–8 minutes to remove residual ethanol. The DNA pellets were then re-suspended in 200 μ l TE buffer, pH 8.0, and stored at -20°C .

2.4.2 RNA Extraction Using the TRI Reagent Method

Total RNA was extracted using TRI Reagent (T9424 - TRI Reagent®, Sigma-Aldrich Chemical Co. Ltd., and Dorset, United Kingdom). Approximately 100 mg of fresh leaf material was pulverised in liquid nitrogen using a clean pre-chilled pestle and mortar (see Section 2.5.1). The powdered frozen samples were transferred to pre-chilled 1.5 ml sterile microfuge tubes, and then 1 ml TRI Reagent was added and mixed, vortexed briefly, and incubated on ice for 5 minutes. Chloroform (200 μ l) was added into the mixture, shaken vigorously for 15 seconds and then incubated further on ice for 10 minutes. The samples were then centrifuged at 13,000 rpm for 15 minutes at 4°C and the top supernatant-containing RNA was transferred to a fresh 1.5 ml microfuge tube and mixed with 0.5 ml of Isopropanol. The samples were allowed to stand on ice for 10 minutes, centrifuged at 30,000 rpm for 10 minutes at 4°C and the supernatant discarded. The RNA pellet was washed once with 1ml ice cold 75% ethanol. After all traces of ethanol had been removed, the pellets were re-suspended in 20 μ l DEPC-treated dH₂O. RNA samples were subsequently DNase-treated to remove any genomic DNA contamination using Ambion's TURBO DNA-free kit according to the manufacturer's instructions. The quality (purity) of RNA was determined by the ratio of absorbance at A260 nm to A280 nm using a nano-drop spectrophotometer (NanoPhotometer, Pearl, Imlen). Following Sambrook and Russell (2001), the concentration was obtained by measuring absorbance at 260 nm where an absorbance of 1 means 50 $\mu\text{g}/\text{mL}$ of DNA and 38 $\mu\text{g}/\text{mL}$ of RNA. The purity of the samples was measured by the ratio of 260/280. An A260p/A280 ratio of between 1.8 and 2.0 indicates that the nucleic acid is generally free from protein contamination.

Alternately, total RNA was extracted using the RNeasy® Plant Mini Kit (QIAGEN Sample and Assay Technologies Cat. No. 74903) following the manufacturer's instructions. Approximately 100 mg of fresh plant materials were pulverised in liquid nitrogen using a pre-chilled pestle and mortar; 450µl Buffer RLT was then added to the powdered frozen samples, which were transferred to the lysate in a QIA shredder spin column (lilac) and centrifuged for 2 minutes at 13,000 rpm. The supernatant of the flow-through was then transferred to a new microfuge tube and 200µL of 75% ethanol was added and mixed immediately by pipetting. The samples were transferred to an RNeasy mini spin column (pink) and centrifuged at 13,000 rpm for 15 seconds. The flow-through was discarded and 700 µl Buffer RW1 was added to the RNeasy spin column. The samples were centrifuged at 13,000 rpm for 15 seconds, the flow-through was discarded and 500µl Buffer RPE was added to the RNeasy spin column. The samples were centrifuged at 13,000 rpm for 15 seconds, the flow-through was discarded and 500 µl was added to the RNeasy spin column. The samples were again centrifuged at 10,000 rpm for 2 minutes and the flow-through was discarded. The RNeasy spin column was then placed in a new 1.5 ml collection tube. Next, 50µl RNase-free water was added directly to the spin column membrane. The samples were centrifuged at 10,000 rpm for 1 minute to elute the RNA, and samples were then stored at -80°C until required.

2.4.3 RNA Treatment with DNase

The RNA samples were treated with RNAase-free DNase to remove DNA (DNAfree, Ambion® ThermoFischer; Cat. No. AM1907) according to the manufacturer's instructions. Approximately 5 µg of RNA was incubated with 4 units of DNase I and 1 x DNase buffer at 37°C for 1 hour. The reaction was stopped by the addition of DNase inactivation reagent to the reaction mix. The samples were incubated for 5 minutes at room temperature and centrifuged at 12,000 Rpm at room temperature and the pellets discarded. Samples were then stored at -80°C until required.

2.4.4 cDNA Synthesis

Two micrograms of total RNA were used with a High Capacity Reverse Transcription Kit (Catalogue number: 4368814; Applied Biosystems, USA) following the manufacturer's instructions. A single 20 μ I RT-PCR reaction was performed for each RNA sample using GoTaq® G2 Colourless Master Mix and DNA polymerase according to the manufacturer's instructions (Invitrogen). The thermal cycler conditions used were 25°C for 10 minutes, 37°C for 2 hours, and 85°C for 5 minutes. This method generates cDNA using random primers. The cDNA samples were subsequently diluted tenfold and stored at -80°C.

2.4.5 PCR Primers

PCR primers were designed for each of the genes of interest after alignment of all the available DNA sequences deposited in the public gene banks using CLUSTALW (Love, Huber & Anders, 2014). PCR primers were designed to the Consensus Coding Sequence of the gene of interest using the CLC Genomics Workbench version 7 package (v7.1) (QIAGEN Bioinformatics). All the primers were supplied by Eurofin MWG Operon. The working concentration of the primers was then prepared by diluting 10 μ l of stock into 90 μ l of sterile dH₂O. The primers and their annealing temperature used in this study are listed in Table 2.1 below.

Table 2.1: Details of PCR for Barley Sequences Studied

Gene	Primers	Annealing Temp (°C)	Estimated Size gDNA Template	Estimated Size cDNA Template
<i>HvACTIN</i>	For 5' GCC GTG CTT TCC CTC TAT G	58	620b p	235bp
	Rev 5' CAG GTC CAT CTC CCC TTA			
<i>HvCBF10A</i>	For 5' CCT CTT CCA ACG AGA ACG CGT C	58,56,54	659bp	659bp
	Rev 5' CCC GAA TTC TCC GTT ATC C			
<i>HvCBF15A</i>	For 5' GCC GTC GTT GTC CTC TCA	59,57,55	642bp	642bp
	Rev 5' CCA TCG GTA TCC CAG CAC			

<i>HvCBF 6</i>	For 5'	AAC TAC TAC TAC TCG CCC TC	61	560bp	560bp
	Rev 5'	TAA AGG TCC CAT CCC ATG C			
<i>HvCBF2C</i>	For 5'	GGG GGC AAG AGT ACA GGA	58	479bp	479
	Rev 5'	GGT GGG AAC GAT GGA GAG			
<i>HvCBF9</i>	For 5'	CAG CGG AGG CAG ATT ATT	55	282bp	282bp
	Rev 5'	GCC TGA AGA CAT GTA GAA CT			
<i>HvCBF4B</i>	For 5'	ATG GAC GTC GCC GAC ATC GC	64,60,56	498bp	498bp
	Rev 5'	GCC GGA CGA GAT GTA AAA C			
<i>HvCBF14</i>	For 5'	CAC CGC TAA GGA GAT CAA G	58	235bp	235bp
	Rev 5'	CGA CTC TAT GAA CAT GCC C			
<i>HvCBF16</i>	For 5'	CTC AAC TTC CCC GAC TCC	58	279bp	279bp
	Rev 5'	CAG GTC CAT CTC CCC AGA			
<i>HvCBF3</i>	For 5'	CCT CAA CTT CGC CGA TTC	54	294bp	294bp
	Rev 5'	GGG AAC AAG TCA AGC CTG			
<i>HvCBF12C</i>	For 5'	TCA GCT CCC CTT CCT CAT CTA	56,53,50	314bp	314bp
	Rev 5'	GGA GTC CGG AAA GTT GAG			
<i>HvCBF6B</i>	For 5'	CAA GAA GGT CAA CCA GAC G	58	362bp	362bp
	Rev 5'	GCG CTG AAG GGT TAG ATG TTA			
<i>HvDHN5</i>	For 5'	AGA AGG GCG TCA TGG AAA A	60,57,54	271bp	271bp
	Rev 5'	CCG TAG GTC TCA GTG GTA T			
<i>HvCOR 14b</i>	For 5'	CTT CTT CTT CCG TGC TGC	62,60,58	528bp	424bp
	Rev 5'	CAT TTG CTG ACA TCC TCA AC			
<i>HvCO 1</i>	For 5'	GCA AAA GGA GTA CGT AGA G	55,53,50	1302bp	289bp
	Rev 5'	GAA GTG GTG TCT GAA GTG			
<i>HvVRN1</i>	For 5'	TAT GAG CGC TAC TCT TAT GC	57,55,53	1374bp	257bp
	Rev 5'	TGA AGC TCA GAA ATG GAT TCG			
<i>HvVRN2</i>	For 5'	CAT CAT CAC CAT CAT CAG	55,52,50	1455bp	444bp
	Rev 5'	GGA CTC GTA GCG GAT TTG			
<i>HvVRN3</i>	For 5'	GAA CCA CCA ACC TCA GG	57,55,52	960bp	427bp
	Rev 5'	CGC TGG CAG TTG AAG TA			

Annealing temperatures were determined empirically using gDNA from barley cultivars Belgravia (spring) and California (winter). Temperature programs were run (50°C – 62°C) at 2°C intervals to establish the optimum annealing temperature. Where single amplicons could not be generated, touchdown PCR was used and the corresponding three temperatures indicated (3, 3, and 30 cycles). Estimates of the expected amplicon size for each fragment using gDNA and cDNA template were determined using the *cv Morex* reference genome (Consortium, 2012).

2.5 Cloning PCR Fragment for Sequence Analysis

HvACTIN primers were designed for the use of a standard control; all primers were used to amplify the gene of interest for cloning and sequencing purposes. Annealing temperature was supplied with the primers; however, PCR temperature profiles were used to give an accurate temperature. 'TD' indicates that the touch-down PCR program was used to avoid nonspecific binding. The ideal PCR primers, which are oligonucleotides, are typically between 18–30 nucleotide base pairs in length (see Table 2.1).

2.5.1 PCR Amplification

The PCR reaction consisted of 10 µl of GoTaq DNA polymerase (Promega, USA M300), 0.5µl of each of the forward and reverse primers (FP and RP), 1–2ng of DNA/cDNA template and dH₂O combined to make a final volume of 25 µl. The PCR conditions were an initial denaturing at 95°C for 2 minutes, followed by 30 cycles of amplification at 94°C for 30 seconds, annealing for 60 seconds (temperature dependant on primer temperature), an extension at 72°C for 60 seconds, then a final extension at 72°C for 5 minutes.

Temperature profile experiments were conducted for each amplified gene sequence to empirically determine an optimal annealing temperature. This involved running a temperature profile in 2°C steps from 6°C below to 6°C above the provided annealing temperature. The resulting products were run on agarose gels and the fragment size and purity of product assessed. Once an appropriate annealing temperature was established, appropriate controls were run (genomic template (gDNA), FP only, RP only, FP + RP) to confirm that the authentic amplicon was generated.

2.5.2 Purification of PCR Amplicon with Qi A Quick Gel Extraction Kit

To isolate the amplified fragment of DNA from the agarose gel, the QIAquick Gel Extraction Kit (Qiagen Cat no. 28704) was used, following the manufacturer's protocol. A 25 µl PCR reaction was set up, comprising 10µl GoTaq Colourless Master Mix, 1 µl of each FP and RP

and 2,3 μl templates and dH_2O combined to make a final volume of 25 μl , and a PCR was run. The PCR products were then resolved in a 1.5% agarose gel electrophoresis and then visualised under UV. Bands of the correct size were excised from the gel using a clean sharp scalpel and purified using the QIAquick Gel Extraction Kit.

2.5.3 Cloning of Amplicons into TOPO 2.1 Vector

In the next step, 4 μl purified PCR fragment was added to 1 μl salt solution and 1 μl TOPO vector 2.1 (Invitrogen, TOPO (pCR2.1) in a TA cloning kit according to the manufacturer's instructions. The reaction was mixed gently and incubated for 5 minutes at room temperature (RT). Then, 6 μl of the TOPO cloning reaction was added to 100 μl freshly thawed competent *Escherichia coli* DH5 α cells and mixed gently (gently pipetted up and down). The sample was then incubated on ice for 20 minutes, and afterwards heat shocked at 42°C for 30 seconds in a water bath. The tubes were then transferred onto ice for 2 minutes, and 250 μl SOC (super optimal with catabolic repressor) medium (RT) added. The Eppendorf tubes were shaken horizontally at 37°C, 200 rpm for 1 hour. A tenfold serial dilution of the cells was prepared to X10, 000 and 100 μl of each dilution plated on selection plates (L-broth (LB) 50 $\mu\text{g}/\text{ml}$ kanamycin). The plates were sealed with Parafilm and incubated at 37°C overnight.

2.5.4 Colony PCR

For the colony PCR reaction, approximately half of a single colony was scraped off from a plate with a sterile pipette in a laminar flow hood using a sterile P20 tip, and placed in 20 μl sterile dH_2O for 5 minutes. Then, 5 μl of the sample was streaked onto a fresh agar plate (LB 50 $\mu\text{g}/\text{ml}$ kanamycin), the plate was sealed with Parafilm and incubated at 37°C overnight. The cells were suspended by mixing up and down; this was then used as the template to conduct PCR. Next, 20 μl PCR reaction mix was made, comprising 10 μl GoTaq Master Mix, 0.5 μl of each primer, and 9 μl of suspended cells, and PCR was run. Overnight cultures were set up for colonies with the expected right band size. Half of the colonies that remained were dabbed using a sterile P20 tip in 5 ml LB containing 50 $\mu\text{g}/\text{ml}$ kanamycin.

2.5.5 Purification of Plasmid from *E. coli*

Plasmid was extracted from overnight bacterial cultures using Promega Wizard plus PureYield Plasmid Minipreps DNA Purification System (Cat no. A1330) as per the manufacturer's protocol. For long-term storage of plasmids, glycerol stocks were prepared by adding 8ml of plasmid culture to 50% glycerol, flash freezing in liquid nitrogen and storing at -80°C. All plasmid cultures were sent to Eurofins Genomics for sequencing.

2.5.6 Quantification of DNA and RNA

Nucleic acid concentration in samples was estimated using nano-drop (NanoPhotometer, Pearl, Imlen). A 2 µL aliquot volume of the sample was calibrated against a water blank and the absorbance measured at 230 nm, 260 nm and 280 nm. According to Sambrook and Russell (2001), the concentration was obtained by measuring absorbance at 260 nm, where an absorbance of 1 means 50 µg/mL of DNA and 38 µg/mL of RNA. The purity of the samples was measured using the ratio of 260/280. The DNA was stored at -20°C until required. Then, 5 µl of the sample was used as a template to conduct PCR to confirm the presence of insert (see Table 4.1 in Chapter 4).

2.5.7 Agarose Gel Electrophoresis of gDNA and cDNA

Gel electrophoresis of gDNA and cDNA fragments were performed using 1% and 1.5% agarose, respectively, and 0.5X TBE buffer diluted from 5X TBE buffer (Tris-borate-EDTA) following the standard protocol (40 mM Tris-acetate, 1 mM EDTA, 54 g boric acid, pH 8.0). Then, 10 µl SYBR Safe Gel Stain (Invitrogen, Paisley, UK) was added to the gel and mixed thoroughly for staining. All the gels for gDNA and cDNA were run in TBE buffer at 100 V for approximately 20 minutes, gDNA and cDNA samples were loaded alongside a molecular weight marker (1kb DNA Ladder, Promega, Southampton, United Kingdom), separated by electrophoresis and visualised by UV illumination.

2.5.8 Agarose Gel Electrophoresis of RNA

Where required, integrity of RNA was checked using agarose gel electrophoresis: 1 µg of RNA (see Section 2.4.2.) was separated on a 1.5 (w/v) agarose gel containing 10% formaldehyde and 1 x MOPS buffer, pH 7.0 (20 mM MOPS, 5 mM sodium acetate, 1 mM EDTA (Sambrook & Russell, 2001)). Before loading, the RNA was mixed with 1% (v/v) formaldehyde, 30 % (v/v) formamide, 1 x MOPS pH8.0, and 0.1 volumes of ethidium bromide as a staining agent. RNA mixtures were heated at 65 °C for 10 minutes, cooled on ice, then mixed with 0.2 volumes of loading dye (Promega UK, Ltd., Southampton, United Kingdom) then loaded on the MOPS gel. Electrophoresis was performed in 1 x MOPS buffer pH 7.0 for 2 hours at 100 V and visualised by UV illumination. RNA integrity was assessed by the presence of defined bands.

2.5.9 DNA Sequencing

For the DNA sequencing, 15 µl of confirmed DNA (plasmid) with a concentration of 50–100ng/µl was sent for sequencing to MWG-Eurofins (see Table 4.1, in Chapter 4). The determined fragment sequence was then used to interrogate the barley databases in the public domain using BLASTn hosted at the NCBI.

2.6 RNA Sequencing

Total RNA was purified using the Qiagen RNeasy Plant Mini Prep Kit (Cat no. 74904) and was sent for RNA-seq analysis at the Glasgow Polyomics Facility, University of Glasgow. Paired-end reads were performed on approximately 35 million cDNA sequences generated from each of three biological replicates of samples prepared from the different cold-acclimation condition times and abscisic acid applications. A quality control check was first performed on each of the RNA samples using Biorad Bioanalyses to determine the extent of degradation and the associated RIN (RNA integrity number). In all cases, analysis was performed only if RINs of over 7.5 (out of a possible 10) were achieved. Reads were performed on an Illumina 500 instrument.

2.7 Statistical Analysis

2.7.1 General Statistics

Data were analysed using the SPSS Statistics package (IBM). The Analysis of Variance General Linear Model (GLIM) was used in most cases and, where appropriate, data Log₁₀ or square root transformations were applied to ensure the data sets conformed to a normal distribution. Differences between levels of experimental factors were assessed using Tukey's *a posteriori* tests. In some cases where the explanatory variables were continuous, regression lines were fitted using the GLIM Covariance routine.

The five-parameter logistic model that was fitted to the electrolyte leakage curves (see Section 2.3 and Chapter 3) was solved using the Solver iterative routine in Microsoft Excel. The model was written to minimise the errors of fit and took the following form:

$$\% \text{ Cell Lysis} = \text{Min} + \frac{\text{Max} - \text{Min}}{\left[1 + \left(\frac{\text{Temp}}{\text{LT}_{50}} \right)^{\text{Slope}} \right]^{\text{Sym}}}$$

Min = Minimum leakage (%)
Max = Maximum leakage (100%)
Temp = Temperature
*LT*₅₀ = Empirically determined temperature causing 50% leakage
Slope = Slope factor (Hill factor)
Sym = Symmetry factor

2.7.2 Analysis of Transcriptome Data Sets

The RNA-seq experiments described in this thesis generated experimental data sets with a relatively low number of replicates (n=3), each containing a large number of elements (circa 30,000 sequences) scored with one of two outcomes (significant change from controls, or not). The statistical problem was to establish whether any sequence identified as 'significantly different from controls' in one experimental treatment (averaged across the n=3 replicates), and also identified as such in a second experimental treatment, was genuinely co-regulated by the treatment or was the result of random changes in transcript abundance.

There are potentially several legitimate ways to determine the probability of random coincidence, but in this study two independent methods were used. One calculates the probability of obtaining x successes (significantly different from controls) in a sample of n genes from a total population of N genes which contains k successes using the appropriate probability (hypergeometric) distribution. The other uses set theory to estimate probabilities from which standard deviations and limits can be calculated.

2.7.2.1 Calculation of the Hypergeometric Probability Mass Function

Consider an experiment where the transcript abundances of two treatments ($T1$ and $T2$) are compared with a control (CI). A contrast of the difference in transcript abundance between CI and $T1$, and CI and $T2$, generates two data sets. The total number of genes in the experimental population is identical, say $N= 30,000$ genes. Assume that in the first contrast (CI vs. $T1$) $k = 50$ genes were identified in N as significantly different from controls (i.e., k successes in N), but these were the result of random effects. The probability of identifying one of these genes (a success) in a second contrast (trial) is k/N (or $p= 50/30,000 = 0.00166r$). If, in a second contrast (CI vs. $T2$) $n = 40$ genes are identified as significantly different from controls, the probability that $x = 20$ of these were also in the set k is given by the hypergeometric probability mass function (PMF), as follows:

$$h(x, N, n, k) = [{}_k C_x] \cdot [{}_{N-k} C_{n-x}] \div [{}_N C_n]$$

Equation 2.1

Where:

N = number of items in population = 30,000
 n = number of items in sample = 40
 k = number successes in $N = 50$
 x = number of successes in sample = 20
 $[C]$ indicates the number of combinations given by the subscripts.

Microsoft Excel provides a function (HypGeo) for calculating hypergeometric function probabilities. Feeding the values above into the function generates a probability of $p \leq 4.47 \cdot 10^{-47}$ and the conclusion is that it is highly unlikely the 20 sequences in the intersection of

the two data sets (*CI* vs. *T1*) and (*CI* vs. *T2*) (i.e., common to both sets) have arisen by random effects on transcript abundance; these are most likely to have arisen because treatments *T1* and *T2* have induced all or most of them.

2.7.2.2 Calculation of Probabilities from Set Theory

From the example used above, the probability of randomly drawing one of the k successes from the total population is $k/N = 0.00166r$. Similarly, the probability of drawing one of the n successes is $n/N = 0.00133r$. From set theory, the probability of drawing at random an element (gene) that appears in both a set of randomly selected genes (set $|A|$) when it was previously randomly selected in set $|B|$ is given as the conditional probability:

$p = [|B| \mid |A|]$; that is, the probability the element will be in $|B|$ given that it was already present in $|A|$:

$$p = \frac{p|A| * p|B|}{p|A|}$$

Equation 2.2

If n individuals are drawn from N without replacement, the expected number of successes x is given as:

$$Ex = n * p$$

Equation 2.3

And the standard deviation is given as:

$$St\ Dev = \sqrt{\frac{k * n}{N^2(N - 1)} (N - k)(N - n)}$$

Equation 2.4

Given the observed number of successes (x) and the expected number of successes (Ex), and the standard deviation, the number of standard deviations between x and Ex can be calculated and visualised on a graph. Figure 2.2 presents a plot showing the associated hypergeometric

distribution, x , and Ex . When the number of observations is large (>30), and the $x-Ex$ difference of 1.70, 2.46, and 3.38 standard deviations (one-tail test) is normally taken probabilities of <0.05 , <0.01 , <0.001 .

2.7.2.3 Set Theory Manipulations

Sets are defined as collections of elements (here, barley sequences) that form part of a universe of all possible elements (barley sequences). Sets are normally given the notation $|A|$ or $\{A\}$. The complement of set $|A|$ is the set of elements that are in the defined universe ($|U|$) but not in $|A|$, and is written $|U| \setminus |A|$; hence, $|A| + [|U| \setminus |A|] = |U|$. Similarly, the relative complement of sets $|A|$ and $|B|$, written $|A| \setminus |B|$, will be the set of elements that are in $|A|$ but not in $|B|$. The intersection of sets $|A|$ and $|B|$, written $|A| \cap |B|$ is the set of elements that are in both $|A|$ and $|B|$, i.e., those that are common to both sets. The union of $|A|$ and $|B|$, written as $|A| \cup |B|$, is a set that contains all of the elements that are in $|A|$ or in $|B|$. The conditional probability of two sets, written $[|B| \mid |A|]$, is the probability of an element appearing in $|B|$ given that it has already appeared in $|A|$ (see Equation 2.2); note, $|B| \mid |A| \neq |A| \mid |B|$. These set manipulations can be easily viewed using Euler (or Venn) diagrams

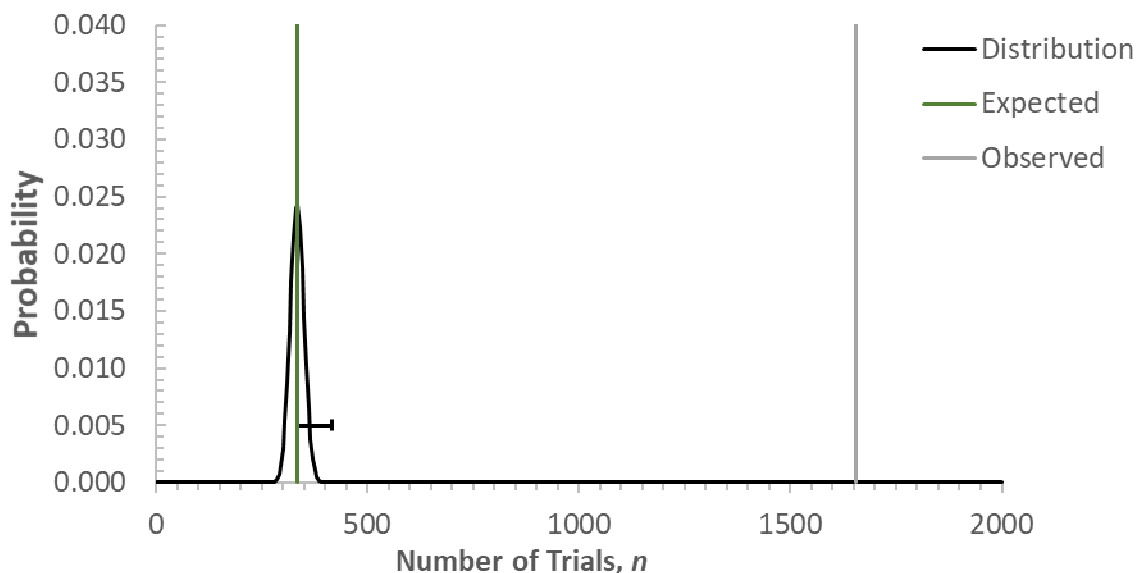
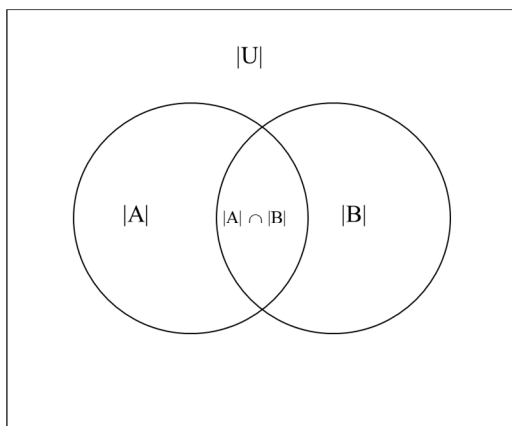


Figure 2.2: The Observed and Expected Number of Sequences Calculated from Set Theory.

The observed and calculated number of successes (genes) appearing in the intersections of sets $|A|$ and $|B|$. The expected value, Ex , was calculated from the conditional probability $p = [|B| / |A|]$; the blue line is the hypergeometric distribution calculated from the data presented in Section 5.3 (0 v 1 week and 0 v 2 week). In that experiment, $N = 30,339$; $k = 3693$; $n = 2739$; $x = 1654$. Here, $(x - Ex) / \text{St Dev} = 19.9$, and the probability that these genes randomly appeared in both sets is $\ll 0.001$. The horizontal error bar shows five standard deviations ($p < 0.001$) from the expected value.



- $|U|$ = Set of all element in the defined Universe (box); here the full set of barley genes $\approx 39,000$
- $|A| \cap |B|$ = Intersection of $|A|$ and $|B|$; set of all elements in $|A|$ and $|B|$
- $|U| \setminus |A|$ = Complement of $|U|$ and $|A|$; set of all elements in $|U|$ that are not in $|A|$
- $|A| \setminus |B|$ = Relative Complement of $|A|$ and $|B|$; set of all elements in $|A|$ that are not in $|B|$
- $|A| \cup |B|$ = Union of $|A|$ and $|B|$; set of all elements that are in either $|A|$ or $|B|$
- $|A| | |B|$ = Conditional Probability; probability of an element appearing in $|A|$ given that it has already appeared in $|B|$.

Figure 2.3: Explanation of Set Theory Manipulations Used in This Study.
See text for further details.

Chapter 3 The Effect of Photoperiod and Temperature on the Induction of Cold Acclimation in Cereals

3.1 Introduction

Freezing injury is an economically important abiotic factor that limits the yields and range of arable crops. The majority of harvests that have financial significance are susceptible to drops in temperature below 10°C (Ohnishi et al., 2010). An example is crops of the *poaceae* family, which have significant yields and thus high financial importance, notably wheat (*Triticum aestivum* L.), barley (*Hordeum vulgare* L.), and rye (*Secale cereale* L.). The yields from these crops account for approximately one third of the overall global yield of grains. Thus, improving the durability of these harvests against freezing injury has been the focus of many breeding programmes in areas frequently exposed to particularly hard winters. Temperate cereals can adapt to tolerate frosty conditions (Ohnishi et al., 2010), however, genotypic variations exist within each species with respect to their tolerance of freezing temperatures (Limin & Fowler, 2002).

Plants use environmental signals to sense or detect changes in the seasons. Transition from warm to cool seasons can result in the activation of mechanisms that initiate cold acclimation. Two of the key environmental signals in autumn are decreases in temperature and reduction in the length of photoperiod (Welling, 2004). The process of cold acclimation in perennial plants (Weiser, 1970; Welling et al., 2002; Puhakainen et al., 2004) and in herbaceous plants (Lee et al., 2012; Fowler et al., 2001) develops in a sequential manner in response to changes in photoperiod and temperature. These studies show that deep cold acclimation occurs when plants are exposed to both cool temperature and a decreasing photoperiod (i.e., increased night length). Dalmannsdottir et al. (2016) showed that changes in the regular pattern of photoperiod and temperature in autumn could delay the process of cold acclimation. Bertrand et al. (2017) studied the effect of photoperiod prior to cold acclimation in alfalfa (*Medicago sativa* L.), and showed that the length of photoperiod prior to initiating cold acclimation had an effect on freezing tolerance. Specifically, it was observed that the length of period affected the level of cryoprotective sugars (sucrose and raffinose-family oligosaccharides) that are believed to play a cryoprotective role, and that

short photoperiods lead to an induction of gene coding for the enzymes involved in their synthesis.

It is known that the biochemical and physiological states of plants are affected by changes in photoperiod, and that cold-acclimated plants are more resistant to photoinhibition and have an increased rate of photosynthesis (Oquist & Huner, 1993). Reduction in photoperiod results in the depletion of particular sugars, such as sucrose in *Arabidopsis* (Gibon et al., 2009) and poplar (Hoffman et al., 2010). This is believed to exert a downstream effect on the plant's ability to initiate and sustain cold acclimation, since sugars have been implicated in the response of plants to development of cold tolerance and survival of freezing temperatures.

The mechanism by which light affects cold acclimation response in plants have been of interest to researchers for several decades. For instance, Williams et al. (1972) showed that exposure of the woody plants *Cornus* and *Weigela* to brief pulses of red light during a dark period leads to suppression of cold acclimation, an effect that can be reversed by consequent exposure to far red light. It was also shown by McKenzie et al (1974) that exposure to far red light at dusk promotes cold acclimation in red osier dogwood (*Cornus stolonifera*). These early studies provided evidence of a strong correlation between Photoperiod sensed by Phytochrome and cold acclimation.

Detailed discussions on the relationship between temperature and photoperiod in the development of the cold response in plants have been provided in recent review papers (Maibam et al., 2013; Kurepin et al., 2013; Lorenzo et al., 2016). Based on the findings of these studies, there appears to be a clear justification for further investigation into how photoperiod length and temperature interact in determining cold acclimation and survival of winter damage in plants. While such a correlation has been shown in perennial and some herbaceous plants, the combination of these two factors has not been examined fully in barley. It is reported that a combination of high light treatment and low temperatures, but not temperature alone, leads to the accumulation of COR14b (a marker for CA) transcripts in barley (Crosatti et al., 1999; Rapacz et al., 2008), although the precise role of this protein is still unknown. These studies additionally provide evidence of an interdependent effect of photoperiod and temperature on cold acclimation in plants, including cereal crops.

3.2 Research Objectives

The main objectives for the work described in this chapter were to evaluate the cold-hardiness of spring (*cv.* Belgravia) and winter (*cv.* California) barley, and two cultivars of rye (Forage and Kapitan). Experiments were designed to assess the roles of photoperiod, non-freezing low night temperatures, and length of the cold acclimation period on conferring freezing tolerance upon these cultivars. To achieve this, a reliable and sensitive method should be used to assess frost damage, but this requires a resolution of better than $\pm 1^\circ\text{C}$. The electrolyte leakage method, which has been widely used to assess frost tolerance (cell lysis) in plants (Maier et al., 1994), has the potential to achieve this resolution, but a review of the literature where this method has been used revealed that this level of precision is rarely achieved. It was necessary, therefore, to refine and develop this method to achieve the required level of sensitivity.

3.3 Methods for Measurement of Freezing Tolerance in Plants

Winter cereal cultivars do not all have the same ability to withstand the extreme temperatures of winter. Winter survival data collected from field trials (Fowler et al., 2014) shows that there is often complete winterkill of some cultivars, while others survive the winter undamaged. These observations demonstrate that cultivar differences in winter survival potential can be significant (Fowler & Thomashow, 2002). Survival data from field trials that involved different levels of winter stress has been used to produce a comparative measure of cultivar winter-hardiness potential; this measure is known as the cultivar's Field Survival Index (FSI) (Fowler et al., 1981; 2002).

In experiments set up under controlled conditions in laboratories, other forms of assessment are used. One of the methods to assess freezing damage is estimating the electrolyte leakage from cells using conductivity measurements (Sukumaran & Weiser, 1972; Hawkins et al., 2002; Zhang & Willison, 1987). The data is expressed as an LT_{50} value, which represents the temperature at which 50% of the cells have lysed to cause electrolyte leakage; this can be expressed as a percentage between 0% (representing no damaged cells) and 100% (representing complete cell lysis, obtained by freezing samples to -196°C for an hour). Samples, usually leaf discs, are exposed to a range of freezing temperatures to induce damage, and the temperature at which 50% of the cells have lysed (LT_{50}) is used as a measure

of cold tolerance. Determinations of these values are generally carried out in a laboratory as an alternative to FSI assessments, which are more time-consuming as they generally require multiple-year studies (Fowler et al., 2014).

The underlying principle of the electrolyte leakage method relates to the intactness of the cell membrane; much of the frost damage to plants arises from ice crystal penetration from the apoplast across the plasma membrane into the cell, and from expansion-induced lysis which occurs on thawing (Steponkus, 1984). If tissues are suspended in a small volume of de-ionised water during the freezing process, a resulting rise in electrical conductivity proportional to the fraction of lysed cells can be observed.

3.4 Assessment of Frost Tolerance (LT₅₀) in Rye and Barley to Establish Conditions for Cold Acclimation Experiments

To assess frost tolerance, plants were grown in soil (see Section 2.1.1) for 3 weeks post-germination and exposed to different regimes of photoperiod and night temperatures for up to 4 weeks (see Section 2.1.2). Plants were then exposed to one night of freezing conditions (0°C to -30°C), and damage to mature leaves was assessed (see Section 2.1.2). Winter and spring cultivars of barley, and the two cultivars of rye, were used for the experiments. As an example, Figure 3.1 shows the effects of cold exposure for one night on non-acclimated rye (*Secale cereale*) cv. Kapitan. The results showed that exposure to a single night with temperatures of -4°C led to some minor damage, however, the plants did survive. When the temperature was further decreased to -7°C, all plants died.

Based on the frost sensitivity of rye, the cold acclimation regime outlined in Figure 3.2 was designed. Four regimes were used in combination, with two photoperiods (Long Day, LD; Short Day, SD), and two non-freezing night temperatures (Warm Temperature, WT; Low Temperature, LT). All plants were grown in the WT regime for 3 weeks, prior to one of the four Cold Acclimation (CA) regimes being imposed for up to a further 4 weeks, as described in Section 2.1.2 (see also Fig. 3.2).

Some justification of the experimental CA regimes described in Figure 3.2 is required. In an experimental setting, cold acclimation is most typically induced through constant day/night temperatures in the range of +2° to +4°C (e.g., Gusta et al., 2013). The rationale for this is that the interpretation of results will be easier; control plants are grown at a

constant temperature of +15°C to +20°C and this compares with CA plants grown at +2°C to +4°C. Whilst this procedure undoubtedly induces a measure of cold acclimation, it is unclear whether it produces full cold acclimation. Cool night temperatures of 4°C should trigger changes at the transcriptional level, but with cool day temperatures it is possible that the full effects of these are not realised at the translational and post-translational level.

The effects of temperature during the developmental stages of cereals is of great interest to agronomists and farmers who wish to predict crop yields. One of the important predictors of yield is the number of growing degree days (GDDs); GDDs can be calculated as follows:

$$\mathbf{GDDs = \sum_1^n \mathbf{Average\ Daily\ Temperature} - \mathbf{Baseline\ Temperature}}$$

Where n is the number of days (or hours) of growth. The baseline temperature (T_b) is cultivar- and process-specific and is the temperature at which a particular physiological process ceases. For temperate cereals growing at high latitudes, T_b values ranging from 1.5° to 6.5°C are used, but 4.5° to 5.5°C is normally used for spring cereals (Sharratt, 1999; Bongard et al., 2018; OMAFRA, 2017). For the experiments described in this chapter, plants were grown for up to 7 weeks (49 days). If a constant temperature CA regime of +2° is used, this would produce a GDD of approximately 25 (49*(2-1.5)) for the lower T_b value and 0 for the upper T_b value. If a constant CA temperature of +4°C is used, the GDDs would be 125 and 0, respectively. In all cases, the development of barley would cease in these conditions, as a GDD of at least 250 is required to reach the five-leaf (7-week) stage (OMAFRA, 2017). Conducting experiments on plants that have had their normal pattern of autumn or spring development curtailed could generate results that contain artefacts and, for this reason, the more natural CA regime was adopted. Calculation of the GDDs for 7-week old plants in the four regimes indicated that all regimes would generate values of more than 403 at the 7-week stage (Fig. 3.3), giving some confidence that the experiments would not be a physiological and would be likely to have some real meaning.

In North America and northern Europe, autumn and spring days have average day/night temperatures of circa +16°C / +4°C (UK Met. Office, 2019) and a photoperiod of approximately 9 hours. It was decided, therefore, to use the photoperiod and temperature regime presented in Figure 3.2 to trigger CA in the experimental plants.

It is not clear why the growth of cereal crops electively ceases when temperatures drop below the T_b . Transcription, translation, and post-translational processes in plants are subject to thermodynamic control and will be severely limited at $+2^{\circ}\text{C}$ to $+4^{\circ}\text{C}$. It is conceivable that some of the proteins essential for full cold acclimation do not accumulate to a sufficient level and, hence, only partial cold acclimation is established. A good example to help illustrate this point is the promoter of flowering in higher plants, *CONSTANS*. The continual synthesis and breakdown of the *CONSTANS* protein occurs in leaf tissue and these temperature-dependent processes are regulated by photoperiod. If the accumulation of a critical factor involved in CA was also dependent on a balance in the rates of synthesis and degradation, the protein might not accumulate to the threshold level at constant low temperatures.

The data generated from the CA regimes outlined in Figure 3.2 will be more complex than that produced from experiments where constant day/night temperatures are used and where simple comparisons where only one variable changes are made. For example, differences that arise from comparisons between plants exposed to the same photoperiod (LD/WT with LD/LT, and SD/WT with SD/LT) can be attributed to the effects of night temperatures alone, as this is the only variable in the experimental treatment (Fig. 3.2). In contrast, observed changes between plants with the same night temperature but different night periods (LD/WT with SD/WT and LD/LT with SD/LT) are more complex and cannot be directly attributed to photoperiod alone. In these cases, the duration of exposure to night temperature also changes (15h vs. 8h); differences may arise as a result of changes triggered by the photoperiod-sensing or temperature-sensing pathways. Chapter 5 presents whole genome expression profile data from plants exposed to these experimental regimes, and methods involving set theory are presented to separate the effects of these two factors (see Section 5.2.6).



Figure 3.1: Survival of Non-Acclimated Rye (*Secale cereale*) cv. Kapitan Exposed to One Night of Freezing Temperatures.

Experimental plants were germinated and grown as described in the Materials and Methods chapter (Section 2.1.1) at the 3-weeks post-emergence stage. The plants were grown in Long Day/Warm Temperature conditions (LD/WT; 8h nights at 16°C) from emergence to the 3-week stage. The non-acclimated plants were then exposed to a single night at the temperatures indicated, and then allowed to remain under LD/WT conditions for a week to recover.

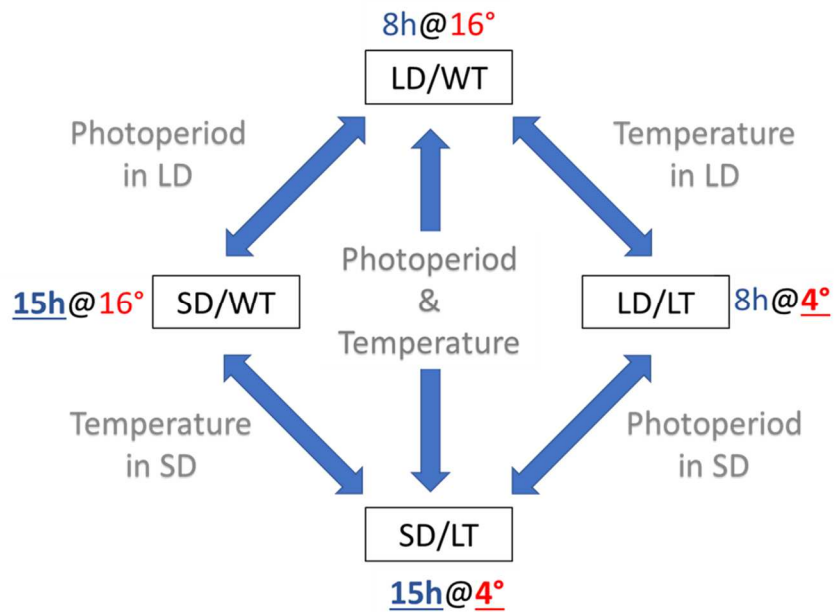


Figure 3.2: Cold Acclimation Regimes for Barley and Rye.

Experimental plants (barley and rye) were germinated and grown as described in Materials and Methods (Section 2.1.1). Three weeks later, the plants were exposed to different light and temperature regimes, as indicated above (Section 2.1.1). Plants were initially grown for 3 weeks under Long Days and Warm Temperatures (LD/WT, 8h nights at 16°C), and then either left in the same conditions or exposed to a combination of Short Days (15h nights) and Low Temperatures (+4°C nights) for up to a further 4 weeks to acclimate to the cold. The diagram highlights the contrasts between the expected data sets. Night length (rather than day length) is presented in blue (8h or 16h) and night temperature in red (+16°C or +4°C); CA-inducing conditions are in bold and underlined.

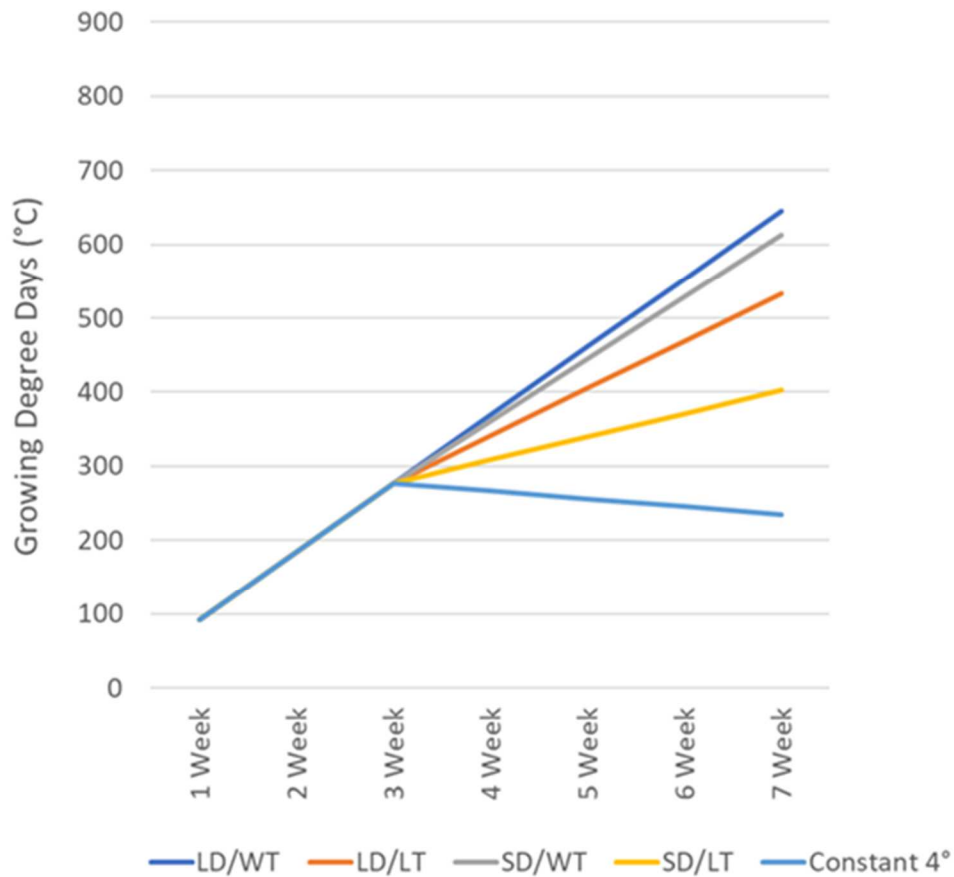


Figure 3.3: Calculated GDD for Cold-Acclimated Barley Plants.

The number of GDDs was calculated as described in the text. Calculations were based on growth for 3 weeks in a 16h photoperiod with a 20°C /16°C day/night temperature followed by a further 4 weeks under one of the four indicated cold-acclimation regimes (see Fig. 3.2 for details). In addition, a calculation was included for plants exposed to a constant 4°C day/night temperature; the graph clearly indicates that no growth would occur after the initial 3-week germination, an abnormal developmental pattern. GDD was calculated using a base temperature of 5.5°C. It is important to recognise that GDD can be expressed in units of temperature or time (here °C). Although its name implies it is a measure of the number of days, in fact, GDD is a summation of the time plants are exposed to growth-promoting temperatures.

3.5 Development of a Reproducible Method for Assessing Frost Damage

Careful examination of the literature and the results from Figure 3.1 indicated, at an early stage of the project, that there was a need to develop methods for assessing the effects of photoperiod and night temperatures on frost tolerance within an accuracy of less than ± 1 °C. One quantitative method that has been routinely used is the LT_{50} , the temperature that lyses 50% of the cells. LT_{50} has been used in many other studies but is not normally sensitive over a -3°C to -5°C temperature range, and so visual inspection of damage has been extensively used for screening in *Arabidopsis*. The lack of quantitative reliability is due to low levels of replication (biological and experimental) and to the use of too few freezing temperatures. Therefore, prior to assessing cold tolerance and cold acclimation in barley and rye, it was necessary to develop robust and reliable methods for assessing freezing injury.

Examination of published works where the LT_{50} method has been used showed that the method often does not meet the requirements of robustness and reliability that might be needed ($\pm 0.2^{\circ}\text{C}$ precision). Furthermore, the range of temperatures used and the variability with which percentage of cell lysis was determined does not normally allow LT_{50} to be assessed with a precision of less than $\pm 2.0^{\circ}$ to 3.0°C (e.g., Sarhadi et al., 2010; Xin & Browse, 2000; Jaglo-Ottosen et al., 1998). For these reasons, considerable effort was invested into developing a protocol based on existing methods that, with an appropriate level of replication, could estimate LT_{50} with $\pm 0.2^{\circ}\text{C}$ precision. The results of these experiments are presented in Figure 3.4. Each data point in the graph represents the average of three biological replicates (each containing five leaf discs) and their corresponding standard errors (not visible due to symbol size). Published methods routinely present standard error bars that are 5 to 15% of the average percentage of electrolyte leakage (Sarhadi et al., 2010; Xin & Browse, 2000; Jaglo-Ottosen et al., 1998). In contrast, the methods used in this study generated standard error bars that were consistently less than 1.5% of the average values. Clearly, these technical developments are a significant improvement on many of the published methods and will now allow frost injury to be assessed with a significant improvement in precision.

3.6 Quantitative Determination of Lethal Temperatures (LT₅₀)

3.6.1 Measurement of Freezing Tolerance (LT₅₀) in Rye *cv.* Forage

Figure 3.4 shows the LT₅₀ curves for Rye cultivars Forage. The graphs show the effects of 0, 1, 2, 3 and 4 weeks exposure to Short Days and Long Days. The effects of night Low Temperatures (+4°C) and SD on subsequent tolerance of a single frost event is presented. Note: by increasing the level of replication (5 leaf disks per replicate, 3 replicates per temperature point), and by using a one-degree C temperature interval over the critical LT₅₀ temperature range, the variability between replicates was reduced to less than 0.5° C; consequently, the standard error bars for % electrolyte leakage are small and obscured by the symbols (Figs 3.4 – 3.7). Complete lysis of all cells in the tissue is represented by 100% and where no damage occurs by 0%. The standard errors for each average value were small and obscured by the symbols used. A five-parameter logistic model was found to best fit the data and subsequently, a non-linear regression algorithm was used on all data sets. In most cases, the model fits the data well, but for some data sets (e.g. week 2 Panel A, Week 3 panel B), this was not the case. Regardless, it is clear that prolonged exposure to cold acclimation night temperatures of +4°C improved frost tolerance (Table 3.1). For NA Forage plants in LD (short nights) the LT₅₀ value decreased from -6.0°C to -12.2°C after 4 weeks of exposure to night temperatures of +4°C (Fig 3.4b). For plants exposed to SD (long nights) the LT₅₀ value decreased from -7.8°C to -22.2°C with increasing exposure to cool night temperatures (Fig 3.4a; Table 3.1). A fixed factor ANOVA statistical analysis was performed on these data and this showed that there was a significant ($p < 0.001$) interaction between the main factors of Photoperiod and Time of exposure to cool night temperatures indicating some CA processes were triggered by long nights, some by low night temperature, and some by a synergistic interaction between both signals (Appendix A3.1).

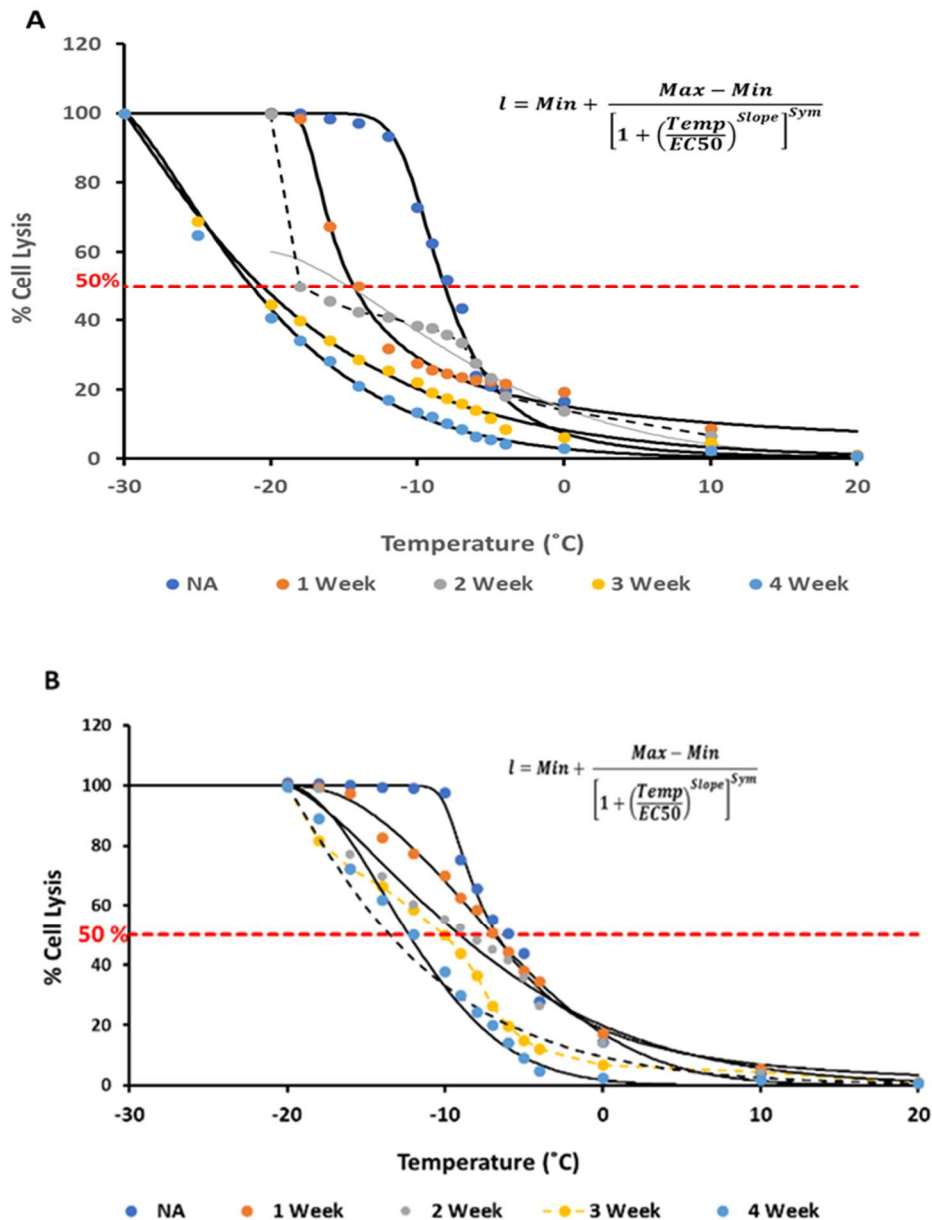


Figure 3.4: Effect of Cold Acclimation on the Freezing Tolerance (LT₅₀) of Rye Forage leaves.

Leaf discs of rye (*Secale cereale*) cv. Forage were exposed to SD and LD CA conditions (+4°C night temperatures), for up to 4 weeks, as described in Section 2.1.1. Tissue damage was estimated as the percentage solute leakage from samples held at each of the indicated temperatures for 60 minutes. The average values and standard errors of n=3 biological replicates are presented. A five-parameter logistic regression model was applied to the data. A value of 100% indicates that all of the cells were damaged (produced by freezing samples to -196°C); 0%, no cells were damaged. Panel A, SD (15h nights at +4°C); Panel B, LD (8h nights at +4°C). Plants were acclimated for up to 4 weeks. The average ± SE of three biological samples, each containing five experimental replicates (7 mm diameter leaf discs), are presented; note, the SE bars are too small to be seen with the symbols.

Table 3.1: Freezing Tolerance in Rye (*Secale cereale*) cv. Forage

Plants were grown and treated (see Sections 2.1.1 and 2.3) and three biological replicate samples containing five freshly cut 7 mm diameter leaf discs from mature sections of the third to fifth emergent leaf. A five-parameter logistic curve was fitted to each of the three replicate curves, LT_{50} determined, and the average and standard error (SE) calculated; values in the table are presented as °C. SD treatment, 15h nights at +4°C for 0 to 4 weeks; LD treatment, 8h nights at +4°C for 0 to 4 weeks. For a full statistical analysis, see Appendix A3.1.

Rye	Short DAY					Rye	Long DAY				
CV Forrage	Weeks of Acclimation at +4°C					CV Forrage	Weeks of Acclimation at +4°C				
Replicates	0 week	1 weeks	2 weeks	3 weeks	4 weeks	Replicates	0 week	1 weeks	2 weeks	3 weeks	4 weeks
a	-7.8	-14.0	-18.0	-21.2	-22.2	a	-6.0	-7.0	-8.0	-10.0	-12.2
b	-7.8	-14.0	-18.0	-21.2	-22.2	b	-6.0	-7.0	-8.0	-10.0	-12.2
c	-7.8	-14.0	-18.0	-21.2	-22.2	c	-6.0	-7.0	-8.0	-10.0	-12.2
Average	-7.8	-14.0	-18.0	-21.2	-22.2	Average	-6.0	-7.0	-8.0	-10.0	-12.2
SE	0.0	0.0	0.0	0.0	0.0	SE	0.0	0.0	0.0	0.0	0.0

3.6.2 Measurement of Freezing Tolerance (LT_{50}) in Rye cv. Kapitan

To examine the effects of cold acclimation on rye (*Secale cereale*) cv. Kapitan leaf tissue, plants were grown and treated as described in Section 2.1.1, and LT_{50} measurements taken.

Figure 3.5 shows the LT_{50} curves for the rye cultivar Kapitan. The plots show the effects of 0, 1, 2, 3, and 4 weeks' exposure to night temperatures of +4°C in SD and LD. For fully NA plants (8h nights for 0 weeks at +4°C), the LT_{50} was -6.0°C and reduced to -10.1°C after 4 weeks' exposure to 8h at +4°C night temperatures. In contrast, the LT_{50} value of Kapitan plants exposed to SD (15h nights at +4°C) reduced from -6.6°C to -17.9°C over the 4-week period. A fixed-factor ANOVA analysis was performed on this data, and showed a significant interaction ($p < 0.0010$) between the main factors of photoperiod and duration of exposure to cool night temperatures, indicating that some CA processes were triggered by long nights, some by low night temperature, and some by a synergistic effect of both factors (see Appendix A3.2).

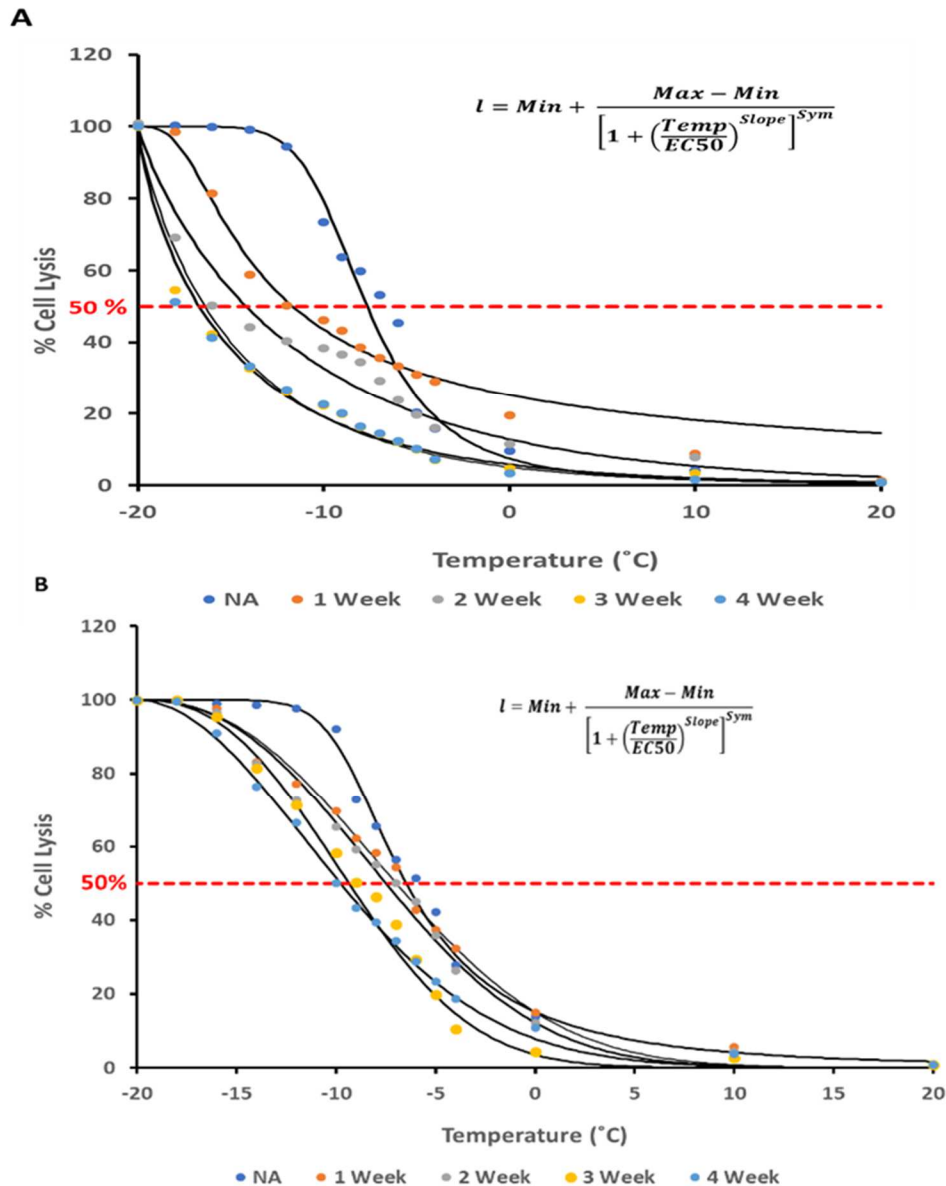


Figure 3.5: Effect of Cold Acclimation on The Freezing Tolerance (LT_{50}) of Rye (*Secale cereale*) cv. Kapitan Leaves.

Leaf discs of rye (*Secale cereale*) cv. Kapitan were exposed to SD and LD CA conditions (+4°C night temperatures), for up to 4 weeks, as described in Section 2.1.1. Tissue damage was estimated as the percentage solute leakage from samples held at each of the indicated temperatures for 60 minutes. The average values and standard errors of n=3 biological replicates are presented. A five-parameter logistic regression model was applied to the data. A value of 100% represents all of the cells were damaged (produced by freezing samples to -196°C); 0%, no cells were damaged. Panel A, SD (15h nights at +4°C); Panel B, LD (8h nights at +4°C). Plants were acclimated for up to 4 weeks. The average \pm SE of three biological samples, each containing five experimental replicates (7 mm diameter leaf discs), are presented; note, the SE bars are too small to be seen with the symbols.

Table 3.2: Freezing Tolerance in Rye (*Secale cereale*) cv. Kapitan

Plants were grown and treated (see Sections 2.1.1 and 2.3) and three biological replicate samples containing five freshly cut 7mm diameter leaf discs from mature sections of the third to fifth emergent leaf. A five-parameter logistic curve was fitted to each of the three replicate curves, LT_{50} determined, and the average and standard error (SE) calculated; values in the table are presented as °C. SD treatment, 15h nights at +4°C for 0 to 4 weeks; LD treatment, 8h nights at +4°C for 0 to 4 weeks. For a full statistical analysis, see Appendix A3.2.

Rye	Short DAY					Rye	Long DAY				
cv kapitan	Weeks of Acclimation at +4°C					CV kapitan	Weeks of Acclimation at +4°C				
Replicates	0 week	1 weeks	2 weeks	3 weeks	4 weeks	Replicates	0 week	1 weeks	2 weeks	3 weeks	4 weeks
a	-6.6	-12.1	-16.1	-17.3	-17.9	a	-6	-6.5	-7	-9	-10.1
b	-6.6	-12	-16	-17.2	-17.9	b	-6	-6.5	-7	-9	-10.1
c	-6.6	-12	-16	-17.2	-17.9	c	-6	-6.6	-7.1	-9.1	-10.1
Average	-6.60	-12.03	-16.03	-17.23	-17.90	Average	-6.0	-6.5	-7.0	-9.0	-10.1
SE	0.00	0.03	0.03	0.03	0.00	SE	0.0	0.0	0.0	0.0	0.0

3.6.3 Measurement of Freezing Tolerance (LT_{50}) in Spring Barley cv. Belgravia Leaves

Figure 3.6 shows the effect of cold acclimation on the spring barley (*Hordeum vulgare* L.) cv. Belgravia leaf tissue LT_{50} values. Belgravia plants were grown and treated as described in Section 2.1.1, and LT_{50} measurements collected as described in Section 2.3. A five-parameter logistic model was applied to each of the three replicate curves for each treatment, and the average and standard error for LT_{50} calculated. In NA Belgravia plants (8h nights, 0 weeks at +4°C) the LT_{50} was -5.5°C (Fig. 3.5b, Table 3.3) but with prolonged exposure (8h nights at 4°C for 4 weeks) this declined to -14.0°C. In SD, the LT_{50} value declined from -6.7°C (15h nights at +4°C for 0 weeks) to -15.2°C (15h nights for 4 weeks at +4°C) (Fig. 3.5a, Table 3.3). A fixed-factor ANOVA analysis was performed on this data, and showed a significant interaction ($p < 0.001$) between the main factors of photoperiod and time of exposure to cool night temperatures, indicating that some CA processes were triggered by long nights, some by low night temperature, and some by a synergistic effect of both factors (see Appendix A3.3).

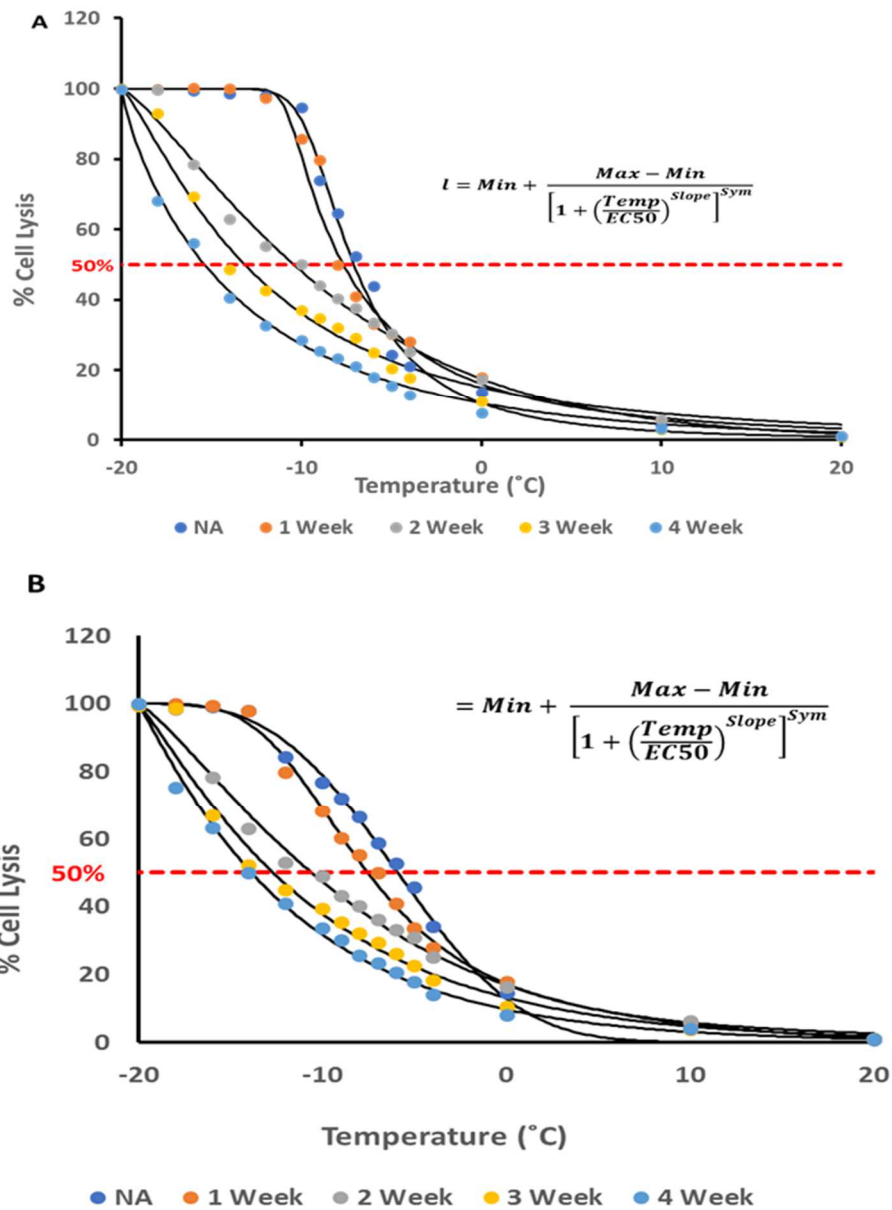


Figure 3.6: Effect of Cold Acclimation on The Freezing Tolerance (LT₅₀) of Spring Barley *cv.* Belgravia Leaves.

Leaf discs of spring barley (*Hordeum vulgare*) *cv.* Belgravia were exposed to SD and LD CA conditions (+4°C night temperatures), for up to 4 weeks, as described in Section 2.1.1. Tissue damage was estimated as the percentage solute leakage from samples held at each of the indicated temperatures for 60 minutes. The average values and standard errors of n=3 biological replicates are presented. A five-parameter logistic regression model was applied to the data. A value of 100% indicates that all of the cells were damaged (produced by freezing samples to -196°C); 0%, no cells were damaged. Panel A, SD (15h nights at +4°C); Panel B, LD (8h nights at +4°C). Plants were acclimated for up to 4 weeks. The average ± SE of three biological samples, each containing five experimental replicates (7 mm diameter leaf discs), are presented; note, the SE bars are too small to be seen with the symbols.

Table 3.3: Freezing Tolerance of Spring Barley (*Hordeum vulgare*) cv. Belgravia Leaves.

Plants were grown and treated (see Sections 2.1.1 and 2.3) and three biological replicate samples containing five freshly cut 7mm diameter leaf discs from mature sections of the third to fifth emergent leaf. A five-parameter logistic curve was fitted to each of the three replicate curves, LT_{50} determined, and the average and standard error (SE) calculated; values in the table are presented as °C. SD treatment, 15h nights at +4°C for 0 to 4 weeks. LD treatment, 8h nights at +4°C for 0 to 4 weeks. For a full statistical analysis, see Appendix A3.3

Barley	Short DAY					Barley	Long DAY				
CV Belgravia	Weeks of Acclimation at + 4°C					CV Belgravia	Weeks of Acclimation at + 4°C				
Replicates	0 week	1 weeks	2 weeks	3 weeks	4 weeks	Replicates	0 week	1 weeks	2 weeks	3 weeks	4 weeks
a	-6.7	-8.0	-10.0	-14.1	-15.2	a	-5.5	-7.0	-10.6	-13.4	-14.0
b	-6.7	-8.0	-10.0	-14.0	-15.2	b	-5.5	-7.0	-10.6	-13.4	-14.0
c	-6.7	-8.0	-10.0	-14.0	-15.2	c	-5.5	-7.0	-10.6	-13.4	-14.0
Average	-6.7	-8.0	-10.0	-14.0	-15.2	Average	-5.5	-7.0	-10.6	-13.4	-14.0
SE	0.0	0.0	0.0	0.0	0.0	SE	0.0	0.0	0.0	0.0	0.0

3.6.4 Measurement of Freezing Tolerance (LT_{50}) of Winter Barley cv. California Leaves

Figure 3.7 shows the effect of cold acclimation on winter barley (*Hordeum vulgare* L.) cv. California leaf LT_{50} values. California plants were grown and treated as described in Sections 2.1.1 and 2.3. A five-parameter logistic model was applied to each of the three replicate curves (see Section 3.6.3 for details). In NA plants (8h nights 0 weeks at +4°C) the LT_{50} value was -7.0°C and this reduced to -16.0°C after 4 weeks of exposure (see Table 3.4 and Fig. 3.7B). For plants in SD, the LT_{50} value reduced from -9.0°C to -18.2°C over the 4-week period (15h nights at +4°C, 0–4 weeks) (see Table 3.4 and Fig. 3.7A). This data indicates that both photoperiod and time of exposure to low night temperatures decrease LT_{50} and improve frost tolerance. A fixed-factor ANOVA analysis was performed on this data, and showed a significant interaction ($p < 0.001$) between the main factors of photoperiod and time of exposure to cool night temperatures, indicating that some CA processes were triggered by long nights, some by low night temperature, and some by a synergistic effect of both factors (see Appendix A3.4).

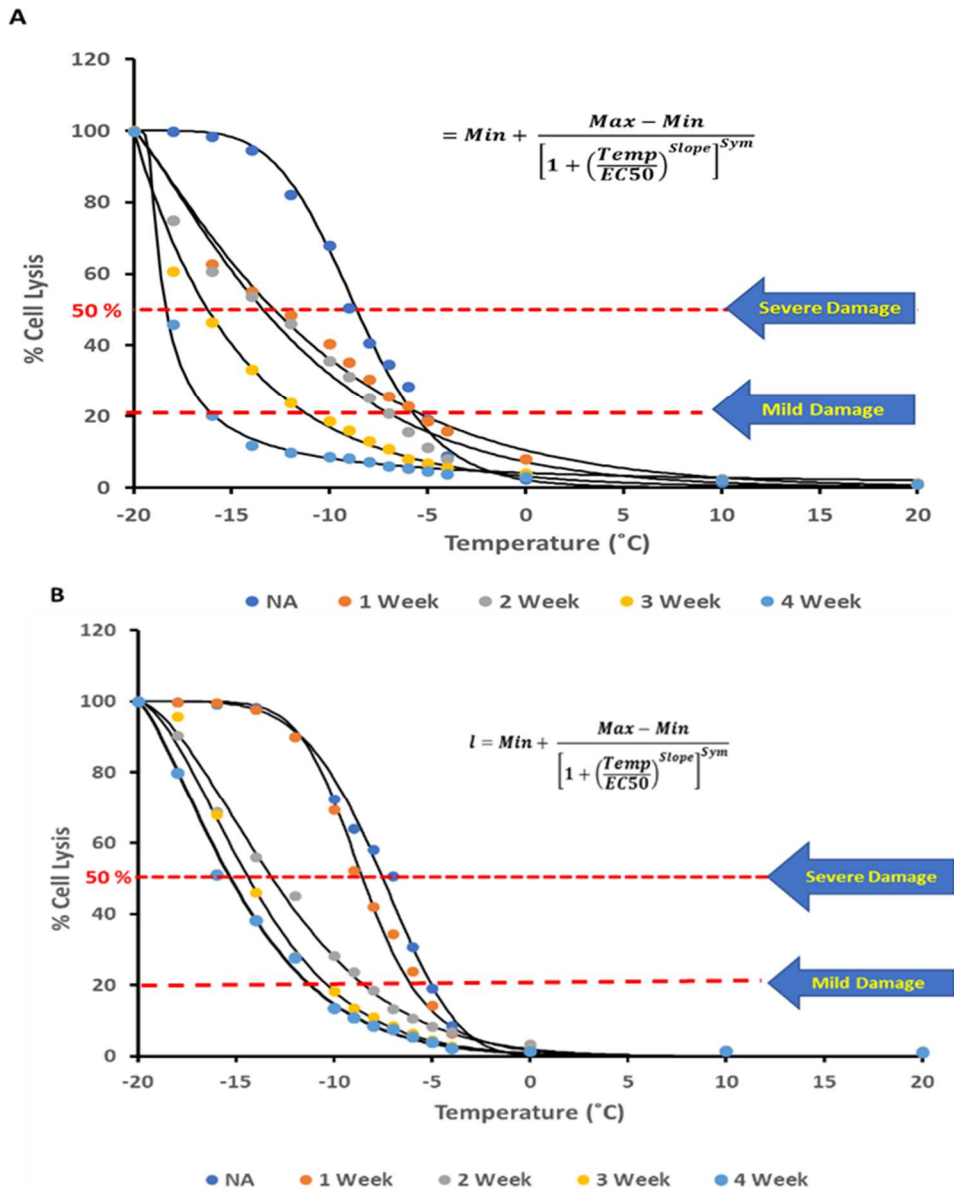


Figure 3.7: Effect of Cold Acclimation on The Freezing Tolerance (LT₅₀) of Winter Barley *cv.* California Leaves.

Leaf discs of winter barley (*Hordeum vulgare*) *cv.* California were exposed to SD and LD CA conditions (+4°C night temperatures), for up to 4 weeks, as described in Section 2.1.1. Tissue damage was estimated as the percentage solute leakage from samples held at each of the indicated temperatures for 60 minutes. The average values and standard errors of n=3 biological replicates are presented. A five-parameter logistic regression model was applied to the data. A value of 100% indicates that all of the cells were damaged (produced by freezing samples to -196°C); 0%, no cells were damaged. Panel A, SD (15h nights at +4°C); Panel B, LD (8h nights at +4°C). Plants were acclimated for up to 4 weeks. The average ± SE of three biological samples, each containing five experimental replicates (7 mm diameter leaf discs), are presented; note, the SE bars are too small to be seen with the symbols.

Table 3.4: Freezing Tolerance of Winter Barley (*Hordeum vulgare*) cv. California Leaves.

Plants were grown and treated (see Sections 2.1.1 and 2.3) and three biological replicate samples containing five freshly cut 7mm diameter leaf discs from mature sections of the third to fifth emergent leaf. A five-parameter logistic curve was fitted to each of the three replicate curves, LT_{50} determined, and the average and standard error (SE) calculated; values in the table are presented as °C. SD treatment, 15h nights at +4°C for 0 to 4 weeks; LD treatment, 8h nights at +4°C for 0 to 4 weeks. For a full statistical analysis, see Appendix A3.4.

Barley	Short DAY					Barley	Long DAY				
CV California	Weeks of Acclimation at + 4°C					CV California	Weeks of Acclimation at + 4°C				
Replicates	0 week	1 week	2 weeks	3 weeks	4 weeks	Replicates	0 week	1 week	2 weeks	3 weeks	4 weeks
a	-9.0	-12.3	-13.3	-16.5	-18.2	a	-7.0	-8.8	-12.9	-14.4	-16.0
b	-9.0	-12.3	-13.3	-16.5	-18.2	b	-7.0	-8.8	-12.9	-14.4	-16.0
c	-9.0	-12.3	-13.3	-16.5	-18.2	c	-7.0	-8.8	-12.9	-14.4	-16.0
Average	-9.00	-12.30	-13.30	-16.50	-18.20	Average	-7.0	-8.8	-12.9	-14.4	-16.0
SE	0.00	0.00	0.00	0.00	0.00	SE	0.0	0.0	0.0	0.0	0.0

3.7 Summary of the Effect of Photoperiod and Night Temperatures on Barley and Rye Cold Acclimation

Figure 3.8 shows a summary of the effects of photoperiod and low night temperature in enabling cold acclimatisation in rye (*Secale cereale*) and barley (*Hordeum vulgare*) cultivars. With respect to rye, both photoperiod and a low temperature are required for full cold acclimation (see Figs. 3.8A and 3.8B), whereas with barley, photoperiod has only a modest effect (see. Figs. 3.8C and 3.8D). Therefore, temperature is the primary requirement for cold acclimation in barley.

It is important to exercise some caution when attributing the increased frost tolerance observed in SD rye to photoperiod alone. Plants exposed to SD conditions received 15h of +4°C night temperatures whereas LD plants received only 8h of +4°C each night. It is

conceivable that the improved frost tolerance observed in SD was attributable to the length of exposure to +4°C night temperature and not a combination of photoperiod and temperature. It is important to make this distinction because, if the former is true, signalling is perceived through a temperature-sensing pathway only, whereas the latter case would arise from additional signalling through a light-sensing pathway.

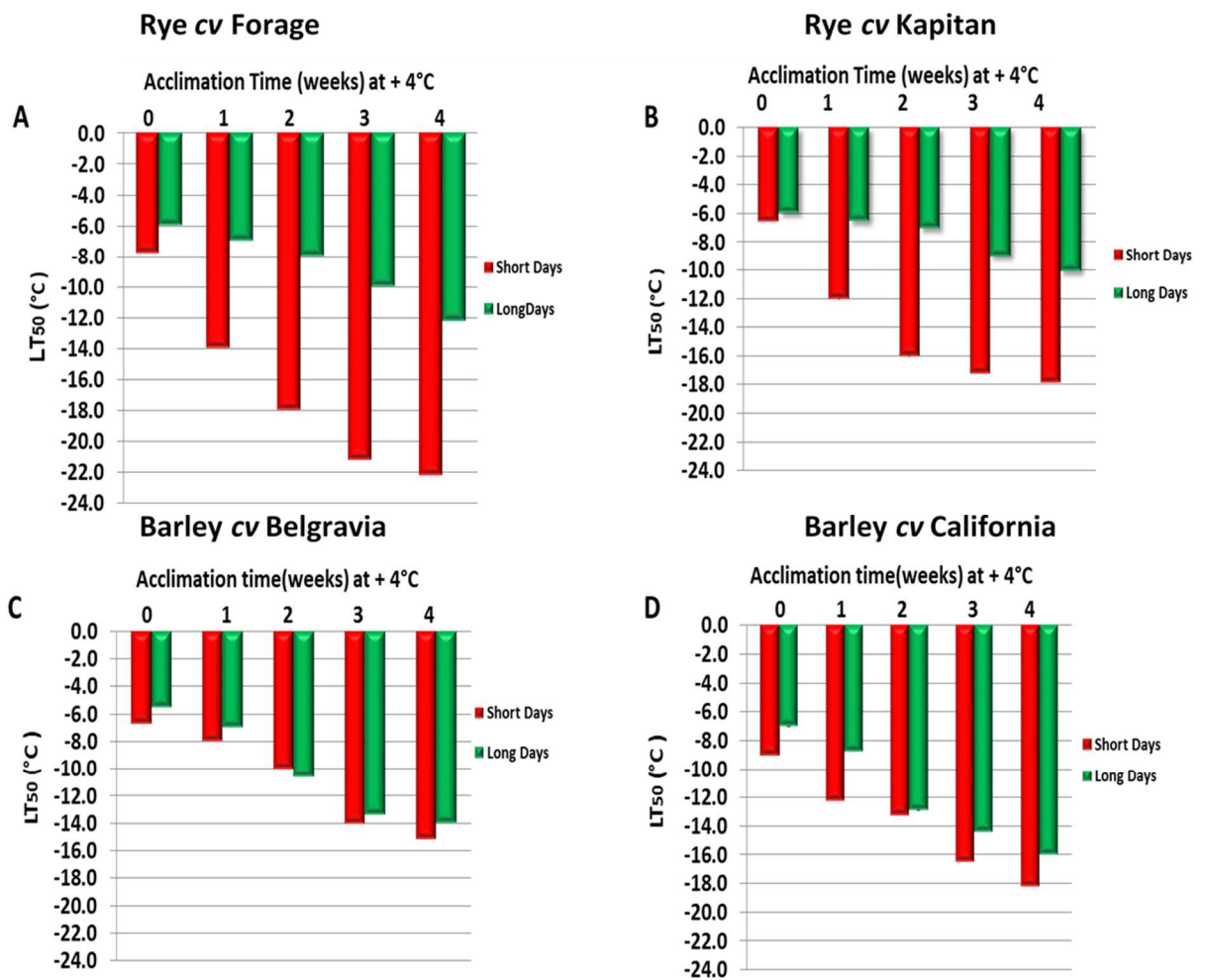


Figure 3.8: The Effects of Photoperiod and Night Temperatures on Cold Acclimation in Rye (*Secale cereale*) and Barley (*Hordeum vulgare*).

Plants were grown in both LD and SD photoperiod regimes (4°C night for 0–4 weeks) as described in Section 2.1.1, and LT₅₀ values determined using the methods outlined in Section 2.3. The error bars in the above graphs represent the average \pm SE of three biological samples, each containing n=5 experimental replicates; note, SE were small and barely visible. For a full statistical analysis see Appendix A3.1 - A3.4

3.8 Comparison of the Effects of Photoperiod and Temperature on Mild and Severe Damage to Spring and Winter Barley

Although Tables 3.3 and 3.4 indicate that increasing night length from 8h to 15h has only a modest effect on frost tolerance in barley (at 4 weeks LT_{50} improvement of -14.0° to -15.2° C for *cv.* Belgravia, and -16.0° C to -18.2° C for *cv.* California), further inspection of Figures 3.6 and 3.7 indicates there may be a more dramatic effect after 4 weeks (*cf.* 4-week curves of Figs. 3.6A with 3.7B and 3.7A). It appears that the shape of the 4-week curve changes for *cv.* California in 15h nights compared with 8h nights (Fig. 3.7) and with the spring *cv.* Belgravia (Fig. 3.6); thus, although changes in LT_{50} were modest, the temperature that induced 20% cell lysis was noticeably lower. To quantify this response, the LT_{20} (temperature that induced 20% cell lysis) was calculated and termed 'mild damage' and LT_{50} referred to as 'severe damage'. This data is summarised in Table 3.5, and clearly shows that for *cv.* California, 4 weeks of CA produced a 2.2° C improvement in LT_{50} (*cf.* 15 h vs. 8h nights), whereas a 5.0° C improvement in LT_{20} was observed over the same time period (Table 3.5). Figure 3.9 presents in graphical form the data for the effects of CA severe (LT_{50}) and mild (LT_{20}) damage in winter and spring barley. Surprisingly, at the 2- and 3-week stage, the combination of short night and low night temperature (8h at $+4^{\circ}$ C) was more effective in conferring CA on the winter cultivar California than long nights (15h at $+4^{\circ}$ C), but, as stated previously, this effect was reversed at the 4-week stage (Fig. 3.9C).

Appendix A3.5 and A3.6 present fixed-factor ANOVA analyses of the LT_{20} data for *cv.* California and Belgravia. The conclusion was that there was a significant interaction between the main factors (night temperature and day/night length) on LT_{20} in both barley cultivars, but the effect was more pronounced in the winter cultivar California. These are significant new findings that have not been reported before. The implications of these observations are discussed further at the end of this chapter.

Table 3.5: Effect of Cold Acclimation on The Freezing Tolerance (LT₅₀) Severe Damage and (LT₂₀) Mild Damage to Winter and Spring Barley Cultivars.

The LT₅₀ values (°C) were estimated empirically from each of the leakage curves, as described in Section 2.3 and Figure 3.7. The LT₂₀ values (°C) were calculated in a similar fashion, but 20% cell lysis was used. Details of the growth and acclimation conditions are given in the legend of Figure 3.7. Values are the averages (bold face type) and standard errors (SE) from three biological replicates. For a full statistical analysis, see Appendix A3.5 and A3.6.

LT ₅₀	Long Day					LT ₅₀	Short Day				
	0	1	2	3	4		0	1	2	3	4
Belgravia	-5.5	-7.0	-10.6	-13.4	-14.0	Belgravia	-6.7	-8.0	-10.0	-14.1	-15.2
	0.0	0.0	0.1	0.0	0.0		0.0	0.1	0.6	0.0	0.1
California	-7.0	-8.8	-12.9	-14.4	-16.0	California	-9.0	-12.3	-13.3	-16.5	-18.2
	0.0	0.0	0.0	0.0	0.0		0.0	0.0	0.0	0.0	0.0
LT ₂₀	Long Day					LT ₂₀	Short Day				
	0	1	2	3	4		0	1	2	3	4
Belgravia	-1.1	-0.9	-1.7	-4.4	-5.8	Belgravia	-3.3	-0.8	-1.3	-4.8	-6.7
	0.1	0.1	0.1	0.1	0.1		0.2	0.1	0.1	0.0	0.1
California	-5.1	-5.6	-8.3	-10.4	-10.9	California	-5.1	-5.3	-6.8	-6.7	-15.9
	0.0	0.0	0.1	0.0	0.0		0.0	0.1	0.0	0.0	0.1

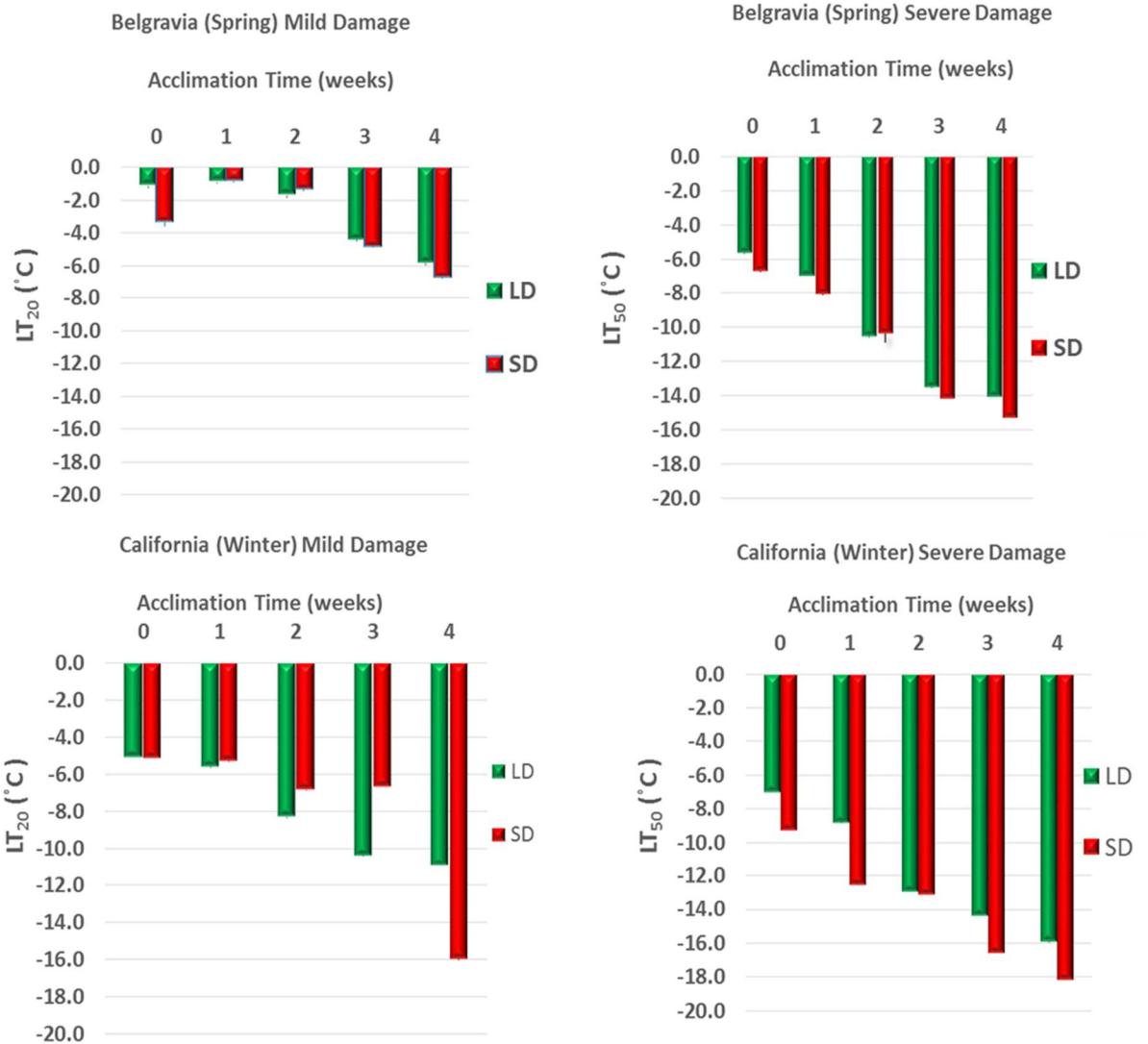


Figure 3.9: Comparing The Effects of Photoperiod and Temperature on Mild and Severe Damage to Spring and Winter Barley.

The above graphs show the effects of photoperiod and temperature on mild and severe damage to spring and winter barley. Plants were grown in both LD and SD photoperiod regimes (4°C night for 0–4 weeks) as described in the Materials and Methods section (Section 2.1.1). After this time, leaf disc samples and LT₅₀ measurements were taken to assess cold tolerance. The bars in the above graphs represent the average ± SE of three biological samples, each containing n=5 experimental replicates. For a full statistical analysis see Appendix A3.3 - A3.6

3.9 Discussion

The acclimation of winter cereals, such as barley, to freezing temperatures is reported to increase upon exposure to decreased temperatures and day length (Uemura et al., 2006; Hayes et al., 1993; Jackson, 2009; Galibra et al., 2009; Crosatti et al., 1999; Rapacz et al., 2008; Bertrand et al., 2017; Gray et al., 1997). Low temperatures trigger various genetic and metabolic alterations in plants, which result in the development of cold acclimation (Limin & Fowler, 1993; 2002). In Chapter 1, a review of the traits that are required to provide resistance to freezing injury, or ‘winter hardiness’, was provided.

Winter barley is more susceptible to frost damage than winter wheat or winter rye. Progress toward increasing the tolerance of winter cereals to frost using either conventional breeding or gene manipulation technologies has been slow, due to under-developed genetic and research resources, and to the large number of genes that confer the trait (Limin & Fowler, 2002; Fowler, 2008). To gain deeper insight into the environmental factors that trigger frost tolerance in rye and barley, a number of experiments were conducted and the results have been reported in this chapter.

The first objective of this study was to develop a robust method for measuring frost damage in foliar tissues. Modifications were made to the electrolyte leakage method for assessing freeze-induced cell lysis, a major contributor to plant frost damage. By measuring temperature-induced electrolyte leakage in one-degree steps over the -4°C to -10°C range (and every 2°C beyond this), and by increasing the level of replication, the lethal temperature which caused 50% leakage (50% cell lysis) – the LT_{50} – could be determined with a resolution of $< \pm 0.5^{\circ}\text{C}$. Although time-consuming, this approach provided sufficient resolution to identify subtle differences in CA caused by night temperature and photoperiod.

The second objective of this study was to use the methods mentioned in the previous paragraph to confirm and quantify the roles of photoperiod and low night temperature in triggering CA in rye and barley. Two cultivars of rye (*cv.* Forage and *cv.* Kapitan) and a spring (*cv.* Belgravia) and winter (*cv.* California) barley were exposed to 8h or 15h night periods at either +16°C or +4°C; day temperature was 20°C. These regimes, with diurnal changes in length of the dark period and temperature, were chosen as they more closely reflect the real conditions found in autumn in northern latitudes, where temperate small-grained cereals are grown. Under these more natural conditions, the higher day temperature

should allow signalling events triggered during the cool night periods to be fully manifest at the protein level, thereby better representing the changes that occur in the field.

The results presented in this chapter show that freezing tolerance in barley and rye is inherently different. In this work, attempts were made to separate the effects of photoperiod and night temperature using acclimation regimes showing a diurnal change in temperature as well as light level (see Section 3.4). This contrasts with most previous studies, where temperature has been held constant during a diurnal light cycle. Whilst there are significant advantages of adopting the regimes used in this study, one disadvantage is that changes that are attributable to photoperiod may in fact have resulted from the length of exposure to night temperatures of 4°C. Plants that are exposed to LD and SD differ in the duration of the light and dark cycle but also in the length of exposure to 4°C (8h nights at 4°C vs. 15h nights at 4°C, respectively). Hence, differences may be attributable to photoperiod or to low temperature ‘dosage’. These effects can be separated at the transcriptome level using set theory (see Chapter 5), but for the discussions in this chapter, the term ‘photoperiod’ will be used in recognition of the fact that responses resulting from a change in day length might arise from the duration of the cool night period. Regardless, the experiments reported in Section 3.6 show that ‘photoperiod’ and low temperatures affect barley and rye differently, and that some subtle differences occur between cultivars of the same species.

Rye *cv.* Forage was the most cold-tolerant of the cultivars assessed, developing an LT_{50} of -12.2°C and -22.0°C after 4 weeks’ exposure to 8h and 15h nights, respectively (see Table 3.1 and Fig. 3.4). This raises the question of whether the 9.8°C improvement in LT_{50} observed with long night periods is attributable to sensing of the length of the light and dark cycle or to the length of exposure to +4°C. Some insight might be gained by considering the effects of the light/dark cycle length on the LT_{50} of 3-week-old plants (0 weeks of treatment, see Fig. 3.2). When Forage plants were grown to the 3-week stage in 15h nights at +16°C, a LT_{50} of -7.8°C was measured, whereas when grown for the same period for 8h at +16°C the value was -6.0°C. These LT_{50} values are statistically significant ($p < 0.05$) (see Appendix A3.1) and the small 1.8°C difference presumably arose from the differences in the light/dark cycle length (true photoperiod) and/or temperature (16h or 9h light at +20°C and 8h or 15h dark at +16°C). It is conceivable that the LT_{50} of -7.8°C in long nights arose from differences in temperature (a 7h reduction in the period at +20°C or a 7h increase in the period at +16°C). However, as neither of these temperatures would be expected to induce CA, it seems

more likely that the difference in LT_{50} arose from photoperiod being sensed through the phytochrome signalling pathway. Regardless, for 3-week-old plants, the effect of changing the light/dark cycle in warm temperatures had only a minor effect on cold tolerance. These findings, albeit on 3-week-old Forage plants, suggest that photoperiod plays only a minor role in CA in this rye cultivar.

Rye *cv.* Kapitan developed an LT_{50} of -10.1°C (8h nights) and -17.9°C (15h nights) after 4 weeks of exposure, a difference of 7.8°C (see Table 3.2, Fig. 3.5 and Appendix A3.2ii) (*cf.* 15 28 vs. 8 28). Again, this significant improvement ($p < 0.05$) may have arisen from signalling events via a light-sensing or temperature-sensing pathway (or both). Looking at the changes in LT_{50} of 3-week-old plants (0 weeks of treatment, see Table 3.2) the changes are modest, 0.6°C although they are significantly different ($p < 0.05$, see Appendix A3.2ii) (*cf.* 15 0 vs. 8 0). For the reasons outlined in the preceding paragraph, it seems reasonable to conclude that photoperiod plays only a minor role in CA in 3-week-old Kapitan plants, and it seems more likely, therefore, that the 7.8°C difference observed after 4 weeks of treatment was due to the increased night period at $+4^{\circ}\text{C}$, not photoperiod *per se*.

Taken together, these results show that low night temperatures induced a significant improvement in rye cold tolerance when grown in 8h nights, and an even greater improvement when grown in 15h nights. The modest improvements observed from changing photoperiod alone in warm night temperatures (Week 0) suggest that photoperiod alone (signalling via the light-sensing pathways only) plays only a minor role in CA in rye. Alternatively, the CA factors of low night temperature and photoperiod might not be additive but more-than-additive; in other words, an interaction or synergism might exist arising from cross-talk between the temperature-sensing and light-sensing pathways. One way to determine which of these possibilities is correct would be to expose plants to the same 8h and 15h night regimes but to interrupt the 15h night with pulses of white light. It is well established that the CA factor photoperiod is sensed by phytochrome in plants (Section 1.14.3), and that prolonged darkness leads to the accumulation of P_{fr} , this must be in the form of phytochrome, which leads to CA. By interrupting the 15h night period with brief flashes of light, the CA-active P_{fr} form will be rapidly converted to the CA-inactive Pr form, thereby removing any light-sensing signalling component. Comparing the LT_{50} of plants with a 15h interrupted dark period with those receiving 15h of un-interrupted darkness should resolve this issue.

Comparison of cold tolerance in the spring barley *cv.* Belgravia and winter barley *cv.* California showed that the latter is more cold-hardy (Tables 3.3 and 3.4). In *cv.* Belgravia, the LT_{50} was -14.0°C and -15.2°C in 8h and 15h nights, respectively. Comparison of the effects of photoperiod alone (3-week-old plants, Week 0 of CA treatment, see Fig. 3.2) showed a modest 1.2°C improvement in 15h nights (-5.5°C to -6.7°C , see Table 3.3). A similar improvement of 1.2°C was found after 4 weeks of exposure to low temperatures; the corresponding values were -14.0°C and -15.2°C (Table 3.3; Appendix A3.3). These results suggest that the effects of photoperiod alone CA are minimal but, unlike in rye, it acts in a purely additive way, with most CA responses occurring through the temperature-sensing pathway(s).

The winter barley *cv.* California showed a very similar pattern to *cv.* Belgravia, but was more cold-hardy. After 4 weeks' exposure to 8h nights, LT_{50} was -16.0°C , and in 15h nights it was 18.2°C (Table 3.4; Appendix A3.4). 'Photoperiod' alone, therefore, produced an improvement of 2.2°C at Week 0, and also after 4 weeks of exposure to low temperatures (Table 3.4). It seems that in both cultivars of barley, exposure to night temperatures of $+4^{\circ}\text{C}$ for 8h nights is sufficient to develop almost full CA; increasing the duration of the night period to 15h produces only a 1.2°C (Belgravia) to 2.2°C (California) improvement in cold-hardiness. The conclusions are, therefore, that either the light/dark cycle, or an additional 7h of cool night temperatures has only a minor effect on barley's cold-hardiness.

Table 3.6 summarises the relative improvements in CA that are attributable to photoperiod and temperature in rye and barley. For rye, full cold acclimation (100%) requires exposure to both long nights and low night temperatures; when applied alone photoperiod achieves only 5-11% and temperature 34-38% of the CA achieved when they are applied in combination. In contrast, for barley photoperiod and temperature alone account for 12-18% and 80-88%, respectively, of the full CA achieved when they are applied in combination. The implications are clear. For barley 8hr exposure to cool night temperatures is sufficient to achieve over 80% of full CA; a further 7hr exposure (15hr cool nights) produces an almost additive effect (although the ANOVA analysis presented in Appendix A3.3 & A3.4 indicates a significant interaction). For rye, increasing the duration of cool nights produces a more-than-additive response in CA suggesting a strong interaction between these two CA factors. As discussed above, this may arise from an interaction between temperature-sensing and photoperiod-sensing signalling pathways, or from a non-linear 'temperature 'dosage' effect.

Table 3.6 The Contribution of Night Length (Photoperiod) to Full Cold Acclimation in Rye and Barley Cultivars

The average LT_{50} values ($^{\circ}C$) are presented for the four cultivars exposed to the cold acclimation factors low night temperatures ($4^{\circ}C$) and night duration (15 h) for 4 weeks. The relative contribution of Photoperiod alone (15h minus 8h nights at $16^{\circ}C$) and Temperature alone ($4^{\circ}C$ minus $16^{\circ}C$ in 8h nights) are expressed as a ratio of the full cold acclimation (15h at $4^{\circ}C$ minus 8h at $16^{\circ}C$, set as 100%). Data from Tables 3.1-3.4.

	Night Temperature ($^{\circ}C$)	16	16	4	4	Photo-period Only	Temperature Only	Both Temp & Photo ($^{\circ}C$, 100 %)
	Night Duration (h)	8	15	8	15			
<i>Secale cereale</i>	Forage	-6.0	-7.8	-12.2	-22.2	11%	38%	16.2
Rye	Kapitan	-6.0	-6.6	-10.1	-17.9	5%	34%	11.9
<i>Hordeum vulgare</i>	Belgravia	-5.5	-6.7	-14.0	-15.2	12%	88%	9.7
Barley	California	-7.0	-9.0	-16.0	-18.2	18%	80%	11.2

In addition to these temperature-induced changes in LT_{50} , it was mentioned in Section 3.6.4 that there were significant changes to the LT_{20} after 4 weeks, which appear to be associated with the length of the light and dark periods. In this section, this was explained as a possible effect of a light-sensing signalling pathway that triggered tolerance to mild frost conditions. This term photoperiod is perhaps not particularly informative and requires further clarification. What can be observed in these curves (Figs. 3.7A and 3.7B) is that after 4 weeks' exposure to cool 15h nights, the shape of the curve changes so that much lower temperatures are required to produce 20% cell damage. A possible explanation of this observation is that there are several tissues in barley leaves that have different capacities to develop frost tolerance, such that some tissues are more sensitive to damage than others. In *cv.* California, it might be that cold acclimation in these tissues only requires exposure to cool long nights. Regardless, it is not clear whether this improved tolerance to frost damage operates through temperature-sensing or light-sensing signalling pathways.

It was mentioned in Sections 3.6.1 and 3.6.2 that, on occasions, the five-parameter logistic model did not fit the % cell lysis curves (see Figs. 3.2 and 3.3); this was not the case for either of the barley cultivars. The reasons for this are unclear but may be associated with the

narrower width of rye leaves compared with those of barley. Attempts were made to take leaf discs avoiding the main mid-rib, but for rye this was not always possible and it proved to be impractical to use smaller leaf discs. Consequently, the heterogeneity of leaf tissues in the rye samples may have contributed to the problem. To avoid artefacts arising from poor-fitting curves, the LT_{50} values were derived empirically by inspecting the curves and not calculated from the fitted models.

The observation that short photoperiod increased freezing tolerance in both Forage and Kapitan cultivars of rye (Fig. 3.8) agrees with some studies where the effect of SD or LD on adaptation to freezing temperature was observed. Bertrand et al. (2017) studied the effect of photoperiod on freezing tolerance in two cultivars of alfalfa plants, and the results showed that the effects vary with each cultivar. Freezing tolerance tests carried out at -16°C showed that for *cv.* 6010, a 40% survival rate was observed after exposure to 16h nights, and a 60% survival rate with exposure to 14h nights. In contrast, for *cv.* Evolution, long nights resulted in a survival rate of 82% compared with 54% in short nights.

The results in this study are in agreement with the findings of Mahfoozi et al. (2000), who showed that freezing tolerance of an SD-sensitive barley genotype was similar regardless of whether the plants were grown in LD or SD regimes. In contrast, growing the highly SD-sensitive barley cultivar Dicktoo (a winter barley) in SD resulted in an increased level and/or longer retention of low temperature tolerance. In another study on Dicktoo, a delayed transition of the crown meristem from the vegetative to the reproductive stage was observed (Fowler et al., 2001). This was associated with increased and sustained level of cold tolerance as a result of increased expression of cold tolerance genes in leaves.

The mechanism by which photoperiod affects the rate and extent of cold acclimation is not fully understood. However, a number of studies in the past two decades have provided some information on this. The experimental evidence suggests that there is a link between photoperiod and the expression of *VRNI*. For instance, Dhillon et al. (2010) showed that *VRNI* is involved in the down-regulation of the cold-acclimation pathway in temperate cereals. In photoperiod-sensitive plants, longer photoperiods lead to an increase in accumulation of the *VRNI* transcript. In contrast, shorter photoperiods slow down transcript accumulation. In wheat and barley, it is known that delay in vernalisation in plants exposed to short photoperiods is associated with an increase in freezing tolerance (Fowler et al., 2001;

Limin & Fowler, 2006). It follows from the findings of these papers that photoperiod plays a role in *VRN1* regulation.

Recent studies suggest that the combined effect of photoperiod and temperature on cold tolerance in cereals is strongly linked to the expression of CBF genes (Novak et al., 2015; Skinner et al., 2018). The effect of temperature and photoperiod will be examined in Chapter 4.

It is important to bear in mind that a key difference in this study is that plants were exposed to light for the different photoperiods prior to and after exposure to cool night temperatures so treatments were administered at the same time. This limits the extent to which comparisons can be drawn between this work and related studies that were discussed above. The evidence from the literature indicates that plants use a coordinated response to develop cold acclimation and freezing tolerance in autumn and winter. This is reported to involve a sequential effect of decrease in length of photoperiod and decrease in temperature (Crosatti et al., 1999; Rapacz et al., 2008). The gradual decrease in light exposure is viewed to trigger a set of genetic, biochemical, and physiological events that prepares the plant for cold tolerance (Bertrand et al., 2017). It is further suggested that full cold acclimation and freezing tolerance is dependent on the initial trigger due to shortening of daylight. This implies that it would have been more ideal to separate the two treatments of low temperature and photoperiod in this study. However, for several reasons that seems not to be the case. First, as demonstrated above, photoperiod has very little effect on CA in barley or rye in the absence of low night temperatures. Second, shorter cool nights are almost as effective as longer cool nights in conferring CA on barley, although there is a stronger synergistic effect in rye. Finally, the experiments described here, where plants are exposed to alternating diurnal temperature, better replicate natural conditions, are more likely to reflect the changes that occur in the field.

3.9.1 Summary and Conclusions

- There is strong evidence for a temperature-sensing signalling pathway(s) in both rye and barley.
- There is some evidence that a light-sensing pathway(s) may contribute to cold acclimation in rye and that the different parts of this pathway(s) act synergistically with the temperature-sensing pathway. It is perhaps more likely, though, that cold acclimation in rye is triggered through temperature-sensing pathways only but full cold acclimation is achieved after prolonged exposure to cool night temperatures (> 8h). Further experiments on the freezing tolerance of plants exposed to long night periods at 4°C interrupted with short pulses of white light should resolve this issue.
- There is little evidence that light-sensing pathways play a major role in conferring tolerance to severe frost events in barley; signalling through temperature-sensing pathways appears to confer almost full cold acclimation.
- There is some evidence that in winter barley only, signalling through a light-sensing pathway may confer a measure of tolerance on a sub-population of frost-sensitive cells in leaves.

The findings reported in this chapter are novel and have not been reported before; they were uncovered as a result of the refined protocol developed for measuring freezing injury.

Chapter 4 Expression of Key Plant Cold Acclimation Orthologues in Spring and Winter Barley

4.1 Introduction

Chapter 1 summarised details of the cold acclimation process in *Arabidopsis* (Sections 1.5 – 1.11); both the influences of photoperiod and low night temperatures were considered, and the process was understood to be activated through ABA-dependent and ABA-independent signalling pathways. In Chapter 3 evidence was provided suggesting the cold acclimation process in tribe Triticeae was somewhat different from the model proposed for *Arabidopsis*, and differences between rye (*S. cereale*) and barley (*H. vulgare*) were observed. These results indicate a highly significant response to both cool night temperatures alone (4°C) and the duration of the night period alone (15hr) in both cultivars of rye and of barley. For rye, low night temperatures alone and photoperiod alone induced 30-40% and 5-11%, respectively, of the observed full CA achieved when both factors were combined (Table 3.6). In contrast, for barley, photoperiod alone produced (12-18%), whilst temperature alone produced 80-88% of the reaction achieved when the two factors were applied together. It was therefore concluded that full cold acclimation in barley can be confirmed when there are 8hr nights at 4°C; neither photoperiod nor increased duration of the cool night period to 15hrs play an important role.

The key questions that still need to be addressed to understand the regulation of cold acclimation in cereals include the following: (1) CBF transcription factors, which play a significant role in cold acclimation in *Arabidopsis* (estimated to contribute 20% to the full CA response, see Section 1.14.4), questioning to what extent multiple CBF sequences encoded at the *FR2* locus in barley are involved?; (2) what transcriptional changes occur in barley homologues of *CBF* sequences in response to changes in photoperiod and night temperature?; (3) the vernalization gene *VRN1* in the *FRI* locus is reported to both augment and suppress CA in small grained cereals (Section 1.14), but what exactly is its role in barley?; and (4) What role, if any, do barley homologues of key *Arabidopsis* CA sequences play in barley CA (e.g. *DHN5*, *COR15A*, etc.).

The aims of the work described in this chapter were to provide a more detailed account of the importance of transcriptional regulation of homologues in the above sequences (reported to be important in *Arabidopsis* CA) for conferring frost tolerance upon spring (*cv.* Belgravia) and winter (*cv.* California) lines. The plan was to answer some of these questions by assessing the role of different combinations of photoperiod and night temperature on the transcriptional regulation of *VRN1* at the *FRI* locus, and the *HvCBFs* at the *FR2* locus, in barley leaves, using semi-quantitative and quantitative reverse transcription PRC (RT-PCR); see Section 4.4). The objective was to identify and compare the expression levels of some of the key sequences implicated in cold tolerance in cereals as induced by combinations of Temperature and Photoperiod in a spring and a winter barley cultivar.

4.2 Protocols for Quantifying Transcriptional Changes of Cold Acclimation Genes

To perform transcript profiling in a reproducible and reliable way, it is necessary to first establish robust protocols for quantifying the transcriptional changes of the homologues of sequences reportedly involved in cold acclimation in plants.

Spring (*cv.* Belgravia) and winter (*cv.* California) lines of barley were grown in soil and subjected to photoperiod and temperature regimes as described in Section 2.1.1. After 0, 1, 2, 3 or 4 weeks of cold acclimation, total RNA was prepared and cDNA synthesised for quantification by PCR (Section 2.4.4 and Section 2.5).

4.3 Primer Design and Amplification of Sequences Involved in Cold Acclimation

4.3.1 PCR Primer Design for *HvVRN1*, *HvVRN1*, & *HvVRN3*

The GenBank database contains fourteen *HvVRN1* and eleven *HvVRN3* full length barley cDNA sequences; in addition, there are two full length and one partial cDNA sequences deposited for *HvVRN2*. However, none of these sequences are from the cultivars Belgravia

or California, as used in this study. Preliminary CLUSTALW alignments of the *HvVRNI* DNA accessions revealed some between-cultivar sequence divergence, and it follows that the design of PCR primers could be confounded if SNPs were to appear in the regions where the primers anneal. Therefore, it seemed sensible to design ‘universal’ PCR primers from a consensus sequence for a gene derived from all the available cultivars; this was expected to improve the probability of successfully generating amplicons from the target genes in cvs. Belgravia and California.

The GenBank database was interrogated using the ENTREZ portal (<https://www.ncbi.nlm.nih.gov/nucleotide/>), and the search criteria, ‘gene name’ (i.e. *VRNI* [All Fields]) and ‘*Hordeum vulgare* [Organism]’. Full length sequences were downloaded in ‘GenBank (full)’ format and imported into CLC Workbench for further analysis. PCR primers for each of the *VRN* sequences were then designed from the CLUSTALW alignments of the homologues, and regions of complete sequence identity were selected for forward and reverse primers and the CLC Workbench Primer Design package was used to identify suitable primer pairs based on the default rules for PCR primer design. The gene structure and primers for each of the *VRN* sequences are presented in Figs 4.1, 4.2, & 4.3. Table 4.1 presents a summary of forward and reverse primer sequence, the empirically determined annealing temperature(s), amplicon sizes, and confirmation that the amplicons were generated from the intended template (by amplicon sequencing). The amplicon sequences were used to search the Morex full genome database (http://plants.ensembl.org/Hordeum_vulgare/Info/Index) and the most likely gene then identified based on the homology scores. CLUSTALW DNA alignments were then performed on the CLC Workbench of the amplicon sequence, the identified Morex homologue, and the original GenBank accession(s) used to design the PCR primers. The purpose of performing these alignments was two-fold. First, it was necessary to confirm that the PCR primers amplified the intended target sequence; second, by comparing the amplicon sizes with the amplicon size predicted from the sequences of other cultivars, and then to gain some insight into between-cultivar variation in gene structure and splice variants. For all but three of the original 18 sequences, amplicon sequencing provided strong evidence suggesting the primer pairs amplified the intended gene.

For *HvVRNI*, CLUSTALW cDNA alignments showed complete homology (100% identical) between the overlapping regions of the 257 bp cv. California amplicon and the six published

HvVRN1 sequences from the 6 other cultivars (Fig A4.1A, Appendix). Alignment of this amplicon with the 9 different *HvVRN1* transcript variants predicted from the Morex genome database (HORVU5Hr1G095630) also showed a strong homology in overlapping regions. Morex variants .4 and .5 would not have generated an amplicon with the *HvVRN1* primers, and variant .7 would have produced a slightly larger fragment (Fig A4.1B, Appendix).

A similar approach was used to design the PCR primers for *HvVRN2* and *HvVRN3* from *cvs.* California and Belgravia. The gene structures of *HvVRN2* (a suppressor of flowering that is structurally unrelated to functionally equivalent Arabidopsis *AtFLC*) and *HvVRN3* (a homologue of the Arabidopsis promoter of flowering *AtFT*) are shown in Fig 4.2 and 4.3, and further details on primer design are provided in Figs A4.2 and A4.3, (Appendix) and Table 4.1. Briefly, the primer pair designed to amplify the *HvVRN2* fragment generated amplicons of approximately 1,400 - 1,500 bp from the gDNA template prepared with *cvs.* California (Fig 4.4) and Belgravia (data not presented). The fragment from *cv.* California was cloned and sequenced and then found to be 100% identical in the overlapping regions to the GenBank accessions used for the primer design (Fig A4.2, Appendix). The predicted size of the *HvVRN2* cDNA was 444bp.

Details of the *HvVRN3* gene structure are provided in Fig 4.3. Briefly, 11 barley homologues of *VRN3* show a similar structure: three exons and two introns. The alignment of these 11 GenBank accessions provided a consensus sequence enabling the CLC Workbench Primer Design routine to identify suitable sites in exon 1 and exon 3 (Table 4.1 & Fig A4.3, Appendix). The predicted sizes of the amplicons were 960 bp and 427 bp when gDNA and cDNA were used as templates respectively. When gDNA was used as template, a fragment of approximately 1,000 bp was generated (Fig 4.3). Sequencing showed this *cv.* California gDNA amplicon was 1374 bp, and when *cv.* California gDNA was used as template it was 100% identical to 10 of the eleven sequences used in the primers design.

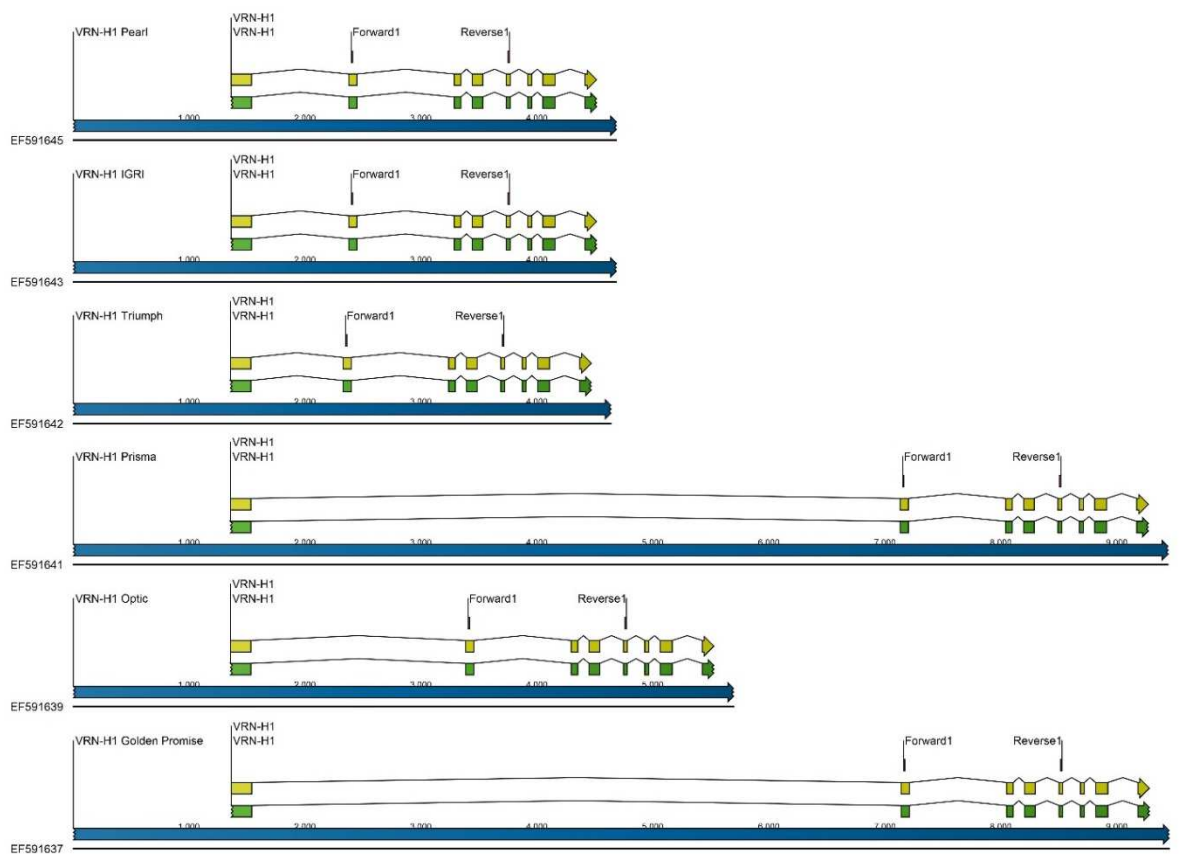


Figure 4.1. Gene Structure of *HvVRN1* from Six Barley Cultivars.

Of the 14 *HvVRN1* sequences available in the GenBank databases, 9 were identical in their ORFs; the six variants are shown above, for *cvs.* Pearl, IGRI, Triumph, Prisma, Optic and Golden Promise. The GenBank accession numbers for these sequences are indicated on the left. The primers were designed to regions in the ORFs, avoiding intron/exon boundaries; the Forward1 primer annealed to a completely conserved sequence in exon 2 and Reverse1 to exon 3 (indicated as red vertical marks). The sequence of these primers, their empirically determined annealing temperatures, and the expected size of the gDNA and cDNA amplicons are presented in Table 4.1. Figure A4.1B in the Appendix presents the full CLUSTALW alignment of the transcripts of these sequences. In this figure the dark blue bar indicates the transcription product prior to processing; the yellow bars the exons with introns (connecting black lines); and the green, the Genbank ‘gene sequence’. Note the much larger size of the first intron in *cvs.* Prisma and Golden Promise, which has been implicated in the epigenetic control of *VRN1* expression during vernalization (see Section 1.14.). Originally, it was believed spring cultivars had large deletions in the first intron, which prevented chromatin condensation and the *VRN-1* transcriptional silencing reported to occur in autumn in winter cultivars. However, it is now known that epigenetic control of *VRN1* expression is more complex, as all the cultivars above except for Prisma are spring varieties, including Golden Promise.

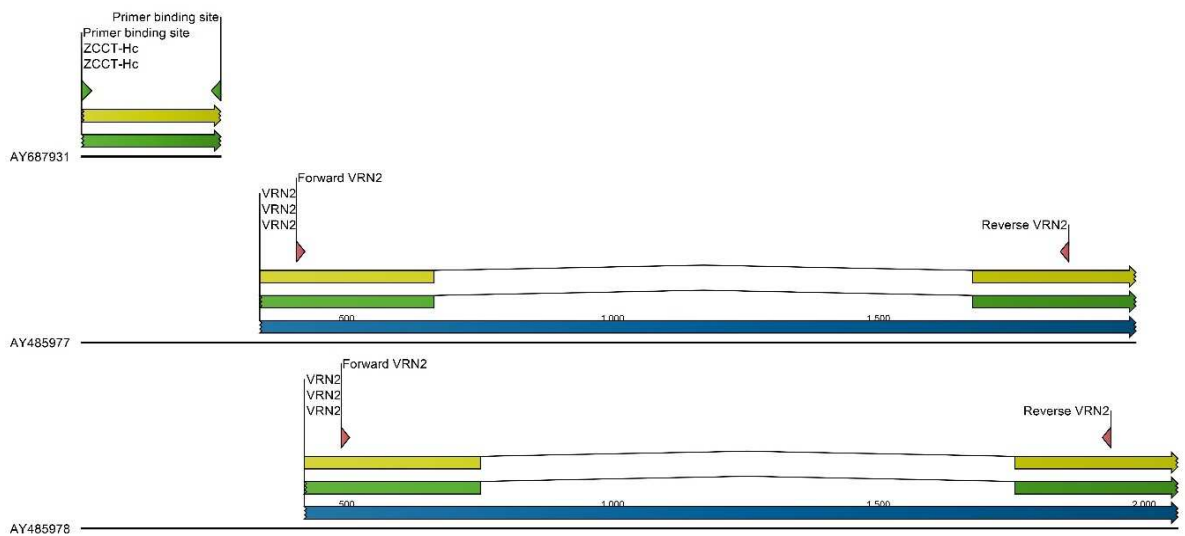


Figure 4.2. Gene Structure of Barley *HvVRN2* from Three Barley Cultivars.

Two full length and one partial sequence for *HvVRN2* were found in the GenBank database; AY485977 and AY485978 (both winter *cv.* Dairokkuku), AY687931 (*cv.* Hayakiso). The CLC Workbench CLUSTALW alignments for these three sequences (see Appendix Fig A4.2) showed sufficient homology in the first and second exon of the full length sequences to allow the PCR primer pairs to be designed; their positions are indicated by the red markers (Forward VRN, Reverse VRN; see Table 4.1 for details). BLAST interrogation of the Morex genome sequence (ICBS v2) identified five genes with over 93% homology: HORVU1Hr089840 (100%); HORVU3Hr 1G117890 (100%); HORVU6Hr1G084390 (100%); HORVU6Hr1G084390 (100%); HORVU6Hr1G021460 (93%); HORVU7Hr 1G052210 (96%).

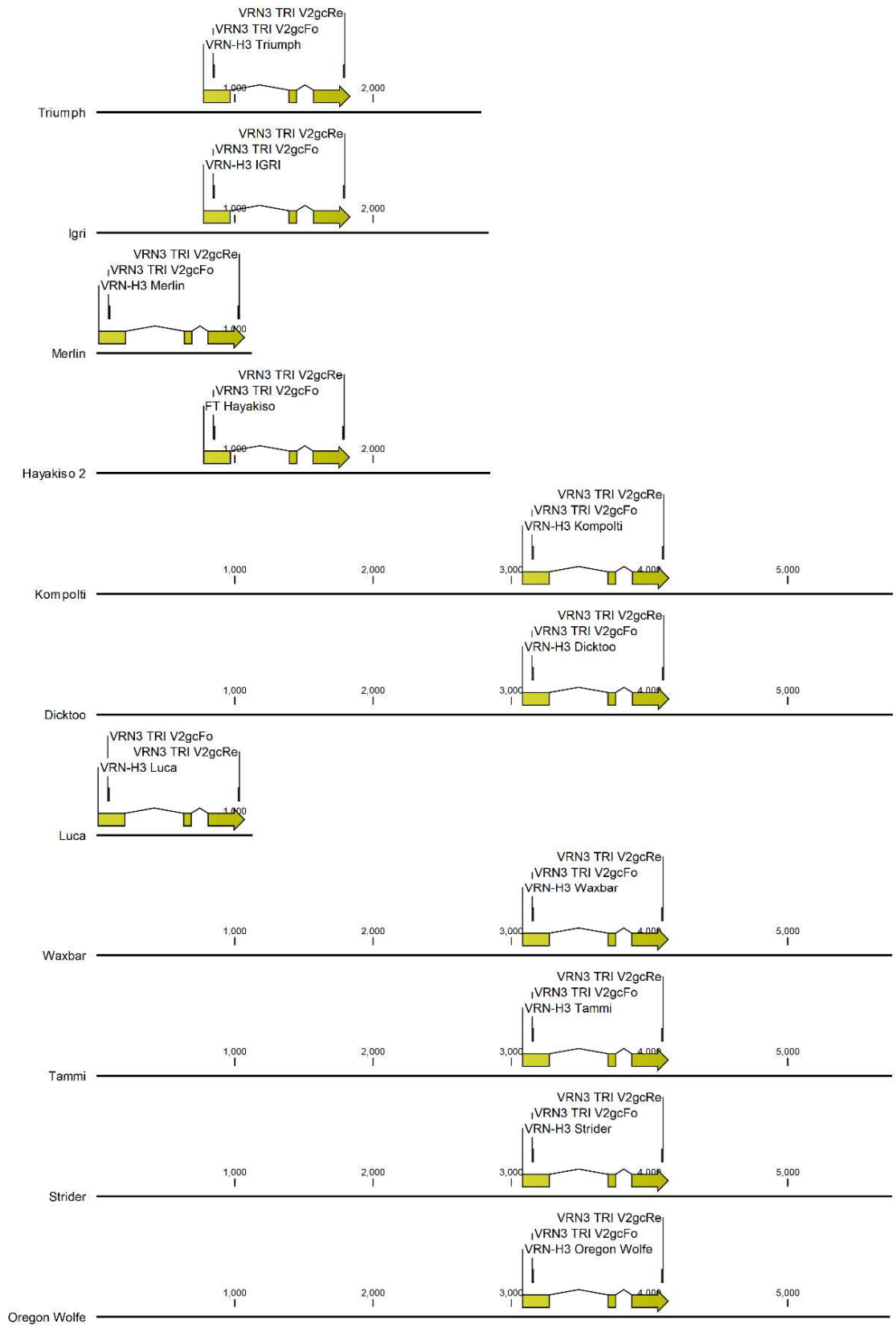


Figure 4.3. Gene Structure of *HvVRN3* Sequences from Eleven Barley Cultivars.

Eleven homologues of *HvVRN3* were deposited in the GenBank databases, and CLC Workbench CLUSTALW and Primer Design routines found regions of complete conservation in exon 1 and exon 3, which were suited to designing ‘universal’ PCR primers (*VRN3*TRI V2gcFo – Forward, and *VRN3* TRI V2gcRe – Reverse); their position is indicated by vertical red lines. The sequence of these primers, their empirically determined annealing temperatures, and the expected size of the gDNA and cDNA amplicons are given in Table 4.1. The solid black line represents the pre-mRNA sequence before processing, the numbers indicate bases from the transcriptional start site; and the yellow boxes are the exons with connecting zig-zag lines depicting introns. Figure A4.3 in the Appendix presents the full alignment for the predicted transcripts of these sequences.

Table 4.1: Summary of PCR Results for Cold Acclimation Sequences in Barley.

The table shows the empirically determined PCR primer annealing temperatures for each of the sequences indicated. Primers were designed either from the cultivar Morex genome sequence (*HvCBF* sequences) or from CLUSTALW alignments of cDNA sequences, taken from a range of cultivars and deposited in public data bases. The anticipated size of the products using a genomic or cDNA template is shown. Letter codes for cultivars (*cv*) indicate a product was successfully amplified from *cvs.* Belgravia (B) and California (C). Plus (+) signs indicate completion of each stage confirming amplicon authenticity; a cross (x) indicates failure at that stage.

Gene		Primers	Annealing Temperature (°C)	Estimated Size gDNA Template (bp)	Estimated Size cDNA Template (bp)	cv	Clone	Confirmed by Colony PCR	Confirmed by Sequencing
<i>HvACTIN</i>	For 5'	GCC GTG CTT TCC CTC TAT G	58	620	235bp	B, C	+	+	+
	Rev 5'	CAG GTC CAT CTC CCC TTA							
<i>HvCBF10A</i>	For 5'	CCT CTT CCA ACG AGA ACG CGT C	58,56,54	659	659bp	B, C	+	+	x
	Rev 5'	CCC GAA TTC TCC GTT ATC C							
<i>HvCBF15A</i>	For 5'	GCC GTC GTT GTC CTC TCA	59,57,55	642	642bp	B, C	+	+	+
	Rev 5'	CCA TCG GTA TCC CAG CAC							
<i>HvCBF 6A</i>	For 5'	AAC TAC TAC TAC TCG CCC TC	61	560	560bp	B, C	+	+	+
	Rev 5'	TAA AGG TCC CAT CCC ATG TC							
<i>HvCBF2C</i>	For 5'	GGG GGC AAG AGT ACA GGA	58	479	479	B, C	+	+	+
	Rev 5'	GGT GGG AAC GAT GGA GAG							
<i>HvCBF9</i>	For 5'	CAG CGG AGG CAG ATT ATT	55	282	282bp	B, C	+	+	+
	Rev 5'	GCC TGA AGA CAT GTA GAA CT							

Gene		Primers	Annealing Temperature (°C)	Estimated Size gDNA Template (bp)	Estimated Size cDNA Template (bp)	cv	Clone	Confirmed by Colony PCR	Confirmed by Sequencing
<i>HvCBF4B</i>	For 5'	ATG GAC GTC GCC GAC ATC GC	64,60,56	498	498	B, C	+	+	x
	Rev 5'	GCC GGA CGA GAT GTA AAA C							
<i>HvCBF14</i>	For 5'	CAC CGC TAA GGA GAT CAA G	58	235	235	B, C	+	+	+
	Rev 5'	CGA CTC TAT GAA CAT GCC C							
<i>HvCBF16</i>	For 5'	CTC AAC TTC CCC GAC TCC	58	279	279	B, C	+	+	+
	Rev 5'	CAG GTC CAT CTC CCC AGA							
<i>HvCBF3</i>	For 5'	CCT CAA CTT CGC CGA TTC	54	294	294	B, C	+	+	+
	Rev 5'	GGG AAC AAG TCA AGC CTG							
<i>HvCBF12C</i>	For 5'	TCA GCT CCC CTT CCT CAT CTA	56,53,50	314	314	B, C	+	+	+
	Rev 5'	GGA GTC CGG AAA GTT GAG							
<i>HvCBF6B</i>	For 5'	CAA GAA GGT CAA CCA GAC G	58	362	362	B, C	+	+	+
	Rev 5'	GCG CTG AAG GGT TAG ATG TTA							
<i>HvDHN5</i>	For 5'	AGA AGG GCG TCA TGG AAA A	60,57,54	271	271	B,C	+	+	x
	Rev 5'	CCG TAG GTC TCA GTG GTA T							
<i>HvCOR 14b</i>	For 5'	CTT CTT CTT CCG TGC TGC	62,60,58	528	424	B,C	+	+	+
	Rev 5'	CAT TTG CTC ACA TCC TCA AC							
<i>Hv CO 1</i>	For 5'	GCA AAA GGA GTA CGT AGA G	55,53,50	1302	289	B	+	+	+

Gene		Primers	Annealing Temperature (°C)	Estimated Size gDNA Template (bp)	Estimated Size cDNA Template (bp)	cv	Clone	Confirmed by Colony PCR	Confirmed by Sequencing
	Rev 5'	GAA GTG GTG TCT GAA GTG							
<i>HvVRN1</i>	For 5'	TAT GAG CGC TAC TCT TAT GC	57,55,53	1374	257	B,C	+	+	+
	Rev 5'	TGA AGC TCA GAA ATG GAT TCG							
<i>HvVRN2</i>	For 5'	CAT CAT CAC CAT CAT CAG	55,52,50	1455	444	C	+	+	+
	Rev 5'	GGA CTC GTA GCG GAT TTG							
<i>HvVRN3</i>	For 5'	GAA CCA CCA ACC TCA GG	57,55,52	960	427	C	+	+	+
	Rev 5'	CGC TGG CAG TTG AAG TA							

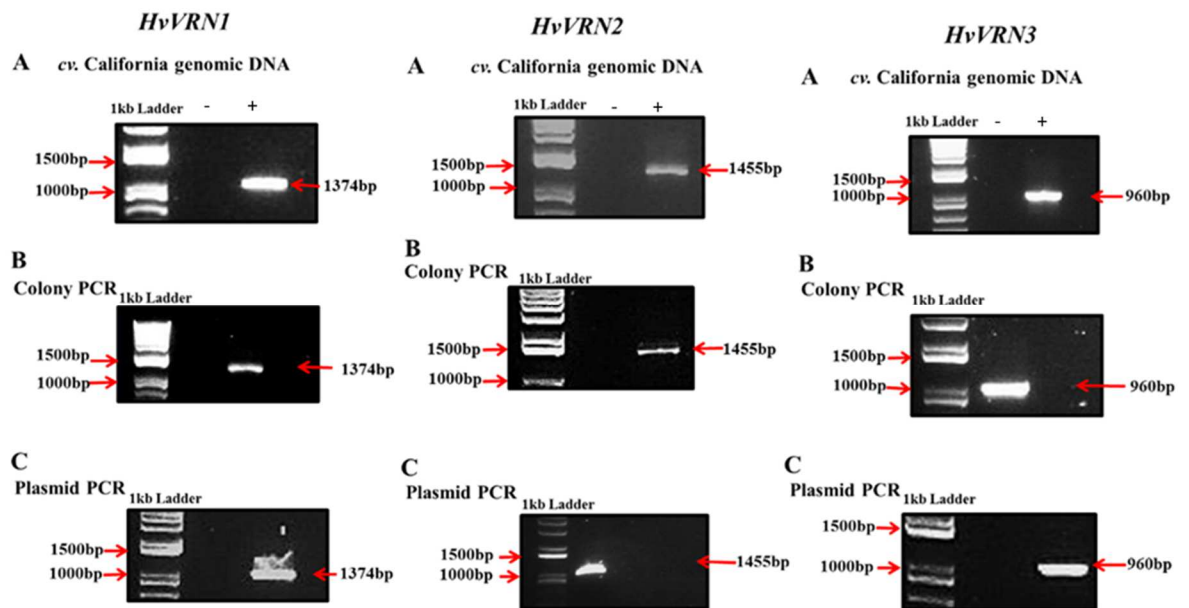


Figure 4.4: Agarose Gel Electrophoresis Images of the PCR Amplicons Generated for Barley *HvVRN1*, *HvVRN2* and *HvVRN3*.

The amplicons were generated from the *cv. California* gDNA template, and similar experiments were conducted using a template from *cv. Belgravia* (not presented). Panel A; shows direct amplification from *cv. California* gDNA template. Panel B; colony PCR of several biological replicates of gDNA amplicons, cloned into pTOPO2.3 and transformed into *E. coli* DH α . Panel C; amplicons generated using purified plasmid from colonies in Panel B prior to sequencing. The sizes of the amplicons were determined by sequencing, and are indicated on the right of each image. The + and - symbols indicate positive (plus gDNA template) and negative (no gDNA template) controls. The DNA size markers (1 kb ladder) in the left lane are 100, 200, 300, 400, 500, 650, 850, 1000, 1500, and 2000 bp.

4.3.2 PCR Primer Design for *HvActin*, *HvDHN5*, *HvCO1*, & *HvCOR14b*

A similar approach to that described above (Section 4.3.1) was used to design the PCR primer pairs for the four sequences.

A search of the GenBank using the ENTREZ portal using the criteria ‘Actin [All Fields] AND *Hordeum vulgare* [Organism]’ identified one accession (AY145451), but the cultivar was not specified. The accession is a 1,421bp mRNA, with a coding region of 1,133bp; there was no indication of introns. As no other barley actin genes were annotated in the GenBank database, PCR primer pairs were designed according to AY145451, and details of these primers are presented in Table 4.1. Preliminary experiments revealed the primers produced an amplicon of between 500 and 650bp when California gDNA was used as template (Fig 4.5). A similar result was found when gDNA from *cv. Belgravia* was used (data not

presented). Analysis of the AY145451 sequence, however, indicated that the amplicon should be 234bp (Fig A4.4, Appendix). It is conceivable this actin gene contains an intron of approximately 400bp between the forward and reverse primer sites, and if so, this would account for the discrepancy between the predicted and observed amplicon sizes. It was decided to clone the amplicon regardless, and then to confirm its origins by sequencing. Alignment of the amplicon sequence with AY145451 showed over 99% sequence identity in the regions where the two sequences overlapped, suggesting the *cv.* California and Belgravia contain homologues of AY145451 and do contain introns. Further, cDNA was prepared from leaf samples of both cultivars to serve as a template for the PCR primer pairs. Figure 4.4A shows an amplicon of approximately 230bp was generated, providing further evidence that these primers generate an amplicon from a barley actin gene containing an intron, making them suitable for quantitative PCR analysis.

A BLAST search of the Morex genome (ICBS v2) was performed using AY145451 as the query sequence. Only 1 gene showed significant homology at the DNA level (HORVU1Hr1G002840; 100% identity over approximately 800 bases), and a further 6 returned >83% identity (HORVU1Hr1G047440, HORVU3Hr1G083380, HORVU4Hr1G008310, HORVU5Hr1G000180, HORVU5Hr1G039850, HORVU5Hr1G117900). CLUSTALW alignments (using CLC Workbench) of AY145451 and HORVU1Hr1G002840, and of the 7 Morex homologues, are presented in Fig A4.4 (Appendix). Although HORVU1Hr1G002840 is the closest Morex homologue of the actin gene AY145451, there is sufficient sequence divergence to conclude they might be different loci. Furthermore, although there is clear sequence homology between the 7 Morex actin sequences, there is sufficient sequence divergence to conclude that they probably encode different proteins in the formation of microfilaments.

From these results it can be concluded that HORVU1Hr1G002840 on chromosome 1 is probably the Morex homologue of AY145451. Sequencing has therefore shown that amplicons of 620bp and 235bp can be generated from *cvs.* California and Belgravia when gDNA and cDNA are used as templates, and Fig 4.5 shows an amplicon of approximately 600bp was generated from the *cv.* California gDNA template. Moreover, an amplicon of approximately 250bp was generated using *cv.* California cDNA, and similar results were obtained when the template prepared from *cv.* Belgravia was used (data not presented). The sequencing of these amplicons confirmed their identity as an *HvActin* gene, with sizes of 630bp and 235bp from gDNA and cDNA template, respectively.

Interrogation of the GenBank database for the barley *COR14b* sequence identified only one accession (AJ512944, from *cv.* Aurea). BLAST interrogation of the barley Morex genome database (IBSC v2; http://plants.ensembl.org/Hordeum_vulgare/Info/Index) using the FASTA sequence file of AJ512944 identified just one sequence with extensive homology, HORVU2Hr1G099820 (E-val of 0.0) and therefore this gene on chromosome 2 appears to be the only COR14b homologue in barley. A graphical representation of the gene structure, and a CLUSTALW alignment of accession AJ512944 and HORV2Hr1G099820 is presented in Fig A4.5 (Appendix). Figure 4.6 presents the results from the preliminary PCR experiments. The results indicate that an amplicon of approximately 500bp was generated when the template used was gDNA from *cv.* California. The fragment was cloned and sequenced and found to be over 99% identical to a fragment from the AJ512944 sequence. These results confirmed the primer pair could be used to quantify the expression of *HvCOR14b* with quantitative RT-PCR.

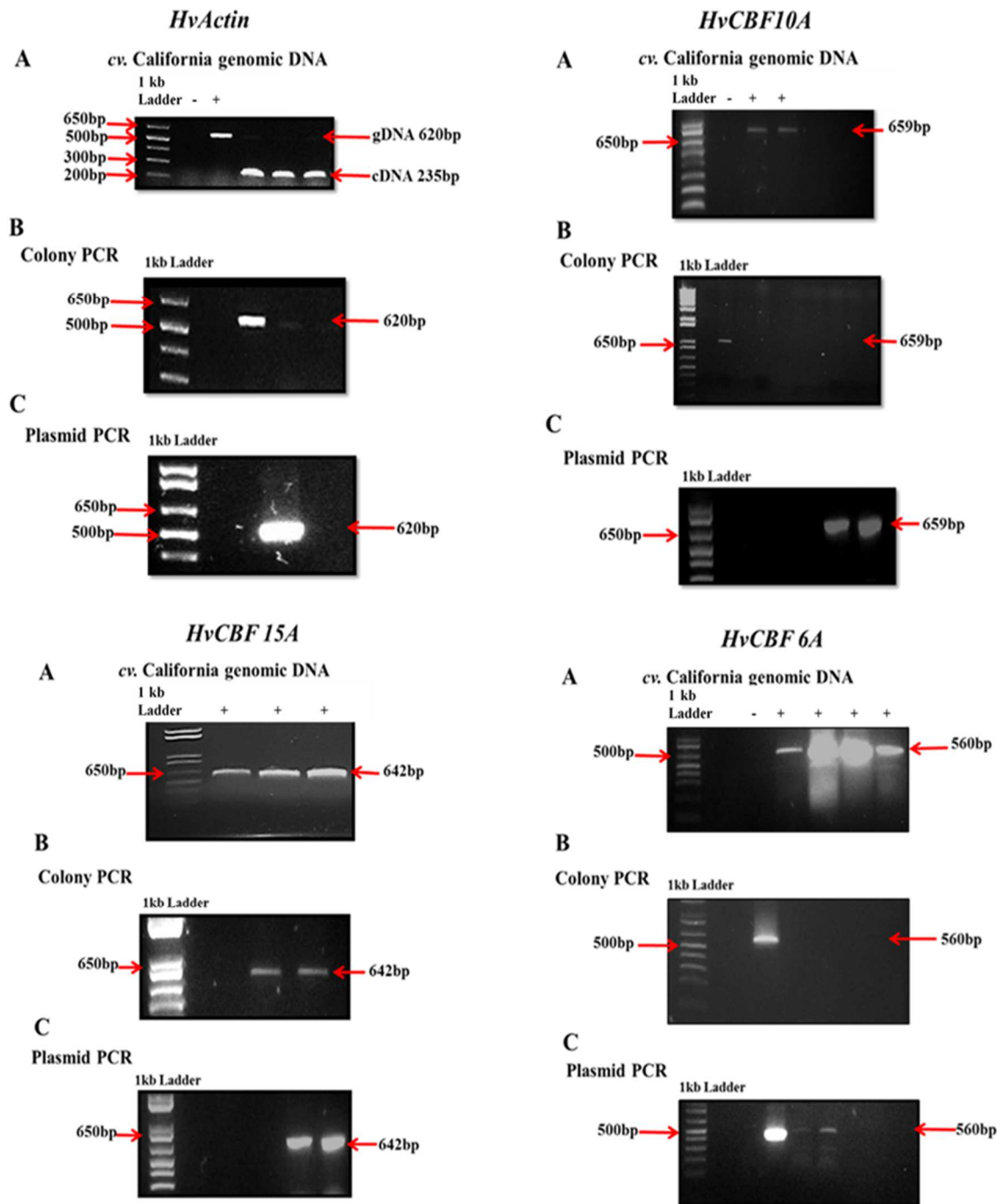


Figure 4.5: Agarose Gel Electrophoresis Images of the PCR Amplicons for Barley *HvActin*, *HvCBF10A*, *HvCBF15A*, and *HvCBF6A*.

Panel A; direct amplification from the *cv. California* gDNA template. Panel B; colony PCR of several biological replicates of gDNA amplicons cloned into pTOPO2.3 and transformed into *E. coli* DH α . Panel C; amplicons generated from purified plasmid from colonies in Panel B prior to sequencing. The sizes of the amplicons were determined by sequencing, and appear on the right of each image. The + and - symbols indicate positive (plus gDNA template) and negative (no gDNA template) controls. The DNA size markers (1 kb ladder) in the left lane are on the 100, 200, 300, 400, 500, 650, 850, 1000, 1500, and 2000 bp.

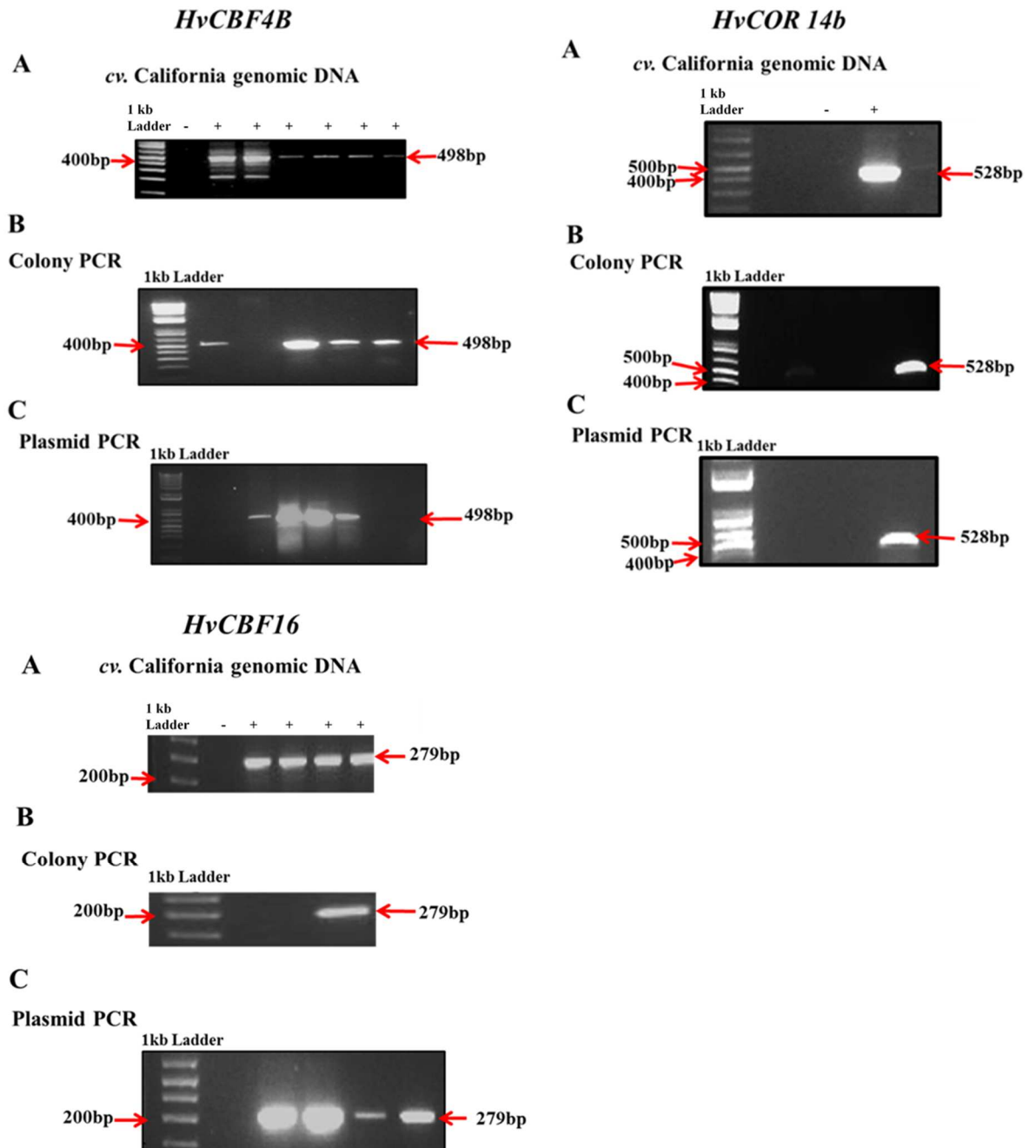


Figure 4.6: Agarose Gel Electrophoresis Images of PCR Amplicons of Barley *HvCBF4B*, *HvCOR14b*, and *HvCBF16*

Panel A; direct amplification from the *cv. California* gDNA template. The + and - symbols indicate positive (plus gDNA template) and negative (no gDNA template) controls. Panel B; colony PCR of several biological replicates of gDNA amplicons, cloned into pTOPO2.3 and transformed into *E. coli* DH α . Panel C; amplicons generated from purified plasmid from the colonies in Panel B prior to sequencing. The sizes of the amplicons were determined by sequencing and are indicated on the right of each image. The DNA size markers (1 kb ladder) in the left lane are on the 100, 200, 300, 400, 500, 650, 850, 1000, 1500, and 2000 bp.

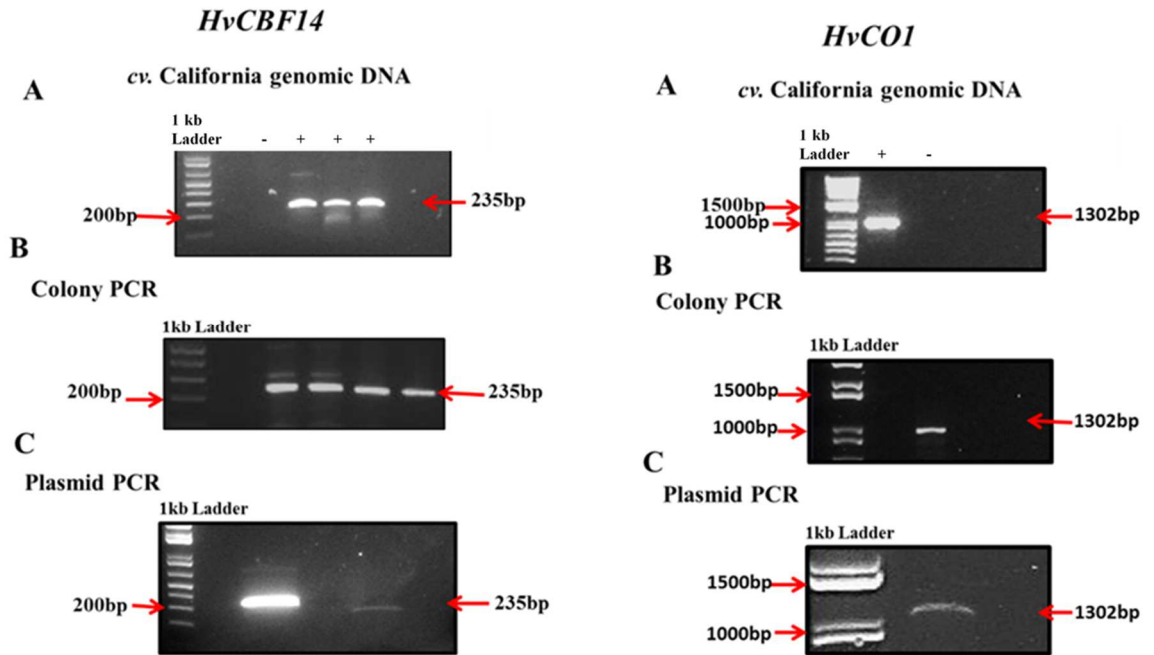


Figure 4.7: Agarose Gel Electrophoresis Images of the PCR Amplicons of Barley *HvCOR14b* and *HvCO1*.

The amplicons were generated from the *cv. California* gDNA template; similar experiments were conducted using a template from *cv. Belgravia* (not presented). Panel A; direct amplification from the *cv. California* gDNA template (3 or more biological replicates). Panel B; colony PCR of several biological replicates of gDNA amplicons cloned into pTOPO2.3 and transformed into *E. coli* DH α . Panel C; amplicon generated from purified plasmid prior to sequencing. The sizes of the amplicons were determined by sequencing, and are indicated on the right of each image. The DNA size markers (1 kb ladder) in the left lane are on the 100, 200, 300, 400, 500, 650, 850, 1000, 1500, and 2000 bp.

Interrogation of the GenBank database using the search criteria ‘CO1 [All Fields] OR CONSTANS1 [All Fields] AND *Hordeum vulgare* [Organism]’ returned two full length sequences: AF490468 (*cv. Morex*) and AF490467 (*cv. Igri*). The *HvCO1* gene appears to contain 1 intron and the CLUSTALW alignments of the *Morex* and *Igri* sequences were used to design suitable PCR primer pairs (CLC Workbench Primer Design routine). The chosen primers are presented in Table 4.1, and the predicted *HvCO1* gene structure and the CLUSTALW alignments are presented in Fig A4.6. The primers were then used with gDNA prepared from *cv. California* to generate an amplicon, and the results presented in Fig 4.7. A fragment of between 1,000 and 1,500bp was then generated which was then cloned and sequenced. Alignment of this sequence with the AF490467 and AF 490468 GenBank accessions showed over 95% sequence identity, providing confidence that the amplicon of 1302bp was the product of an authentic barley *CO1* gene.

In 2017, the GenBank database returned 5 full length accessions when the search criteria ‘Dehydrin [All Fields] AND Hordeum vulgare [Organism]’ was used (KC963076 (*HvDHN5*, *cv.* Steptoe), AF181454 (*HvDHN4*, *cv.* Morex), AF181455 (*HvDHN5*, *cv.* Morex), AF043096 (*HvDHN5*, *cv.* Dicktoo), and AF043089 (*HvDHN3*, *cv.* Dicktoo)). These sequences were aligned using the CLUSTALW (CLC Workbench) set at the default settings (Fig A4.7 Appendix). Three of these GenBank accessions were annotated as *DHN5*, with 1 *DHN4* and 1 *DHN3*. Forward and reverse primers were designed to achieve consensus with the *DHN5* sequences (CLC Workbench, Primer Design routine) as this was expected to increase the likelihood that the primers would be ‘universal’ and generate a product from *cv.* Belgravia and California (see Table 4.1). Figure 4.8 present the preliminary PCR results when these primers were used to generate amplicons from *cv.* California gDNA. A product of between 200 and 300bp was generated, cloned, and sequenced, and the result compared with the 3 *DHN5* sequences (KC963076, AF181455, AF043096). The amplicon was 271bp and showed low homology (<30%) with all 3 of the Morex *HvDHN5* sequences (Fig A4.7 Appendix). A BLAST search of the full Morex genome database (IBSC v2) indicated the closest match in the Morex genome in the 91bp region on chromosome 5 (chr5H; 378047602-378047692; 84.6% identical); no genes are indicated at this location on either strand. Amplicons of a similar size were generated when gDNA from *cv.* Belgravia was used as template. The failure to generate an authentic product for *HvDHN5* from either cultivar is disappointing. This may have been a result of sequence differences in the PCR primer binding sites (i.e. the presence of SNPs).

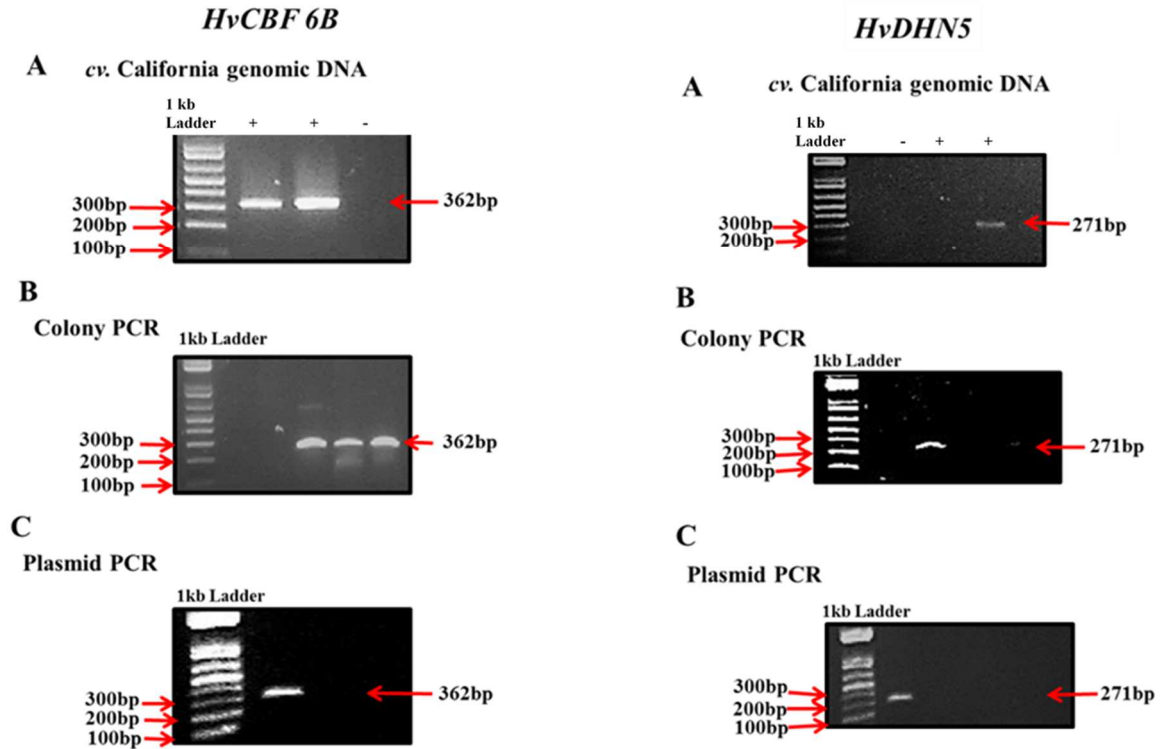


Figure 4.8: Agarose Gel Electrophoresis Images of the PCR Amplicons of Barley *HvCBF6B* and *HvDHN5*

The amplicons were generated from the *cv. California* gDNA template; similar experiments were conducted using a template from *cv. Belgravia* (not presented). Panel A; direct amplification from *cv. California* gDNA template (3 biological replicates). Panel B; colony PCR of 3 replicates of gDNA amplicons, cloned into pTOPO2.3 and transformed into *E. coli* DH α . Panel C; amplicon generated from purified plasmid prior to sequencing. The sizes of the amplicons were determined by sequencing, and are indicated on the right of each image. The + and – symbols indicate the presence or absence of the gDNA template in the PCR reactions. DNA size markers (1 kb ladder) are in the left lane; 100, 200, 300, 400, 500, 650, 850, 1000, 1500, and 2000 bp.

4.3.3 PCR Primer Design to the *CBF* Sequences in the Barley *FR2* Locus.

Section 1.14 reviewed the importance of the *FR2* locus in conferring cold tolerance to members of the Triticeae tribe, including barley. During the first Morex sequencing project (IBSC v1, 2012), sequencing BAC (Bacterial Artificial Chromosome, GenBank accession KF686739) was physically mapped to the approximate position of the genetic map of the *FR2* locus. The BAC contains 26 clones and 42 ordered pieces. Figure 4.8 presents the gene order and structure of the *CBF* genes in *FR2*; other genes in this accession, which do not encode *CBF* transcription factors have been removed to enhance clarity.

None of the *CBF* genes in the *FR2* locus are reported to contain introns, which simplifies the primer design process. Attempts were made to establish consensus sequences from different cultivars for each of the 13 Morex *CBF* genes encoded in this BAC, to assist in the design of ‘universal’ PCR primers to produce amplicons from *cvs.* California and Belgravia. The Morex sequence for each gene was used as a query sequence, to interrogate the GenBank database using the BLAST search tool. For each of the 13 genes, multiple sequences were returned from a variety of cultivars; however, it was not clear which were homologues of the *FR2* locus *CBF* gene. This made it difficult to establish a consensus sequence. After many attempts to generate authentic amplicons from *FR2 CBF* genes in *cvs.* California and Belgravia using ‘universal’ PCR primers, a new strategy was adopted. Primers were subsequently designed using the CLC Workbench Primer Design routine and Morex *CBF* sequences. The sequences of these primers are presented in Table 4.1. PCR experiments were undertaken, and after optimisation, amplicons of the expected size (*cf* Morex sequence) were generated from both *cvs.* California and Belgravia. Figures 4.5 – 4.8, & 4.10 presents the results from the preliminary PCR experiments and shows that amplicons could be generated from 11 of the *CBF* genes; note, no products could be generated from either *cv.* California or Belgravia gDNA template for *HvCBF2A* or *HvCBF12*. Amplicons from each of the 11 *HvCBF* genes were sequenced and the results used as BLAST query sequences to search the full Morex genome database (IBSC v2). In all cases the amplicons showed a strong homology with the intended target gene in the *FR2* locus (Table 4.2). These results suggest PCR primers which have been designed to amplify each of the *FR2 HvCBF* genes can be used to quantify changes in expression level while barley plants undergo cold acclimation.

With confirmation that gene-specific primer pairs could be used to amplify 14 (in Belgravia) or 15 (in California) authentic sequences reportedly involved in cold acclimation, cDNA samples (3 biological replicates) were prepared from each of the four acclimation treatments (LD/WT, LD/LT, SD/WT, SD/LT), at each of the five time points (0, 1, 2, 3 and 4 weeks). This was replicated for both cultivars.

Table 4.2 Morex Genome Location for Individual GenBank *HvCBF* Genes

A BAC sequencing clone deposited in the GenBank database (KF686739) is reported to span part of the barley *FR2* locus. In silico techniques were used to mask the gene structure and published (IBSC v1, 2012) along with a IBSC v1 index (MLOC_XXXXX) and a common gene name (*HvCBFx*). The second physical barley genome map (IBSC v2, 2017) uses a different index system (HORVUxHr1GXXXXXX). The table provides the new Morex gene index ID for the *HvCBF* genes encoded in KF686739. The direction of the arrows indicates the gene is encoded on the + or – strand. The % Identity column indicates the homology between the sequenced *cv.* California amplicon (used as the query sequence) and the closest Morex homologue (identified by BLAST searches of the IBSC v2 Morex full genome). Amplicons of the Morex *HvCBF12* homologue could not be cloned from cvs California or Belgravia.

Gene Name	Orientation	% Identity	IBSC Gene ID
<i>HvCBF9</i>	⇒	>99	HORVU5Hr1G080230
<i>HvCBF2C</i>	⇐	>99	HORVU5Hr1G080220
<i>HvCBF4B</i>	⇒	>99	HORVU5Hr1G080300
<i>HvCBF2A</i>	⇐	?	HORVU5Hr1G080310
<i>HvCBF12C</i>	⇒	99.7	HORVU5Hr1G080340
<i>HvCBF14</i>	⇐	99.1	HORVU5Hr1G080350
<i>HvCBF15A</i>	⇒	>99	HORVU5Hr1G080380
<i>HvCBF12</i>	⇐	?	?
<i>HvCBF16</i>	⇒	>99	HORVU5Hr1G080440
<i>HvCBF3</i>	⇒	>99	HORVU5Hr1G080420
<i>HvCBF6B</i>	⇒	>99	HORVU5Hr1G080390
<i>HvCBF10A</i>	⇒	>99	HORVU5Hr1G080430
<i>HvCBF6</i>	⇐	>99	HORVU5Hr1G080450

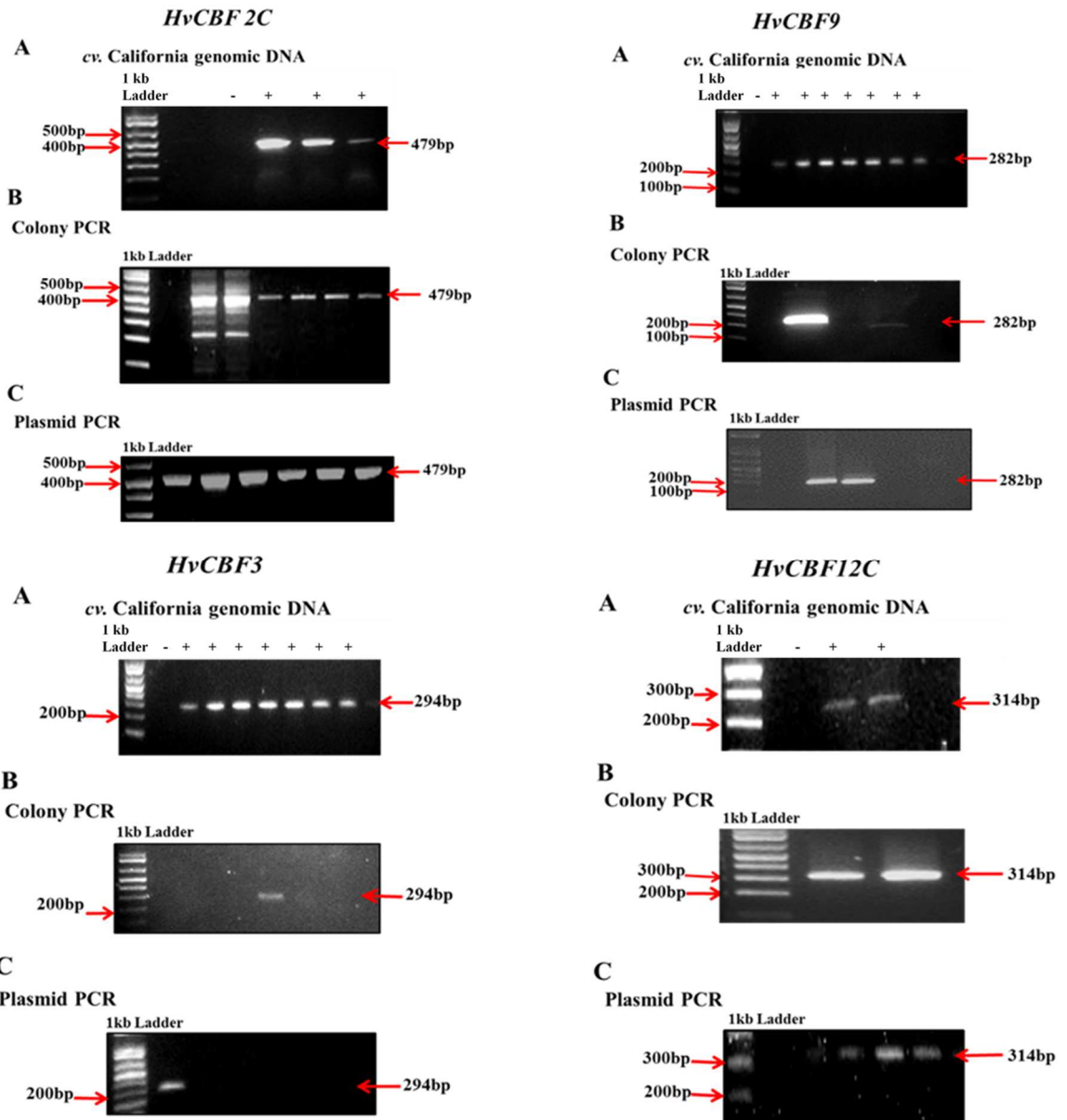


Figure 4.9: Agarose Gel Electrophoresis Images of the PCR Amplicons of Barley *HvCBF2C*, *HvCBF9*, *HvCBF3*, and *HvCBF12C*.

The amplicons were generated from the *cv. California* gDNA template; similar experiments were conducted using template from *cv. Belgravia* (not presented). Panel A; direct amplification from *cv. California* gDNA template (3 or more biological replicates). Panel B; colony PCR of several biological replicates of gDNA amplicons cloned into pTOPO2.3 and transformed into *E. coli* DH5 α . Panel C; amplicon generated from purified plasmid prior to sequencing. The sizes of the amplicons were determined by sequencing, and are indicated to the right of each image. The DNA size markers (1 kb ladder) in the left lane are on the 100, 200, 300, 400, 500, 650, 850, 1000, 1500, and 2000 bp.

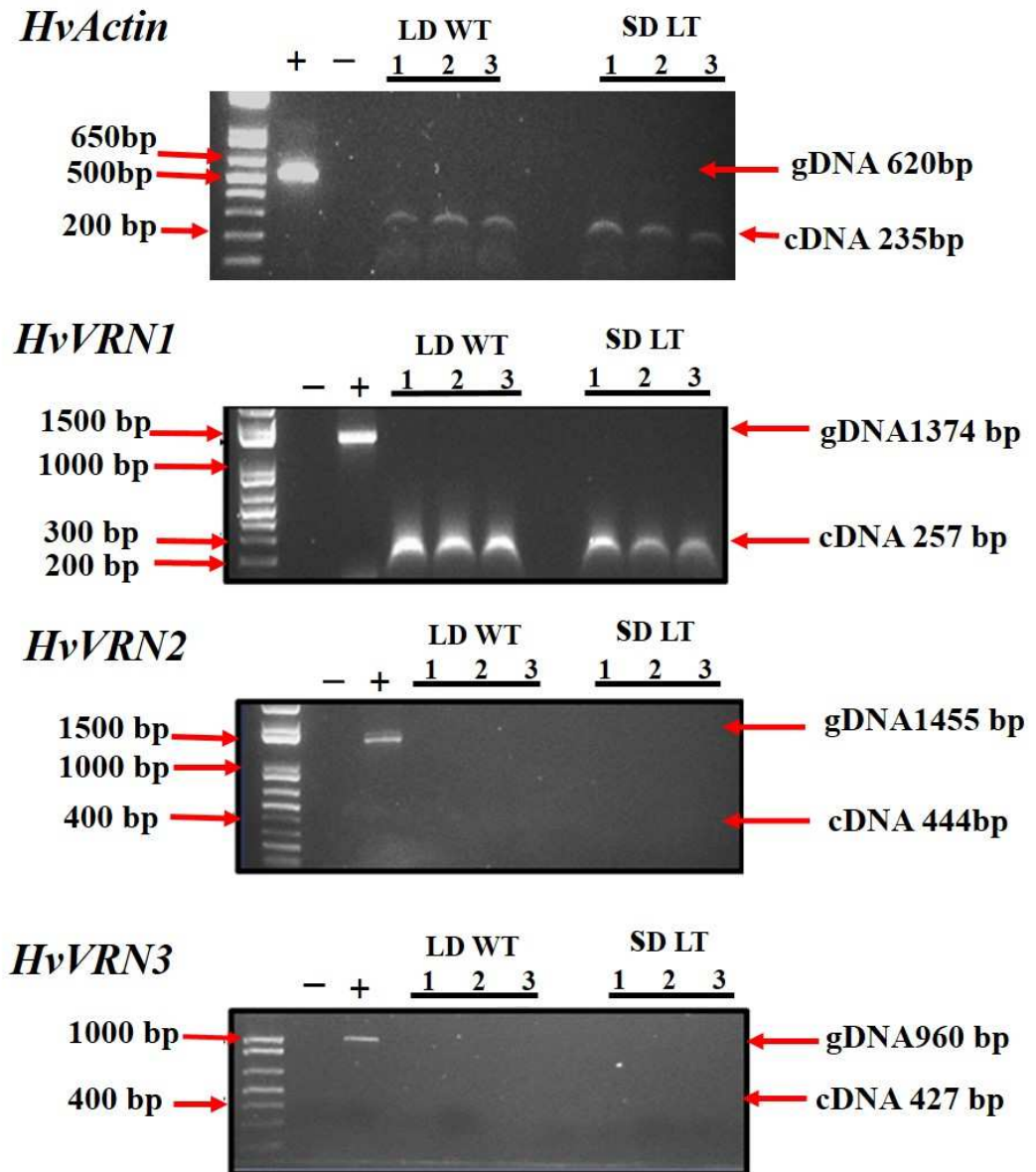


Figure 4.10: Semi-quantitative RT-PCR of *HvVRN1*, *HvVRN2*, and *HvVRN3* expression in Non-Acclimated and Cold-acclimated Leaves of Barley *cv.* California.

Plants were grown to the 3-week stage in non-acclimating conditions, before exposure to cold acclimation conditions for 2 weeks (SD/LT) or not (LD/WT), Section 2.1.1. RNA was extracted from 3 biological replicates and cDNA synthesised. PCR reactions were performed using gene-specific primers, and the conditions indicated (see Fig. 4.8). (+) indicates a positive control containing gDNA template, (-) indicates a negative control with no template. For the full experimental conditions see Section 2.4.5 to Section 2.5.2. The sizes of the gDNA and cDNA amplicons (from sequencing) are given on the right of the images; DNA size markers (1kb ladder) are shown on the left (100, 200, 300, 400, 500, 650, 850, 1000, 1500, 2000 and 3000 bp). The number codes 1, 2, and 3 indicate the replicated pools of cDNA used for the template (i.e. 1 indicates the same pool of cDNA as that used for each of the sequences). The volume of the template was adjusted to give a similar input level of cDNA, which was then confirmed by the intensity of the control *HvActin* bands.

4.4 Semi-Quantitative RT-PCR.

Plants of both cultivars, Belgravia and California, were germinated and grown in soil (Section 2.1.1) under Long Day (LD) and Warm Night Temperatures (WT) conditions for a period of three weeks; the conditions were a 15/9 hour photoperiod at 20/16°C day/night temperatures. Plants were then acclimated to the following conditions LD/WT, LD/LT, SD/WT, SD/LT (Short Days, SD were 9/15 hour day/night photoperiod; Low Temperatures, LT were 20/4 °C day/night temperatures) for a period lasting up to a further 4 weeks (i.e. plants up to 7 weeks old). Mature leaves were harvested two hours after dawn each week, at the 3, 4, 5, 6, and 7 week old stage (i.e. after 0, 1, 2, 3 and 4 weeks of acclimation) and stored at -80°C. Leaf material was then retrieved, and total RNA isolated using the phenol extraction method. Nucleic acid purity and abundance were assessed spectrophotometrically, and denaturing (RNA) gels were run to confirm that minimal degradation had occurred (Section 2.5.8). Total RNA was prepared for the three biological replicates for each treatment at each sampling time (3 replicates x 4 CA treatments x 5 weeks = 60 samples for each cultivar). In some cases, a PCR product of the expected size was generated (e.g. Table 4.1); however, in others, spurious bands or no bands at all were synthesised (data not presented). Due to the inconsistent quality of the cDNA generated, the experiment was scaled back to focus on generating good quality cDNA from plants acclimated for 2 weeks under the four conditions (i.e. 3 biological replicates x 4 treatments = 12 samples). For all the cDNA samples the primer pairs for *HvActin* generated fragments that produced strong bands of the expected size when analysed on agarose gels, providing assurance that good quality cDNA had been prepared.

The currently accepted model for the induction of cold tolerance in winter cereals predicts *HvVRN1* is not expressed in leaves in summer and autumn seasons (von Zitzewitz et al., 2005; Sasani et al., 2009), but begins to accumulate in winter with the onset of SD and LT. Figure 4.10 presents the results from the preliminary semi-quantitative RT-PCR (sqRT-PCR) experiments regarding cDNA samples using gene-specific primers for *HvVRN1*, *HvVRN2*, and *HvVRN3*. It is apparent from these results that *HvVRN1* is expressed in the leaves of non-acclimated plants (LD/WT) at a level similar to those exposed to SD/LT. Furthermore, in the non-acclimated winter line (LD/WT), the accepted model for the control of flowering in winter cereals suggests that *HvVRN3* expression is regulated by circadian clock-dependent transcription of two genes, a promoter flowering *HvCO1* and a suppressor of flowering *HvVRN2* (Galiba et al., 2009; Fowler et al., 2014). Figure 4.10 clearly shows the model is inconsistent with the data; the transcription of both *HvVRN2* and *HvVRN3*

remain low in both summer/autumn and early winter conditions. These findings suggest the accepted model for the induction of cold tolerance (and flowering) in *cv. California* requires revision, and the planned experiments for qRT-PCR on cold-regulated sequences in barley as based on the currently accepted model might prove premature.

For this reason, it was decided to undertake a full transcriptome profile of non-acclimated and cold acclimated leaves from *cv. California*, in order to better understand the cold acclimation process. These experiments are described in Section 2.1.1.

4.5 Evidence that *cv. California* is not a cold-tolerant winter barley

The finding that *cv. California*, a line described by Limagrain who developed and now distribute the germplasm, as their most cold-tolerant winter barley, does not trigger cold acclimation by the pathway described in the literature for winter lines, prompted an experiment to confirm if it can indeed be classified as a winter line (i.e. unable to flower in spring unless it has undergone a period of vernalization in winter). Plants of *cv. California* were sown in soil and grown for 3 weeks in LD/WT. Half the plants were then transferred to give SD/LT conditions for 5 weeks, to induce vernalization, and the remainder were kept in LD/WT. After this period all the plants were grown in LD/WT and permitted to flower.

Careful monitoring of the time to flowering in both sets of plants clearly showed all the plants flowered at approximately the same time (Data not shown). This indicates that *cv. California*, despite the claims by Limagrain, is a cold tolerant spring (i.e. a facultative) line, not a winter line. Undoubtedly, *California* is advertised and sold as a winter line, planted by farmers in the autumn and harvested the following summer; thus, in that sense it could be considered a winter line. From a genetic perspective, however, with no vernalization requirement for flowering, it is a facultative line. Little work on the induction of cold tolerance in spring or facultative cereals has been published to date. Consequently, it is not possible to compare these findings with those in the literature with regard to the expression pattern of VRN sequences in spring and facultative cultivars. Further work is required to fully characterise the genotype of *cv. California*. Notwithstanding these findings, it appears that winter and facultative lines might be equally cold tolerant, and the model developed to explain the induction of cold tolerance in winter lines may not apply to facultative 'winter' lines. This is a novel finding.

4.6 Discussion

The work described in this chapter was intended to characterise the role of *HvCBF* genes in conferring cold tolerance on a spring (*cv.* Belgravia) and a winter (*cv.* California) line, by investigating the effects of different combinations of photoperiod and night temperature on the activation of key CA sequences, including those encoded in the *FR1* and *FR2* loci. To do this, primers were designed to anneal to the target gene, and PCR performed on both gDNA and cDNA samples. The resulting fragments were cloned and then sequenced and 15 were confirmed as having been amplified from the intended target gene.

After robust PRC protocols were established for 15 of the sequences previously implicated in cold acclimation in cereals, preliminary experiments revealed some discrepancies with the published model which underpins the work described in this chapter. The model for the transcriptional induction of cold tolerance involving *HvVRN1* does not appear to apply for the commercial winter cultivar California (*HvVRN1* is expressed in both non-acclimated and cold acclimated leaves). In addition, neither *HvVRN2* or *HvVRN3* acclimated in leaves in the autumn cast doubt on the role of these sequences in cross-talk between CA and the flowering pathways. Furthermore, studies on the abundance of transcripts encoded at the *FR2* locus (*HvCBF* genes for example) generated inconsistent results, and the reasons for this are unclear. It is conceivable that the expression of these sequences is not tightly controlled by the cold acclimation conditions applied in this study.

Other factors that were not well controlled in these experiments might have affected expression, and accounted for the high variability observed between biological replicates. One obvious factor identified is the endogenous circadian rhythms present in leaf tissues. In the experiments presented here, care was taken to harvest the leaf tissue of a similar development stage two hours post dawn. Whilst this should minimise the extraneous factors that could affect gene expression, the duration and the different temperature during the night period are very likely to affect normal circadian rhythms, delaying some processes and accelerating others. Transition from a cool night (4°C) to a warm day (20°C) could lead to a delay in the onset of morning circadian rhythms that do not occur during the transition from a warm night (16°C). This may well culminate in very different patterns of gene expression two hours post dawn, which are wholly unrelated to the cold acclimation process.

Another possibility that could account for the inconsistent results is the sheer scale of the experiment, which introduced technical difficulties complicating the attainment of consistent results. Semi quantitative and qRT-PCR are techniques which are routinely used, and work

well for a relatively small number of genes on a relatively large number of cDNA samples. In the experiments reported here, the abundance of the 15 genes was screened in over 120 (3 replicates x 4 CA treatments x 5 time points) cDNA pools for the two cultivars.

The original intention was to gain some insight into the role of these 15 genes in the cold acclimation process. The strategy was to first compare the expression of each individual gene over time and between the CA treatments for each cultivar (3 x 4 x 5 = 60 cDNA pools for each cultivar), and then to compare the responses of the two cultivars. Finally, it was hoped that it would be possible to better understand the co-expression of two or more genes across time and treatment in the two cultivars. To achieve this aim, the amount of cDNA in each pool must first be standardised by performing actin PCR experiments. Once normalisation is achieved, the abundance of any gene can then be assessed between pools, enabling comparisons of transcript abundance across time, also in terms of CA treatment, and cultivar. In practice, to keep the workload manageable, one gene was assayed at a time (i.e. 60 different pools of cDNA from one cultivar were used at one time). In all cases, positive and negative gDNA template controls were run alongside the 60 cDNA template samples. However, it was not unusual for several of the cDNA pools to provide erratic results where the replicates produce one, two or no amplicons. One of the reasons for this was most likely 'contamination' of the primer stock solutions or of other PCR ingredients (as evidenced by the absence of a positive control gDNA band). Consultation with colleagues confirmed that it is not unusual when a large number of cDNA pools are used together. Regardless, wherever these failures occurred, several or sometimes all 60 of the samples had to be run again using fresh ingredients. Occasionally, failure was attributed to 'contamination' of the cDNA pools themselves (as evidenced by the presence of a positive gDNA control amplicon but no actin amplicon from the cDNA pool). Consequently, a fresh pool of cDNA was synthesised, and this used with the other pools in a repeat experiment of 60 samples. In theory, this approach should ensure progress; in practice the relatively few failures created a greater problem. A standard reaction to generate cDNA produces approximately 50 μ L of sample. Quantification of the cDNA concentration (using actin) indicated that between 0.5 and 3.0 μ L was required to generate a visible gel fragment; therefore, one standard pool of cDNA was sufficient to complete between 16 and 100 reactions. The lower number provided barely sufficient cDNA to assay all 15 genes, and if a failure occurred, a rapid depletion of the cDNA pools followed. Bulking-up the cDNA synthesis to produce pools of 250 μ L helped, but the problem remained a substantial one, frequently requiring re-normalisation, resulting in a further depletion of the cDNA pools.

One way around this problem would be to use qRT-PCR (quantitative RT-PCR), as normalisation is achieved for each sample. The original plan for this work was to first use sqRT-PCR to establish which transcriptional changes are likely to be important, and to then use the more expensive but robust qRT-PCR method to quantify changes. With 1,800 samples to assay, the cost would have been similar to those incurred with a transcriptome-wide analysis, such as RNA-Seq. The major advantage with transcriptome-wide methods is that changes in the levels of all transcripts are monitored, so not only the few key sequences reported in the literature are important. For these reasons, it was decided to abandon the work using sqRT-PCR and qRT-PCR and to use the RNA-Seq instead; this work is described in Chapter 5.

Chapter 5 Changes in Leaf Transcript Abundance Accompanying Barley Cold Acclimation

5.1 Introduction

As a result of the unexpected finding that the widely accepted model for the induction of the cold-acclimation process may not be applicable to barley *cv.* California (Chapters 3 and 4), the focus of the research was shifted toward a transcriptome-wide approach to obtain information on gene or sequence changes during the cold-acclimation process. A genome-wide approach using RNA-Seq analysis was expected to provide information on differential expressed genes (DEGs) in acclimated leaf tissue. The design of the experiments, the findings, and the discussion of the data are presented here in Chapter 5.

5.2 Acclimation Condition Experiment

To assess the role of cool night temperatures and photoperiod on the cold-acclimation process in winter barley, four acclimation regimes were chosen. These were coded Long Days/Warm Temperatures (LD/WT), Long Days/Low Temperatures (LD/LT), Short Days/Warm Temperatures (SD/WT), and Short Days/Low Temperatures (SD/LT). Samples exposed to LD/WT were used as non-acclimated controls; LD/LT and SD/WT were considered to be partially cold acclimated by cool night temperatures and photoperiod, respectively; SD/LT was considered to be fully acclimated. The experiments presented in Section 2.1.2 on the extent of cold acclimation (LT_{50} measurements) suggested that after 2 weeks' exposure the cold acclimation process had begun, but full resistance to freezing temperatures was not achieved for at least 4 weeks (Figs. 3.6 and 3.7). It is likely that during the cold-acclimation process there are many transient changes in gene expression and to gain a full understanding of these changes a range of time points, perhaps every 24 hours, should be used. With four experimental conditions, a minimum of three biological replicates per treatment, and the inclusion of multiple time points, the experiment would have been too cumbersome and costly to undertake in this study. For these reasons, it was decided to assess the effects of experimental conditions on changes in the gene expression profiles after 2 weeks of exposure.

5.2.1 Plant Treatment and RNA Preparation

Three biological replicates were prepared from frozen mature leaf tissue of 5-week old plants of winter barley (*cv.* California) treated for 2 weeks under the four cold-acclimation regimes (4 x 3 = 12 samples). Purified total RNA was prepared using a Qiagen Plant RNEasy Mini Kit and contaminating DNA removed using an Ambicon RNase-Free DNase Kit, according to the manufacturer's instructions (Section 2.4.3). The quality and quantity of RNA was assessed by running samples on a denaturing gel to assess the integrity of ribosomal bands, and through spectrophotometric analysis (Section 2.4). Samples were kept frozen at -80°C until required, and then sent to the Glasgow Polyomics Facility at the University of Glasgow for processing.

5.2.2 Development of RNA-Seq Analysis Protocols for Barley

A quality assurance (QA) assessment was first carried out on all samples to ensure the RNA was of sufficient quality for sequencing. This was achieved using an Agilent 2100 Bioanalyser, which performs capillary electrophoresis on samples to separate fragments according to size. A typical electrophoretogram is presented (Fig. 5.1), which shows the expected clear 25S, 23S, 18S, and 16S ribosomal bands from green plant tissues and no evidence of small RNA fragments, providing confidence of minimal RNA degradation. An RIN (RNA integrity number) value was also generated; RINs range from 0 (total degradation) to 10 (completely intact), and values of over 7 are normally required for sequencing. Initially, several samples failed this QA test and consequently fresh samples were prepared. Table 5.1 presents the QA data for the samples that were subsequently sequenced.

Although there are well-established protocols for high-throughput sequencing (NGS) of samples from many organisms, at the time of writing there were no established methods for quantifying gene expression levels in barley or with downstream robust processing of the sequence data. This is, in part, due to the large genome size of barley (5.3 Gb, roughly 40 times larger than *Arabidopsis*) containing approximately 39,000 genes (*cf.* *Arabidopsis* with 27,000 genes). The computing power required to analyse large genomes increases exponentially with genome size, and methods developed for organisms with smaller genomes become cumbersome when applied to organisms such as barley. Another reason that well-established methods for analysing RNA-Seq data have (until very recently) not

been developed is the lack of a reliable, fully annotated physical map of the barley genome. The first physical map was published in 2012 by the International Barley Sequencing Consortium (IBSC, 2012), but it contains many errors and almost completely lacks annotation. All of the experiments reported in this chapter were first analysed using this map. After completion of this analysis, the IBSC published a second independent map at the end of 2017 (IBSC, 2017). Consequently, the data from all experiments was analysed a second time, in 2018. By mid-2019, significant gene ontology annotation had been added to the map, providing a much more useful resource. The results presented in this chapter were compiled using the 2017 (V2) map and annotated in August 2019.

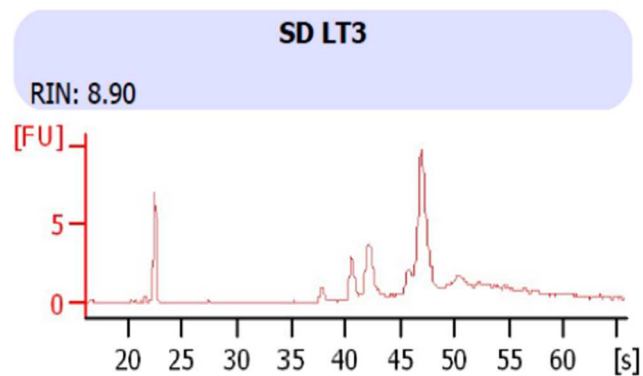


Figure 5.1: Barley Total RNA Electrophoretogram from Agilent 2100 Bioanalyser.

The electrophoretogram shows RNA fluorescence (arbitrary units) eluting from the capillary with time (in seconds). The peak at 23s is a standard marker that is added to each sample. The peaks at ~37s, 41s, 43s, and 47s are the 16S, 18S, 23S, and 25S ribosomal subunits, respectively, found in green higher plant tissues. The disperse ‘hump’ appearing between 40s and 65s is considered to be mRNA and ideally should not be degraded. Any RNA breakdown results in a deterioration of the ribosomal peaks and an appearance of fragments (‘noise’) in the trace between 23s and 38s (not apparent in this sample). The RIN value is calculated by the instrument based on the integrity of the ribosomal bands and the appearance of low molecular weight fragments. RIN values range from 0 (totally fragmented) to 10 (completely intact); values of over 7.0 are considered suitable for RNA-Seq analysis.

Table 5.1: Summary of Sample RNA Quality (RIN Number).

Total RNA was prepared and sent for quality control analysis by an Agilent 2100 Bioanalyser. For each sample, an analysis of RNA fragment size was performed using capillary electrophoresis and a RNA integrity number (RIN) was calculated. Samples with values over 7.0 are considered ‘good’ and suitable for sequencing. All the treatments produced samples with some RNA degradation, but this was particularly problematic with the non-acclimated controls (LD/WT). # indicates the replicate independent sample number; and the numbers in parentheses indicate the number of extractions required to obtain good quality RNA.

Sample Name	RIN Number	Sample Name	RIN Number
LD-WT		SD-WT	
#1 (2)	8.40	#1 (1)	8.10
#2 (3)	8.40	#2 (2)	8.20
#3 (4)	8.10	#3 (3)	8.00
LD-LT		SD-LT	
#1 (1)	8.80	#1 (1)	8.50
#2 (2)	8.70	#2 (2)	8.40
#3 (3)	8.60	#3 (3)	8.90

5.2.3 cDNA synthesis

In the next step, complementary DNA (cDNA) was generated from RNA samples that passed the QA tests using a TruSeq RNA Transcription Kit, and paired-end sequencing was performed using an Illumina NextSeq™ 500 platform (Section 2.6). Files containing the raw cDNA reads (75 bp) were then provided by the Glasgow Polyomics Facility and further analysed using the Glasgow University Galaxy Server (see Section 5.2.4).

5.2.4 Analyses of Data Quality from RNA-Seq Data Sets

As no customised methods were available for barley RNA-Seq analysis, all protocols had to be developed ‘in-house’. A pipeline was written on the University of Glasgow Galaxy server to download the barley genome (V2) and perform the range of data manipulations that are required to analyse the RNA-Seq datasets. A graphical representation of this pipeline is presented in Figure 5.2, and a brief description of these procedures follows.

The 12 forward and 12 reverse Illumina output ‘readfiles’ were provided in Fastqcsanger format and pooled into two data bins (Raw Barley forward reads, R1; Raw Barley reverse reads, R2; see Fig. 5.2). The datasets in these bins were then tested twice for read quality using the FastQC package (<https://www.bioinformatics.babraham.ac.uk/projects/fastqc/>) – once using the raw data, and once after ambiguous/poor quality sequences were trimmed from the 75 bp reads using the Trim Galore package (www.bioinformatics.babraham.ac.uk/projects/trim_galore/).

Comparison of the two FastQC output files allowed an assessment of whether trimming (i.e., to produce shorter, less ambiguous sequences) improved the dataset or whether the raw data (longer, more ambiguous sequences) would provide more useful information (Fig. 5.2).

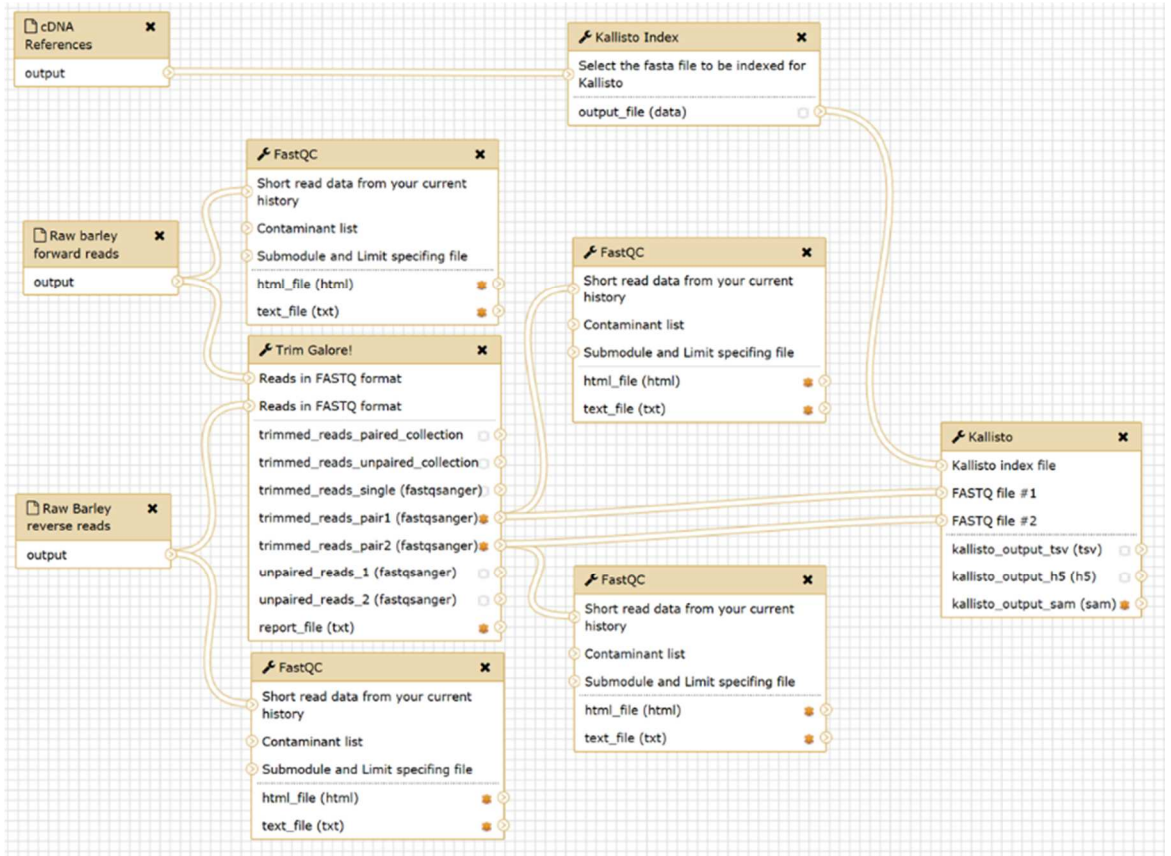


Figure 5.2: Workflow for Automated Quality Control and Kallisto Alignment of Barley (*cv.* California) RNA-Seq Reads to the Barley (*cv.* Morex) cDNA Library.

Paired-end reads were collected and used as input for FastQC to assess the quality of data. In addition, the same raw data files were used as input for Trim Galore to remove sequencing ambiguities and sequencing primers at the ends of the reads; the output from Trim Galore was then re-assessed by FastQC to confirm improvements. The barley cDNA reference genome (*Hordeum vulgare*.Hv_IBSC_PGSA-v2.cdna.all.fa) containing 63.7 Mb of sequences was used for alignment of the pooled reads of all forward and reverse replicates and treatments to generate a Kallisto index file of all expressed sequences. The forward (R1) and reverse (R2) output files from Trim Galore for each of the experimental treatments and their replicates, along with the Kallisto index file, were then used as input for Kallisto to generate paired statistics relating to the abundance of each sequence in each of the experimental treatments.

In all cases, improvements were observed after trimming and, consequently, the trimmed files were analysed further. A summary of the basic statistical analysis performed by FastQC on each of the 24 data files is presented in Table 5.2, and some graphical output is provided in Appendix A5.7.

There were between 28.4 and 52.3 million paired-end reads in the samples. Trim Galore removed between 0.24 and 1.5 million reads (compare the '.fastq' and '_trimmed' files for each replicate; Table 5.2); none of the reads were considered 'poor quality', although some were masked and sequences removed so that only partial reads (sequence length) were used in the subsequent alignments.

The quality of the reads can be visualised from the FastQC graphical output and typical outputs from a good (R1) and poorer (R2) quality dataset are presented in the Appendix A5.1. The 'per base sequence quality' plot indicated that the 'forward' (R1) reads were always of better quality than the reverse reads (R2); this is a general rule for paired-end sequencing. Figure A5.1 shows an example of the average quality of each base (from 1–75) in a dataset of approximately 49.3 million reads (Table 5.2) from a high quality (SD-WT3 R1) and poorer quality (SD-WT3 R2) dataset. A value of 36 is considered a perfect sequence (where all 75 bases are usable); a score of above 20 is usable sequence. The 'whisker and box' plots represent the middle two quartiles (50% of values, yellow box); the horizontal red line is the median value. The whiskers show the lowest 10% to 90% range of values, and the blue line is the average. For the forward (R1) reads, over 90% had scores of over 32, up to base 64, but even above this only a small percentage of bases had scores below 28. This is again reflected in the 'Per sequence quality scores' plot (Fig A5.2). There was little ambiguity with base calling, as the 'Per base N content' plot showed a very low percentage level of N (base) calling and no biasing across the 75 base reads. The 'Adapter content' plot (Fig A5.3) shows little contamination of the reads with the PCR primer adapters ligated to either end of the cDNA molecules, at least for bases 1–63, providing further confidence that the datasets were of good quality. Of more concern, however, are the 'Per base sequence content', 'Per sequence GC content', 'Sequence duplication levels', and 'K-mer content' plots (Fig A5.4 - Fig A5.7). The 'Per base sequence content' plot (Fig A5.7) should have generated near-parallel lines for each of the four bases at each of the positions in the reads, indicating no positional bias. It is clear, however, that this is not the case for bases 1–10, indicating that the ends of these forward reads may require some further trimming to remove any bias. This is further highlighted in the 'K-mer content' plot (Fig A5.6), which again

indicates the presence of repetitive sequences at the ends of some of the 75 bp cDNA fragments. The ‘Sequence duplication levels’ plot (Fig A5.7) indicated that the removal of some repetitive sequences would improve the dataset (red line), and this option was subsequently selected. Overall, the FastQC analysis indicated that the data are of very good quality, but may benefit from further trimming of the ends to remove some of the issues highlighted above.

To summarise, there were between 28.4 and 52.3 million paired-end reads in the samples. Trim Galore removed between 0.24 and 1.5 million reads (compare ‘.fastq’ and ‘_trimmed’ files for each replicate) so that none of the reads were considered poor quality, although some of the sequences were masked and only partial reads (sequence length) were used in the subsequent alignments.

5.2.5 Alignment of RNA-Seq Datasets with Barley cDNA Library: Kallisto Pseudo-Alignment of Reads

After quality control of the data files, the next stage in the analysis pipeline was to align each of the trimmed reads (circa 800 million per experiment) to the barley genome. Until recently, this has been achieved by aligning to the full genome sequence using alignment tools such as HiSAT2 (Kim et al., 2015); however, with large genomes such as barley (5.3 Gb) containing repetitive sequences, this approach requires huge computational resources, is time consuming, and prone to errors. For these reasons, it was decided to align the reads to a barley cDNA library (63.7 Mb) rather than the full barley genome (IBSC, 2017). This approach should reduce the ambiguities that might arise from repetitive sequences and greatly reduce the computing resources required. To achieve alignment to the barley cDNA reference library, the Kallisto package was used (Bray et al., 2016). Kallisto quantifies the abundances of transcripts from RNA-Seq data or other high-throughput sequencing technologies using ‘pseudoalignments’ to rapidly determine the compatibility of reads with target cDNAs. Kallisto first pools all of the reads in an experiment, regardless of treatment, and aligns each of the reads to the cDNA reference genome (IBSC, 2017) to generate a Kallisto index (or expression) file (Fig. 5.2); this is a list of all detected sequences in the experiment. Once this has been achieved, the reads in each of the replicate datasets are aligned to the full length cDNAs in the compiled Kallisto index file, and counts for each gene are recorded in each dataset. It has been estimated that with standard RNA-Seq data,

Kallisto can quantify 30 million reads of higher eukaryote sequences in less than 3 minutes on a desktop computer, and generation of the Kallisto index file takes approximately 10 minutes (Bray et al., 2016). The barley cDNA reference genome (*Hordeum_vulgare.Hv_IBSC_PGSSB-v2.cdna.all.fa*) was downloaded from the Ensembl Plants portal ([ftp://ftp.ensemblgenomes.org/pub/plants /release-38/fasta/hordeum_vulgare/cdna/](ftp://ftp.ensemblgenomes.org/pub/plants/release-38/fasta/hordeum_vulgare/cdna/)). This resource was made available by the International Barley Sequencing Consortium and curated in the Plant Genomes and Systems Biology database at Gatersleben, Germany (IBSC, 2017).

Table 5.2: FastQC Basic Statistics of High-Throughput Sequencing Data Sets from Barley Leaves Cold Adapted for 2 Weeks.

The Forward (R1) and Reverse (R2) output files from Trim Galore! for each of the experimental treatments and their replicates. Long Days (LD), Short Days (SD), Warm Nights (WT), Cool Nights (LT). Between 28.4 to 52.3 million paired end reads were made in the samples. Trim Galore! removed between 0.24 and 1.5 million reads (compare the ‘.fastq’ and ‘_trimmed’ files for each replicate;); none of the reads were considered ‘Poor Quality’ although some were masked and sequence removed so that only partial reads (Sequence Length) were used in the subsequent alignments. See text for full details.

Filename	Total Sequences	Poor Quality Sequences	Sequence Length	%GC
LD-LT1_R1.fastq	31651894	0	35-75	53
LD-LT1_R1_trimmed	30653685	0	20-75	53
LD-LT1_R2.fastq	31651894	0	35-75	55
LD-LT1_R2_trimmed	30653685	0	20-75	54
LD-LT2_R1.fastq	29921224	0	35-75	52
LD-LT2_R1_trimmed	28406465	0	20-75	52
LD-LT2_R2.fastq	29921224	0	35-75	54
LD-LT2_R2_trimmed	28406465	0	20-75	54
LD-LT3_R1.fastq	47349439	0	75	53
LD-LT3_R1_trimmed	46866974	0	20-75	53
LD-LT3_R2.fastq	47349439	0	75	55
LD-LT3_R2_trimmed	46866974	0	20-75	55
LD-WT1_R1.fastq	29737204	0	35-75	54
LD-WT1_R1_trimmed	28675826	0	20-75	54
LD-WT1_R2.fastq	29737204	0	35-75	56
LD-WT1_R2_trimmed	28675826	0	20-75	56
LD-WT2_R1.fastq	31198124	0	35-75	55
LD-WT2_R1_trimmed	30045813	0	20-75	55
LD-WT2_R2.fastq	31198124	0	35-75	57
LD-WT2_R2_trimmed	30045813	0	20-75	57
LD-WT3_R1.fastq	52303379	0	75	53
LD-WT3_R1_trimmed	51733013	0	20-75	53
LD-WT3_R2.fastq	52303379	0	75	55
LD-WT3_R2_trimmed	51733013	0	20-75	55
SD-LT1_R1.fastq	29317914	0	35-75	51
SD-LT1_R1_trimmed	28382924	0	20-75	51
SD-LT1_R2.fastq	29317914	0	35-75	52
SD-LT1_R2_trimmed	28382924	0	20-75	52
SD-LT2_R1.fastq	31688736	0	35-75	55
SD-LT2_R1_trimmed	31073180	0	20-75	55
SD-LT2_R2.fastq	31688736	0	35-75	56
SD-LT2_R2_trimmed	31073180	0	20-75	56
SD-LT3_R1.fastq	49733691	0	75	53
SD-LT3_R1_trimmed	49198311	0	20-75	53
SD-LT3_R2.fastq	49733691	0	75	55
SD-LT3_R2_trimmed	49198311	0	20-75	55
SD-WT1_R1.fastq	30679449	0	35-75	51
SD-WT1_R1_trimmed	29511744	0	20-75	51
SD-WT1_R2.fastq	30679449	0	35-75	53
SD-WT1_R2_trimmed	29511744	0	20-75	53
SD-WT2_R1.fastq	29638082	0	35-75	53
SD-WT2_R1_trimmed	28798947	0	20-75	53
SD-WT2_R2.fastq	29638082	0	35-75	54
SD-WT2_R2_trimmed	28798947	0	20-75	54
SD-WT3_R1.fastq	49269494	0	75	52
SD-WT3_R1_trimmed	49025470	0	20-75	52
SD-WT3_R2.fastq	49269494	0	75	54
SD-WT3_R2_trimmed	49025470	0	20-75	54

5.2.5.1 Statistical Analysis of Experimental Treatments

Kallisto generated tab-separated variable (.tsv) output files for each of the experimental treatment replicates based on the forward (R1) and reverse (R2) reads for each replicate. These .tsv files were then analysed using the DESeq2 package to resolve statistical patterns of changes in the transcript profiles between the experimental cold-acclimation treatments (Love et al., 2014). The DESeq2 package and submodules were downloaded from the BioConductor portal (<https://bioconductor.org/packages/release/bioc/html/DESeq2.html>), incorporated into R-script and run through R-Studio on a laptop computer. DESeq2 was set up to make pair-wise comparisons between each of the four treatments (LD/WT, LD/LT, SD/WT, SD/LT), a total of six pair-wise contrasts, and to generate abundance changes and adjusted statistical probabilities for each gene. DESeq2 output is in the form of comma-separated variable (.csv) files, which can be imported into Microsoft Excel for further analysis. In addition, several other calculations/plots were created for each of these comparisons: two-dimensional Principal Component Analysis (PCA), gene dispersion plots, gene standard deviation plots, heatmaps of gene expression (consistency in expression level across replicates), volcano plots (p-value versus expression level), and gene plots (expression change versus average abundance). Some examples of these are presented in Appendix A5.

Table 5.3 presents a summary of the statistical analysis performed by DESeq2. There was evidence that reads for 39,809 unique sequences were detected by Kallisto amongst the 12 pooled samples and these sequences constituted the Kallisto index file (Fig. 5.2), but the presence of many of these was found in only one of the replicates, or they were recorded at very low abundance (< 0 BaseMean, a measure of transcript abundance in any sample) and their reliability was uncertain. Nonetheless, these sequences were included in further analyses. With four acclimation treatments, DESeq2 generated six pair-wise gene comparison tables (.csv files). These datasets were then filtered in Microsoft Excel using the following criteria:

- Selection for significant changes between the two treatments using the default Benjamini-Hochberg adjusted p-value ($p_{adj} < 0.1$); this compensates for the increased uncertainty incurred when making multiple sequence comparisons between two treatments.

- Removal of sequences with a low BaseMean score. The BaseMean score is a measure of the normalised abundance of a gene across all treatments in a pair-wise comparison that compensates for differences in sequencing depth. It is calculated as $\log_2\text{FoldChange}/\log_2\text{FoldSE}$. Genes for which the BaseMean score was too low to generate a $\log_2\text{FoldChange}$ were deleted from the list (BaseMean >1.0).
- Selection of significant sequences ($p_{\text{adj}} < 0.1$) showing a >2-fold, >5-fold, and >10-fold *increase* in abundance in the cold-acclimated samples over the non- or partially-acclimated samples.
- Selection of significant sequences ($p_{\text{adj}} < 0.1$) showing a >2-fold, >5-fold, and >10-fold *decrease* in abundance in the cold-acclimated samples over the non- or partially-acclimated samples.

Table 5.3: Summary of DESeq2 Pair-wise Treatment Comparisons for Expressed Genes in *Hordeum vulgare* (cv. California) Leaves Exposed for 2 Weeks to Different Cold-Acclimation Conditions.

RNA-Seq analysis was performed on three independent biological replicates from mature barley leaves exposed to four cold acclimation conditions for 2 weeks (Section 2.1.1). Tables of the normalised abundance for each detected gene in each of the replicates were generated by DESeq2 as .csv files, which were then filtered in Microsoft Excel. The number of genes with significantly different abundances ($p_{\text{adj}} < 0.1$, Benjamini-Hochberg correction) is presented. The other columns present the number of significantly differentially abundant genes at the 2-fold, 5-fold, and 10-fold levels. ‘Upregulated’ refers to genes that were higher in the more cold-acclimated samples (SD/LT > LD/LT > SD/WT > LD/WT). LD, Long Days; SD, Short Days; WT, Warm Night Temperatures; LT, Low Night Temperatures. See Section 2.1.1 for full experimental conditions.

	#Genes	Significant	Up-regulated >2x	Up-regulated 5x	Up-regulated 10x	Down-regulated 2x	Down-regulated 5x	Down-regulated 10x
LDWT v LDLT	30,912	474	291	36	2	110	3	1
LDLT v SDLT	30,912	87	71	1	0	10	0	0
SDWT v LDLT	30,912	81	54	14	1	18	1	0
LDWT v SDLT	30,912	93	52	11	1	30	6	1
LDWT v SDWT	30,912	6	2	0	0	3	1	0
SDWT v SDLT	30,912	42	37	20	0	3	0	0

Figure 5.3 presents a two-dimensional PCA plot that provides a visual summary of the covariance between the samples. Normally, it is expected that replicates receiving the same treatment would cluster in the same region of the graph, and ideally it is hoped the clustering arises from the applied treatments. Figure 5.3 has identified an experimental factor (Principal Component 1; PC1) that accounts for 40% of the variance in the gene expression amongst the samples, whilst a second component (Principal Component 2; PC2) accounts for 23%. Approximately 63% of the variance found in these datasets, therefore, was due to these two unidentified factors. It is clear from Figure 5.3 that not all of the treatment replicates cluster together. Considering the first dimension only (PC1), broadly, the samples exposed to WT tend to occur at the extremes of the range (<-30 or above +30) whereas the LT-treated samples occur between -22 and + 22. Two of the replicates for LD/LT (red) cluster around -20, the third, however, is located at around +15. Similarly, two of the replicates for LD/WT (green) cluster around +30, whilst the third is located at -35. Two of the SD/LT replicates cluster between -5 and -19 but the third is at +21, whereas the SD/WT replicates do not cluster at all with respect to PC1.

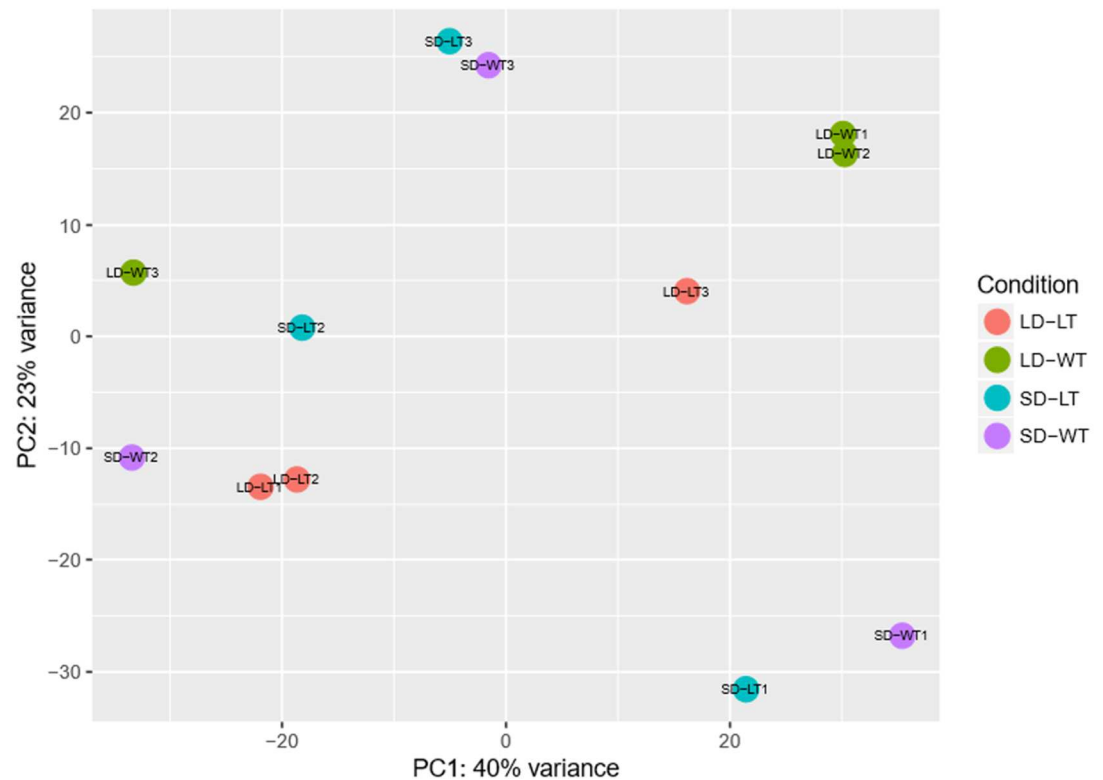


Figure 5.3: Two-Dimensional Principal Component Analysis of Transcript Profiles in Cold-Acclimated *Hordeum vulgare* (cv. California) Leaves.

Plants were grown in LD (16/8-hour photoperiod) and WT (20°/16°C day/night) for 4 weeks (LD/WT) and then exposed for a further 2 weeks to partial (LD/LT, or SD/WT), or full (SD/LT). Mature sections of the third and fourth leaves of plants were then harvested, frozen immediately to -80°C, and total RNA was subsequently prepared for RNA-Seq analysis (Section 2.6). NGS sequencing was performed on cDNA generated from these pools of RNA (Sections 2.6 and 5.2.3) and analysed by Kallisto and DESeq2. The PCA variance was calculated using the relative abundance of each sequence expressed as rlog₂ (regularised Log₂) transformation of the normalised values recorded.

Further, the variance in gene expression between replicates is not well explained by PC2 (Fig. 5.3). The replicates for the LD/LT cluster between +4 and -14, and those for LD/WT between +18 and +6, but those for SD show no clustering at all (+28 to -32). These results suggest that although the cold-acclimation treatments that were applied may have induced consistent changes in gene expression, there were other unknown and uncontrolled factors that exerted a stronger influence on transcription. It is not clear what these other factors might be, as PCA does not provide insight into this; this point is discussed further in the Discussion section at the end of this chapter.

Although PCA revealed that the acclimation treatments were not the only major factors affecting gene expression, this does not mean that important acclimation-induced changes were not included in the datasets; rather, these changes were obscured by other transcriptional events not strongly related to the acclimation conditions. Figure 5.4 presents the 'Heat map' plots for five of the pair-wise treatment comparisons. These are presented to emphasise the effects of partial cold acclimation conditions (SD alone; LT alone) and full cold acclimation conditions (SD and LT). It was clear there were sequences in each of the three treatment replicates whose expression correlated when exposed to the different cold-acclimating regimes.

Comparison of the effects of temperature alone showed that a larger set of significant ($p_{adj} < 0.1$) differentially expressed sequences were identifiable when plants were exposed to LT in LD (partial cold acclimation) compared with exposure in SD (full cold acclimation) (see Figs. 5.4b and c for heat maps). LT appears to have resulted mainly in increases (red) in transcript abundance, although some decreases (blue) were also observed. A similar pattern was observed when plants were exposed to LT in SD, but, as mentioned above, there were fewer significant changes.

Surprisingly, only a few sequences appeared to be affected by changes in photoperiod when plants were exposed to WT (Fig. 5.4a). Again, SD (partial acclimation) induced both an increase (red) and decrease (blue) in expression. When plants were exposed to different photoperiods at low temperatures, DESeq2 identified over 100 sequences that appeared to be co-regulated across the three replicates for photoperiod (Fig. 5.4b). What appeared to be common between these two pair-wise comparisons was that more significant changes were identified when samples exposed to LD and LT were considered (Figs. 5.4b and c). The implications of this observation will be discussed further in the Discussion section at the end of this chapter.

One of the concerns regarding this analysis was that in one of the pair-wise comparisons (Fig. 5.4 b) replicate (SD/LT1) appeared to be more similar to the LD replicates than it was to its other two SD replicates (SD/LT2 and SD/LT3). This irregularity is not present when the same dataset (SD/LT1) is used in other comparisons (Fig. 5.4d and e). This inconsistency is difficult to reconcile. For this reason, DESeq2 was run again with the SD/LT1 replicate omitted (i.e., with 11 samples), but very similar lists of differentially regulated genes were obtained (data not presented). Given this result, and the consistency between the SD/LT replicates when other comparisons were made, the SD/LT1 sample was included in all further analyses.

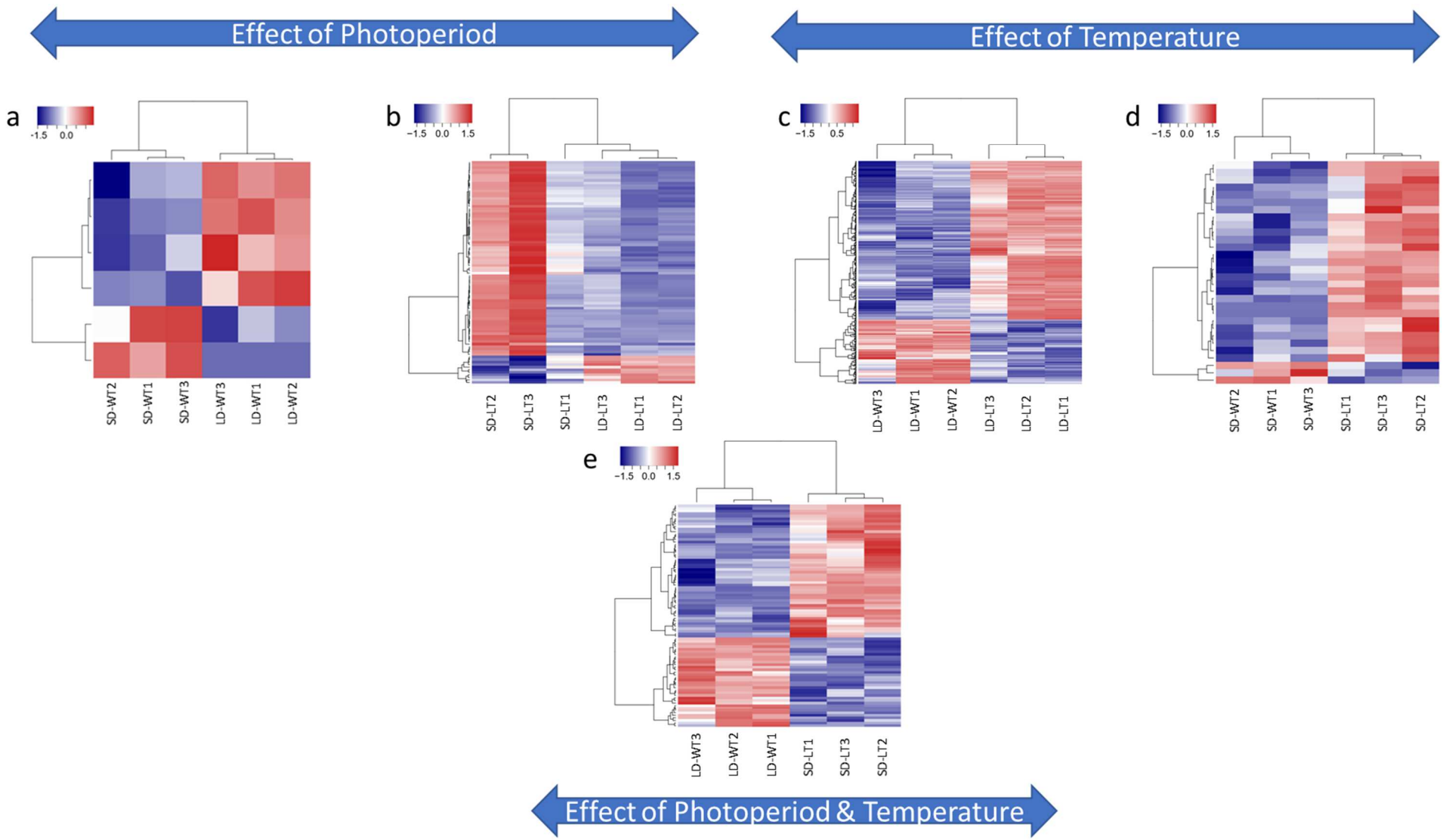


Figure 5.4: DESeq2 Barley Gene Expression Heat Maps: Comparison of Cold-Acclimation Treatments.

Five-week old plants were exposed for 2 weeks to all combinations of photoperiod (LD or SD; 16h or 8h light) and night temperature (WT or LT; 16° or 4°) (see Section 2.1.1). Total RNA was extracted and purified 2 hours post-dawn and cDNA generated for sequencing using an Illumina NextSeq 500 sequencer and a TrueSeq RNA Kit (see Section 2.6). The raw read datasets (3 replicates x 4 treatments x 2 paired-end reads = 24 files) were trimmed to remove low quality sequences, aligned to the barley cDNA data base (ICBS, 2017) using the pseudo-alignment program Kallisto, and the output was analysed using the DESeq2 statistical package (Section 5.2.5.1). Code: LD, Long Days; SD, Short Days; WT, Warm Temperatures; LT, Low Temperatures). The pair-wise comparison LD/LT versus SD/WT was not included, as the comparison is somewhat meaningless. Sequences that met the DESeq2 search criteria are represented as horizontal red (upregulated) or blue (downregulated) lines.

From the full set of 30,912 detected filtered genes, the six comparisons with controls showed that the different acclimation conditions induced 507 ‘upregulated’ and 174 ‘downregulated’ sequences that met the filter criteria ($p_{adj} < 0.1$, >2-fold change, BaseMean score > 0; Table 5.3). These sequences should fall into one of four groups. Some are likely to have been included in these sets by random events not directly related to cold acclimation and can be considered ‘not of prime interest’. Others may have been influenced by the transition to SD (photoperiod) or to LT (temperature) alone, and others by interactions arising between products of the two transitions. One way of establishing which sequences fall into which class is to use set theory and Venn (or Euler) diagrams.

It was pointed out in Chapter 3 (Section 3.4) that the data generated from the CA regimes used in this study will generate complex data and, thus, that caution should be exercised in terms of drawing firm conclusions. Comparisons of the datasets generated from plants where the length of the night period was identical (i.e., LD/WT with LD/LT, and SD/WT with SD/LT, see Fig. 3.2) allow differences induced by night temperature alone to be assessed. Datasets containing these differences will be referred to as |T| (LD) and |T| (SD). Comparisons between datasets where there was a difference in photoperiod (night length) were more difficult to interpret. Figure 3.2b shows, in bold typeface, the treatment factors that induced cold acclimation (15h nights and 4°C). Comparing these datasets for photoperiod effects, LD/WT with SD/WT, and LD/LT with SD/LT, shows that, although night temperature does not change, the duration of exposure to the night temperature does (15 hours or 8 hours). Hence, differences between either of these contrasts could be attributed to photoperiod (increased length of the dark period) or an increased period of

exposure to cool temperatures (an additional 7h at 4°C). Similar issues will arise from comparison of the non-acclimated plants (LD/WT) with the fully acclimated plants (SD/LT). At face value, it seems the effects of temperature and photoperiod on gene expression cannot be separated, but this is not the case. To identify which sequences were affected by cool night temperatures alone, by photoperiod alone, or by an interaction (synergy) of both, Set Theory can be applied and viewed using Venn (Euler) diagrams.

In this experiment, the transcriptome consisted of 30,912 barley sequences. It was expected that the majority of these sequences would be unresponsive to cold acclimation (CA) and would be designated (U), but that some may be responsive to low night temperatures alone (T), or to long nights alone (photoperiod, P), or to an interaction (I) between both factors. For the purpose of these experiments, therefore, the transcriptome of barley was considered to consist of four classes of sequences; T, P, I, and U.

The 12 Kallisto output sequence datasets (four treatments with three replicates) contain abundances for each of the 30,912 detected genes isolated from plants exposed to one of the four CA regimes: LD/WT (no CA); LD/LT (low temperatures only); SD/WT (long night periods only); SD/LT (both low temperatures and long night periods). It was expected that the set |LDLT| (8h night at 4°C) would vary from |LDWT| (8h night at 16°C) only in a difference in abundance of the T class of sequences, which would be contained in set |T'| (Table 5.4). Similarly, |SDLT| (15h night at 4°C) would differ from |SDWT| (15h night at 16°C) only by abundance differences in the T and I classes of genes and represented in set |TI|. Finally, |SDLT| and |LDWT| would differ in the T, P, and I classes of sequences and represented in set |TPI|. Set theory was then used to reveal the sequences that respond to temperature alone, to photoperiod alone, and to a combination of both, by determining the complements and intersects of the appropriate pairs of sets (Table 5.4).

Table 5.4: Identification of Sequences regulated by Temperature Alone, Photoperiod Alone, or by an Interaction of Both Using Set Manipulations.

Each dataset contains 30,912 sequences that respond to temperature alone (T genes), photoperiod alone (P genes), an interaction of both (I genes), or are unresponsive (U genes) to CA. Sets (LD/WT) that contained non-acclimated levels of gene abundances are shown in grey font (i.e., T, P, I, and U); sets where altered levels were detected are shown in black font (T, P, and I). DESeq 2 and spreadsheet filtering was used to identify the relative complement of pairs of datasets (i.e., subtracts) and these are shown in the column ‘Set Manipulations’ along with two further complements and intersects/unions of the derived sets. The normal convention for set manipulations was followed: the relative complement of $|A| \setminus |B|$ is $|C|$, a set that contains all elements in $|A|$ that are *not* in $|B|$ (some conventions present this as $|B|^c |A| = |C|$); the intersect $|A| \cap |B|$ is $|C|$, which contains elements that are common in $|A|$ and $|B|$; the union $|A| \cup |B|$ is $|C|$, which contains all of the elements that are either in $|A|$ or in $|B|$. The set $|T'|$ indicates sequences that responded to low temperature alone for a duration of 8 hours, whereas set $|T|$ indicates sequences that responded to low temperatures alone for a duration of 15 hours (see text for further details).

Set Manipulation	CA Factors Involved	Gene Class in Derived Set	Number of Sequences in Set	
			Up	Down
$ LDLT \setminus LDWT $	<u>T'PIU</u> - <u>TPIU</u>	$ T' $	291	110
$ SDLT \setminus SDWT $	<u>TPIU</u> - <u>TPIU</u>	$ TI $	37	3
$ SDLT \setminus LDWT $	<u>TPIU</u> - <u>TPIU</u>	$ TPI $	52	30
$ TPI \cap TI \cap T' $	In all three sets	$ T $	18	0
$ TPI ^c (TI \cup T')$	TPI <i>not</i> (TI or T')	$ P $	8	16
$(TPI \cap TI)^c T' $	In TPI and TI, <i>not</i> T'	$ I $	6	0

5.2.5.2 Upregulated Sequences

Figure 5.5 shows that 18 sequences were responsive to low temperatures alone (appear in the intersect of (are common to) |T'|, |TI|, and |TPI|); eight sequences were responsive to photoperiod alone (appear exclusively in |TPI| but not |TI| or |T'|); and six sequences appeared to be responsive to the combined effects of temperature and photoperiod (interaction). These sequences are listed in Table 5.5 and their corresponding annotations and GO activities are presented.

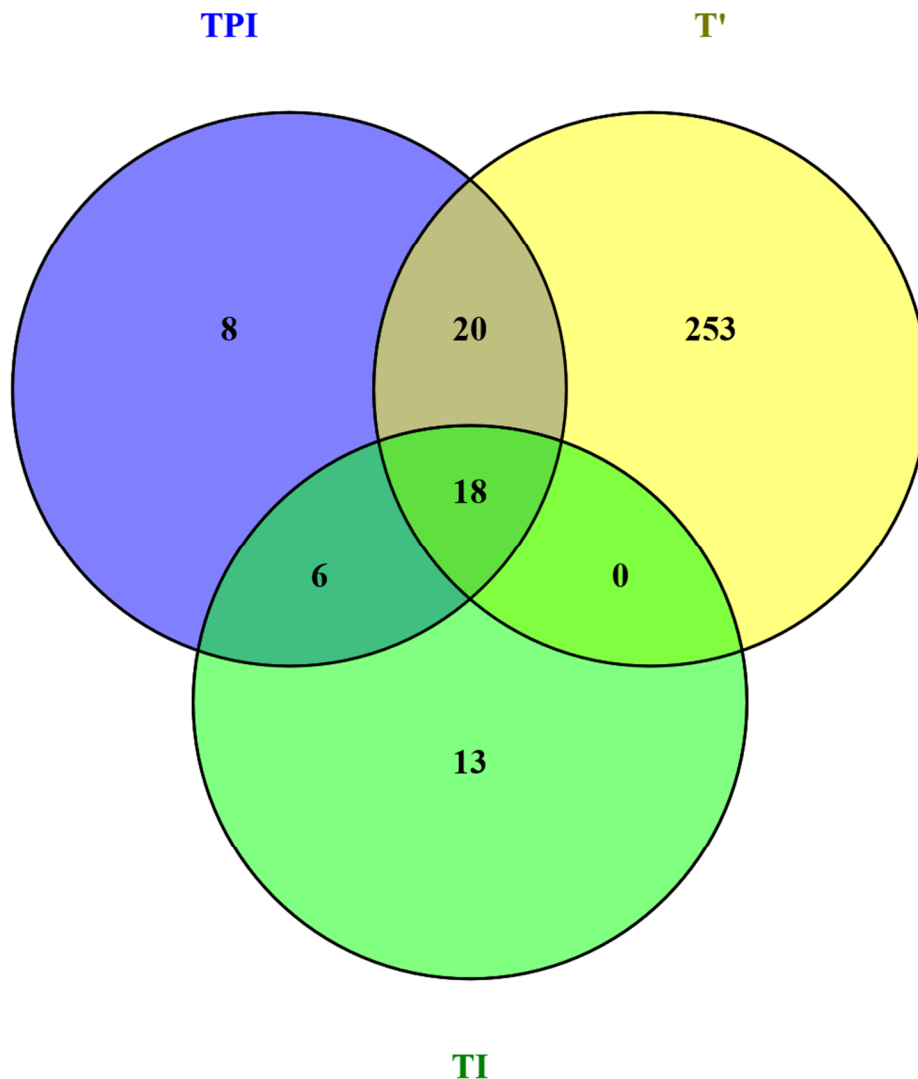


Figure 5.5: Venn Diagram Identifying Cold Acclimation Barley Sequences Upregulated by Temperature Alone, Photoperiod Alone, and a Combination of Both Factors.

TPI, the set of sequences responsive to: P (photoperiod) alone (15h dark); T (temperature) alone (4°C for 15h); I (interaction) between P and T; T', the set of sequences responsive to 4°C for 8h. TI, the set of sequences responsive to T and I; T', the set of sequences responsive to 4°C for 8h. The eight sequences exclusive to TPI were responsive to P alone. The 18 sequences at the intersect of all three sets were responsive to T alone. The six sequences at the intersect of TPI and TI were only responsive to an interaction of low night temperatures and photoperiod. Diagram reproduced from the Venny online resource page (Oliveros, J.C. (2007–2015). (<https://bioinfogp.cnb.csic.es/tools/venny/index.html>)).

It was expected that no elements would appear exclusively in |T'|, |TI| or only in the intersect of |T'| and |TPI|, but 253, 13, and 20 sequences were identified, respectively. This discrepancy may have arisen in part from the different treatments for low temperature. Set |T'| contains the elements that were upregulated by exposure of tissues to 8h nights at 4°C, whereas in sets |TI| and |TPI| the samples were exposed to 15h nights at 4°C. It is for this reason that the group of sequences responsive to 8h at 4°C temperatures alone are designated T', whilst those responsive to 15h at 4°C temperatures alone are designated as T. A full discussion on why only 38 (20+18) sequences of the 291 (20+18+253) sequences in |T'| were found after 15h at 4°C is presented in the Discussion section at the end of this chapter.

Table 5.5: Identification of Upregulated Cold Acclimation Sequences in Barley Induced by Photoperiod Alone, Low Night Temperatures Alone, and a Combination of Both Factors.

Sequences with a greater than two-fold increase are shown along with some annotation from the UniProt online resource. Sequences presented with a bold face sequence ID were also identified in an independent parallel experiment, described in Section 5.2. The average and standard error is given for the fold change in expression level for: |P| sequences, derived from a single complement; |I| sequences, derived from two complements; |T| sequences, derived from three complements.

Sequence ID	UniProt Link	Gene Annotation	GO Annotation	Fold Change
 P 				
HORVU3Hr1G073280	https://www.uniprot.org/uniprot/M0WFD0	Uncharacterised protein		4.3 -
HORVU6Hr1G014270	https://www.uniprot.org/uniprot/F2D3G5	Predicted protein; FAD-binding oxidoreductase.	D-arabinono-1,4-lactone oxidase activity; FAD binding	3.4 -
HORVU3Hr1G086940	https://www.uniprot.org/uniprot/F2DFC5	Predicted protein; P-loop containing nucleoside triphosphate hydrolase.	All organs;	3.2 -
HORVU3Hr1G029770	https://www.uniprot.org/uniprot/M0VW66	PlsC domain-containing protein; Phospholipid/glycerol acyltransferase.	Glycerol-3-phosphate 2-O-acyltransferase activity; cutin biosynthetic process	3.0 -
HORVU2Hr1G043830	https://www.uniprot.org/uniprot/A0A287HUH4	Formin-like protein; Formin, FH2 domain.	All organs; involved in cytoskeleton re-arrangement	2.8 -

Sequence ID	UniProt Link	Gene Annotation	GO Annotation	Fold Change
HORVU7Hr1G035050	https://www.uniprot.org/uniprot/A0A287W0E4	PMR5N domain-containing protein; similar c-terminal PMR5N to ESK1.	The plant proteins PMR5 and ESK1 have an N-terminal C-rich predicted sugar binding domain followed by the PC-Esterase (acyl esterase) domain	2.4 -
HORVU2Hr1G100720	https://www.uniprot.org/uniprot/A0A287J6B1	CUE domain-containing protein; Ubiquitin system component CUE; This domain may be involved in binding ubiquitin-conjugating enzymes (UBCs). CUE domains also occur in two proteins of the IL-1 signal transduction pathway, tollip and TAB2.	DNA-binding transcription activator activity, RNA polymerase II-specific	2.3 -
HORVU1Hr1G065070	https://www.uniprot.org/uniprot/M0WIR0	Uncharacterised protein; Kinase; responsive to ABA, microtubule re-organisation	protein tyrosine phosphatase activity; cortical microtubule organisation; response to abscisic acid	2.1 -
[T]				
HORVU4Hr1G083250	https://www.uniprot.org/uniprot/A0A287PWH6	Uncharacterised protein		12.3 (2.0)
HORVU2Hr1G099820	https://www.uniprot.org/uniprot/A0A287J5K1	Uncharacterised protein; >90% identity to COR14b; expresses in leaves/shoots; responds to photoperiod.		6.5 (0.9)
HORVU3Hr1G112020	https://www.uniprot.org/uniprot/M0UUU9	Uncharacterised protein; induced by water deficit stress (WDS) [1], or abscisic acid (ABA) stress; caryopsis, embryo and root.		7.1 (1.4)

Sequence ID	UniProt Link	Gene Annotation	GO Annotation	Fold Change
HORVU1Hr1G058310	https://www.uniprot.org/uniprot/A0A287FSH4	Protein kinase domain-containing protein.	ATP-binding; Serine/Threonine Kinase	6.1 (0.8)
HORVU7Hr1G007800	https://www.uniprot.org/uniprot/A0A287VG01	Uncharacterised protein; late embryogenesis abundant protein, LEA_1 subgroup.	Embryo development	6.5 (1.6)
HORVU5Hr1G001750	https://www.uniprot.org/uniprot/F2DNS7	Predicted protein; transmembrane domain; Modifying wall lignin-1/2.	Modifying wall lignin-1/2	5.8 (0.4)
HORVU2Hr1G028920	https://www.uniprot.org/uniprot/A0A287HIJ4	Uncharacterised protein; Harbinger transposase-derived protein.	Hydrolase activity, acting on ester bonds.	4.8 (0.7)
HORVU2Hr1G099830	https://www.uniprot.org/uniprot/A0A287J5G3	Uncharacterised protein; Harbinger transposase-derived protein; >90% identity with Cold-responsive protein WCOR15-2A from <i>Triticum dicoccoides</i> ; shoot.		5.1 (0.3)
HORVU5Hr1G098190	https://www.uniprot.org/uniprot/A0A287SG76	Uncharacterised protein; Cold-regulated 413 protein. This family can be classified into two groups: the cold-regulated (COR)413-plasma membrane and COR413-thylakoid membrane groups. Highly conserved phosphorylation site and a glycosylphosphatidylinositol-anchoring site at the C-terminal end.	Integral component of membrane; expressed in all tissues.	4.9 (0.2)
HORVU3Hr1G058990	https://www.uniprot.org/uniprot/A0A287L7N1	CTP synthase; catalysis of the reaction: ATP + UTP + NH ₃ = ADP + phosphate + CTP.	Catalysis of the reaction: ATP + UTP + NH ₃ = ADP + phosphate + CTP; expressed in all tissues.	5.7 (1.0)
HORVU7Hr1G012310	https://www.uniprot.org/uniprot/A0A287VIT5	Uncharacterised protein; late embryogenesis abundant protein, LEA_1 subgroup.		5.3 (0.9)

Sequence ID	UniProt Link	Gene Annotation	GO Annotation	Fold Change
HORVU5Hr1G098920	https://www.uniprot.org/uniprot/A0A287SGQ5	Pectin acetylerase; Pectinacetylerase /NOTUM.	Hydrolase activity; cell wall organisation.	3.6 (0.3)
HORVU6Hr1G086820	https://www.uniprot.org/uniprot/A0A287V1V7	Uncharacterised protein		4.9 (0.5)
HORVU2Hr1G043980	https://www.uniprot.org/uniprot/A0A287HU83	Uncharacterised protein; signal peptide.		4.2 (0.6)
HORVU4Hr1G057000	https://www.uniprot.org/uniprot/A0A287P6C5	Low temperature-induced protein It101.1; MPM3 - Proteolipid membrane potential modulator.	Integral component of membrane; all organs	3.5 (0.1)
HORVU0Hr1G003190	https://www.uniprot.org/uniprot/A0A287DV56	Uncharacterised protein.	Roots, inflorescence, and embryo	3.4 (0.7)
HORVU3Hr1G006940	https://www.uniprot.org/uniprot/F2EBD5	Predicted protein; HSP20-like chaperone.	Shoots and internodes mainly	2.8 (0.2)
HORVU6Hr1G060540	https://www.uniprot.org/uniprot/M0VB12	Protein kinase domain-containing protein; plasma membrane; transmembrane receptor protein serine/threonine kinase activity.	Reactions, triggered in response to the presence of a foreign body or the occurrence of an injury, which result in restriction of damage to the organism attacked or prevention/recovery from the infection caused by the attack.	3.1 (0.6)

Sequence ID	UniProt Link	Gene Annotation	GO Annotation	Fold Change
[I]				
HORVU3Hr1G112520	https://www.uniprot.org/uniprot/A0A287MQJ7	Uncharacterised protein.	Carboxylic acid metabolic process; carboxy-lyase activity; pyridoxal phosphate binding.	5.3 (0.6)
HORVU2Hr1G073210	https://www.uniprot.org/uniprot/A0A287IFF2	Glyco_hydro_32C domain-containing protein; C-terminal domain of glycosyl hydrolase family 32; Concanavalin A-like lectin/glucanase domain	All parts, especially flowers, caryopsis, root and shoot.	7.1 (2.4)
HORVU2Hr1G103550	https://www.uniprot.org/uniprot/A0A287J913	Uncharacterised protein; glycine rich protein.		4.3 (0.2)
HORVU1Hr1G005120	https://www.uniprot.org/uniprot/A0A287EIM2	Uncharacterised protein	All organs; amino acid transmembrane transporter activity; protein domain specific binding; responsive to cold, glucose, sucrose, wounding and JA.	4.7 (0.9)
HORVU7Hr1G009800	https://www.uniprot.org/uniprot/A0A287VHI9	Uncharacterised protein; transporter, OPT superfamily. Oligopeptide	all orgns, especially roots and shoots; transmembrane transport.	3.2 (0.5)

Sequence ID	UniProt Link	Gene Annotation	GO Annotation	Fold Change
HORVU1Hr1G055000	https://www.uniprot.org/uniprot/A0A287FNZ2	Uncharacterised protein; vacuolar protein sorting-associated protein 62.	All organs; Vps62 is a vacuolar protein sorting (VPS) protein required for cytoplasm to vacuole targeting of proteins	2.3 (0.2)

5.2.5.3 Downregulated Sequences

Figure 5.6 presents the Venn diagram for the downregulated sequences. From these data, it would appear that 16 sequences were responsive to photoperiod alone, as they do not appear in the sets |T| or |TI|. No sequences appear in the intersects of all three sets, indicating that none of the downregulated sequences were responsive to temperature alone. Similarly, no sequences appear in the intersect of |TPI| and |TI| only, suggesting no sequences responded to the combined effects of temperature and photoperiod (I). The data, therefore, suggests there is no evidence that downregulated sequences respond to anything other than photoperiod. However, some explanation is required to account for the 112 (95+14+1+2) sequences that were significantly downregulated but could not be assigned to the |T| or |I| groups of responsive genes. This is provided in the Discussion section at the end of this chapter.

Table 5.6 presents the identities and corresponding annotations of the 16 sequences identified in Figure 5.6 as responsive to photoperiod alone, as well as some of those whose regulation is uncertain (14 designated as T, and three designated as I).

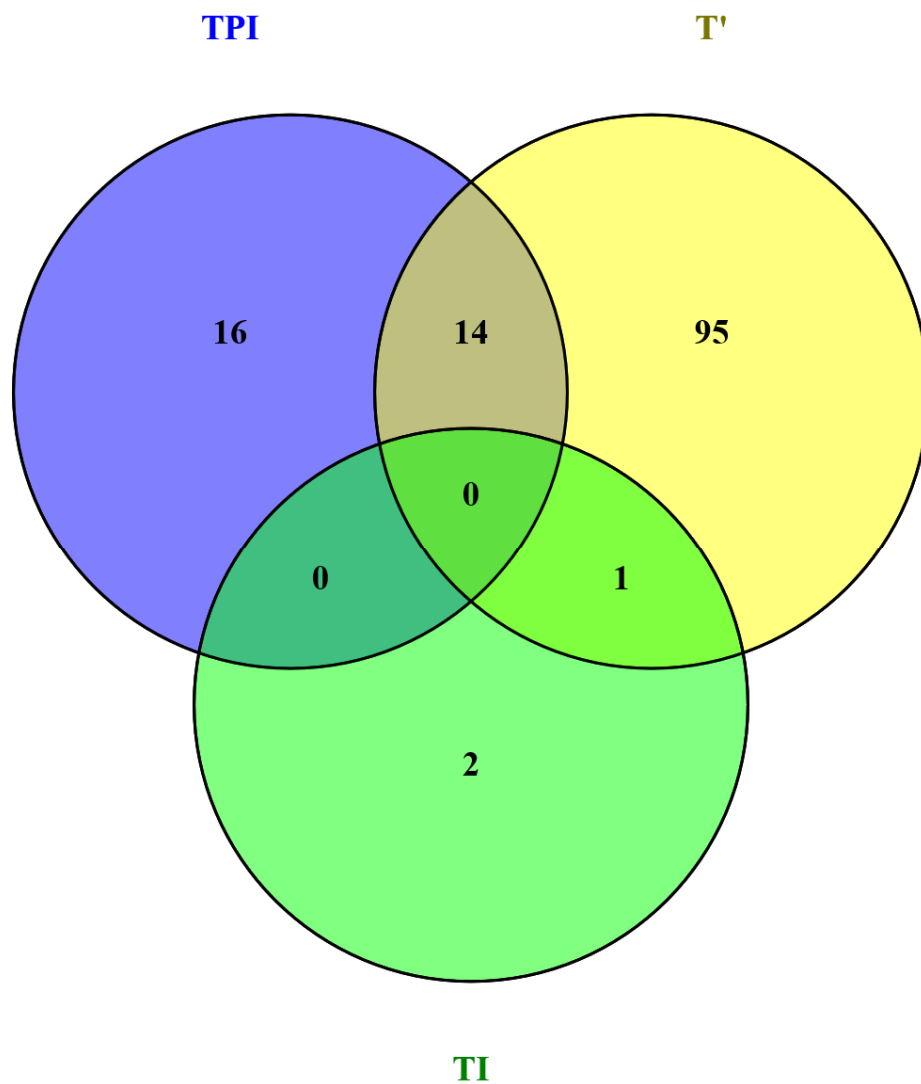


Figure 5.6: Venn Diagram Identifying Cold-Acclimation Barley Sequences Downregulated by Temperature Alone, Photoperiod Alone, and a Combination of Both Factors.

TPI, the set of sequences responsive to: P (Photoperiod) alone (15h dark); T (temperature) alone (4°C for 15h); I (Interaction) between P and T; T' (Temperature) alone (4°C for 8hr). TI set of sequences responsive to T and I; T' set of sequences responsive to 4°C for 8h. The 16 sequences exclusive to TPI are responsive to P alone. Diagram reproduced from the Venny online resource page (Oliveros, J.C. (2007-2015) Venny <http://bioinfogp.cnb.csic.es/tools/venny/index.html>).

Table 5.6: Identification of Downregulated Cold-Acclimation Sequences in Barley Suppressed by Photoperiod Alone, Low Night Temperatures Alone, and a Combination of Both Factors

Sequences with a greater than two-fold decrease are shown along with some annotations from the UniProt online resource. Sequences presented with a bold face Sequence ID were also identified in an independent parallel experiment, described in Section 5.2. The average and standard error is given for the fold change in expression level for: |P| sequences, derived from a single complement; |I| sequences, derived from two complements; |T| sequences, derived from three complements.

Sequence ID	UniProt Link	Gene Annotation	GO Annotation	Fold Change
 P 				
HORVU7Hr1G027540	https://www.uniprot.org/uniprot/A0A287VU35	Uncharacterised protein; Glutathione S-transferase, C-terminal-like; auxin-regulated proteins in plants.	Glutathione transferase activity; glutathione metabolic process.	5.6 -
HORVU5Hr1G125460	https://www.uniprot.org/uniprot/A0A287T3G4	Uncharacterised protein; membrane protein; AWPM-19-like; 19kDa membrane proteins responsive to abscisic acid; involved in freezing tolerance.	The increased presence of this protein leads to greater tolerance of freezing.	5.1 -
HORVU5Hr1G052730	https://www.uniprot.org/uniprot/F2E0Y6	Predicted protein		4.5 -
HORVU2Hr1G108340	https://www.uniprot.org/uniprot/A0A287JDF9	Uncharacterised protein		4.3 -
HORVU2Hr1G012280	https://www.uniprot.org/uniprot/A0A287H365	UDPGT domain-containing protein; UDP-glycosyltransferase family, conserved site; anthocyanin biosynthesis.	Transferase activity, transferring hexosyl groups; Plants flavonol O(3)-glucosyltransferase (2.4.1.91). An enzyme that catalyses the	4.2 -

Sequence ID	UniProt Link	Gene Annotation	GO Annotation	Fold Change
			transfer of glucose from UDP-glucose to a flavanol. This reaction is essential and one of the last steps in anthocyanin pigment biosynthesis.	
HORVU5Hr1G091840	https://www.uniprot.org/uniprot/F2EGA4	Predicted protein; membrane protein; signal peptide.		4.0 -
HORVU2Hr1G019900	https://www.uniprot.org/uniprot/F2D3N9	Predicted protein; flowering-promoting factor 1.	Regulation of flower development	4.0 -
HORVU2Hr1G071450	https://www.uniprot.org/uniprot/A0A287IDQ1	Nudix hydrolase domain-containing protein	Hydrolase activity; 'NUDIX hydrolases' (NUcleoside DIphosphate linked to some other moiety X.	3.9 -
HORVU0Hr1G020630	https://www.uniprot.org/uniprot/M0UGG8	Uncharacterised protein	S-adenosylmethionine-dependent methyltransferase activity	3.8 -
HORVU4Hr1G060670	https://www.uniprot.org/uniprot/M0UJ08	WD_REPEATS_REGION domain-containing protein; possible G proteins (beta subunit is a beta-propeller), TAFII transcription factor, and E3 ubiquitin ligase.	WD40/YVTN repeat-like-containing domain superfamily	3.6 -
HORVU7Hr1G025700	https://www.uniprot.org/uniprot/A0A287VRE2	Uncharacterised protein; MADS MEF2-like; transcription factor, K-box.	DNA-binding transcription factor activity; protein dimerization activity; RNA polymerase II regulatory region sequence-specific DNA binding.	3.4 -

Sequence ID	UniProt Link	Gene Annotation	GO Annotation	Fold Change
HORVU3Hr1G026920	https://www.uniprot.org/uniprot/F2EFN3	Predicted protein; Metallothionein.		3.0 -
HORVU3Hr1G070440	https://www.uniprot.org/uniprot/A0A287LJE6	X8 domain-containing protein; X8 domain.	Hydrolase activity, hydrolysing O-glycosyl compounds; carbohydrate metabolic process.	2.8 -
HORVU6Hr1G006840	https://www.uniprot.org/uniprot/F2EEP9	Predicted protein		2.7 -
HORVU3Hr1G066410	https://www.uniprot.org/uniprot/A0A287LFB7	DEK_C domain-containing protein; DEK, C-terminal, chromatin remodelling.	Transcription coactivator activity; positive regulation of transcription initiation from RNA polymerase II promoter.	2.3 -
HORVU6Hr1G012400	https://www.uniprot.org/uniprot/A0A287TC39	Uncharacterised protein		2.2 -

Sequence ID	UniProt Link	Gene Annotation	GO Annotation	Fold Change
[T]				
HORVU1Hr1G093560	https://www.uniprot.org/uniprot/A0A287GSM9	Uncharacterised protein; RNA catabolic process.	Endoribonuclease activity; ribonuclease T2 activity; plant T2 RNases are expressed during leaf senescence in order to scavenge phosphate from ribonucleotides. They are also expressed in response to wounding or pathogen invasion.	11.3 (0.3)
HORVU6Hr1G005050	-	Non-translating CDS; 1016bp.		4.9 (0.7)
HORVU0Hr1G000340	https://www.uniprot.org/uniprot/A0A287DTM8	Uncharacterised protein	Pyridoxal phosphate binding; trans-sulfuration	4.4 (0.9)
HORVU2Hr1G024120	https://www.uniprot.org/uniprot/A0A287HE24	Terpene_synth domain-containing protein	Terpene synthase activity.	4.4 (0.8)
HORVU1Hr1G090890	https://www.uniprot.org/uniprot/F2DDZ8	Predicted protein; DUF 761.		4.0 (0.7)
HORVU0Hr1G027640	https://www.uniprot.org/uniprot/A0A287E9M2	Uncharacterised protein; zinc finger, FYVE/PHD-type; plant homeodomain (PHD) zinc finger domain has a C4HC3-type motif, and is widely distributed in eukaryotes, being found in many chromatin regulatory factors.		4.5 (0.3)

Sequence ID	UniProt Link	Gene Annotation	GO Annotation	Fold Change
HORVU5Hr1G007890	https://www.uniprot.org/uniprot/F2ELJ6	Predicted protein; CCAAT-binding TF, conserved site; Diverse DNA-binding proteins are known to bind the CCAAT box, a common cis-acting element found in the promoter and enhancer regions of a large number of genes in eukaryotes. Amongst these proteins is one known as the CCAAT-binding factor (CBF) or nuclear transcription factor Y (NF-Y).	DNA binding; DNA-binding transcription factor activity; CCAAT-binding factor, conserved site.	3.6 (0.3)
HORVU3Hr1G002000	https://www.uniprot.org/uniprot/M0XC35	Germin-like protein	Manganese ion binding; Cupin 1 protein.	3.1 (0.6)
HORVU3Hr1G013840	https://www.uniprot.org/uniprot/A0A287K5T6	Uncharacterised protein; Metallothionein, family 15, plant.	Metal ion binding	3.7 (0.4)
HORVU5Hr1G085550	https://www.uniprot.org/uniprot/A0A287S3H5	Uncharacterised protein; F-box-like domain superfamily.		2.9 (0.1)
HORVU5Hr1G092700	https://www.uniprot.org/uniprot/A0A287S921	Uncharacterised protein; nuclear transcription factor Y subunit A.	DNA-binding transcription factor activity; protein dimerization activity; RNA polymerase II regulatory region sequence-specific DNA binding.	3.0 (0.1)
HORVU2Hr1G097980	https://www.uniprot.org/uniprot/A0A287J347	Uncharacterised protein; protein of unknown function DUF761.		2.6 (0.1)
HORVU3Hr1G070880	https://www.uniprot.org/uniprot/M0WWL9	HPt domain-containing protein; two-component histidine signalling; signal	Phosphorelay signal transduction system	2.5 (0.0)

Sequence ID	UniProt Link	Gene Annotation	GO Annotation	Fold Change
		transduction histidine kinase, phosphotransfer (Hpt) domain.		
HORVU3Hr1G024920	https://www.uniprot.org/uniprot/A0A287KGR6	Uncharacterised protein		2.1 (0.1)
[I]				
HORVU2Hr1G030600	https://www.uniprot.org/uniprot/F2E0L1	Predicted protein; EF-hand domain pair	Calcium ion binding	4.5 -
HORVU2Hr1G003480	https://www.uniprot.org/uniprot/A0A287GXE7	Uncharacterised protein; Cytochrome P450.	Heme binding; iron ion binding; oxidoreductase activity, acting on paired donors, with incorporation or reduction of molecular oxygen, NAD(P)H as one donor, and incorporation of one atom of oxygen.	4.5 -
HORVU2Hr1G015930	https://www.uniprot.org/uniprot/A0A287H618	Protein kinase domain-containing protein; armadillo-like helical; Serine/threonine-protein kinase, active site.		2.1 -

A full list of the sequences presented in Figures 5.5 and 5.6 is presented in Appendix A5.2.

5.2.5.4 Hypergeometric Probability

The question now arises as to whether the sequences identified in Tables 5.4 and 5.5 are the result of random events (transcriptional ‘noise’), or are genuinely the result of the effects of the factors indicated. This problem can be addressed by considering the following. The sets |T’|, |TI|, and |TPI| were derived from comparisons (i.e., abundance differences, or complements) performed by DESeq2, and the Benjamini-Hochberg p_{adj} statistic was provided for each sequence in these complements. Therefore, the Benjamini-Hochberg statistic is the appropriate probability to use for the P (photoperiod alone) sequences, as they were identified as the residual (complement) sub-set of |TPI| once |T| and |I| had been removed (Table 5.4, Figs. 5.5 and 5.6). Sequences in the |T| and |I| set, however, were identified by intersections of three or two sets, respectively, and were therefore identified by more than one complement and so a greater statistical certainty could be calculated for these. The appropriate probability for these sequences was calculated using the Hypergeometric Probability function. A full explanation of the development of this approach is given in Section 2.7.

From Table 5.4 and Fig 5.5, it is clear the six sequences identified as responsive to I were derived from the intersection of |TPI| and |TI| ($|TPI| \cap |TI|$). The probability that these six sequences appeared randomly in the 52 sequences of |TPI| (selected from a total of 30,912 sequences), and also appeared randomly among the 37 sequences of |TI| was calculated by the Hypergeometric Probability Mass Function (*pmf*) and found to be $3.73 \cdot 10^{-11}$; thus, it was concluded that there is very strong evidence that these sequences are upregulated by an interaction between photoperiod and temperature. Another way of visualising this result is to calculate the most likely, or expected, number of sequences that would appear in the intersect if only random factors were present; the answer is much closer to 0 than 1 (0.062, standard deviation of 0.249) meaning the most likely outcome was no common sequences between |TPI| and |TI|. A plot of the hypergeometric distribution for these two sets displaying the expected (Ex) and observed (x) number of sequences is presented in Figure 5.7. The range between the observed and expected number of sequences can be expressed in units of standard deviations ($(6 - 0.062)/0.249 = 23.3$); a range of 5 standard deviations is approximately equivalent to $p < 0.001$. Table 5.7 also shows the probabilities that the 18 sequences that appeared in the intersect of all three sets ($|TPI| \cap |TI| \cap |T’| = |T|$) were extremely likely to have arisen from the effects of temperature alone. Figure 5.7 also presents these results in a graphical form. The presented hypergeometric *pmf* is given as $< 2.957 \cdot 10^{-27}$ but this is the *pmf* for the intersect $|TI| \cap |T’|$ only; the true probability of these 18 sequences appearing in all three

sets is the product of the *pmf* for the intersection $|TPI| \cap |TI|$ and $|TI| \cap |T'|$, which is $3.731 \cdot 10^{11} * 2.957 \cdot 10^{-27} = 1.10 \cdot 10^{-37}$.

The probability that the 16 sequences were downregulated by photoperiod (Fig. 5.6) is given by the Benjamini-Hochberg statistic calculated by DESeq2, as these were identified as the residual sequences in $|TPI|$ once T and I sequences were removed. No sequences were found at the intersection of $|TPI|$ and $|TI|$ or the intersection of all three sets, so it appears as though no sequences were downregulated by temperature alone or by a combination of temperature and photoperiod.

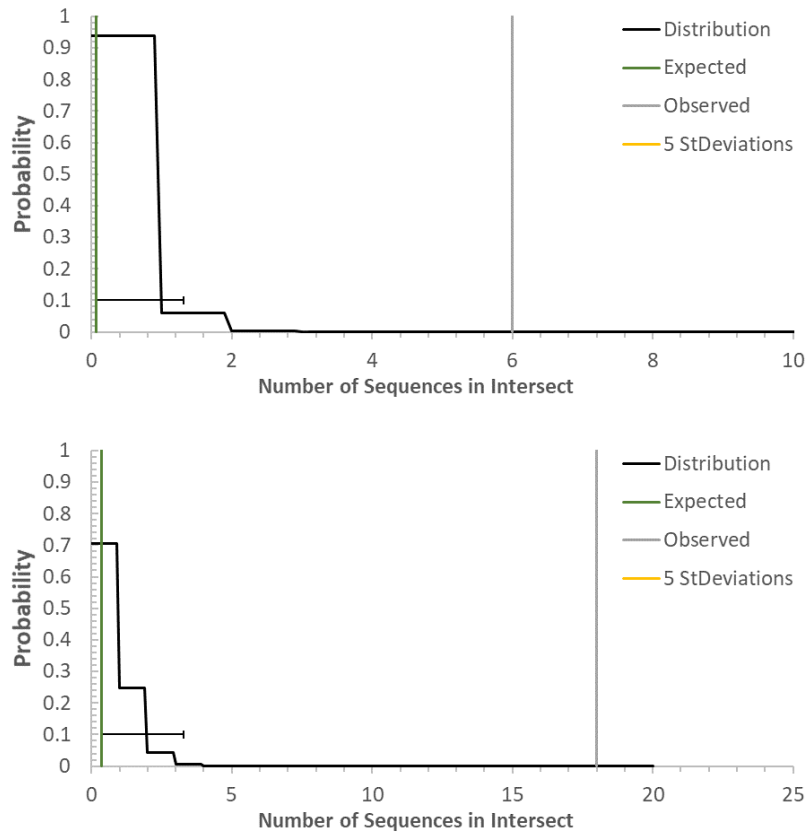


Figure 5.7: Hypergeometric Distribution for Intersection of Sequences in Independent RNA-Seq Experiments.

The hypergeometric distribution (black line) was calculated using the parameters shown in Table 5.7 for sequences found at the intersection of two RNA-Seq data sets (see Figs. 5.5 and 5.6). Upper panel, upregulated sequences of $|TPI| \cap |TI|$ (used to identify $|I|$ sequences); lower panel, upregulated sequences of $|TI| \cap |T'|$ (used to calculate $|T|$ sequences); see text for details. In both cases, the most likely outcome (expected value) was close to zero, much less than one common sequence. The horizontal line shows the range of 5 standard deviations ($p < 0.001$) from the expected outcome.

Table 5.7: Hypergeometric Probabilities for Sequences Transcriptionally Regulated by Cold Acclimation.

The hypergeometric probability mass function (*pmf*) was calculated for the comparison sets shown. k , the number of sequences (>2-fold change) identified in the first set; n , number of sequences identified in the second set; N , total number of detected genes in the experiment; x , the number of sequences appearing in an intersect (in two or more sets); the probability of selecting one gene from N is given as $p=k/N$. The hypergeometric *pmf* was calculated from the values N , n , k , and x (Section 2.7). In addition to this statistical approach, the hypergeometric distribution for all values of n was constructed using the conditional probability for x calculated from set theory ($p(\{A\} | \{B\})$). From this, an expected value for the average of the distribution can be calculated ($E(x)$) and the observed (x) and expected ($E(x)$) values compared. A standard deviation (*St Dev*) can also be calculated as well as the number of standard deviations between x and $E(x)$ (*St Dev Range*). Normally, standard deviation ranges exceeding 2, 3, and 5 are indicative of probabilities of <0.05, <0.01, and <0.001. See Section 2.7 for a full explanation.

Intersection (Common Genes)	<i>n</i>	<i>x</i>	<i>k</i>	<i>N</i>	<i>pmf</i>	$p(\{A\} \cap \{B\})$	<i>E(x)</i>	<i>St Dev</i>	<i>St Dev Range</i>
Upregulated									
$ TPI ^c (TI \cup T') = P $	Probabilities for each individual sequence given by the Benjamini-Hochberg adjusted statistic from DESeq2								
$(TPI \cap TI ^c T' = I $	37	6	52	30,912	$3.731 \cdot 10^{-11}$	$1.197 \cdot 10^{-3}$	0.062	0.249	23.3
$ TPI \cap TI \cap T' = T $	291	18	37	30,912	$< 2.957 \cdot 10^{-27}$	$< 1.197 \cdot 10^{-3}$	0.348	0.587	<30.1
Downregulated									
$ TPI ^c (TI \cup T') = P $	Probabilities for each individual sequence given by the Benjamini-Hochberg adjusted statistic from DESeq2								
$(TPI \cap TI ^c T' = I $	3	0	30	39,809	n/s	n/s	n/s	n/s	n/s
$ TPI \cap TI \cap T' = T $	110	0	30	30912	n/s	n/s	n/s	n/s	n/s

5.3 Full Cold Acclimation Time-Series Experiment

In, Section 5.2.1 an RNA-Seq experiment that attempted to identify genes that are differentially expressed two weeks after transition to short days, low night temperatures, or both in combination, was described. It was hoped that this approach would identify sequences that, after two weeks' exposure respond to the partial cold-acclimation factors of photoperiod and temperature, and those that respond through an interaction of both. Although sequences were identified through this approach, the time-dependent expression of these sequences has not been investigated. It is likely that exposure to cold-acclimation conditions induces transient changes in transcript abundance that occurs within hours or days of exposure, or possibly after 2 weeks. For this reason, and to provide a more complete description of cold acclimation in barley, it was decided to undertake an RNA-Seq Time Series experiment where 3-week old non-acclimated plants grown in Long Days and Warm Night Temperatures would be exposed to Short Days and Low Night Temperatures for 0, 1, 2, 3, and 4 weeks. Winter barley plants of the cultivar California were grown, cold acclimated by exposure to SD/LT (full cold acclimation) for up to 4 weeks; three biological replicates per time point were prepared, and RNA-Seq performed as before (Section 5.2.1).

5.3.1 Quality Control and Statistical Analysis of RNA-Seq Datasets

All RNA samples generated an RIN of over 7.5, demonstrating a good quality template, and cDNA was subsequently generated from these. The resulting cDNA was then pair-end sequenced using an Illumina NextSeq™ 500 platform and the raw forward and reverse reads used as input for the Kallisto analysis pipeline that was developed and mounted on the University of Glasgow Galaxy server (Section 5.2.2). Briefly, between 28 and 53 million usable reads were present in each of the raw data sets; some TrimGalore trimming was required but all sets were deemed 'good quality' for sequencing (Table 5.8). The 'forward' and 'reverse' paired-end reads were then used as input for Kallisto and the output .csv files were analysed by DESeq2 (Sections 5.2.4 and 5.2.5; Fig. 5.2).

Table 5.8: Fast QC Basic Statistics of High-Throughput Sequencing Datasets from Barley Leaves Fully Cold Adapted for Up To 4 Weeks.

The forward (R1) and reverse (R2) Samples were grown as described in Section 5.3. LD-WT, non-acclimating (Long Days, Warm Temperature); SD-LT, fully-acclimating (Short Days, Low Temperature) conditions for 0 to 4 weeks (W0 – W4). Forward (R1) and Reverse (R2) paired-end read output files from Trim Galore!. None of the raw input files were considered by TrimGalore! To be of ‘Poor Quality’ although some further trimming was recommended; these were masked, and end sequence trimmed so that only partial reads (Sequence Length) were used in the subsequent alignments. See text for details.

Filename	Total Sequences	# Poor quality	Sequence length	%GC
0W-LD-WT-1_R1.fastq	29737204	0	35-75	54
0W-LD-WT-1_R1_trimmed	28675826	0	20-75	54
0W-LD-WT-1_R2.fastq	29737204	0	35-75	56
0W-LD-WT-1_R2_trimmed	28675826	0	20-75	56
0W-LD-WT-2_R1.fastq	31198124	0	35-75	55
0W-LD-WT-2_R1_trimmed	30045813	0	20-75	55
0W-LD-WT-2_R2.fastq	31198124	0	35-75	57
0W-LD-WT-2_R2_trimmed	30045813	0	20-75	57
0W-LD-WT-3_R1.fastq	52303379	0	75	53
0W-LD-WT-3_R1_trimmed	51733013	0	20-75	53
0W-LD-WT-3_R2.fastq	52303379	0	75	55
0W-LD-WT-3_R2_trimmed	51733013	0	20-75	55
1W-SD-LT-1_S1_R1.fastq	43022717	0	32-75	54
1W-SD-LT-1_S1_R1_trimmed	42659467	0	20-75	54
1W-SD-LT-1_S1_R2.fastq	43022717	0	32-75	56
1W-SD-LT-1_S1_R2_trimmed	42659467	0	20-75	56
1W-SD-LT-2_S4_R1.fastq	39405864	0	32-75	54
1W-SD-LT-2_S4_R1_trimmed	39060591	0	20-75	54
1W-SD-LT-2_S4_R2.fastq	39405864	0	32-75	56
1W-SD-LT-2_S4_R2_trimmed	39060591	0	20-75	56
1W-SD-LT-3_S7_R1.fastq	40683246	0	32-75	54
1W-SD-LT-3_S7_R1_trimmed	40311566	0	20-75	54
1W-SD-LT-3_S7_R2.fastq	40683246	0	32-75	56
1W-SD-LT-3_S7_R2_trimmed	40311566	0	20-75	56
2W-SD-LT-1_S10_R1.fastq	39690435	0	32-75	54
2W-SD-LT-1_S10_R1_trimmed	39416514	0	20-75	54
2W-SD-LT-1_S10_R2.fastq	39690435	0	32-75	55
2W-SD-LT-1_S10_R2_trimmed	39416514	0	20-75	55
2W-SD-LT-2_S2_R1.fastq	38728903	0	32-75	54
2W-SD-LT-2_S2_R1_trimmed	38328915	0	20-75	54
2W-SD-LT-2_S2_R2.fastq	38728903	0	32-75	56
2W-SD-LT-2_S2_R2_trimmed	38328915	0	20-75	56
2W-SD-LT-3_S5_R1.fastq	38653790	0	32-75	54
2W-SD-LT-3_S5_R1_trimmed	38171936	0	20-75	54
2W-SD-LT-3_S5_R2.fastq	38653790	0	32-75	56
2W-SD-LT-3_S5_R2_trimmed	38171936	0	20-75	56
3W-SD-LT-2_S8_R1.fastq	39779606	0	32-75	52
3W-SD-LT-2_S8_R1_trimmed	39358269	0	20-75	52
3W-SD-LT-2_S8_R2.fastq	39779606	0	32-75	55
3W-SD-LT-2_S8_R2_trimmed	39358269	0	20-75	55
3W-SD-LT-3_S11_R1.fastq	31739904	0	32-75	54
3W-SD-LT-3_S11_R1_trimmed	30396925	0	20-75	54
3W-SD-LT-3_S11_R2.fastq	31739904	0	32-75	57
3W-SD-LT-3_S11_R2_trimmed	30396925	0	20-75	57
3W-SD-LT6_S3_R1.fastq	34573990	0	32-75	53
3W-SD-LT6_S3_R1_trimmed	33683255	0	20-75	54
3W-SD-LT6_S3_R2.fastq	34573990	0	32-75	56
3W-SD-LT6_S3_R2_trimmed	33683255	0	20-75	56
4W-SD-LT-1_S6_R1.fastq	32728214	0	32-75	54
4W-SD-LT-1_S6_R1_trimmed	32168274	0	20-75	54
4W-SD-LT-1_S6_R2.fastq	32728214	0	32-75	56
4W-SD-LT-1_S6_R2_trimmed	32168274	0	20-75	56
4W-SD-LT-4_S9_R1.fastq	30551567	0	32-75	53
4W-SD-LT-4_S9_R1_trimmed	29997115	0	20-75	54

Filename	Total Sequences	# Poor quality	Sequence length	%GC
4W-SD-LT-4_S9_R2.fastq	30551567	0	32-75	56
4W-SD-LT-4_S9_R2_trimmed	29997115	0	20-75	56
4W-SD-LT-6_S12_R1.fastq	30460966	0	32-75	54
4W-SD-LT-6_S12_R1_trimmed	29935915	0	20-75	55
4W-SD-LT-6_S12_R2.fastq	30460966	0	32-75	57
4W-SD-LT-6_S12_R2_trimmed	29935915	0	20-75	57

The PCA output from DESeq2 is presented in Figure 5.8a. The datasets are tightly clustered together but one of the controls (0 W-3) is clearly an outlier. For this reason, it was omitted from the analysis and DESeq2 run again with 14 instead of 15 samples. The PCA for this second analysis is presented in Figure 5.8b. Approximately 50% of the variance in gene expression between the five datasets was attributable to PCA factor 1, and 39% to PCA factor 2. In total, therefore, 89% of the variance in the datasets was attributable to two factors; encouragingly these two unknown factors separated the datasets well. Table 5.9 summarises gene expression patterns in the pair-wise comparisons of the filtered datasets. Compared with the 2-week acclimation ‘condition’ experiment described in Section 5.2 (Table 5.3), a far greater number of sequences that met the filter criteria and which responded to full cold-acclimation conditions were identified when compared with non-acclimated controls (Table 5.9). Of particular note is that, after 2 weeks exposure to full cold-acclimation conditions, 3,693 sequences were identified as upregulated and 5,051 as downregulated by 2-fold or more (Table 5.9); this compares with 52 and 30 sequences (LD/WT versus. SD/LT), respectively, for the corresponding treatments shown in Table 5.3.

Table 5.9 provides a summary of the changes observed in the datasets. Kallisto identified 30,339 sequences that appeared in at least one time point dataset. Pair-wise comparisons between the time points suggested up to 16,050 sequences responded to full cold acclimation in all comparisons apart from the 3-week versus 4-week sets, where few differences were detected. Filtering of these significant changes in Excel using the criteria of $p_{adj} < 0.1$, > 2 -fold change, BaseMean score > 1 , reduced the datasets; a list of these is presented in digital format on the accompanying digital media storage device. Heat map plots of these datasets are presented in Figure 5.9 and clearly indicate good correlation for gene regulation by cold acclimation across the replicate samples, giving added confidence the datasets contain useful information on the regulation of genes by cold-acclimation conditions.

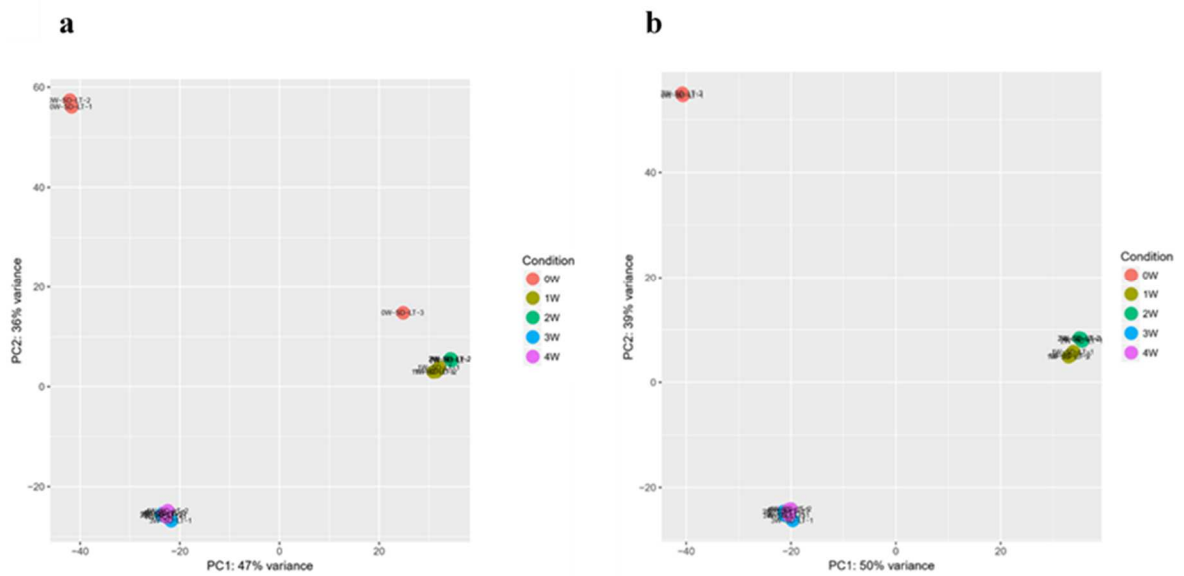


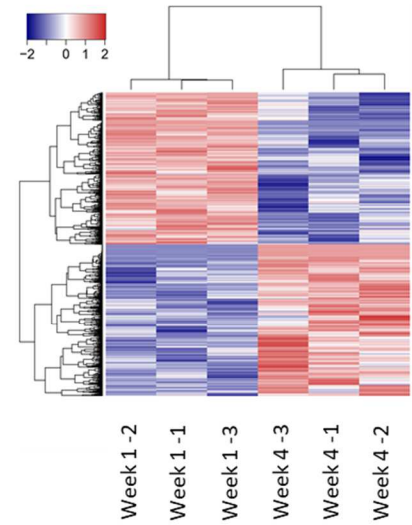
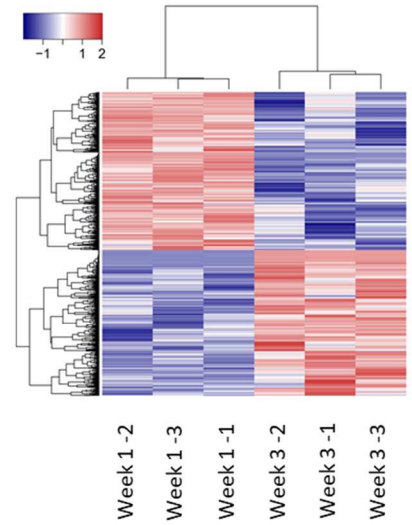
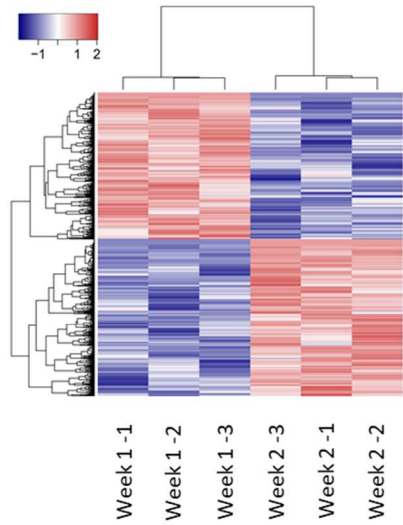
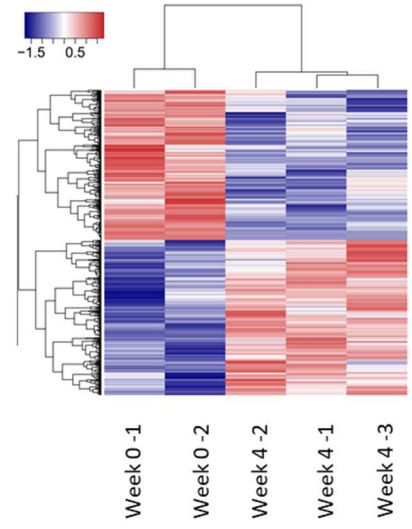
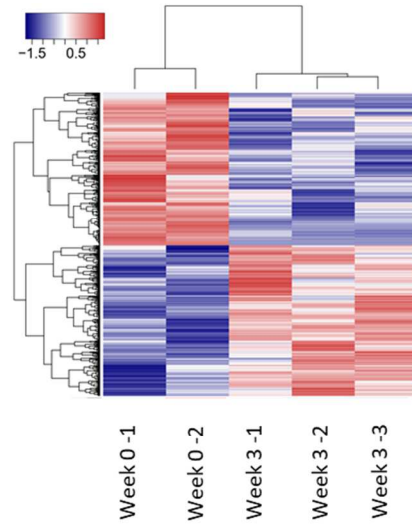
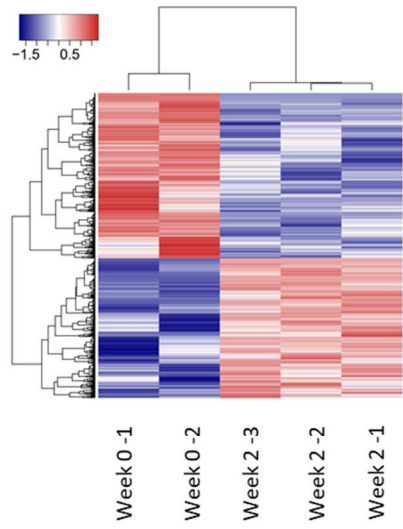
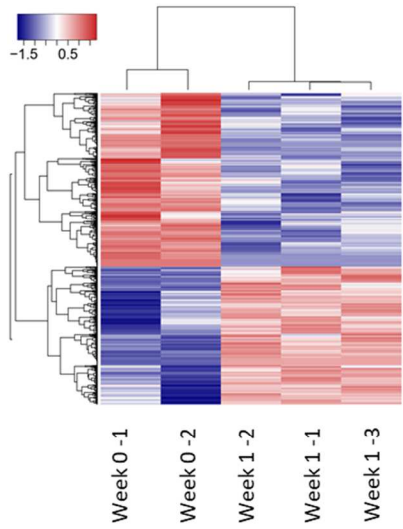
Figure 5.8: Two-Dimensional Principal Component Analysis of a Time-Series Transcript Profile in Cold-Acclimated *Hordeum vulgare* (cv. California) Leaves.

Plants were grown in LD (16/8h photoperiod) and WT (20°/16°C day/night) for 4 weeks (LD/WT) and then exposed for a further two weeks to a full cold-acclimation regime (SD/LT). Mature sections of the third and fourth leaves of plants were then harvested, frozen immediately to -80°C, and total RNA was subsequently prepared for RNA-Seq analysis (Section 2.6). NGS sequencing was performed on cDNA generated from these pools of RNA (Sections 2.6 and 5.2.3) and analysed by Kallisto and DESeq2. The PCA variance was calculated using the relative abundance of each sequence, expressed as rlog2 (regularised Log2) transformation of the normalised values recorded.

Table 5.9: Summary of DESeq2 Pair-wise Time-Dependent Comparisons for Expressed Genes in *Hordeum vulgare* (cv. California) Leaves Exposed to Short Days and Low Temperatures.

RNA-Seq analysis was performed on three biological replicates of mature barley leaves exposed to Short Days and Low Night Temperatures for 0–4 weeks (Section 2.1.2). Tables of the normalised abundance for each detected gene in each of the replicates were generated by DESeq2 as .csv files, which were then filtered in Microsoft Excel spreadsheets. The number of genes with significantly different abundances ($p_{adj} < 0.1$, Benjamini-Hochberg correction) is presented. The other columns present the number of significantly differentially abundant genes at the 2-fold, 5-fold, and 10-fold levels. ‘Upregulated’ refers to genes that were higher in the cold-acclimated sample; see Section 2.1.2 for full experimental conditions. In this table, Wk0 v Wk1, for example, is equivalent to the relative complement of sets $|Wk1| \setminus |Wk0|$, sequences that are in set $|Wk1|$ but not in set $|Wk0|$.

	#Genes	Significant (20384)	Up-regulated >2x	Up-regulated >5x	Up-regulated >10x	Down-regulated >2x	Down-regulated >5x	Down-regulated >10x
Wk0 v Wk1	30339	14943	2739	688	211	5610	2568	1345
Wk0 v Wk2	30339	15864	3693	1120	407	5051	1919	971
Wk0 v Wk3	30339	12229	1787	261	49	3272	1389	772
Wk0 v Wk4	30339	12268	1933	281	52	3294	1379	781
Wk1 v Wk2	30339	13753	3376	1394	567	2269	366	111
Wk2 v Wk3	30339	16050	4122	1170	518	4437	1286	439
Wk3 v Wk4	30339	34	5	4	4	8	4	4



/cont.

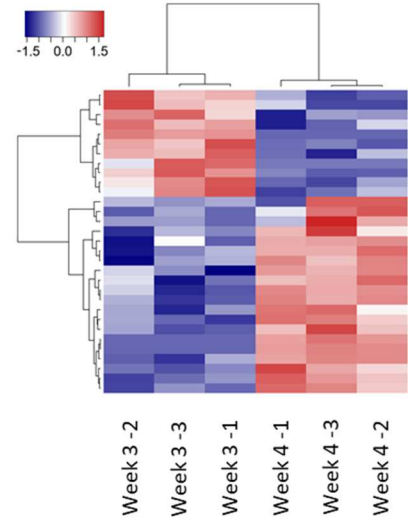
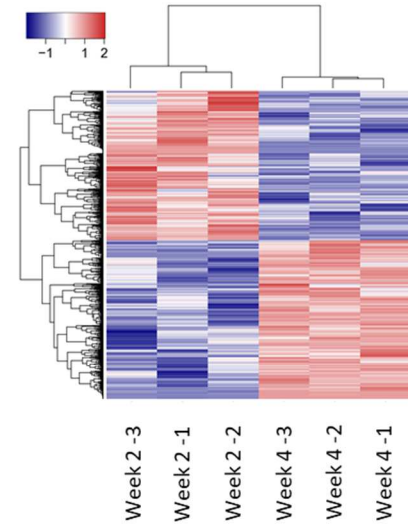
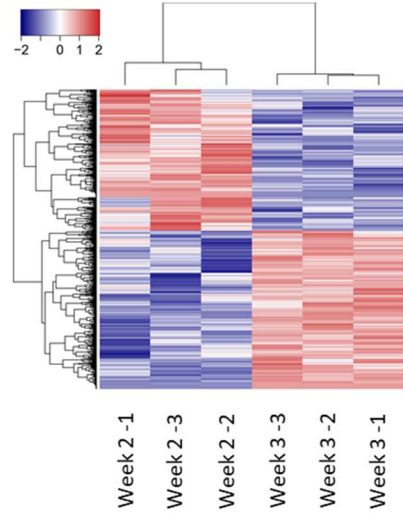


Figure 5.9: DESeq2 Barley Gene Expression Heat Maps: Comparison of Time-Series Samples for Cold Acclimation Treatment.

Plants grown in Long Days and Warm Night Temperatures (16h, 16°C) for 4 weeks and then exposed to Short Days and Low Night Temperatures (8h and 4°C) for up to 4 weeks; see Section 2.2. Total RNA was extracted and purified 2 hours post-dawn and cDNA generated for sequencing using an Illumina NextSeq 500 Sequencer and TrueSeq RNA Kit (see Sections 5.2.1 to 5.2.4). The raw read datasets (3 replicates x 5 time points x 2 paired-end reads = 30 files) were trimmed to remove low quality sequences, aligned to the barley cDNA database (IBSC, 2017) using the pseudo-alignment programme Kallisto, and the output analysed by the DESeq2 statistical package (Sections 5.2.4 and 5.2.5). One of the 0-week replicates (Weeks 0–3) was omitted as PCA analysis suggested it was an outlier (see Fig. 5.8).

5.3.2 An RNA-Seq Validity Check; Comparison of Two Independent |TPI| Datasets.

Before progressing to discuss the Cold Acclimation Time Series results, a check of the validity of the RNA-Seq method for this experiment is provided. In Section 5.2, a dataset was derived from the relative complement of sequences that were in |SDLT| for two weeks but not in |LDWT|, i.e., $|SDLT| \setminus |LDWT| = |TPI|$. In this section (Section 5.3.2) a similar comparison is made between the relative complement of Wk0 v Wk2; the derived set is $|SDLT| \setminus |LDWT| = |TPI|$ and, therefore, these two derived sets should contain similar sequences. Sequences that are common to both of these sets can be viewed at their intersect in a Venn diagram, this is presented in Figure 5.10. The set |TPI| from Section 5.2 (Experiment 1) contains 52 upregulated sequences ($n=52$ from $N=30912$ total sequences detected; Table 5.3), whereas the set |TPI| from Section 5.3 (Experiment 2) contains 3,693 upregulated sequences ($k=3,693$ from $N=30,339$ total sequences detected; Table 5.9). A total of 48 sequences appear in the intersect of these two sets (x) and the Hypergeometric Probability Mass Function (*pmf*) can be calculated as $n=52$, $k=3693$, $x=48$, and $N=30,339$. These calculations are presented in Table 5.10 and a graphical representation is presented in Figure 5.11. It is clear from these results that, given the sizes of k and n , the expected number of common sequences was 6.3 for upregulated genes (whereas 48 were observed) and 5 for downregulated genes (whereas 22 were observed). The probabilities that these common genes appeared in both datasets due to random factors alone are $<1 \cdot 10^{-38}$ and $<1 \cdot 10^{-11}$, respectively. The conclusion is that the methods used to cold-acclimate plants, sequence their transcriptomes, and analyse the resulting data are robust and allow genes responsive to T, P, and I to be identified. The sequences that occur in the intersects of Figure 5.10 are shown in bold typeface in Tables 5.5

and 5.6. It is also clear that these two experiments are not identical; Experiment 1 identified 52 upregulated and 30 downregulated sequences, whereas Experiment 2 revealed 3,693 and 5,051 sequences, respectively. Possible reasons for this are given in the Discussions section at the end of this chapter. A similar comparison can be made for downregulated sequences

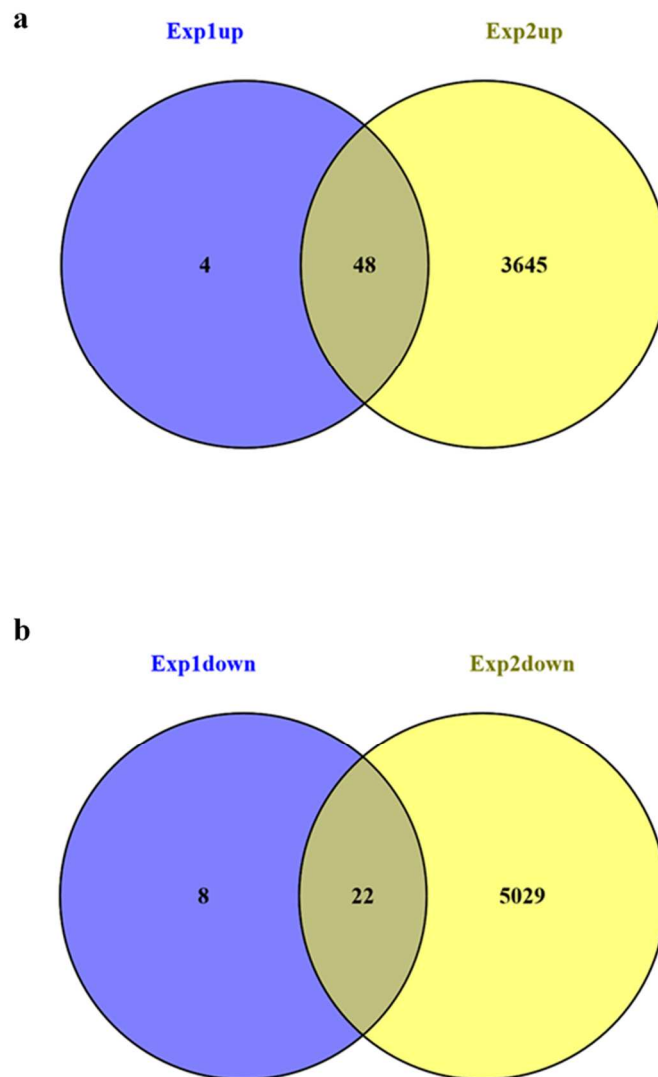


Figure 5.10: Venn Diagram Comparing TPI-Responsive Sequences Derived from Two Independent Experiments.

Two sets of sequences were responsive to temperature alone, photoperiod alone, and an interaction between both (TPI sequences); these were determined from the relative complement of samples from plants fully acclimated for 2 weeks and non-acclimated plants ($|\text{SDLT}| \setminus |\text{LDWT}| = |\text{TPI}|$; Tables 5.3 and 5.9). Experiment 1 is described in Section 5.2; Experiment 2 is described in Section 5.3. The Venn diagrams above show a comparison of these two $|\text{TPI}|$ datasets for upregulated sequences (a) and downregulated sequences (b). Diagram reproduced from the Venny online resource page (Oliveros, J.C. (2007–2015). (<https://bioinfogp.cnb.csic.es/tools/venny/index.html>)).

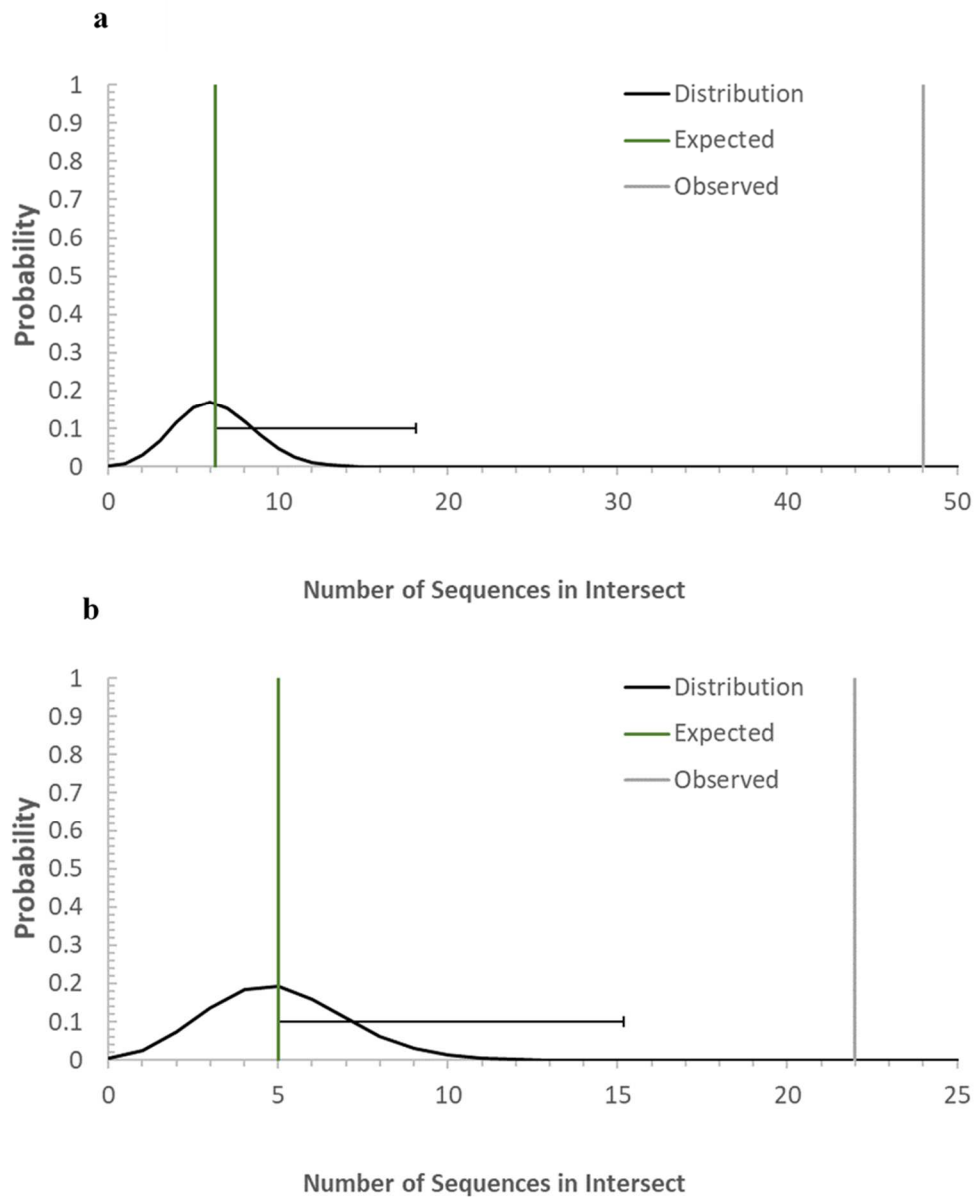


Figure 5.11: Hypergeometric distribution for Intersection of sequences in two independent RNA-Seq experiments.

The hypergeometric distribution (black line) was calculated using the parameters shown in Table 5.4 for sequences found at the intersection of two independent experiments to derive |TPI| responsive sequences in RNA-Seq datasets (see Fig. 5.10). The relative complements of $|\text{SDLT}| \setminus |\text{LDWT} = |\text{TPI}|$ set was used to determine upregulated (panel a) and downregulated (panel b) sequences (see text for details). In both cases, the most likely outcome (expected value) was 5 or 6, whereas the observed outcome was much more than 5 standard deviations ($p < 0.001$) away (horizontal error bar).

Table 5.10: Hypergeometric Probabilities for TPI Sequences Derived from Two Independent Cold-Acclimation Experiments.

The hypergeometric probability mass function (*pmf*) was calculated for the comparison sets shown. *k*, the number of sequences (>2-fold change) identified in the first set; *n*, number of sequences identified in the second set; *N*, total number of detected genes in the experiment; *x*, the number of sequences appearing in the intersect; the probability of selecting one gene from *N* is given as $p=k/N$. The hypergeometric *pmf* is calculated from the values *N*, *n*, *k*, and *x* (Section 2.7). In addition to this statistical approach, the hypergeometric distribution for all values of *n* was constructed using the conditional probability for *x* calculated from set theory ($p(\{A\} | \{B\})$). From this, an expected value for the average of the distribution could be calculated ($E(x)$) and the observed (*x*) and expected ($E(x)$) values compared. The standard deviation (*St Dev*) was also calculated as well as the number of standard deviations between *x* and $E(x)$ (*St Dev Range*). Normally, standard deviation ranges exceeding 2, 3, and 5 are indicative of probabilities of <0.05, <0.01, and <0.001. See Section 2.7 for a full explanation.

Response	<i>k</i>	<i>n</i>	<i>x</i>	<i>N</i>	<i>pmf</i>	$p\{A\} \{B\}$	Exp	St Dev	St Dev Range
Up	52	3693	48	30339	$1.55 \cdot 10^{-39}$	$1.71 \cdot 10^{-3}$	6.33	2.36	17.7
Down	30	5051	22	30339	$9.79 \cdot 10^{-12}$	$9.89 \cdot 10^{-4}$	4.99	2.04	8.3

5.3.3 Time-Dependent Changes Compared with Non-Acclimated Controls

The filtered time series datasets were then further analysed for common genes, and the results are presented in Venn diagrams (Figs. 5.12 and 5.13). Hypergeometric probabilities were calculated to determine whether the common sequences appearing in the intersections between these time series datasets were likely to have arisen through random transcriptional changes (transcriptional ‘noise’) or from the experimental cold-acclimation conditions.

Initially, sets containing sequences responsive to T, P, and I were derived ($|TPI|$) by finding the relative complements of fully acclimated samples and non-acclimated samples ($|\{SDLT\} \setminus \{LDWT\}| = |TPI|$) (see Table 5.4) at each time point (1–4 weeks). During the first week of cold acclimation, 2,739 sequences appeared to be upregulated (Fig. 5.12; Table 5.9). Many of these sequences were transiently elevated levels for only 1 week (874), 1 to 2 weeks (1133), 1 to 3

weeks (53), and 1 to 4 weeks (393). After 2 weeks of cold acclimation, a further 1,664 TPI sequences were transiently upregulated for just the 2-week period, 43 for the 2 to 3 week period, and 270 for the 2 to 4 week period. After 3 weeks of cold acclimation, a further 150 TPI sequences were upregulated for just the 3-week period, and 702 for the 3 to 4 week period. Finally, after 4 weeks of cold acclimation, a further 242 TPI sequences were upregulated. These transient changes are represented in a graphical form in Figure 5.14a.

Figure 5.13 presents a Venn diagram showing the sequences that were down-regulated by cold acclimation. During the first week of cold acclimation, a total of 5,610 sequences were downregulated. Of these, 1,797 sequences were downregulated but only for the first week. A further 1,579 sequences were down regulated for Week 1 and Week 2, 96 for Weeks 1 to 3, and 1,531 remained downregulated for the whole of the 4-week period. A further 1,724 sequences (1316+43+318+47) were downregulated after 2 weeks of cold acclimation; of these, 1,316 were downregulated for Week 2 only, 43 for Weeks 2 and 3, and 318 for Weeks 2 to 4. After 3 weeks of cold acclimation, a further 270 TPI sequences were downregulated for just the 3-week period, and 591 for the 3–4 week period. Finally, 260 TPI sequences were downregulated for the 4-week period only. These transient changes are presented in graphical form in Figure 5.14b.

It is clear from Figures 5.12 and 5.13 that other sequences were detected that appeared in the intersects of the four sets (e.g., in Fig. 5.12, 22 sequences appear to be upregulated after 1 week and 3 weeks only) but the erratic appearance of these with respect to time gives some cause for concern, and raises the question of whether it is possible that a sequence can be upregulated after one week, return to base level the next, and be upregulated again the following week. Whilst it is conceivable that some sequences respond in this way, it is also possible that these changes were unrelated to the cold-acclimation process. This will be discussed further at the end of this chapter.

Table 5.11 presents the hypergeometric probabilities that the sequences appearing in the intersects of these data sets are likely to have arisen through random transcriptional events, or were regulated by the cold-acclimation conditions.

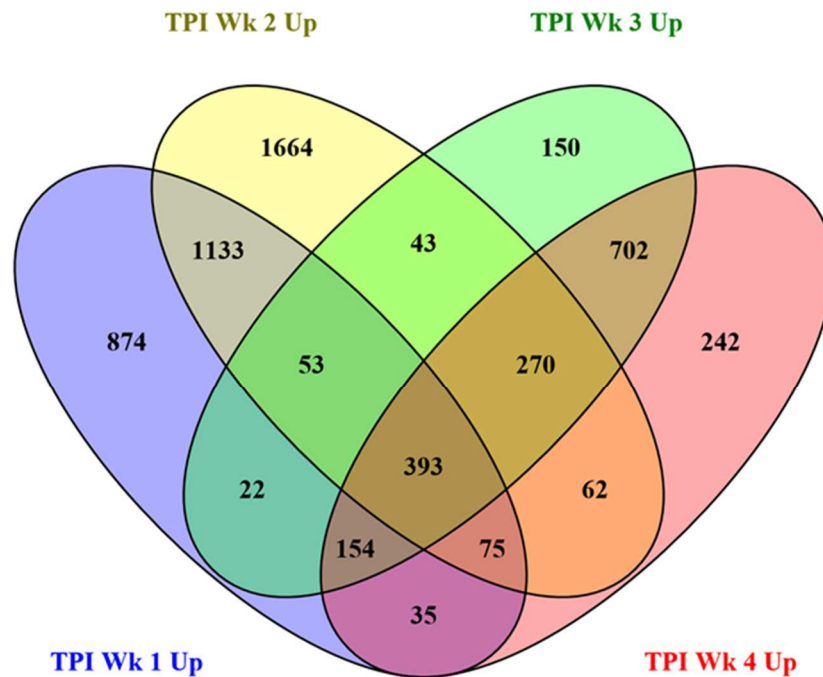


Figure 5.12: Venn Diagram of Time-Series Changes in Barley Genes ‘Upregulated’ by Transition to Both Short Days and Low Temperatures.

Samples were prepared as described in Figure 5.9 and the datasets from the relative complements of each time point with non-acclimated (control) plants were derived (e.g., $|Wk1| \setminus |Wk0| = |TPI\ Wk1|$). The datasets were filtered for significance (Benjamini-Hochberg $p_{adj}=0.1$) and only those showing a > 2-fold increase over controls and a BaseMean abundance score of >1.0 are presented. Diagram reproduced from the Venny online resource page (Oliveros, J.C. (2007–2015) Venny. An interactive tool for comparing lists with Venn's diagrams. (<https://bioinfogp.cnb.csic.es/tools/venny/index.html>).

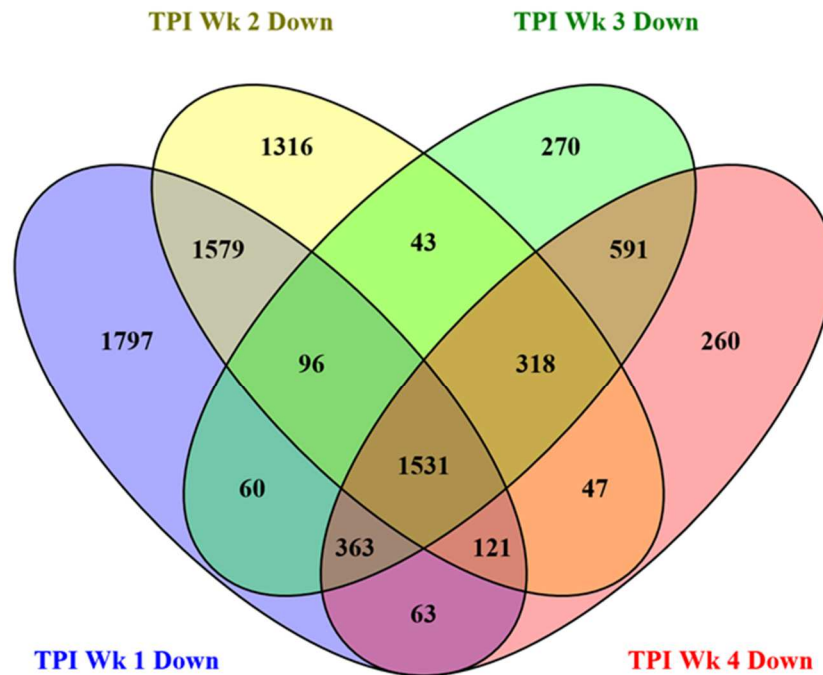


Figure 5.13: Venn Diagram of Time-Series Changes in Barley Genes ‘Downregulated’ by Transition to Both Short Days and Low Temperatures.

Samples were prepared as described in Figure 5.9 and the datasets from the relative complements of each time point with non-acclimated (control) plants were derived (e.g., $|Wk1| \setminus |Wk0| = |TPI\ Wk1|$). The datasets were filtered for significance (Benjamini-Hochberg $p_{adj}=0.1$) and only those showing a > 2 -fold increase over controls and a BaseMean abundance score of >1.0 are presented. Diagram reproduced from the Venny online resource page (Oliveros, J.C. (2007–2015) Venny. An interactive tool for comparing lists with Venn's diagrams. (<https://bioinfogp.cnb.csic.es/tools/venny/index.html>)).

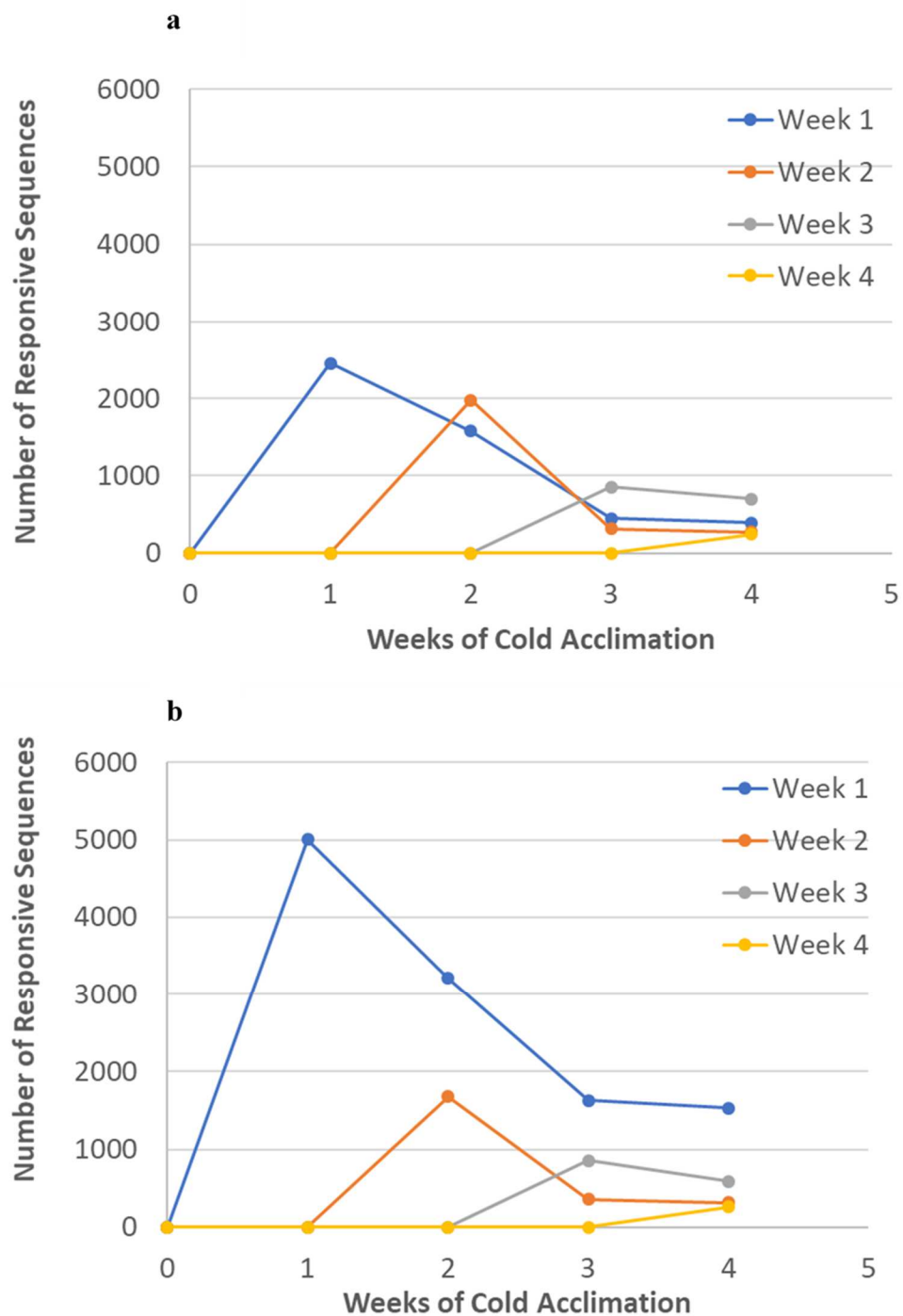


Figure 5.14: Transient Changes in Gene Expression Accompanying Exposure to Cold Acclimation Conditions.

The number of TPI sequences responsive to full cold-acclimation conditions. A, upregulated sequences; B, downregulated sequences. See Figures 5.12 and 5.13 for further details.

Table 5.11: Comparisons of Common Genes Regulated by Transition to Short Days and Low Temperatures: Time Series *cf.* Non-Acclimated Controls.

The hypergeometric probability mass function (*pmf*) was calculated for the comparison sets shown. The first set, chosen arbitrarily, contained k successes (the number of genes with >2-fold change), which were selected from a total population of N detected genes in the experiment; the probability of selecting one successful gene from N is given as $p=k/N$. The second set contained n genes (>2-fold change), x of which appeared in the intersection of the two sets. The hypergeometric *pmf* was calculated from the values N , n , k , and x . In addition to this statistical approach, the hypergeometric distribution for all values of n was constructed using the conditional probability for x calculated from set theory ($p(\{A\} | \{B\})$). From this, an expected value for the average of the distribution could be calculated ($E(x)$) and the observed (x) and expected ($E(x)$) values compared. A standard deviation (*St Dev*) was also calculated as well as the number of standard deviations between x and $E(x)$ (*St Dev Range*). Normally, standard deviation ranges exceeding 2, 3, and 5 are indicative of probabilities of <0.05, <0.01, and <0.001. See Section 2.7 for a full explanation.

Intersection (Common Genes)	n	x	k	N	pmf	$p(\{A\} \{B\})$	$E(x)$	<i>St Dev</i>	<i>St Dev Range</i>
Upregulated									
TPI 1Wk ∩ TPI 2Wk	3693	1654	2739	30,339	$< 1 \cdot 10^{-255}$	$1.217 \cdot 10^{-1}$	449.5	19.9	60.6
TPI 2Wk ∩ TPI 3Wk	3693	759	1787	30,339	$5.5 \cdot 10^{-205}$	$5.890 \cdot 10^{-2}$	217.5	14.3	37.8
TPI 3Wk ∩ TPI 4Wk	1933	1519	1787	30,339	$3.0 \cdot 10^{-213}$	$6.371 \cdot 10^{-2}$	123.2	10.7	130.0
TPI 1Wk ∩ TPI 2Wk ∩ TPI 3Wk	$< 1 \cdot 10^{-255} * 5.5 \cdot 10^{-205} =$				$< 1 \cdot 10^{-255}$				
TPI 2Wk ∩ TPI 3Wk ∩ TPI 4Wk	$5.5 \cdot 10^{-205} * 3.0 \cdot 10^{-213} =$				$< 1 \cdot 10^{-255}$				
TPI 1Wk ∩ TPI 2Wk ∩ TPI 3Wk ∩ TPI 4Wk	$< 1 \cdot 10^{-255} * 5.5 \cdot 10^{-205} * 3.0 \cdot 10^{-213} =$				$< 1 \cdot 10^{-255}$				

Downregulated									
 TPI 1Wk ∩ TPI 2Wk 	5610	3327	5051	30,339	$< 1 \cdot 10^{-255}$	$1.665 \cdot 10^{-1}$	840.90	26.5	93.9
 TPI 2Wk ∩ TPI 3Wk 	5051	1988	3272	30,339	$< 1 \cdot 10^{-255}$	$1.087 \cdot 10^{-1}$	544.7	22.1	65.5
 TPI 3Wk ∩ TPI 4Wk 	3294	1122	3272	30,339	$< 1 \cdot 10^{-255}$	$1.086 \cdot 10^{-1}$	357.6	17.9	42.8
 TPI 1Wk ∩ TPI 2Wk ∩ TPI 3Wk 	$< 1 \cdot 10^{-255} * < 1 \cdot 10^{-255} =$				$< 1 \cdot 10^{-255}$				
 TPI 2Wk ∩ TPI 3Wk ∩ TPI 4Wk 	$< 1 \cdot 10^{-255} * < 1 \cdot 10^{-255} =$				$< 1 \cdot 10^{-255}$				
 TPI 1Wk ∩ TPI 2Wk ∩ TPI 3Wk ∩ TPI 4Wk 	$< 1 \cdot 10^{-255} * < 1 \cdot 10^{-255} < 1 \cdot 10^{-255} =$				$< 1 \cdot 10^{-255}$				

Table 5.11 shows that the sequences appearing in the intersections (x) between the different sets are highly significant. This is confirmed by the hypergeometric probability mass function (pmf) for the observed number in the intersections (x), and from set theory calculations where, in all cases, the observed and expected ($E(x)$) values were more than 5 standard deviations apart ($p < 0.001$). From these findings, it seems the bulk of the identified sequences responded to the cold-acclimation conditions, although it is possible a few may have arisen from random transcriptional events. The list of genes that appeared in the different intersections is too large to present in this chapter but is included in the Appendix, and electronic copies have been included in the digital media accompanying this thesis. A brief description of some of the more interesting sequences is included in Appendix Tables A5.3, A5.3.1, and A5.6

5.4 Role of ABA in Barley Cold Acclimation

It has long been established that the plant growth regulator abscisic acid (ABA) is synthesised in plants in response to a range of environmental factors, including low temperatures (Cutler, et al. 2010). In Chapter 1, evidence was presented that low temperatures and photoperiod trigger ABA-dependent and ABA-independent responses in the model plant *Arabidopsis*. In Chapter 3, however, some evidence was provided that the cold-acclimation process in barley differs from that in *Arabidopsis* and rye, in that exposure to low night temperatures alone appears to confer full cold acclimation; short photoperiods are not required. This raises the question, ‘do ABA-dependent and ABA-independent cold-acclimation pathways operate in barley?’ Cold acclimation can be induced in chickpea (*Cicer arietinum*) plants grown in warm conditions and long days by spraying foliage with solutions of ABA (Bakht et al., 2017; Bakht, et al., 2013). It was decided to use a similar approach to determine if exogenous applications of ABA would induce partial or full cold acclimation in barley.

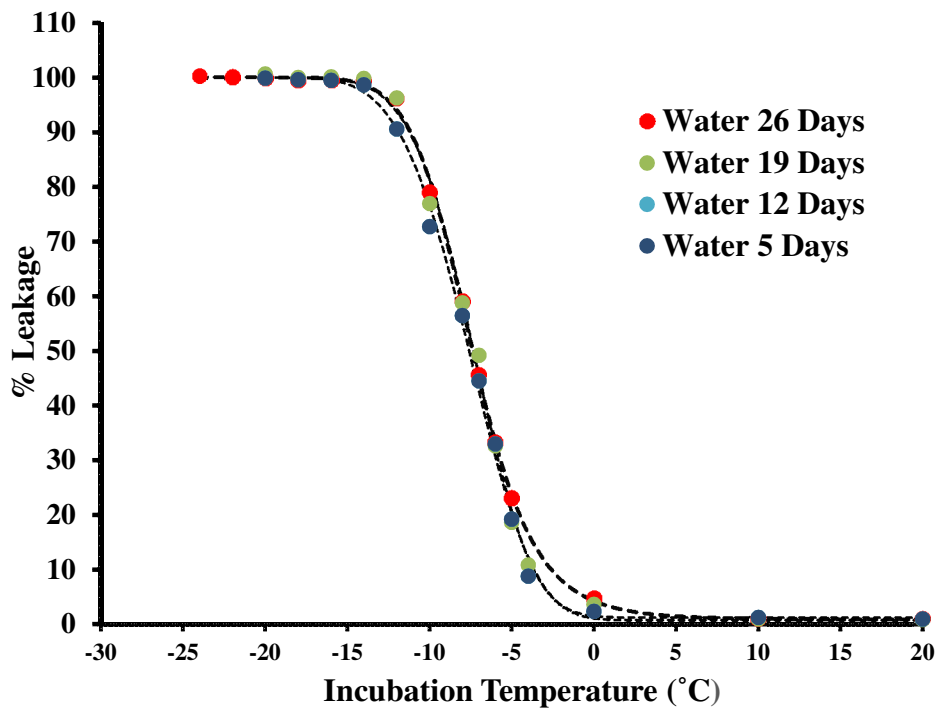
5.4.1 Assessment of Cold Tolerance in Barley Plants Sprayed with ABA

Plants of *Hordeum vulgare* cv. California were germinated and grown in non-acclimating conditions (16/8h and 20°/16°C day/night) for up to 7 weeks. At the 3-week stage, the foliage was sprayed every second day with 10 mL of deionised water containing either 0, 10⁻⁵, or 10⁻⁴ M ABA (Section 2.3.1). After 0, 1, 2, 3, or 4 weeks of ABA treatment, samples were

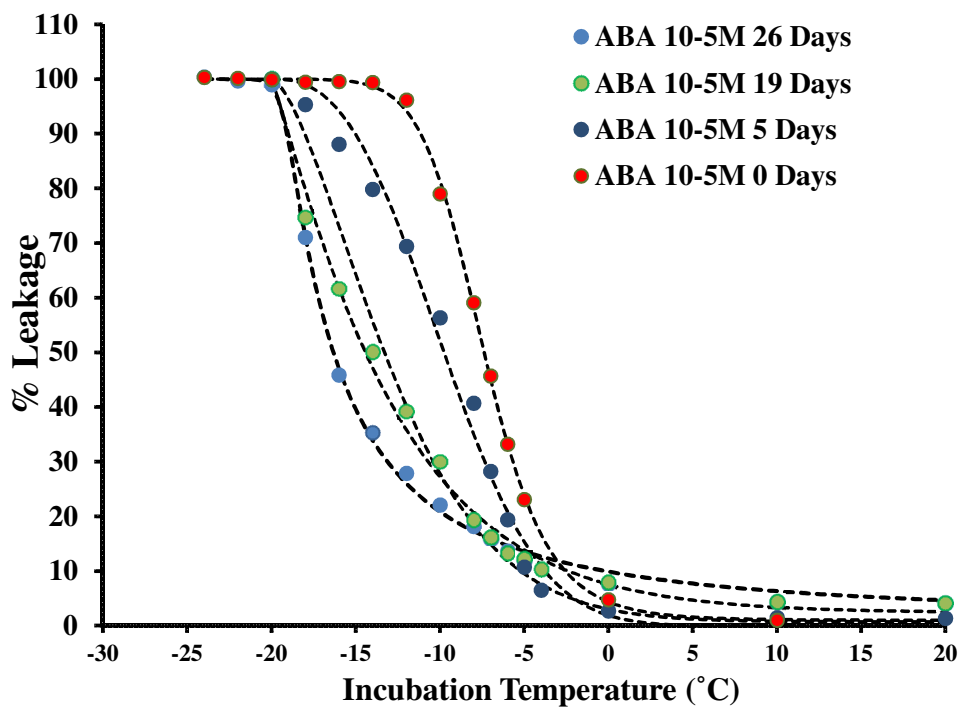
removed, leaves were briefly washed with deionised water, and leaf disc samples removed for LT_{50} measurements to assess the level of cold tolerance (Section 2.3).

Figure 5.15 presents the results of these experiments. Spraying with water alone had no discernible effect on LT_{50} ; even after 26 days (13 spraying events), the LT_{50} remained between -7.2° and -7.6°C , similar to that of unsprayed, non-acclimated controls (Fig. 5.15a). Spraying with 10^{-5} or 10^{-4} M ABA progressively decreased the LT_{50} value; after 26 days, these values had decreased to -16.2°C and -18.2°C , respectively (Table 5.12). Comparison of Table 3.4 with Table 5.12, and Figure 3.7 with Figure 5.15, shows that after 4 weeks of treatment, spraying the California cultivar grown in non-acclimating conditions (8h nights at 16°C) with 10^{-4} M ABA was equally effective in inducing cold tolerance as exposure to SD and LT in the absence of foliar exogenous ABA application; both treatments reduced the LT_{50} from $-7.0^{\circ}/-9.0^{\circ}\text{C}$ to -18.2°C .

a



b



C

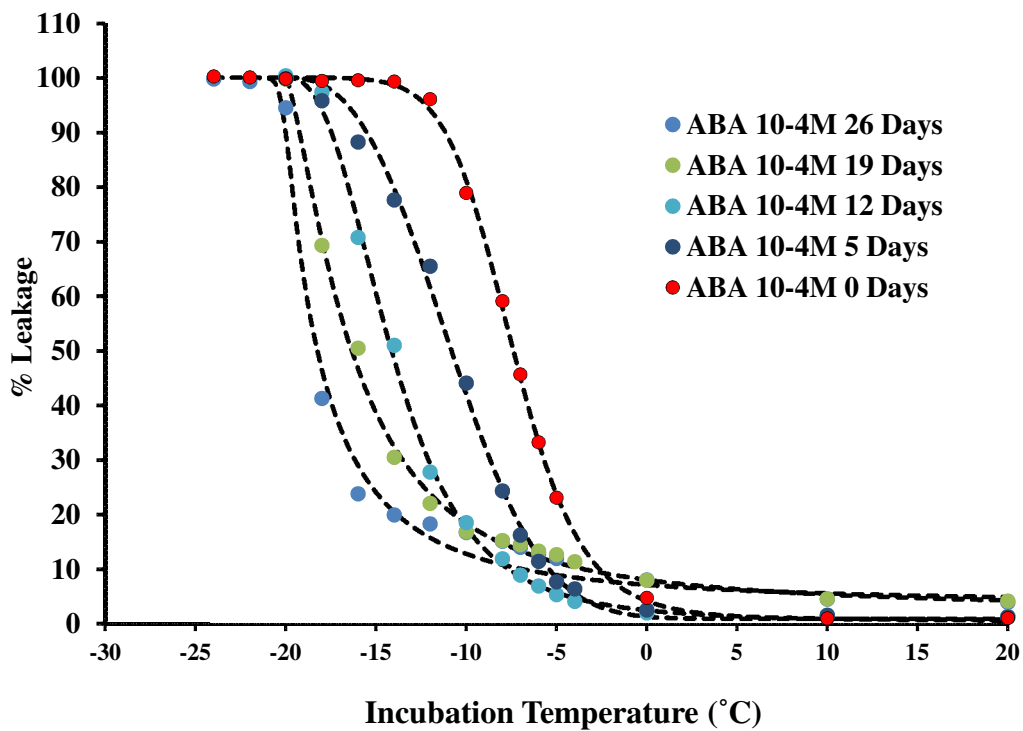


Figure 5.15: The Effect of ABA Applications of Barley Leaf Cold Tolerance (LT_{50}).

Plants were grown as described in Section 2.1.2 and treated with water, 10^{-5} M or 10^{-4} M ABA as described in Section 5.4, for the times indicated. Tissue damage was estimated as the percentage solute leakage from samples held at each of the indicated temperatures for 60 minutes (Section 2.3). The average values and standard errors of $n=3$ replicates are presented. A four-parameter logistic regression model was applied to the data. A value of 100% indicates that all cells were lysed; 0%, that no cells were damaged. Three-week-old plants were sprayed every second day with 10 mL of deionised water containing 0, 10^{-5} , or 10^{-4} M ABA for up to 26 days. Percentage leakage curves for 0 M ABA (a), 10^{-5} M ABA (b), and 10^{-4} M ABA (c)

Table 5.12: Freezing Tolerance in Barley Cultivar California Leaves Induced by ABA Application.

Plants were grown as in the non-acclimating conditions described in Section 2.1.2 and treated with water, 10^{-5} M or 10^{-4} M ABA as described in Section 5.4. The LT_{50} values were measured and used as an estimate of cold tolerance (Section 2.3). The values are the average \pm SE (in parentheses) of three biological replicates (n=3); each replicate contained five independent leaf disc samples.

	0 Days	5 Days	12 Days	19 days	26 Days
0 M ABA	-7.2 (0.1)	-7.2 (0.0)	-7.3 (0.2)	-7.3 (0.0)	-7.6 (0.0)
10^{-5} M ABA	-7.4 (0.1)	-9.8 (0.1)	-13.2 (0.2)	-14.4 (0.2)	-16.2 (0.2)
10^{-4} M ABA	-7.4 (0.0)	-10.8 (0.0)	-14.0 (0.1)	-16.2 (0.3)	-18.2 (0.1)

Given these findings, it would be interesting to compare the transcriptome profiles of plants cold acclimated by the environmental factors of SD and LT with those of plants treated with 10^{-4} M ABA (see Section 5.4.1).

5.4.2 Transcriptome Profile of Barley *cv.* California Leaves Treated with Exogenous ABA Applications.

Plants were grown and treated with ABA as described in Section 5.4, leaf tissue was harvested and total RNA extracted and purified (Sections 2.6 and 5.2). Samples were then sent to the University of Glasgow Polyomics Facility for quality control assessment, cDNA synthesis, and high-throughput DNA sequencing using an Illumina NextSeq™ 500 platform (Sections 2.6 and 5.2). The raw sequence was then used as input for the Galaxy server pipeline that was developed; details of the trimmed sequence are provided in Table 5.13. To summarise, between 22.8 and 35.9 million paired-end reads were present in the 30 datasets (5 time points x 3 replicates x 2 paired reads = 30 data files). None of the datasets were considered poor quality by the FastQC package, although extensive trimming was required (Table 5.13). Following this stage, the output from Trim Galore was used as input for the Kallisto cDNA alignment package (Fig. 5.2). The Kallisto output was then analysed by DESeq2 and the .csv output filtered in Microsoft Excel using the criteria mentioned in Section 5.2.5.

Table 5.13: FastQC Basic Statistics of High-Throughput Sequencing Datasets from Barley Leaves Cold-Adapted by 10^{-4} M ABA Application.

Plants were grown in non-acclimating conditions (Long Days, Warm Temperature) for 3 weeks and then sprayed every two days with 10^{-4} M ABA. Samples were taken at the commencement of spraying (0W) and every week thereafter up to 4 weeks (4W). Forward (R1) and Reverse (R2) paired-end read output files from Trim Galore!. None of the raw input files were considered by TrimGalore! To be of ‘Poor Quality’ although some further trimming was recommended; these were masked, and end sequence trimmed (*cf* files with fastq and trimmerd suffixes) so that only partial reads (Sequence Length) were used in the subsequent alignments. See text for details.

Filename	Total Sequences	Sequences flagged as poor quality	Sequence length	%GC
ABA-0W1_S8_R1_001.fastq	24887789	0	35-75	53
ABA-0W1_S8_R1_001_trimmed	23490854	0	20-75	52
ABA-0W1_S8_R2_001.fastq	24887789	0	35-75	55
ABA-0W1_S8_R2_001_trimmed	23490854	0	20-75	56
ABA-0W2_S1_R1_001.fastq	31586971	0	35-75	52
ABA-0W2_S1_R1_001_trimmed	30839564	0	20-75	52
ABA-0W2_S1_R2_001.fastq	31586971	0	35-75	53
ABA-0W2_S1_R2_001_trimmed	30839564	0	20-75	53
ABA-0W3_S7_R1_001.fastq	31748692	0	35-75	55
ABA-0W3_S7_R2_001.fastq	31748692	0	35-75	58
ABA-0W3_S7_R1_001_trimmed	31085208	0	20-75	55
ABA-0W3_S7_R2_001_trimmed	31085208	0	20-75	58
ABA-1W1_S9_R1_001.fastq	28617779	0	35-75	51
ABA-1W1_S9_R2_001.fastq	28617779	0	35-75	52
ABA-1W1_S9_R1_001_trimmed	27611059	0	20-75	51
ABA-1W1_S9_R2_001_trimmed	27611059	0	20-75	53
ABA-1W2_S10_R1_001.fastq	27108575	0	35-75	50
ABA-1W2_S10_R2_001.fastq	27108575	0	35-75	51
ABA-1W2_S10_R1_001_trimmed	26112375	0	20-75	50
ABA-1W2_S10_R2_001_trimmed	26112375	0	20-75	52
ABA-1W3_S11_R1_001.fastq	23644369	0	35-75	49
ABA-1W3_S11_R2_001.fastq	23644369	0	35-75	50
ABA-1W3_S11_R1_001_trimmed	22893775	0	20-75	49
ABA-1W3_S11_R2_001_trimmed	22893775	0	20-75	50
ABA-2W1_S12_R1_001.fastq	34086708	0	35-75	52
ABA-2W1_S12_R2_001.fastq	34086708	0	35-75	53
ABA-2W1_S12_R1_001_trimmed	32894757	0	20-75	52
ABA-2W1_S12_R2_001_trimmed	32894757	0	20-75	54
ABA-2W2_S13_R1_001.fastq	28258986	0	35-75	51
ABA-2W2_S13_R2_001.fastq	28258986	0	35-75	53
ABA-2W2_S13_R1_001_trimmed	27189330	0	20-75	51
ABA-2W2_S13_R2_001_trimmed	27189330	0	20-75	53
ABA-2W3_S14_R1_001.fastq	30503912	0	35-75	51
ABA-2W3_S14_R2_001.fastq	30503912	0	35-75	53
ABA-2W3_S14_R1_001_trimmed	29479715	0	20-75	51
ABA-2W3_S14_R2_001_trimmed	29479715	0	20-75	53
ABA-3W1_S5_R1_001.fastq	31358623	0	35-75	52
ABA-3W1_S5_R2_001.fastq	31358623	0	35-75	53
ABA-3W1_S5_R1_001_trimmed	30911701	0	20-75	52
ABA-3W1_S5_R2_001_trimmed	30911701	0	20-75	54
ABA-3W2_S2_R1_001.fastq	35492559	0	35-75	54
ABA-3W2_S2_R2_001.fastq	35492559	0	35-75	56
ABA-3W2_S2_R1_001_trimmed	34719551	0	20-75	54
ABA-3W2_S2_R2_001_trimmed	34719551	0	20-75	56
ABA-3W3_S15_R1_001.fastq	28984988	0	35-75	51
ABA-3W3_S15_R2_001.fastq	28984988	0	35-75	53
ABA-3W3_S15_R1_001_trimmed	27658490	0	20-75	51
ABA-3W3_S15_R2_001_trimmed	27658490	0	20-75	54
ABA-4W1_S6_R1_001.fastq	34417868	0	35-75	50
ABA-4W1_S6_R2_001.fastq	34417868	0	35-75	52
ABA-4W1_S6_R1_001_trimmed	33687519	0	20-75	50
ABA-4W1_S6_R2_001_trimmed	33687519	0	20-75	52
ABA-4W2_S3_R1_001.fastq	35980518	0	35-75	55
ABA-4W2_S3_R2_001.fastq	35980518	0	35-75	56
ABA-4W2_S3_R1_001_trimmed	35282736	0	20-75	55
ABA-4W2_S3_R2_001_trimmed	35282736	0	20-75	56
ABA-4W3_S4_R1_001.fastq	33689960	0	35-75	53
ABA-4W3_S4_R2_001.fastq	33689960	0	35-75	55
ABA-4W3_S4_R1_001_trimmed	33052716	0	20-75	53
ABA-4W3_S4_R2_001_trimmed	33052716	0	20-75	55

The PCA performed by DESeq2 suggested that one of the 0-week replicates (ABA 0W2) was an outlier (Fig. 5.16a). The first principal component accounted for 72% of the variance in gene expression between the datasets, but sample ABA 0W2 separated at +22 whereas the other two replicates clustered below -20; furthermore, this sample generated a value of over +20 for the second principal component, whereas the other replicates generated values of below -5. In addition, pair-wise analysis of the criteria-filtered datasets showed no differential expression of any genes when the ABA 0W and ABA 3W samples were contrasted. For this reason, the ABA 0W2 sample plus all of the ABA 3W samples were removed and DESeq2 run again. The corresponding PCA plot for this analysis is presented in Figure 5.16b. The first component was then shown to account for 79% of the variance found in the datasets, but there was still some evidence of outliers. Considering PC1 first, the 0W samples clustered between -19 and -23 (red symbols), and the 1W samples between +30 and +34 (green symbols), and the 2W samples around -15 (blue symbols). One of the 4W replicates (purple), however, separated at +30 while the other two replicates clustered at -20 (Fig. 5.16b). There is a compelling case for considering the 4W1 replicate as an outlier and remove it from the analysis, but as four replicates had already been removed, it was decided not to deplete the analysis any further, so the sample was included. Consideration of PC2 shows a reasonably good clustering of replicates apart from the two 0W samples, one generating a value of +10, the other a value of -13. As PC2 only accounted for 7% of the variance, and because there were only two 0W replicates left, no further action was taken to remove outliers.

DESeq2 analysis of the 11 remaining datasets showed Kallisto aligned 29,133 sequences. After filtering for significant changes between the pair-wise comparisons (Benjamini-Hochberg adjusted $p_{adj} < 0.1$), between 37 and 9,494 sequences with a calculable Log2fold change were found (Table 5.14). Most of the changes in sequence abundance occurred between Week 0 and Week 1 (5-day samples), and more downregulated sequences were detected than upregulated. Broadly, most of these changes appeared to be transient, occurring in Week 1; after 4 weeks (26 days), only two genes showed a significant increase in abundance compared with controls (Day 0), and only 20 showed a significant decrease (Table 5.14).

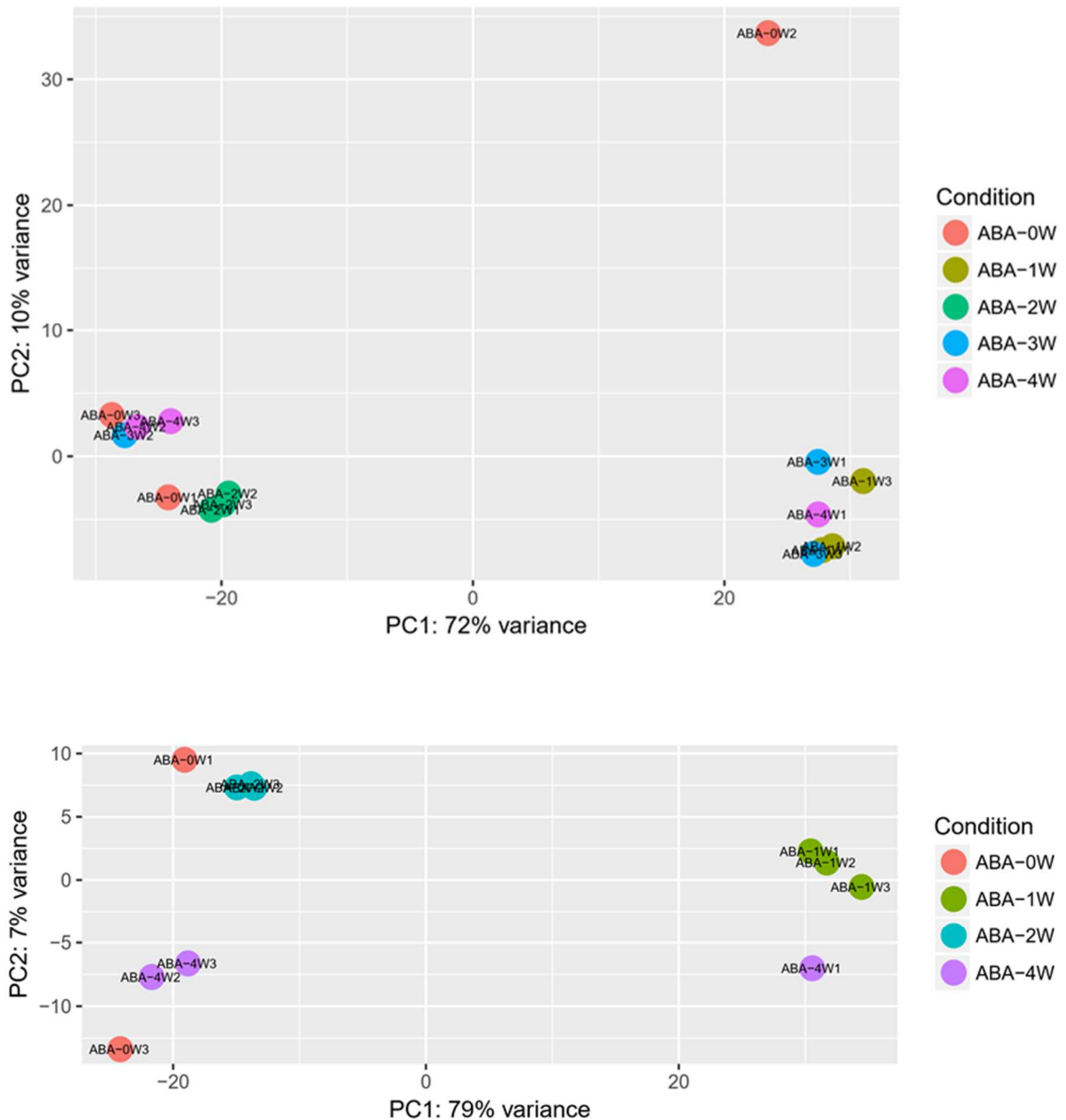


Figure 5.16: Two-Dimensional Principal Component Analysis of Transcript Profiles in Cold-Acclimated *Hordeum vulgare* (cv. California) Leaves Treated with ABA.

Plants were grown in LD (16/8h photoperiod) and WT (20°/16°C day/night, LD/WT). After 3 weeks, plants were sprayed with 10 mL of deionised water containing 0, 10⁻⁵, or 10⁻⁴ M ABA every second day for up to 4 weeks (26 days). Mature sections of the third and fourth leaves of plants were then harvested, frozen immediately to -80°C, and subsequently total RNA was prepared for RNA-Seq analysis (Sections 2.6 and 5.2.3). NGS sequencing was performed on cDNA generated from these pools of RNA (Section 5.2) and analysed by Kallisto and DESeq2. The PCA variance was calculated using the relative abundance of each sequence, expressed as rlog2 (regularised Log2), and transformation of the normalised values recorded.

Table 5.14: Summary of Winter Barley (*cv.* California) Leaf Sequences Identified by DESeq2 as Responsive to Foliar Applications of ABA.

RNA-Seq analysis was performed on three biological replicates of mature barley leaves treated with ABA (see Fig. 5.15). Tables of the normalised abundance for each detected gene in each of the replicates were generated by DESeq2 as .csv files and the relative complement of $|+ABA| \setminus |-ABA| = |TPI|$ determined. These derived sets were then filtered in Microsoft Excel spreadsheets using the criteria of significance ($p_{adj} < 0.1$, Benjamini-Hochberg correction, BaseMean abundance score > 1.0) at the >2 -fold, >5 -fold, or > 10 -fold levels. ‘Upregulated’ refers to genes that were higher than in Week 0 samples. In this table, ABA Wk0 vs. ABA Wk1, for example, is equivalent to the relative complement of sets $|ABA\ Wk1| \setminus |ABA\ Wk0|$, sequences that show significantly different abundances in set $|ABA\ Wk1|$ from set $|ABA\ Wk0|$.

	#Genes	Significant (20384)	Up- regulated >2x	Up- regulated >5x	Up- regulated >10x	Down- regulated >2x	Down- regulated >5x	Down- regulated >10x
ABA WK0 v WK1	29133	9494	1273	21	0	3196	357	12
ABA WK0 v WK2	29133	3966	191	6	0	930	4	0
ABA WK0 v WK4	29133	37	2	0	0	20	9	1

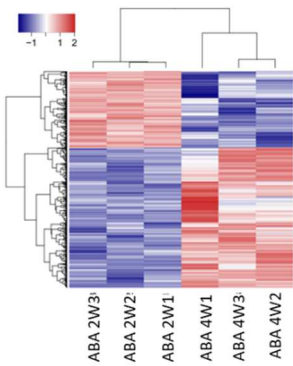
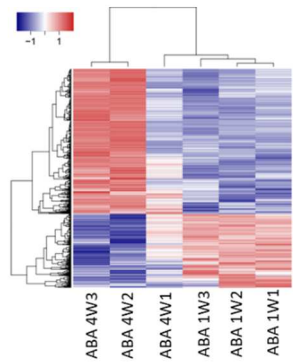
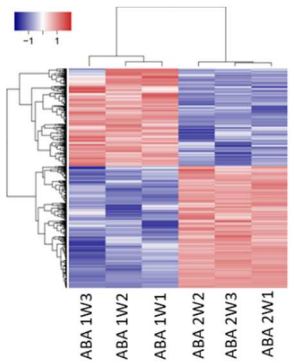
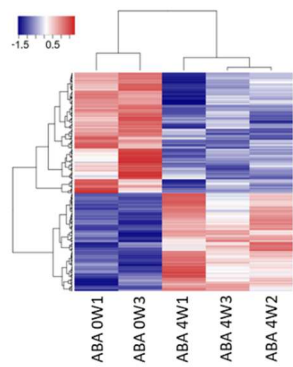
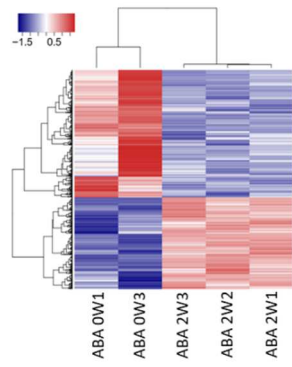
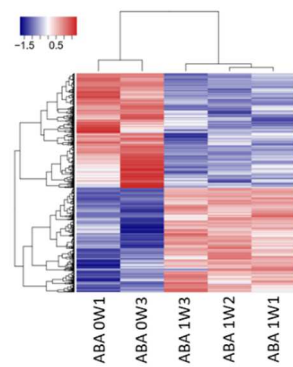


Figure 5.17: Time Series Heat Maps for Barley Sequences Responsive to Exogenous Foliar ABA Application.

Leaves of 3-week-old plants grown in Long Days and Warm Night Temperatures (16h, 16°C) were sprayed with 10 mL 10^{-4} M ABA every second day for up to 4 weeks (26 days). Total RNA was extracted and purified 2 hours post-dawn and cDNA generated for sequencing using an Illumina NextSeq 500 Sequencer and TrueSeq RNA Kit (see Sections 2.6 and 5.2). The raw read data sets (3 replicates x 5 time points x 2 paired-end reads = 30 files) were trimmed to remove low quality sequences, aligned to the barley cDNA database (ICBS, 2017) using the pseudo-alignment programme Kallisto, and the output analysed by the DESeq2 statistical package (Section 5.2). One of the 0-week replicates (Weeks 0–3), and all of the 3-week replicates were omitted for the reasons given in the text.

Despite the concerns of outlier replicates in this experiment, consideration of the gene expression heat maps suggested some sequences were strongly, and reproducibly, influenced by the application of ABA in a time-dependent manner. Figure 5.17 clearly shows good correlation for some sequences across the replicates providing confidence that, despite the removal of some outlier datasets, the depleted analysis still retained some useful information. The lists of genes filtered into the relative complements of the datasets summarised in Table 5.14 were then further analysed using Venn diagrams and set theory.

Figure 5.18 presents a Venn diagram of genes upregulated by ABA application, and Table 5.15 presents a statistical summary of the sequences found in these datasets and their intersections. Calculation of the hypergeometric *pmf* using the observed number of genes in the respective intersections suggested, in all cases, a very high degree of significance (Table 5.15). Furthermore, calculation of the expected number of sequences appearing in the intersections ($E(x)$) and their standard deviations using set theory confirmed these findings. In all cases, the observed number of intersecting genes (x) exceeded the expected number ($E(x)$) that might arise from purely random processes by $p < 6.5 \cdot 10^{-3}$ to $< 6.9 \cdot 10^{-5}$. A similar conclusion can be drawn from the downregulated sequences (Fig. 5.19 and Table 5.15). Here, both the hypergeometric *pmf* and the standard deviation range suggested high significance. The conclusion is that the identified filtered sequences were induced by ABA application in a time-dependent manner, and that these changes correlate well with the measured changes in transcript abundance and cold tolerance in leaves.

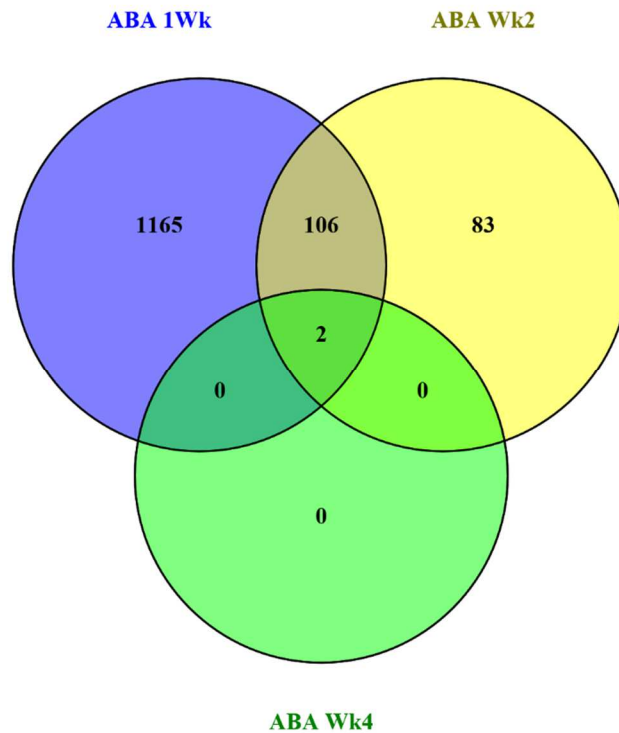


Figure 5.18: Venn Diagram of Time-Dependent Increases in Barley Leaf Gene Abundance Induced by ABA Application.

Samples were prepared as described in Figure 5.17 and the datasets derived from, for example, the relative complements of $|+ABA\ xWeeks| \setminus |-ABA| = |ABA\ Wkx|$; sequences whose abundance is significantly different in $|+ABA|$ from $|-ABA|$. Untreated samples (0-week or -ABA) were used as the controls. The datasets were filtered for significance (Benjamini-Hochberg $p_{adj}=0.1$), showing a > 2 -fold increase over the controls, and a BaseMean abundance score of >1.0 are presented. Diagram reproduced from the Venny online resource page (Oliveros, J.C. (2007–2015) Venny. An interactive tool for comparing lists with Venn's diagrams. (<https://bioinfogp.cnb.csic.es/tools/venny/index.html>)).

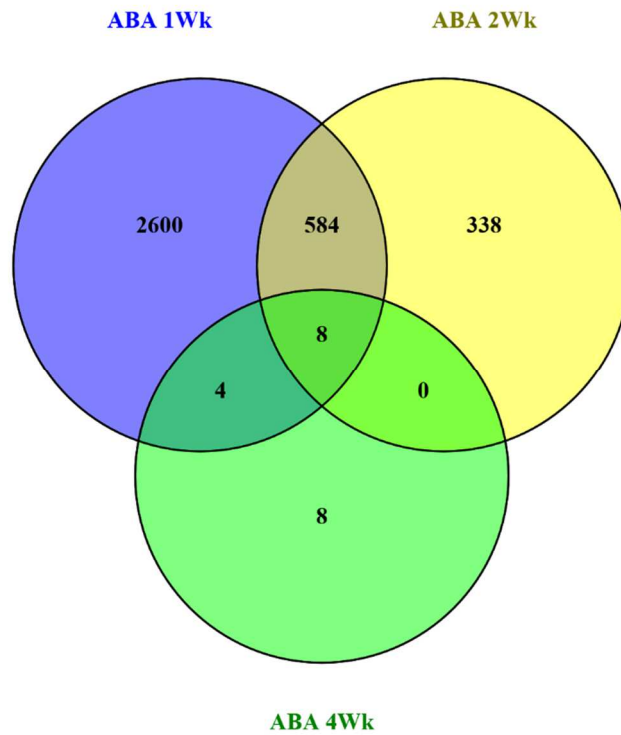


Figure 5.19: Venn Diagram of Time-Dependent Decreases in Barley Leaf Gene Abundance Induced by ABA Application.

Samples were prepared as described in Figure 5.17 and the datasets derived from, for example, the relative complements of $|+ABA\ xWeeks| \setminus |-ABA| = |ABA\ Wkx|$; sequences whose abundance is significantly different in $|+ABA|$ from $|-ABA|$. Untreated samples (0-week or -ABA) were used as the controls. The datasets were filtered for significance (Benjamini-Hochberg $p_{adj}=0.1$), showing a > 2 -fold increase over the controls, and a BaseMean abundance score >1.0 is presented. Diagram reproduced from the Venny online resource page (Oliveros, J.C. (2007–2015) Venny. An interactive tool for comparing lists with Venn's diagrams. (<https://bioinfogp.cnb.csic.es/tools/venny/index.html>)).

Table 5.15: Hypergeometric Probabilities for Common Genes Regulated by ABA Application.

The hypergeometric *pmf* was calculated for the comparison sets shown. The first set, chosen arbitrarily, contained k successes (the number of genes with >2-fold change) selected from a total population of N detected genes in the experiment; the probability of selecting one successful gene from N is given as $p=k/N$. The second set contained n genes (>2-fold change), x of which appeared in the intersection of the two sets. The hypergeometric *pmf* is calculated from the values N , n , k , and x . In addition to this statistical approach, the hypergeometric distribution for all values of n was constructed using the conditional probability for x calculated from set theory ($p(\{A\} | \{B\})$). From this, an expected value for the average of the distribution could be calculated ($E(x)$) and the observed (x) and expected ($E(x)$) values compared. A standard deviation (*St Dev*) was also calculated, as well as the number of standard deviations between x and $E(x)$ (*St Dev Range*). Normally, standard deviation ranges exceeding 2, 3, and 5 are indicative of probabilities of <0.05, <0.01, and <0.001. See Section 2.7 for a full explanation.

Intersection (Common Genes)	n	x	k	N	pmf	$p(\{A\} \{B\})$	$E(x)$	<i>St Dev</i>	<i>St Dev Range</i>
ABA Upregulated									
$ ABA\ 1Wk \cap ABA\ 2Wk $	1273	108	191	29,133	$3.23 \cdot 10^{-181}$	$6.56 \cdot 10^{-3}$	1.25	1.115	95.7
$ ABA\ 1Wk \cap ABA\ 4Wk $	1273	2	2	29,133	$1.91 \cdot 10^{-3}$	$6.87 \cdot 10^{-5}$	$8.73 \cdot 10^{-3}$	0.289	6.6
$ ABA\ 2Wk \cap ABA\ 4Wk $	191	2	2	29,133	$4.28 \cdot 10^{-5}$	$6.87 \cdot 10^{-5}$	$1.32 \cdot 10^{-2}$	0.114	17.4
$ ABA\ 1Wk \cap ABA\ 2Wk \cap ABA\ 4Wk $	$3.23 \cdot 10^{-181} * 1.91 \cdot 10^{-3} * 4.28 \cdot 10^{-5} =$				$1.61 \cdot 10^{-102}$				

ABA Downregulated										
ABA 1Wk ∩ ABA 2Wk	3196	592	930	29,133	$<1 \cdot 10^{-255}$	$1.16 \cdot 10^{-2}$	30.2	5.21	106.3	
ABA 1Wk ∩ ABA 4Wk	3196	12	20	29,133	$3.05 \cdot 10^{-3}$	$2.75 \cdot 10^{-4}$	0.71	0.81	4.07	
ABA 2Wk ∩ ABA 4Wk	938	8	20	29,133	n/s	n/s	n/s	n/s	n/s	
ABA 1Wk ∩ ABA 2Wk ∩ ABA 4Wk	$<1 \cdot 10^{-255} * 3.05 \cdot 10^{-3} =$				$<3.05 \cdot 10^{-258}$					

Figure 5.18 shows that the number of ABA-responsive genes declined over time from the onset of ABA application; 1,273 (1,165 + 106 + 2) sequences were upregulated during the first week of exposure. Of these, 1,165 were upregulated for Week 1 only, 106 for Weeks 1 and 2; and only two for Weeks 1–4. A further 83 sequences were upregulated after 2 weeks of ABA treatment, but no new sequences appeared after 4 weeks. These findings suggest that a major change in gene expression occurs within 1 week of ABA application, but most of these changes (1,165) were transient, returning to base levels by 2 weeks following ABA treatment. Lists of these genes are presented in Appendix A5.4, Table A5.7.

Figure 5.19 presents the Venn diagram for the filtered downregulated sequences induced by ABA application. Most of the changes occurred within the first week of ABA application (Fig. 5.20); 3,196 sequences (2,600+584+8+4) were significantly downregulated during this period. After 2 weeks of ABA treatment, 930 sequences were significantly downregulated; 338 were induced between Week 1 and Week 2, and 592 (584+8) of the sequences downregulated after 1 week were still downregulated after 2 weeks (*cf.* Figs. 5.19 and 5.20). After 4 weeks, 20 (8+8+4) sequences were downregulated; eight were downregulated for Week 4 only, but a further eight appear to be suppressed over the full 4-week period.

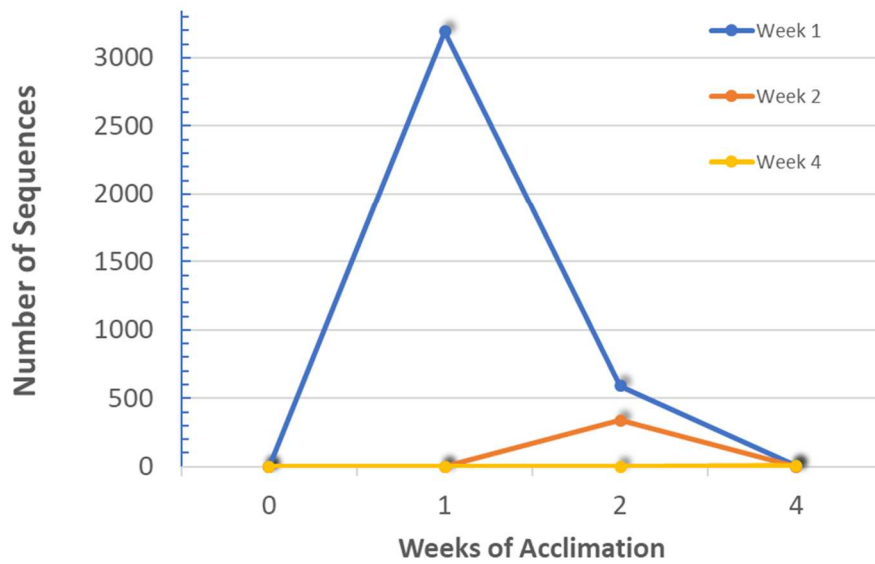
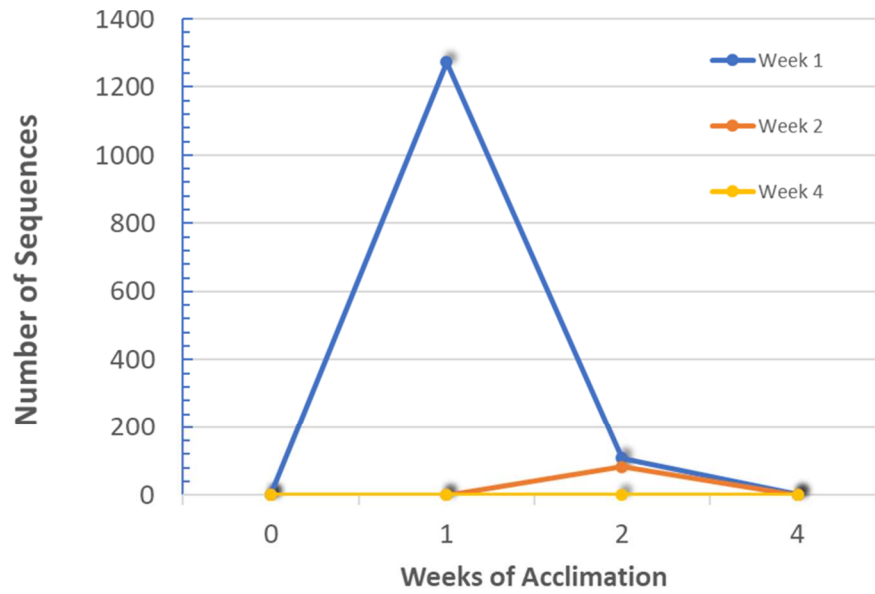


Figure 5.20: Transient Changes in Gene Expression Resulting from Exogenous Foliar ABA Application.

The number of sequences responsive to up to 4 weeks of exogenous 10^{-4} M ABA application. **a**, up regulated; **b**, down regulated. See Figures 5.18 and 5.19 for further details.

5.4.3 An RNA-Seq Validity Check; Comparison of Transcriptome of Cold Acclimation Time Series and ABA Time Series

In Section 5.3, data on the transcriptome of the leaves of a winter barley cultivar exposed to full cold-acclimation conditions (15h nights at 4°C) for up to 4 weeks were presented. In Section 5.4, the transcriptome of barley leaves of the same cultivar exposed to exogenous foliar ABA applications (8h nights at 16°C) for up to 4 weeks was presented. From measurements on the LT_{50} of leaves, it appears that both treatments induced full cold acclimation (Figs. 3.7 and 5.15; Tables 3.4 and 5.12). A comparison of these data might reveal which transcriptional events are triggered by ABA, a subset of which may confer cold tolerance.

A full comparison of the three ABA time points (Weeks 1, 2 and 4) with the four cold acclimation time points (TPI Weeks 1–4) is complicated to analyse. Figures 5.14 and 5.20 present the number of transcriptional changes that occurred in these samples over the 4-week treatment period. These results suggest that some sequences responded relatively quickly, after 1 week, whilst some responded only after 2, 3, or 4 weeks of treatment. Further, some sequences responded transiently for a single week, whilst some responded for up to 4 weeks. This pattern of change suggests operons involving transcriptional cascades may be operating to induce cold acclimation (*cf.* the ICE-1/CBF/COR operon in *Arabidopsis*; see Fig. 1.12). The time series experiments reported in Sections 5.3 and 5.4 are of low resolution with respect to time (weekly samples), and there is perhaps little value comparing the ABA and cold acclimation treatments in a time-dependent manner ($|ABA\ Wk1| \cap |TPI\ Wk1|$, $|ABA\ Wk2| \cap |TPI\ Wk2|$, etc.). For these two reasons, it was decided to pool the transcriptional changes recorded for ABA treatment regardless of time, and similarly with the cold acclimation changes, and to compare these pooled datasets (i.e.. $[|ABA\ Wk1| \cup |ABA\ Wk2| \cup |ABA\ Wk4|] \cap [|TPI\ Wk1| \cup |TPI\ Wk2| \cup |TPI\ Wk3| \cup |TPI\ Wk4|]$). Figures 5.21 and 5.22 present Venn diagrams for upregulated and downregulated unique sequences, respectively. Figure 5.21 shows that, of the 1,356 (1,050+306) unique sequences upregulated by 1–4 weeks of ABA treatment, 306 were also found in the 4,713 (4,407+306) unique TPI sequences upregulated by 1–4 weeks of cold acclimation. A summary of the statistical significance of these findings

is presented in Table 5.16. Figure 5.22 shows that of the 3,542 (2,108+1434) unique sequences downregulated by 1–4 weeks of exogenous ABA treatment, 1,434 were also found in the 8,034 (6,600+1,434) unique TPI sequences that were downregulated (Table 5.16).

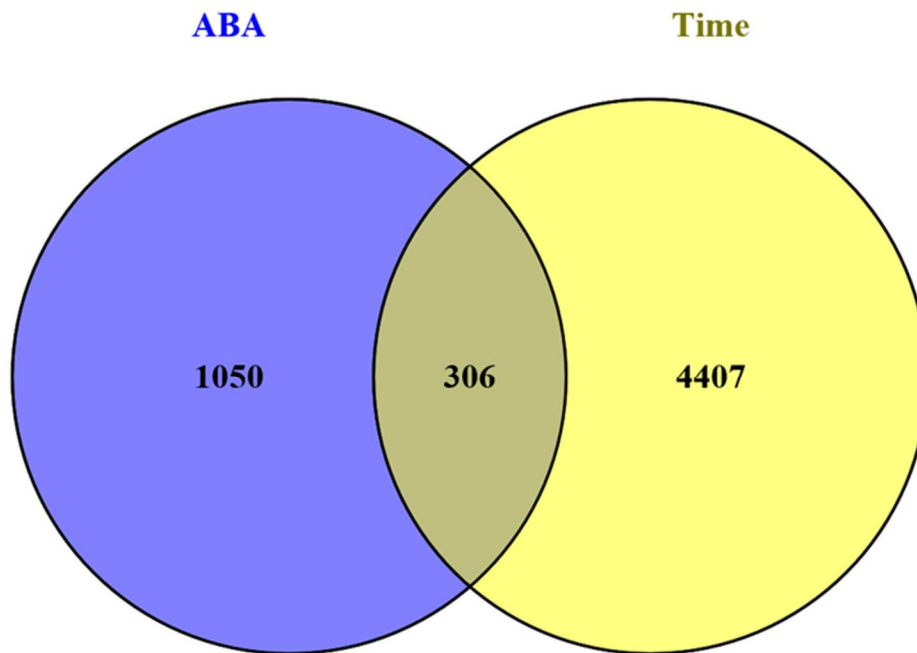


Figure 5.21: Venn Diagram Comparing All Sequences Induced by up to 4 Weeks of Foliar ABA Application and Cold Acclimation.

All unique sequences upregulated by 1, 2, or 4 weeks of foliar ABA application (ABA; see Fig. 5.18) and 1–4 weeks of full cold-acclimation (15h night at 4°C; see Fig. 5.12) were compared.

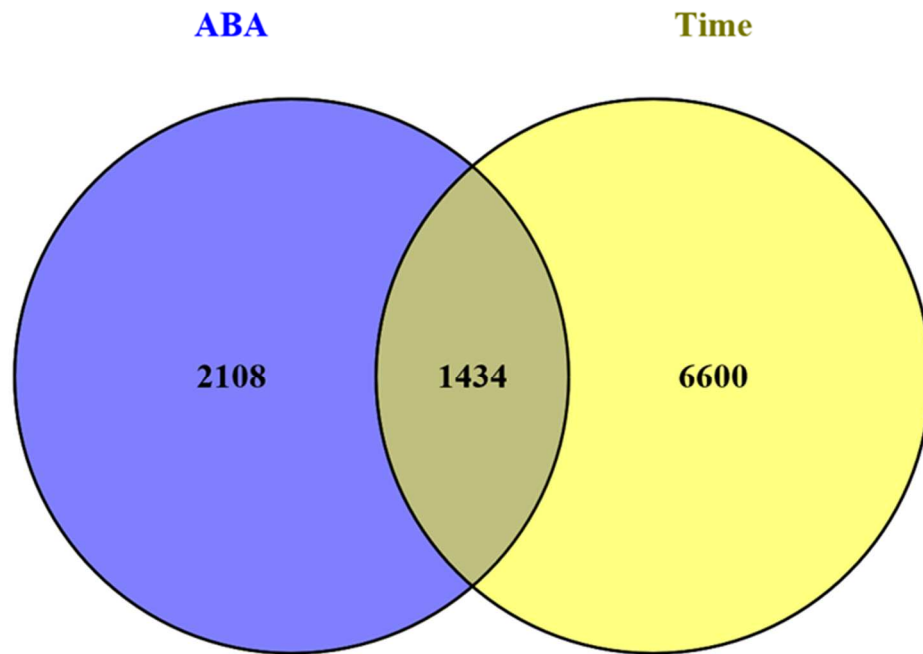


Figure 5.22: Venn Diagram Comparing All Sequences Suppressed by up to 4 Weeks of Foliar ABA Application and Cold Acclimation.

All unique sequences upregulated by 1, 2, or 4 weeks of foliar ABA application (ABA; see Fig. 5.19) and 1–4 weeks of full cold acclimation (15h night at 4°C; see Fig. 5.13) were compared.

Table 5.16: Hypergeometric Probabilities for Common Genes Regulated by ABA Application and Cold Acclimation.

The hypergeometric *pmf* was calculated for the comparison sets shown. The first set, chosen arbitrarily, contained k successes (the number of genes with >2-fold change) selected from a total population of N detected genes in the experiment; the probability of selecting one successful gene from N is given as $p=k/N$. The second set contained n genes (>2-fold change), x of which appeared in the intersection of the two sets. The hypergeometric *pmf* is calculated from the values N , n , k , and x . In addition to this statistical approach, the hypergeometric distribution for all values of n was constructed using the conditional probability for x calculated from set theory ($p(\{A\} | \{B\})$). From this, an expected value for the average of the distribution could be calculated ($E(x)$) and the observed (x) and expected ($E(x)$) values compared. A standard deviation (*St Dev*) was also calculated, as well as the number of standard deviations between x and $E(x)$ (*St Dev Range*). Normally, standard deviation ranges exceeding 2, 3, and 5 are indicative of probabilities of <0.05, <0.01, and <0.001. See Section 2.7 for a full explanation. $|ABA\ Wk1-4| = [|ABA\ Wk1| \cup |ABA\ Wk2| \cup |ABA\ Wk4|]$; see Fig 5.18. $|TPI\ Wk1-4| = [|TPI\ Wk1| \cup |TPI\ Wk2| \cup |TPI\ Wk3| \cup |TPI\ Wk4|]$ – see Figure 5.12.

Intersection (Common Genes)	<i>n</i>	<i>x</i>	<i>k</i>	<i>N</i>	<i>pmf</i>	$p(\{A\} \{B\})$	<i>E(x)</i>	<i>St Dev</i>	<i>St Dev Range</i>
Upregulated									
$ ABA\ Wk1-4 \cap TPI\ Wk1-4 $	1356	306	4713	29,133	$8.18 \cdot 10^{-11}$	$4.65 \cdot 10^{-2}$	219.4	13.2	6.5
ABA Downregulated									
$ ABA\ Wk1-4 \cap TPI\ Wk1-4 $	3542	1434	8034	29,133	$5.74 \cdot 10^{-11}$	$1.216 \cdot 10^{-1}$	967	24.9	18.3

5.5 Discussion

In this chapter, transcriptomic analysis of cold response in barley was investigated with the aim of understanding the cold-acclimation process in winter genotypes. Plants were exposed to cold treatment in a setting of three different experimental treatments. Total RNA was prepared from treated plants, cDNA was generated from these samples, and high-throughput Next Generation Sequencing (NGS) technology was used to sequence approximately 800 million paired-end reads. Although, methods have been developed and published for routinely aligning reads from plants with a relatively small genome – such as *Arabidopsis* (130 Mb) and rice (420 Mb) – to their respective sequenced genomes, no established method is available for aligning the reads from a plant with a large genome, such as barley (5,800 Mb). While an improved genome map of barley has recently been published (IBSC, 2017), the computational resources required to undertake this task are significant. Consequently, where transcriptome analysis of barley has been undertaken, microarray technology has been used (Greenup et al., 2011). Due to the lack of published protocols, and the size of the barley genome, a method was developed where reads were (pseudo)aligned to a barley cDNA library (63.7Mb) using the package Kallisto (Bray et al., 2016). Kallisto identifies the gene from which each read originates and collects ‘counts’ of the number of reads for each identified gene in the datasets. Statistical analysis was then performed using the DESeq2 package, which provides statistical analysis for expression patterns between the experimental treatments; an R-Script procedure was modified for barley, and Microsoft Excel spreadsheets and pivot tables used to filter the data (Sections 5.2–5.4).

When genome-wide transcriptome profiles have been established by microarray technology, it is generally considered wise to confirm any finding using qRT-PCR on the same pool of mRNA. This is deemed to be necessary because microarray technology relies on the hybridisation of probes to cDNA generated from the harvested mRNA, and hybridisation tends to generate a large number of false positives. This generally arises from the inability to control the hybridisation and wash temperatures sufficiently to prevent hybridisation between the probe and an unintended target sequence that contains a small number of base pair mismatches. Consequently, amplicons are subsequently generated from the same batch of mRNA by qRT-PCR, and these are normally sequenced to confirm their authenticity (18–24 bases). This authentication is sufficient to adopt the qRT-PCR result, should there be a

discrepancy with the microarray result. The 18–24 base pair sequence of the amplicon generated by RT-PCR is, therefore, taken as strong evidence for a positive result. RNA-Seq also uses RT-PCR to generate many amplicons, all of which are sequenced, but these are between 75 and 150 bases. The question that now arises is whether a positive result using RNA-Seq needs to be confirmed by qRT-PCR, and if a discrepancy should arise, which result should be believed; the single 18–24 base sequence, or the much longer multiple sequences generated by RNA-Seq? For this reason, confirmatory qRT-PCR is not often performed after RNA-Seq.

There is an additional possible source of error; the possibility that genuine differences in the pools of mRNA used in the experiments exist, but that these differences are not correlated to the processes under investigation. The only way to confirm if this is the case is to increase the level of replication by preparing fresh mRNA samples to provide genuine biological replicates for either qRT-PCR or RNA-Seq. The approach usually adopted with RNA-Seq is confirmation of results using RNA-Seq again on fresh biological samples. This was not done in this study due to time and cost constraints, but should be undertaken to confirm the findings.

5.5.1 Identification of Cold Tolerance Genes

The first experiment described in this chapter was designed to identify gene sequences that confer cold tolerance on barley and respond to low night temperatures alone, short days alone, or a combination of both, after 2 weeks of treatment (Section 5.2). Although the quality of sequencing was considered to be high, preliminary analysis performed by DESeq2 suggested there was significant variance between the biological replicates, which decreases the sensitivity of the analysis. Specifically, a PCA indicated that most of the variance in the datasets was not generated by the experimental conditions of night temperature and photoperiod (Fig. 5.3). Great care was taken to isolate RNA from plants exactly 2 hours post-dawn. This was done in an attempt to avoid changes in transcript abundance that result from circadian rhythms or other time-dependent factors. Regardless, major fold changes in the abundance of several sequences that are known to be controlled by the circadian clock were detected, including several chlorophyll *a/b*-binding (*CAB*) light-harvesting sequences (McClung, 2006); see Appendix Table A5.1. One possible explanation for this is the effect

of differences in night temperatures on circadian rhythms. It is conceivable that a cool night temperature of 4°C slows the circadian clock, compared with leaves of control plants that were exposed to 16°C night temperatures. At dawn, when the circadian clock is usually synchronised, plants that have experienced a warm night may be able to progress on to the next diurnal phase more rapidly than those that have been exposed to low temperatures, hence a lag develops in the expression of genes under the control of the circadian clock, such as *CABs*. This lag will result in the detection of different transcript abundances when samples are compared. It is believed that several clock-associated proteins, including the pseudo-response regulators, act to compensate for temperature effects on the circadian clock, but it is not clear to what extent these mechanisms are successful in barley. A possible alternative explanation is based on the recent finding by Skinner et al. (2018) that expression of several wheat *CBFs*, and possibly many other cold acclimation-induced genes too, show ultradian rhythms (i.e., two or more full periods in 24 hours). If this is the case, reliable estimates for the expression level of a sequence will be highly dependent on the time of day sampling was performed.

The failure of a PCA to separate the experimental biological replicates into clusters does not mean the experiment has failed. It is conceivable that the detected changes in transcript abundance were random and no sensible temperature-induced or photoperiod-induced pattern was present in the data sets, but it is also conceivable that meaningful changes were present but obscured by the effects of circadian or ultradian rhythms. With hindsight, it is clear that the 2-hour point post-dawn when samples were collected could have allowed certain changes in gene expression to be missed. Future experiments should take this into consideration and samples should be collected throughout a 24-hour period at each of the time points (0, 1, 2, 3, and 4 weeks of CA). More biological replication might have resolved this by reducing the variance ('noise') in gene expression 2 hours post-dawn, and it is recommended that, in addition to taking extra care with the time of sample collection, more than three replicates should be used – perhaps 6–10. RNA-Seq is still a relatively expensive method, however, and it might not be possible to resource experiments at this level. It was primarily for cost reasons that a wider range of sampling times was not used at each weekly time point in this study.

Regardless of the issues highlighted by the PCA analysis, four sets of upregulated and downregulated sequences were derived and set theory used to produce subsets of relative

complements (Table 5.4). These subsets contained differentially abundant sequences that were responsive to temperature alone ($|T'$), to both temperature alone and photoperiod alone, and to an interaction of both ($|TPI|$), and to temperature alone and interaction ($|TI|$). These sequences were identified as significant according to the Benjamini-Hochberg $p_{adj} < 0.1$ statistic calculated by the DESseq2 package (Section 5.2). This calculation is required because multiple t -tests (treatment versus control) for each gene are inappropriate, but even with this correction, with over 30,000 sequences detected, inevitably some false positives will be included. Many of these false positives can be removed, however, by determining the sequences that appear in the intersections of the $|T'|$, $|TI|$, and $|TPI|$ (Figs. 5.5 and 5.6). If sequences appear in these datasets through random events ('transcriptional noise') rather than through differences in temperature and photoperiod, the hypergeometric probability distribution can be used to calculate the probability that the same sequences will appear in two or three sets (i.e., in their intersections). As far as the author is aware, this is a new and novel approach for removing false positives from lists of transcripts. Table 5.7 presents these probabilities and it is concluded that there is an extremely high probability the 18 upregulated sequences in the $|T|$ ($p < 10^{-26}$) and the six upregulated sequences in $|I|$ ($p < 10^{-10}$) were responsive to low night temperature and a combination (interaction) of low night temperature and photoperiod (Tables 5.5). What is less certain is how many of the eight upregulated sequences in $|P|$ were false positives, as these were residual sequences not appearing in an intersect and therefore carried only the Benjamini-Hochberg probability of $p_{adj} < 0.1$. In this experiment, none of the downregulated sequences in the $|T'|$, $|TI|$, and $|TPI|$ subsets appeared in the relevant intersections. Therefore, at this stage, the role of CA factors in their expression has been predicted by the Benjamini-Hochberg $p_{adj} < 0.1$ statistic, and it follows that some of these might have been false positives (Table 5.6).

Some justification is required to explain why the temperature subset $|T'|$ was used in this analysis and not the subset $|T|$. In Section 5.2.2, it was pointed out that the use of more natural cold-acclimation regimes where both day and night temperatures and photoperiod cycle makes interpretation of results more complicated. Temperature-responsive sequences in the subsets of $|TPI|$ and $|TI|$ received 15 hours at $+4^{\circ}\text{C}$ (T), whereas subset $|T'|$ received only 8 hours at $+4^{\circ}\text{C}$ (Table 5.4). The analyses of these subsets is complicated, therefore, and this may in part account for why so many sequences appeared outside of the three expected sectors ($|TPI| \cap |TI| \cap |T'| = |T|$; $[|TPI| \cap |TI|] \setminus |T'| = |I|$; $|TPI| \setminus [|TI| \cup |T'|] = |P|$). In theory, all of the sequences in the three subsets should have appeared in one of these sectors.

5.5.2 Time-dependent Expression of Cold Tolerance Genes

The second RNA-Seq experiment was undertaken to profile transcript abundance changes that occurred with time after exposure to full cold-acclimation conditions (i.e., the T, P, and I sequences). Ideally, samples should be collected over the initial few hours and days following exposure to the first night of low temperatures, as well as the longer weekly time intervals used here. The main reason for undertaking the current study, however, was to investigate changes that occur after several days or weeks of cold acclimation, as the early signalling events have been extensively studied over the last three decades. Regardless, it would have been desirable to map transcriptome changes using RNA-Seq over the full time range, from the early events occurring after minutes or hours to those occurring after weeks of cold acclimation. The major advantage of a genome-wide approach is that no assumptions are made regarding which sequences are important (unlike northern blot or PCR-based methods).

Quality control analysis undertaken by the FastQC package indicated the sequenced data was of high quality (Table 5.8) and the resulting PCA analysis showed very good clustering of the replicates, although one outlier appeared and was subsequently removed (Fig. 5.8). A large number of significant upregulated and downregulated sequences were found; 5,872 upregulated (Fig. 5.12) and 5,455 downregulated (Fig. 5.13) sequences (Table 5.9). It is unclear why this experiment identified far more significant changes than the previous RNA-Seq experiment. One possibility is that there was less variability between the biological replicates of the time series experiment, thereby allowing between-treatment differences to be resolved with greater precision. It was stated above that the probability of a sequence appearing in a single set is given by the Benjamini-Hochberg statistic, but where intersections have occurred (i.e., where sequences have appeared in consecutive time sets), the hypergeometric probability distribution can be used to calculate significance with greater precision. The statistical analysis of the identified upregulated and downregulated TPI sequences showed that these differences are extremely unlikely to have arisen through random changes in transcript abundance and appear to have resulted from exposure to low night temperatures and long nights (Table 5.11). The observed pattern of change with time was complex; some sequences were transiently expressed only within the first or second

week, others were expressed at later times, whilst others were expressed throughout the time series (Fig. 5.14). A selection of these sequences is presented in the Appendix Table A5.6, and the full list is included on the accompanying digital storage device.

To confirm that these observed changes are consistent, the experiment should be repeated with more biological replicates, and more time points should be included, particularly over the initial few hours and days after treatment so that a more comprehensive understanding of the signalling events that accompany cold acclimation can be established. However, comparison of the set of TPI sequences identified after 2 weeks of cold acclimation in this experiment with the set of TPI sequences identified after 2 weeks of treatment from the experiment described in Section 5.2 provides a validity check; a similar set of sequences should appear in both sets. Calculations of the probability that TPI sequences occur in the TPI sets from both experiments are presented in Table 5.10 and these up and downregulated sequences have been presented in bold type face in Tables 5.5 and 5.6, respectively. A discussion of a selection of these sequences is presented in Chapter 6.

5.5.3 Role of ABA in the Cold-Acclimation Process in Barley

The final set of experiments was designed to investigate the role of ABA in the cold acclimation process in barley. The plant growth regulator ABA is known to be induced during the cold-acclimation process and, in turn, ABA acts as a second messenger that confers partial cold tolerance on *Arabidopsis* (Cutler et al., 2010). What is not known is to what extent the full cold-acclimation response in barley is mediated through the ABA signalling pathway. To address this question, leaves of winter barley (*cv.* California) were sprayed with solutions of ABA for up to 4 weeks and cold tolerance assessed by estimating the LT₅₀. The results were somewhat unexpected, suggesting that, unlike *Arabidopsis*, full cold tolerance can be conferred on barley by foliar application of exogenous ABA, implying that all of the environmental cues for cold acclimation feed through ABA signalling pathways (Fig. 5.15). The ability to confer full cold tolerance on barley leaves without exposing them to low night temperatures and short photoperiods could improve the resolution of experiments attempting to establish the accompanying changes in transcript profile, as temperature- and photoperiod-dependent changes that are unrelated to cold acclimation will not be included. Unfortunately, this RNA-Seq experiment proved to be less

than ideal. The initial PCA showed that the variance between the biological replicates was large, making differences between treatments difficult to establish (Fig. 5.16). Furthermore, no differences were found between non-acclimated controls and one of the time points (Week 3). Consequently, four replicates were excluded from further analysis, which undoubtedly reduced the sensitivity of the experiment. Notwithstanding these difficulties, the remaining datasets were analysed and some statistically significant differences were observed (Table 5.15). In total 1,356 upregulated and 3,542 downregulated sequences were significantly changed by ABA over the 4-week experimental period (Figs. 5.18 and 5.19), and it appears extremely unlikely that these changes arose from random events controlling transcript abundance (Table 5.15). A summary of some of these sequences is presented in Appendix Table A5.8 and a full list is included on the accompanying USB SD drive.

A comparison can be made between the time-series sets of TPI sequences identified in the experiments described in Section 5.3 and those from the time series ABA experiments in Section 5.4. For simplicity, the datasets within each time series experiment were pooled and comparisons made between the upregulated (Fig. 5.21) and downregulated (Fig. 5.22) combined sets. A total of 306 sequences were found in both the 1,356 pooled upregulated ABA set and the 4,713 pooled upregulated time series set (Fig. 5.21). Similarly, a total of 1,434 sequences were found in both the 3,547 pooled downregulated ABA set and the 8,034 downregulated time series set (Fig. 5.22). It is clear from these findings that the two time series experiments identified a set of sequences whose expression appears to be regulated by both ABA and cold acclimation. Some caution should be applied, however, before firm conclusions can be drawn.

First, it should be emphasised that not all of the transcriptional changes induced by exposure to low night temperatures, long night periods, or ABA treatment are necessarily involved in the cold-acclimation process in barley. It is quite feasible that many of these transcriptional changes occur in response to these environmental factors but do not confer improved freezing tolerance.

Second, although sets of sequences were identified that were common between the experiments described in Sections 5.2 and 5.3, and between those described in Sections 5.3 and 5.4, there were no common sequences found between the experiments reported in Sections 5.2 and 5.4 (data not presented). It is unclear why this should be; further RNA-Seq experiments are required to confirm and resolve the changes reported here

Chapter 6 General Discussion

6.1 Genomic Studies of Economically Important Plants

Over the last decade, methods have been developed for rapidly sequencing the genomes, transcriptomes, and proteomes of higher eukaryotes. This breakthrough in technology has revolutionised research strategies in the biomedical sciences, including plant biology. It is now possible to identify molecular changes that occur at the DNA, RNA, or protein level of many higher eukaryote species, and even to characterise changes that occur between individuals of the same species. Understandably, humans have been the focus of these developments, but these technologies are now being applied to other higher eukaryotes. In plant biology, focus was initially placed on species that met sensible criteria for development as model systems; these included small diploid genomes, physically small species, and those with rapid life cycles. Initially, *Arabidopsis thaliana*, and more recently rice (*Oryza sativa*), have been developed as experimental models, but as the genomic and post-genomic eras have developed it has become clear that model systems cannot provide a detailed understanding of economically important plants such as the small-grained cereals (wheat, barley, oats, etc.) and beans (*Phaseolus vulgaris*, *Glycine max*, *Vicia faba*, etc.). Approximately half of the genes found in *Arabidopsis* have identifiable homologues in rice, but around 40% of *Arabidopsis* genes have homologues in humans. From this, it might be concluded that many metabolic and developmental processes in higher eukaryotes are similar and that this accounts for much of the gene homology (e.g., sequences involved in respiration, cell division, etc.), but major differences occur between the genomes of quite closely related species, reflecting important but subtle differences in their morphology, physiology, and life strategies. Consequently, there is now increasing pressure to extend studies beyond model systems and into commercially important crop plants, despite the fact that the experimental tools to undertake such studies are immature and not fully developed.

6.2 Rationale for Studying Cold Acclimation in Barley

In this study, the decision was made to investigate the cold-acclimation process in barley (*Hordeum vulgare* L.) a member of the *Triticeae* tribe (which includes bread wheat, durum wheat, and rye). There were several reasons for choosing barley: it is diploid and its genetics are therefore relatively simple and easy to interpret; it is the world's fourth most economically important grain; unlike maize and rice, it is relatively cold tolerant, growing in temperate latitudes up to 70° N; and the genome of one cultivar, Morex, has been sequenced twice, in 2012 (IBSC, 2012) and in 2017 (IBSC, 2017). There are, however, several limitations when using barley: until very recently, few open-access bioinformatic tools were available to exploit the plethora of molecular data that is now being generated; experimental approaches to test hypotheses generated from sequencing information are limited, as plant collections and methods to perform forward and reverse genetics are underdeveloped; there are many cultivars grown globally, but *cv.* Morex has now been superseded, making the design of universal PCR primer pairs for the sequences of interest problematic. There are also good reasons to choose to investigate cold tolerance in this important crop. Food security is a major concern for humanity in the 21st century, and there is an imperative to produce more food. This can be achieved by increasing the range of the major crops, including barley, and also by increasing yields. Over the last 10,000 years, our ancestors have selected and bred the progenitors of modern crops to produce good yields in a wide range of habitats that are very different from those where they originated, including northern Europe, North America, and Asia, where severe winter conditions in early autumn or late spring can decimate crops. Long days and a plentiful water supply result in a very high seasonal productivity in these northern regions and wild grasses survive well, tolerating the freezing conditions of deep winter and sporadic early autumn and late spring frost. Domesticated small-grained cereals that have their origins in sub-tropical regions do not survive well, however, and their current northern range is constrained by their lack of cold tolerance. A strong case can be made for placing more focus on developing cereals with improved cold tolerance to exploit the high seasonal productivity of these northern regions, rather than concentrating on developing plants to tolerate the conditions found in unexploited arid semi-deserts in the tropics and sub-tropics.

6.3 The Role of Night Duration and Temperature in Freezing Tolerance

To embark on a successful programme to identify and manipulate the key genetic sequences involved in cold tolerance it is imperative to first develop a robust, sensitive, and reliable method for quantifying the degree of cold tolerance. Studies where clear phenotypes are not definable are likely to fail. In Chapter 3, the development of the standard LT₅₀ method to provide precision in cold tolerance assessments to within 0.3°C was described. These methods were then used to assess the role of photoperiod and low night temperatures on cold tolerance in two cultivars of rye (*Secale cereale* L.) and a spring and winter cultivar of barley (*Hordeum vulgare* L.). The improved precision allowed clear differences between and within the species to be established. Rye requires both short days (long nights) and low night temperatures (+4°C) to confer full cold tolerance, and the data presented in Chapter 3 suggests that the signalling pathways activated by these two cues appears to act in a more than additive fashion. In contrast, frost tolerance in barley appears to be activated almost exclusively by exposure to low night temperatures for 8 hours; there does not seem to be a major advantage to exposing plants to cool nights for longer. It was, therefore, concluded that either the photoperiod-sensing signalling pathway has a discernible but minor role in barley cold acclimation, or that the temperature-sensing pathway is almost fully activated in cool 8-hour nights. Furthermore, the effects of long night periods and low night temperature appear to be additive. As far as the author is aware, these findings are novel and warrant further investigation.

In Chapter 1, a comprehensive overview of the current understanding of the light (photoperiod)-sensing and low temperature-sensing signalling pathways in plants was provided. The work presented in Chapter 3 did not resolve whether both signalling pathways are involved in cold acclimation in rye or whether the increased frost tolerance observed in 15-hour nights arises from longer exposure to low night temperatures, but experiments were proposed to resolve this issue. Briefly, the proposed experiments involve exposing rye plants to 4°C nights for 15 hours, and interrupting the night period with brief flashes of white light. Photoperiod in leaves is sensed by phytochrome C and the flashes of light should convert the Pr form that accumulates in the dark to the Pfr form, thereby signalling short night periods. It is strongly recommended that these experiments are carried out on rye. Regardless, the conclusion from the present study is that there is currently no strong evidence to support the notion that cold acclimation in the *Triticeae* tribe is triggered in part by

photoperiod. This contrasts with the findings from other studies, where a role for photoperiod was implicated (Hayes et al., 1993; Tondelli et al., 2006; von Zitzewitz et al., 2005; von Zitzewitz et al., 2011; Jackson, 2009; Fowler et al., 2014; Singh et al., 2017); in many of these studies, cold acclimation was conferred by exposure of plants to constant low day/night temperatures. These divergent conclusions, therefore, may have arisen from the different cold-acclimation regimes used.

One way to unravel the signalling pathways in rye will involve transcriptome or proteome analysis of plants subjected to cold-acclimation regimes similar to those described in Chapter 2 and used throughout this thesis for the experiments on barley. By activating the photoperiod pathway alone, the temperature pathway alone, and both at the same time, an outline of the cold-acclimation processes in rye should emerge. At the time of writing, however, a full genome map of rye is not available and alignment of rye reads to a cDNA library using Kallisto would have to be performed; it is not clear whether this is feasible at this stage. The experience gained by undertaking transcriptome profiling experiments in barley has highlighted the importance of collecting time series data, and care should be taken to ensure an appropriate level of replication and good choice of time points (see below). Once time-dependent changes, ranging from an hour to weeks of cold-acclimation treatment, have been characterised, it will be interesting to compare these with the pattern in barley so that a better understanding can be gained of the different responses of the two species.

6.4 Identification of Sequences Involved in Frost Tolerance in Barley

Cold acclimation in plants is evidently a complex process. Although great strides have been made over the last 20 years in scientific understanding of the molecular events that accompany the cold-acclimation process in model plants and small-grained cereals, there is still no strong consensus on the details. In Chapter 1, a description was provided of the events that have been proposed for wheat and barley; these involve regulation of the expression of the MADS box transcription factor *VRN1* in leaves, encoded in the *FR1* locus of chromosome 5, and its subsequent role in controlling the transcription of several CBF transcription factors located in the *FR2* locus 20 centimorgans proximal to *FR1*. The evidence for this model has come from classic QTL studies (mainly on wheat) on the F2 generation of crosses between cold-tolerant and cold-sensitive lines, which identified the

FR1 and *FR2* loci, and from the recent sequencing of these two regions (Galibra et al., 2009). In Chapter 4, a limited set of results is presented from a series of experiments that aimed to quantify changes in the transcript abundance of key sequences implicated in this model. It was intended to assess transcript abundance by designing universal PCR primer pairs for each of these key sequences, and to use initially sqRT-PCR to confirm the methods were robust, before embarking on qRT-PCR to carefully quantify changes. A huge amount of effort was expended on this work but, despite this, consistent results could not be obtained, and the approach was eventually abandoned. One of the problems with this approach was the design of universal PCR primer pairs. The only barley cultivar to be sequenced at the time of writing was Morex, and initially this was used to design primers. It quickly became evident, however, that there were significant sequence differences between Morex and the spring and winter cultivars that were used in this study. It was then decided to use sequences from any barley cultivar deposited in the public databases in an attempt to generate universal PCR primer pairs. All of the available sequences for a particular barley sequence (for some there was only one entry from a single cultivar, for others there were many entries from several cultivars) was downloaded and aligned using ClustalW, and from these alignments consensus regions were identified and primers designed for these. Chapter 4 presented the results of the primer design stage. In total, attempts were made to develop universal PCR primers for 18 key sequences: *HvActin*; 11 *HvCBF* sequences reported to be located in *FR2*; *HvVRN1* (in leaves reported to control cold acclimation), plus *HvCONSTANS1*, *HvVRN2*, and *HvVRN3* to control flowering in winter lines; two classic ‘cold stress response’ sequences, a dehydrin (*HvDHN5*), and *HvCOR14a*. Of these 18 sequences, sqRT-PCR using genomic and cDNA templates, only two *HvCBF* sequences failed to generate amplicons which, after confirmatory sequencing, were considered to be authentic. The sequence of these amplicons derived from *cv.* Belgravia or California were sometimes identical to that for Morex, but sometimes this was not the case. BLAST searches of the Morex genome with these fragments often indicated high homology with several loci, and so in some cases it could not be established with confidence that the amplicons were generated from the intended template. This difficulty has confounded the results, as it is not possible to state with certainty that the observed changes from PCR experiments truly reflected changes in the transcript abundance of the target gene.

Another compounding issue was the sheer scale of these PCR experiments. With the appropriate positive and negative controls, sqRT-PCR is a reliable method for detecting the

presence or absence of a transcript in a sample. When the intention is to assess the abundance of 16 sequences in each sample, and with a limited amount of cDNA template synthesised each time, there is little room for error. It was not uncommon for PCR reactions that routinely work to fail for no apparent reason; normally, these reactions are simply repeated, but with a limited amount of template, sometimes that was not possible and a fresh batch of cDNA had to be prepared and calibrated with Actin, and all 16 sequences re-run with the fresh batch of cDNA. This required a considerable amount of work and was further compounded by the required level of biological replication (normally a minimum of three replicates per experimental treatment), and the number of treatments. When treatments such as photoperiod, temperature, and time were factors in the experiment, each with three biological replicates, and each replicate was used to assess the abundance of 16 sequences, the workload became unmanageable. As an alternative, quantitative PCR, qRT-PCR, is a fool-proof approach but it is costly and first requires confirmation from sqRT-PCR.

Despite these difficulties, the author persisted with this approach, but the final decision to abandon it was made when results for *HvVRN1*, *HvVRN2*, and *HvVRN3* accumulated (Fig. 4.3). Although sequencing of amplicons had suggested they were authentic, and appropriate controls were used, the pattern of expression in the leaves of the winter line California were not as expected. *HvVRN1* was not induced in cold-acclimation conditions, as expected, but constitutively expressed. *HvVRN2* was not detected in non-acclimated or acclimated samples; it should have been present in at least the former. *HvVRN3* was also not detected in non-acclimated or acclimated leaves. This raised the question of whether the model for flowering and the activation of cold tolerance in winter barley was wrong (Section 1.17.3), or the sqRT-PCR experiments did not report the abundance of the correct sequences. For the above reasons, it was decided to use RNA-Seq to assess genome-wide changes in transcript abundance rather than focus on a selection of 16 key sequences using PCR methods.

6.5 Genome-wide Transcriptome Analysis of Cold Acclimation in Barley

It is only recently, and after beginning this PhD project, that reports have appeared in the literature on transcriptome profiling in barley using RNA-Seq (Brandt et al., 2018; Hübner et al., 2015; Kintlová et al., 2017; Luan et al., 2017; Tang et al., 2017). These have relied on more conventional methods aligning reads against the published genomes, and due to the

large computational resources required, the datasets have been small compared with those used in this study. To align and analyse datasets of >800 million reads, as were used in this study, an alternative method was required with lower computational requirements. In another RNA-Seq barley study from our laboratory, alignments were achieved using the conventional Tuxedo suite of programs (<https://galaxyproject.org/>); when 400 million reads were aligned on a server the computation took over 3 weeks to complete. For this reason, it was decided to adopt a new method for the analysis of barley data using a cDNA database and the Kallisto pseudo-alignment package (Sections 5.2.5); with this approach, alignment of >800 million reads never took more than 12 hours. Section 5.2.4 presented an account of the development of these methods using the University of Glasgow Galaxy server. This approach has several major advantages for experimental biologists. The underlying complexities associated with the curation of multi-core servers and advanced bioinformatics is removed from the user, who develops 'pipelines' of workflow to ensure each part of the multi-stage analysis progresses smoothly. Kallisto aligns each of the reads to a cDNA and then counts the number of reads that align to each detected sequence. For this study, the output was then analysed by DESeq2 (Section 5.2.5.1); this compares the number of reads for each gene in the replicates of one experimental treatment with those from another, and calculates a statistical probability of a difference in abundance. This procedure can be run on a Galaxy server, but the program is difficult to control; no one has yet provided a robust pipeline that includes DESeq2. For this reason, DESeq2 was downloaded and run on a laptop using a modified R-script. Finally, Microsoft Excel spreadsheets containing Pivot Tables were developed to filter and present the data. The workflow pipeline is an open source resource and mounted on the University of Glasgow Galaxy server (<http://heighliner.cvr.gla.ac.uk/root/>).

The initial RNA-Seq experiment contained samples exposed for 2 weeks to four cold-acclimation conditions: non-acclimated; partially cold acclimated by low night temperatures alone; partially cold acclimated by photoperiod alone; fully cold acclimated by both photoperiod and low night temperatures. The last two treatments were shown to induce a significant level of cold tolerance in barley (Sections 3.6.4 and 3.7). Care was taken to ensure samples were harvested exactly 2 hours post-dawn to minimise the effects of circadian-controlled transcription. Preliminary PCA showed that, on a global scale, there were major changes occurring in the transcription of some genes, changes that were not directly related to the experimental conditions (some replicates did not show strong clustering in the PCA

plots). In such cases, the outlier replicate datasets are normally removed, but in this experiment removal of all outlier datasets would have reduced the experiment to a meaningless level. It was pointed out in Chapter 5 that a high degree of unaccounted-for variance in a PCA plot (poor clustering of replicates) does not mean treatment-induced patterns are not contained within the datasets, it is simply that these patterns are obscured by patterns arising from other, unknown and uncontrolled factors. Consequently, a full analysis was undertaken and lists of differentially abundant upregulated and downregulated genes were produced. The question then arises as to which of the genes in these lists were genuinely regulated by the imposed experimental acclimation conditions. At the time of writing, none of the sequences in the genomic or cDNA databases contained any information other than their unique gene ID and chromosome location. Consequently, to gain information on the possible function of a sequence, the unique ID of each sequence had to be used to interrogate online resources, such as Ensembl Plants (<http://plants.ensembl.org/index.html>), which links directly to other resources such as InterPro (<http://www.ebi.ac.uk/interpro/>) and Panther (<http://www.pantherdb.org/>), from which some limited functional annotation could be obtained. The lists of differentially abundant genes contain thousands of sequences and it was not feasible to determine annotations for all of these. An alternative approach is to perform a GO enrichment analysis using the Gene Ontology (GO) database (<http://geneontology.org/page/go-enrichment-analysis>); unfortunately, it was not possible to process these lists because barley is not yet one of the supported species. For this reason, it was decided to reduce the list of identified sequences by looking for those that appeared in more than one dataset. In addition to reducing the number of genes in the list, this approach will also allow further statistical tests to be performed to confirm that the genes common to both datasets have not appeared as a result of random factors. In Section 2.7, the developed statistical approach was described and, in most cases, the common genes that intersected between sets were highly likely to have appeared due to the experimental treatments and not from random processes. The lists of intersecting sequences were presented in Chapter 5, and possible functions of each of these were determined individually using the Ensembl Plants online resource and embedded links. These annotated lists can be used to identify the processes that are induced by cold acclimation, but the approach is limited. Attention is usually drawn to sequences in the lists that appeal to the preconceptions of the experimenter; thus, models of dubious reliability can result. These lists also contain many sequences annotated with functions that have tenuous links to cold acclimation, and it is easy to

overlook these. Mainly for this reason, a few of the sequences that have previously been implicated in cold acclimation were highlighted in Section 5.4. No further attempts have been made to construct a hypothetical signalling pathway; GO enrichment analysis for barley must first be developed.

6.6 Time Series Transcriptome Analyses of Cold-Acclimated Barley

Chapter 5 also reported the results of an RNA-Seq time series experiment. Here, plants were exposed to non-acclimating conditions (0 weeks) and to full acclimating conditions (low night temperatures and photoperiod) for up to 4 weeks. The costs of RNA-Seq prevented the collection of samples at many time points, and so the experiment was reduced to sampling each week for up to 4 weeks (5 time points with 3 replicates at each time point = 15 samples). A time series experiment has some advantages and disadvantages when compared with the acclimation conditions experiment described above. Its major advantage is that sampling over the initial few hours of exposure to acclimating conditions could identify the early transcriptional events that invoked a full cold acclimation response; sampling at a later time can indicate which sequences are transiently up or downregulated, and in which this persists for the duration of the cold-acclimation period. The cost limitations of this experiment, however, meant that the early events were not monitored, which is a weakness of this experimental plan (see below). Regardless, extensive lists of several thousand upregulated and downregulated sequences were compiled to contrast differences in gene abundance with non-acclimated leaves (0 weeks) after 1 week, 2 weeks, 3 weeks, and 4 weeks from exposure to low night temperatures. Most of the changes occurred during the first week of exposure; fewer differences were detected at later times. There was clear evidence of transient changes and set analysis showed that some changes persisted for the 4-week period. The sequences that appeared in more than one list (i.e., differentially abundant in two or more consecutive time points) were statistically analysed and it was found to be highly likely that their abundance was regulated by the experimental treatment and not by random changes. The gene IDs of these common genes appearing in two or more consecutive time points were used one at a time to determine possible gene function using the Ensembl Plants online portal (see above). Lists of these annotated genes were presented in Section 5.4, but time-dependent

models of the signalling events relating to cold acclimation were not developed; this can be attempted when GO enrichment analysis resources for barley become available.

6.7 Transcriptome Analysis of ABA-Treated Barley Leaves

Both the experimental ‘Condition’ and ‘Time Series’ RNA-Seq experiments discussed above contained samples that were exposed to different photoperiod and night temperature regimes. Analysis of the resulting data produced lists of genes that were differentially abundant between two treatments and that are known to be regulated by the circadian clock based on dawn/dusk temperature switches. In Chapter 5, it was hypothesised that these differences had arisen not because they were involved in cold acclimation but from unintended delays imposed on the circadian clock. For that reason, it was decided to undertake a third RNA-Seq experiment where cold acclimation was induced in plants grown in constant non-acclimating conditions (LD and WT) and sprayed with the plant growth regulator abscisic acid (ABA); samples were collected weekly for up to 4 weeks of treatment (Section 5.3 and 5.4). This treatment was shown to confer full cold tolerance on barley and so RNA-Seq analysis was performed. Unfortunately, there were technical issues with some samples; these were removed but, inevitably, with a reduction in the level of replication, the sensitivity of the experiment was compromised. Nonetheless, extensive lists of differentially abundant sequences were generated for the remaining time point comparisons, and set analysis identified common sequences that appeared at more than two consecutive time points. Some functional annotation for these sequences was gleaned from the Ensembl Plants online portal and these were also presented in Section 5.4.

Finally, it is reasonable to assume that some of the identified sequences should have appeared in all of the RNA-Seq experiments if they are truly regulated by cold-acclimation conditions. Section 5.4 provides lists of these genes; some of them have previously been implicated in cold acclimation, which gives confidence that the experimental approach used in the experiments reported in this thesis has some validity. The appearance of some other sequences is puzzling, however, as these have, at best, a tenuous link to cold acclimation. A better understanding of the signalling mechanisms conferring cold tolerance in barley will hopefully be acquired following the development of more extensive bioinformatics resources in barley, including GO enrichment analysis.

6.8 Limitations of the Current Study

It is clear that a major weakness of this study was the long gap between treatments and sample collection. Previous studies have shown that changes in transcriptomic profile are detectable as early as a few hours following treatments, while the accompanying changes in phenotypes may not be observable for days. Walia et al. (2006) carried out transcriptional profiling of barley in response to salinity stress, and found that several abiotic stress (heat, drought, cold)-related genes were responsive to salinity stress and, significantly, the transcript changes were detected very early after exposure to the salt stress. A similar early response in transcriptional pattern was reported in an earlier study on the effect of salt and drought stress on barley (Ozturk et al., 2002). Another example was observed in the study by Opitz et al. (2015), which showed that acute drought stress that does not result in phenotypic changes in maize plants led to considerable changes in root tissue transcriptome. More recently, Osthoff et al. (2019) observed changes in transcriptome profile after 6 hours of exposing barley to combined water deficit and salt stress. These examples illustrate the need for an experimental design that captures possible transcriptional changes at earlier time points. Future studies on transcriptome changes accompanying cold acclimation in barley would need to include this important element, which is missing in the present study. Interestingly, the analyses carried out by Osthoff et al. (2019) showed that between 60% and 80% of the gene expression changes observed 6 hours after the stress treatment were still present 24 hours after the treatment. Therefore, while the lack of data at the early time points was a major limitation of this study, the list of consistent differentially expressed genes could still provide some insight into barley's transcriptional response to cold acclimation in the longer term.

6.9 Conclusion and Future Perspectives

Genome-wide transcriptome analyses of the effect of stress conditions on barley are gaining increasing attention. Hübner et al. (2015) carried out RNA-Seq analyses of the effect of drought stress on wild barley *Hordeum spontaneum*; their results identified differentially expressed genes that are known to be involved in altering metabolism and giving cells and

tissues the flexibility to alter growth and adapt to stress conditions. Kintlova et al. (2017) studied the transcriptome of barley (*Hordeum vulgare* L., cv. Morex) under three different heavy metal stress conditions: copper, zinc, and cadmium. Luan et al. (2017) adopted a proteomic approach to investigate the hypoxic stress response in barley (*Hordeum vulgare* L.) during waterlogging. Similar to the other studies mentioned above, stress induced the expression of genes and proteins involved in energy metabolism and cellular transport.

Despite the disappointment of not being able to develop hypothetical signalling pathways for cold acclimation in barley, the work presented in this thesis does provide some novel findings and suggests optimism for the future. Evidence for clear differences in the role of photoperiod and temperature in barley and rye cold acclimation was presented. It would be interesting to investigate the cold-acclimation process in other small-grained cereals, including wheat, and it is recommended that these experiments be undertaken. Transcriptome profiling in barley using RNA-Seq has significant advantages over other methods. The work presented in this thesis has shown that the approach is feasible, and rigorous statistical analysis has demonstrated the validity of the approach. The RNA-Seq experiments reported here have not led to a more detailed understanding of the molecular events that induce cold tolerance in barley, but development of better bioinformatic resources for this important crop species is surely imminent and the results presented here could then be analysed in more depth. It is also recommended that resources be found to sequence a more comprehensive time series, ranging from hours (to capture early changes) to weeks. There may also be some merit in collecting more biological samples; three were used in this study, but high variance between replicates arose sporadically. A higher level of biological replication would allow outlier samples to be removed without significantly reducing the sensitivity of the analysis.

These experiments provide a framework for more detailed time-series analyses on the changes in the transcriptome profiles of low-temperature-induced cold acclimation in barley plants. These may provide some insight into how low temperatures predispose leaf tissue to adapt to and survive the freezing conditions that prevail in winter, allowing over-wintering lines to establish biomass early in the spring and thereby leading to higher yields by harvest. In addition, the role of hormones such as ABA and auxin in promoting survival of freezing temperatures should be explored further, as it is clear that the cold acclimation process in

barley, and possibly in other small-grained cereals, is quite different from that in *Arabidopsis*.

Chapter 4 presents the results of RT-PCR experiments that were intended to establish the importance of transcriptional regulation of genes in the *FR1* and *FR2* locus on the long arm of chromosome 5 (see Section 1.13). Results from these experiments suggested that the generally accepted model, that cold acclimation regulates the MADS box transcription factor *VRNI* expression in *FR1* and this subsequently, directly or indirectly, regulates the transcription of *CBF* sequences at the *FR2* locus may not be correct. The RT-PCR experiments in Chapter 4 showed *VRNI* was expressed in both acclimated and non-acclimated barley leaves that had clearly established a significant degree of cold tolerance (see Section 3.6). For this reason, the RT-PCR approach was abandoned for an RNA-Seq approach. Analyses of all of the RNA-Seq files showed that *HvVRNI* (HORVU5Hr1G095630) was expressed in the leaves of plants of all three RNA-Seq experiments (Sections 5.2, 5.3, and 5.4) regardless of treatment level, albeit at a low level, but only in two (1 week and 2 weeks exposure to long, low night temperatures) was there a significant difference with non-acclimated samples (a \log_2 change of +2.1; $p < 0.03$). In one treatment (ABA treatment for 1 week) *HvVRNI* transcript levels decreased compared with non-acclimated controls ($\log_2 -1.09$, $p = 0.095$). These modest changes, coupled with the low level of significance, suggest the finding from the RT-PCR experiments in Chapter 4 were correct, *HvVRNI* is not strongly regulated at the transcriptional level in response to cold acclimating conditions. If it does play an important role in activating the *FR2* locus in barley, it does so at the posttranscriptional level.

HvVRNI has been implicated in cold acclimation as it maps closely to the well-established cold acclimation QTL, *FR1*; there is only weak physical evidence that it modulates cold acclimation (see Section 1.14). Another gene of unknown function, HORVU5Hr1G095660 that also maps to the *FR1* locus was found by RNA-Seq to be up regulated by the application of ABA but only after 1 and 2 weeks ($\log_2 > +1.5$, $p < 0.07$). Again, HORVU5Hr1G095660 was found in all samples but the abundances (BaseMean scores) were typically much higher than those of *HvVRNI* giving more confidence for its involvement in the cold acclimation process. HORVU5Hr1G095660 is predicted to have four splice variants and encode a protein of 128 – 209 amino acids; it is encoded in the large first intron of *HvVRNI* (see Fig 4.1). Several other sequences (e.g. HORVu5Hr1G098190, HORVu5Hr1G098190,

HORVu5Hr1G093640) also map quite closely to *FRI* and their transcription appeared to respond in a semi-consistent way to low night temperatures. Whether any of these are involved in *FRI*-mediated regulation of cold acclimation remains to be confirmed.

6.10 Addendum

Whilst the RNA-Seq transcriptome profiling experiments and analyses were underway, new and improved resources and methods became available that offer significant improvements to barley research. Initially, a full RNA-Seq analysis on the datasets was performed using the IBSC 2012 (Version 1) of the barley genome. At the writing-up stage of this thesis, the IBSC 2017 (Version 2) was published, and it was clear that re-analysing the datasets using this physical map could offer significant advantages. Subsequently, this was carried out, but the lack of GO annotation for barley made it difficult to draw firm conclusions on which metabolic and signalling pathways play important roles in cold acclimation. Nonetheless, by analysing each individual sequence in turn using the Ensembl Plant barley portal (https://plants.ensembl.org/Hordeum_vulgare/Info/Index), some information was gathered and used to annotate the genes; these annotations are included in Tables 5.5 and 5.6. It is emphasised that these annotations were derived from historical tags that have been assigned to the sequences based on a range of criteria used by different research groups; these tags were not independently verified *in silico* or confirmed by experimentation, and their validity should, therefore, be questioned. This approach was necessary at the time because a more rigorous approach for assigning annotation to sequences was not available for barley, although this was possible for model organisms through the development of gene ontology (GO) methods. Gene ontology resources are based on curator confirmation of annotations, and existing annotations are graded; the highest grades are given where annotations have been confirmed by experimentation, and association based on general and domain homology of proteins is also weighted for the degree of identity/homology. In order to provide statistical inference of higher-order function (involvement in known pathways, etc.) a normalised transcriptome is required, that is, the transcriptome of the non-stressed, pathogen-free organism at various stages of development. The abundance of transcripts from an experiment that are known to be involved in identified processes, pathways, and families of proteins can then be compared with those from the normalised set, and higher-

order responses identified. Thus, GO analyses provide a much more robust indication of the function and location of gene products.

In 2019, the Panther Gene Ontology Resource (<http://geneontology.org/>) began supporting *Hordeum vulgare* (domesticated barley), making it possible to apply GO analysis to the datasets reported in this thesis. A full GO analysis has begun, but these resource developments became available too late to be included in this thesis before the submission deadline.

6.10.1 GO Analyses of TPI Sequences Responsive to Full Cold-Acclimation Conditions for Two Weeks

A GO analysis has been performed on two datasets derived from the three RNA-Seq experiments: the up and downregulated sets of the combined T, P and I sequences from the Condition experiment (Section 5.2); the up- and downregulated sequences from the intersections of the Time Series (Section 5.3) and ABA (Section 5.4) experiments. The results from these GO analyses are presented in Tables A6.1–A6.6 in the Appendix.

For these analyses, it was decided to use the combined sets of 32 T, P, and I upregulated sequences (18, 8, and 6, respectively = 32; Fig. 5.5) and a table of these sequences and their respective GO annotations is presented in Appendix Table A6.1. However, Figure 5.6 shows that there were no sequences that appeared in the appropriate intersects to provide firm additional statistical evidence for the T and I sequences. To allow some GO analyses, it was decided to compile and analyse a set of 33 sequences (16 from $|TPI| \setminus [|TI| \cup |T'|]$, 14 from $|TPI| \cap |T'|$, and three from $|TI|$); each of these sequences was at least identified as significant using the Benjamini-Hochberg $p_{adj} < 0.1$ statistic. Due to the low number of TPI sequences in these two GO analyses, no sensible statistical analyses were provided but tables of the GO annotations for each of the sequences are presented (Appendix 6.1 and 6.2). For the 32 upregulated sequences that appeared in the appropriate intersects of Figure 5.5, GO generated annotation for 32. Of these 32 sequences, only one provided evidence for involvement in a known pathway: HORVU7Hr1G027540 encodes a cysteine protease that is involved in CTP biosynthesis. It is not currently clear why barley plants would upregulate CTP biosynthesis in response to cold-acclimation conditions, or whether this leads to an

improvement in frost tolerance. Several other sequences of interest were identified, despite the failure of GO analyses to place them in known pathways. These include: phosphatases and kinases; several proteins involved in cell wall biosynthesis/the cell wall matrix/protein trafficking; a protein involved in the unfolded protein response (a common response to abiotic stress); and two sequences that may be involved in the regulation of transcription, one a regulator of RNA Pol II activity (HORVU2Hr1G100720) and an acyltransferase involved in macromolecule modifications (chromatin re-organisation, or perhaps cell wall structure, HORVU3Hr1G029770).

For the set of 33 downregulated sequences (Fig. 5.6) GO analyses again failed to generate any statistics, most likely due to the low number of genes in this dataset. GO did generate annotation for 32 of the 33 sequences, and these are summarised in Table A6.2. The one sequence that GO failed to generate annotation for (HORVU6Hr1G005050) encoded a 1010bp non-translated RNA and was identified with high probability as an authentic sequence upregulated by temperature (appeared as one of the 18 sequences in the intersection $[TPI] \cap [TI] \cap [T']$). It is feasible that this RNA is a long non-coding RNA (lncRNA) involved in the regulation of the expression of sequences involved in frost tolerance. Further experiments will be required to establish if this is the case. Of the remaining 32 downregulated sequences, eight were assigned a role in a known biological pathway. Five were assigned a role in the regulation of transcription (letters in parentheses indicate activation by T, P, or I): three in the regulation of RNA Pol II (HORVU5Hr1G007890 (T), HORVU5Hr1G092700 (T), HORVU3Hr1G066410 (P)); one is a MADS box transcription factor (HORVU7Hr1G0254700 (P)) implicated in ovule development (but these samples were prepared from leaves); and one is involved in RNA stability (HORVU1Hr1G093560 (T)). Two were assigned roles in signalling; a sequence involved in a phosphorylation cascade evoking cytokinin-mediated responses (HORVU3Hr1G070880 (T)), and a phosphatase (HORVU2Hr1G071450 (P)). Two other sequences were implicated in general metabolism: HORVU0Hr1G000340 (T) cystathionine β -lyase, involved in methionine biosynthesis; and HORVU7Hr1G027540 (P), involved in glutathione metabolism. Other sequences of possible interest were also annotated but no involvement in a biological pathway was identified; for example, a serine/threonine kinase (HORVU2Hr1G015930) implicated in the hedgehog phosphorylation cascade signalling pathway. All of these sequences were downregulated by cold acclimation but it remains to be established if their downregulation leads to an improvement in frost tolerance. In Chapter 1, evidence was

reviewed that suggested rapid growth and cold tolerance are antagonistic traits in plants. When plants undergo cold acclimation, the processes involved in growth are suppressed; this response is reversed in the spring. Several of the downregulated sequences identified in this analysis may well be involved in promoting rapid growth, and, if so, it would be expected that their expression levels would be suppressed. Clearly, further experiments are required to establish their role in conditioning plants for winter.

6.10.2 GO Analyses of Sequences Responsive to up to Four Weeks of Full Cold-Acclimation Conditions and Foliar ABA Application

The up and downregulated sets of sequences that were used in this GO analyses were described in Section 5.4.3. The pooled upregulated ABA set contained 1,356 sequences and the pooled upregulated time series contained 4,713 sequences. Their intersection contained 306 common sequences, and these are presented in the Appendix Table A5.8 (see also Fig. 5.21). GO analysis was performed on this set and the statistical inferences for the different GO classes of sequences are presented in the Appendix Table A6.3. For all GO classes the probability of involvement was $p < 0.05$, and in some cases $p < 0.0001$, giving some confidence that the annotations are correct. Table A6.4 presents only the sequences that generated GO pathway information. Five sequences were identified: a gene encoding the α -subunit of the F1 complex of the mitochondrial ATP synthase (HORVU0Hr1G019950); a gene encoding a helicase protein involved in DNA replication/repair (HORVU3Hr1G082930); a serine/threonine phosphatase involved in the regulation of the phosphorylation state of target proteins (HORVUHr1G019950); a Rootletin isoform involved in nicotinic acetylcholine receptor signalling; and a sequence in the well-established universal WNT signalling pathway. The requirement for increasing bioenergetic processes, such as mitochondrial ATP biosynthesis in response to cold stress, is perhaps not surprising, neither is the need for helicases for DNA repair and chromatin remodelling. Rootletin is a protein that associates with the cytoskeleton and is involved with centrosome cohesion before mitosis; a role for a re-organisation of the cytoskeleton was discussed in Section 1.6.2, and it is feasible that this sequence is involved in adapting the behaviour of dehydrating cells to withstand freeze-induced cell lysis or modulating cell division. The involvement of protein phosphatase implicated in the mammalian Epidermal Growth Factor

(EGF) receptor is a little more difficult to understand. It is not surprising that phosphorylation cascades are activated in response to cold acclimation, and parts of the mammalian EGF signalling pathway are known to be present in plants. It is feasible that this phosphatase is involved in an EGF/RAS/MEK/MAPK/MYC signalling pathway that is activated on exposure to cold-acclimating conditions.

Perhaps of greatest interest is the sequence HORVU1Hr1G019290, a DNA helicase that has been implicated in the animal WNT signalling pathway. WNT is a portmanteau for a signalling pathway first uncovered in a wingless *Drosophila* deletion mutant (Wingless Int-1) and that has since been found in eukaryotes. The signal cascade is triggered by binding the extracellular WNT glycoprotein to a G-protein coupled receptor, FRIZZLED. The glycosylation state of WNT is highly variable and this may be related to its activity. To augment and amplify some responses, co-receptors are required; these include membrane-associated lipoproteins and tyrosine kinases. The activated FRIZZLED then interacts with the cytoplasmic phosphoprotein DISHEVELLED, which has three distinct domains, each involved with three discrete downstream responses. These are termed as follows: the Canonical β -Catenin-dependent pathway; the Non-canonical PCP (Planar Cell Polarity) pathway; and the Non-canonical Calcium signalling pathway. Several components of the WNT pathway are known to exist in plants and Figure 6.1 presents an overview of these.

In the Canonical β -Catenin pathway, activated DISHEVELLED suppresses the activity of the kinase GSK3, which is an essential component of the β -Catenin Destruction Complex that targets β -Catenin for destruction. WNT signalling through this pathway, therefore, leads to the accumulation of β -Catenin in the cytoplasm and eventually in the nucleus, where it interacts with a variety of transcription factors to modulate transcription of target genes.

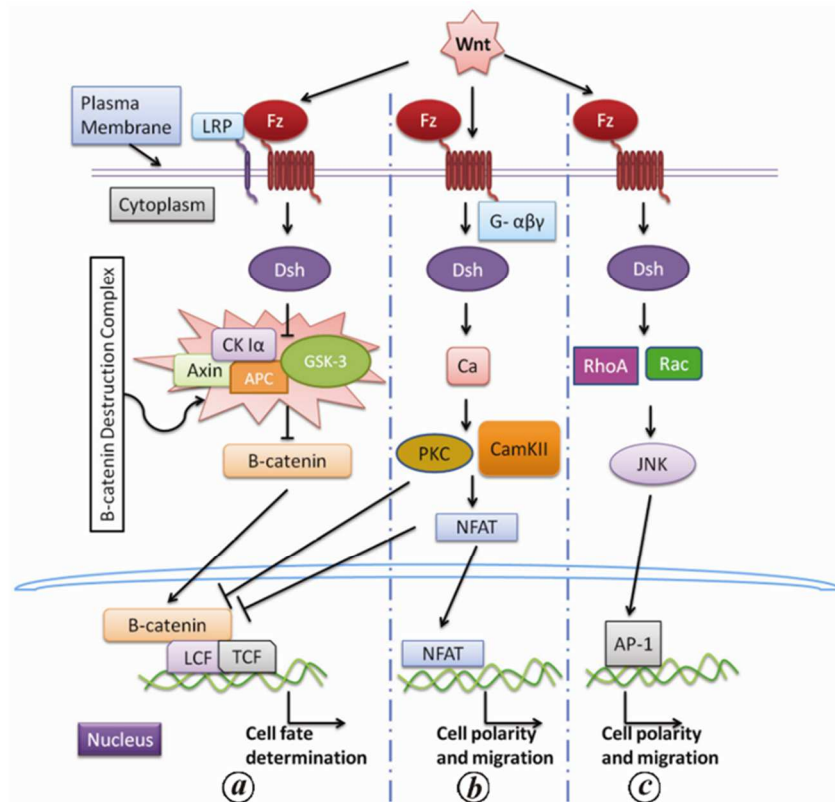


Figure 6.1: Overview of WNT Signalling Pathway in Plants.

Representation of three WNT signalling pathways that may operate in plants. The WNT-Canonical/ β -Catenin pathway; the WNT-calcium pathway; the WNT-Planar Cell Polarity pathway. Fz, FRIZZLED; Dsh, DISHEVELLED; GSK-3, Glycogen Synthase Kinase-3; LRP, Low-density Lipoprotein Receptor; APC, *Adenomatosis Polyposis Coli*; CKI, Casein Kinase I; TCF, T-cell factor; LEF, Lymphoid Enhancer-binding Factor; Ca, Calcium; PKC, Protein Kinase C; CamKII, calmodulin-dependent kinase II; NFAT, Nuclear Factor of Activated T cells; RhoA, Ras homologue gene family, member A; RAC, Ras-related GTPase; JNK, c- JUN-N-terminal Kinase; AP-1, Activator Protein-1. Diagram reproduced from Das and Kumar (2016).

The Non-canonical PCP pathway is also triggered by the activation of DISHEVELLED, which activates JNK-dependent transcription factors through the small GTPases RAC1 and RhoA; these, in turn, interact with JUN Kinase (JNK) and Activator Protein-1 (AP-1), which regulates cell polarity through modifications to the cytoskeleton.

The initial events in the WNT Calcium pathway are similar, involving the activation of DISHEVELLED via WNT and FRIZZLED, but here, DSH activates calcium-binding proteins such as Protein Kinase C (PKC) and Calmodulin-dependent Kinase II (CamKII). This causes the release of free calcium from the ER, which activates NFAT, a transcription

factor. There is some evidence from mammals that the WNT β -Catenin and WNT PCP pathways may be antagonistic (Das and Kumar, 2016). The presence of the WNT signalling pathway in plants could explain some of the well-established cold-acclimation processes in plants. Many studies on stress responses in plants have implicated modifications to the cell wall matrix; the appearance of specific glycoproteins in the extracellular space might trigger the activation of FRIZZLED (Section 6.10.2). The β -Catenin pathway is known to activate chromatin re-modelling, and changes in chromatin structure have been implicated in vernalisation in a range of plants (Section 1.14.2). A central role for increases in cytoplasmic calcium in triggering cold acclimation has long been known, but how this is triggered remains to be discovered (Section 1.14). It is also known that, after cold acclimation, the response of freeze-induced dehydration in cells is different compared with non-acclimated cells, and this helps to prevent expansion-induced lysis upon thawing (Section 1.4.2). It seems likely there is a role for the cytoskeleton in this process, but that has not been investigated in any depth. Signalling through the WNT PCP pathway could trigger these responses.

At present, all of the above is conjecture. Further experiments are required to determine whether any of these identified sequences play a role in conferring frost tolerance. After confirmation that these sequences are regulated by low night temperature, photoperiod, plus an interaction of both, and by ABA applications, progress will require work with mutant lines. The standard approach is to generate loss-of-function knockout (gene deletion) or knockdown (RNAi silencing) lines as well as gain-of-function over-expressing lines. The technology for generating knockdown and over-expressing lines is now well established for barley, and indeed was available in the author's host lab at Glasgow. Knockout lines in barley that enable forward genetic screens are more difficult to procure. Traditionally, this has been achieved in cereals by making TILLING collections, where single genes have been deleted and mapped, but these collections are incomplete and not available for public use. Gene editing *in vivo* using CRISPR may offer a way forward for generating knockout lines.

6.10.3 Confirmation of Identified Cold Acclimation Sequences Using CRISPR

Chapter 1 provides an overview of the many responses in plants to cold acclimation: levels of compatible solutes; production of high concentrations of small proteins in the chloroplast (*COR14A*, *COR15*, etc.) and cytoplasm (*LEA* proteins, *Dehydrins*, etc.). The role these responses play in conferring cold tolerance, however, has not been established and remains conjecture. The sequences identified in this thesis that respond to temperature (T), photoperiod (P), or to both (interaction, I), are also correlative observations and it should not be inferred that any of them confer cold tolerance. To confirm which of these sequences do confer cold tolerance, targeted mutagenesis could be used. CRISPR is a new technology that could be used to edit the barley genome and modify gene function. CRISPR (Clustered Regularly Interspaced Short Palindromic Repeats), were discovered in the genomes of archaea and eubacteria in the 1990s that contained copies of viral genes. The CRISPR-Cas9 system evolved as a method of genome editing that exploits a natural DNA-cutting enzyme in bacteria, called Cas9 (CRISPR-associated protein 9), to target and edit particular foreign genes (Fig. 6.2). This ability to identify specific DNA sequences with precision and edit them was quickly recognised as an ideal tool for editing genes. The protein Cas9 can be used in conjunction with engineered CRISPR sequences to locate specific sequences, excise them from the chromosome, and replace it with a different sequence allowing gene editing *in situ* without the requirement to clone, edit, and transform chimeras back into the host organism. CRISPR-Cas9 editing can now be performed in cereals and this opens up the prospect of making targeted gene knockouts or over-expressors for performing forward genetic experiments in the important crops species in the tribe Triticeae.

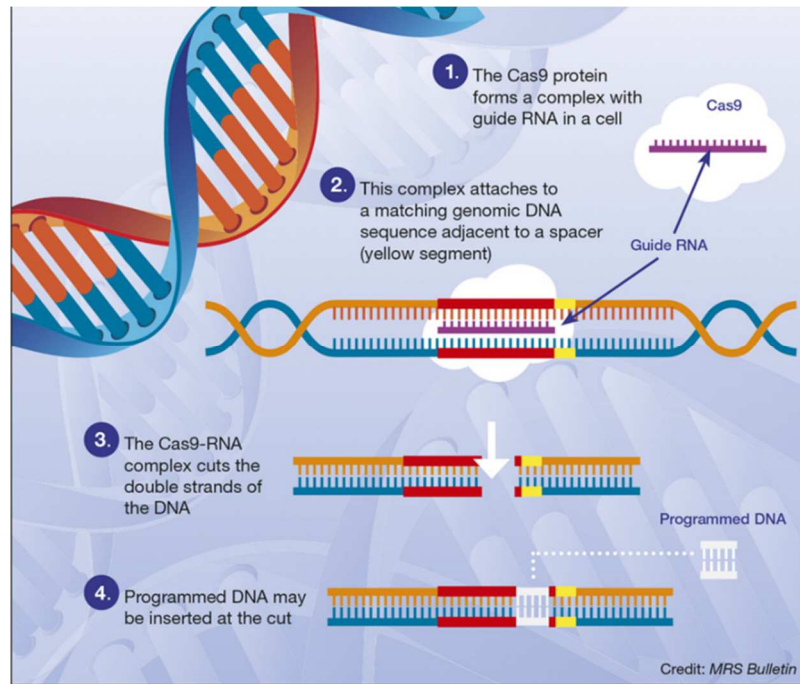


Figure 6.2: CRISPR-Cas9 is a method that is used to target and alter specific sequences with the ability to replace removed sequence with new sequences. Diagram reproduced from Ball (2016).

References

- ABBASI, F., ONODERA, H., TOKI, S., TANAKA, H. & KOMATSU, S. 2004. OsCDPK13, a calcium-dependent protein kinase gene from rice, is induced by cold and gibberellin in rice leaf sheath. *Plant molecular biology*, 55, 541-552.
- AGARWAL, M., HAO, Y., KAPOOR, A., DONG, C.-H., FUJII, H., ZHENG, X. & ZHU, J.-K. 2006a. A R2R3 type MYB transcription factor is involved in the cold regulation of CBF genes and in acquired freezing tolerance. *Journal of Biological Chemistry*, 281, 37636-37645.
- AGARWAL, P. & JHA, B. 2010. Transcription factors in plants and ABA dependent and independent abiotic stress signalling. *Biologia Plantarum*, 54, 201-212.
- AGARWAL, P. K., AGARWAL, P., REDDY, M. & SOPORY, S. K. 2006b. Role of DREB transcription factors in abiotic and biotic stress tolerance in plants. *Plant cell reports*, 25, 1263-1274.
- AKHTAR, M., JAISWAL, A., TAJ, G., JAISWAL, J., QURESHI, M. & SINGH, N. 2012. DREB1/CBF transcription factors: their structure, function and role in abiotic stress tolerance in plants. *Journal of genetics*, 91, 385-395.
- ALDON, D., MBENGUE, M., MAZARS, C. & GALAUD, J.-P. 2018. Calcium signalling in plant biotic interactions. *International journal of molecular sciences*, 19, 665.
- ALI, G., SRIVASTAVA, P. & IQBAL, M. 1999. Proline accumulation, protein pattern and photosynthesis in *Bacopa monniera* regenerants grown under NaCl stress. *Biologia Plantarum*, 42, 89-95.
- ALI, M. B., HAHN, E.-J. & PAEK, K.-Y. 2005. Effects of temperature on oxidative stress defense systems, lipid peroxidation and lipoxygenase activity in *Phalaenopsis*. *Plant physiology and Biochemistry*, 43, 213-223.
- ALLAGULOVA, C. R., GIMALOV, F., SHAKIROVA, F. & VAKHITOV, V. 2003a. The plant dehydrins: structure and putative functions. *Biochemistry (Moscow)*, 68, 945-951.
- ALLAGULOVA, C. R., GIMALOV, F. R., SHAKIROVA, F. M. & VAKHITOV, V. A. 2003b. The Plant Dehydrins: Structure and Putative Functions. *Biochemistry (Moscow) Biochemistry (Moscow)*, 68, 945-951.
- ALONSO-BLANCO, C., GOMEZ-MENA, C., LLORENTE, F., KOORNNEEF, M., SALINAS, J. & MARTÍNEZ-ZAPATER, J. M. 2005. Genetic and molecular analyses of natural variation indicate CBF2 as a candidate gene for underlying a freezing tolerance quantitative trait locus in *Arabidopsis*. *Plant Physiology*, 139, 1304-1312.
- ALONSO, A., QUEIROZ, C. S. & MAGALHÃES, A. C. 1997. Chilling stress leads to increased cell membrane rigidity in roots of coffee (*Coffea arabica* L.) seedlings. *Biochimica et Biophysica Acta (BBA)-Biomembranes*, 1323, 75-84.

- AMASINO, R. 2004. Vernalization, competence, and the epigenetic memory of winter. *The Plant Cell*, 16, 2553-2559.
- ANCHORDOGUY, T. J., RUDOLPH, A. S., CARPENTER, J. F. & CROWE, J. H. 1987. Modes of interaction of cryoprotectants with membrane phospholipids during freezing. *Cryobiology*, 24, 324-331.
- ANOWER, M. R., FENNELL, A., BOE, A., MOTT, I. W., PEEL, M. D. & WU, Y. 2016. Physiological and molecular characterisation of lucerne (*Medicago sativa* L.) germplasm with improved seedling freezing tolerance. *Crop and Pasture Science*, 67, 655-665.
- ANTIKAINEN, M. & GRIFFITH, M. 1997. Antifreeze protein accumulation in freezing-tolerant cereals. *Physiologia Plantarum*, 99, 423-432.
- APPENDINO, M. & SLAFER, G. A. 2003. Earliness per se and its dependence upon temperature in diploid wheat lines differing in the major gene *Eps-A m 1* alleles. *The Journal of Agricultural Science*, 141, 149-154.
- ASENSI-FABADO, M.-A., AMTMANN, A. & PERRELLA, G. 2017. Plant responses to abiotic stress: the chromatin context of transcriptional regulation. *Biochimica et Biophysica Acta (BBA)-Gene Regulatory Mechanisms*, 1860, 106-122.
- ATİCİ, Ö. & NALBANTOĞLU, B. 2003. Antifreeze proteins in higher plants. *Phytochemistry*, 64, 1187-1196.
- BADAWI, M., DANYLUK, J., BOUCHO, B., HOUDE, M. & SARHAN, F. 2007. The CBF gene family in hexaploid wheat and its relationship to the phylogenetic complexity of cereal CBFs. *Molecular genetics and genomics*, 277, 533-554.
- BADAWI, M., REDDY, Y. V., AGHARBAOUI, Z., TOMINAGA, Y., DANYLUK, J., SARHAN, F. & HOUDE, M. 2008. Structure and functional analysis of wheat ICE (inducer of CBF expression) genes. *Plant and Cell Physiology*, 49, 1237-1249.
- BADR, A., SCH, R., RABEY, H. E., EFFGEN, S., IBRAHIM, H., POZZI, C., ROHDE, W. & SALAMINI, F. 2000. On the origin and domestication history of barley (*Hordeum vulgare*). *Molecular biology and evolution*, 17, 499-510.
- BÅGA, M., CHODAPARAMBIL, S. V., LIMIN, A. E., PECAR, M., FOWLER, D. B. & CHIBBAR, R. N. 2007. Identification of quantitative trait loci and associated candidate genes for low-temperature tolerance in cold-hardy winter wheat. *Functional & integrative genomics*, 7, 53-68.
- BÅGA, M., FOWLER, D. B. & CHIBBAR, R. N. 2009. Identification of genomic regions determining the phenological development leading to floral transition in wheat (*Triticum aestivum* L.). *Journal of experimental botany*, 60, 3575-3585.
- BAJWA, V. S., SHUKLA, M. R., SHERIF, S. M., MURCH, S. J. & SAXENA, P. K. 2014. Role of melatonin in alleviating cold stress in *A rabidopsis thaliana*. *Journal of pineal research*, 56, 238-245.

- BAKER, E. H., BRADFORD, K. J., BRYANT, J. A. & ROST, T. L. 1995. A comparison of desiccation-related proteins (dehydrin and QP47) in peas (*Pisum sativum*). *Seed Science Research*, 5, 185-193.
- BAKER, S. S., WILHELM, K. S. & THOMASHOW, M. F. 1994. The 5'-region of *Arabidopsis thaliana* cor15a has cis-acting elements that confer cold-, drought- and ABA-regulated gene expression. *Plant molecular biology*, 24, 701-713.
- BALK, J., CONNORTON, J., WAN, Y., LOVEGROVE, A., MOORE, K., UAUY, C., SHARP, P. & SHEWRY, P. 2019. Improving wheat as a source of iron and zinc for global nutrition. *Nutrition Bulletin*.
- BALL, P. (2016). CRISPR: Implications for materials science. *MRS Bulletin*, 41(11), 832-835. doi:10.1557/mrs.2016.250
- BANERJEE, A., WANI, S. H. & ROYCHOUDHURY, A. 2017. Epigenetic control of plant cold responses. *Frontiers in plant science*, 8, 1643.
- BARRERO-GIL, J. & SALINAS, J. 2013. Post-translational regulation of cold acclimation response. *Plant Science*, 205, 48-54.
- BARRERO-GIL, J. & SALINAS, J. 2018. Gene Regulatory Networks Mediating Cold Acclimation: The CBF Pathway. *Survival Strategies in Extreme Cold and Desiccation*. Springer.
- BARRETT, C. B. 2010. Measuring food insecurity. *Science*, 327, 825-828.
- BARTELS, D. & SUNKAR, R. 2005. Drought and salt tolerance in plants. *Critical reviews in plant sciences*, 24, 23-58.
- BAUMANN, K. 2017. Stress responses: membrane-to-nucleus signals modulate plant cold tolerance. *Nature Reviews Molecular Cell Biology*, 18, 276.
- BEALES, J., TURNER, A., GRIFFITHS, S., SNAPE, J. & LAURIE, D. 2007a. A pseudo-response regulator is misexpressed in the photoperiod insensitive. Ppd-D1a.
- BEALES, J., TURNER, A., GRIFFITHS, S., SNAPE, J. W. & LAURIE, D. A. 2007b. A pseudo-response regulator is misexpressed in the photoperiod insensitive Ppd-D1a mutant of wheat (*Triticum aestivum* L.). *Theoretical and Applied Genetics*, 115, 721-733.
- BECK, E. H., HEIM, R. & HANSEN, J. 2004. Plant resistance to cold stress: mechanisms and environmental signals triggering frost hardening and dehardening. *Journal of biosciences*, 29, 449-459.
- BERTRAND, A., BIPFUBUSA, M., CLAESSENS, A., ROCHER, S. & CASTONGUAY, Y. 2017. Effect of photoperiod prior to cold acclimation on freezing tolerance and carbohydrate metabolism in alfalfa (*Medicago sativa* L.). *Plant Science*, 264, 122-128.
- BLUEMEL, M., DALLY, N. & JUNG, C. 2015. Flowering time regulation in crops—what did we learn from *Arabidopsis*? *Current opinion in biotechnology*, 32, 121-129.

- BLUM, A. 2018. *Plant Breeding for Stress Environments: 0*, CRC press.
- BOLOURI-MOGHADDAM, M. R., LE ROY, K., XIANG, L., ROLLAND, F. & VAN DEN ENDE, W. 2010. Sugar signalling and antioxidant network connections in plant cells. *The FEBS journal*, 277, 2022-2037.
- BONGARD, P., OELKE, E., SIMMONS, S., 2019. Spring barley growth and development guide. College of Food, Agricultural and Natural Resource Sciences. University of Minnesota Extension Guide. <https://extension.umn.edu/growing-small-grains/spring-barley-growth-and-development-guide>
- BORLAUG, N. E. 2007. Sixty-two years of fighting hunger: personal recollections. *Euphytica*, 157, 287-297.
- BOUCHÉ, F., DETRY, N. & PÉRILLEUX, C. 2015. Heat can erase epigenetic marks of vernalization in Arabidopsis. *Plant signaling & behavior*, 10, e990799.
- BOUCHÉ, N., SCHARLAT, A., SNEDDEN, W., BOUCHEZ, D. & FROMM, H. 2002. A novel family of calmodulin-binding transcription activators in multicellular organisms. *Journal of Biological Chemistry*, 277, 21851-21861.
- BOUDSOCQ, M. & SHEEN, J. 2013. CDPKs in immune and stress signaling. *Trends in plant science*, 18, 30-40.
- BRADY, S. M., ORLANDO, D. A., LEE, J.-Y., WANG, J. Y., KOCH, J., DINNENY, J. R., MACE, D., OHLER, U. & BENFEY, P. N. 2007. A high-resolution root spatiotemporal map reveals dominant expression patterns. *Science*, 318, 801-806.
- BRAVO, L. A., GALLARDO, J., NAVARRETE, A., OLAVE, N., MARTÍNEZ, J., ALBERDI, M., CLOSE, T. J. & CORCUERA, L. J. 2003. Cryoprotective activity of a cold-induced dehydrin purified from barley. *Physiologia Plantarum*, 118, 262-269.
- BRAY, E. A., MOSES, M. S., CHUNG, E. & IMAI, R. 1996. The role of abscisic acid in the regulation of gene expression during drought stress. *Physical Stresses in Plants*. Springer.
- BRAY, N. L., PIMENTEL, H., MELSTED, P. & PACHTER, L. 2016. Near-optimal probabilistic RNA-seq quantification. *Nature biotechnology*, 34, 525.
- BREDOW, M. & WALKER, V. K. 2017. Ice-binding proteins in plants. *Frontiers in plant science*, 8, 2153.
- BREMER, A., WOLFF, M., THALHAMMER, A. & HINCHA, D. K. 2017. Folding of intrinsically disordered plant LEA proteins is driven by glycerol-induced crowding and the presence of membranes. *The FEBS journal*, 284, 919-936.
- BROWN, L. R. 2011. Can the United States feed China. *Washington Post*, 03-11.
- BROWN, L. R. & KANE, H. 1995. *Full house: Reassessing the earth's population carrying capacity*, Earthscan.

- BROWSE, J. & XIN, Z. 2001. Temperature sensing and cold acclimation. *Current opinion in plant biology*, 4, 241-246.
- BRUINSMA, J. 2017. *World agriculture: towards 2015/2030: an FAO study*, Routledge.
- BRUSH, R. A., GRIFFITH, M. & MLYNARZ, A. 1994. Characterization and quantification of intrinsic ice nucleators in winter rye (*Secale cereale*) leaves. *Plant physiology*, 104, 725-735.
- BURCHETT, S., NIVEN, S. & FULLER, M. P. 2006. The effect of cold-acclimation on the water relations and freezing tolerance of *Hordeum vulgare* L. *CryoLetters*, 27, 295-303.
- BUSH, D. S. 1995. Calcium regulation in plant cells and its role in signaling. *Annual review of plant biology*, 46, 95-122.
- BYUN, Y. J., KOO, M. Y., JOO, H. J., HA-LEE, Y. M. & LEE, D. H. 2014. Comparative analysis of gene expression under cold acclimation, deacclimation and reacclimation in *Arabidopsis*. *Physiologia plantarum*, 152, 256-274.
- CAMPOLI, C., MATUS-CÁDIZ, M. A., POZNIAK, C. J., CATTIVELLI, L. & FOWLER, D. B. 2009. Comparative expression of Cbf genes in the Triticeae under different acclimation induction temperatures. *Molecular Genetics and Genomics*, 282, 141-152.
- CANDAN, A. P., GRAELL, J. & LARRIGAUDIÈRE, C. 2008. Roles of climacteric ethylene in the development of chilling injury in plums. *Postharvest Biology and Technology*, 47, 107-112.
- CANDAT, A., POUPART, P., ANDRIEU, J.-P., CHEVROLLIER, A., REYNIER, P., ROGNIAUX, H., AVELANGE-MACHEREL, M.-H. & MACHEREL, D. 2013. Experimental determination of organelle targeting-peptide cleavage sites using transient expression of green fluorescent protein translational fusions. *Analytical biochemistry*, 434, 44-51.
- CANEL, C., BAILEY-SERRES, J. N. & ROOSE, M. L. 1995. Pummelo fruit transcript homologous to ripening-induced genes. *Plant physiology*, 108, 1323.
- CANELLA, D., GILMOUR, S. J., KUHN, L. A. & THOMASHOW, M. F. 2010. DNA binding by the *Arabidopsis* CBF1 transcription factor requires the PKKP/RAGR_xKFxETRHP signature sequence. *Biochimica et Biophysica Acta (BBA)-Gene Regulatory Mechanisms*, 1799, 454-462.
- CARPENTER, B. & WATSON, T. 1994. More people more pollution. *US News and World Report*, 117, 63-5.
- CASAO ACERETE, C., KARSAI, I., IGARTUA ARREGUI, E., GRACIA GIMENO, M. P., VEISZ, O. B. & CASAS CENDOYA, A. M. 2011. Adaptation of barley to mild winters: A role for PPDH2.

- CATALÁ, R., LÓPEZ-COBOLLO, R., CASTELLANO, M. M., ANGOSTO, T., ALONSO, J. M., ECKER, J. R. & SALINAS, J. 2014. The Arabidopsis 14-3-3 protein RARE COLD INDUCIBLE 1A links low-temperature response and ethylene biosynthesis to regulate freezing tolerance and cold acclimation. *The Plant Cell*, 26, 3326-3342.
- CATTIVELLI, L. & BARTELS, D. 1989. Cold-induced mRNAs accumulate with different kinetics in barley coleoptiles. *Planta*, 178, 184-188.
- CENSUS, B. O. T., BUREAU, U. C. & PRESS, H. S. B. 2004. *Statistical abstract of the United States: The national data book*, National Technical Information Service, US Department of Commerce.
- CHANG, M.-C., CHIEN, W.-F., CHAO, C.-H. & LU, M.-K. 2010. Effects of cold stress on alterations of physiochemical and chemical properties of rice polysaccharides. *Carbohydrate Polymers*, 80, 373-376.
- CHANG, S., CHANG, T., SONG, Q., ZHU, X.-G. & DENG, Q. 2016. Photosynthetic and agronomic traits of an elite hybrid rice Y-Liang-You 900 with a record-high yield. *Field crops research*, 187, 49-57.
- CHEN, J., YANG, X., HUANG, X., DUAN, S., LONG, C., CHEN, J. & RONG, J. 2017. Leaf transcriptome analysis of a subtropical evergreen broadleaf plant, wild oil-tea camellia (*Camellia oleifera*), revealing candidate genes for cold acclimation. *BMC genomics*, 18, 211.
- CHEN, T. H. & MURATA, N. 2008. Glycinebetaine: an effective protectant against abiotic stress in plants. *Trends in plant science*, 13, 499-505.
- CHEN, T. H. & MURATA, N. 2011. Glycinebetaine protects plants against abiotic stress: mechanisms and biotechnological applications. *Plant, cell & environment*, 34, 1-20.
- CHENG, C., GAO, X., FENG, B., SHEEN, J., SHAN, L. & HE, P. 2013a. Plant immune response to pathogens differs with changing temperatures. *Nature communications*, 4, 2530.
- CHENG, M.-C., LIAO, P.-M., KUO, W.-W. & LIN, T.-P. 2013b. The Arabidopsis ETHYLENE-RESPONSE-FACTOR1 regulates abiotic-stress-responsive gene expression by binding to different cis-acting elements in response to different stress signals. *Plant Physiology*, pp. 113.221911.
- CHINNUSAMY, V., OHTA, M., KANRAR, S., LEE, B.-H., HONG, X., AGARWAL, M. & ZHU, J.-K. 2003. ICE1: a regulator of cold-induced transcriptome and freezing tolerance in Arabidopsis. *Genes & development*, 17, 1043-1054.
- CHINNUSAMY, V., ZHU, J.-K. & SUNKAR, R. 2010. Gene regulation during cold stress acclimation in plants. *Plant Stress Tolerance*. Springer.
- CHINNUSAMY, V., ZHU, J. & ZHU, J.-K. 2006a. Gene regulation during cold acclimation in plants. *Physiol Plant Physiologia Plantarum*, 126, 52-61.

- CHINNUSAMY, V., ZHU, J. & ZHU, J.-K. 2007. Cold stress regulation of gene expression in plants. *Trends in plant science*, 12, 444-451.
- CHINNUSAMY, V., ZHU, J. & ZHU, J. K. 2006b. Gene regulation during cold acclimation in plants. *Physiologia Plantarum*, 126, 52-61.
- CHRIS, S. & MAARTEN, K. 2002. A fortunate choice: the history of Arabidopsis as a model plant. *Nature Reviews Genetics*, 3, 883.
- CLAPHAM, D. E. 2007. Calcium signaling. *Cell*, 131, 1047-1058.
- CLOSE, T. J. 1997. Dehydrins: a commonality in the response of plants to dehydration and low temperature. *Physiologia Plantarum*, 100, 291-296.
- COCKRAM, J., CHIAPPARINO, E., TAYLOR, S. A., STAMATI, K., DONINI, P., LAURIE, D. A. & O'SULLIVAN, D. M. 2007. Haplotype analysis of vernalization loci in European barley germplasm reveals novel VRN-H1 alleles and a predominant winter VRN-H1/VRN-H2 multi-locus haplotype. *Theoretical and Applied Genetics*, 115, 993-1001.
- CONSORTIUM, I. B. G. S. 2012. A physical, genetic and functional sequence assembly of the barley genome. *Nature*, 491, 711.
- CONSTANTINIDOU, H. & MENKISSOGLU, O. 1992. Characteristics and importance of heterogeneous ice nuclei associated with citrus fruits. *Journal of experimental botany*, 43, 585-591.
- COOK, D., FOWLER, S., FIEHN, O. & THOMASHOW, M. F. 2004. A prominent role for the CBF cold response pathway in configuring the low-temperature metabolome of Arabidopsis. *Proceedings of the National Academy of Sciences*, 101, 15243-15248.
- CROSATTI, C., DE LAURETO, P. P., BASSI, R. & CATTIVELLI, L. 1999. The interaction between cold and light controls the expression of the cold-regulated barley gene cor14b and the accumulation of the corresponding protein. *Plant Physiology*, 119, 671-680.
- CROWE, J. H., CARPENTER, J. F., CROWE, L. M. & ANCHORDOGUY, T. J. 1990. Are freezing and dehydration similar stress vectors? A comparison of modes of interaction of stabilizing solutes with biomolecules. *Cryobiology*, 27, 219-231.
- CURTIS, B. 2002. Wheat in the world. Bread wheat: Improvement and production.
- CURTIS, T. & HALFORD, N. 2014. Food security: the challenge of increasing wheat yield and the importance of not compromising food safety. *Annals of Applied Biology*, 164, 354-372.
- DAHAL, K., GADAPATI, W., SAVITCH, L. V., SINGH, J. & HÜNER, N. P. 2012. Cold acclimation and BnCBF17-over-expression enhance photosynthetic performance and energy conversion efficiency during long-term growth of Brassica napus under elevated CO₂ conditions. *Planta*, 236, 1639-1652.

- DALMANNSDOTTIR, S., RAPACZ, M., JØRGENSEN, M., ØSTREM, L., LARSEN, A., RØDVEN, R. & ROGNLI, O. 2016. Temperature before cold acclimation affects cold tolerance and photoacclimation in timothy (*Phleum pratense* L.), perennial ryegrass (*Lolium perenne* L.) and red clover (*Trifolium pratense* L.). *Journal of agronomy and crop science*, 202, 320-330.
- DAS, J., KUMAR, R. 2016 Plant Wnt: deciphering a novel signalling pathway in plants. *Current Science*, 111 (8), 1319-1324.
- DANYLUK, J., KANE, N. A., BRETON, G., LIMIN, A. E., FOWLER, D. B. & SARHAN, F. 2003. TaVRT-1, a putative transcription factor associated with vegetative to reproductive transition in cereals. *Plant Physiology*, 132, 1849-1860.
- DAVIES, P. L. 2014. Ice-binding proteins: a remarkable diversity of structures for stopping and starting ice growth. *Trends in biochemical sciences*, 39, 548-555.
- DEAL, R. B., TOPP, C. N., MCKINNEY, E. C. & MEAGHER, R. B. 2007. Repression of flowering in *Arabidopsis* requires activation of FLOWERING LOCUS C expression by the histone variant H2A. *The Plant Cell*, 19, 74-83.
- DEFALCO, T. A., BENDER, K. W. & SNEDDEN, W. A. 2010. Breaking the code: Ca²⁺ sensors in plant signalling. *Biochemical Journal*, 425, 27-40.
- DEFALCO, T. A., MARSHALL, C. B., MUNRO, K., KANG, H.-G., MOEDER, W., IKURA, M., SNEDDEN, W. A. & YOSHIOKA, K. 2016. Multiple calmodulin-binding sites positively and negatively regulate *Arabidopsis* CYCLIC NUCLEOTIDE-GATED CHANNEL12. *The Plant Cell*, tpc. 00870.2015.
- DENISON, C., KIRKPATRICK, D. S. & GYGI, S. P. 2005. Proteomic insights into ubiquitin and ubiquitin-like proteins. *Current opinion in chemical biology*, 9, 69-75.
- DEPAUW, R., MALHI, S., BULLOCK, P., GAN, Y., MCKENZIE, R., LARNEY, F., JANZEN, H., CUTFORTH, H. & WANG, H. 2011. Wheat production in northern high latitudes—Canadian example. *The world wheat book: a history of wheat breeding*. Edited by W. Angus, A. Bonjean, and M. Van Ginkel. Lavoisier Publishing, Paris, France, 607-651.
- DEVASAGAYAM, T., TILAK, J., BOLOOR, K., SANE, K. S., GHASKADBI, S. S. & LELE, R. 2004. Free radicals and antioxidants in human health: current status and future prospects. *Japi*, 52, 4.
- DEVRIES, A. L. & WOHLSCHLAG, D. E. 1969. Freezing resistance in some Antarctic fishes. *Science*, 163, 1073-1075.
- DHILLON, T., PEARCE, S. P., STOCKINGER, E. J., DISTELFELD, A., LI, C., KNOX, A. K., VASHEGYI, I., VÁGÚJFALVI, A., GALIBA, G. & DUBCOVSKY, J. 2010. Regulation of freezing tolerance and flowering in temperate cereals: the *VRN1* connection. *Plant Physiology*, 153, 1846-1858.
- DIAMOND, J. GUNS, GERMS and STEEL (London: Vintage, 1998). *The prologue of this book gives a good overview of the literature on the subject of early humans as known*

at the end of the previous century. The point in time of our appearance outside Africa is still best described as, 70.

- DÍAZ, A., ZIKHALI, M., TURNER, A. S., ISAAC, P. & LAURIE, D. A. 2012. Copy number variation affecting the Photoperiod-B1 and Vernalization-A1 genes is associated with altered flowering time in wheat (*Triticum aestivum*). *PloS one*, 7, e33234.
- DIEHL, R. C., GUINN, E. J., CAPP, M. W., TSODIKOV, O. V. & RECORD JR, M. T. 2013. Quantifying additive interactions of the osmolyte proline with individual functional groups of proteins: comparisons with urea and glycine betaine, interpretation of m-values. *Biochemistry*, 52, 5997-6010.
- DIETZ, K.-J., VOGEL, M. O. & VIEHHAUSER, A. 2010. AP2/EREBP transcription factors are part of gene regulatory networks and integrate metabolic, hormonal and environmental signals in stress acclimation and retrograde signalling. *Protoplasma*, 245, 3-14.
- DING, Y., JIA, Y., SHI, Y., ZHANG, X., SONG, C., GONG, Z. & YANG, S. 2018. OST1-mediated BTF3L phosphorylation positively regulates CBFs during plant cold responses. *The EMBO journal*, 37, e98228.
- DING, Y., LI, H., ZHANG, X., XIE, Q., GONG, Z. & YANG, S. 2015. OST1 kinase modulates freezing tolerance by enhancing ICE1 stability in Arabidopsis. *Developmental cell*, 32, 278-289.
- DINNENY, J. R., LONG, T. A., WANG, J. Y., JUNG, J. W., MACE, D., POINTER, S., BARRON, C., BRADY, S. M., SCHIEFELBEIN, J. & BENFEY, P. N. 2008. Cell identity mediates the response of Arabidopsis roots to abiotic stress. *Science*, 320, 942-945.
- DISTELFELD, A., LI, C. & DUBCOVSKY, J. 2009a. Regulation of flowering in temperate cereals. *Current opinion in plant biology*, 12, 178-184.
- DISTELFELD, A., TRANQUILLI, G., LI, C., YAN, L. & DUBCOVSKY, J. 2009b. Genetic and molecular characterization of the *VRN2* loci in tetraploid wheat. *Plant physiology*, 149, 245-257.
- DO HEO, W., LEE, S. H., KIM, M. C., KIM, J. C., CHUNG, W. S., CHUN, H. J., LEE, K. J., PARK, C. Y., PARK, H. C. & CHOI, J. Y. 1999. Involvement of specific calmodulin isoforms in salicylic acid-independent activation of plant disease resistance responses. *Proceedings of the National Academy of Sciences*, 96, 766-771.
- DODD, I. C., EGEE, G. & DAVIES, W. J. 2008. Abscisic acid signalling when soil moisture is heterogeneous: decreased photoperiod sap flow from drying roots limits abscisic acid export to the shoots. *Plant, Cell & Environment*, 31, 1263-1274.
- DODD, I. C., EGEE, G., WATTS, C. W. & WHALLEY, W. R. 2010. Root water potential integrates discrete soil physical properties to influence ABA signalling during partial rootzone drying. *Journal of Experimental Botany*, 61, 3543-3551.

- DOHERTY, C. J., VAN BUSKIRK, H. A., MYERS, S. J. & THOMASHOW, M. F. 2009. Roles for Arabidopsis CAMTA transcription factors in cold-regulated gene expression and freezing tolerance. *The Plant Cell*, 21, 972-984.
- DONG, C.-H., AGARWAL, M., ZHANG, Y., XIE, Q. & ZHU, J.-K. 2006. The negative regulator of plant cold responses, HOS1, is a RING E3 ligase that mediates the ubiquitination and degradation of ICE1. *Proceedings of the National Academy of Sciences*, 103, 8281-8286.
- DONG, C.-H., ZOLMAN, B. K., BARTEL, B., LEE, B.-H., STEVENSON, B., AGARWAL, M. & ZHU, J.-K. 2009. Disruption of Arabidopsis CHY1 reveals an important role of metabolic status in plant cold stress signaling. *Molecular plant*, 2, 59-72.
- DONG, M. A., FARRÉ, E. M. & THOMASHOW, M. F. 2011. Circadian clock-associated 1 and late elongated hypocotyl regulate expression of the C-repeat binding factor (CBF) pathway in Arabidopsis. *Proceedings of the National Academy of Sciences*, 201103741.
- DUBCOVSKY, J., LJAVETZKY, D., APPENDINO, L. & TRANQUILLI, G. 1998. Comparative RFLP mapping of Triticum monococcum genes controlling vernalization requirement. *Theoretical and Applied Genetics*, 97, 968-975.
- DUBCOVSKY, J., LOUKOIANOV, A., FU, D., VALARIK, M., SANCHEZ, A. & YAN, L. 2006. Effect of photoperiod on the regulation of wheat vernalization genes *VRN1* and *VRN2*. *Plant molecular biology*, 60, 469-480.
- DUBOUZET, J. G., SAKUMA, Y., ITO, Y., KASUGA, M., DUBOUZET, E. G., MIURA, S., SEKI, M., SHINOZAKI, K. & YAMAGUCHI-SHINOZAKI, K. 2003. OsDREB genes in rice, *Oryza sativa* L., encode transcription activators that function in drought-, high-salt-and cold-responsive gene expression. *The Plant Journal*, 33, 751-763.
- DUMAN, J. G. 1994. Purification and characterization of a thermal hysteresis protein from a plant, the bittersweet nightshade *Solanum dulcamara*. *Biochimica et Biophysica Acta (BBA)-Protein Structure and Molecular Enzymology*, 1206, 129-135.
- DUMAN, J. G. & WISNIEWSKI, M. J. 2014. The use of antifreeze proteins for frost protection in sensitive crop plants. *Environmental and Experimental Botany*, 106, 60-69.
- DUNKER, A. K., BABU, M. M., BARBAR, E., BLACKLEDGE, M., BONDOS, S. E., DOSZTÁNYI, Z., DYSON, H. J., FORMAN-KAY, J., FUXREITER, M. & GSPONER, J. 2013. What's in a name? Why these proteins are intrinsically disordered: Why these proteins are intrinsically disordered. *Intrinsically disordered proteins*, 1, e24157.
- DURE III, L., GREENWAY, S. C. & GALAU, G. A. 1981. Developmental biochemistry of cottonseed embryogenesis and germination: changing messenger ribonucleic acid populations as shown by in vitro and in vivo protein synthesis. *Biochemistry*, 20, 4162-4168.

- DURVASULA, A., FULGIONE, A., GUTAKER, R. M., ALACAKAPTAN, S. I., FLOOD, P. J., NETO, C., TSUCHIMATSU, T., BURBANO, H. A., PICÓ, F. X. & ALONSO-BLANCO, C. 2017. African genomes illuminate the early history and transition to selfing in *Arabidopsis thaliana*. *Proceedings of the National Academy of Sciences*, 201616736.
- ENDO, M., SHIMIZU, H., NOHALES, M. A., ARAKI, T. & KAY, S. A. 2014. Tissue-specific clocks in *Arabidopsis* show asymmetric coupling. *Nature*, 515, 419.
- FAN, M., SHEN, J., YUAN, L., JIANG, R., CHEN, X., DAVIES, W. J. & ZHANG, F. 2011. Improving crop productivity and resource use efficiency to ensure food security and environmental quality in China. *Journal of experimental botany*, 63, 13-24.
- FAO, F. 2012. Agriculture Organization of the United Nations. 2012. *FAO statistical yearbook*.
- FAO, I. 2016. WFP (2015), The State of Food Insecurity in the World 2015. Meeting the 2015 international hunger targets: taking stock of uneven progress. *Food and Agriculture Organization Publications, Rome*.
- FELDMAN, M. 2000. Origin of cultivated wheat. *The World Wheat Book, A history of wheat breeding*.
- FERRÁNDIZ, C., GU, Q., MARTIENSSEN, R. & YANOFSKY, M. F. 2000. Redundant regulation of meristem identity and plant architecture by FRUITFULL, APETALA1 and CAULIFLOWER. *Development*, 127, 725-734.
- FINKA, A., QUENDET, A. F. H., MAATHUIS, F. J., SAIDI, Y. & GOLOUBINOFF, P. 2012. Plasma membrane cyclic nucleotide gated calcium channels control land plant thermal sensing and acquired thermotolerance. *The Plant Cell*, tpc. 112.095844.
- FINKELSTEIN, R. 2013a. Abscisic acid synthesis and response. *The Arabidopsis book/American Society of Plant Biologists*, 11.
- FINKELSTEIN, R. 2013b. Abscisic acid synthesis and response. *Arabidopsis Book 11*: e0166.
- FISCHER, R. & EDMEADES, G. O. 2010. Breeding and cereal yield progress.
- FLOOD, R. G. & HALLORAN, G. 1986. Genetics and physiology of vernalization response in wheat. *Advances in agronomy*. Elsevier.
- FOOD, U. 2016. Agriculture Organization Corporate Statistical Database [Faostat](2017). *Production/Crops, Persimmons, Food and Agriculture Organization of the United Nations: Division of Statistics*. Available from: <http://faostat3.fao.org/browse/Q/QC/E> [last accessed 19 April 2016].
- FOWLER, D., BYRNS, B. & GREER, K. 2014. Overwinter low-temperature responses of cereals: analyses and simulation. *Crop Science*, 54, 2395-2405.

- FOWLER, D., CHAUVIN, L., LIMIN, A. & SARHAN, F. 1996. The regulatory role of vernalization in the expression of low-temperature-induced genes in wheat and rye. *Theoretical and Applied Genetics*, 93, 554-559.
- FOWLER, D. & LIMIN, A. 2004. Interactions among factors regulating phenological development and acclimation rate determine low-temperature tolerance in wheat. *Annals of Botany*, 94, 717-724.
- FOWLER, D., LIMIN, A. & RITCHIE, J. 1999. Low-temperature tolerance in cereals: model and genetic interpretation. *Crop Science*, 39, 626-633.
- FOWLER, D. B., BRETON, G., LIMIN, A. E., MAHFOOZI, S. & SARHAN, F. 2001. Photoperiod and temperature interactions regulate low-temperature-induced gene expression in barley. *Plant Physiology*, 127, 1676-1681.
- FOWLER, S. & THOMASHOW, M. F. 2002. Arabidopsis transcriptome profiling indicates that multiple regulatory pathways are activated during cold acclimation in addition to the CBF cold response pathway. *The Plant Cell*, 14, 1675-1690.
- FRANCIA, E., BARABASCHI, D., TONDELLI, A., LAIDÒ, G., RIZZA, F., STANCA, A. M., BUSCONI, M., FOGHER, C., STOCKINGER, E. J. & PECCHIONI, N. 2007. Fine mapping of a HvCBF gene cluster at the frost resistance locus Fr-H2 in barley. *Theoretical and Applied Genetics*, 115, 1083-1091.
- FRANCIA, E., RIZZA, F., CATTIVELLI, L., STANCA, A. M., GALIBA, G., TOTH, B., HAYES, P. M., SKINNER, J. S. & PECCHIONI, N. 2004. Two loci on chromosome 5H determine low-temperature tolerance in a 'Nure'(winter)×'Tremois'(spring) barley map. *Theoretical and Applied Genetics*, 108, 670-680.
- FRANKLIN-TONG, V. E., RIDE, J. P., READ, N. D., TREWAVAS, A. J. & FRANKLIN, F. C. H. 1993. The self-incompatibility response in *Papaver rhoeas* is mediated by cytosolic free calcium. *The Plant Journal*, 4, 163-177.
- FRICANO, A., RIZZA, F., FACCIOLI, P., PAGANI, D., PAVAN, P., STELLA, A., ROSSINI, L., PIFFANELLI, P. & CATTIVELLI, L. 2009. Genetic variants of HvCbf14 are statistically associated with frost tolerance in a European germplasm collection of *Hordeum vulgare*. *Theoretical and Applied Genetics*, 119, 1335-1348.
- FUJIKAWA, S., JITSUYAMA, Y. & KURODA, K. 1999. Determination of the role of cold acclimation-induced diverse changes in plant cells from the viewpoint of avoidance of freezing injury. *Journal of Plant Research*, 112, 237-244.
- FUJITA, M., FUJITA, Y., NOUTOSHI, Y., TAKAHASHI, F., NARUSAKA, Y., YAMAGUCHI-SHINOZAKI, K. & SHINOZAKI, K. 2006. Crosstalk between abiotic and biotic stress responses: a current view from the points of convergence in the stress signaling networks. *Current opinion in plant biology*, 9, 436-442.
- FUJITA, Y., FUJITA, M., SHINOZAKI, K. & YAMAGUCHI-SHINOZAKI, K. 2011. ABA-mediated transcriptional regulation in response to osmotic stress in plants. *Journal of plant research*, 124, 509-525.

- FUJITA, Y., YOSHIDA, T. & YAMAGUCHI-SHINOZAKI, K. 2013. Pivotal role of the AREB/ABF-SnRK2 pathway in ABRE-mediated transcription in response to osmotic stress in plants. *Physiologia plantarum*, 147, 15-27.
- FURSOVA, O. V., POGORELKO, G. V. & TARASOV, V. A. 2009. Identification of ICE2, a gene involved in cold acclimation which determines freezing tolerance in *Arabidopsis thaliana*. *Gene*, 429, 98-103.
- GALIBA, G., QUARRIE, S. A., SUTKA, J., MORGOUNOV, A. & SNAPE, J. W. 1995. RFLP mapping of the vernalization (*VRN1*) and frost resistance (*FRI*) genes on chromosome 5A of wheat. *Theoretical and Applied Genetics*, 90, 1174-1179.
- GALIBA, G., VAGUJFALVI, A., LI, C., SOLTESZ, A. & DUBCOVSKY, J. 2009a. Regulatory genes involved in the determination of frost tolerance in temperate cereals. *Plant Science*, 176, 12-19.
- GALIBA, G., VÁGÚJFALVI, A., LI, C., SOLTÉSZ, A. & DUBCOVSKY, J. 2009b. Regulatory genes involved in the determination of frost tolerance in temperate cereals. *Plant Science*, 176, 12-19.
- GELVIN, S. B. 2017. Integration of *Agrobacterium* T-DNA into the plant genome. *Annual review of genetics*, 51, 195-217.
- GIBERTI, S., FUNCK, D. & FORLANI, G. 2014. Δ 1-pyrroline-5-carboxylate reductase from *Arabidopsis thaliana*: stimulation or inhibition by chloride ions and feedback regulation by proline depend on whether NADPH or NADH acts as co-substrate. *New Phytologist*, 202, 911-919.
- GIBON, Y., PYL, E. T., SULPICE, R., LUNN, J. E., HOEHNE, M., GUENTHER, M. & STITT, M. 2009. Adjustment of growth, starch turnover, protein content and central metabolism to a decrease of the carbon supply when *Arabidopsis* is grown in very short photoperiods. *Plant, Cell & Environment*, 32, 859-874.
- GILL, S. S. & TUTEJA, N. 2010. Reactive oxygen species and antioxidant machinery in abiotic stress tolerance in crop plants. *Plant physiology and biochemistry*, 48, 909-930.
- GILMOUR, S. J., FOWLER, S. G. & THOMASHOW, M. F. 2004. *Arabidopsis* transcriptional activators CBF1, CBF2, and CBF3 have matching functional activities. *Plant molecular biology*, 54, 767-781.
- GILMOUR, S. J., HAJELA, R. K. & THOMASHOW, M. F. 1988. Cold acclimation in *Arabidopsis thaliana*. *Plant Physiology*, 87, 745-750.
- GILMOUR, S. J., SEBOLT, A. M., SALAZAR, M. P., EVERARD, J. D. & THOMASHOW, M. F. 2000. Overexpression of the *Arabidopsis* CBF3 transcriptional activator mimics multiple biochemical changes associated with cold acclimation. *Plant physiology*, 124, 1854-1865.

- GILMOUR, S. J. & THOMASHOW, M. F. 1991. Cold acclimation and cold-regulated gene expression in ABA mutants of *Arabidopsis thaliana*. *Plant molecular biology*, 17, 1233-1240.
- GILMOUR, S. J., ZARKA, D. G., STOCKINGER, E. J., SALAZAR, M. P., HOUGHTON, J. M. & THOMASHOW, M. F. 1998. Low temperature regulation of the Arabidopsis CBF family of AP2 transcriptional activators as an early step in cold-induced COR gene expression. *The Plant Journal*, 16, 433-442.
- GILROY, S., READ, N. & TREWAVAS, A. 1990. Elevation of cytoplasmic calcium by caged calcium or caged inositol trisphosphate initiates stomatal closure. *Nature*, 346, 769.
- GIRI, J. 2011. Glycinebetaine and abiotic stress tolerance in plants. *Plant signaling & behavior*, 6, 1746-1751.
- GOMEZ, D., VANZETTI, L., HELGUERA, M., LOMBARDO, L., FRASCHINA, J. & MIRALLES, D. J. 2014. Effect of *VRN1*, *Ppd-1* genes and earliness per se on heading time in Argentinean bread wheat cultivars. *Field Crops Research*, 158, 73-81.
- GONG, M., VAN DER LUIT, A. H., KNIGHT, M. R. & TREWAVAS, A. J. 1998. Heat-shock-induced changes in intracellular Ca²⁺ level in tobacco seedlings in relation to thermotolerance. *Plant Physiology*, 116, 429-437.
- GONG, Z., LEE, H., XIONG, L., JAGENDORF, A., STEVENSON, B. & ZHU, J.-K. 2002. RNA helicase-like protein as an early regulator of transcription factors for plant chilling and freezing tolerance. *Proceedings of the National Academy of Sciences*, 99, 11507-11512.
- GOULAS, E., SCHUBERT, M., KIESELBACH, T., KLECZKOWSKI, L. A., GARDESTRÖM, P., SCHRÖDER, W. & HURRY, V. 2006. The chloroplast lumen and stromal proteomes of *Arabidopsis thaliana* show differential sensitivity to short- and long-term exposure to low temperature. *The Plant Journal*, 47, 720-734.
- GOUW, J. W., KRIJGSVELD, J. & HECK, A. J. 2010. Quantitative proteomics by metabolic labeling of model organisms. *Molecular & cellular proteomics*, 9, 11-24.
- GREENUP, A., PEACOCK, W. J., DENNIS, E. S. & TREVASKIS, B. 2009. The molecular biology of seasonal flowering-responses in *Arabidopsis* and the cereals. *Annals of botany*, 103, 1165-1172.
- GRIFFITH, M. & YAISH, M. W. 2004. Antifreeze proteins in overwintering plants: a tale of two activities. *Trends in plant science*, 9, 399-405.
- GROSS, D. C., PROEBSTING, E. L. & MACCRINDLE-ZIMMERMAN, H. 1988. Development, distribution, and characteristics of intrinsic, nonbacterial ice nuclei in *Prunus* wood. *Plant physiology*, 88, 915-922.
- GUO, L., YANG, H., ZHANG, X. & YANG, S. 2013. Lipid transfer protein 3 as a target of MYB96 mediates freezing and drought stress in *Arabidopsis*. *Journal of experimental botany*, 64, 1755-1767.

- GUO, X., LIU, D. & CHONG, K. 2018. Cold signaling in plants: Insights into mechanisms and regulation. *Journal of integrative plant biology*, 60, 745-756.
- GUO, X., XU, S. & CHONG, K. 2017. Cold signal shuttles from membrane to nucleus. *Molecular cell*, 66, 7-8.
- GUO, Y., XIONG, L., ISHITANI, M. & ZHU, J.-K. 2002. An Arabidopsis mutation in translation elongation factor 2 causes superinduction of CBF/DREB1 transcription factor genes but blocks the induction of their downstream targets under low temperatures. *Proceedings of the National Academy of Sciences*, 99, 7786-7791.
- GUPTA, A. K. & KAUR, N. 2005. Sugar signalling and gene expression in relation to carbohydrate metabolism under abiotic stresses in plants. *Journal of biosciences*, 30, 761-776.
- GUSTA, L., WISNIEWSKI, M., NESBITT, N. & GUSTA, M. 2004. The effect of water, sugars, and proteins on the pattern of ice nucleation and propagation in acclimated and nonacclimated canola leaves. *Plant Physiology*, 135, 1642-1653.
- GUY, C., KAPLAN, F., KOPKA, J., SELBIG, J. & HINCHA, D. K. 2008. Metabolomics of temperature stress. *Physiologia plantarum*, 132, 220-235.
- GUY, C., NIEMI, K. J. & BRAMBL, R. 1985a. Altered gene expression during cold acclimation of spinach. *Proceedings of the National Academy of Sciences*, 82, 3673-3677.
- GUY, C. L. & HASKELL, D. 1987. Induction of freezing tolerance in spinach is associated with the synthesis of cold acclimation induced proteins. *Plant Physiology*, 84, 872-878.
- GUY, C. L., NIEMI, K. J. & BRAMBL, R. 1985b. Altered gene expression during cold acclimation of spinach. *Proceedings of the National Academy of Sciences*, 82, 3673-3677.
- HAAKE, V., COOK, D., RIECHMANN, J., PINEDA, O., THOMASHOW, M. F. & ZHANG, J. Z. 2002. Transcription factor CBF4 is a regulator of drought adaptation in Arabidopsis. *Plant physiology*, 130, 639-648.
- HAAS, M., SCHREIBER, M. & MASCHER, M. 2018. Domestication and crop evolution of wheat and barley: Genes, genomics, and future directions. *Journal of integrative plant biology*.
- HAJELA, R. K., HORVATH, D. P., GILMOUR, S. J. & THOMASHOW, M. F. 1990. Molecular cloning and expression of cor (cold-regulated) genes in Arabidopsis thaliana. *Plant Physiology*, 93, 1246-1252.
- HANANO, S. & GOTO, K. 2011. Arabidopsis TERMINAL FLOWER1 is involved in the regulation of flowering time and inflorescence development through transcriptional repression. *The Plant Cell*, tpc. 111.088641.

- HAND, S. C., MENZE, M. A., TONER, M., BOSWELL, L. & MOORE, D. 2011. LEA proteins during water stress: not just for plants anymore. *Annual review of physiology*, 73, 115-134.
- HANIN, M., BRINI, F., EBEL, C., TODA, Y., TAKEDA, S. & MASMOUDI, K. 2011. Plant dehydrins and stress tolerance: versatile proteins for complex mechanisms. *Plant signaling & behavior*, 6, 1503-1509.
- HARLAN, J. R. & ZOHARY, D. 1966. Distribution of wild wheats and barley. *Science*, 153, 1074-1080.
- HASAN KHAN, Z., KUMAR, B., DHATTERWAL, P., MEHROTRA, S. & MEHROTRA, R. 2017. Transcriptional regulatory network of cis-regulatory elements (Cres) and transcription factors (TFs) in plants during abiotic stress. *International Journal of Plant Biology & Research*.
- HASHIMOTO, K. & KUDLA, J. 2011. Calcium decoding mechanisms in plants. *Biochimie*, 93, 2054-2059.
- HAYES, P. M., BLAKE, T., CHEN, T. H., TRAGOONRUNG, S., CHEN, F., PAN, A. & LIU, B. 1993. Quantitative trait loci on barley (*Hordeum vulgare* L.) chromosome 7 associated with components of winterhardiness. *Genome*, 36, 66-71.
- HAYYAN, M., HASHIM, M. A. & ALNASHEF, I. M. 2016. Superoxide ion: generation and chemical implications. *Chemical reviews*, 116, 3029-3085.
- HEIDARVAND, L. & MAALI-AMIRI, R. 2013. Physio-biochemical and proteome analysis of chickpea in early phases of cold stress. *Journal of plant physiology*, 170, 459-469.
- HEMMING, M. N., PEACOCK, W. J., DENNIS, E. S. & TREVASKIS, B. 2008. Low-temperature and daylength cues are integrated to regulate FLOWERING LOCUS T in barley. *Plant Physiology*, 147, 355-366.
- HINCHA, D. K. & THALHAMMER, A. 2012. LEA proteins: IDPs with versatile functions in cellular dehydration tolerance. Portland Press Limited.
- HLAVÁČKOVÁ, I., VÍTÁMVÁS, P., ŠANTRŮČEK, J., KOSOVÁ, K., ZELENKOVÁ, S., PRÁŠIL, I., OVESNÁ, J., HYNEK, R. & KODÍČEK, M. 2013. Proteins involved in distinct phases of cold hardening process in frost resistant winter barley (*Hordeum vulgare* L.) cv Luxor. *International journal of molecular sciences*, 14, 8000-8024.
- HOFFMAN, D. E., JONSSON, P., BYLESJÖ, M., TRYGG, J., ANTTI, H., ERIKSSON, M. E. & MORITZ, T. 2010. Changes in diurnal patterns within the *Populus* transcriptome and metabolome in response to photoperiod variation. *Plant, cell & environment*, 33, 1298-1313.
- HOLMSTRUP, M., BOUVRAIS, H., WESTH, P., WANG, C., SLOTSBO, S., WAAGNER, D., ENGGROB, K. & IPSEN, J. H. 2014. Lipophilic contaminants influence cold tolerance of invertebrates through changes in cell membrane fluidity. *Environmental science & technology*, 48, 9797-9803.

- HON, W.-C., GRIFFITH, M., MLYNARZ, A., KWOK, Y. C. & YANG, D. S. 1995. Antifreeze proteins in winter rye are similar to pathogenesis-related proteins. *Plant Physiology*, 109, 879-889.
- HONG, J. H., SAVINA, M., DU, J., DEVENDRAN, A., RAMAKANTH, K. K., TIAN, X., SIM, W. S., MIRONOVA, V. V. & XU, J. 2017. A sacrifice-for-survival mechanism protects root stem cell niche from chilling stress. *Cell*, 170, 102-113. e14.
- HONG, Z., LAKKINENI, K., ZHANG, Z. & VERMA, D. P. S. 2000. Removal of feedback inhibition of Δ 1-pyrroline-5-carboxylate synthetase results in increased proline accumulation and protection of plants from osmotic stress. *Plant physiology*, 122, 1129-1136.
- HOQUE, M. A., OKUMA, E., BANU, M. N. A., NAKAMURA, Y., SHIMOISHI, Y. & MURATA, Y. 2007. Exogenous proline mitigates the detrimental effects of salt stress more than exogenous betaine by increasing antioxidant enzyme activities. *Journal of Plant Physiology*, 164, 553-561.
- HU, R., WANG, Z., WU, P., TANG, J. & HOU, X. 2015. Identification and abiotic stress analysis of calmodulin-binding transcription activator/signal responsive genes in non-heading Chinese cabbage ('*Brassica campestris*' ssp. '*chinensis*' Makino). *Plant Omics*, 8, 141.
- HU, Y., JIANG, L., WANG, F. & YU, D. 2013. Jasmonate regulates the inducer of CBF expression–c-repeat binding factor/DRE binding factor1 cascade and freezing tolerance in Arabidopsis. *The Plant Cell*, 25, 2907-2924.
- HUA, J. 2009. From freezing to scorching, transcriptional responses to temperature variations in plants. *Current opinion in plant biology*, 12, 568-573.
- HUANG, G.-T., MA, S.-L., BAI, L.-P., ZHANG, L., MA, H., JIA, P., LIU, J., ZHONG, M. & GUO, Z.-F. 2012. Signal transduction during cold, salt, and drought stresses in plants. *Molecular biology reports*, 39, 969-987.
- HUANG, J., PRAY, C. & ROZELLE, S. 2002. Enhancing the crops to feed the poor. *nature*, 418, 678.
- HUGHES, M. A. & DUNN, M. A. 1996. The molecular biology of plant acclimation to low temperature. *Journal of Experimental Botany*, 47, 291-305.
- HURRY, V., STRAND, Å., FURBANK, R. & STITT, M. 2000. The role of inorganic phosphate in the development of freezing tolerance and the acclimatization of photosynthesis to low temperature is revealed by the pho mutants of Arabidopsis thaliana. *The Plant Journal*, 24, 383-396.
- HURRY, V., TOBIAESON, M., KRÖMER, S., GARDESTRÖM, P. & ÖQUIST, G. 1995a. Mitochondria contribute to increased photosynthetic capacity of leaves of winter rye (*Secale cereale* L.) following cold-hardening. *Plant, Cell & Environment*, 18, 69-76.
- HURRY, V. M., STRAND, A., TOBIAESON, M., GARDESTROM, P. & OQUIST, G. 1995b. Cold hardening of spring and winter wheat and rape results in differential

- effects on growth, carbon metabolism, and carbohydrate content. *Plant Physiology*, 109, 697-706.
- INGRAM, J. & BARTELS, D. 1996. The molecular basis of dehydration tolerance in plants. *Annual review of plant biology*, 47, 377-403.
- INITIATIVE, A. G. 2000. Analysis of the genome sequence of the flowering plant *Arabidopsis thaliana*. *nature*, 408, 796.
- ISHIKAWA, M. 1984. Deep supercooling in most tissues of wintering *Sasa senanensis* and its mechanism in leaf blade tissues. *Plant physiology*, 75, 196-202.
- ISHITANI, M., XIONG, L., LEE, H., STEVENSON, B. & ZHU, J.-K. 1998. HOS1, a genetic locus involved in cold-responsive gene expression in *Arabidopsis*. *The Plant Cell*, 10, 1151-1161.
- ISWARI, S. & PALTA, J. P. 1989. Plasma membrane ATPase activity following reversible and irreversible freezing injury. *Plant physiology*, 90, 1088-1095.
- JACKSON, S. D. 2009. Plant responses to photoperiod. *New Phytologist*, 181, 517-531.
- JAGLO-OTTOSEN, K. R., GILMOUR, S. J., ZARKA, D. G., SCHABENBERGER, O. & THOMASHOW, M. F. 1998. *Arabidopsis* CBF1 overexpression induces COR genes and enhances freezing tolerance. *Science*, 280, 104-106.
- JAGLO, K. R., KLEFF, S., AMUNDSEN, K. L., ZHANG, X., HAAKE, V., ZHANG, J. Z., DEITS, T. & THOMASHOW, M. F. 2001. Components of the *Arabidopsis* C-repeat/dehydration-responsive element binding factor cold-response pathway are conserved in *Brassica napus* and other plant species. *Plant physiology*, 127, 910-917.
- JANICKA-RUSSAK, M., KABAŁA, K. & BURZYŃSKI, M. 2012a. Different effect of cadmium and copper on H⁺-ATPase activity in plasma membrane vesicles from *Cucumis sativus* roots. *Journal of experimental botany*, 63, 4133-4142.
- JANICKA-RUSSAK, M., KABAŁA, K., WADOWIKOWSKA, A. & KŁOBUS, G. 2012b. Response of plasma membrane H⁺-ATPase to low temperature in cucumber roots. *Journal of plant research*, 125, 291-300.
- JANSKÁ, A., MARŠÍK, P., ZELENKOVÁ, S. & OVESNÁ, J. 2010. Cold stress and acclimation—what is important for metabolic adjustment? *Plant Biology*, 12, 395-405.
- JEKNIĆ, Z., PILLMAN, K. A., DHILLON, T., SKINNER, J. S., VEISZ, O., CUESTA-MARCOS, A., HAYES, P. M., JACOBS, A. K., CHEN, T. H. & STOCKINGER, E. J. 2014. Hv-CBF2A overexpression in barley accelerates COR gene transcript accumulation and acquisition of freezing tolerance during cold acclimation. *Plant molecular biology*, 84, 67-82.
- JIANG, B., SHI, Y., ZHANG, X., XIN, X., QI, L., GUO, H., LI, J. & YANG, S. 2017. PIF3 is a negative regulator of the CBF pathway and freezing tolerance in *Arabidopsis*. *Proceedings of the National Academy of Sciences*, 114, E6695-E6702.

- JOAZEIRO, C. A. & WEISSMAN, A. M. 2000. RING finger proteins: mediators of ubiquitin ligase activity. *Cell*, 102, 549-552.
- JOSHI, R., WANI, S. H., SINGH, B., BOHRA, A., DAR, Z. A., LONE, A. A., PAREEK, A. & SINGLA-PAREEK, S. L. 2016. Transcription factors and plants response to drought stress: current understanding and future directions. *Frontiers in plant science*, 7, 1029.
- JUNG, J.-H., SEO, P. J. & PARK, C.-M. 2012. The E3 ubiquitin ligase HOS1 regulates Arabidopsis flowering by mediating CONSTANS degradation under cold stress. *Journal of Biological Chemistry*, 287, 43277-43287.
- KAMATA, T. & UEMURA, M. 2004. Solute accumulation in wheat seedlings during cold acclimation: contribution to increased freezing tolerance. *CryoLetters*, 25, 311-322.
- KAMRAN, A., IQBAL, M. & SPANER, D. 2014. Flowering time in wheat (*Triticum aestivum* L.): a key factor for global adaptability. *Euphytica*, 197, 1-26.
- KANT, L., AMRAPALI, S. & BABU, B. K. 2016. Barley. *Genetic and Genomic Resources for Grain Cereals Improvement*. Elsevier.
- KAPLAN, F. & GUY, C. L. 2004. β -Amylase induction and the protective role of maltose during temperature shock. *Plant Physiology*, 135, 1674-1684.
- KAPLAN, F., KOPKA, J., SUNG, D. Y., ZHAO, W., POPP, M., PORAT, R. & GUY, C. L. 2007. Transcript and metabolite profiling during cold acclimation of Arabidopsis reveals an intricate relationship of cold-regulated gene expression with modifications in metabolite content. *The Plant Journal*, 50, 967-981.
- KARSAI, I., SZÚCS, P., KŐSZEGI, B., HAYES, P. M., CASAS, A., BEDŐ, Z. & VEISZ, O. 2008. Effects of photo and thermo cycles on flowering time in barley: a genetical phenomics approach. *Journal of Experimental Botany*, 59, 2707-2715.
- KAUR, N. & GUPTA, A. K. 2005. Signal transduction pathways under abiotic stresses in plants. *Curr. Sci*, 88, 1771-1780.
- KEUNEN, E., PESHEV, D., VANGRONSVELD, J., VAN DEN ENDE, W. & CUYPERS, A. 2013. Plant sugars are crucial players in the oxidative challenge during abiotic stress: extending the traditional concept. *Plant, cell & environment*, 36, 1242-1255.
- KIDOKORO, S., WATANABE, K., OHORI, T., MORIWAKI, T., MARUYAMA, K., MIZOI, J., MYINT PHYU SIN HTWE, N., FUJITA, Y., SEKITA, S. & SHINOZAKI, K. 2015. Soybean DREB 1/CBF-type transcription factors function in heat and drought as well as cold stress-responsive gene expression. *The Plant Journal*, 81, 505-518.
- KIDOKORO, S., YONEDA, K., TAKASAKI, H., TAKAHASHI, F., SHINOZAKI, K. & YAMAGUCHI-SHINOZAKI, K. 2017. Different cold-signaling pathways function in the responses to rapid and gradual decreases in temperature. *The Plant Cell*, 29, 760-774.

- KIKUCHI, R., KAWAHIGASHI, H., ANDO, T., TONOOKA, T. & HANDA, H. 2009. Molecular and functional characterization of PEBP genes in barley reveal the diversification of their roles in flowering. *Plant physiology*, 149, 1341-1353.
- KIM, K.-N., CHEONG, Y. H., GRANT, J. J., PANDEY, G. K. & LUAN, S. 2003. CIPK3, a calcium sensor-associated protein kinase that regulates abscisic acid and cold signal transduction in Arabidopsis. *The Plant Cell*, 15, 411-423.
- KIM, Y., PARK, S., GILMOUR, S. J. & THOMASHOW, M. F. 2013. Roles of CAMTA transcription factors and salicylic acid in configuring the low-temperature transcriptome and freezing tolerance of Arabidopsis. *The Plant Journal*, 75, 364-376.
- KIM, Y. S., LEE, M., LEE, J.-H., LEE, H.-J. & PARK, C.-M. 2015. The unified ICE-CBF pathway provides a transcriptional feedback control of freezing tolerance during cold acclimation in Arabidopsis. *Plant molecular biology*, 89, 187-201.
- KINTLOVÁ, M., BLAVET, N., CEGAN, R. & HOBZA, R. 2017. Transcriptome of barley under three different heavy metal stress reaction. *Genomics data*, 13, 15-17.
- KIRBY, E. 1988. Analysis of leaf, stem and ear growth in wheat from terminal spikelet stage to anthesis. *Field Crops Research*, 18, 127-140.
- KISELEVA, A. A., POTOKINA, E. K. & SALINA, E. A. 2017. Features of Ppd-B1 expression regulation and their impact on the flowering time of wheat near-isogenic lines. *BMC plant biology*, 17, 172.
- KISHOR, P. K., SANGAM, S., AMRUTHA, R., LAXMI, P. S., NAIDU, K., RAO, K., RAO, S., REDDY, K., THERIAPPAN, P. & SREENIVASULU, N. 2005. Regulation of proline biosynthesis, degradation, uptake and transport in higher plants: its implications in plant growth and abiotic stress tolerance. *Curr Sci*, 88, 424-438.
- KISHORE, G. M. & SHEWMAKER, C. 1999. Biotechnology: Enhancing human nutrition in developing and developed worlds. *Proceedings of the National Academy of Sciences*, 96, 5968-5972.
- KLOTKE, J., KOPKA, J., GATZKE, N. & HEYER, A. 2004. Impact of soluble sugar concentrations on the acquisition of freezing tolerance in accessions of Arabidopsis thaliana with contrasting cold adaptation—evidence for a role of raffinose in cold acclimation. *Plant, Cell & Environment*, 27, 1395-1404.
- KNIGHT, H., TREWAVAS, A. J. & KNIGHT, M. R. 1996. Cold calcium signaling in Arabidopsis involves two cellular pools and a change in calcium signature after acclimation. *The Plant Cell*, 8, 489-503.
- KNIGHT, H., ZARKA, D. G., OKAMOTO, H., THOMASHOW, M. F. & KNIGHT, M. R. 2004. Abscisic acid induces CBF gene transcription and subsequent induction of cold-regulated genes via the CRT promoter element. *Plant physiology*, 135, 1710-1717.

- KNIGHT, M. R., CAMPBELL, A. K., SMITH, S. M. & TREWAVAS, A. J. 1991a. Recombinant aequorin as a probe for cytosolic free Ca²⁺ in *Escherichia coli*. *FEBS letters*, 282, 405-408.
- KNIGHT, M. R., CAMPBELL, A. K., SMITH, S. M. & TREWAVAS, A. J. 1991b. Transgenic plant aequorin reports the effects of touch and cold-shock and elicitors on cytoplasmic calcium. *Nature*, 352, 524.
- KNOX, A. K., DHILLON, T., CHENG, H., TONDELLI, A., PECCHIONI, N. & STOCKINGER, E. J. 2010. CBF gene copy number variation at Frost Resistance-2 is associated with levels of freezing tolerance in temperate-climate cereals. *Theoretical and Applied Genetics*, 121, 21-35.
- KNOX, A. K., LI, C., VÁGÚJFALVI, A., GALIBA, G., STOCKINGER, E. J. & DUBCOVSKY, J. 2008a. Identification of candidate CBF genes for the frost tolerance locus Fr-A m 2 in *Triticum monococcum*. *Plant Molecular Biology*, 67, 257-270.
- KNOX, A. K., LI, C., VÁGÚJFALVI, A., GALIBA, G., STOCKINGER, E. J. & DUBCOVSKY, J. 2008b. Identification of candidate CBF genes for the frost tolerance locus Fr-A m 2 in *Triticum monococcum*. *Plant molecular biology*, 67, 257-270.
- KOCSY, G., ATHMER, B., PEROVIC, D., HIMMELBACH, A., SZÚCS, A., VASHEGYI, I., SCHWEIZER, P., GALIBA, G. & STEIN, N. 2010. Regulation of gene expression by chromosome 5A during cold hardening in wheat. *Molecular genetics and genomics*, 283, 351-363.
- KOCSY, G., LAURIE, R., SZALAI, G., SZILÁGYI, V., SIMON-SARKADI, L., GALIBA, G. & DE RONDE, J. A. 2005. Genetic manipulation of proline levels affects antioxidants in soybean subjected to simultaneous drought and heat stresses. *Physiologia Plantarum*, 124, 227-235.
- KOCSY, G., TÓTH, B., BERZY, T., SZALAI, G., JEDNÁKOVITS, A. & GALIBA, G. 2001. Glutathione reductase activity and chilling tolerance are induced by a hydroxylamine derivative BRX-156 in maize and soybean. *Plant Science*, 160, 943-950.
- KOMATSU, M., TOBITA, H., WATANABE, M., YAZAKI, K., KOIKE, T. & KITAO, M. 2013. Photosynthetic downregulation in leaves of the Japanese white birch grown under elevated CO₂ concentration does not change their temperature-dependent susceptibility to photoinhibition. *Physiologia plantarum*, 147, 159-168.
- KOMATSU, S., YANG, G., KHAN, M., ONODERA, H., TOKI, S. & YAMAGUCHI, M. 2007. Over-expression of calcium-dependent protein kinase 13 and calreticulin interacting protein 1 confers cold tolerance on rice plants. *Molecular Genetics and Genomics*, 277, 713.
- KOORNNEEF, M., JORNA, M., BRINKHORST-VAN DER SWAN, D. & KARSSSEN, C. 1982. The isolation of abscisic acid (ABA) deficient mutants by selection of induced

revertants in non-germinating gibberellin sensitive lines of *Arabidopsis thaliana* (L.) Heynh. *Theoretical and Applied Genetics*, 61, 385-393.

- KOORNNEEF, M. & MEINKE, D. 2010. The development of *Arabidopsis* as a model plant. *The Plant Journal*, 61, 909-921.
- KORN, M., PETEREK, S., MOCK, H. P., HEYER, A. G. & HINCHA, D. K. 2008. Heterosis in the freezing tolerance, and sugar and flavonoid contents of crosses between *Arabidopsis thaliana* accessions of widely varying freezing tolerance. *Plant, cell & environment*, 31, 813-827.
- KÖRNER, C. 2016. Plant adaptation to cold climates. *F1000Research*, 5.
- KOSTER, K. L. & LYNCH, D. V. 1992. Solute accumulation and compartmentation during the cold acclimation of Puma rye. *Plant Physiology*, 98, 108-113.
- KREPS, J. A., WU, Y., CHANG, H.-S., ZHU, T., WANG, X. & HARPER, J. F. 2002. Transcriptome changes for *Arabidopsis* in response to salt, osmotic, and cold stress. *Plant physiology*, 130, 2129-2141.
- KUDLA, J., BECKER, D., GRILL, E., HEDRICH, R., HIPPLER, M., KUMMER, U., PARNISKE, M., ROMEIS, T. & SCHUMACHER, K. 2018. Advances and current challenges in calcium signaling. *New Phytologist*, 218, 414-431.
- KUDO, M., KIDOKORO, S., YOSHIDA, T., MIZOI, J., KOJIMA, M., TAKEBAYASHI, Y., SAKAKIBARA, H., FERNIE, A. R., SHINOZAKI, K. & YAMAGUCHI-SHINOZAKI, K. 2018. A gene-stacking approach to overcome the trade-off between drought stress tolerance and growth in *Arabidopsis*. *The Plant Journal*.
- KUMAR, S., MALIK, J., THAKUR, P., KAISTHA, S., SHARMA, K. D., UPADHYAYA, H., BERGER, J. & NAYYAR, H. 2011. Growth and metabolic responses of contrasting chickpea (*Cicer arietinum* L.) genotypes to chilling stress at reproductive phase. *Acta physiologiae plantarum*, 33, 779-787.
- KUMAR, S. V. & WIGGE, P. A. 2010. H2A. Z-containing nucleosomes mediate the thermosensory response in *Arabidopsis*. *Cell*, 140, 136-147.
- KUME, S., KOBAYASHI, F., ISHIBASHI, M., OHNO, R., NAKAMURA, C. & TAKUMI, S. 2005. Differential and coordinated expression of Cbf and Cor/Lea genes during long-term cold acclimation in two wheat cultivars showing distinct levels of freezing tolerance. *Genes & Genetic Systems*, 80, 185-197.
- KUREPIN, L., DAHAL, K., SAVITCH, L., SINGH, J., BODE, R., IVANOV, A., HURRY, V. & HUENER, N. 2013a. Role of CBFs as integrators of chloroplast redox, phytochrome and plant hormone signaling during cold acclimation. *International journal of molecular sciences*, 14, 12729-12763.
- KUREPIN, L. V., DAHAL, K. P., SAVITCH, L. V., SINGH, J., BODE, R., IVANOV, A. G., HURRY, V. & HUENER, N. 2013b. Role of CBFs as integrators of chloroplast redox, phytochrome and plant hormone signaling during cold acclimation. *International Journal of Molecular Sciences*, 14, 12729-12763.

- LAMESCH, P., BERARDINI, T. Z., LI, D., SWARBRECK, D., WILKS, C., SASIDHARAN, R., MULLER, R., DREHER, K., ALEXANDER, D. L. & GARCIA-HERNANDEZ, M. 2011. The Arabidopsis Information Resource (TAIR): improved gene annotation and new tools. *Nucleic acids research*, 40, D1202-D1210.
- LANTICAN, R. M. 2001a. *The science and practice of crop production*, SEAMEO Regional Center for Graduate Study and Research in Agriculture (SEAMEO SEARCA).
- LANTICAN, R. M. 2001b. The science and practice of crop production. *Regional Textbooks*.
- LATA, C., YADAV, A. & PRASAD, M. 2011. Role of plant transcription factors in abiotic stress tolerance. *Abiotic stress response in plants-Physiological, biochemical and genetic perspectives*. InTech.
- LAURIE, D., PRATCHETT, N., SNAPE, J. & BEZANT, J. 1995. RFLP mapping of five major genes and eight quantitative trait loci controlling flowering time in a winter x spring barley (*Hordeum vulgare* L.) cross. *Genome*, 38, 575-585.
- LAURIE, D. A. 1997. Comparative genetics of flowering time. *Oryza: From Molecule to Plant*. Springer.
- LAURIE, D. A., PRATCHETT, N., BEZANT, J. H. & SNAPE, J. W. 1994. Genetic analysis of a photoperiod response gene on the short arm of chromosome 2 (2H) of *Hordeum vulgare* (barley). *Heredity*, 72, 619.
- LAW, C., WORLAND, A. & GIORGI, B. 1976. The genetic control of ear-emergence time by chromosomes 5A and 5D of wheat. *Heredity*, 36, 49.
- LAW, J. A. & JACOBSEN, S. E. 2010. Establishing, maintaining and modifying DNA methylation patterns in plants and animals. *Nature Reviews Genetics*, 11, 204.
- LAZARO, A., VALVERDE, F., PIÑEIRO, M. & JARILLO, J. A. 2012. The Arabidopsis E3 ubiquitin ligase HOS1 negatively regulates CONSTANS abundance in the photoperiodic control of flowering. *The Plant Cell*, 24, 982-999.
- LEE, B.-H., HENDERSON, D. A. & ZHU, J.-K. 2005. The Arabidopsis cold-responsive transcriptome and its regulation by ICE1. *The Plant Cell*, 17, 3155-3175.
- LEE, B.-H., LEE, H., XIONG, L. & ZHU, J.-K. 2002. A mitochondrial complex I defect impairs cold-regulated nuclear gene expression. *The Plant Cell*, 14, 1235-1251.
- LEE, C.-M. & THOMASHOW, M. F. 2012a. Photoperiodic regulation of the C-repeat binding factor (CBF) cold acclimation pathway and freezing tolerance in *Arabidopsis thaliana*. *Proceedings of the National Academy of Sciences*, 109, 15054-15059.
- LEE, C.-M. & THOMASHOW, M. F. 2012b. Photoperiodic regulation of the C-repeat binding factor (CBF) cold acclimation pathway and freezing tolerance in *Arabidopsis thaliana*. *Proceedings of the National Academy of Sciences*, 201211295.
- LEE, H., XIONG, L., GONG, Z., ISHITANI, M., STEVENSON, B. & ZHU, J.-K. 2001. The Arabidopsis HOS1 gene negatively regulates cold signal transduction and

- encodes a RING finger protein that displays cold-regulated nucleo–cytoplasmic partitioning. *Genes & development*, 15, 912-924.
- LEE, H., YOO, S. J., LEE, J. H., KIM, W., YOO, S. K., FITZGERALD, H., CARRINGTON, J. C. & AHN, J. H. 2010a. Genetic framework for flowering-time regulation by ambient temperature-responsive miRNAs in Arabidopsis. *Nucleic acids research*, 38, 3081-3093.
- LEE, H. G. & SEO, P. J. 2015. The MYB 96–HHP module integrates cold and abscisic acid signaling to activate the CBF–COR pathway in Arabidopsis. *The Plant Journal*, 82, 962-977.
- LEE, R. E., WARREN, G. J. & GUSTA, L. V. 1995. *Biological ice nucleation and its applications*.
- LEE, S.-J., KANG, J.-Y., PARK, H.-J., KIM, M. D., BAE, M. S., CHOI, H.-I. & KIM, S. Y. 2010b. DREB2C interacts with ABF2, a bZIP protein regulating ABA-responsive gene expression, and its overexpression affects ABA sensitivity. *Plant physiology*, pp. 110.154617.
- LEE, S.-K., KIM, B.-G., KWON, T.-R., JEONG, M.-J., PARK, S.-R., LEE, J.-W., BYUN, M.-O., KWON, H.-B., MATTHEWS, B. F. & HONG, C.-B. 2011. Overexpression of the mitogen-activated protein kinase gene OsMAPK33 enhances sensitivity to salt stress in rice (*Oryza sativa* L.). *Journal of biosciences*, 36, 139-151.
- LEHTI-SHIU, M. D. & SHIU, S.-H. 2012. Diversity, classification and function of the plant protein kinase superfamily. *Phil. Trans. R. Soc. B*, 367, 2619-2639.
- LEVITT, J. 1980a. Chilling temperatures-Chilling injury and resistance. *Responses of plants to environmental stresses*. Academic Press, London, New York, 23.
- LEVITT, J. 1980b. *Responses of Plants to Environmental Stress, Volume 1: Chilling, Freezing, and High Temperature Stresses*, Academic Press.
- LEVITT, J. 1980c. *Responses of Plants to Environmental Stresses (Physiological Ecology): Chilling, freezing, and high temperature stresses*.
- LI, A., WANG, X., LESEBERG, C. H., JIA, J. & MAO, L. 2008. Biotic and abiotic stress responses through calcium-dependent protein kinase (CDPK) signaling in wheat (*Triticum aestivum* L.). *Plant signaling & behavior*, 3, 654-656.
- LI, H., DING, Y., SHI, Y., ZHANG, X., ZHANG, S., GONG, Z. & YANG, S. 2017. MPK3- and MPK6-mediated ICE1 phosphorylation negatively regulates ICE1 stability and freezing tolerance in Arabidopsis. *Developmental cell*, 43, 630-642. e4.
- LIMIN, A. E. & FOWLER, D. B. 2006. Low-temperature tolerance and genetic potential in wheat (*Triticum aestivum* L.): response to photoperiod, vernalization, and plant development. *Planta*, 224, 360-366.

- LIN, C. & THOMASHOW, M. F. 1992. DNA sequence analysis of a complementary DNA for cold-regulated Arabidopsis gene cor15 and characterization of the COR 15 polypeptide. *Plant physiology*, 99, 519-525.
- LINDLÖF, A. 2010. Interplay between low-temperature pathways and light reduction. *Plant signaling & behavior*, 5, 820-825.
- LISSARRE, M., OHTA, M., SATO, A. & MIURA, K. 2010. Cold-responsive gene regulation during cold acclimation in plants. *Plant signaling & behavior*, 5, 948-952.
- LIU, C. & ZHANG, T. 2017. Expansion and stress responses of the AP2/EREBP superfamily in cotton. *BMC genomics*, 18, 118.
- LIU, Q., KASUGA, M., SAKUMA, Y., ABE, H., MIURA, S., YAMAGUCHI-SHINOZAKI, K. & SHINOZAKI, K. 1998. Two transcription factors, DREB1 and DREB2, with an EREBP/AP2 DNA binding domain separate two cellular signal transduction pathways in drought- and low-temperature-responsive gene expression, respectively, in Arabidopsis. *The Plant Cell*, 10, 1391-1406.
- LIU, Y. & ZHOU, J. 2018. MAPping kinase regulation of ICE1 in freezing tolerance. *Trends in plant science*, 23, 91-93.
- LIU, Z., JIA, Y., DING, Y., SHI, Y., LI, Z., GUO, Y., GONG, Z. & YANG, S. 2017. Plasma membrane CRPK1-mediated phosphorylation of 14-3-3 proteins induces their nuclear import to fine-tune CBF signaling during cold response. *Molecular cell*, 66, 117-128. e5.
- LORENZO, C. D., SANCHEZ-LAMAS, M., ANTONIETTI, M. S. & CERDÁN, P. D. 2016. Emerging hubs in plant light and temperature signaling. *Photochemistry and photobiology*, 92, 3-13.
- LOS, D. A., MIRONOV, K. S. & ALLAKHVERDIEV, S. I. 2013. Regulatory role of membrane fluidity in gene expression and physiological functions. *Photosynthesis research*, 116, 489-509.
- LOS, D. A. & MURATA, N. 2004. Membrane fluidity and its roles in the perception of environmental signals. *Biochimica et Biophysica Acta (BBA)-Biomembranes*, 1666, 142-157.
- LUAN, S., KUDLA, J., RODRIGUEZ-CONCEPCION, M., YALOVSKY, S. & GRUISSEM, W. 2002. Calmodulins and calcineurin B-like proteins: Calcium sensors for specific signal response coupling in plants. *The Plant Cell*, 14, S389-S400.
- LUAN, H., SHEN, H., PAN, Y., GUO, B., LY, C., XU, R. 2018 Elucidating the hypoxic stress response in barley (*Hordeum vulgare* L.) during waterlogging: A proteomic approach. *Sci Rep.* 8, 9655
- LUKATKIN, A. S., BRAZAITYTE, A., BOBINAS, C. & DUCHOVSKIS, P. 2012. Chilling injury in chilling-sensitive plants: a review. *Agriculture*, 99, 111-124.

- LUO, D., NIU, X., YU, J., YAN, J., GOU, X., LU, B.-R. & LIU, Y. 2012. Rice choline monooxygenase (OsCMO) protein functions in enhancing glycine betaine biosynthesis in transgenic tobacco but does not accumulate in rice (*Oryza sativa* L. ssp. japonica). *Plant cell reports*, 31, 1625-1635.
- MAEDA, O., LUCAS, L., SILVA, F., TANNO, K.-I. & FULLER, D. Q. 2016. Narrowing the harvest: Increasing sickle investment and the rise of domesticated cereal agriculture in the Fertile Crescent. *Quaternary Science Reviews*, 145, 226-237.
- MAGOME, H., YAMAGUCHI, S., HANADA, A., KAMIYA, Y. & ODA, K. 2008. The DDF1 transcriptional activator upregulates expression of a gibberellin-deactivating gene, GA2ox7, under high-salinity stress in Arabidopsis. *The Plant Journal*, 56, 613-626.
- MAHAJAN, S. & TUTEJA, N. 2005. Cold, salinity and drought stresses: an overview. *Archives of biochemistry and biophysics*, 444, 139-158.
- MAHFOOZI, S., LIMIN, A. & FOWLER, D. 2001. Developmental regulation of low-temperature tolerance in winter wheat. *Annals of Botany*, 87, 751-757.
- MAHFOOZI, S., LIMIN, A., HAYES, P., HUCL, P. & FOWLER, D. 2000. Influence of photoperiod response on the expression of cold hardiness in wheat and barley. *Canadian journal of plant science*, 80, 721-724.
- MAIBAM, P., NAWKAR, G. M., PARK, J. H., SAHI, V. P., LEE, S. Y. & KANG, C. H. 2013. The influence of light quality, circadian rhythm, and photoperiod on the CBF-mediated freezing tolerance. *International journal of molecular sciences*, 14, 11527-11543.
- MANN, M. & JENSEN, O. N. 2003. Proteomic analysis of post-translational modifications. *Nature biotechnology*, 21, 255.
- MANTYLA, E., LANG, V. & PALVA, E. T. 1995. Role of abscisic acid in drought-induced freezing tolerance, cold acclimation, and accumulation of LT178 and RAB18 proteins in Arabidopsis thaliana. *Plant Physiology*, 107, 141-148.
- MARCH-DÍAZ, R., GARCÍA-DOMÍNGUEZ, M., LOZANO-JUSTE, J., LEÓN, J., FLORENCIO, F. J. & REYES, J. C. 2008. Histone H2A. Z and homologues of components of the SWR1 complex are required to control immunity in Arabidopsis. *The Plant Journal*, 53, 475-487.
- MAROZSÁN-TÓTH, Z., VASHEGYI, I., GALIBA, G. & TÓTH, B. 2015. The cold response of CBF genes in barley is regulated by distinct signaling mechanisms. *Journal of plant physiology*, 181, 42-49.
- MARUYAMA, K., TODAKA, D., MIZOI, J., YOSHIDA, T., KIDOKORO, S., MATSUKURA, S., TAKASAKI, H., SAKURAI, T., YAMAMOTO, Y. Y. & YOSHIWARA, K. 2011. Identification of cis-acting promoter elements in cold-and dehydration-induced transcriptional pathways in Arabidopsis, rice, and soybean. *DNA research*, 19, 37-49.

- MATTEUCCI, M., D'ANGELI, S., ERRICO, S., LAMANNA, R., PERROTTA, G. & ALTAMURA, M. 2011. Cold affects the transcription of fatty acid desaturases and oil quality in the fruit of *Olea europaea* L. genotypes with different cold hardiness. *Journal of experimental botany*, 62, 3403-3420.
- MAURYA, J. P. & BHALERAJ, R. P. 2017. Photoperiod-and temperature-mediated control of growth cessation and dormancy in trees: a molecular perspective. *Annals of Botany*, 120, 351-360.
- MAZUR, P. 1969. Freezing injury in plants. *Annual Review of Plant Physiology*, 20, 419-448.
- MCAINSH, M. R. & PITTMAN, J. K. 2009. Shaping the calcium signature. *New Phytologist*, 181, 275-294.
- MCCLUNG, C. R. & DAVIS, S. J. 2010. Ambient thermometers in plants: from physiological outputs towards mechanisms of thermal sensing. *Current Biology*, 20, R1086-R1092.
- MCCORMACK, E., TSAI, Y.-C. & BRAAM, J. 2005. Handling calcium signaling: arabidopsis CaMs and CMLs. *Trends in plant science*, 10, 383-389.
- MCKENZIE, J., WEISER, C. & BURKE, M. 1974. Effects of Red and Far Red Light on the Initiation of Cold Acclimation in *Cornus stolonifera* Michx. *Plant physiology*, 53, 783-789.
- MCKOWN, R., KUROKI, G. & WARREN, G. 1996. Cold responses of Arabidopsis mutants impaired in freezing tolerance. *Journal of Experimental Botany*, 47, 1919-1925.
- MCLAREN, W., GIL, L., HUNT, S. E., RIAT, H. S., RITCHIE, G. R., THORMANN, A., FLICEK, P. & CUNNINGHAM, F. 2016. The ensembl variant effect predictor. *Genome biology*, 17, 122.
- MEDINA, J., CATALÁ, R. & SALINAS, J. 2011. The CBFs: three Arabidopsis transcription factors to cold acclimate. *Plant Science*, 180, 3-11.
- MEGHA, S., BASU, U. & KAV, N. N. 2014. Metabolic engineering of cold tolerance in plants. *Biocatalysis and Agricultural Biotechnology*, 3, 88-95.
- MEHROTRA, R., BHALOTHIA, P., BANSAL, P., BASANTANI, M. K., BHARTI, V. & MEHROTRA, S. 2014. Abscisic acid and abiotic stress tolerance—Different tiers of regulation. *Journal of plant physiology*, 171, 486-496.
- METZGER, M. B., HRISTOVA, V. A. & WEISSMAN, A. M. 2012. HECT and RING finger families of E3 ubiquitin ligases at a glance. *J Cell Sci*, 125, 531-537.
- MEZA-BASSO, L., ALBERDI, M., RAYNAL, M., FERRERO-CADINANOS, M.-L. & DELSENY, M. 1986. Changes in protein synthesis in rapeseed (*Brassica napus*) seedlings during a low temperature treatment. *Plant physiology*, 82, 733-738.

- MILLER, A. K., GALIBA, G. & DUBCOVSKY, J. 2006. A cluster of 11 CBF transcription factors is located at the frost tolerance locus Fr-A m 2 in *Triticum monococcum*. *Molecular Genetics and Genomics*, 275, 193-203.
- MINORSKY, P. 1985. An heuristic hypothesis of chilling injury in plants: a role for calcium as the primary physiological transducer of injury. *Plant, Cell & Environment*, 8, 75-94.
- MINORSKY, P. & SPANSWICK, R. 1989. Electrophysiological evidence for a role for calcium in temperature sensing by roots of cucumber seedlings. *Plant, Cell & Environment*, 12, 137-143.
- MIRALLES, D. & RICHARDS, R. 2000. Responses of leaf and tiller emergence and primordium initiation in wheat and barley to interchanged photoperiod. *Annals of Botany*, 85, 655-663.
- MITTLER, R., VANDERAUWERA, S., SUZUKI, N., MILLER, G., TOGNETTI, V. B., VANDEPOELE, K., GOLLERY, M., SHULAEV, V. & VAN BREUSEGEM, F. 2011. ROS signaling: the new wave? *Trends in plant science*, 16, 300-309.
- MIURA, K., JIN, J. B., LEE, J., YOO, C. Y., STIRM, V., MIURA, T., ASHWORTH, E. N., BRESSAN, R. A., YUN, D.-J. & HASEGAWA, P. M. 2007. SIZ1-mediated sumoylation of ICE1 controls CBF3/DREB1A expression and freezing tolerance in *Arabidopsis*. *The Plant Cell*, 19, 1403-1414.
- MIZOI, J., SHINOZAKI, K. & YAMAGUCHI-SHINOZAKI, K. 2012. AP2/ERF family transcription factors in plant abiotic stress responses. *Biochimica et Biophysica Acta (BBA)-Gene Regulatory Mechanisms*, 1819, 86-96.
- MOHAPATRA, S. S., POOLE, R. J. & DHINDSA, R. S. 1987. Changes in protein patterns and translatable messenger RNA populations during cold acclimation of alfalfa. *Plant physiology*, 84, 1172-1176.
- MOLASSIOTIS, A. & FOTOPOULOS, V. 2011. Oxidative and nitrosative signaling in plants: two branches in the same tree? *Plant Signaling & Behavior*, 6, 210-214.
- MOLINA-CANO, J., FRA-MON, P., SALCEDO, G., ARAGONCILLO, C., DE TOGORES, F. R. & GARCÍA-OLMEDO, F. 1987. Morocco as a possible domestication center for barley: biochemical and agromorphological evidence. *Theoretical and Applied Genetics*, 73, 531-536.
- MOLINARI, H. B. C., MARUR, C. J., DAROS, E., DE CAMPOS, M. K. F., DE CARVALHO, J. F. R. P., FILHO, J. C. B., PEREIRA, L. F. P. & VIEIRA, L. G. E. 2007. Evaluation of the stress-inducible production of proline in transgenic sugarcane (*Saccharum* spp.): osmotic adjustment, chlorophyll fluorescence and oxidative stress. *Physiologia Plantarum*, 130, 218-229.
- MONROY, A. F., DRYANOVA, A., MALETTE, B., OREN, D. H., FARAJALLA, M. R., LIU, W., DANYLUK, J., UBAYASENA, L. W., KANE, K. & SCOLES, G. J. 2007. Regulatory gene candidates and gene expression analysis of cold acclimation in winter and spring wheat. *Plant Molecular Biology*, 64, 409-423.

- MU, D., LIANG, Y., ZHANG, W. & WANG, Y. 2018. Investigation on Tree Molecular Genome of Arabidopsis Thaliana for Internet of Things. *IEEE Access*.
- MUTHUSWAMY, S. & MEIER, I. 2011. Genetic and environmental changes in SUMO homeostasis lead to nuclear mRNA retention in plants. *Planta*, 233, 201-208.
- NAKASHIMA, K., ITO, Y. & YAMAGUCHI-SHINOZAKI, K. 2009. Transcriptional regulatory networks in response to abiotic stresses in Arabidopsis and grasses. *Plant physiology*, 149, 88-95.
- NAKASHIMA, K., SHINWARI, Z. K., SAKUMA, Y., SEKI, M., MIURA, S., SHINOZAKI, K. & YAMAGUCHI-SHINOZAKI, K. 2000. Organization and expression of two Arabidopsis DREB2 genes encoding DRE-binding proteins involved in dehydration-and high-salinity-responsive gene expression. *Plant molecular biology*, 42, 657-665.
- NAKASHIMA, K., YAMAGUCHI-SHINOZAKI, K. & SHINOZAKI, K. 2014. The transcriptional regulatory network in the drought response and its crosstalk in abiotic stress responses including drought, cold, and heat. *Frontiers in plant science*, 5, 170.
- NANJO, T., KOBAYASHI, M., YOSHIBA, Y., KAKUBARI, Y., YAMAGUCHI-SHINOZAKI, K. & SHINOZAKI, K. 1999. Antisense suppression of proline degradation improves tolerance to freezing and salinity in Arabidopsis thaliana. *Febs Letters*, 461, 205-210.
- NATIONS, U. 2016. World population ageing 1950-2050. United Nations, Department of Economic and Social Affairs, Population Division.
- NAVARRO, M., MARQUE, G., AYAX, C., KELLER, G., BORGES, J., MARQUE, C. & TEULIERES, C. 2009. Complementary regulation of four Eucalyptus CBF genes under various cold conditions. *Journal of experimental botany*, 60, 2713-2724.
- NEVO, E. 1992. Origin, evolution, population genetics and resources for breeding of wild barley, *Hordeum spontaneum*, in the Fertile Crescent. *Barley: genetics, biochemistry, molecular biology and biotechnology*, 19-43.
- NG, L. M., MELCHER, K., TEH, B. T. & XU, H. E. 2014. Abscisic acid perception and signaling: structural mechanisms and applications. *Acta Pharmacologica Sinica*, 35, 567.
- NILSSON-LEISSNER, G. 1929. Death from low temperature and resistance of plants to cold. *The Quarterly Review of Biology*, 4, 113-117.
- NISHIDA, I. & MURATA, N. 1996. Chilling sensitivity in plants and cyanobacteria: the crucial contribution of membrane lipids. *Annual review of plant biology*, 47, 541-568.
- NISHIYAMA, Y., YAMAMOTO, H., ALLAKHVERDIEV, S. I., INABA, M., YOKOTA, A. & MURATA, N. 2001. Oxidative stress inhibits the repair of photodamage to the photosynthetic machinery. *The EMBO journal*, 20, 5587-5594.

- NIU, X., ZHENG, W., LU, B.-R., REN, G., HUANG, W., WANG, S., LIU, J., TANG, Z., LUO, D. & WANG, Y. 2007. An unusual posttranscriptional processing in two betaine aldehyde dehydrogenase loci of cereal crops directed by short, direct repeats in response to stress conditions. *Plant physiology*, 143, 1929-1942.
- NOH, S. A., PARK, S. H., HUH, G. H., PAEK, K.-H., SHIN, J. S. & BAE, J. M. 2009. Growth retardation and differential regulation of expansin genes in chilling-stressed sweetpotato. *Plant Biotechnology Reports*, 3, 75-85.
- NOVÁK, A., BOLDIZSÁR, Á., ÁDÁM, É., KOZMA-BOGNÁR, L., MAJLÁTH, I., BĀGA, M., TÓTH, B., CHIBBAR, R. & GALIBA, G. 2015. Light-quality and temperature-dependent CBF14 gene expression modulates freezing tolerance in cereals. *Journal of experimental botany*, 67, 1285-1295.
- NOVILLO, F., ALONSO, J. M., ECKER, J. R. & SALINAS, J. 2004. CBF2/DREB1C is a negative regulator of CBF1/DREB1B and CBF3/DREB1A expression and plays a central role in stress tolerance in Arabidopsis. *Proceedings of the National Academy of Sciences*, 101, 3985-3990.
- OAKLEY, C. G., ÅGREN, J., ATCHISON, R. A. & SCHEMSKE, D. W. 2014. QTL mapping of freezing tolerance: links to fitness and adaptive trade-offs. *Molecular Ecology*, 23, 4304-4315.
- OH, S. J., KWON, C. W., CHOI, D. W., SONG, S. I. & KIM, J. K. 2007. Expression of barley HvCBF4 enhances tolerance to abiotic stress in transgenic rice. *Plant Biotechnology Journal*, 5, 646-656.
- OLVERA-CARRILLO, Y., CAMPOS, F., REYES, J. L., GARCIARRUBIO, A. & COVARRUBIAS, A. A. 2010. Functional analysis of the group 4 late embryogenesis abundant proteins reveals their relevance in the adaptive response during water deficit in Arabidopsis. *Plant physiology*, 154, 373-390.
- [OMAFRA] ONTARIO MINISTRY OF AGRICULTURE, FOOD AND RURAL AFFAIRS, 2017. Agronomy Guide for Field Crops. Publication 811
- OPITZ, N., MARCON, C., PASCHOLD, A., MALIK, W. A., LITHIO, A., BRANDT, R., PIEPHO, H.-P., NETTLETON, D. & HOCHHOLDINGER, F. 2015. Extensive tissue-specific transcriptomic plasticity in maize primary roots upon water deficit. *Journal of Experimental Botany*, 67, 1095-1107.
- ÖQUIST, G. & HUNER, N. P. 1993. Cold-hardening-induced resistance to photoinhibition of photosynthesis in winter rye is dependent upon an increased capacity for photosynthesis. *Planta*, 189, 150-156.
- ÖRVAR, B. L., SANGWAN, V., OMANN, F. & DHINDSA, R. S. 2000. Early steps in cold sensing by plant cells: the role of actin cytoskeleton and membrane fluidity. *The Plant Journal*, 23, 785-794.
- OSTHOFF, A., DALLE ROSE, P. D., BALDAUF, J. A., PIEPHO, H.-P. & HOCHHOLDINGER, F. 2019. Transcriptomic reprogramming of barley seminal roots by combined water deficit and salt stress. *BMC genomics*, 20, 325.

- OZDEN, M., DEMIREL, U. & KAHRAMAN, A. 2009. Effects of proline on antioxidant system in leaves of grapevine (*Vitis vinifera* L.) exposed to oxidative stress by H₂O₂. *Scientia Horticulturae*, 119, 163-168.
- ÖZTÜRK, L. & DEMİR, Y. 2002. In vivo and in vitro protective role of proline. *Plant Growth Regulation*, 38, 259-264.
- OZTURK, Z. N., TALAMÉ, V., DEYHOLOS, M., MICHALOWSKI, C. B., GALBRAITH, D. W., GOZUKIRMIZI, N., TUBEROSA, R. & BOHNERT, H. J. 2002. Monitoring large-scale changes in transcript abundance in drought-and salt-stressed barley. *Plant molecular biology*, 48, 551-573.
- PADMANABHAN, V., DIAS, D. M. & NEWTON, R. J. 1997. Expression analysis of a gene family in loblolly pine (*Pinus taeda* L.) induced by water deficit stress. *Plant molecular biology*, 35, 801-807.
- PALTA, J. P., LEVITT, J. & STADELMANN, E. J. 1977. Freezing injury in onion bulb cells: II. Post-thawing injury or recovery. *Plant physiology*, 60, 398-401.
- PALTA, J. P. & WEISS, L. S. 2018. ICE FORMATION AND FREEZING INJURY: ANOVERVIEW ON THE SURVIVAL MECHANISMS AND MOLECULAR ASPECTS OF INJURY AND COLD ACCLIMATION IN HERBACEOUS PLANTS. *Advances in plant cold hardiness*, 11.
- PAPAGEORGIU, G. C. & MURATA, N. 1995. The unusually strong stabilizing effects of glycine betaine on the structure and function of the oxygen-evolving photosystem II complex. *Photosynthesis Research*, 44, 243-252.
- PAREEK, A., KHURANA, A., K SHARMA, A. & KUMAR, R. 2017. An Overview of Signaling Regulons During Cold Stress Tolerance in Plants. *Current genomics*, 18, 498-511.
- PARK, H. J., PARK, H. C., LEE, S. Y., BOHNERT, H. J. & YUN, D.-J. 2011. Ubiquitin and ubiquitin-like modifiers in plants. *Journal of Plant Biology*, 54, 275.
- PARK, S., LEE, C. M., DOHERTY, C. J., GILMOUR, S. J., KIM, Y. & THOMASHOW, M. F. 2015. Regulation of the Arabidopsis CBF regulon by a complex low-temperature regulatory network. *The Plant Journal*, 82, 193-207.
- PEARCE, R. S. 1999. Molecular analysis of acclimation to cold. *Plant growth regulation*, 29, 47-76.
- PEARCE, R. S. 2001. Plant freezing and damage. *Annals of botany*, 87, 417-424.
- PENFIELD, S. 2008. Temperature perception and signal transduction in plants. *New Phytologist*, 179, 615-628.
- PÉREZ-GIANMARCO, T. I., SLAFER, G. A. & GONZÁLEZ, F. G. 2018. Wheat pre-anthesis development as affected by photoperiod sensitivity genes (*Ppd-1*) under contrasting photoperiods. *Functional Plant Biology*, 45, 645-657.

- PIMENTEL, D., HUANG, X., CORDOVA, A. & PIMENTEL, M. 1997. Impact of population growth on food supplies and environment. *Population & Environment*, 19, 9-14.
- PLIETH, C., HANSEN, U. P., KNIGHT, H. & KNIGHT, M. R. 1999. Temperature sensing by plants: the primary characteristics of signal perception and calcium response. *The Plant Journal*, 18, 491-497.
- POCOCK, T. H., HURRY, V., SAVITCH, L. V. & HUNER, N. P. 2001. Susceptibility to low-temperature photoinhibition and the acquisition of freezing tolerance in winter and spring wheat: The role of growth temperature and irradiance. *Physiologia Plantarum*, 113, 499-506.
- PRESTON, J. C. & SANDVE, S. R. 2013. Adaptation to seasonality and the winter freeze. *Frontiers in plant science*, 4, 167.
- PUÉRTOLAS, J., CONESA, M. R., BALLESTER, C. & DODD, I. C. 2014. Local root abscisic acid (ABA) accumulation depends on the spatial distribution of soil moisture in potato: implications for ABA signalling under heterogeneous soil drying. *Journal of experimental botany*, 66, 2325-2334.
- PUHAKAINEN, T., HESS, M. W., MÄKELÄ, P., SVENSSON, J., HEINO, P. & PALVA, E. T. 2004a. Overexpression of multiple dehydrin genes enhances tolerance to freezing stress in Arabidopsis. *Plant molecular biology*, 54, 743-753.
- PUHAKAINEN, T., LI, C., BOIJE-MALM, M., KANGASJÄRVI, J., HEINO, P. & PALVA, E. T. 2004b. Short-day potentiation of low temperature-induced gene expression of a C-repeat-binding factor-controlled gene during cold acclimation in silver birch. *Plant Physiology*, 136, 4299-4307.
- PURANIK, S., SAHU, P. P., SRIVASTAVA, P. S. & PRASAD, M. 2012. NAC proteins: regulation and role in stress tolerance. *Trends in plant science*, 17, 369-381.
- PYOTT, D. E., SHEEHAN, E. & MOLNAR, A. 2016. Engineering of CRISPR/Cas9-mediated potyvirus resistance in transgene-free Arabidopsis plants. *Molecular plant pathology*, 17, 1276-1288.
- QI, J., SONG, C. P., WANG, B., ZHOU, J., KANGASJÄRVI, J., ZHU, J. K. & GONG, Z. 2018. Reactive oxygen species signaling and stomatal movement in plant responses to drought stress and pathogen attack. *Journal of integrative plant biology*, 60, 805-826.
- RADA, F., GOLDSTEIN, G., AZÓCAR, A. & MEINZER, F. 1985. Freezing avoidance in Andean giant rosette plants. *Plant, Cell & Environment*, 8, 501-507.
- RAKSHIT, R., PATRA, A., PAL, D., -KUMAR, M. & SINGH, R. 2012. Effect of elevated CO₂ and temperature on nitrogen dynamics and microbial activity during wheat (*Triticum aestivum* L.) growth on a subtropical inceptisol in India. *Journal of agronomy and crop science*, 198, 452-465.

- RAPACZ, M., WOLANIN, B., HURA, K. & TYRKA, M. 2008. The effects of cold acclimation on photosynthetic apparatus and the expression of COR14b in four genotypes of barley (*Hordeum vulgare*) contrasting in their tolerance to freezing and high-light treatment in cold conditions. *Annals of botany*, 101, 689-699.
- RASOOL, S., URWAT, U., NAZIR, M., ZARGAR, S. M. & ZARGAR, M. 2018. Cross Talk Between Phytohormone Signaling Pathways Under Abiotic Stress Conditions and Their Metabolic Engineering for Conferring Abiotic Stress Tolerance. *Abiotic Stress-Mediated Sensing and Signaling in Plants: An Omics Perspective*. Springer.
- REAM, T. S., WOODS, D. P., SCHWARTZ, C. J., SANABRIA, C. P., MAHOY, J. A., WALTERS, E. M., KAEPLER, H. F. & AMASINO, R. M. 2014. Interaction of photoperiod and vernalization determines flowering time of *Brachypodium distachyon*. *Plant physiology*, 164, 694-709.
- REDDY, A. S., ALI, G. S., CELESNIK, H. & DAY, I. S. 2011. Coping with stresses: roles of calcium-and calcium/calmodulin-regulated gene expression. *The Plant Cell*, 23, 2010-2032.
- REHMAN, S. & MAHMOOD, T. 2015. Functional role of DREB and ERF transcription factors: regulating stress-responsive network in plants. *Acta Physiologiae Plantarum*, 37, 178.
- REJEB, K. B., ABDELLY, C. & SAVOURÉ, A. 2014. How reactive oxygen species and proline face stress together. *Plant Physiology and Biochemistry*, 80, 278-284.
- RHODES, D. & HANSON, A. 1993. Quaternary ammonium and tertiary sulfonium compounds in higher plants. *Annual review of plant biology*, 44, 357-384.
- RIHAN, H. Z., AL-ISSAWI, M. & FULLER, M. P. 2017. Advances in physiological and molecular aspects of plant cold tolerance. *Journal of Plant Interactions*, 12, 143-157.
- ROBERTS, D. 1990. Identification of loci on chromosome 5A of wheat involved in control of cold hardiness, vernalization, leaf length, rosette growth habit, and height of hardened plants. *Genome*, 33, 247-259.
- ROHDE, P., HINCHA, D. K. & HEYER, A. G. 2004. Heterosis in the freezing tolerance of crosses between two *Arabidopsis thaliana* accessions (Columbia-0 and C24) that show differences in non-acclimated and acclimated freezing tolerance. *The Plant Journal*, 38, 790-799.
- ROMERO, I., FUERTES, A., BENITO, M., MALPICA, J., LEYVA, A. & PAZ-ARES, J. 1998. More than 80R2R3-MYB regulatory genes in the genome of *Arabidopsis thaliana*. *The Plant journal: for cell and molecular biology*, 14, 273-284.
- ROUDIER, F., FERNANDEZ, A. G., FUJITA, M., HIMMELSPACH, R., BORNER, G. H., SCHINDELMAN, G., SONG, S., BASKIN, T. I., DUPREE, P. & WASTENEYS, G. O. 2005. COBRA, an *Arabidopsis* extracellular glycosyl-phosphatidyl inositol-anchored protein, specifically controls highly anisotropic expansion through its involvement in cellulose microfibril orientation. *The Plant Cell*, 17, 1749-1763.

- RUELLAND, E., VAULTIER, M.-N., ZACHOWSKI, A. & HURRY, V. 2009. Cold signalling and cold acclimation in plants. *Advances in botanical research*, 49, 35-150.
- RUELLAND, E. & ZACHOWSKI, A. 2010. How plants sense temperature. *Environmental and experimental botany*, 69, 225-232.
- SAGISAKA, S., MATSUDA, Y., OKUDA, T. & OZEKI, S. 1991. Relationship between wintering ability of winter wheat and the extent of depression of carbohydrate reserves: basal metabolic rate under snow determines longevity of plants. *Soil Science and Plant Nutrition*, 37, 531-541.
- SAH, S. K., REDDY, K. R. & LI, J. 2016. Abscisic acid and abiotic stress tolerance in crop plants. *Frontiers in plant science*, 7, 571.
- SAKAI, A. & LARCHER, W. 1987a. Frost survival of plants ecological studies 62. Springer-Verlag, Berlin, Germany.
- SAKAI, A. & LARCHER, W. 1987b. Low temperature and frost as environmental factors. *Frost Survival of Plants*. Springer.
- SAKAI, A. & LARCHER, W. 2012. *Frost survival of plants: responses and adaptation to freezing stress*, Springer Science & Business Media.
- SAKUMA, Y., LIU, Q., DUBOUZET, J. G., ABE, H., SHINOZAKI, K. & YAMAGUCHI-SHINOZAKI, K. 2002. DNA-binding specificity of the ERF/AP2 domain of Arabidopsis DREBs, transcription factors involved in dehydration-and cold-inducible gene expression. *Biochemical and biophysical research communications*, 290, 998-1009.
- ŠAMAJOVÁ, O., PLÍHAL, O., AL-YOUSIF, M., HIRT, H. & ŠAMAJ, J. 2013. Improvement of stress tolerance in plants by genetic manipulation of mitogen-activated protein kinases. *Biotechnology Advances*, 31, 118-128.
- SAMARAH, N. H. 2016. Understanding how plants respond to drought stress at the molecular and whole plant levels. *Drought Stress Tolerance in Plants, Vol 2*. Springer.
- SANDERS, D., PELLOUX, J., BROWNLEE, C. & HARPER, J. F. 2002. Calcium at the crossroads of signaling. *The Plant Cell*, 14, S401-S417.
- SANGHERA, G. S., WANI, S. H., HUSSAIN, W. & SINGH, N. 2011. Engineering cold stress tolerance in crop plants. *Current genomics*, 12, 30.
- SARHADI, E., MAHFOOZI, S., HOSSEINI, S. A. & SALEKDEH, G. H. 2010. Cold acclimation proteome analysis reveals close link between the up-regulation of low-temperature associated proteins and vernalization fulfillment. *Journal of proteome research*, 9, 5658-5667.
- SARHAN, F., DANYLUK, J., BADAWI, M., REDDY, Y. V., TOMINAGA, Y., AGHARBAOUI, Z. & HOUDE, M. 2008. Structure and Functional Analysis of

- Wheat ICE (Inducer of CBF Expression) Genes. *Plant and Cell Physiology*, 49, 1237-1249.
- SASAKI, K., KIM, M.-H. & IMAI, R. 2007. Arabidopsis COLD SHOCK DOMAIN PROTEIN2 is a RNA chaperone that is regulated by cold and developmental signals. *Biochemical and Biophysical Research Communications*, 364, 633-638.
- SASANI, S., HEMMING, M. N., OLIVER, S. N., GREENUP, A., TAVAKKOL-AFSHARI, R., MAHFOOZI, S., POUSTINI, K., SHARIFI, H.-R., DENNIS, E. S. & PEACOCK, W. J. 2009. The influence of vernalization and daylength on expression of flowering-time genes in the shoot apex and leaves of barley (*Hordeum vulgare*). *Journal of Experimental Botany*, 60, 2169-2178.
- SATHEESH, V., CHIDAMBARANATHAN, P., JAGANNADHAM, P., KOHLI, D., JAIN, P., BHAT, S. & SRINIVASAN, R. 2014. A polyketide cyclase/dehydrase and lipid transport superfamily gene of Arabidopsis and its orthologue of chickpea exhibit rapid response to wounding. *Ind J Genet Pl Breed*, 74, 463-70.
- SAVITCH, L. V., ALLARD, G., SEKI, M., ROBERT, L. S., TINKER, N. A., HUNER, N. P., SHINOZAKI, K. & SINGH, J. 2005. The effect of overexpression of two Brassica CBF/DREB1-like transcription factors on photosynthetic capacity and freezing tolerance in Brassica napus. *Plant and Cell Physiology*, 46, 1525-1539.
- SAWASDIKOSOL, S., PRATT, J. C., MENG, W., ECK, M. J. & BURAKOFF, S. J. 2000. Adapting to multiple personalities: Cbl is also a RING finger ubiquitin ligase. *Biochimica et Biophysica Acta (BBA)/Reviews on Cancer*, 1471, M1-M12.
- SCHIEBER, M. & CHANDEL, N. S. 2014a. ROS function in redox signaling and oxidative stress. *Current biology*, 24, R453-R462.
- SCHIEBER, M. & CHANDEL, N. S. 2014b. TOR signaling couples oxygen sensing to lifespan in *C. elegans*. *Cell reports*, 9, 9-15.
- SCHINDELMAN, G., MORIKAMI, A., JUNG, J., BASKIN, T. I., CARPITA, N. C., DERBYSHIRE, P., MCCANN, M. C. & BENFEY, P. N. 2001. COBRA encodes a putative GPI-anchored protein, which is polarly localized and necessary for oriented cell expansion in Arabidopsis. *Genes & Development*, 15, 1115-1127.
- SEKI, M., ISHIDA, J., NARUSAKA, M., FUJITA, M., NANJO, T., UMEZAWA, T., KAMIYA, A., NAKAJIMA, M., ENJU, A. & SAKURAI, T. 2002a. Monitoring the expression pattern of around 7,000 Arabidopsis genes under ABA treatments using a full-length cDNA microarray. *Functional & integrative genomics*, 2, 282-291.
- SEKI, M., KAMEI, A., YAMAGUCHI-SHINOZAKI, K. & SHINOZAKI, K. 2003. Molecular responses to drought, salinity and frost: common and different paths for plant protection. *Current opinion in biotechnology*, 14, 194-199.
- SEKI, M., NARUSAKA, M., ABE, H., KASUGA, M., YAMAGUCHI-SHINOZAKI, K., CARNINCI, P., HAYASHIZAKI, Y. & SHINOZAKI, K. 2001. Monitoring the expression pattern of 1300 Arabidopsis genes under drought and cold stresses by using a full-length cDNA microarray. *The Plant Cell*, 13, 61-72.

- SEKI, M., NARUSAKA, M., ISHIDA, J., NANJO, T., FUJITA, M., OONO, Y., KAMIYA, A., NAKAJIMA, M., ENJU, A. & SAKURAI, T. 2002b. Monitoring the expression profiles of 7000 Arabidopsis genes under drought, cold and high-salinity stresses using a full-length cDNA microarray. *The Plant Journal*, 31, 279-292.
- SEO, P. J., XIANG, F., QIAO, M., PARK, J.-Y., LEE, Y. N., KIM, S.-G., LEE, Y.-H., PARK, W. J. & PARK, C.-M. 2009. The MYB96 transcription factor mediates abscisic acid signaling during drought stress response in Arabidopsis. *Plant Physiology*, 151, 275-289.
- SHACKLOCK, P., READ, N. & TREWAVAS, A. 1992. Cytosolic free calcium mediates red light-induced photomorphogenesis. *Nature*, 358, 753.
- SHAKHATREH, Y., HADDAD, N., ALRABABAH, M., GRANDO, S. & CECCARELLI, S. 2010. Phenotypic diversity in wild barley (*Hordeum vulgare* L. ssp. *spontaneum* (C. Koch) Thell.) accessions collected in Jordan. *Genetic Resources and Crop Evolution*, 57, 131-146.
- SHAO, H., WANG, H. & TANG, X. 2015. NAC transcription factors in plant multiple abiotic stress responses: progress and prospects. *Frontiers in plant science*, 6, 902.
- SHARMA, S., VILLAMOR, J. G. & VERSLUES, P. E. 2011. Essential role of tissue-specific proline synthesis and catabolism in growth and redox balance at low water potential. *Plant physiology*, 157, 292-304.
- SHARRATT, B. 1999. Thermal requirements for barley maturation and leaf development in interior Alaska. *Field Crops Research*, 63, 179-184.
- SHI, Y., DING, Y. & YANG, S. 2014. Cold signal transduction and its interplay with phytohormones during cold acclimation. *Plant and Cell Physiology*, 56, 7-15.
- SHI, Y., DING, Y. & YANG, S. 2018. Molecular regulation of CBF signaling in cold acclimation. *Trends in plant science*.
- SHI, Y., HUANG, J., SUN, T., WANG, X., ZHU, C., AI, Y. & GU, H. 2017. The precise regulation of different COR genes by individual CBF transcription factors in Arabidopsis thaliana. *Journal of integrative plant biology*, 59, 118-133.
- SHI, Y., TIAN, S., HOU, L., HUANG, X., ZHANG, X., GUO, H. & YANG, S. 2012. Ethylene signaling negatively regulates freezing tolerance by repressing expression of CBF and type-A ARR genes in Arabidopsis. *The Plant Cell*, tpc. 112.098640.
- SHINOZAKI, K. & YAMAGUCHI-SHINOZAKI, K. 1996. Molecular responses to drought and cold stress. *Current Opinion in Biotechnology*, 7, 161-167.
- SHINOZAKI, K. & YAMAGUCHI-SHINOZAKI, K. 1997. Gene expression and signal transduction in water-stress response. *Plant physiology*, 115, 327.
- SHINOZAKI, K. & YAMAGUCHI-SHINOZAKI, K. 2000. Molecular responses to dehydration and low temperature: differences and cross-talk between two stress signaling pathways. *Current opinion in plant biology*, 3, 217-223.

- SHINOZAKI, K. & YAMAGUCHI-SHINOZAKI, K. 2007. Gene networks involved in drought stress response and tolerance. *Journal of experimental botany*, 58, 221-227.
- SHINWARI, Z. K., NAKASHIMA, K., MIURA, S., KASUGA, M., SEKI, M., YAMAGUCHI-SHINOZAKI, K. & SHINOZAKI, K. 1998. An Arabidopsis gene family encoding DRE/CRT binding proteins involved in low-temperature-responsive gene expression. *Biochemical and biophysical research communications*, 250, 161-170.
- SHU, Y., LIU, Y., ZHANG, J., SONG, L. & GUO, C. 2016. Genome-wide analysis of the AP2/ERF superfamily genes and their responses to abiotic stress in *Medicago truncatula*. *Frontiers in plant science*, 6, 1247.
- SIMINOVITCH, D. & CLOUTIER, Y. 1982. Twenty-four-hour induction of freezing and drought tolerance in plumules of winter rye seedlings by desiccation stress at room temperature in the dark. *Plant Physiology*, 69, 250-255.
- SINCLAIR, T. R. & RUFTY, T. W. 2012. Nitrogen and water resources commonly limit crop yield increases, not necessarily plant genetics. *Global Food Security*, 1, 94-98.
- SINCLAIR, T. R. & SINCLAIR, C. J. 2010. *Bread, beer and the seeds of change: agriculture's imprint on world history*, Cabi.
- SINGH, R. K., SVYSTUN, T., ALDAHMAH, B., JÖNSSON, A. M. & BHALERAJ, R. P. 2017. Photoperiod- and temperature-mediated control of phenology in trees—a molecular perspective. *New Phytologist*, 213, 511-524.
- SINGLE, W. 1964. Studies on frost injury to wheat. II. Ice formation within the plant. *Australian Journal of Agricultural Research*, 15, 869-875.
- SKINNER, D. Z. 2015. Genes upregulated in winter wheat (*Triticum aestivum* L.) during mild freezing and subsequent thawing suggest sequential activation of multiple response mechanisms. *PLoS One*, 10, e0133166.
- SKINNER, D. Z., BELLINGER, B., HISCOX, W. & HELMS, G. L. 2018. Evidence of cyclical light/dark-regulated expression of freezing tolerance in young winter wheat plants. *PloS one*, 13, e0198042.
- SKINNER, J. S., VON ZITZEWITZ, J., SZÜCS, P., MARQUEZ-CEDILLO, L., FILICHKIN, T., AMUNDSEN, K., STOCKINGER, E. J., THOMAS, M. F., CHEN, T. H. & HAYES, P. M. 2005. Structural, functional, and phylogenetic characterization of a large CBF gene family in barley. *Plant molecular biology*, 59, 533-551.
- SLAFER, G., REYNOLDS, M., PASK, A. & MULLAN, D. 2012. Wheat development: its role in phenotyping and improving crop adaptation. *Physiological breeding I: interdisciplinary approaches to improve crop adaptation*. (Eds MP Reynolds, AJD Pask, DM Mullan) pp, 107-121.
- SMALLWOOD, M. & BOWLES, D. J. 2002. Plants in a cold climate. *Philosophical Transactions of the Royal Society of London B: Biological Sciences*, 357, 831-847.

- SNAPE, J., BUTTERWORTH, K., WHITECHURCH, E. & WORLAND, A. 2001a. Waiting for fine times: genetics of flowering time in wheat. *Wheat in a global environment*. Springer.
- SNAPE, J., LAW, C. & WORLAND, A. 1976. Chromosome variation for loci controlling ear emergence time on chromosome 5A of wheat. *Heredity*, 37, 335.
- SNAPE, J., SARMA, R., QUARRIE, S. A., FISH, L., GALIBA, G. & SUTKA, J. 2001b. Mapping genes for flowering time and frost tolerance in cereals using precise genetic stocks. *Euphytica*, 120, 309.
- SOLÉ, R., LEVIN, S., HIGGINS, P. A., MASTRANDREA, M. D. & SCHNEIDER, S. H. 2002. Philosophical Transactions of the Royal Society of London. Series B: Biological Sciences: 357 (1421). *Philosophical Transactions of the Royal Society of London B: Biological Sciences*, 357.
- SOLTIS, P. S., MARCHANT, D. B., VAN DE PEER, Y. & SOLTIS, D. E. 2015. Polyploidy and genome evolution in plants. *Current opinion in genetics & development*, 35, 119-125.
- SONG, Y., LIU, L., FENG, Y., WEI, Y., YUE, X., HE, W., ZHANG, H. & AN, L. 2015a. Chilling- and freezing-induced alterations in cytosine methylation and its association with the cold tolerance of an alpine subnival plant, *Chorispora bungeana*. *PLoS One*, 10, e0135485.
- SONG, Y. H., SHIM, J. S., KINMONTH-SCHULTZ, H. A. & IMAIZUMI, T. 2015b. Photoperiodic flowering: time measurement mechanisms in leaves. *Annual review of plant biology*, 66, 441-464.
- SREENIVASULU, N., HARSHAVARDHAN, V. T., GOVIND, G., SEILER, C. & KOHLI, A. 2012. Contrapuntal role of ABA: does it mediate stress tolerance or plant growth retardation under long-term drought stress? *Gene*, 506, 265-273.
- STEINDAL, A. L. H., RØDVEN, R., HANSEN, E. & MØLMANN, J. 2015. Effects of photoperiod, growth temperature and cold acclimatisation on glucosinolates, sugars and fatty acids in kale. *Food chemistry*, 174, 44-51.
- STELMAKH, A. 1990. Geographic distribution of Vrn-genes in landraces and improved varieties of spring bread wheat. *Euphytica*, 45, 113-118.
- STEPONKUS, P., LYNCH, D. & UEMURA, M. 1990a. The influence of cold acclimation on the lipid composition and cryobehaviour of the plasma membrane of isolated rye protoplasts. *Phil. Trans. R. Soc. Lond. B*, 326, 571-583.
- STEPONKUS, P., LYNCH, D. & UEMURA, M. 1990b. The influence of cold acclimation on the lipid composition and cryobehaviour of the plasma membrane of isolated rye protoplasts. *Philosophical Transactions of the Royal Society of London. B, Biological Sciences*, 326, 571-583.

- STEPONKUS, P., MYERS, S., LYNCH, D., GARDNER, L., BRONSHTEYN, V., LEIBO, S., RALL, W., PITT, R., LIN, T.-T. & MACLNTYRE, R. 1990c. Cryopreservation of *Drosophila melanogaster* embryos. *Nature*, 345, 170.
- STEPONKUS, P. & WEBB, M. 1992. Freeze-induced dehydration and membrane destabilization in plants. *Water and life*. Springer.
- STEPONKUS, P. L. 1984. Role of the plasma membrane in freezing injury and cold acclimation. *Annual Review of Plant Physiology*, 35, 543-584.
- STEPONKUS, P. L., UEMURA, M., BALSAMO, R. A., ARVINTE, T. & LYNCH, D. V. 1988. Transformation of the cryobehavior of rye protoplasts by modification of the plasma membrane lipid composition. *Proceedings of the National Academy of Sciences*, 85, 9026-9030.
- STITT, M. & HURRY, V. 2002. A plant for all seasons: alterations in photosynthetic carbon metabolism during cold acclimation in *Arabidopsis*. *Current opinion in plant biology*, 5, 199-206.
- STOCKINGER, E., CHENG, H. & SKINNER, J. 2006. Structural organization of barley CBF genes coincident with QTLs for cold hardiness. *Cold hardiness in plants: molecular genetics, cell biology and physiology*. CABI Publishing Oxon, UK, 53-63.
- STOCKINGER, E. J., GILMOUR, S. J. & THOMASHOW, M. F. 1997. *Arabidopsis thaliana* CBF1 encodes an AP2 domain-containing transcriptional activator that binds to the C-repeat/DRE, a cis-acting DNA regulatory element that stimulates transcription in response to low temperature and water deficit. *Proceedings of the National Academy of Sciences*, 94, 1035-1040.
- STOCKINGER, E. J., MAO, Y., REGIER, M. K., TRIEZENBERG, S. J. & THOMASHOW, M. F. 2001. Transcriptional adaptor and histone acetyltransferase proteins in *Arabidopsis* and their interactions with CBF1, a transcriptional activator involved in cold-regulated gene expression. *Nucleic acids research*, 29, 1524-1533.
- STOCKINGER, E. J., SKINNER, J. S., GARDNER, K. G., FRANCIJA, E. & PECCHIONI, N. 2007. Expression levels of barley Cbf genes at the Frost resistance-H2 locus are dependent upon alleles at Fr-H1 and Fr-H2. *The Plant Journal*, 51, 308-321.
- STRAND, Å., FOYER, C., GUSTAFSSON, P., GARDESTRÖM, P. & HURRY, V. 2003. Altering flux through the sucrose biosynthesis pathway in transgenic *Arabidopsis thaliana* modifies photosynthetic acclimation at low temperatures and the development of freezing tolerance. *Plant, Cell & Environment*, 26, 523-535.
- SU, C., CHEN, K., DING, Q., MOU, Y., YANG, R., ZHAO, M., MA, B., XU, Z., MA, Y. & PAN, Y. 2018. Proteomic Analysis of the Function of a Novel Cold-Regulated Multispanning Transmembrane Protein COR413-PM1 in *Arabidopsis*. *International journal of molecular sciences*, 19, 2572.
- SUH, J., JEUNG, J., LEE, J., CHOI, Y., YEA, J., VIRK, P., MACKILL, D. & JENA, K. 2010. Identification and analysis of QTLs controlling cold tolerance at the

- reproductive stage and validation of effective QTLs in cold-tolerant genotypes of rice (*Oryza sativa* L.). *Theoretical and Applied Genetics*, 120, 985-995.
- SUNKAR, R., LI, Y.-F. & JAGADEESWARAN, G. 2012. Functions of microRNAs in plant stress responses. *Trends in plant science*, 17, 196-203.
- SUTKA, J. 1994. Genetic control of frost tolerance in wheat (*Triticum aestivum* L.). *Euphytica*, 77, 277-282.
- SUTKA, J. & SNAPE, J. W. 1989. Location of a gene for frost resistance on chromosome 5A of wheat. *Euphytica*, 42, 41-44.
- SUTTON, F., CHEN, D.-G., GE, X. & KENEFICK, D. 2009. Cbf genes of the Fr-A2 allele are differentially regulated between long-term cold acclimated crown tissue of freeze-resistant and-susceptible, winter wheat mutant lines. *BMC Plant Biology*, 9, 34.
- SZABADOS, L. & SAVOURE, A. 2010. Proline: a multifunctional amino acid. *Trends in plant science*, 15, 89-97.
- TAKAHASHI, D., LI, B., NAKAYAMA, T., KAWAMURA, Y. & UEMURA, M. 2013. Plant plasma membrane proteomics for improving cold tolerance. *Frontiers in plant science*, 4, 90.
- TAKUMI, S., KOIKE, A., NAKATA, M., KUME, S., OHNO, R. & NAKAMURA, C. 2003. Cold-specific and light-stimulated expression of a wheat (*Triticum aestivum* L.) Cor gene Wcor15 encoding a chloroplast-targeted protein. *Journal of Experimental Botany*, 54, 2265-2274.
- TALEEI, A., MIRFAKHRAEE, R., MARDI, M., ZALI, A. & MAHFOUZI, C. 2010. QTL markers associated with low temperature tolerance in winter wheat. *International journal of bio-science and bio-technology*, 2, 39-47.
- TANG, M., LÜ, S., JING, Y., ZHOU, X., SUN, J. & SHEN, S. 2005. Isolation and identification of a cold-inducible gene encoding a putative DRE-binding transcription factor from *Festuca arundinacea*. *Plant Physiology and Biochemistry*, 43, 233-239.
- TANOU, G., MINAS, I. S., SCOSSA, F., BELGHAZI, M., XANTHOPOULOU, A., GANOPOULOS, I., MADESIS, P., FERNIE, A. & MOLASSIOTIS, A. 2017. Exploring priming responses involved in peach fruit acclimation to cold stress. *Scientific reports*, 7, 11358.
- TANTAU, H., BALKO, C., BRETTSCHEIDER, B., MELZ, G. & DÖRFFLING, K. 2004. Improved frost tolerance and winter survival in winter barley (*Hordeum vulgare* L.) by in vitro selection of proline overaccumulating lines. *Euphytica*, 139, 19-32.
- TANTAU, H. & DÖRFFLING, K. 1991. In vitro-selection of hydroxyproline-resistant cell lines of wheat (*Triticum aestivum*): accumulation of proline, decrease in osmotic potential, and increase in frost tolerance. *Physiologia Plantarum*, 82, 243-248.

- TEIGE, M., SCHEIKL, E., EULGEM, T., DÓCZI, R., ICHIMURA, K., SHINOZAKI, K., DANGL, J. L. & HIRT, H. 2004. The MKK2 pathway mediates cold and salt stress signaling in Arabidopsis. *Molecular cell*, 15, 141-152.
- THALHAMMER, A., BRYANT, G., SULPICE, R. & HINCHA, D. K. 2014a. Disordered cold regulated15 proteins protect chloroplast membranes during freezing through binding and folding, but do not stabilize chloroplast enzymes in vivo. *Plant physiology*, 166, 190-201.
- THALHAMMER, A., BRYANT, G., SULPICE, R. & HINCHA, D. K. 2014b. Disordered COR15 proteins protect chloroplast membranes during freezing through binding and folding, but do not stabilize chloroplast enzymes in-vivo. *Plant physiology*, pp. 114.245399.
- THALHAMMER, A., HINCHA, D. K. & ZUTHER, E. 2014c. Measuring freezing tolerance: electrolyte leakage and chlorophyll fluorescence assays. *Plant Cold Acclimation*. Springer.
- THALHAMMER, A., HUNDERTMARK, M., POPOVA, A. V., SECKLER, R. & HINCHA, D. K. 2010. Interaction of two intrinsically disordered plant stress proteins (COR15A and COR15B) with lipid membranes in the dry state. *Biochimica et Biophysica Acta (BBA)-Biomembranes*, 1798, 1812-1820.
- THEOCHARIS, A., CLÉMENT, C. & BARKA, E. A. 2012. Physiological and molecular changes in plants grown at low temperatures. *Planta*, 235, 1091-1105.
- THOMASHOW, M. 1999a. Plant cold tolerance. *Molecular responses to cold, drought, heat and salt stress in higher plants*, 61-80.
- THOMASHOW, M. F. 1998. Role of cold-responsive genes in plant freezing tolerance. *Plant physiology*, 118, 1-8.
- THOMASHOW, M. F. 1999b. Plant cold acclimation: freezing tolerance genes and regulatory mechanisms. *Annual review of plant biology*, 50, 571-599.
- THOMASHOW, M. F. 2001. So what's new in the field of plant cold acclimation? Lots! *Plant physiology*, 125, 89-93.
- THOMASHOW, M. F. 2010. Molecular basis of plant cold acclimation: insights gained from studying the CBF cold response pathway. *Plant physiology*, 154, 571-577.
- THOMASHOW, M. F., STOCKINGER, E. J., JAGLO-OTTOSEN, K. R., GILMOUR, S. J. & ZARKA, D. G. 1997. Function and regulation of Arabidopsis thaliana COR (cold-regulated) genes. *Acta Physiologiae Plantarum*, 19, 497-504.
- TIEFENBACHER, J. P., HAGELMAN, R. R. & CECORA, R. J. 2000. *California Citrus Freeze of December 1998: Place, Perception and Choice: Developing a Disaster Reconstruction Model*, Natural Hazards Center.

- TILMAN, D., BALZER, C., HILL, J. & BEFORT, B. L. 2011. Global food demand and the sustainable intensification of agriculture. *Proceedings of the National Academy of Sciences*, 108, 20260-20264.
- TODAKA, D., NAKASHIMA, K., SHINOZAKI, K. & YAMAGUCHI-SHINOZAKI, K. 2012. Toward understanding transcriptional regulatory networks in abiotic stress responses and tolerance in rice. *Rice*, 5, 6.
- TOENNIESSEN, G. H., O'TOOLE, J. C. & DEVRIES, J. 2003. Advances in plant biotechnology and its adoption in developing countries. *Current opinion in plant biology*, 6, 191-198.
- TONDELLI, A., FRANCIA, E., BARABASCHI, D., APRILE, A., SKINNER, J. S., STOCKINGER, E. J., STANCA, A. M. & PECCHIONI, N. 2006. Mapping regulatory genes as candidates for cold and drought stress tolerance in barley. *Theoretical and Applied Genetics*, 112, 445-454.
- TONDELLI, A., FRANCIA, E., BARABASCHI, D., PASQUARIELLO, M. & PECCHIONI, N. 2011. Inside the CBF locus in Poaceae. *Plant science*, 180, 39-45.
- TONDELLI, A., PAGANI, D., GHAFOORI, I. N., RAHIMI, M., ATAEI, R., RIZZA, F., FLAVELL, A. J. & CATTIVELLI, L. 2014. Allelic variation at Fr-H1/Vrn-H1 and Fr-H2 loci is the main determinant of frost tolerance in spring barley. *Environmental and experimental botany*, 106, 148-155.
- TÓTH, B., GALIBA, G., FEHÉR, E., SUTKA, J. & SNAPE, J. W. 2003. Mapping genes affecting flowering time and frost resistance on chromosome 5B of wheat. *Theoretical and Applied Genetics*, 107, 509-514.
- TRANQUILLI, G. & DUBCOVSKY, J. 2000. Epistatic interaction between vernalization genes Vrn-Am1 and Vrn-Am2 in diploid wheat. *Journal of Heredity*, 91, 304-306.
- TREVASKIS, B., HEMMING, M. N., DENNIS, E. S. & PEACOCK, W. J. 2007. The molecular basis of vernalization-induced flowering in cereals. *Trends in plant science*, 12, 352-357.
- TRUMAN, W., SREEKANTA, S., LU, Y., BETHKE, G., TSUDA, K., KATAGIRI, F. & GLAZEBROOK, J. 2013. The Calmodulin Binding Protein 60 Family Includes Both Negative and Positive Regulators of Plant Immunity. *Plant physiology*, pp. 113.227108.
- TSUDA, K., TSVETANOV, S., TAKUMI, S., MORI, N., ATANASSOV, A. & NAKAMURA, C. 2000. New members of a cold-responsive group-3 Lea/Rab-related Cor gene family from common wheat (*Triticum aestivum* L.). *Genes & genetic systems*, 75, 179-188.
- TUNNACLIFFE, A., HINCHA, D. K., LEPRINCE, O. & MACHEREL, D. 2010. LEA proteins: versatility of form and function. *Dormancy and resistance in harsh environments*. Springer.

- TURNER, A., BEALES, J., FAURE, S., DUNFORD, R. P. & LAURIE, D. A. 2005. The pseudo-response regulator Ppd-H1 provides adaptation to photoperiod in barley. *Science*, 310, 1031-1034.
- TURSMAN, D. & DUMAN, J. G. 1995. Cryoprotective effects of thermal hysteresis protein on survivorship of frozen gut cells from the freeze-tolerant centipede *Lithobius forficatus*. *Journal of Experimental Zoology*, 272, 249-257.
- TUTEJA, N. 2007. Abscisic acid and abiotic stress signaling. *Plant signaling & behavior*, 2, 135-138.
- TYYSTJÄRVI, E. 2013. Photoinhibition of photosystem II. *International review of cell and molecular biology*. Elsevier.
- UEMURA, M., JOSEPH, R. A. & STEPONKUS, P. L. 1995. Cold acclimation of *Arabidopsis thaliana* (effect on plasma membrane lipid composition and freeze-induced lesions). *Plant physiology*, 109, 15-30.
- UEMURA, M., TOMINAGA, Y., NAKAGAWARA, C., SHIGEMATSU, S., MINAMI, A. & KAWAMURA, Y. 2006. Responses of the plasma membrane to low temperatures. *Physiologia Plantarum*, 126, 81-89.
- UEMURA, M. & YOSHIDA, S. 1984. Involvement of plasma membrane alterations in cold acclimation of winter rye seedlings (*Secale cereale* L. cv Puma). *Plant physiology*, 75, 818-826.
- UK Meteorological Office 2019 <https://www.metoffice.gov.uk/weather/world/canada>
- UK Meteorological Office 2019 <https://www.metoffice.gov.uk/weather/world/poland>
- USMAN, M. G., RAFII, M. Y., MARTINI, M. Y., YUSUFF, O. A., ISMAIL, M. R. & MIAH, G. 2017. Molecular analysis of Hsp70 mechanisms in plants and their function in response to stress. *Biotechnology and Genetic Engineering Reviews*, 33, 26-39.
- VÁGÚJFALVI, A., APRILE, A., MILLER, A., DUBCOVSKY, J., DELUGU, G., GALIBA, G. & CATTIVELLI, L. 2005. The expression of several Cbf genes at the Fr-A2 locus is linked to frost resistance in wheat. *Molecular Genetics and Genomics*, 274, 506-514.
- VÁGÚJFALVI, A., GALIBA, G., CATTIVELLI, L. & DUBCOVSKY, J. 2003. The cold-regulated transcriptional activator Cbf3 is linked to the frost-tolerance locus Fr-A2 on wheat chromosome 5A. *Molecular Genetics and Genomics*, 269, 60-67.
- VALLURU, R., LAMMENS, W., CLAUPEIN, W. & VAN DEN ENDE, W. 2008. Freezing tolerance by vesicle-mediated fructan transport. *Trends in Plant Science*, 13, 409-414.
- VANBUREN, R., BRYANT, D., EDGER, P. P., TANG, H., BURGESS, D., CHALLABATHULA, D., SPITTLE, K., HALL, R., GU, J. & LYONS, E. 2015.

- Single-molecule sequencing of the desiccation-tolerant grass *Oropetium thomaeum*. *Nature*, 527, 508.
- VASHEGYI, I., VGJFALVI, A., GALIBA, G. & DUBCOVSKY, J. 2010. Regulation of freezing tolerance and flowering in temperate cereals: the *VRN1* connection. *Plant Physiol*, 153, 1846-1858 Diederichsen.
- VERMEULEN, S. J., CAMPBELL, B. M. & INGRAM, J. S. 2012. Climate change and food systems. *Annual review of environment and resources*, 37.
- VERSLUES, P. E. & SHARP, R. E. 1998. Role of amino acids in abiotic stress resistance. *Plant amino acids: biochemistry and biotechnology*, 319.
- VIGELAND, M. D., SPANNAGL, M., ASP, T., PAINA, C., RUDI, H., ROGNLI, O. A., FJELLHEIM, S. & SANDVE, S. R. 2013. Evidence for adaptive evolution of low-temperature stress response genes in a Pooidae grass ancestor. *New Phytologist*, 199, 1060-1068.
- VISWANATHAN, C. & ZHU, J.-K. 2002. Molecular genetic analysis of cold-regulated gene transcription. *Philosophical Transactions of the Royal Society of London. Series B: Biological Sciences*, 357, 877-886.
- VÍTÁMVÁS, P., PRÁŠIL, I. T., KOSOVA, K., PLANCHON, S. & RENAUT, J. 2012. Analysis of proteome and frost tolerance in chromosome 5A and 5B reciprocal substitution lines between two winter wheats during long-term cold acclimation. *Proteomics*, 12, 68-85.
- VOGEL, J. T., ZARKA, D. G., VAN BUSKIRK, H. A., FOWLER, S. G. & THOMASHOW, M. F. 2005. Roles of the CBF2 and ZAT12 transcription factors in configuring the low temperature transcriptome of *Arabidopsis*. *The Plant Journal*, 41, 195-211.
- VON BOTHMER, R. & JACOBSEN, N. 1985. Origin, taxonomy, and related species. *Barley*, 19-56.
- VON ZITZEWITZ, J., CUESTA-MARCOS, A., CONDON, F., CASTRO, A. J., CHAO, S., COREY, A., FILICHKIN, T., FISK, S. P., GUTIERREZ, L. & HAGGARD, K. 2011. The genetics of winterhardiness in barley: perspectives from genome-wide association mapping. *The Plant Genome*, 4, 76-91.
- VON ZITZEWITZ, J., SZŰCS, P., DUBCOVSKY, J., YAN, L., FRANCIÀ, E., PECCHIONI, N., CASAS, A., CHEN, T. H., HAYES, P. M. & SKINNER, J. S. 2005. Molecular and structural characterization of barley vernalization genes. *Plant molecular biology*, 59, 449-467.
- VYSE, K., PAGTER, M., ZUTHER, E. & HINCHA, D. K. 2019. Deacclimation after cold acclimation—a crucial, but widely neglected part of plant winter survival. *Journal of experimental botany*, 70, 4595-4604.

- WALIA, H., WILSON, C., WAHID, A., CONDAMINE, P., CUI, X. & CLOSE, T. J. 2006. Expression analysis of barley (*Hordeum vulgare* L.) during salinity stress. *Functional & integrative genomics*, 6, 143.
- WANG, D.-Z., JIN, Y.-N., DING, X.-H., WANG, W.-J., ZHAI, S.-S., BAI, L.-P. & GUO, Z.-F. 2017. Gene regulation and signal transduction in the ICE–CBF–COR signaling pathway during cold stress in plants. *Biochemistry (Moscow)*, 82, 1103-1117.
- WANG, J.-T., GOULD, J. H., PADMANABHAN, V. & NEWTON, R. J. 2002. Analysis and localization of the water-deficit stress-induced gene (Ip3). *Journal of plant growth regulation*, 21, 469-478.
- WANG, K., BAI, Z.-Y., LIANG, Q.-Y., LIU, Q.-L., ZHANG, L., PAN, Y.-Z., LIU, G.-L., JIANG, B.-B., ZHANG, F. & JIA, Y. 2018. Transcriptome analysis of chrysanthemum (*Dendranthema grandiflorum*) in response to low temperature stress. *BMC genomics*, 19, 319.
- WANG, Z., CHENG, K., WAN, L., YAN, L., JIANG, H., LIU, S., LEI, Y. & LIAO, B. 2015. Genome-wide analysis of the basic leucine zipper (bZIP) transcription factor gene family in six legume genomes. *BMC genomics*, 16, 1053.
- WANI, S., CHANDER, G., SAHRAWAT, K. L. & RAO, P. N. 2014. Integrated nutrient management using deoiled *Jatropha* cake for sustained and economic food production. *International Journal of Plant Production*, 8, 549-562.
- WANI, S. & KUMAR, V. 2015. Plant stress tolerance: engineering ABA: a Potent phytohormone. *Transcriptomics*, 3, 1000113.
- WARREN, G. J. 1998. Cold stress: manipulating freezing tolerance in plants. *Current Biology*, 8, R514-R516.
- WEBB, M. S., UEMURA, M. & STEPONKUS, P. L. 1994. A comparison of freezing injury in oat and rye: two cereals at the extremes of freezing tolerance. *Plant Physiology*, 104, 467-478.
- WEI, M., XU, X. & LI, C. 2017. Identification and expression of CAMTA genes in *Populus trichocarpa* under biotic and abiotic stress. *Scientific reports*, 7, 17910.
- WEISER, C. 1970. Cold resistance and injury in woody plants: knowledge of hardy plant adaptations to freezing stress may help us to reduce winter damage. *Science*, 169, 1269-1278.
- WELLING, A., MORITZ, T., PALVA, E. T. & JUNTILA, O. 2002. Independent activation of cold acclimation by low temperature and short photoperiod in hybrid aspen. *Plant Physiology*, 129, 1633-1641.
- WELLING, A., RINNE, P., VIHERRÄ-AARNIO, A., KONTUNEN-SOPPELA, S., HEINO, P. & PALVA, E. T. 2004. Photoperiod and temperature differentially regulate the expression of two dehydrin genes during overwintering of birch (*Betula pubescens* Ehrh.). *Journal of Experimental Botany*, 55, 507-516.

- WHEELER, T. & VON BRAUN, J. 2013. Climate change impacts on global food security. *Science*, 341, 508-513.
- WIEMER, M., CHENG, Y. T., IMKAMPE, J., LI, M., WANG, D., LIPKA, V. & LI, X. 2012. Putative members of the Arabidopsis Nup107-160 nuclear pore sub-complex contribute to pathogen defense. *The Plant Journal*, 70, 796-808.
- WILKINSON, S. & DAVIES, W. J. 2010. Drought, ozone, ABA and ethylene: new insights from cell to plant to community. *Plant, cell & environment*, 33, 510-525.
- WILLIAMS, B., PELLETT, N. & KLEIN, R. 1972. Phytochrome control of growth cessation and initiation of cold acclimation in selected woody plants. *Plant physiology*, 50, 262-265.
- WILSON, P., HENEGHAN, A. & HAYMET, A. 2003. Ice nucleation in nature: supercooling point (SCP) measurements and the role of heterogeneous nucleation. *Cryobiology*, 46, 88-98.
- WINFIELD, M. O., LU, C., WILSON, I. D., COGHILL, J. A. & EDWARDS, K. J. 2010. Plant responses to cold: transcriptome analysis of wheat. *Plant Biotechnology Journal*, 8, 749-771.
- WISNIEWSKI, M., GLENN, D. M., GUSTA, L. & FULLER, M. P. 2008. Using infrared thermography to study freezing in plants. *HortScience*, 43, 1648-1651.
- WOLKERS, W. F., BALASUBRAMANIAN, S. K., ONGSTAD, E. L., ZEC, H. C. & BISCHOF, J. C. 2007. Effects of freezing on membranes and proteins in LNCaP prostate tumor cells. *Biochimica et Biophysica Acta (BBA)-Biomembranes*, 1768, 728-736.
- WRIGHT, S. 1969. An increase in the "inhibitor- β " content of detached wheat leaves following a period of wilting. *Planta*, 86, 10-20.
- XIN, Z. 1998. eskimo1 mutants of Arabidopsis are constitutively freezing-tolerant. *Proceedings of the National Academy of Sciences*, 95, 7799-7804.
- XIN, Z. & BROWSE, J. 2000. Cold comfort farm: the acclimation of plants to freezing temperatures. *Plant, Cell & Environment*, 23, 893-902.
- XIN, Z. & LI, P. H. 1993. Relationship between proline and abscisic acid in the induction of chilling tolerance in maize suspension-cultured cells. *Plant physiology*, 103, 607-613.
- XIN, Z., MANDAOKAR, A., CHEN, J., LAST, R. L. & BROWSE, J. 2007. Arabidopsis ESK1 encodes a novel regulator of freezing tolerance. *The Plant Journal*, 49, 786-799.
- XIONG, L. & YANG, Y. 2003. Disease resistance and abiotic stress tolerance in rice are inversely modulated by an abscisic acid-inducible mitogen-activated protein kinase. *The Plant Cell*, 15, 745-759.

- XIONG, T. C., JAUNEAU, A., RANJEVA, R. & MAZARS, C. 2004. Isolated plant nuclei as mechanical and thermal sensors involved in calcium signalling. *The Plant Journal*, 40, 12-21.
- XU, J., LI, Y., WANG, Y., LIU, H., LEI, L., YANG, H., LIU, G. & REN, D. 2008a. Activation of MAPK kinase 9 induces ethylene and camalexin biosynthesis and enhances sensitivity to salt stress in Arabidopsis. *Journal of Biological Chemistry*, 283, 26996-27006.
- XU, L.-M., ZHOU, L., ZENG, Y.-W., WANG, F.-M., ZHANG, H.-L., SHEN, S.-Q. & LI, Z.-C. 2008b. Identification and mapping of quantitative trait loci for cold tolerance at the booting stage in a japonica rice near-isogenic line. *Plant Science*, 174, 340-347.
- XUE, G. P. & LOVERIDGE, C. W. 2004. HvDRF1 is involved in abscisic acid-mediated gene regulation in barley and produces two forms of AP2 transcriptional activators, interacting preferably with a CT-rich element. *The Plant Journal*, 37, 326-339.
- YADAV, S. K. 2011. Cold stress tolerance mechanisms in plants. *Sustainable Agriculture Volume 2*. Springer.
- YAMADA, T., KURODA, K., JITSUYAMA, Y., TAKEZAWA, D., ARAKAWA, K. & FUJIKAWA, S. 2002. Roles of the plasma membrane and the cell wall in the responses of plant cells to freezing. *Planta*, 215, 770-778.
- YAMAGUCHI-SHINOZAKI, K. & SHINOZAKI, K. 1994. A novel cis-acting element in an Arabidopsis gene is involved in responsiveness to drought, low-temperature, or high-salt stress. *The Plant Cell*, 6, 251-264.
- YAMAGUCHI-SHINOZAKI, K. & SHINOZAKI, K. 2006. Transcriptional regulatory networks in cellular responses and tolerance to dehydration and cold stresses. *Annu. Rev. Plant Biol.*, 57, 781-803.
- YAN, L., FU, D., LI, C., BLECHL, A., TRANQUILLI, G., BONAFEDE, M., SANCHEZ, A., VALARIK, M., YASUDA, S. & DUBCOVSKY, J. 2006. The wheat and barley vernalization gene VRN3 is an orthologue of FT. *Proceedings of the National Academy of Sciences*, 103, 19581-19586.
- YAN, L., HELGUERA, M., KATO, K., FUKUYAMA, S., SHERMAN, J. & DUBCOVSKY, J. 2004a. Allelic variation at the VRN1 promoter region in polyploid wheat. *Theoretical and applied genetics*, 109, 1677-1686.
- YAN, L., LOUKOIANOV, A., BLECHL, A., TRANQUILLI, G., RAMAKRISHNA, W., SANMIGUEL, P., BENNETZEN, J. L., ECHENIQUE, V. & DUBCOVSKY, J. 2004b. The wheat VRN2 gene is a flowering repressor down-regulated by vernalization. *Science*, 303, 1640-1644.
- YAN, L., LOUKOIANOV, A., TRANQUILLI, G., HELGUERA, M., FAHIMA, T. & DUBCOVSKY, J. 2003. Positional cloning of the wheat vernalization gene VRN1. *Proceedings of the National Academy of Sciences*, 100, 6263-6268.

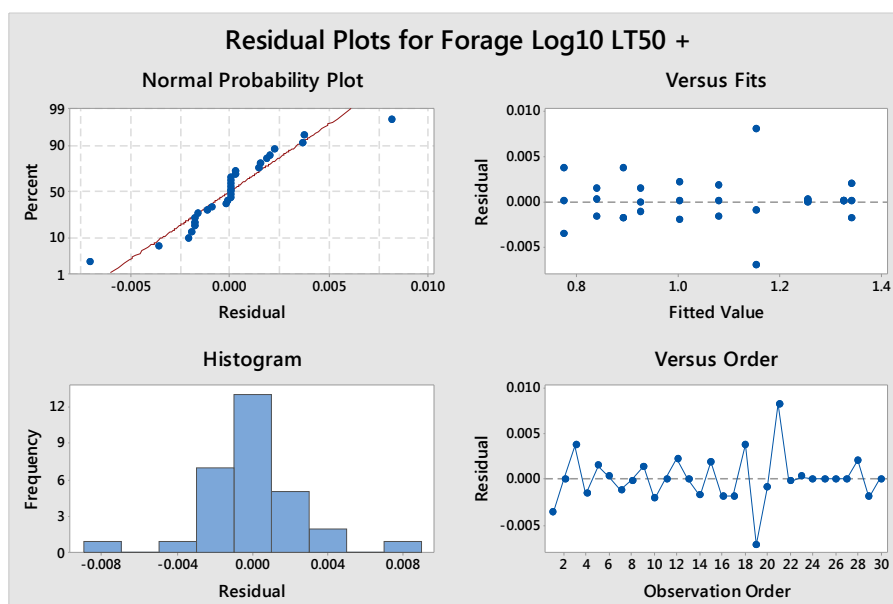
- YANG, C., LI, D., MAO, D., LIU, X., JI, C., LI, X., ZHAO, X., CHENG, Z., CHEN, C. & ZHU, L. 2013. Overexpression of micro RNA 319 impacts leaf morphogenesis and leads to enhanced cold tolerance in rice (*Oryza sativa* L.). *Plant, cell & environment*, 36, 2207-2218.
- YAQOOB, S., BABA, W. N., MASOODI, F., SHAFI, M. & BAZAZ, R. 2018. Effect of sprouting on cake quality from wheat–barley flour blends. *Journal of Food Measurement and Characterization*, 12, 1253-1265.
- YEARBOOK, F. S. 2010. FAO. *Rzym [Tryb dostepuz]* http://www.fao.org/docrep/015/ar n08lrn/a rn08lrn00 htm# Contents_er1 [Data odczytu: maj 2012].
- YIN, X. 2013. Improving ecophysiological simulation models to predict the impact of elevated atmospheric CO₂ concentration on crop productivity. *Annals of botany*, 112, 465-475.
- YOKOI, S., HIGASHI, S.-I., KISHITANI, S., MURATA, N. & TORIYAMA, K. 1998. Introduction of the cDNA for shape Arabidopsis glycerol-3-phosphate acyltransferase (GPAT) confers unsaturation of fatty acids and chilling tolerance of photosynthesis on rice. *Molecular Breeding*, 4, 269-275.
- YOSHIDA, M., ABE, J., MORIYAMA, M. & KUWABARA, T. 1998. Carbohydrate levels among winter wheat cultivars varying in freezing tolerance and snow mold resistance during autumn and winter. *Physiologia Plantarum*, 103, 8-16.
- YOSHIDA, S. & UEMURA, M. 1984. Protein and lipid compositions of isolated plasma membranes from orchard grass (*Dactylis glomerata* L.) and changes during cold acclimation. *Plant Physiology*, 75, 31-37.
- YOSHIDA, T., FUJITA, Y., SAYAMA, H., KIDOKORO, S., MARUYAMA, K., MIZOI, J., SHINOZAKI, K. & YAMAGUCHI-SHINOZAKI, K. 2010a. AREB1, AREB2, and ABF3 are master transcription factors that cooperatively regulate ABRE-dependent ABA signaling involved in drought stress tolerance and require ABA for full activation. *The Plant Journal*, 61, 672-685.
- YOSHIDA, T., MOGAMI, J. & YAMAGUCHI-SHINOZAKI, K. 2014. ABA-dependent and ABA-independent signaling in response to osmotic stress in plants. *Current opinion in plant biology*, 21, 133-139.
- YOSHIDA, T., NISHIDA, H., ZHU, J., NITCHER, R., DISTELFELD, A., AKASHI, Y., KATO, K. & DUBCOVSKY, J. 2010b. Vrn-D4 is a vernalization gene located on the centromeric region of chromosome 5D in hexaploid wheat. *Theoretical and Applied Genetics*, 120, 543-552.
- ZARKA, D. G., VOGEL, J. T., COOK, D. & THOMASHOW, M. F. 2003. Cold induction of Arabidopsis CBF genes involves multiple ICE (inducer of CBF expression) promoter elements and a cold-regulatory circuit that is desensitized by low temperature. *Plant Physiology*, 133, 910-918.
- ZHANG, C. & GUY, C. 2006. In vitro evidence of Hsc70 functioning as a molecular chaperone during cold stress. *Plant Physiology and Biochemistry*, 44, 844-850.

- ZHAO, C., LANG, Z. & ZHU, J.-K. 2015. Cold responsive gene transcription becomes more complex. *Trends in plant science*, 20, 466-468.
- ZHAO, C., WANG, P., SI, T., HSU, C.-C., WANG, L., ZAYED, O., YU, Z., ZHU, Y., DONG, J. & TAO, W. A. 2017. MAP kinase cascades regulate the cold response by modulating ICE1 protein stability. *Developmental cell*, 43, 618-629. e5.
- ZHAO, C., ZHANG, Z., XIE, S., SI, T., LI, Y. & ZHU, J.-K. 2016a. Mutational evidence for the critical role of CBF genes in cold acclimation in Arabidopsis. *Plant physiology*, pp. 00533.2016.
- ZHAO, C., ZHANG, Z., XIE, S., SI, T., LI, Y. & ZHU, J.-K. 2016b. Mutational evidence for the critical role of CBF transcription factors in cold acclimation in Arabidopsis. *Plant physiology*, 171, 2744-2759.
- ZHAO, M.-G., CHEN, L., ZHANG, L.-L. & ZHANG, W.-H. 2009. Nitric reductase-dependent nitric oxide production is involved in cold acclimation and freezing tolerance in Arabidopsis. *Plant physiology*, 151, 755-767.
- ZHEN, Y. & UNGERER, M. C. 2008. Clinal variation in freezing tolerance among natural accessions of Arabidopsis thaliana. *New Phytologist*, 177, 419-427.
- ZHENG, G., LI, L. & LI, W. 2016. Glycerolipidome responses to freezing-and chilling-induced injuries: examples in Arabidopsis and rice. *BMC plant biology*, 16, 70.
- ZHOU, A., LIU, E., LI, H., LI, Y., FENG, S., GONG, S. & WANG, J. 2018. PsCor413pm2, a Plasma Membrane-Localized, Cold-Regulated Protein from Phlox subulata, Confers Low Temperature Tolerance in Arabidopsis. *International journal of molecular sciences*, 19, 2579.
- ZHOU, M., SHEN, C., WU, L., TANG, K. & LIN, J. 2011. CBF-dependent signaling pathway: a key responder to low temperature stress in plants. *Critical reviews in biotechnology*, 31, 186-192.
- ZHU, J.-K. 2016. Abiotic stress signaling and responses in plants. *Cell*, 167, 313-324.
- ZHU, J., DONG, C.-H. & ZHU, J.-K. 2007. Interplay between cold-responsive gene regulation, metabolism and RNA processing during plant cold acclimation. *Current opinion in plant biology*, 10, 290-295.
- ZHU, J., VERSLUES, P. E., ZHENG, X., LEE, B.-H., ZHAN, X., MANABE, Y., SOKOLCHIK, I., ZHU, Y., DONG, C.-H. & ZHU, J.-K. 2005. HOS10 encodes an R2R3-type MYB transcription factor essential for cold acclimation in plants. *Proceedings of the National Academy of Sciences*, 102, 9966-9971.
- ZHU, X., DUNAND, C., SNEDDEN, W. & GALAUD, J.-P. 2015. CaM and CML emergence in the green lineage. *Trends in Plant Science*, 20, 483-489.
- ZHU, X., FENG, Y., LIANG, G., LIU, N. & ZHU, J.-K. 2013. Aequorin-based luminescence imaging reveals stimulus-and tissue-specific Ca²⁺ dynamics in Arabidopsis plants. *Molecular plant*, 6, 444-455.

- ZOHARY, D. & HOPF, M. 1993. Date palm, *Phoenix dactylifera*. *Domestication of plants in the Old World*, 157-162.
- ZOHARY, D. & HOPF, M. 2000. *Domestication of plants in the Old World: The origin and spread of cultivated plants in West Asia, Europe and the Nile Valley*, Oxford University Press.
- ZOHARY, D., HOPF, M. & WEISS, E. 2012. *Domestication of Plants in the Old World: The origin and spread of domesticated plants in Southwest Asia, Europe, and the Mediterranean Basin*, Oxford University Press on Demand.
- ZUTHER, E., BÜCHEL, K., HUNDERTMARK, M., STITT, M., HINCHA, D. K. & HEYER, A. G. 2004. The role of raffinose in the cold acclimation response of *Arabidopsis thaliana*. *Febs Letters*, 576, 169-173.

Appendices

Appendix A3.1 General Linear Model: Forage Log10 LT₅₀ + versus Photoperiod & Acclimation Time To Low Temperatures



Method

Factor coding (-1, 0, +1)

Factor Information

Factor	Type	Levels	Values
Acclimation Photoperiod	Fixed	2	8, 15
Acclimation Time	Fixed	5	0, 7, 14, 21, 28

Analysis of Variance

Source	DF	Adj SS	Adj MS	F-Value	P-Value
Acclimation Time	4	0.53913	0.134783	13679.59	0.000
Acclimation Photoperiod	1	0.54176	0.541761	54985.33	0.000
Acclimation Photoperiod*Acclimation Time	4	0.04774	0.011935	1211.35	0.000
Error	20	0.00020	0.000010		
Total	29	1.12883			

Model Summary

S	R-sq	R-sq(adj)	R-sq(pred)
0.0031389	99.98%	99.97%	99.96%

Coefficients

Term	Coef	SE Coef	T-Value	P-Value	VIF
Constant	1.05896	0.00057	1847.82	0.000	
Acclimation Time					
0	-0.22613	0.00115	-197.29	0.000	1.60
7	-0.06207	0.00115	-54.15	0.000	1.60
14	0.03205	0.00115	27.97	0.000	1.60
21	0.10529	0.00115	91.86	0.000	1.60
Acclimation Photoperiod					
8	-0.134383	0.000573	-234.49	0.000	1.00
Acclimation Photoperiod*Acclimation Time					
8 0	0.07606	0.00115	66.36	0.000	1.60
8 7	-0.02199	0.00115	-19.18	0.000	1.60
8 14	-0.03012	0.00115	-26.28	0.000	1.60
8 21	-0.02770	0.00115	-24.17	0.000	1.60

Fits and Diagnostics for Unusual Observations

Forage					
Log10					
Obs	LT ₅₀ +	Fit	Resid	Std Resid	
19	1.14613	1.15326	-0.00713	-2.78	R
21	1.16137	1.15326	0.00811	3.16	R

R Large residual

Residual Plots for Forage Log10 LT₅₀ +

Comparisons for Forage Log10 LT₅₀ +

Tukey Pairwise Comparisons: Acclimation Photoperiod*Acclimation Time

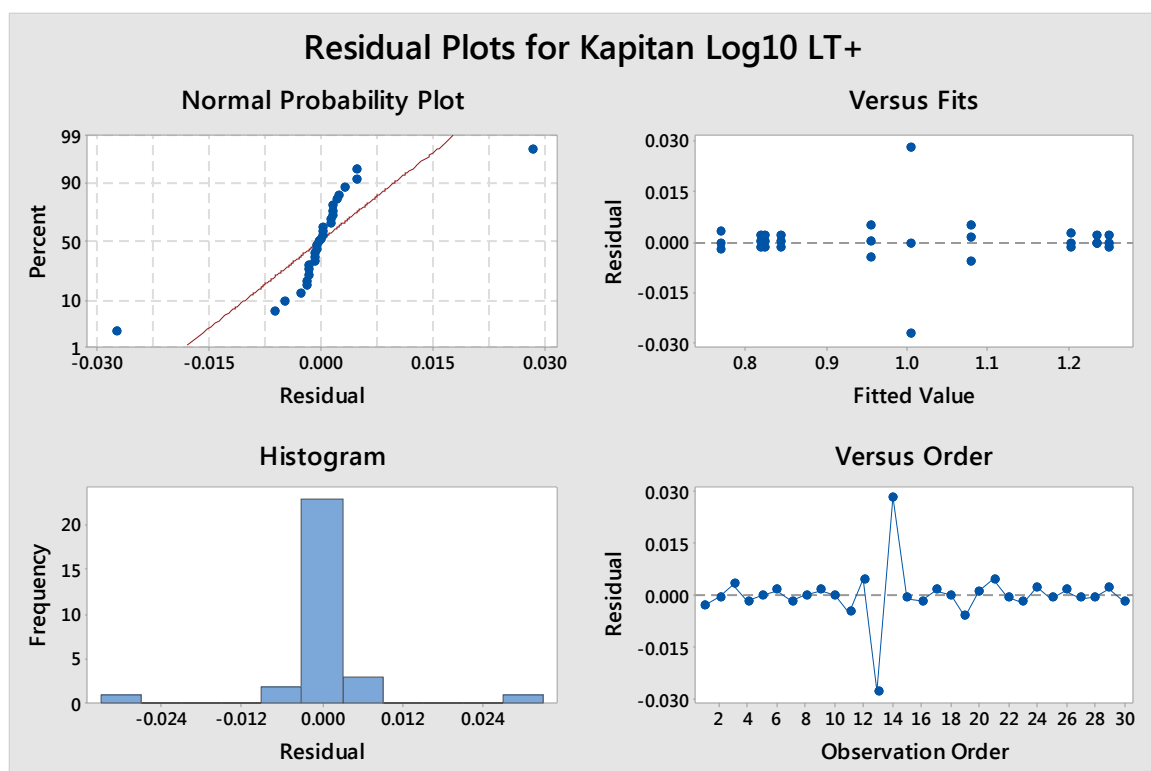
Grouping Information Using the Tukey Method and 95% Confidence

Acclimation			
Photoperiod*Acclimation			
Time	N	Mean	Grouping
15 28	3	1.34044	A
15 21	3	1.32634	B
15 14	3	1.25551	C
15 7	3	1.15326	D
8 28	3	1.07918	E
8 21	3	1.00216	F
8 14	3	0.92651	G
15 0	3	0.89116	H
8 7	3	0.84052	I
8 0	3	0.77451	J

Means that do not share a letter are significantly different.

Appendix A3.2

General Linear Model: Kapitan Log10 LT+ versus Photoperiod & Acclimation Time To Low Temperatures



Method

Factor coding (-1, 0, +1)

Factor Information

Factor	Type	Levels	Values
Acclimation Photoperiod	Fixed	2	8, 15
Acclimation Time	Fixed	5	0, 7, 14, 21, 28

Analysis of Variance

Source	DF	Adj SS	Adj MS	F-Value	P-Value
Acclimation Time	4	0.428107	0.107027	1248.71	0.000
Acclimation Photoperiod	1	0.426060	0.426060	4970.95	0.000
Acclimation Photoperiod*Acclimation Time	4	0.077948	0.019487	227.36	0.000
Error	20	0.001714	0.000086		
Total	29	0.933829			

Model Summary

S	R-sq	R-sq(adj)	R-sq(pred)
0.0092580	99.82%	99.73%	99.59%

Coefficients

Term	Coef	SE Coef	T-Value	P-Value	VIF
Constant	0.99783	0.00169	590.34	0.000	
Acclimation Time					
0	-0.20500	0.00338	-60.64	0.000	1.60
7	-0.04755	0.00338	-14.07	0.000	1.60
14	0.02492	0.00338	7.37	0.000	1.60
21	0.09747	0.00338	28.83	0.000	1.60
Acclimation Photoperiod					
8	-0.11917	0.00169	-70.50	0.000	1.00
Acclimation Photoperiod*Acclimation Time					
8 0	0.09399	0.00338	27.80	0.000	1.60
8 7	-0.00850	0.00338	-2.51	0.021	1.60
8 14	-0.05993	0.00338	-17.73	0.000	1.60
8 21	-0.02190	0.00338	-6.48	0.000	1.60

Fits and Diagnostics for Unusual Observations

Kapitan					
Obs	Log10 LT+	Fit	Resid	Std Resid	
13	0.97772	1.00516	-0.02743	-3.63	R
14	1.03342	1.00516	0.02827	3.74	R

R Large residual

Residual Plots for Kapitan Log10 LT+

Comparisons for Kapitan Log10 LT+

Tukey Pairwise Comparisons: Acclimation Photoperiod*Acclimation Time

Grouping Information Using the Tukey Method and 95% Confidence

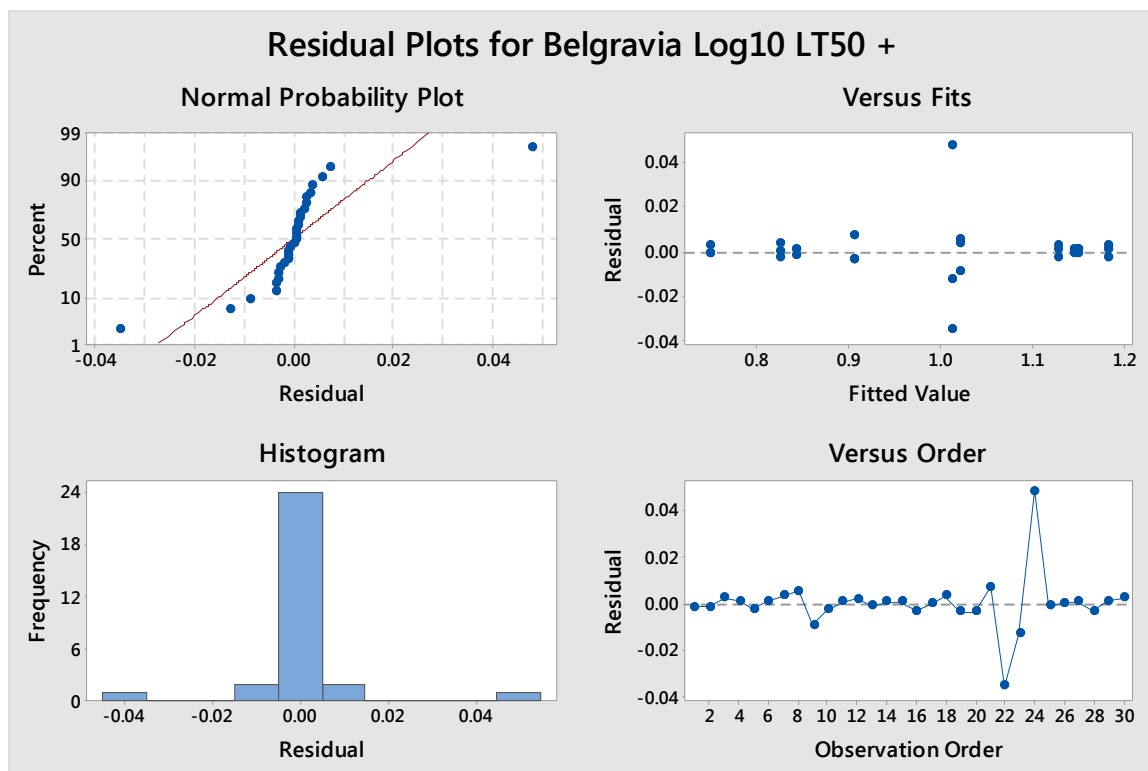
Acclimation

Photoperiod*Acclimation

Time	N	Mean	Grouping
15 28	3	1.25082	A
15 21	3	1.23637	A
15 14	3	1.20185	B
15 7	3	1.07795	C
8 28	3	1.00516	D
8 21	3	0.95422	E
8 14	3	0.84365	F
8 7	3	0.82260	F
15 0	3	0.81800	F
8 0	3	0.76764	G

Means that do not share a letter are significantly different.

Appendix A3.3 General Linear Model: Belgravia Log10 LT₅₀ + versus Photoperiod & Acclimation Time To Low Temperatures



Method

Factor coding (-1, 0, +1)

Factor Information

Factor	Type	Levels	Values
Acclimation Photoperiod	Fixed	2	8, 15
Acclimation Time	Fixed	5	0, 7, 14, 21, 28

Analysis of Variance

Source	DF	Adj SS	Adj MS	F-Value	P-Value
Acclimation Time	4	0.646975	0.161744	817.06	0.000
Acclimation Photoperiod	1	0.010525	0.010525	53.17	0.000
Acclimation Photoperiod*Acclimation Time	4	0.006916	0.001729	8.73	0.000
Error	20	0.003959	0.000198		
Total	29	0.668375			

Model Summary

S	R-sq	R-sq(adj)	R-sq(pred)
0.0140697	99.41%	99.14%	98.67%

Coefficients

Term	Coef	SE Coef	T-Value	P-Value	VIF
Constant	0.99719	0.00257	388.20	0.000	
Acclimation Time					
0	-0.20942	0.00514	-40.76	0.000	1.60
7	-0.12183	0.00514	-23.71	0.000	1.60
14	0.02012	0.00514	3.92	0.001	1.60
21	0.14288	0.00514	27.81	0.000	1.60
Acclimation Photoperiod					
8	-0.01873	0.00257	-7.29	0.000	1.00
Acclimation Photoperiod*Acclimation Time					
8 0	-0.01957	0.00514	-3.81	0.001	1.60
8 7	-0.01257	0.00514	-2.45	0.024	1.60
8 14	0.02324	0.00514	4.52	0.000	1.60
8 21	0.00845	0.00514	1.65	0.116	1.60

Fits and Diagnostics for Unusual Observations

Belgravia					
Log10					
Obs	LT ₅₀ +	Fit	Resid	Std Resid	
22	0.97772	1.01281	-0.03508	-3.05	R
24	1.06070	1.01281	0.04789	4.17	R

R Large residual

Residual Plots for Belgravia Log10 LT₅₀ +

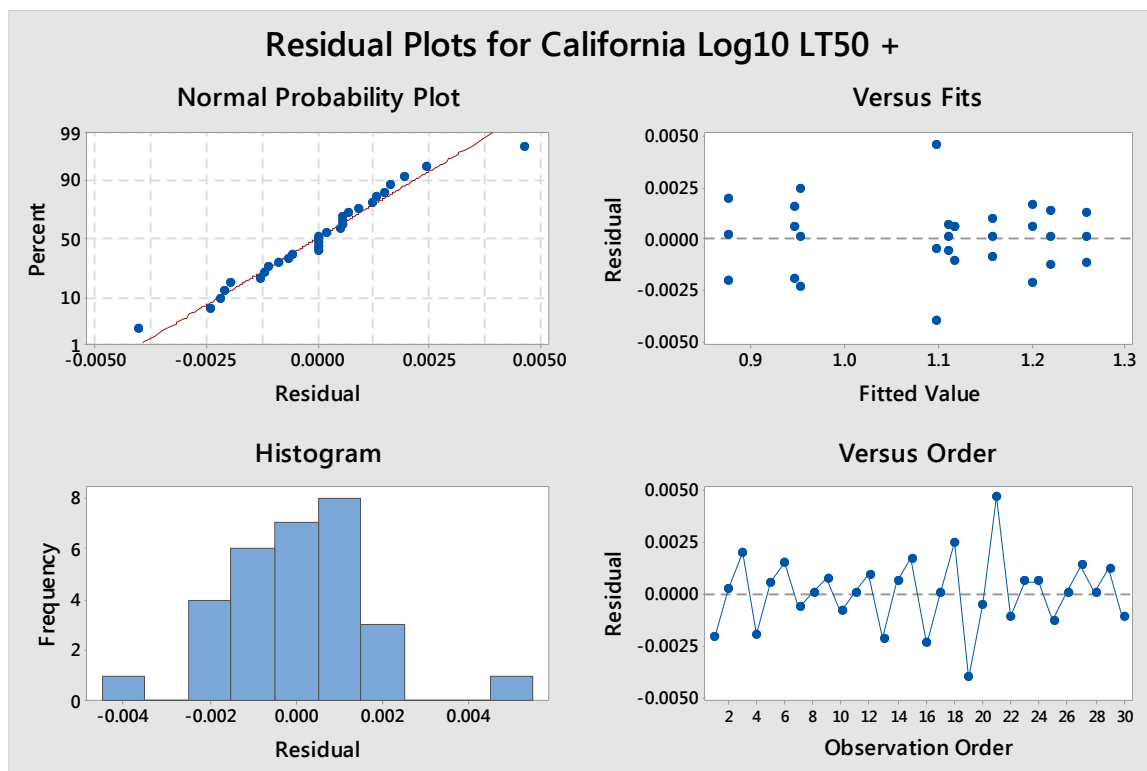
Comparisons for Belgravia Log10 LT₅₀ +

Tukey Pairwise Comparisons: Acclimation Photoperiod*Acclimation Time

Grouping Information Using the Tukey Method and 95% Confidence

Acclimation		Photoperiod*Acclimation		Grouping	
Time	N	Mean			
15 28	3	1.18374	A		
15 21	3	1.15035	A	B	
8 28	3	1.14716	A	B	
8 21	3	1.12979		B	
8 14	3	1.02183			C
15 14	3	1.01281			C
15 7	3	0.90666			D
8 7	3	0.84406			E
15 0	3	0.82607			E
8 0	3	0.74947			F

Appendix A3.4 General Linear Model: California Log10 LT₅₀ + versus Photoperiod & Acclimation Time To Low Temperatures



Method

Factorcoding (-1, 0 +1)

Factor Information

Factor	Type	Levels	Values
Acclimation Photoperiod	Fixed	2	8h, 15h
Acclimation Time	Fixed	5	0, 7, 14, 21, 28

Analysis of Variance

Source	DF	Adj SS	Adj MS	F-Value	P-Value
Acclimation Time	4	0.395148	0.098787	23803.30	0.000
Acclimation Photoperiod	1	0.038385	0.038385	9249.20	0.000
Acclimation Photoperiod*Acclimation Time	4	0.016968	0.004242	1022.13	0.000
Error	20	0.000083	0.000004		
Total	29	0.450584			

Model Summary

S	R-sq	R-sq(adj)	R-sq(pred)
0.0020372	99.98%	99.97%	99.96%

Coefficients

Term	Coef	SE Coef	T-Value	P-Value	VIF
Constant	1.09297	0.00037	2938.57	0.000	
Acclimation Time					
0	-0.180205	0.000744	-242.25	0.000	1.60
7	-0.072236	0.000744	-97.11	0.000	1.60
14	0.020687	0.000744	27.81	0.000	1.60
21	0.094858	0.000744	127.52	0.000	1.60
Acclimation Photoperiod					
9	-0.035770	0.000372	-96.17	0.000	1.00
Acclimation Photoperiod*Acclimation Time					
8 0	-0.003287	0.000744	-4.42	0.000	1.60
8 7	-0.040974	0.000744	-55.08	0.000	1.60
8 14	0.032706	0.000744	43.97	0.000	1.60
8 21	0.004798	0.000744	6.45	0.000	1.60

Fits and Diagnostics for Unusual Observations

California					
Obs	Log10 LT50 +	Fit	Resid	Std Resid	
19	1.09342	1.09747	-0.00405	-2.44	R
21	1.10209	1.09747	0.00462	2.78	R

R Large residual

Residual Plots for California Log10 LT₅₀ +

Tukey Pairwise Comparisons: Acclimation Photoperiod*Acclimation Time

Grouping Information Using the Tukey Method and 95% Confidence

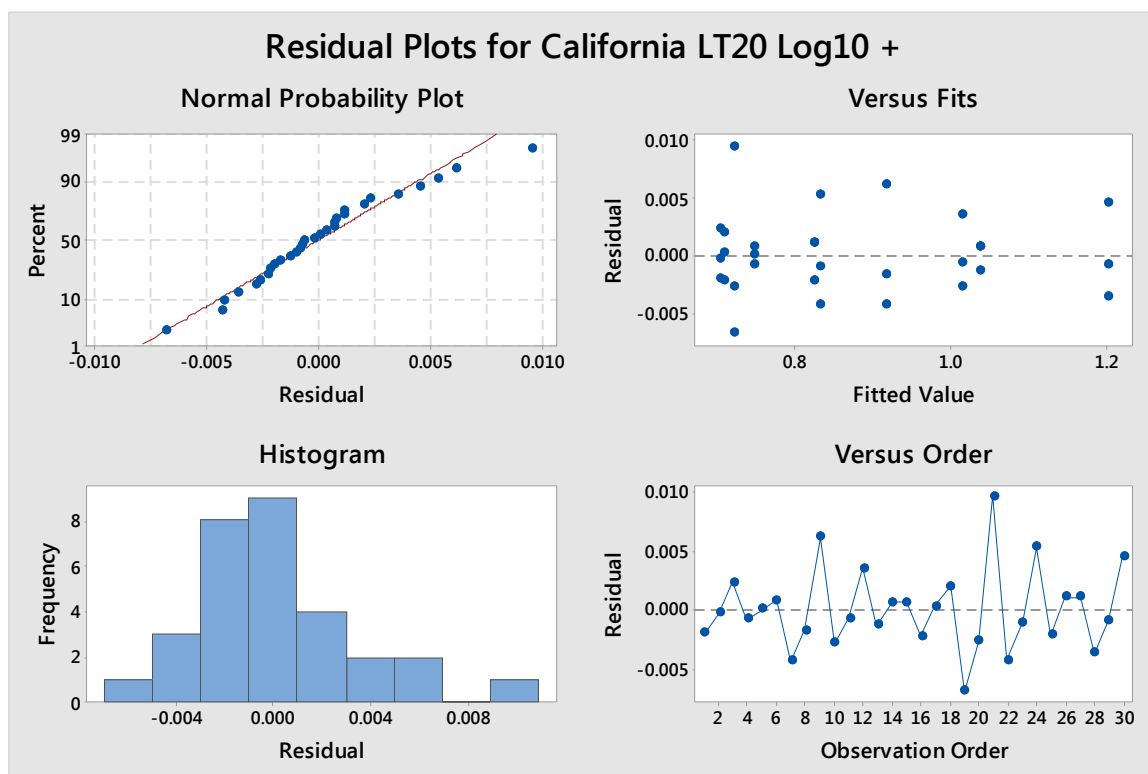
Acclimation

Photoperiod*Acclimation

Time	N	Mean	Grouping
15 28	3	1.25888	A
15 21	3	1.21880	B
8 28	3	1.20085	C
8 21	3	1.15685	D
15 14	3	1.11672	E
8 14	3	1.11059	F
15 7	3	1.09747	G
15 0	3	0.95182	H
8 7	3	0.94399	I
8 0	3	0.87370	J

Means that do not share a letter are significantly different.

Appendix A3.5 General Linear Model: California LT₂₀ Log10 + versus Photoperiod & Acclimation Time To Low Temperatures



Method

Factor coding (-1, 0, +1)

Factor Information

Factor	Type	Levels	Values
Acclimation Photoperiod	Fixed	2	8, 15
Acclimation Time	Fixed	5	0, 7, 14, 21, 28

Analysis of Variance

Source	DF	Adj SS	Adj MS	F-Value	P-Value
Acclimation Time	4	0.659523	0.164881	9816.14	0.000
Acclimation Photoperiod	1	0.005201	0.005201	309.62	0.000
Acclimation Photoperiod*Acclimation Time	4	0.101184	0.025296	1505.99	0.000
Error	20	0.000336	0.000017		
Total	29	0.766243			

Model Summary

S	R-sq	R-sq(adj)	R-sq(pred)
0.0040984	99.96%	99.94%	99.90%

Coefficients

Term	Coef	SE Coef	T-Value	P-Value	VIF
Constant	0.871871	0.000748	1165.19	0.000	
Acclimation Time					
0	-0.16474	0.00150	-110.08	0.000	1.60
7	-0.13635	0.00150	-91.11	0.000	1.60
14	0.00400	0.00150	2.67	0.015	1.60
21	0.04844	0.00150	32.37	0.000	1.60
Acclimation Photoperiod					
8	0.013166	0.000748	17.60	0.000	1.00
Acclimation Photoperiod*Acclimation Time					
8 0	-0.01587	0.00150	-10.60	0.000	1.60
8 7	-0.00050	0.00150	-0.33	0.742	1.60
8 14	0.02915	0.00150	19.48	0.000	1.60
8 21	0.08215	0.00150	54.90	0.000	1.60

Fits and Diagnostics for Unusual Observations

California					
Obs	LT20 Log10 +	Fit	Resid	Std Resid	
19	0.71600	0.72285	-0.00685	-2.05	R
21	0.73239	0.72285	0.00954	2.85	R

R Large residual

Residual Plots for California LT₂₀ Log10 +

Comparisons for California LT₂₀ Log₁₀ +

Tukey Pairwise Comparisons: Acclimation Photoperiod*Acclimation Time

Grouping Information Using the Tukey Method and 95% Confidence

Acclimation

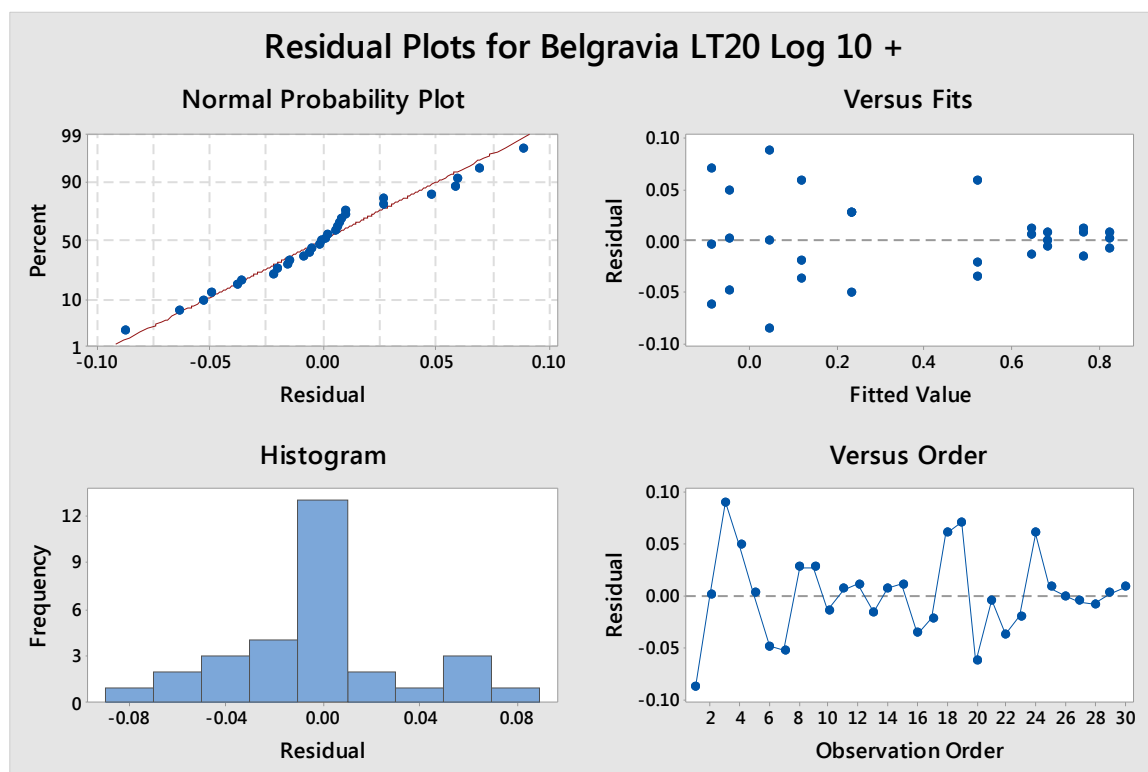
Photoperiod*Acclimation

Time	N	Mean	Grouping
15 28	3	1.20229	A
8 28	3	1.03875	B
9 21	3	1.01563	C
8 14	3	0.91818	D
15 14	3	0.83355	E
15 21	3	0.82499	E
8 7	3	0.74819	F
15 7	3	0.72285	G
15 0	3	0.70983	H
8 0	3	0.70443	H

Means that do not share a letter are significantly different.

Appendix A3.6 General Linear Model: Belgravia LT₂₀ Log 10 + versus Photoperiod & Acclimation Time To Low Temperatures

Method



Factor coding (-1, 0, +1)

Factor Information

Factor	Type	Levels	Values
Acclimation Photoperiod	Fixed	2	8, 15
Acclimation Time	Fixed	5	0, 7, 14, 21, 28

Analysis of Variance

Source	DF	Adj SS	Adj MS	F-Value	P-Value
Acclimation Time	4	3.03585	0.758962	338.45	0.000
Acclimation Photoperiod	1	0.05376	0.053762	23.97	0.000
Acclimation Photoperiod*Acclimation Time	4	0.31945	0.079862	35.61	0.000
Error	20	0.04485	0.002242		
Total	29	3.45391			

Model Summary

S	R-sq	R-sq(adj)	R-sq(pred)
0.0473549	98.70%	98.12%	97.08%

Coefficients

Term	Coef	SE Coef	T-Value	P-Value	VIF
Constant	0.36856	0.00865	42.63	0.000	
Acclimation Time					
0	-0.0872	0.0173	-5.04	0.000	1.60
7	-0.4380	0.0173	-25.33	0.000	1.60
14	-0.1954	0.0173	-11.30	0.000	1.60
21	0.2945	0.0173	17.03	0.000	1.60
Acclimation Photoperiod					
9	-0.04233	0.00865	-4.90	0.000	1.00
Acclimation Photoperiod*Acclimation Time					
8 0	-0.1971	0.0173	-11.40	0.000	1.60
8 7	0.0642	0.0173	3.71	0.001	1.60
8 14	0.0981	0.0173	5.67	0.000	1.60
8 21	0.0226	0.0173	1.31	0.205	1.60

Fits and Diagnostics for Unusual Observations

Belgravia					
LT ₂₀ Log					
Obs	10 +	Fit	Resid	Std Resid	
1	-0.0458	0.0420	-0.0877	-2.27	R
3	0.1303	0.0420	0.0883	2.28	R

R Large residual

Residual Plots for Belgravia LT₂₀ Log 10 +

Comparisons for Belgravia LT₂₀ Log 10 +

Tukey Pairwise Comparisons: Acclimation Photoperiod*Acclimation Time

Grouping Information Using the Tukey Method and 95% Confidence

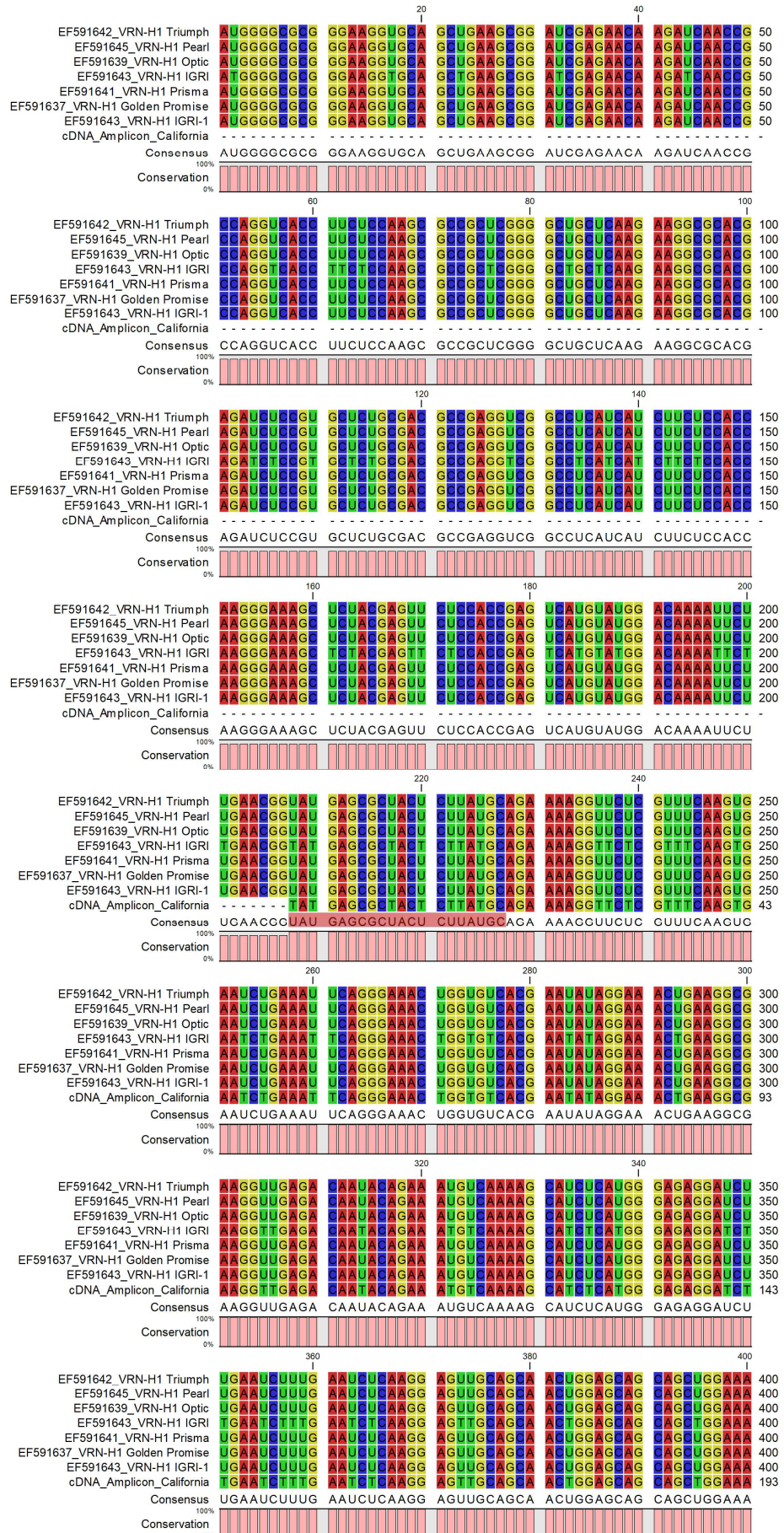
Acclimation

Photoperiod*Acclimation

Time	N	Mean	Grouping
15 28	3	0.824942	A
8 28	3	0.764519	A B
15 21	3	0.682710	B
8 21	3	0.643320	B C
15 0	3	0.520798	C
8 14	3	0.228879	D
15 14	3	0.117394	D E
8 0	3	0.041990	E F
8 7	3	-0.047556	F
15 7	3	-0.091363	F

Means that do not share a letter are significantly different.

Appendix A4.1.



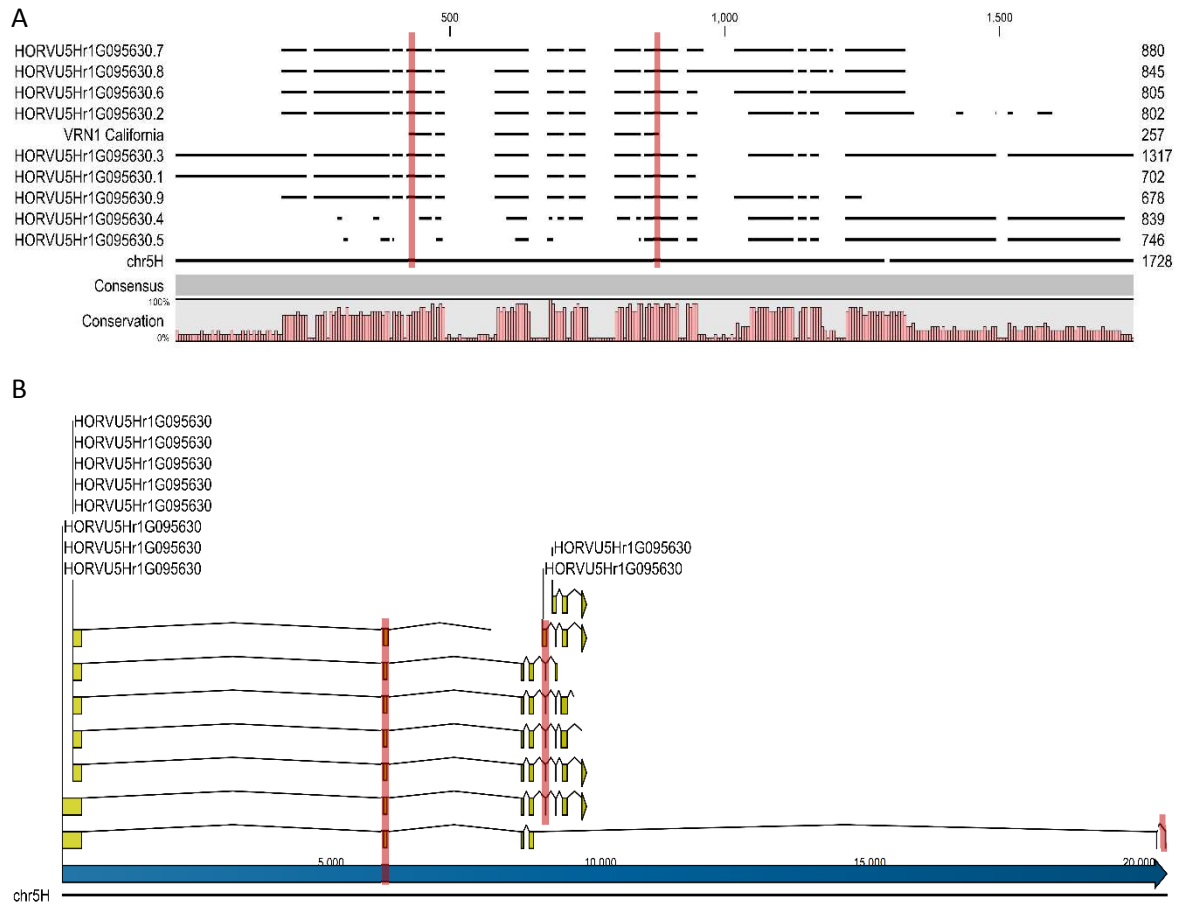


Figure A4.1B. CLUSTALW Alignments of *HvVRN1* cDNA Sequences from cvs California and Morex.

An amplicon of approximately 1,400bp was amplified using the *HvVRN1* primers and California or Belgravia (not shown) gDNA template. The California gDNA amplicon was cloned and sequenced and used as the BLAST query sequence to interrogate the Morex full genome database (IBSC v2, 2017). **Panel A**, the BLAST results showed 100% homology over the full amplicon sequence with HORVU5Hr1G095630 (consistent with the location of *HvVRN1* on the long arm of chromosome 5, **Section 1.14**). Alignments of the predicted 9 Morex splice variants and the sequenced California cDNA to Morex chromosome 5 (chr5) showed 100% identity. Vertical red bars indicate the position of the forward and reverse PCR primers binding sites. **Panel B**, from alignments of the homologous Morex transcript variants with the corresponding region of Morex chromosome 5 it is estimated the *HvVRN1* primers should generate an amplicon of 3,012bp or greater when gDNA is used as template. However, gDNA from both cvs California and Belgravia generated a fragment of between 1,000 and 1,500 bp; sequencing of the California amplicon confirmed the primers generated a 1,374 bp product encoded in the *HvVRN1* gene (HORVU5Hr1G095630). suggesting varietal differences in the size of the intron between exon 2 and exon 5. Left side variant labels, from top: .7; .8; .6; .9; .2; .3; .1. Right side variant labels, from top: .5; .4.

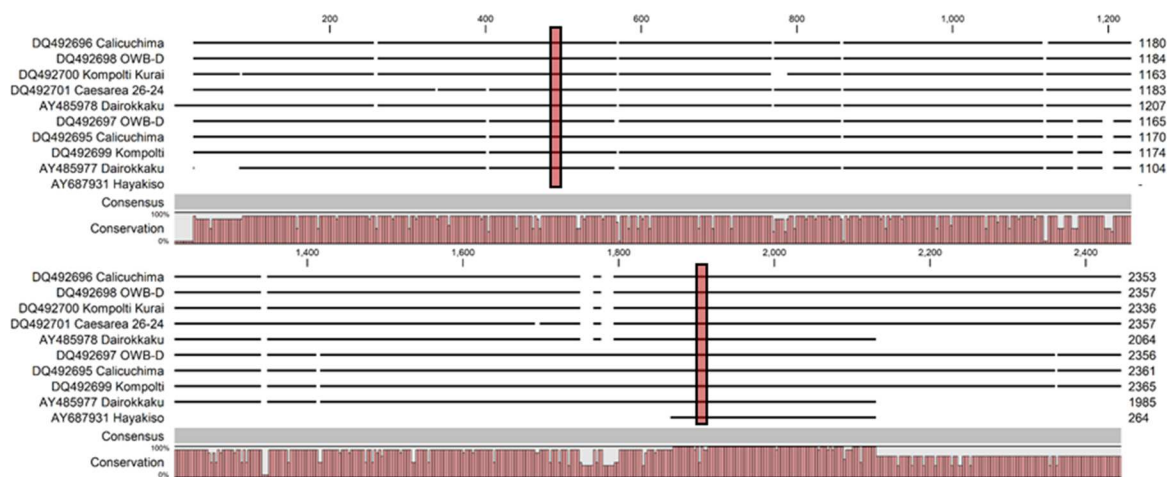


Figure A4.2. CLUSTALW Alignments of *HvVRN2* DNA Sequences from Ten Barley Cultivars.

At the time the work was done (2017) only 3 *VRN2* sequences were deposited in GenBank; see **Fig 4.2**, 2 full length for cv Dairokkaku and a partial sequence for cv Hayakiso). It proved difficult to design PCR primers for the original 3 accessions due to the short length of the partial Hayakiso sequence. Hence, primers were designed to 2 Dairokkaku sequences only. At the time of thesis corrections (2020) there were a further 7 GeneBank accessions for *HvVRN2*; these are included in the CLC Workbench CLUSTALW alignments above. The position of the original Dairokkaku Forward and Reverse primers that anneal to exon 1 and 2, respectively (see **Fig 4.2**) and their position is indicated by vertical red bars (462-479 and 1878-1897, respectively, relative to cv Kompolti Kurai sequence). The primers proved to have 100% sequence homology to 9 of the cultivars, the exception being the partial Hayakiso sequence (there were also two mismatch bases in the Hayakiso Reverse primer region).

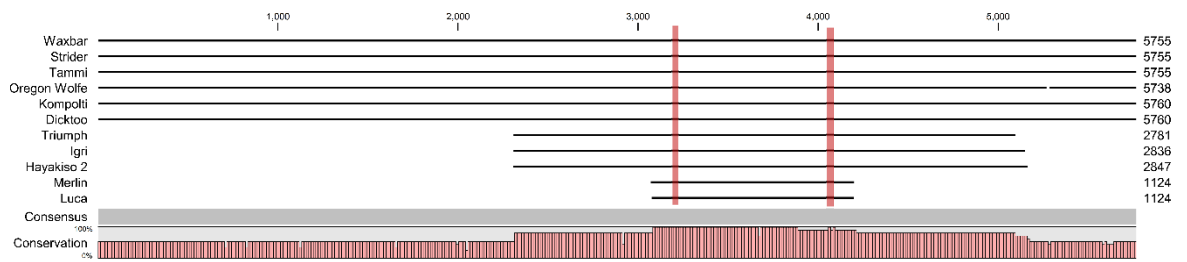


Figure A4.3. CLUSTALW Alignments of *HvVRN3* DNA Sequences from Eleven Barley Cultivars.

Eleven homologues of *HvVRN3* were deposited in the GenBank database and complete conservation were found in exon 1 and exon 3 that were suitable for designing ‘universal’ PCR primers (VRN3TRI V2gcFo – Forward, and VRN3 TRI V2gcRe – Reverse) which are highlighted in pink in the Consensus sequence line. In the region of the forward primer (3153-3169) the sequences were 100% identical whereas in the region of the reverse primer (4096-4112) ten of the sequences were identical although cv. Luca showed some non-conserved variation.

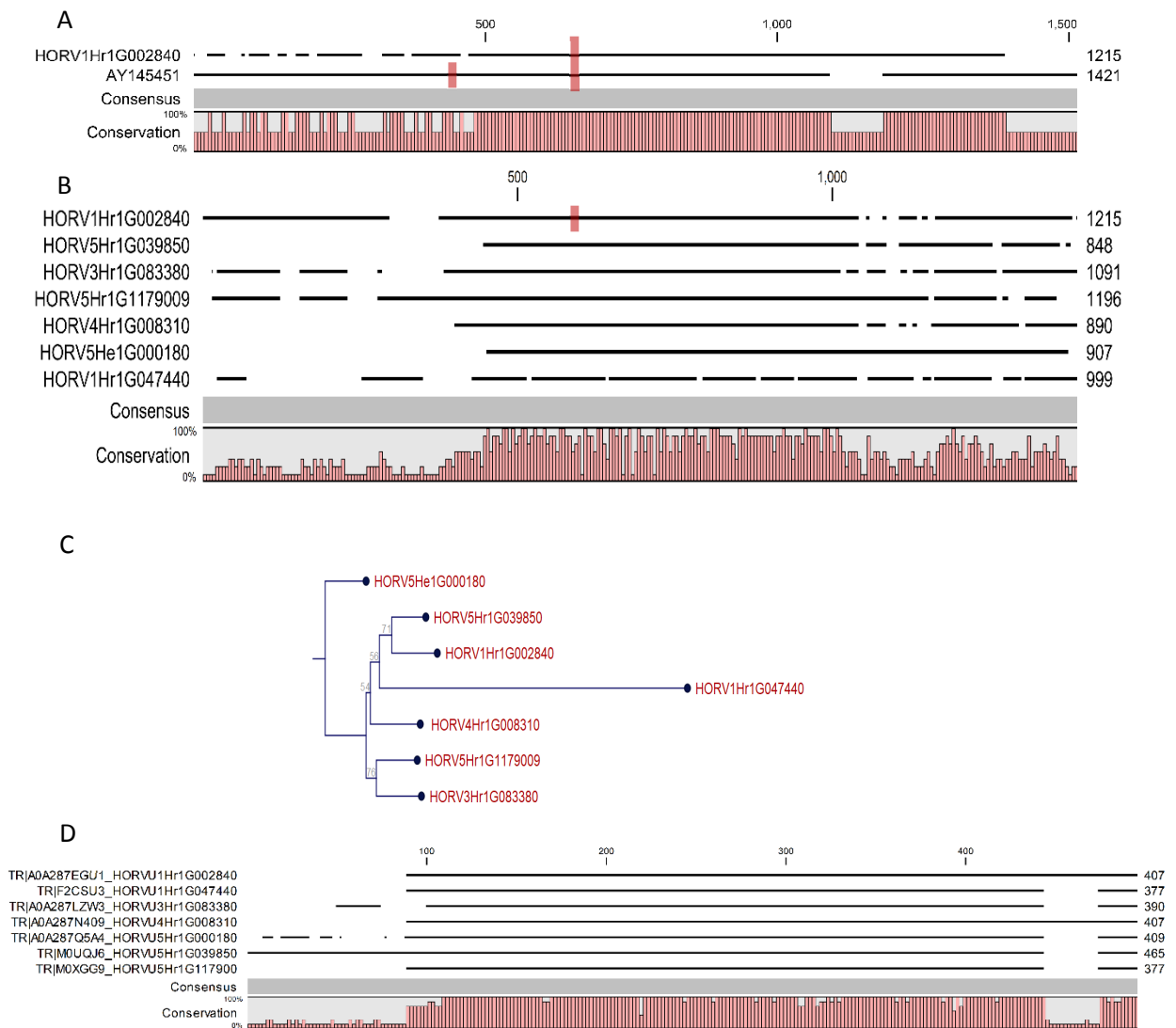


Figure A4.4. CLUSTALW Alignments of *HvActin* DNA Sequences from Barley Cultivars.

Only 1 homologue of *HvActin* (AY145451) was deposited in the GenBank database (2017); the cultivar was not specified in the GenBank annotation. BLAST searches of the full Morex genome databases (IBSC v2) with AY145451 as the query sequence identified 7 genes with > 83% identity over more than 300 bases. **Panel A**, CLUSTALW DNA alignment of AY145451 and HORVU1Hr1G002840 (the most similar Morex sequence); there is 100% sequence identity between 400 and 1,100bp that could be used for PCR primer pair design (primer positions are shown by vertical red bars). **Panel B**, CLUSTALW DNA alignment of the 7 Morex Actin sequences; although there is some consensus there is insufficient sequence consensus to design ‘universal’ Actin primers; the forward primer does not anneal to any of the Morex homologues and the reverse primer binds only to HORVU1Hr1G002840. **Panel C**, cladogram of the 7 Morex actin sequences. **Panel D**, CLUSTAL protein alignments of the 7 Morex actin sequences. It appears that many of SNPs shown in B at the DNA level are silent; closer analysis of the protein polymorphisms indicates many are conservative or semi-conservative substitutions in the region of ~90 – 440 aa.

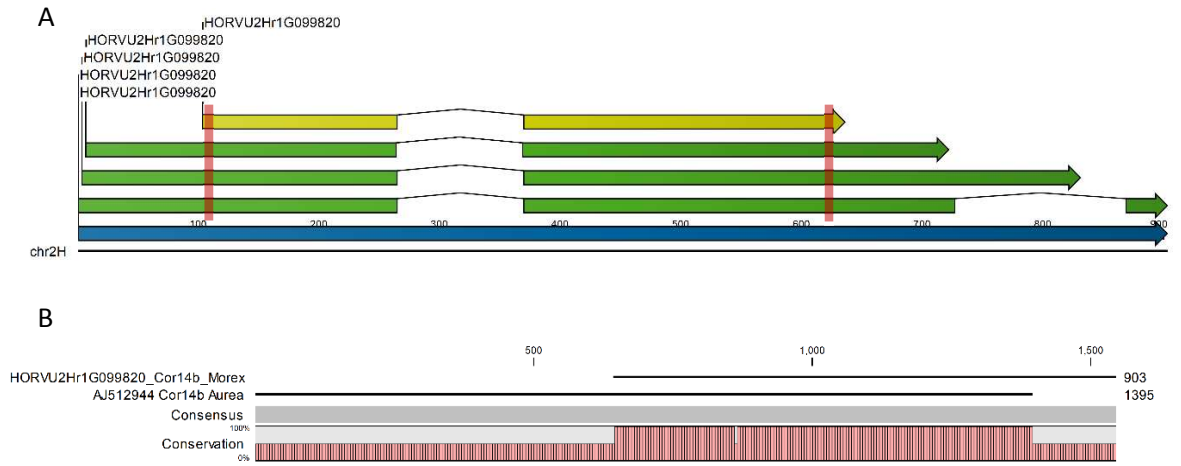


Figure A4.5 Gene Structure and CLUSTALW DNA Alignments of *HvCOR14b* Genes from Barley.

The GenBank accessions AJ512944 was the only sequence annotated as ‘COR14b’ in the database. BLAST interrogation of the *cv* Morex genome database with *cv* Aurea sequence AJ512944 identified HORVU2Hr1G099820 as the most likely homologue (E-val 0.0). **Panel A**, Morex *COR14b* gene structure. Four variants are indicated on the full Morex genome database containing one or two introns. The positions of the primer binding sites designed from the Aurea AJ512944 sequence are shown as vertical red bars. **Panel B**, CLUSTALW alignment of the Morex and Aurea *COR14b* genes. There were only two SNPs in the overlapping 753bp sequence which generated an E-score of 0.0. (see **Section 4.3.2** for further details).

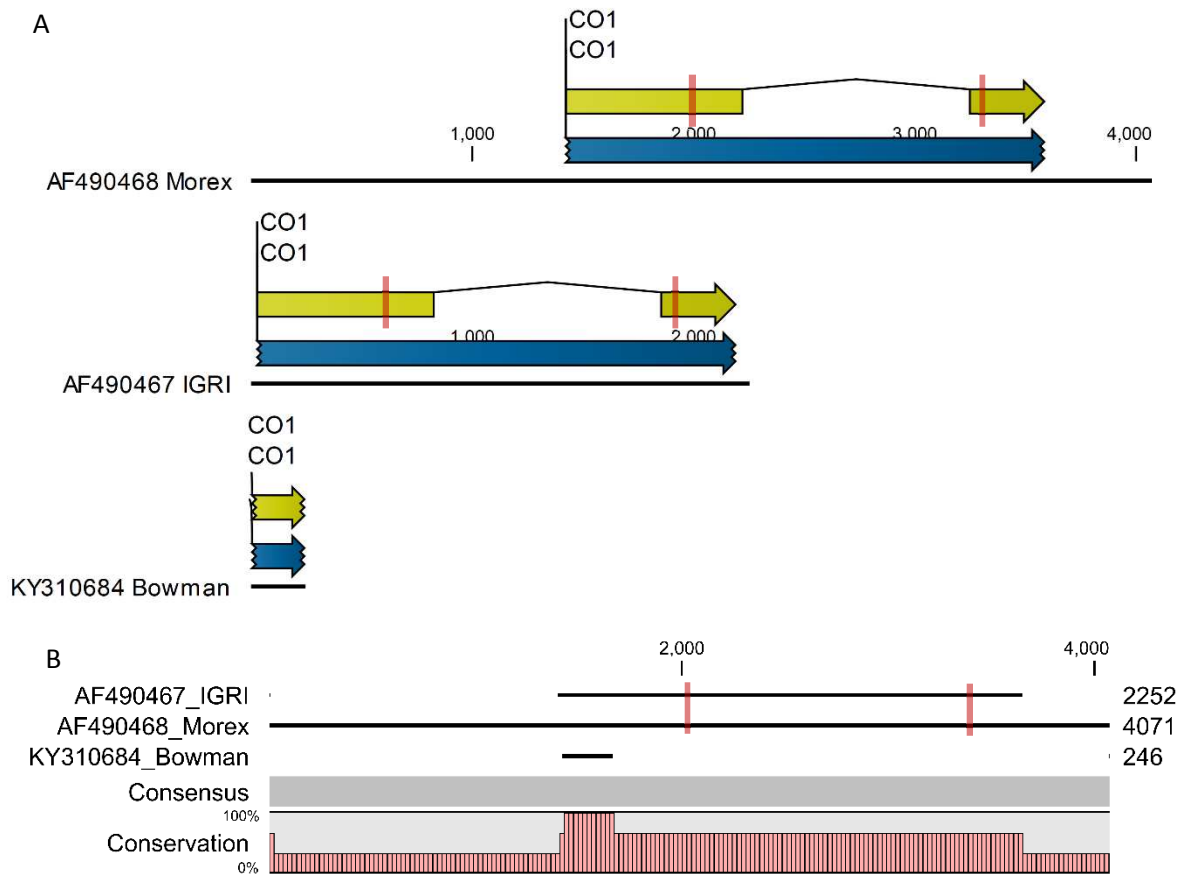


Figure A4.6 Gene Structure and DNA Alignments of Three *HvCO1* (CONSTANS1) Sequences.

The GenBank accessions AF490467 (*cv* IGRI), AF490468 (*cv* Morex), and KY310684 (*cv* Bowman) are presented. **Panel A**, The IGRI and Morex sequences are full length, the Bowman sequence is a ‘partial’. The full coding sequence is shown in green; the yellow bars indicate the exons. The positions of the forward and reverse primer sites are shown as vertical red bars (see **Section 4.3.2** for further details). **Panel B**, CLUSTALW alignment of the 3 Genebank accessions

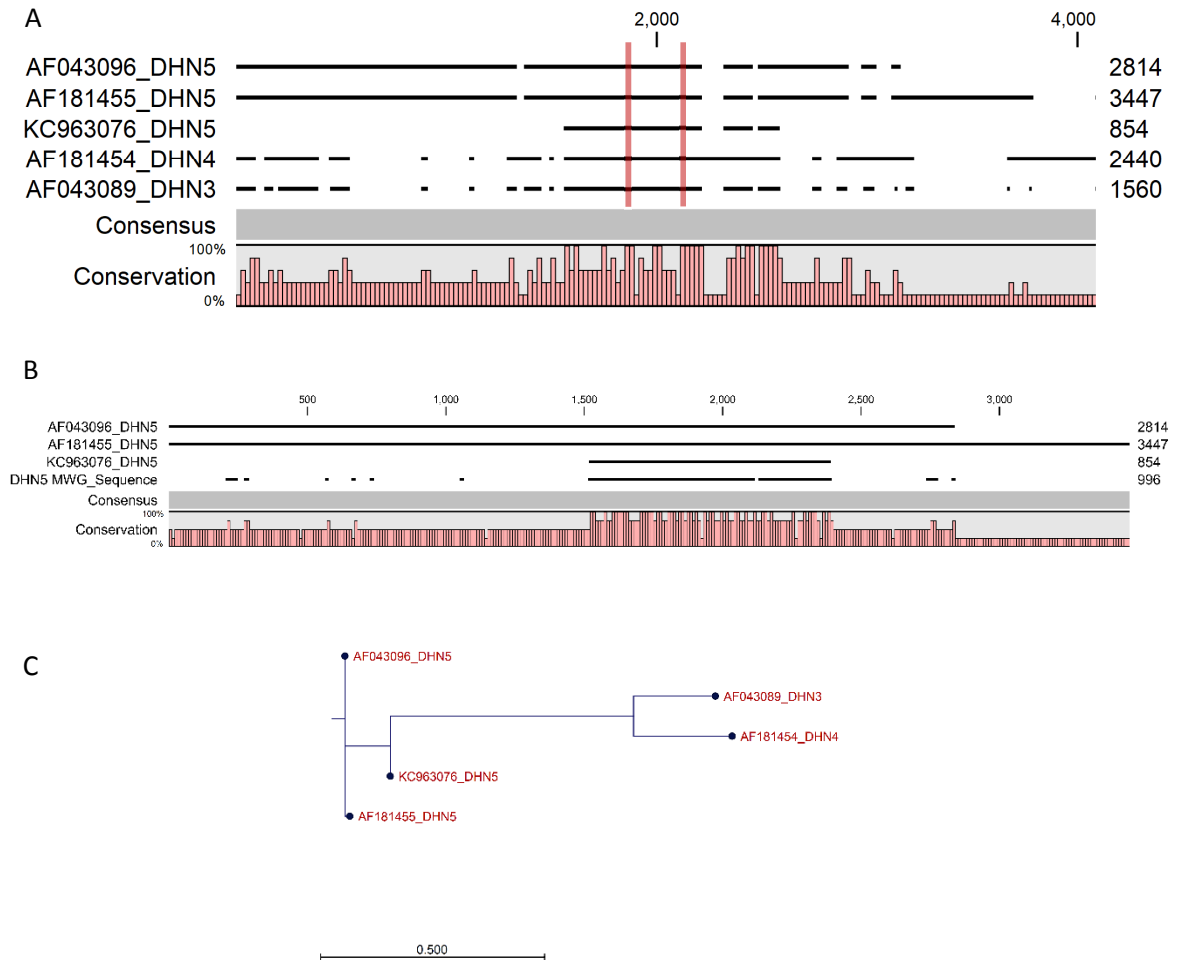
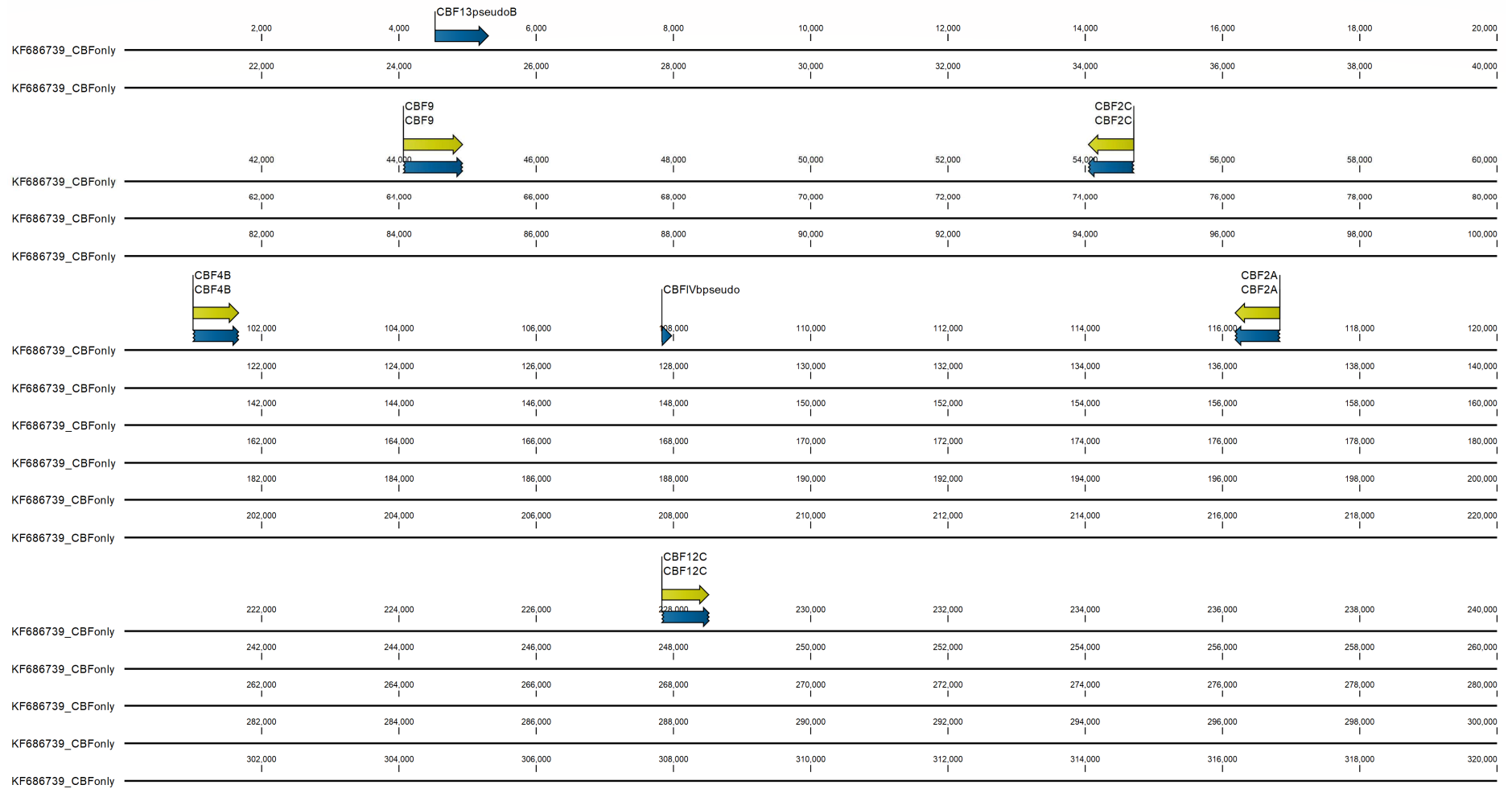


Figure A4.7 CLUSTALW DNA Alignments of Five *HvDHN* (DEHYDRIN) Sequences.

The GenBank accessions AF043096 (*cv* Dicktoo), AF181455 (*cv* Morex), and KC963076 (*cv* Steptoe) are annotated as *HvDHN5* sequences; AF181454(*cv* Morex) and AF043089 (*cv* Dicktoo) are annotated as *HvDHN4* and *HvDHN3*, respectively. **Panel A**, sequence alignments at the DNA and protein (not shown) level did not indicate strong sequence homology although the primers annealed to each of the sequences. **Panel B**, alignment of AF043096, AF181455, KC963078 and sequenced *cv* California *HvDHN5* amplicon. No strong homology exists casting doubt on the suitability of these primers for amplifying *HvDHN5*. **Panel C**, cladogram showing the relationship between these 5 DNA sequences. The positions of the forward and reverse primer sites are shown as vertical red bars (see **Section 4.3.2** for further details).



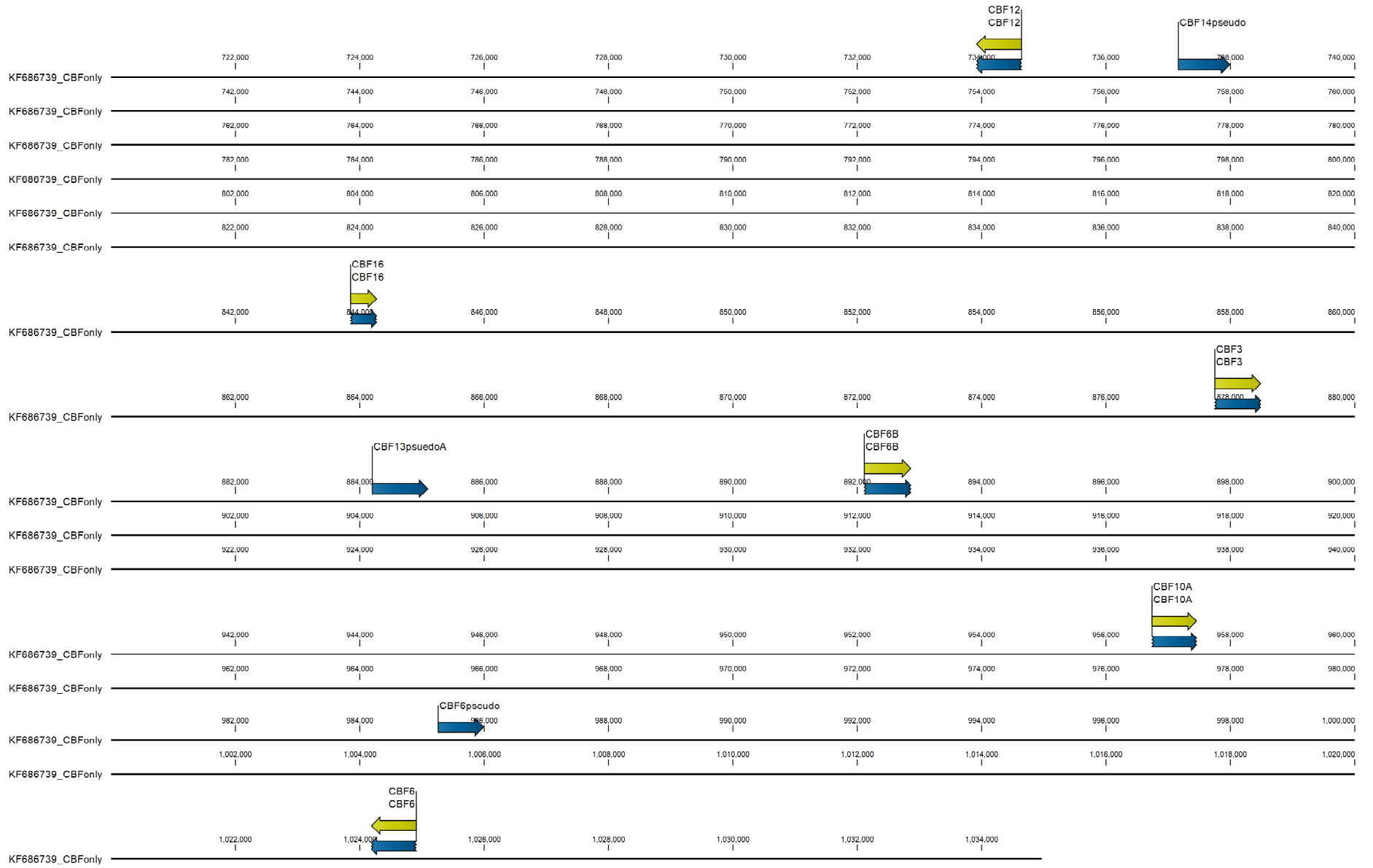


Figure A4.8: *HvCBF* Gene Structure in the *FR2* Locus on Barley Chromosome 5H.

The amplicons were generated from cv California gDNA template; similar experiments were conducted using template from cv Belgravia (not presented). **Panel A**; direct amplification from cv. California gDNA template (3 or more biological replicates). **Panel B**; colony PCR of several biological replicates of gDNA amplicons cloned into pTOPO2.3 and transformed into *E. coli* DH α . **Panel C**; amplicon generated from purified plasmid prior to sequencing. The size of the products was determined from amplicon sequencing and is indicated on the right of each image. The DNA size markers (1 kb ladder) in the left lane are on the 100, 200, 300, 400, 500, 650, 850, 1000, 1500, and 2000 bp.

Appendix A5.1 FastQ Output

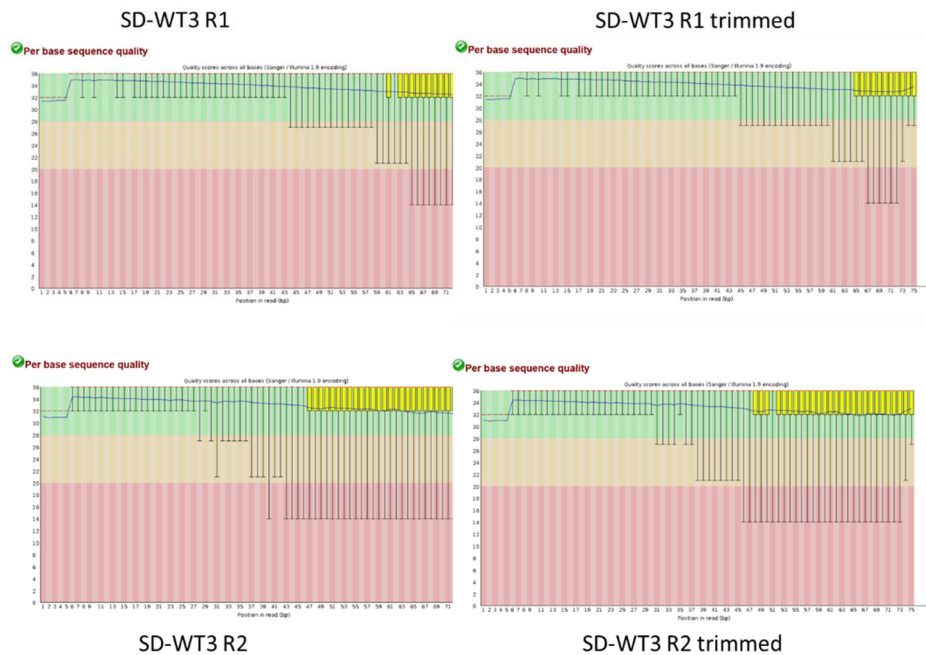


Figure A5.1 FastQC Analysis of RNASeq Reads of Cold Acclimated Barley Leaf Tissue: ‘Per base Quality Sequence’ Plot.

The ‘Per Base Quality Sequence’ plots present the base number along the x-axis and the average quality score on the Y-axis (36 represents perfect sequence, 20 is deemed to be acceptable). The yellow box represents the 25-75% quartiles, and the black error bars the 90% range. The blue line represents the median score for each position in the data set. R 1 and R2 represent the forward and reverse reads for the fragments. Individual sequences in the SD-WT3 pool were trimmed from 75 to 20-to-75 bases (**Table 5.2**); the R2 reads in LD-LT2 were of poorer quality and trimmed more extensively.

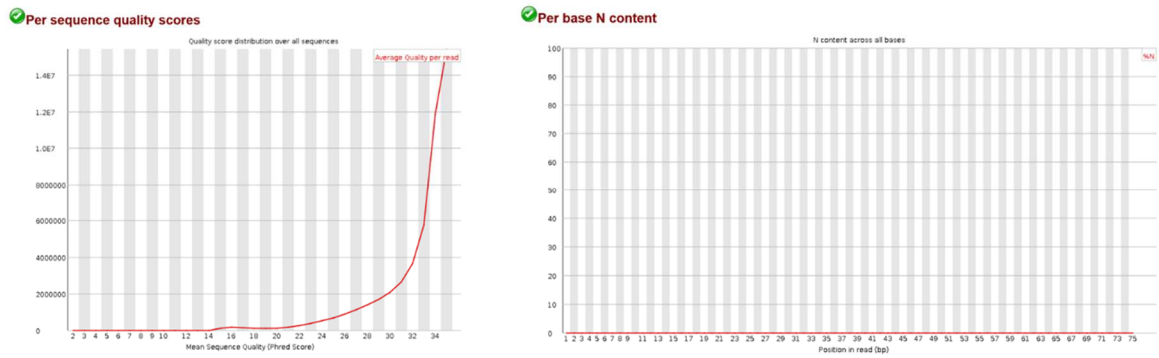


Figure A5.2 FastQC Analysis of RNASeq Reads of Cold Acclimated Barley Leaf Tissue: ‘Per Sequence Quality Scores’ and ‘Per Base N Content’ Plots.

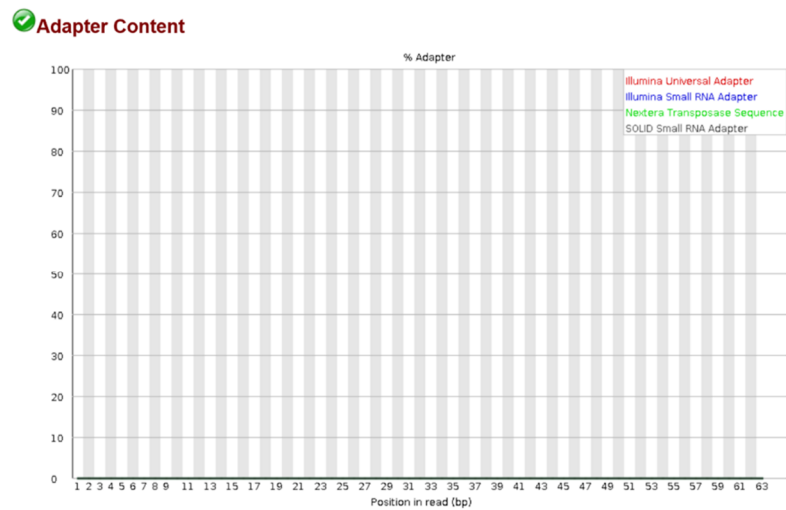
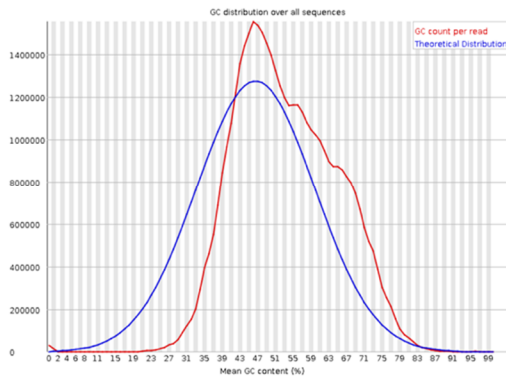


Figure A5.3 FastQC Analysis of RNASeq Reads of Cold Acclimated Barley Leaf Tissue: ‘Adapter Content’ Plot.

❌ Per sequence GC content



⚠ Per sequence GC content

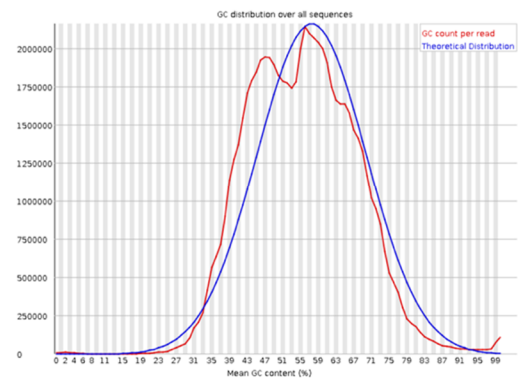
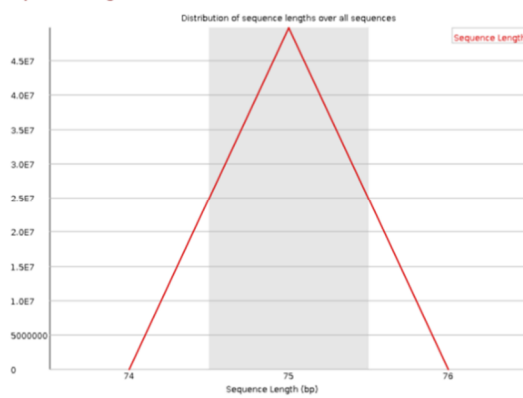


Figure A5.4 FastQC Analysis of RNASeq Reads of Cold Acclimated Barley Leaf Tissue: 'Per Sequence GC Content' Plots.

✅ Sequence Length Distribution



⚠ Sequence Length Distribution

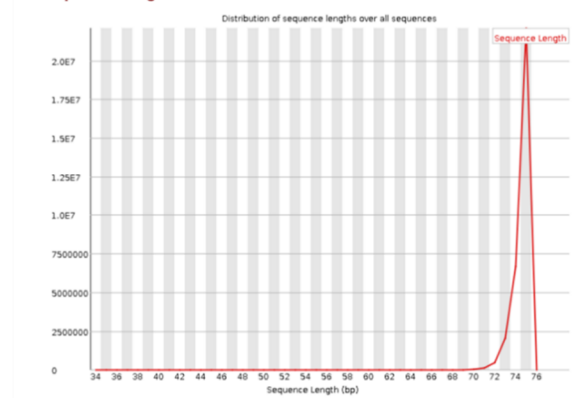


Figure A5.5 FastQC Analysis of RNASeq Reads of Cold Acclimated Barley Leaf Tissue: 'Sequence Length Distribution' Plots.

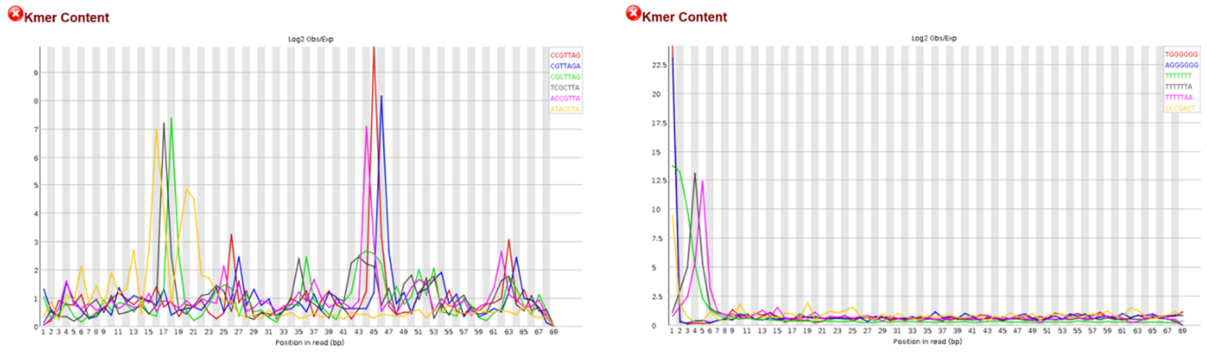


Figure A5.6 FastQC Analysis of RNASeq Reads of Cold Acclimated Barley Leaf Tissue: ‘k-mer Content’ Plots.

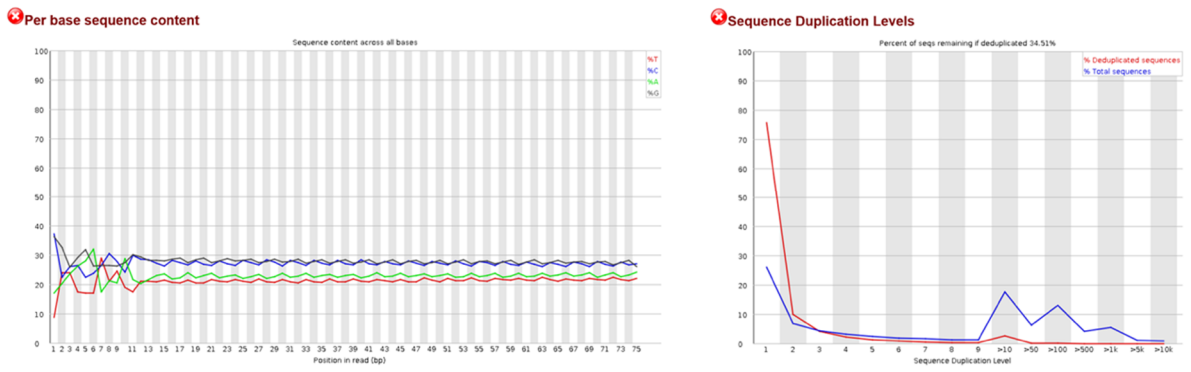


Figure A5.7 FastQC Analysis of RNASeq Reads of Cold Acclimated Barley Leaf Tissue: ‘Per Base Sequence Content’ and ‘Sequence Duplication Levels’ Plots.

Appendix Table A5.1: Lists of Transcript Changes from the Condition RNASeq Experiment

Table A5.1-1 List of Common Upregulated Cold Acclimation Barley Genes Regulated by Transition to Low Night Temperatures.

RNAseq analysis was performed on barley plants that were non-acclimated (LD-WT), partially acclimated by temperature alone (LD-LT and SD-LT), and fully cold acclimated (SD-LT); n=3 biological replicates per treatment. Reads were aligned using Kallisto and pairwise comparisons made and corresponding statistical inference calculated using the DESeq2 package. The resulting comparisons were then filtered by significance (Benjamin-Hochberg $p_{adj} < 0.1$) and then by >2-fold upregulation change ($\log_2 = >1$). The three resulting data sets (LD-WT vs LD-LT; SD-WT vs SD-LT; LD-WT vs SDLT) were then analysed for common sequences (see **Fig 5.5**) and those appearing in the intersections are listed below. A full list of the three data sets are presented in **Appendix 5**.

Gene ID	Base Mean	log2 Fold Change	p_{adj}	Chromosome	Fold Change	Description
6 common elements in "Full" and "Temperature SD":						
HORVU3Hr1G112520	65	2.25	0.0353	chr3H	4.7	Pyridoxal-5-Phosphate Decarboxylase (PTHR11999)
HORVU2Hr1G073210	1161	2.24	0.0281	chr2H	4.7	Concanavalin A-like lectin/glucanase domain superfamily (IPR013320)
HORVU2Hr1G103550	188	2.06	0.0304	chr2H	4.2	Glycine rich protein (IPR010800)

Gene ID	Base Mean	log2 Fold Change	p _{adj}	Chromosome	Fold Change	Description
HORVU1Hr1G005120	16626	1.96	0.0005	chr1H	3.9	Outer Envelope Pore Protein 16-1, Chloroplastic (PTHR15371:SF2)
HORVU7Hr1G009800	3444	1.47	0.0892	chr7H	2.8	Tetrapeptide transporter, OPT1/isp4 (IPR004648)
HORVU1Hr1G055000	6168	1.26	0.0024	chr1H	2.4	?
20 common elements in "Full" and Temperature LD":						
HORVU7Hr1G002360	155	2.15	0.0614	chr7H	4.4	Aspartic peptidase A1 family (IPR001461)
HORVU7Hr1G031680	32	2.04	0.0978	chr7H	4.1	Ionotropic glutamate receptor (IPR001320)
HORVU2Hr1G104080	821	2.29	0.0198	chr2H	4.9	?
HORVU6Hr1G074370	210	2.24	0.0304	chr6H	4.7	Subfamily Not Named (PTHR35547:SF1)
HORVU3Hr1G094320	67	2.11	0.0176	chr3H	4.3	Nucleotide-diphospho-sugar transferase (IPR005069)
HORVU2Hr1G112160	259	1.47	0.0299	chr2H	2.8	WAT1-related protein (IPR030184)
HORVU7Hr1G007810	275	2.89	0.0010	chr7H	7.4	Late embryogenesis abundant protein, LEA_1 subgroup (IPR005513)

Gene ID	Base Mean	log2 Fold Change	p _{adj}	Chromosome	Fold Change	Description
HORVU3Hr1G111160	78	2.02	0.0978	chr3H	4.1	Glycoside hydrolase superfamily (IPR017853)
HORVU3Hr1G039010	12	2.26	0.0374	chr3H	4.8	Polyketide cyclase/dehydrase (IPR019587)
HORVU5Hr1G056300	7	2.36	0.0260	chr5H	5.1	Gamma-Butyrobetaine Hydroxylase-Related (PTHR10696)
HORVU6Hr1G014300	667	1.84	0.0778	chr6H	3.6	Major intrinsic protein, conserved site (IPR022357)
HORVU6Hr1G014650	1385	2.02	0.0253	chr6H	4.0	Family Not Named (PTHR31618)
HORVU3Hr1G002980	690	2.21	0.0150	chr3H	4.6	Glycine-rich domain-containing protein-like (IPR009836)
HORVU2Hr1G082420	3396	1.24	0.0000	chr2H	2.4	Copper amine oxidase, N-terminal (IPR016182)
HORVU3Hr1G053090	513	1.17	0.0561	chr3H	2.2	?
HORVU4Hr1G050930	860	1.82	0.0705	chr4H	3.5	Cytochrome P450 superfamily (IPR036396)
HORVU2Hr1G080460	214	1.92	0.0010	chr2H	3.8	NAC domain superfamily (IPR036093)
HORVU4Hr1G082910	3871	1.42	0.0253	chr4H	2.7	Lyst-Interacting Protein Lip5 Dopamine Responsive Protein Drg-1 (PTHR12741)

Gene ID	Base Mean	log2 Fold Change	p _{adj}	Chromosome	Fold Change	Description
HORVU7Hr1G035300	264	1.55	0.0174	chr7H	2.9	LysM domain (IPR018392)
HORVU1Hr1G016200	2879	1.54	0.0304	chr1H	2.9	AMP-dependent synthetase/ligase (IPR000873)
18 common elements in "Temperature LD", "Full" and "Temperature SD":						
HORVU4Hr1G083250	1447	3.77	0.0000	chr4H	13.7	S-Adenosyl-L-Methionine-Dependent Methyltransferases Superfamily Protein (PTHR12176:SF19)
HORVU6Hr1G086820	198	2.01	0.0565	chr6H	4.0	Family Not Named (PTHR33132)
HORVU5Hr1G001750	1601	2.57	0.0000	chr5H	5.9	?
HORVU2Hr1G099820	17318	2.90	0.0010	chr2H	7.5	?
HORVU3Hr1G112020	759	2.82	0.0010	chr3H	7.0	ABA/WDS induced protein (IPR003496)
HORVU5Hr1G098190	18330	2.37	0.0000	chr5H	5.2	Cold-regulated 413 protein (IPR008892)
HORVU1Hr1G058310	11	2.66	0.0050	chr1H	6.3	Protein kinase-like domain superfamily (IPR011009)

Gene ID	Base Mean	log2 Fold Change	p _{adj}	Chromosome	Fold Change	Description
HORVU3Hr1G058990	526	2.30	0.0002	chr3H	4.9	P-loop containing nucleoside triphosphate hydrolase (IPR027417)
HORVU2Hr1G099830	36825	2.48	0.0152	chr2H	5.6	?
HORVU7Hr1G012310	222	2.25	0.0260	chr7H	4.8	Late embryogenesis abundant protein, LEA_1 subgroup (IPR005513)
HORVU7Hr1G007800	4441	2.64	0.0000	chr7H	6.2	Late embryogenesis abundant protein, LEA_1 subgroup (IPR005513)
HORVU5Hr1G098920	304	2.09	0.0007	chr5H	4.2	Pectinacetylerase/NOTUM (IPR004963)
HORVU2Hr1G028920	144	2.56	0.0004	chr2H	5.9	Nuclease (PTHR22930:SF52)
HORVU4Hr1G057000	11568	1.89	0.0304	chr4H	3.7	Proteolipid membrane potential modulator (IPR000612)
HORVU3Hr1G006940	3952	1.45	0.0054	chr3H	2.7	Small heat shock protein HSP20 (IPR031107)
HORVU2Hr1G043980	105	1.99	0.0304	chr2H	4.0	Protein of unknown function DUF1218 (IPR009606)
HORVU0Hr1G003190	119	1.63	0.0366	chrUn	3.1	Protein of unknown function DUF1218 (IPR009606)
HORVU6Hr1G060540	86	1.41	0.0366	chr6H	2.7	Protein kinase domain (IPR000719)

Gene ID	Base Mean	log2 Fold Change	p _{adj}	Chromosome	Fold Change	Description
8 elements included exclusively in "Full":						
HORVU3Hr1G073280	145	2.10	0.0754	chr3H	4.3	Subfamily Not Named (PTHR34268:SF6)
HORVU6Hr1G014270	141	1.76	0.0485	chr6H	3.4	L-gulonolactone oxidase, plant (IPR010030)
HORVU3Hr1G086940	339	1.66	0.0697	chr3H	3.2	Chitinase (PTHR11177)
HORVU3Hr1G029770	633	1.58	0.0334	chr3H	3.0	Phospholipid/glycerol acyltransferase (IPR002123)
HORVU2Hr1G043830	97	1.49	0.0304	chr2H	2.8	Formin, FH2 domain (IPR015425)
HORVU7Hr1G035050	166	1.24	0.0233	chr7H	2.4	Trichome birefringence-like family (IPR029962)
HORVU2Hr1G100720	3349	1.20	0.0415	chr2H	2.3	Family Not Named (PTHR16223)
HORVU1Hr1G065070	556	1.08	0.0315	chr1H	2.1	Protein kinase-like domain superfamily (IPR011009)

Appendix Table A5.2-2 List of Common Downregulated Cold Acclimation Barley Genes Regulated by Transition to Low Night Temperatures.

RNAseq analysis was performed on barley plants that were non-acclimated (LD-WT), partially acclimated by temperature alone (LD-LT and SD-LT), and fully cold acclimated (SD-LT); n=3 biological replicates per treatment. Reads were aligned using Kallisto and pairwise comparisons made and corresponding statistical inference calculated using the DESeq2 package. The resulting comparisons were then filtered by significance (Benjamin-Hochberg $p_{adj} < 0.1$) and then by >2-fold downregulation change ($\log_2 = > -1$). The three resulting data sets (LD-WT vs LD-LT; SD-WT vs SD-LT; LD-WT vs SDLT) were then analysed for common sequences (see **Fig 5.6**) and those appearing in the intersections are listed below. A full list of the three data sets are presented in **Appendix 5**.

Gene ID	Base Mean	log ₂ Fold Change	p _{adj}	Chromosome	Fold Change	Description
14 common elements in "Temperature LD" and "Full":						
HORVU1Hr1G093560	122	-3.55	0.0000	chr1H	11.7	Ribonuclease Ribonuclease T2 familyT2 family
HORVU0Hr1G027640	31	-2.06	0.0793	chrUn	4.2	Zinc finger, FYVE/PHD-type
HORVU6Hr1G005050	20	-2.50	0.0060	chr6H	5.7	Subfamily Not Named (PTHR33433:SF4)
HORVU3Hr1G013840	22309	-1.73	0.0315	chr3H	3.3	Subfamily Not Named (PTHR33543:SF1)
HORVU2Hr1G024120	193	-2.36	0.0044	chr2H	5.1	Terpenoid Cyclases/Protein Prenyltransferases Superfamily

HORVU0Hr1G000340	138	-2.39	0.0152	chrUn	5.2	Cys/Met metabolism PLP-dependent enzyme family
HORVU5Hr1G007890	583	-1.97	0.0458	chr5H	3.9	Transcription Factor NF-Y Alpha-Related (PTHR12632)
HORVU1Hr1G090890	26	-2.24	0.0304	chr1H	4.7	Protein of unknown function DUF761, plant (IPR008480)
HORVU5Hr1G092700	2145	-1.52	0.0803	chr5H	2.9	Transcription Factor NF-Y Alpha-Related (PTHR12632)
HORVU5Hr1G085550	165	-1.54	0.0646	chr5H	2.9	Subfamily Not Named (PTHR33207:SF4)
HORVU2Hr1G097980	37	-1.40	0.0315	chr2H	2.6	Family Not Named (PTHR34059)
HORVU3Hr1G070880	1169	-1.35	0.0485	chr3H	2.5	HPT domain superfamily (IPR036641)
HORVU3Hr1G002000	28	-1.90	0.0038	chr3H	3.7	Rmlc-Like Cupin Domain Superfamily (IPR011051)
HORVU3Hr1G024920	19019	-1.15	0.0485	chr3H	2.2	?
1 common element in "Temperature LD" and "Temperature SD":						
HORVU2Hr1G015930	155	1.09	0.0199	chr2H	2.1	Serine / Threonine-Protein Kinase 36 (PTHR22983:SF6)
16 elements included exclusively in "Full":						
HORVU7Hr1G027540	16	-2.49	0.0150	chr7H	5.6	Glutathione S-Transferase, GST, Superfamily, GST Domain-Containing (PTHR11260)
HORVU5Hr1G125460	6	-2.35	0.0253	chr5H	5.1	AWPM-19-Like Family Protein (PTHR33294:SF5)

HORVU5Hr1G052730	222	-2.18	0.0050	chr5H	4.5	Copper Transport Protein Atox1-Related (PTHR22814)
HORVU2Hr1G108340	5	-2.10	0.0793	chr2H	4.3	UDP-glucuronosyl and UDP-glucosyl transferase
HORVU2Hr1G012280	9	-2.06	0.0967	chr2H	4.2	Protein of unknown function (DUF1298)
HORVU5Hr1G091840	69	-2.00	0.0931	chr5H	4.0	?
HORVU2Hr1G019900	56	-1.99	0.0334	chr2H	4.0	Family Not Named (PTHR33433)
HORVU2Hr1G071450	9	-1.96	0.0754	chr2H	3.9	NUDIX Hydrolase-Like Domain Superfamily (IPR015797)
HORVU0Hr1G020630	104	-1.91	0.0754	chrUn	3.8	S-adenosyl-L-methionine-dependent Methyltransferase (IPR029063)
HORVU4Hr1G060670	51	-1.83	0.0315	chr4H	3.6	WD40 repeat (IPR001680)
HORVU7Hr1G025700	29	-1.78	0.0561	chr7H	3.4	Transcription factor, MADS-box superfamily (IPR036879)
HORVU3Hr1G026920	44060	-1.57	0.0173	chr3H	3.0	Family Not Named (PTHR33357)
HORVU3Hr1G070440	122	-1.47	0.0931	chr3H	2.8	Glycoside hydrolase superfamily (IPR017853)
HORVU6Hr1G006840	1679	-1.42	0.0458	chr6H	2.7	?
HORVU3Hr1G066410	190	-1.18	0.0088	chr3H	2.3	RNA Polymerase Ii Transcriptional Coactivator (PTHR13215)
HORVU6Hr1G012400	471	-1.13	0.0366	chr6H	2.2	?

Table A5.1-3 List of Common Downregulated Barley Genes Regulated by Transition to Short Days in Warm Night Temperatures.

RNAseq analysis was performed on barley plants that were non-acclimated (LD-WT), partially acclimated by temperature alone (LD-LT and SD-LT), and fully cold acclimated (SD-LT); n=3 biological replicates per treatment. Reads were aligned using Kallisto and pairwise comparisons made and corresponding statistical inference calculated using the DESeq2 package. The resulting comparisons were then filtered by significance (Benjamin-Hochberg $p_{adj} < 0.1$) and then by >2-fold downregulation change ($\log_2 = > -1$). The three resulting data sets (LD-WT vs LD-LT; SD-WT vs SD-LT; LD-WT vs SDLT) were then analysed for common sequences (see **Fig 5.6**) and those appearing in the intersections are listed below. A full list of the three data sets are presented in **Appendix 5**.

Gene ID	Base Mean	log2 Fold Change	p_{adj}	Chromosome	Fold Change	Description
Downregulated: 2 common elements in "Photoperiod WT" and "Full"						
HORVU1Hr1G093560	122	-3.55	0.0000	chr1H	11.7	Ribonuclease T2-like superfamily (IPR036430)
HORVU3Hr1G002000	28	-1.90	0.0038	chr3H	3.7	RmlC-like cupin domain superfamily (IPR011051)

Appendix Table A5.3 Transcript Abundance Changes LDWT v SDLT (Full)

Upregulated

Gene ID	base Mean	log2 Fold Change	pAdj	chromosome
HORVU4Hr1G083250	1447	3.77	0.0000	chr4H
HORVU2Hr1G099820	17318	2.90	0.0010	chr2H
HORVU7Hr1G007810	275	2.89	0.0010	chr7H
HORVU3Hr1G112020	759	2.82	0.0010	chr3H
HORVU1Hr1G058310	11	2.66	0.0050	chr1H
HORVU7Hr1G007800	4441	2.64	0.0000	chr7H
HORVU5Hr1G001750	1601	2.57	0.0000	chr5H
HORVU2Hr1G028920	144	2.56	0.0004	chr2H
HORVU2Hr1G099830	36825	2.48	0.0152	chr2H
HORVU5Hr1G098190	18330	2.37	0.0000	chr5H
HORVU5Hr1G056300	7	2.36	0.0260	chr5H
HORVU3Hr1G058990	526	2.30	0.0002	chr3H
HORVU2Hr1G104080	821	2.29	0.0198	chr2H
HORVU3Hr1G039010	12	2.26	0.0374	chr3H
HORVU7Hr1G012310	222	2.25	0.0260	chr7H
HORVU3Hr1G112520	65	2.25	0.0353	chr3H
HORVU6Hr1G074370	210	2.24	0.0304	chr6H
HORVU2Hr1G073210	1161	2.24	0.0281	chr2H
HORVU3Hr1G002980	690	2.21	0.0150	chr3H
HORVU7Hr1G002360	155	2.15	0.0614	chr7H
HORVU3Hr1G094320	67	2.11	0.0176	chr3H
HORVU3Hr1G073280	145	2.10	0.0754	chr3H
HORVU5Hr1G098920	304	2.09	0.0007	chr5H
HORVU2Hr1G103550	188	2.06	0.0304	chr2H
HORVU7Hr1G031680	32	2.04	0.0978	chr7H
HORVU3Hr1G111160	78	2.02	0.0978	chr3H
HORVU6Hr1G014650	1385	2.02	0.0253	chr6H
HORVU6Hr1G086820	198	2.01	0.0565	chr6H
HORVU2Hr1G043980	105	1.99	0.0304	chr2H
HORVU1Hr1G005120	16626	1.96	0.0005	chr1H
HORVU2Hr1G080460	214	1.92	0.0010	chr2H
HORVU4Hr1G057000	11568	1.89	0.0304	chr4H
HORVU6Hr1G014300	667	1.84	0.0778	chr6H
HORVU4Hr1G050930	860	1.82	0.0705	chr4H
HORVU6Hr1G014270	141	1.76	0.0485	chr6H
HORVU3Hr1G086940	339	1.66	0.0697	chr3H
HORVU0Hr1G003190	119	1.63	0.0366	chrUn
HORVU3Hr1G029770	633	1.58	0.0334	chr3H
HORVU7Hr1G035300	264	1.55	0.0174	chr7H
HORVU1Hr1G016200	2879	1.54	0.0304	chr1H
HORVU2Hr1G043830	97	1.49	0.0304	chr2H
HORVU7Hr1G009800	3444	1.47	0.0892	chr7H
HORVU2Hr1G112160	259	1.47	0.0299	chr2H
HORVU3Hr1G006940	3952	1.45	0.0054	chr3H
HORVU4Hr1G082910	3871	1.42	0.0253	chr4H

Downregulated

Gene ID	base Mean	log2 Fold Change	pAdj	chromosome
HORVU1Hr1G093560	122	-3.55	0.0000	chr1H
HORVU6Hr1G005050	20	-2.50	0.0060	chr6H
HORVU7Hr1G027540	16	-2.49	0.0150	chr7H
HORVU0Hr1G000340	138	-2.39	0.0152	chrUn
HORVU2Hr1G024120	193	-2.36	0.0044	chr2H
HORVU5Hr1G125460	6	-2.35	0.0253	chr5H
HORVU1Hr1G090890	26	-2.24	0.0304	chr1H
HORVU5Hr1G052730	222	-2.18	0.0050	chr5H
HORVU2Hr1G108340	5	-2.10	0.0793	chr2H
HORVU0Hr1G027640	31	-2.06	0.0793	chrUn
HORVU2Hr1G012280	9	-2.06	0.0967	chr2H
HORVU5Hr1G091840	69	-2.00	0.0931	chr5H
HORVU2Hr1G019900	56	-1.99	0.0334	chr2H
HORVU5Hr1G007890	583	-1.97	0.0458	chr5H
HORVU2Hr1G071450	9	-1.96	0.0754	chr2H
HORVU0Hr1G020630	104	-1.91	0.0754	chrUn
HORVU3Hr1G002000	28	-1.90	0.0038	chr3H
HORVU4Hr1G060670	51	-1.83	0.0315	chr4H
HORVU7Hr1G025700	29	-1.78	0.0561	chr7H
HORVU3Hr1G013840	22309	-1.73	0.0315	chr3H
HORVU3Hr1G026920	44060	-1.57	0.0173	chr3H
HORVU5Hr1G085550	165	-1.54	0.0646	chr5H
HORVU5Hr1G092700	2145	-1.52	0.0803	chr5H
HORVU3Hr1G070440	122	-1.47	0.0931	chr3H
HORVU6Hr1G006840	1679	-1.42	0.0458	chr6H
HORVU2Hr1G097980	37	-1.40	0.0315	chr2H
HORVU3Hr1G070880	1169	-1.35	0.0485	chr3H
HORVU3Hr1G066410	190	-1.18	0.0088	chr3H
HORVU3Hr1G024920	19019	-1.15	0.0485	chr3H
HORVU6Hr1G012400	471	-1.13	0.0366	chr6H

Appendix Table A5.4 Transcript Abundance Changes LDWT v LDLT (Temperature LD)

Upregulated

Gene ID	base Mean	log2 Fold Change	pAdj	chromosome
HORVU7Hr1G002360	155	4.18	0.0000	chr7H
HORVU7Hr1G031680	32	3.56	0.0000	chr7H
HORVU2Hr1G104080	821	3.08	0.0000	chr2H
HORVU4Hr1G083250	1,447	3.08	0.0001	chr4H
HORVU2Hr1G082170	65	3.05	0.0000	chr2H
HORVU6Hr1G074370	210	3.02	0.0001	chr6H
HORVU6Hr1G092540	477	3.02	0.0001	chr6H
HORVU7Hr1G003630	108	2.83	0.0008	chr7H
HORVU6Hr1G092200	9	2.76	0.0014	chr6H
HORVU2Hr1G002750	799	2.68	0.0018	chr2H
HORVU7Hr1G020810	40	2.67	0.0023	chr7H
HORVU2Hr1G085260	17	2.62	0.0030	chr2H
HORVU4Hr1G054860	13	2.61	0.0033	chr4H
HORVU3Hr1G105600	1,194	2.61	0.0015	chr3H
HORVU2Hr1G123160	386	2.61	0.0023	chr2H
HORVU2Hr1G108690	30	2.60	0.0031	chr2H
HORVU5Hr1G076410	258	2.53	0.0049	chr5H
HORVU6Hr1G001770	160	2.50	0.0037	chr6H
HORVU3Hr1G108060	9	2.50	0.0054	chr3H
HORVU7Hr1G122430	261	2.47	0.0047	chr7H
HORVU5Hr1G066260	2,226	2.47	0.0044	chr5H
HORVU4Hr1G071300	1,454	2.45	0.0011	chr4H
HORVU5Hr1G115870	2,886	2.44	0.0056	chr5H
HORVU3Hr1G094320	67	2.42	0.0011	chr3H
HORVU6Hr1G020950	90	2.41	0.0022	chr6H
HORVU5Hr1G098630	22	2.40	0.0039	chr5H
HORVU3Hr1G105560	1,280	2.37	0.0106	chr3H
HORVU3Hr1G002520	357	2.35	0.0006	chr3H
HORVU6Hr1G086820	198	2.35	0.0046	chr6H
HORVU3Hr1G105420	2,977	2.35	0.0079	chr3H
HORVU0Hr1G005300	4,979	2.35	0.0082	chrUn
HORVU5Hr1G088260	20	2.34	0.0126	chr5H
HORVU2Hr1G112160	259	2.33	0.0000	chr2H
HORVU5Hr1G001750	1,601	2.33	0.0001	chr5H
HORVU1Hr1G002590	89	2.33	0.0115	chr1H
HORVU5Hr1G124170	31	2.32	0.0068	chr5H
HORVU3Hr1G104940	10,019	2.29	0.0147	chr3H
HORVU6Hr1G092020	130	2.29	0.0098	chr6H
HORVU5Hr1G043460	260	2.29	0.0056	chr5H
HORVU2Hr1G113080	108	2.28	0.0137	chr2H
HORVU2Hr1G017470	911	2.28	0.0060	chr2H
HORVU6Hr1G033060	605	2.27	0.0027	chr6H
HORVU3Hr1G006410	57	2.27	0.0137	chr3H
HORVU3Hr1G105790	129	2.25	0.0182	chr3H
HORVU2Hr1G076060	77	2.24	0.0081	chr2H
HORVU2Hr1G099820	17,318	2.24	0.0197	chr2H

Downregulated

Gene ID	base Mean	log2 Fold Change	pAdj	chromosome
HORVU1Hr1G093560	122	-3.46	0.0000	chr1H
HORVU5Hr1G076970	6,031	-2.45	0.0072	chr5H
HORVU7Hr1G112910	342	-2.35	0.0069	chr7H
HORVU0Hr1G027640	31	-2.26	0.0143	chrUn
HORVU1Hr1G066930	71	-2.26	0.0044	chr1H
HORVU4Hr1G049550	52	-2.24	0.0004	chr4H
HORVU3Hr1G023750	1,159	-2.21	0.0039	chr3H
HORVU5Hr1G063600	39	-2.16	0.0027	chr5H
HORVU4Hr1G087250	77	-2.14	0.0179	chr4H
HORVU6Hr1G066450	119	-2.11	0.0176	chr6H
HORVU6Hr1G005050	20	-2.06	0.0236	chr6H
HORVU3Hr1G013840	22,309	-2.05	0.0018	chr3H
HORVU2Hr1G059780	139	-2.05	0.0106	chr2H
HORVU3Hr1G111580	16	-2.03	0.0421	chr3H
HORVU6Hr1G084010	21	-1.97	0.0382	chr6H
HORVU7Hr1G021120	78	-1.96	0.0056	chr7H
HORVU2Hr1G072960	298	-1.88	0.0562	chr2H
HORVU3Hr1G089300	7	-1.87	0.0735	chr3H
HORVU3Hr1G093260	66	-1.87	0.0595	chr3H
HORVU2Hr1G024120	193	-1.86	0.0280	chr2H
HORVU3Hr1G028410	41	-1.86	0.0441	chr3H
HORVU5Hr1G086660	9	-1.85	0.0729	chr5H
HORVU3Hr1G004410	110	-1.85	0.0793	chr3H
HORVU5Hr1G016090	29	-1.85	0.0411	chr5H
HORVU2Hr1G094810	18	-1.84	0.0767	chr2H
HORVU1Hr1G036490	21	-1.84	0.0833	chr1H
HORVU6Hr1G094070	415	-1.83	0.0596	chr6H
HORVU5Hr1G103990	349	-1.83	0.0347	chr5H
HORVU0Hr1G034800	901	-1.83	0.0475	chrUn
HORVU3Hr1G050700	19	-1.82	0.0208	chr3H
HORVU5Hr1G083990	19,506	-1.82	0.0812	chr5H
HORVU6Hr1G019760	169	-1.81	0.0928	chr6H
HORVU0Hr1G000340	138	-1.80	0.0753	chrUn
HORVU0Hr1G010040	78	-1.79	0.0126	chrUn
HORVU4Hr1G062830	16	-1.79	0.0769	chr4H
HORVU5Hr1G012990	97,434	-1.78	0.0793	chr5H
HORVU5Hr1G114230	644	-1.78	0.0977	chr5H
HORVU4Hr1G078450	32	-1.77	0.0208	chr4H
HORVU1Hr1G088190	20	-1.76	0.0917	chr1H
HORVU2Hr1G073670	68	-1.75	0.0670	chr2H
HORVU1Hr1G070780	30	-1.75	0.0076	chr1H
HORVU4Hr1G055300	66	-1.75	0.0569	chr4H
HORVU5Hr1G007890	583	-1.73	0.0577	chr5H
HORVU4Hr1G018800	370	-1.72	0.0130	chr4H
HORVU1Hr1G090890	26	-1.70	0.0995	chr1H
HORVU5Hr1G017180	20	-1.70	0.0936	chr5H

Appendix Table A5.5 Transcript Abundance Changes SDWT v SDLT (Temperature SD)

Upregulated

Gene ID	base Mean	log2 Fold Change	pAdj	chromosome
HORVU4Hr1G083250	1447	3.88	0.0000	chr4H
HORVU3Hr1G112020	759	3.25	0.0000	chr3H
HORVU2Hr1G073210	1161	3.25	0.0000	chr2H
HORVU7Hr1G007800	4441	3.23	0.0000	chr7H
HORVU3Hr1G058990	526	2.94	0.0000	chr3H
HORVU1Hr1G002100	508	2.88	0.0000	chr1H
HORVU1Hr1G058310	11	2.88	0.0010	chr1H
HORVU2Hr1G099820	17318	2.87	0.0012	chr2H
HORVU7Hr1G012310	222	2.83	0.0005	chr7H
HORVU5Hr1G001750	1601	2.71	0.0000	chr5H
HORVU3Hr1G112520	65	2.56	0.0096	chr3H
HORVU6Hr1G059200	8	2.52	0.0108	chr6H
HORVU6Hr1G086820	198	2.52	0.0034	chr6H
HORVU1Hr1G005120	16626	2.48	0.0000	chr1H
HORVU2Hr1G043980	105	2.40	0.0020	chr2H
HORVU2Hr1G099830	36825	2.37	0.0371	chr2H
HORVU4Hr1G005800	50	2.35	0.0221	chr4H
HORVU2Hr1G028920	144	2.34	0.0019	chr2H
HORVU5Hr1G098190	18330	2.33	0.0000	chr5H
HORVU7Hr1G115640	7	2.32	0.0472	chr7H
HORVU0Hr1G003190	119	2.24	0.0002	chrUn
HORVU3Hr1G000170	221	2.23	0.0002	chr3H
HORVU2Hr1G103550	188	2.16	0.0233	chr2H
HORVU6Hr1G060540	86	2.09	0.0000	chr6H
HORVU2Hr1G000430	553	1.97	0.0371	chr2H
HORVU1Hr1G025440	1367	1.97	0.0000	chr1H
HORVU7Hr1G009800	3444	1.91	0.0043	chr7H
HORVU2Hr1G005310	40	1.86	0.0710	chr2H
HORVU1Hr1G063420	192	1.81	0.0233	chr1H
HORVU4Hr1G057000	11568	1.81	0.0797	chr4H
HORVU7Hr1G078670	686	1.79	0.0155	chr7H
HORVU3Hr1G079210	4664	1.71	0.0467	chr3H
HORVU5Hr1G098920	304	1.62	0.0490	chr5H
HORVU5Hr1G093640	341	1.50	0.0797	chr5H
HORVU3Hr1G006940	3952	1.34	0.0233	chr3H
HORVU6Hr1G032830	536	1.24	0.0781	chr6H
HORVU1Hr1G055000	6168	1.06	0.0465	chr1H

Downregulated

Gene ID	base Mean	log2 Fold Change	pAdj	chromosome
HORVU2Hr1G030600	33	-2.19	0.0768	chr2H
HORVU2Hr1G003480	35	-2.17	0.0990	chr2H
HORVU2Hr1G015930	155	-1.07	0.0990	chr2H

Appendix Table A5.6: Lists of Transcript Changes from the Time Series RNASeq Experiment

Upregulated.

Gene ID	<u>0 v 1 Week</u>		<u>0 v 2 Week</u>		<u>0 v 3 Week</u>		<u>0 v 4 Week</u>		Description
	Log2 Fold Change	p _{adj}	Log2 Fold Change	p _{adj}	Log2 Fold Change	p _{adj}	Log2 Fold Change	p _{adj}	
HORVU2Hr1G099820	12.06	0.0000	11.62	0.0000	10.97	0.0000	10.99	0.0000	LATE EMBRYOGENESIS ABUNDANT PLANTS LEA-RELATED (PTHR23241); Senescence/spartin-associated (IPR009686)
HORVU2Hr1G099830	11.36	0.0000	10.78	0.0000	10.72	0.0000	10.74	0.0000	Cold acclimation protein; coiled coil
HORVU6Hr1G016850	7.60	0.0000	4.48	0.0000	4.82	0.0000	4.85	0.0000	Chlorophyll A-B binding protein (IPR022796)
HORVU3Hr1G039010	6.51	0.0000	7.56	0.0000	6.23	0.0000	6.20	0.0000	Polyketide cyclase/dehydrase (IPR019587); Lipid binding phosphatase activity (PTHR31213)
HORVU4Hr1G080300	6.15	0.0000	8.83	0.0000	3.79	0.0000	3.55	0.0000	AP2/ERF domain (IPR001471)

Gene ID	<u>0 v 1 Week</u>		<u>0 v 2 Week</u>		<u>0 v 3 Week</u>		<u>0 v 4 Week</u>		Description
	Log2 Fold Change	p _{adj}	Log2 Fold Change	p _{adj}	Log2 Fold Change	p _{adj}	Log2 Fold Change	p _{adj}	
HORVU1Hr1G058310	6.03	0.0000	6.61	0.0000	5.30	0.0000	5.26	0.0000	Protein kinase domain (IPR000719)
HORVU1Hr1G089240	5.85	0.0000	2.38	0.0000	3.85	0.0000	3.78	0.0000	Cytochrome c oxidase subunit I (IPR000883)
HORVU7Hr1G021630	5.63	0.0000	3.46	0.0000	5.25	0.0000	5.07	0.0000	GDSL lipase/esterase (IPR001087)
HORVU7Hr1G007810	5.44	0.0000	5.08	0.0000	4.58	0.0000	4.42	0.0000	?
HORVU6Hr1G016890	5.36	0.0000	2.49	0.0000	3.14	0.0000	3.13	0.0000	Chlorophyll A-B binding protein (IPR022796)
HORVU3Hr1G064710	5.31	0.0000	4.90	0.0000	2.28	0.0240	2.46	0.0141	Zinc finger, RING-type (IPR001841)
HORVU1Hr1G088920	5.29	0.0000	1.85	0.0000	3.93	0.0000	3.99	0.0000	Chlorophyll A-B binding protein (IPR022796)
HORVU1Hr1G078380	5.24	0.0000	2.75	0.0000	3.26	0.0000	3.20	0.0000	Chlorophyll A-B binding protein (IPR022796)
HORVU4Hr1G087800	5.04	0.0000	3.10	0.0000	2.33	0.0001	2.36	0.0001	Hydrophobic seed protein (IPR027923)
HORVU5Hr1G119520	5.03	0.0000	7.08	0.0000	3.61	0.0000	3.55	0.0000	Leucine-rich repeat (IPR001611)
HORVU4Hr1G082900	4.86	0.0000	6.02	0.0000	2.89	0.0000	3.02	0.0000	?

Gene ID	<u>0 v 1 Week</u>		<u>0 v 2 Week</u>		<u>0 v 3 Week</u>		<u>0 v 4 Week</u>		Description
	Log2 Fold Change	Padj							
HORVU6Hr1G070060	4.70	0.0000	4.55	0.0000	2.64	0.0000	3.24	0.0000	Hydroxymethylglutaryl-CoA reductase, class I/II (IPR002202)
HORVU1Hr1G002000	4.68	0.0000	5.08	0.0000	2.15	0.0000	2.27	0.0000	Bulb-type lectin domain (IPR001480); S-locus glycoprotein domain (IPR000858); Protein kinase domain (IPR000719);
HORVU3Hr1G058990	4.57	0.0000	5.74	0.0000	1.86	0.0000	1.55	0.0000	CTP synthase, N-terminal (IPR017456); Glutamine amidotransferase (IPR017926)
HORVU5Hr1G056300	4.56	0.0000	4.97	0.0000	3.10	0.0007	2.81	0.0027	TauD/TfdA-like domain (IPR003819)
HORVU3Hr1G114900	4.51	0.0000	2.04	0.0051	3.59	0.0000	3.56	0.0000	Cupin 1 (IPR006045); common in 11S and 7S storage proteins.
HORVU7Hr1G007800	4.46	0.0000	4.93	0.0000	2.76	0.0000	2.66	0.0000	Late embryogenesis abundant protein, LEA-25/LEA-D113 (IPR005513)
HORVU6Hr1G016880	4.39	0.0000	2.25	0.0000	2.78	0.0000	2.76	0.0000	Chlorophyll A-B binding protein (IPR022796)
HORVU1Hr1G089180	4.22	0.0000	1.98	0.0000	2.70	0.0000	2.66	0.0000	Chlorophyll A-B binding protein (IPR022796)
HORVU2Hr1G073210	4.22	0.0000	4.17	0.0000	1.21	0.0108	1.11	0.0209	Glycosyl hydrolase family 32, C-terminal (IPR013189)
HORVU7Hr1G012310	4.18	0.0000	6.86	0.0000	3.71	0.0000	3.69	0.0000	Late embryogenesis abundant protein, LEA-25/LEA-D113 (IPR005513)
HORVU6Hr1G080750	4.15	0.0000	2.77	0.0000	2.19	0.0000	2.30	0.0000	Nitrite/Sulfite reductase ferredoxin-like domain (IPR005117)

Gene ID	<u>0 v 1 Week</u>		<u>0 v 2 Week</u>		<u>0 v 3 Week</u>		<u>0 v 4 Week</u>		Description
	Log2 Fold Change	p _{adj}	Log2 Fold Change	p _{adj}	Log2 Fold Change	p _{adj}	Log2 Fold Change	p _{adj}	
HORVU6Hr1G063480	4.14	0.0000	1.42	0.0000	1.35	0.0000	1.45	0.0000	Pyridoxal-phosphate dependent enzyme (IPR001926)
HORVU7Hr1G090970	4.11	0.0000	4.78	0.0000	4.00	0.0000	4.04	0.0000	Heavy metal-associated domain, HMA (IPR006121)
HORVU2Hr1G033080	4.07	0.0000	3.39	0.0002	2.32	0.0244	3.67	0.0001	COBRA, plant (IPR006918); cell wall biosynthesis
HORVU3Hr1G112020	3.97	0.0000	4.62	0.0000	5.55	0.0000	5.48	0.0000	ABA/WDS induced protein (IPR003496)
HORVU5Hr1G121250	3.91	0.0000	3.70	0.0000	0.72	0.0000	0.67	0.0000	Aspartate/glutamate/uridylate kinase (IPR001048); ACT domain (IPR002912)
HORVU2Hr1G005310	3.91	0.0000	3.32	0.0000	1.54	0.0000	1.54	0.0000	Transferase (IPR003480); EPS1 from Arabinopsis - involved in SA biosynthesis
HORVU1Hr1G088900	3.86	0.0000	1.05	0.0533	2.02	0.0001	2.00	0.0001	Chlorophyll A-B binding protein (IPR022796)
HORVU1Hr1G080120	3.85	0.0000	2.63	0.0000	3.01	0.0000	2.88	0.0000	Sulfotransferase domain (IPR000863)
HORVU4Hr1G079120	3.79	0.0000	4.16	0.0000	2.29	0.0074	2.93	0.0003	Armadillo-type fold (IPR016024)
HORVU4Hr1G013380	3.78	0.0000	2.67	0.0000	1.35	0.0621	1.32	0.0694	Lateral organ boundaries, LOB (IPR004883)
HORVU7Hr1G027270	3.77	0.0000	3.87	0.0000	2.00	0.0000	2.04	0.0000	Multi antimicrobial extrusion protein (IPR002528); PROTEIN DETOXIFICATION 40 (PTHR11206:SF153)

Gene ID	<u>0 v 1 Week</u>		<u>0 v 2 Week</u>		<u>0 v 3 Week</u>		<u>0 v 4 Week</u>		Description
	Log2 Fold Change	p _{adj}	Log2 Fold Change	p _{adj}	Log2 Fold Change	p _{adj}	Log2 Fold Change	p _{adj}	
HORVU5Hr1G014320	3.77	0.0000	0.73	0.0881	1.10	0.0095	1.43	0.0006	F-box domain (IPR001810)
HORVU4Hr1G016730	3.75	0.0000	2.96	0.0000	1.57	0.0000	1.42	0.0000	Peptidase S10, serine carboxypeptidase (IPR001563);
HORVU7Hr1G085510	3.68	0.0000	2.75	0.0000	1.51	0.0000	1.77	0.0000	UDP-glucuronosyl/UDP-glucosyltransferase (IPR002213); maybe involved in flavanol biosynthesis
HORVU4Hr1G071040	3.68	0.0000	3.28	0.0000	1.84	0.0000	1.77	0.0000	Serine acetyltransferase, N-terminal (IPR010493)
HORVU7Hr1G002360	3.67	0.0000	8.57	0.0000	6.71	0.0000	6.52	0.0000	Aspartic peptidase A1 family (IPR001461); Xylanase inhibitor, N-terminal (IPR032861)
HORVU2Hr1G104080	3.67	0.0000	6.78	0.0000	4.26	0.0000	4.21	0.0000	?
HORVU4Hr1G064260	3.65	0.0001	3.40	0.0003	2.33	0.0284	2.98	0.0030	Serine-threonine/tyrosine-protein kinase, catalytic domain (IPR001245)
HORVU4Hr1G018180	3.65	0.0000	2.01	0.0000	-1.40	0.0006	-1.30	0.0016	Fatty acid hydroxylase (IPR006694); lipid biosynthesis
HORVU7Hr1G040370	3.64	0.0000	0.67	0.0000	2.58	0.0000	2.57	0.0000	Chlorophyll A-B binding protein (IPR022796)
HORVU2Hr1G005570	3.64	0.0000	3.39	0.0000	1.40	0.0000	1.65	0.0000	Non-haem dioxygenase N-terminal domain (IPR026992)

Gene ID	<u>0 v 1 Week</u>		<u>0 v 2 Week</u>		<u>0 v 3 Week</u>		<u>0 v 4 Week</u>		Description
	Log2 Fold Change	p _{adj}	Log2 Fold Change	p _{adj}	Log2 Fold Change	p _{adj}	Log2 Fold Change	p _{adj}	
HORVU3Hr1G073110	3.64	0.0000	2.28	0.0000	3.75	0.0000	3.92	0.0000	N-terminal Protein kinase domain (IPR000719); c-terminal NAF domain (IPR004041)

Downregulated.

Gene ID	<u>0 v 1 Week</u>		Description						
	Log2 Fold Change	p _{adj}	Log2 Fold Change	p _{adj}	Log2 Fold Change	p _{adj}	Log2 Fold Change	p _{adj}	
HORVU1Hr1G046400	-4.20	0.0000	-2.18	0.0000	-2.14	0.0000	-2.24	0.0000	
HORVU5Hr1G060730	-2.19	0.0000	-0.44	0.0000	0.72	0.0000	0.70	0.0000	
HORVU3Hr1G027160	-1.95	0.0000	-0.19	0.0014	0.34	0.0000	0.31	0.0000	
HORVU6Hr1G000510	-4.24	0.0000	0.52	0.0004	-0.83	0.0000	-0.83	0.0000	
HORVU2Hr1G006830	-5.80	0.0000	-0.70	0.0001	-1.35	0.0000	-1.28	0.0000	
HORVU2Hr1G089440	-1.58	0.0000	1.40	0.0000	1.18	0.0000	1.13	0.0000	
HORVU7Hr1G001030	-6.96	0.0000	-4.27	0.0000	-3.45	0.0000	-3.48	0.0000	
HORVU4Hr1G012530	-3.29	0.0000	-1.31	0.0000	0.32	0.0146	0.29	0.0319	
HORVU3Hr1G117440	-5.87	0.0000	-1.03	0.0000	-6.40	0.0000	-6.57	0.0000	
HORVU4Hr1G022950	-2.41	0.0000	-0.65	0.0000	0.56	0.0000	0.43	0.0000	
HORVU5Hr1G062290	-5.97	0.0000	-3.04	0.0000	1.13	0.0000	1.00	0.0000	

Gene ID	<u>0 v 1 Week</u>		Description						
	Log2 Fold Change	Padj							
HORVU4Hr1G066270	-5.03	0.0000	-2.22	0.0000	0.62	0.0046	0.61	0.0052	
HORVU5Hr1G019110	-3.91	0.0000	-1.59	0.0000	0.36	0.0244	0.42	0.0085	
HORVU4Hr1G090130	-3.74	0.0000	0.51	0.0006	-1.55	0.0000	-1.88	0.0000	
HORVU1Hr1G029460	-4.01	0.0000	-3.09	0.0000	-3.34	0.0000	-3.35	0.0000	
HORVU5Hr1G093860	-3.39	0.0000	0.55	0.0000	2.03	0.0000	2.02	0.0000	
HORVU3Hr1G067910	-2.23	0.0000	-0.41	0.0000	0.85	0.0000	0.82	0.0000	
HORVU2Hr1G098110	-5.27	0.0000	-4.06	0.0000	0.74	0.0021	0.70	0.0038	
HORVU3Hr1G003980	-5.94	0.0000	-3.95	0.0000	-3.07	0.0000	-3.07	0.0000	
HORVU7Hr1G010230	-2.60	0.0000	-0.81	0.0000	-3.16	0.0000	-3.08	0.0000	
HORVU6Hr1G002300	-3.78	0.0000	-2.03	0.0000	-2.34	0.0000	-2.25	0.0000	
HORVU6Hr1G031960	-1.80	0.0000	-1.33	0.0000	0.45	0.0000	0.42	0.0000	

Gene ID	<u>0 v 1 Week</u>		Description						
	Log2 Fold Change	Padj							
HORVU5Hr1G106640	-5.46	0.0000	-1.51	0.0000	-0.52	0.0623	-0.47	0.0938	
HORVU1Hr1G057880	-4.53	0.0000	-5.11	0.0000	1.36	0.0000	1.42	0.0000	
HORVU3Hr1G030150	-2.23	0.0000	-1.98	0.0000	-0.44	0.0001	-0.51	0.0000	
HORVU3Hr1G059470	-3.52	0.0000	-2.86	0.0000	-3.58	0.0000	-3.46	0.0000	
HORVU7Hr1G002820	-7.15	0.0000	-6.51	0.0000	-2.67	0.0000	-2.61	0.0000	
HORVU1Hr1G068170	-2.13	0.0000	-1.79	0.0000	-1.19	0.0000	-1.23	0.0000	
HORVU3Hr1G087740	-2.82	0.0000	0.86	0.0000	0.86	0.0000	0.89	0.0000	
HORVU7Hr1G001020	-4.34	0.0000	-1.85	0.0000	-2.52	0.0000	-2.29	0.0000	
HORVU1Hr1G016660	-3.58	0.0000	-1.66	0.0000	-4.57	0.0000	-4.30	0.0000	
HORVU3Hr1G009370	-3.47	0.0000	-1.33	0.0000	-4.88	0.0000	-4.63	0.0000	
HORVU0Hr1G009450	-3.85	0.0000	0.87	0.0000	-2.53	0.0000	-2.88	0.0000	

Gene ID	<u>0 v 1 Week</u>		Description						
	Log2 Fold Change	Padj							
HORVU3Hr1G092420	-2.94	0.0000	-2.37	0.0000	-2.65	0.0000	-2.80	0.0000	
HORVU3Hr1G069590	-5.82	0.0000	-1.03	0.0000	-2.10	0.0000	-1.96	0.0000	
HORVU6Hr1G029540	-4.02	0.0000	-3.20	0.0000	0.51	0.0162	0.50	0.0168	
HORVU2Hr1G017400	-2.44	0.0000	0.64	0.0000	0.32	0.0178	0.40	0.0023	
HORVU1Hr1G054240	-4.30	0.0000	-3.53	0.0000	-2.10	0.0000	-2.19	0.0000	
HORVU7Hr1G108570	-2.42	0.0000	-1.23	0.0000	-1.69	0.0000	-1.90	0.0000	
HORVU4Hr1G008270	-1.95	0.0000	-1.62	0.0000	-0.96	0.0000	-0.96	0.0000	
HORVU6Hr1G074940	-3.22	0.0000	-2.29	0.0000	-3.25	0.0000	-3.21	0.0000	
HORVU2Hr1G031310	-3.60	0.0000	-1.16	0.0000	0.64	0.0046	0.61	0.0070	
HORVU6Hr1G061420	-5.90	0.0000	-2.43	0.0000	1.39	0.0000	1.37	0.0000	
HORVU2Hr1G002840	-5.56	0.0000	-2.83	0.0000	0.67	0.0157	0.57	0.0473	

Gene ID	<u>0 v 1 Week</u>		Description						
	Log2 Fold Change	Padj							
HORVU1Hr1G069470	-6.39	0.0000	-5.09	0.0000	-2.56	0.0000	-2.66	0.0000	
HORVU2Hr1G024460	-4.09	0.0000	3.85	0.0000	1.11	0.0000	1.01	0.0000	
HORVU3Hr1G023750	-4.82	0.0000	-2.80	0.0000	-2.03	0.0000	-2.12	0.0000	
HORVU0Hr1G005300	-2.70	0.0000	3.08	0.0000	0.99	0.0000	1.06	0.0000	
HORVU3Hr1G018810	-2.83	0.0000	-2.12	0.0000	-7.52	0.0000	-6.58	0.0000	
HORVU1Hr1G086120	-3.92	0.0000	-3.55	0.0000	0.74	0.0001	0.78	0.0000	
HORVU0Hr1G000910	-2.53	0.0000	1.26	0.0000	-0.68	0.0000	-0.63	0.0000	
HORVU7Hr1G095960	-2.47	0.0000	-1.55	0.0000	0.69	0.0000	0.66	0.0000	
HORVU4Hr1G087400	-7.46	0.0000	-3.72	0.0000	-3.10	0.0000	-2.89	0.0000	
HORVU7Hr1G088260	-3.91	0.0000	-2.70	0.0000	-2.37	0.0000	-2.34	0.0000	
HORVU3Hr1G110330	-1.72	0.0000	-0.90	0.0000	0.56	0.0000	0.55	0.0000	

Gene ID	<u>0 v 1 Week</u>		Description						
	Log2 Fold Change	Padj							
HORVU4Hr1G005900	-1.70	0.0000	-0.53	0.0000	-1.91	0.0000	-1.99	0.0000	
HORVU3Hr1G018430	-3.64	0.0000	-0.68	0.0007	0.37	0.0990	0.43	0.0486	
HORVU4Hr1G072960	-3.04	0.0000	-1.48	0.0000	-2.12	0.0000	-2.20	0.0000	
HORVU2Hr1G115750	-3.08	0.0000	-1.87	0.0000	0.96	0.0000	0.80	0.0000	
HORVU3Hr1G069030	-1.73	0.0000	-0.58	0.0000	0.27	0.0234	0.33	0.0040	
HORVU5Hr1G004370	-7.70	0.0000	-6.64	0.0000	-1.31	0.0000	-1.44	0.0000	
HORVU6Hr1G008720	-8.66	0.0000	-4.73	0.0000	-6.18	0.0000	-7.25	0.0000	
HORVU2Hr1G112830	-3.74	0.0000	-0.49	0.0154	-3.01	0.0000	-3.23	0.0000	
HORVU2Hr1G069950	-1.87	0.0000	0.96	0.0000	0.82	0.0000	0.85	0.0000	
HORVU6Hr1G094070	-6.68	0.0000	-3.54	0.0000	-0.70	0.0432	-0.65	0.0649	
HORVU2Hr1G081540	-5.94	0.0000	0.94	0.0000	-0.65	0.0040	-0.68	0.0026	

Gene ID	<u>0 v 1 Week</u>		Description						
	Log2 Fold Change	Padj							
HORVU2Hr1G103880	-3.48	0.0000	-0.81	0.0001	-1.41	0.0000	-1.44	0.0000	
HORVU3Hr1G009510	-3.04	0.0000	-1.44	0.0000	-3.98	0.0000	-4.60	0.0000	
HORVU4Hr1G021270	-2.07	0.0000	-0.89	0.0000	0.50	0.0005	0.35	0.0176	
HORVU1Hr1G065820	-3.44	0.0000	-1.84	0.0000	-0.64	0.0024	-0.46	0.0404	
HORVU2Hr1G126570	-7.56	0.0000	-5.98	0.0000	-4.30	0.0000	-4.31	0.0000	
HORVU7Hr1G002130	-2.97	0.0000	-1.24	0.0000	-1.05	0.0000	-1.03	0.0000	
HORVU1Hr1G002090	-4.80	0.0000	-1.11	0.0004	-2.42	0.0000	-2.32	0.0000	
HORVU1Hr1G080680	-5.01	0.0000	-2.08	0.0000	0.91	0.0110	0.97	0.0065	
HORVU5Hr1G097270	-2.20	0.0000	2.17	0.0000	1.61	0.0000	1.56	0.0000	
HORVU6Hr1G012110	-3.77	0.0000	-5.63	0.0000	-1.69	0.0000	-1.62	0.0000	
HORVU3Hr1G116200	-1.96	0.0000	-0.89	0.0000	-1.59	0.0000	-1.76	0.0000	

Gene ID	<u>0 v 1 Week</u>		Description						
	Log2 Fold Change	Padj							
HORVU6Hr1G019510	-1.95	0.0000	0.45	0.0006	0.38	0.0056	0.27	0.0635	
HORVU1Hr1G004150	-7.56	0.0000	-1.23	0.0114	-2.06	0.0000	-2.08	0.0000	
HORVU5Hr1G070360	-3.08	0.0000	1.63	0.0000	0.85	0.0001	0.91	0.0000	
HORVU2Hr1G005510	-4.10	0.0000	-3.41	0.0000	-4.15	0.0000	-4.61	0.0000	
HORVU5Hr1G101820	-4.04	0.0000	-1.56	0.0000	-4.08	0.0000	-5.11	0.0000	
HORVU3Hr1G060060	-4.38	0.0000	-1.96	0.0000	-2.68	0.0000	-2.68	0.0000	
HORVU5Hr1G081500	-3.24	0.0000	-0.91	0.0001	0.86	0.0003	0.89	0.0001	
HORVU4Hr1G012330	-2.92	0.0000	-1.39	0.0000	1.06	0.0000	1.04	0.0000	
HORVU6Hr1G070290	-1.88	0.0000	0.32	0.0154	-0.54	0.0000	-0.66	0.0000	
HORVU3Hr1G000160	-5.47	0.0000	-3.58	0.0000	0.65	0.0858	0.72	0.0545	
HORVU3Hr1G116770	-5.56	0.0000	-6.43	0.0000	-8.21	0.0000	-8.67	0.0000	

Gene ID	<u>0 v 1 Week</u>		Description						
	Log2 Fold Change	Padj							
HORVU4Hr1G089910	-1.83	0.0000	-0.76	0.0000	0.52	0.0000	0.59	0.0000	
HORVU4Hr1G089200	-4.57	0.0000	-2.24	0.0000	-6.87	0.0000	-7.08	0.0000	
HORVU2Hr1G103150	-8.01	0.0000	-8.13	0.0000	-2.65	0.0000	-2.61	0.0000	
HORVU2Hr1G126660	-9.97	0.0000	-5.33	0.0000	-4.63	0.0000	-5.10	0.0000	
HORVU6Hr1G076380	-1.72	0.0000	-0.80	0.0000	0.67	0.0000	0.66	0.0000	
HORVU7Hr1G030690	-6.14	0.0000	-3.26	0.0000	-6.78	0.0000	-6.76	0.0000	
HORVU7Hr1G120030	-1.79	0.0000	-2.11	0.0000	-1.35	0.0000	-1.29	0.0000	
HORVU0Hr1G006830	-4.64	0.0000	-2.23	0.0000	0.96	0.0000	0.71	0.0011	
HORVU7Hr1G039260	-1.97	0.0000	-1.66	0.0000	-1.39	0.0000	-1.61	0.0000	
HORVU5Hr1G062940	-2.14	0.0000	-2.30	0.0000	0.74	0.0000	0.68	0.0001	
HORVU3Hr1G009360	-3.19	0.0000	-1.49	0.0000	-3.30	0.0000	-3.42	0.0000	

Appendix Table A.5.7: List of Transcript Changes from the ABA Time Series RNASeq Experiment

Upregulated

Gene ID	base Mean	log2 Fold Change	pAdj	chromosome
HORVU5Hr1G122960	157	2.48	0.0000	chr5H
HORVU2Hr1G042650	35	1.38	0.0340	chr2H
HORVU5Hr1G091790	19	1.38	0.0106	chr5H
HORVU5Hr1G096340	8	1.38	0.0352	chr5H
HORVU6Hr1G058000	15	1.38	0.0316	chr6H
HORVU3Hr1G024430	11	1.38	0.0220	chr3H
HORVU5Hr1G104960	27	1.38	0.0241	chr5H
HORVU6Hr1G053350	9	1.38	0.0337	chr6H
HORVU3Hr1G032370	408	1.38	0.0186	chr3H
HORVU6Hr1G057240	2020	1.37	0.0002	chr6H
HORVU5Hr1G050310	52	1.37	0.0164	chr5H
HORVU0Hr1G015650	7	1.37	0.0352	chrUn
HORVU7Hr1G042410	1646	1.37	0.0001	chr7H
HORVU6Hr1G086440	131	1.37	0.0015	chr6H
HORVU5Hr1G096110	145	1.37	0.0063	chr5H
HORVU5Hr1G060580	36	1.37	0.0155	chr5H
HORVU4Hr1G026570	4479	1.37	0.0108	chr4H
HORVU3Hr1G066210	87	1.37	0.0042	chr3H
HORVU7Hr1G000530	1160	1.37	0.0178	chr7H
HORVU5Hr1G045640	47	1.37	0.0110	chr5H
HORVU7Hr1G009610	1398	1.36	0.0111	chr7H
HORVU7Hr1G061620	173	1.36	0.0185	chr7H
HORVU4Hr1G072060	80	1.36	0.0182	chr4H
HORVU2Hr1G097060	62	1.36	0.0351	chr2H
HORVU1Hr1G053400	14	1.36	0.0240	chr1H
HORVU2Hr1G083450	390	1.36	0.0001	chr2H
HORVU4Hr1G067070	139	1.35	0.0048	chr4H
HORVU3Hr1G021310	175	1.35	0.0037	chr3H
HORVU0Hr1G010910	7	1.35	0.0354	chrUn
HORVU3Hr1G060600	16	1.35	0.0359	chr3H
HORVU7Hr1G082830	38	1.35	0.0351	chr7H
HORVU3Hr1G007290	563	1.35	0.0228	chr3H
HORVU7Hr1G098970	6	1.35	0.0393	chr7H
HORVU2Hr1G089630	72	1.35	0.0027	chr2H
HORVU4Hr1G089290	528	1.34	0.0035	chr4H
HORVU0Hr1G020260	328	1.34	0.0001	chrUn
HORVU7Hr1G064620	15	1.34	0.0255	chr7H
HORVU4Hr1G069990	1191	1.34	0.0002	chr4H
HORVU6Hr1G009910	56	1.34	0.0316	chr6H
HORVU5Hr1G055570	12	1.34	0.0375	chr5H
HORVU7Hr1G066250	14	1.34	0.0344	chr7H
HORVU4Hr1G082110	1721	1.34	0.0012	chr4H
HORVU4Hr1G044140	36	1.33	0.0409	chr4H
HORVU7Hr1G051730	49	1.33	0.0327	chr7H
HORVU4Hr1G068170	1392	1.33	0.0007	chr4H

Downregulated

Gene ID	base Mean	log2 Fold Change	pAdj	chromosome
HORVU7Hr1G010690	28759	-2.71	0.0000	chr7H
HORVU3Hr1G085680	308	-2.57	0.0001	chr3H
HORVU6Hr1G050680	122	-2.53	0.0001	chr6H
HORVU0Hr1G016660	73	-2.51	0.0002	chrUn
HORVU4Hr1G083170	201	-2.50	0.0000	chr4H
HORVU2Hr1G120530	1022	-2.47	0.0000	chr2H
HORVU4Hr1G059260	68	-2.46	0.0001	chr4H
HORVU3Hr1G003980	261	-2.44	0.0002	chr3H
HORVU2Hr1G043890	641	-2.42	0.0000	chr2H
HORVU6Hr1G073500	36	-2.38	0.0003	chr6H
HORVU3Hr1G105780	49	-2.36	0.0003	chr3H
HORVU4Hr1G087250	64	-2.35	0.0001	chr4H
HORVU4Hr1G090090	31	-2.35	0.0003	chr4H
HORVU2Hr1G025380	631	-2.34	0.0003	chr2H
HORVU6Hr1G086190	105	-2.32	0.0002	chr6H
HORVU7Hr1G011810	498	-2.30	0.0000	chr7H
HORVU6Hr1G088140	10	-2.30	0.0004	chr6H
HORVU4Hr1G050390	22	-2.29	0.0001	chr4H
HORVU5Hr1G065350	1346	-2.28	0.0003	chr5H
HORVU7Hr1G036390	47	-2.25	0.0004	chr7H
HORVU3Hr1G030620	37	-2.24	0.0000	chr3H
HORVU0Hr1G013340	98	-2.23	0.0002	chrUn
HORVU7Hr1G010680	42	-2.23	0.0002	chr7H
HORVU7Hr1G030730	32	-2.22	0.0002	chr7H
HORVU2Hr1G105010	644	-2.20	0.0000	chr2H
HORVU1Hr1G007810	6129	-2.19	0.0004	chr1H
HORVU6Hr1G076730	18	-2.18	0.0006	chr6H
HORVU7Hr1G037080	393	-2.18	0.0006	chr7H
HORVU1Hr1G066450	106	-2.17	0.0001	chr1H
HORVU2Hr1G073370	51043	-2.17	0.0005	chr2H
HORVU6Hr1G090220	171	-2.17	0.0008	chr6H
HORVU5Hr1G053020	104	-2.17	0.0003	chr5H
HORVU7Hr1G113270	1424	-2.16	0.0004	chr7H
HORVU5Hr1G070040	54	-2.15	0.0002	chr5H
HORVU2Hr1G105140	142	-2.15	0.0001	chr2H
HORVU5Hr1G055140	132	-2.15	0.0005	chr5H
HORVU2Hr1G108460	139	-2.12	0.0011	chr2H
HORVU5Hr1G097870	6930	-2.12	0.0003	chr5H
HORVU4Hr1G057170	1670	-2.12	0.0007	chr4H
HORVU1Hr1G010230	722	-2.12	0.0008	chr1H
HORVU1Hr1G037610	127	-2.11	0.0007	chr1H
HORVU1Hr1G025440	298	-2.10	0.0002	chr1H
HORVU6Hr1G074940	108	-2.10	0.0002	chr6H
HORVU4Hr1G066230	5689	-2.10	0.0001	chr4H
HORVU1Hr1G090860	17	-2.08	0.0014	chr1H

Appendix Table A5.8 Full List of Barley Sequences Up Regulated by Both Cold Acclimation Conditions and Foliar ABA Application.

Sequences that appeared in the Intersect ABA Up \cap Time Up (see Section 5.4.3).

HORVU1Hr1G057880	HORVU2Hr1G066100	HORVU4Hr1G075090	HORVU5Hr1G042030	HORVU1Hr1G080160	HORVU3Hr1G116010
HORVU0Hr1G034610	HORVU0Hr1G037590	HORVU6Hr1G049160	HORVU7Hr1G051730	HORVU3Hr1G072810	HORVU7Hr1G041300
HORVU2Hr1G066280	HORVU7Hr1G090970	HORVU2Hr1G118820	HORVU1Hr1G091860	HORVU0Hr1G014360	HORVU2Hr1G108530
HORVU3Hr1G007290	HORVU7Hr1G073640	HORVU3Hr1G019840	HORVU0Hr1G034150	HORVU2Hr1G118880	HORVU0Hr1G019950
HORVU5Hr1G077920	HORVU4Hr1G013840	HORVU7Hr1G043880	HORVU0Hr1G035470	HORVU1Hr1G083420	HORVU1Hr1G018600
HORVU2Hr1G017270	HORVU6Hr1G032750	HORVU7Hr1G041230	HORVU7Hr1G056820	HORVU3Hr1G108370	HORVU7Hr1G085130
HORVU2Hr1G012980	HORVU5Hr1G097500	HORVU4Hr1G086660	HORVU4Hr1G050900	HORVU2Hr1G068780	HORVU5Hr1G077700
HORVU4Hr1G056210	HORVU2Hr1G084130	HORVU3Hr1G004840	HORVU6Hr1G086440	HORVU7Hr1G000530	HORVU7Hr1G040970
HORVU5Hr1G123970	HORVU5Hr1G095120	HORVU5Hr1G070360	HORVU4Hr1G054770	HORVU5Hr1G087210	HORVU2Hr1G108690
HORVU3Hr1G013360	HORVU7Hr1G025230	HORVU5Hr1G077580	HORVU7Hr1G020010	HORVU2Hr1G117620	HORVU4Hr1G082910
HORVU7Hr1G111580	HORVU7Hr1G096870	HORVU1Hr1G063450	HORVU2Hr1G086550	HORVU4Hr1G016840	HORVU6Hr1G054180
HORVU2Hr1G088640	HORVU1Hr1G057940	HORVU0Hr1G005160	HORVU2Hr1G107250	HORVU6Hr1G037020	HORVU1Hr1G057410
HORVU1Hr1G092640	HORVU2Hr1G107150	HORVU3Hr1G052880	HORVU2Hr1G105190	HORVU5Hr1G062290	HORVU5Hr1G067920
HORVU6Hr1G021780	HORVU0Hr1G020210	HORVU6Hr1G086860	HORVU3Hr1G117780	HORVU6Hr1G066840	HORVU7Hr1G083370
HORVU5Hr1G073990	AGP50755	HORVU6Hr1G049200	HORVU5Hr1G056420	HORVU7Hr1G098830	HORVU3Hr1G078140
HORVU4Hr1G079710	HORVU5Hr1G010560	HORVU1Hr1G015210	HORVU3Hr1G018390	HORVU2Hr1G097060	HORVU7Hr1G088600
HORVU2Hr1G113250	HORVU3Hr1G000600	HORVU2Hr1G082170	HORVU5Hr1G034830	HORVU0Hr1G003950	HORVU3Hr1G014270
HORVU5Hr1G080430	HORVU2Hr1G060510	HORVU2Hr1G041590	HORVU7Hr1G040790	HORVU1Hr1G025060	HORVU1Hr1G072590
HORVU7Hr1G003880	HORVU7Hr1G034560	HORVU4Hr1G000420	HORVU5Hr1G095170	HORVU0Hr1G018190	HORVU2Hr1G117400
HORVU0Hr1G016480	HORVU4Hr1G061060	HORVU7Hr1G036410	HORVU1Hr1G081410	HORVU4Hr1G069990	HORVU5Hr1G081860
HORVU5Hr1G018410	HORVU6Hr1G004420	HORVU1Hr1G055000	HORVU4Hr1G062330	HORVU1Hr1G045220	HORVU2Hr1G108280
HORVU5Hr1G045360	HORVU2Hr1G046420	HORVU7Hr1G041260	HORVU2Hr1G076970	HORVU6Hr1G051760	HORVU7Hr1G095500
HORVU3Hr1G095820	HORVU6Hr1G031360	HORVU6Hr1G068370	HORVU2Hr1G041780	HORVU7Hr1G034350	HORVU7Hr1G101800
HORVU5Hr1G106470	HORVU6Hr1G084670	HORVU2Hr1G096820	HORVU6Hr1G068620	HORVU5Hr1G060580	HORVU5Hr1G120550
HORVU3Hr1G032370	HORVU0Hr1G002390	HORVU1Hr1G059760	HORVU7Hr1G073050	HORVU6Hr1G045800	HORVU0Hr1G034550
HORVU2Hr1G100720	HORVU4Hr1G072060	HORVU2Hr1G032780	HORVU4Hr1G029060	HORVU5Hr1G000640	HORVU3Hr1G109230

HORVU1Hr1G038010	HORVU6Hr1G010050	HORVU3Hr1G075250	HORVU6Hr1G028790	HORVU6Hr1G057240	HORVU3Hr1G066420
HORVU7Hr1G098970	HORVU3Hr1G088850	HORVU2Hr1G105430	HORVU2Hr1G100210	HORVU7Hr1G032420	HORVU2Hr1G083560
HORVU4Hr1G076960	HORVU1Hr1G080360	HORVU0Hr1G004910	HORVU3Hr1G056550	HORVU4Hr1G064670	HORVU4Hr1G082110
HORVU2Hr1G017950	HORVU5Hr1G086970	HORVU7Hr1G024980	HORVU5Hr1G073970	HORVU7Hr1G005270	HORVU3Hr1G087050
HORVU7Hr1G061620	HORVU3Hr1G114150	HORVU1Hr1G075620	HORVU2Hr1G063220	HORVU3Hr1G043250	HORVU5Hr1G120420
HORVU3Hr1G069010	HORVU2Hr1G017740	HORVU3Hr1G031220	HORVU7Hr1G075350	HORVU4Hr1G056470	HORVU5Hr1G093960
HORVU2Hr1G107180	HORVU4Hr1G062060	HORVU1Hr1G000210	HORVU6Hr1G053550	HORVU4Hr1G076820	HORVU5Hr1G008050
HORVU3Hr1G108100	HORVU0Hr1G020130	HORVU3Hr1G109740	HORVU3Hr1G014660	HORVU7Hr1G029290	HORVU2Hr1G019180
HORVU0Hr1G026710	HORVU2Hr1G016000	HORVU5Hr1G056130	HORVU6Hr1G071770	HORVU4Hr1G054580	HORVU1Hr1G067490
HORVU1Hr1G068200	HORVU3Hr1G034020	HORVU6Hr1G004770	HORVU7Hr1G072570	HORVU7Hr1G024960	HORVU1Hr1G091370
HORVU2Hr1G126950	HORVU0Hr1G040270	HORVU3Hr1G016610	HORVU2Hr1G036590	HORVU2Hr1G097150	HORVU5Hr1G070800
HORVU3Hr1G019330	HORVU2Hr1G075230	HORVU5Hr1G100150	HORVU5Hr1G049180	HORVU1Hr1G056100	HORVU2Hr1G076380
HORVU3Hr1G083990	HORVU3Hr1G079410	HORVU3Hr1G040840	HORVU1Hr1G019290	HORVU0Hr1G039620	HORVU5Hr1G084740
HORVU3Hr1G093550	HORVU1Hr1G014010	HORVU7Hr1G073370	HORVU0Hr1G006050	HORVU5Hr1G061950	HORVU5Hr1G043090
HORVU4Hr1G008980	HORVU3Hr1G074250	HORVU4Hr1G000040	HORVU6Hr1G045410	HORVU6Hr1G095000	HORVU3Hr1G067590
HORVU3Hr1G109370	HORVU3Hr1G002550	HORVU2Hr1G113830	HORVU0Hr1G015530	HORVU5Hr1G084010	HORVU3Hr1G028670
HORVU7Hr1G027230	HORVU1Hr1G025010	HORVU1Hr1G068860	HORVU1Hr1G068530	HORVU2Hr1G118120	HORVU6Hr1G001960
HORVU0Hr1G008670	HORVU1Hr1G036040	HORVU5Hr1G108670	HORVU3Hr1G062900	HORVU2Hr1G111760	HORVU5Hr1G049470
HORVU4Hr1G015890	HORVU3Hr1G082930	HORVU0Hr1G038510	HORVU0Hr1G008030	HORVU6Hr1G072640	HORVU3Hr1G087770
HORVU2Hr1G053190	HORVU3Hr1G110580	HORVU1Hr1G059050	HORVU2Hr1G067350	HORVU1Hr1G079680	HORVU0Hr1G024980
HORVU0Hr1G031430	HORVU0Hr1G036370	HORVU6Hr1G049230	HORVU3Hr1G109380	HORVU1Hr1G029770	HORVU1Hr1G029540
HORVU6Hr1G009100	HORVU5Hr1G010450	HORVU0Hr1G002020	HORVU2Hr1G048510	HORVU4Hr1G045340	HORVU6Hr1G004380
HORVU2Hr1G048500	HORVU2Hr1G035340	HORVU4Hr1G087510	HORVU6Hr1G057370	HORVU6Hr1G002630	HORVU4Hr1G044370
HORVU3Hr1G002230	HORVU3Hr1G059230	HORVU3Hr1G020260	HORVU1Hr1G094810	HORVU6Hr1G014230	HORVU3Hr1G024880
HORVU7Hr1G011100	HORVU7Hr1G030370	HORVU0Hr1G017960	HORVU2Hr1G038480	HORVU6Hr1G091430	HORVU5Hr1G122950

Appendix Table A5.9 Full List of Barley Sequences Down Regulated by Both Cold Acclimation Conditions and Foliar ABA Application.

Sequences that appeared in the Intersect ABA Down \cap Time Down (see **Section 5.4.3**).

HORVU2Hr1G108460	HORVU7Hr1G040740	HORVU1Hr1G090860	HORVU5Hr1G115160	HORVU3Hr1G010190	HORVU1Hr1G007830
HORVU2Hr1G119050	HORVU1Hr1G007790	HORVU0Hr1G022690	HORVU2Hr1G012460	HORVU7Hr1G091100	HORVU4Hr1G009380
HORVU5Hr1G025560	HORVU7Hr1G040730	HORVU2Hr1G073680	HORVU6Hr1G055440	HORVU5Hr1G055140	HORVU6Hr1G005050
HORVU1Hr1G044000	HORVU6Hr1G086190	HORVU7Hr1G043250	HORVU4Hr1G069100	HORVU2Hr1G089340	HORVU1Hr1G089520
HORVU7Hr1G117710	HORVU5Hr1G098360	HORVU3Hr1G064470	HORVU5Hr1G123550	HORVU3Hr1G106140	HORVU4Hr1G085680
HORVU5Hr1G016730	HORVU5Hr1G062450	HORVU6Hr1G005060	HORVU5Hr1G125850	HORVU6Hr1G005420	HORVU3Hr1G052490
HORVU2Hr1G089350	HORVU4Hr1G062890	HORVU1Hr1G065630	HORVU5Hr1G011780	HORVU3Hr1G090410	HORVU1Hr1G071380
HORVU7Hr1G021950	HORVU4Hr1G074470	HORVU6Hr1G019760	HORVU2Hr1G080140	HORVU5Hr1G097440	HORVU1Hr1G004580
HORVU3Hr1G105420	HORVU2Hr1G023540	HORVU4Hr1G026170	HORVU6Hr1G010740	HORVU7Hr1G032740	HORVU2Hr1G006720
HORVU1Hr1G075580	HORVU7Hr1G001070	HORVU5Hr1G075660	HORVU4Hr1G002600	HORVU4Hr1G071370	HORVU3Hr1G085100
HORVU1Hr1G007810	HORVU3Hr1G084220	HORVU3Hr1G020850	HORVU0Hr1G008830	HORVU2Hr1G090410	HORVU0Hr1G000760
HORVU3Hr1G083470	HORVU1Hr1G043910	HORVU2Hr1G022540	HORVU3Hr1G034100	HORVU3Hr1G014590	HORVU1Hr1G000170
HORVU1Hr1G072250	HORVU3Hr1G116580	HORVU1Hr1G049280	HORVU7Hr1G099720	HORVU2Hr1G119090	HORVU4Hr1G085590
HORVU2Hr1G062670	HORVU7Hr1G102030	HORVU6Hr1G070610	HORVU2Hr1G006910	HORVU1Hr1G038130	HORVU5Hr1G060460
HORVU1Hr1G065150	HORVU1Hr1G039820	HORVU7Hr1G024220	HORVU2Hr1G010990	HORVU2Hr1G028780	HORVU0Hr1G012890
HORVU2Hr1G037360	HORVU2Hr1G028430	HORVU0Hr1G005210	HORVU7Hr1G099980	HORVU5Hr1G117440	HORVU5Hr1G071720
HORVU7Hr1G083550	HORVU7Hr1G119200	HORVU1Hr1G026780	HORVU3Hr1G063030	HORVU5Hr1G080300	HORVU5Hr1G106010
HORVU3Hr1G003480	HORVU2Hr1G120530	HORVU3Hr1G085680	HORVU2Hr1G114440	HORVU2Hr1G018570	HORVU3Hr1G109330
HORVU3Hr1G071220	HORVU2Hr1G007540	HORVU3Hr1G089370	HORVU7Hr1G118770	HORVU2Hr1G103980	HORVU4Hr1G002710
HORVU6Hr1G060440	HORVU3Hr1G049390	HORVU6Hr1G010890	HORVU4Hr1G060280	HORVU7Hr1G073190	HORVU4Hr1G087250
HORVU7Hr1G037000	HORVU0Hr1G017230	HORVU5Hr1G079930	HORVU7Hr1G089300	HORVU3Hr1G026600	HORVU1Hr1G018480
HORVU7Hr1G089480	HORVU4Hr1G087760	HORVU6Hr1G073170	HORVU3Hr1G035210	HORVU3Hr1G096910	HORVU5Hr1G047000
HORVU7Hr1G045000	HORVU6Hr1G084860	HORVU2Hr1G004550	HORVU7Hr1G002390	HORVU3Hr1G071800	HORVU4Hr1G000850
HORVU1Hr1G070480	HORVU1Hr1G049430	HORVU2Hr1G105010	HORVU4Hr1G074530	HORVU2Hr1G072150	HORVU0Hr1G010040

HORVU2Hr1G018900	HORVU1Hr1G089540	HORVU3Hr1G022780	HORVU2Hr1G077970	HORVU2Hr1G126740	HORVU3Hr1G073150
HORVU2Hr1G009800	HORVU0Hr1G003810	HORVU1Hr1G007800	HORVU5Hr1G112130	HORVU3Hr1G003980	HORVU5Hr1G075810
HORVU1Hr1G087600	HORVU7Hr1G098440	HORVU2Hr1G043890	HORVU3Hr1G100190	HORVU5Hr1G005180	HORVU7Hr1G030800
HORVU4Hr1G015000	HORVU7Hr1G037080	HORVU1Hr1G086020	HORVU1Hr1G053990	HORVU6Hr1G004090	HORVU1Hr1G010250
HORVU3Hr1G044660	HORVU2Hr1G102110	HORVU7Hr1G000970	HORVU7Hr1G011810	HORVU2Hr1G114390	HORVU3Hr1G093260
HORVU4Hr1G071330	HORVU6Hr1G059940	HORVU7Hr1G095080	HORVU7Hr1G107360	HORVU5Hr1G112580	HORVU2Hr1G085270
HORVU4Hr1G002390	HORVU4Hr1G006140	HORVU2Hr1G108580	HORVU5Hr1G105930	HORVU3Hr1G059480	HORVU2Hr1G111600
HORVU1Hr1G093220	HORVU7Hr1G020920	HORVU2Hr1G000420	HORVU5Hr1G018220	HORVU3Hr1G083320	HORVU3Hr1G006440
HORVU4Hr1G076040	HORVU7Hr1G036720	HORVU6Hr1G033060	HORVU3Hr1G087430	HORVU7Hr1G098670	HORVU4Hr1G013150
HORVU5Hr1G086670	HORVU6Hr1G092750	HORVU7Hr1G030730	HORVU1Hr1G089700	HORVU7Hr1G036960	HORVU5Hr1G123920
HORVU4Hr1G019740	HORVU2Hr1G114680	HORVU2Hr1G089970	HORVU3Hr1G028410	HORVU1Hr1G089620	HORVU1Hr1G037550
HORVU6Hr1G032670	HORVU1Hr1G043920	HORVU3Hr1G035470	HORVU7Hr1G120060	HORVU3Hr1G057880	HORVU3Hr1G057890
HORVU2Hr1G072120	HORVU2Hr1G109120	HORVU0Hr1G009860	HORVU0Hr1G014040	HORVU4Hr1G066870	HORVU1Hr1G080040
HORVU1Hr1G082410	HORVU4Hr1G052770	HORVU7Hr1G054610	HORVU5Hr1G070540	HORVU5Hr1G082990	HORVU3Hr1G083540
HORVU2Hr1G080350	HORVU7Hr1G111310	HORVU4Hr1G020030	HORVU5Hr1G052760	HORVU5Hr1G002090	HORVU2Hr1G118550
HORVU1Hr1G001570	HORVU2Hr1G074990	HORVU6Hr1G012090	HORVU3Hr1G083520	HORVU7Hr1G055890	HORVU2Hr1G115640
HORVU0Hr1G016350	HORVU3Hr1G111080	HORVU5Hr1G010130	HORVU0Hr1G002990	HORVU5Hr1G120630	HORVU2Hr1G013740
HORVU3Hr1G081150	HORVU3Hr1G007280	HORVU1Hr1G076710	HORVU2Hr1G059780	HORVU2Hr1G000140	HORVU1Hr1G004670
HORVU6Hr1G069910	HORVU7Hr1G100100	HORVU3Hr1G027220	HORVU6Hr1G037700	HORVU2Hr1G028590	HORVU3Hr1G002040
HORVU0Hr1G002950	HORVU7Hr1G074030	HORVU7Hr1G119220	HORVU3Hr1G004190	HORVU7Hr1G117800	HORVU4Hr1G054870
HORVU1Hr1G088840	HORVU7Hr1G102170	HORVU3Hr1G016860	HORVU1Hr1G067230	HORVU7Hr1G037240	HORVU3Hr1G009980
HORVU3Hr1G084590	HORVU6Hr1G000070	HORVU1Hr1G017410	HORVU2Hr1G105140	HORVU5Hr1G124880	HORVU0Hr1G021920
HORVU2Hr1G037140	HORVU6Hr1G070220	HORVU1Hr1G007850	HORVU3Hr1G083760	HORVU1Hr1G093660	HORVU1Hr1G041890
HORVU3Hr1G083770	HORVU2Hr1G093210	HORVU6Hr1G037610	HORVU4Hr1G059950	HORVU3Hr1G000280	HORVU1Hr1G007840
HORVU3Hr1G029250	HORVU5Hr1G048180	HORVU3Hr1G098280	HORVU1Hr1G059290	HORVU7Hr1G018540	HORVU2Hr1G083490
HORVU4Hr1G074620	HORVU4Hr1G046590	HORVU3Hr1G013840	HORVU4Hr1G073730	HORVU3Hr1G064120	HORVU7Hr1G049140
HORVU1Hr1G066450	HORVU4Hr1G089990	HORVU2Hr1G093070	HORVU7Hr1G019530	HORVU5Hr1G094700	HORVU6Hr1G062960
HORVU5Hr1G052150	HORVU0Hr1G002880	HORVU2Hr1G010800	HORVU3Hr1G084120	HORVU2Hr1G124490	HORVU7Hr1G105500
HORVU1Hr1G015050	HORVU4Hr1G072500	HORVU4Hr1G013760	HORVU2Hr1G097940	HORVU7Hr1G002260	HORVU3Hr1G098730
HORVU1Hr1G020690	HORVU7Hr1G092510	HORVU7Hr1G115230	HORVU5Hr1G070040	HORVU2Hr1G072210	HORVU3Hr1G114800
HORVU7Hr1G036780	HORVU5Hr1G068500	HORVU0Hr1G009140	HORVU0Hr1G027640	HORVU4Hr1G006100	HORVU2Hr1G032970
HORVU5Hr1G002150	HORVU5Hr1G096490	HORVU7Hr1G098260	HORVU2Hr1G017310	HORVU1Hr1G091400	HORVU5Hr1G017360

HORVU6Hr1G076380	HORVU0Hr1G020630	HORVU3Hr1G087540	HORVU2Hr1G022640	HORVU2Hr1G122920	HORVU2Hr1G037700
HORVU6Hr1G077520	HORVU2Hr1G030600	HORVU1Hr1G093780	HORVU1Hr1G002760	HORVU7Hr1G078690	HORVU4Hr1G088780
HORVU1Hr1G020720	HORVU4Hr1G004260	HORVU4Hr1G006480	HORVU2Hr1G001620	HORVU6Hr1G062820	HORVU7Hr1G023030
HORVU7Hr1G030810	HORVU0Hr1G038850	HORVU6Hr1G067620	HORVU2Hr1G124740	HORVU6Hr1G064740	HORVU2Hr1G090690
HORVU0Hr1G022110	HORVU5Hr1G048100	HORVU6Hr1G022590	HORVU3Hr1G116790	HORVU5Hr1G068800	HORVU7Hr1G044150
HORVU4Hr1G077730	HORVU0Hr1G000780	HORVU4Hr1G087230	HORVU7Hr1G115500	HORVU7Hr1G010990	HORVU4Hr1G070480
HORVU4Hr1G022580	HORVU7Hr1G081770	HORVU2Hr1G091990	HORVU7Hr1G118340	HORVU0Hr1G017530	HORVU5Hr1G002120
HORVU7Hr1G086690	HORVU6Hr1G074940	HORVU2Hr1G099710	HORVU0Hr1G000340	HORVU7Hr1G119930	HORVU6Hr1G092270
HORVU0Hr1G000620	HORVU7Hr1G096410	HORVU3Hr1G066220	HORVU4Hr1G013180	HORVU3Hr1G054120	HORVU1Hr1G072050
HORVU1Hr1G072890	HORVU7Hr1G057330	HORVU4Hr1G062540	HORVU6Hr1G020570	HORVU5Hr1G085780	HORVU3Hr1G008400
HORVU6Hr1G056000	HORVU5Hr1G079950	HORVU6Hr1G091230	HORVU5Hr1G061730	HORVU3Hr1G005430	HORVU3Hr1G087720
HORVU4Hr1G053150	HORVU2Hr1G097540	HORVU5Hr1G124380	HORVU1Hr1G053950	HORVU5Hr1G086620	HORVU3Hr1G023280
HORVU3Hr1G081640	HORVU3Hr1G072020	HORVU1Hr1G090870	HORVU7Hr1G091180	HORVU7Hr1G088510	HORVU7Hr1G038980
HORVU2Hr1G102710	HORVU5Hr1G083100	HORVU5Hr1G061040	HORVU2Hr1G005620	HORVU3Hr1G037450	HORVU3Hr1G112150
HORVU7Hr1G024660	HORVU6Hr1G084900	HORVU1Hr1G054000	HORVU3Hr1G005420	HORVU5Hr1G057780	HORVU6Hr1G094480
HORVU3Hr1G077660	HORVU7Hr1G022010	HORVU7Hr1G048970	HORVU3Hr1G030950	HORVU3Hr1G001060	HORVU2Hr1G059790
HORVU7Hr1G044100	HORVU3Hr1G070220	HORVU2Hr1G009970	HORVU7Hr1G105950	HORVU1Hr1G059090	HORVU4Hr1G076000
HORVU2Hr1G003900	HORVU5Hr1G098340	HORVU4Hr1G073310	HORVU6Hr1G037000	HORVU4Hr1G087780	HORVU6Hr1G018040
HORVU6Hr1G062140	HORVU5Hr1G074820	HORVU2Hr1G047050	HORVU4Hr1G016590	HORVU7Hr1G100740	HORVU1Hr1G043880
HORVU3Hr1G029750	HORVU5Hr1G109290	HORVU3Hr1G084170	HORVU6Hr1G000130	HORVU7Hr1G027580	HORVU7Hr1G098400
HORVU7Hr1G098320	HORVU2Hr1G033880	HORVU1Hr1G027400	HORVU2Hr1G105050	HORVU4Hr1G069070	HORVU5Hr1G010960
HORVU4Hr1G067410	HORVU6Hr1G088440	HORVU2Hr1G093670	HORVU1Hr1G078740	HORVU2Hr1G017900	HORVU5Hr1G097730
HORVU2Hr1G125120	HORVU4Hr1G018640	HORVU0Hr1G009050	HORVU1Hr1G024180	HORVU1Hr1G025530	HORVU5Hr1G020880
HORVU7Hr1G120420	HORVU1Hr1G088680	HORVU6Hr1G005250	HORVU5Hr1G005310	HORVU2Hr1G072880	HORVU4Hr1G056250
HORVU6Hr1G033310	HORVU4Hr1G086110	HORVU7Hr1G095490	HORVU5Hr1G055200	HORVU2Hr1G105930	HORVU2Hr1G007490
HORVU4Hr1G062830	HORVU5Hr1G060140	HORVU6Hr1G054420	HORVU7Hr1G049860	HORVU7Hr1G018100	HORVU7Hr1G116650
HORVU1Hr1G065770	HORVU3Hr1G089550	HORVU4Hr1G062730	HORVU6Hr1G018350	HORVU3Hr1G097860	HORVU7Hr1G045280
HORVU7Hr1G024270	HORVU2Hr1G034970	HORVU7Hr1G066170	HORVU3Hr1G022370	HORVU1Hr1G093900	HORVU3Hr1G024200
HORVU6Hr1G011620	HORVU2Hr1G019500	HORVU0Hr1G003220	HORVU6Hr1G000030	HORVU7Hr1G085650	HORVU1Hr1G059660
HORVU2Hr1G118050	HORVU7Hr1G120340	HORVU1Hr1G011990	HORVU4Hr1G083100	HORVU2Hr1G028580	HORVU2Hr1G005340
HORVU5Hr1G107000	HORVU0Hr1G015930	HORVU2Hr1G075610	HORVU6Hr1G078260	HORVU6Hr1G058820	HORVU4Hr1G072360
HORVU3Hr1G015640	HORVU7Hr1G023700	HORVU2Hr1G045970	HORVU0Hr1G022030	HORVU6Hr1G008640	HORVU2Hr1G108350

HORVU1Hr1G050720	HORVU7Hr1G114000	HORVU2Hr1G060650	HORVU2Hr1G041040	HORVU4Hr1G014480	HORVU3Hr1G095070
HORVU4Hr1G012750	HORVU6Hr1G003460	HORVU1Hr1G092310	HORVU2Hr1G109590	HORVU3Hr1G095400	HORVU0Hr1G014510
HORVU7Hr1G075040	HORVU5Hr1G073310	HORVU3Hr1G057240	HORVU3Hr1G058810	HORVU7Hr1G098280	HORVU4Hr1G005320
HORVU5Hr1G075470	HORVU7Hr1G085450	HORVU0Hr1G003900	HORVU5Hr1G118520	HORVU1Hr1G066930	HORVU7Hr1G032330
HORVU0Hr1G003480	HORVU3Hr1G074000	HORVU5Hr1G095410	HORVU2Hr1G041080	HORVU3Hr1G031260	HORVU1Hr1G054020
HORVU7Hr1G072910	HORVU3Hr1G073860	HORVU0Hr1G020360	HORVU4Hr1G047240	HORVU7Hr1G091860	HORVU3Hr1G092470
HORVU3Hr1G075150	HORVU1Hr1G051780	HORVU5Hr1G094820	HORVU1Hr1G021620	HORVU5Hr1G021610	HORVU6Hr1G088550
HORVU1Hr1G087530	HORVU3Hr1G083160	HORVU6Hr1G018070	HORVU2Hr1G081050	HORVU3Hr1G061130	HORVU4Hr1G002900
HORVU3Hr1G023230	HORVU1Hr1G058630	HORVU4Hr1G018660	HORVU3Hr1G078780	HORVU5Hr1G044200	HORVU2Hr1G121440
HORVU2Hr1G062910	HORVU2Hr1G085280	HORVU3Hr1G069200	HORVU5Hr1G085680	HORVU0Hr1G040220	HORVU1Hr1G079450
HORVU5Hr1G034100	HORVU4Hr1G008440	HORVU3Hr1G022340	HORVU2Hr1G061190	HORVU6Hr1G026230	HORVU0Hr1G017400
HORVU0Hr1G019700	HORVU2Hr1G032190	HORVU5Hr1G120250	HORVU2Hr1G124930	HORVU1Hr1G092540	HORVU1Hr1G026400
HORVU4Hr1G073090	HORVU5Hr1G115340	HORVU5Hr1G096540	HORVU1Hr1G066530	HORVU3Hr1G060310	HORVU4Hr1G084230
HORVU3Hr1G099760	HORVU6Hr1G073560	HORVU4Hr1G018180	HORVU3Hr1G031130	HORVU7Hr1G026150	HORVU4Hr1G014970
HORVU3Hr1G088360	HORVU5Hr1G063360	HORVU2Hr1G066000	HORVU3Hr1G010240	HORVU7Hr1G024990	HORVU1Hr1G009030
HORVU2Hr1G118570	HORVU3Hr1G062250	HORVU2Hr1G123760	HORVU5Hr1G073140	HORVU1Hr1G001220	HORVU5Hr1G123540
HORVU3Hr1G017590	HORVU4Hr1G018070	HORVU1Hr1G041720	HORVU1Hr1G087630	HORVU5Hr1G089070	HORVU7Hr1G110760
HORVU2Hr1G112250	HORVU2Hr1G039050	HORVU5Hr1G045580	HORVU5Hr1G002130	HORVU2Hr1G127640	HORVU1Hr1G083700
HORVU3Hr1G003470	HORVU2Hr1G091220	HORVU7Hr1G108570	HORVU5Hr1G002110	HORVU1Hr1G078290	HORVU4Hr1G060870
HORVU3Hr1G067280	HORVU4Hr1G066230	HORVU3Hr1G058600	HORVU5Hr1G097260	HORVU4Hr1G090090	HORVU1Hr1G028520
HORVU7Hr1G056600	HORVU3Hr1G064640	HORVU1Hr1G003060	HORVU3Hr1G015850	HORVU7Hr1G040170	HORVU6Hr1G054580
HORVU5Hr1G112340	HORVU2Hr1G044360	HORVU0Hr1G015180	HORVU5Hr1G073580	HORVU6Hr1G083660	HORVU3Hr1G114970
HORVU3Hr1G111960	HORVU1Hr1G060200	HORVU5Hr1G067170	HORVU4Hr1G000490	HORVU6Hr1G088140	HORVU0Hr1G010810
HORVU2Hr1G076010	HORVU1Hr1G037570	HORVU5Hr1G114540	HORVU4Hr1G060170	HORVU1Hr1G043820	HORVU1Hr1G065710
HORVU3Hr1G068810	HORVU3Hr1G070240	HORVU7Hr1G001310	HORVU3Hr1G058830	HORVU1Hr1G026520	HORVU0Hr1G039020
HORVU4Hr1G000290	HORVU6Hr1G091630	HORVU6Hr1G021520	HORVU6Hr1G051500	HORVU6Hr1G073500	HORVU4Hr1G046610
HORVU1Hr1G024070	HORVU7Hr1G052870	HORVU1Hr1G068430	HORVU1Hr1G043040	HORVU7Hr1G088140	HORVU3Hr1G095340
HORVU6Hr1G062380	HORVU7Hr1G057260	HORVU1Hr1G008120	HORVU0Hr1G007790	HORVU7Hr1G083680	HORVU3Hr1G078560
HORVU6Hr1G011970	HORVU2Hr1G103930	HORVU7Hr1G089540	HORVU4Hr1G071170	HORVU2Hr1G007350	HORVU7Hr1G076070
HORVU1Hr1G070720	HORVU2Hr1G100220	HORVU7Hr1G116060	HORVU2Hr1G117900	HORVU2Hr1G024160	HORVU4Hr1G078350
HORVU1Hr1G028200	HORVU4Hr1G069660	HORVU1Hr1G037650	HORVU5Hr1G089050	HORVU4Hr1G057450	HORVU0Hr1G040540
HORVU2Hr1G021150	HORVU3Hr1G096360	HORVU4Hr1G012560	HORVU6Hr1G073300	HORVU1Hr1G055470	HORVU7Hr1G053470

HORVU1Hr1G048760	HORVU5Hr1G073440	HORVU4Hr1G060140	HORVU5Hr1G112060	HORVU7Hr1G055330	HORVU2Hr1G045590
HORVU4Hr1G012000	HORVU7Hr1G108530	HORVU2Hr1G109420	HORVU5Hr1G109580	HORVU6Hr1G025620	HORVU1Hr1G052290
HORVU0Hr1G028710	HORVU5Hr1G027980	HORVU0Hr1G017440	HORVU1Hr1G090950	HORVU5Hr1G045850	HORVU1Hr1G070640
HORVU3Hr1G101230	HORVU2Hr1G109430	HORVU5Hr1G046520	HORVU7Hr1G116770	HORVU2Hr1G101470	HORVU5Hr1G058910
HORVU7Hr1G019680	HORVU1Hr1G083900	HORVU2Hr1G036810	HORVU6Hr1G004930	HORVU5Hr1G062720	HORVU6Hr1G081950
HORVU2Hr1G124880	HORVU4Hr1G003480	HORVU5Hr1G107120	HORVU4Hr1G076050	HORVU7Hr1G029260	HORVU2Hr1G018480
HORVU5Hr1G052190	HORVU6Hr1G018640	HORVU3Hr1G059810	HORVU4Hr1G003400	HORVU4Hr1G005250	HORVU2Hr1G069060
HORVU5Hr1G099470	HORVU2Hr1G011060	HORVU0Hr1G009280	HORVU3Hr1G094900	HORVU7Hr1G010150	HORVU4Hr1G065110
HORVU2Hr1G112060	HORVU5Hr1G014730	HORVU0Hr1G005510	HORVU6Hr1G053090	HORVU4Hr1G087520	HORVU5Hr1G016600
HORVU2Hr1G017880	HORVU4Hr1G028720	HORVU5Hr1G000730	HORVU0Hr1G031730	HORVU3Hr1G097950	HORVU5Hr1G116660
HORVU4Hr1G077350	HORVU4Hr1G017610	HORVU1Hr1G025390	HORVU5Hr1G041960	HORVU2Hr1G046370	HORVU4Hr1G059260
HORVU4Hr1G043680	HORVU7Hr1G088260	HORVU3Hr1G021190	HORVU2Hr1G015720	HORVU3Hr1G006100	HORVU6Hr1G066780
HORVU0Hr1G015220	HORVU7Hr1G048330	HORVU2Hr1G110720	HORVU5Hr1G044330	HORVU5Hr1G097150	HORVU6Hr1G082060
HORVU5Hr1G063390	HORVU4Hr1G063730	HORVU4Hr1G071790	HORVU4Hr1G048970	HORVU1Hr1G018010	HORVU7Hr1G091780
HORVU4Hr1G085290	HORVU2Hr1G018440	HORVU5Hr1G050270	HORVU5Hr1G081310	HORVU7Hr1G028290	HORVU1Hr1G073330
HORVU4Hr1G076940	HORVU1Hr1G069830	HORVU3Hr1G069080	HORVU7Hr1G119340	HORVU7Hr1G108460	HORVU2Hr1G099550
HORVU2Hr1G099590	HORVU1Hr1G081210	HORVU4Hr1G021260	HORVU2Hr1G034860	HORVU5Hr1G080860	HORVU3Hr1G086200
HORVU5Hr1G109680	HORVU5Hr1G080220	HORVU6Hr1G077620	HORVU2Hr1G087370	HORVU3Hr1G069470	HORVU5Hr1G017100
HORVU2Hr1G062350	HORVU7Hr1G025670	HORVU7Hr1G105410	HORVU6Hr1G059090	HORVU7Hr1G087240	HORVU5Hr1G111240
HORVU4Hr1G049960	HORVU2Hr1G071470	HORVU5Hr1G095010	HORVU2Hr1G096500	HORVU5Hr1G094890	HORVU0Hr1G022330
HORVU5Hr1G096360	HORVU1Hr1G090890	HORVU6Hr1G054430	HORVU1Hr1G071430	HORVU5Hr1G093410	HORVU2Hr1G083030
HORVU6Hr1G066720	HORVU2Hr1G090170	HORVU7Hr1G051430	HORVU0Hr1G007370	HORVU2Hr1G120090	HORVU7Hr1G036390
HORVU3Hr1G006220	HORVU2Hr1G044830	HORVU2Hr1G104300	HORVU2Hr1G085340	HORVU1Hr1G076890	HORVU4Hr1G006450
HORVU6Hr1G083690	HORVU7Hr1G014410	HORVU3Hr1G024920	HORVU3Hr1G097390	HORVU2Hr1G065040	HORVU1Hr1G056270
HORVU2Hr1G001330	HORVU5Hr1G027740	HORVU5Hr1G115900	HORVU2Hr1G104630	HORVU5Hr1G069510	HORVU5Hr1G066190
HORVU1Hr1G084620	HORVU7Hr1G009380	HORVU6Hr1G075130	HORVU5Hr1G088530	HORVU3Hr1G029400	HORVU2Hr1G037550
HORVU6Hr1G000540	HORVU5Hr1G007430	HORVU0Hr1G024200	HORVU5Hr1G094220	HORVU2Hr1G109640	HORVU5Hr1G080310
HORVU3Hr1G092520	HORVU4Hr1G074400	HORVU1Hr1G002900	HORVU6Hr1G023740	HORVU4Hr1G065240	HORVU7Hr1G101530
HORVU0Hr1G039750	HORVU7Hr1G104660	HORVU3Hr1G056830	HORVU2Hr1G035020	HORVU2Hr1G085160	HORVU3Hr1G027240
HORVU6Hr1G045900	HORVU4Hr1G079600	HORVU4Hr1G072960	HORVU5Hr1G117910	HORVU2Hr1G105340	HORVU2Hr1G093960
HORVU1Hr1G044560	HORVU0Hr1G028210	HORVU6Hr1G083600	HORVU5Hr1G057220	HORVU5Hr1G098310	HORVU3Hr1G005380
HORVU7Hr1G042000	HORVU4Hr1G082970	HORVU7Hr1G026630	HORVU2Hr1G074210	HORVU7Hr1G120560	HORVU0Hr1G038430

HORVU3Hr1G071750	HORVU7Hr1G094210	HORVU2Hr1G082330	HORVU3Hr1G007970	HORVU7Hr1G064180	HORVU1Hr1G047090
HORVU7Hr1G111010	HORVU3Hr1G081140	HORVU3Hr1G080190	HORVU6Hr1G073850	HORVU1Hr1G076480	HORVU3Hr1G000720
HORVU6Hr1G009690	HORVU5Hr1G042330	HORVU1Hr1G017970	HORVU3Hr1G028710	HORVU4Hr1G048110	HORVU2Hr1G115160
HORVU1Hr1G024060	HORVU3Hr1G043160	HORVU7Hr1G122210	HORVU6Hr1G032810	HORVU1Hr1G051360	HORVU7Hr1G027860
HORVU7Hr1G100060	HORVU1Hr1G000450	HORVU1Hr1G060620	HORVU6Hr1G054890	HORVU3Hr1G022840	HORVU6Hr1G053000
HORVU5Hr1G000910	HORVU2Hr1G109470	HORVU4Hr1G081210	HORVU7Hr1G091580	HORVU7Hr1G038940	HORVU1Hr1G016840
HORVU2Hr1G108820	HORVU2Hr1G035160	HORVU2Hr1G097980	HORVU5Hr1G122510	HORVU7Hr1G084610	HORVU2Hr1G048280
HORVU0Hr1G018320	HORVU2Hr1G085990	HORVU7Hr1G027760	HORVU5Hr1G070260	HORVU2Hr1G093400	HORVU3Hr1G090270
HORVU1Hr1G090300	HORVU7Hr1G020770	HORVU5Hr1G062510	HORVU3Hr1G109540	HORVU3Hr1G017100	HORVU7Hr1G021310
HORVU3Hr1G015310	HORVU1Hr1G065270	HORVU2Hr1G077460	HORVU1Hr1G086450	HORVU7Hr1G046760	HORVU5Hr1G073290
HORVU2Hr1G027690	HORVU6Hr1G081930	HORVU1Hr1G072720	HORVU7Hr1G000870	HORVU2Hr1G032320	HORVU2Hr1G065720
HORVU7Hr1G038530	HORVU4Hr1G006350	HORVU2Hr1G098330	HORVU2Hr1G013760	HORVU7Hr1G022510	HORVU1Hr1G025870
HORVU2Hr1G040790	HORVU5Hr1G112560	HORVU6Hr1G089730	HORVU3Hr1G083670	HORVU3Hr1G096740	HORVU3Hr1G057860
HORVU6Hr1G070900	HORVU4Hr1G015550	HORVU5Hr1G066630	HORVU1Hr1G066410	HORVU3Hr1G066450	HORVU2Hr1G124430
HORVU7Hr1G063020	HORVU2Hr1G022500	HORVU4Hr1G011120	HORVU3Hr1G030090	HORVU2Hr1G005830	HORVU6Hr1G078700
HORVU3Hr1G013400	HORVU1Hr1G049470	HORVU1Hr1G093670	HORVU6Hr1G095240	HORVU1Hr1G081020	HORVU3Hr1G007960
HORVU1Hr1G000560	HORVU2Hr1G012810	HORVU5Hr1G023720	HORVU1Hr1G071210	HORVU3Hr1G011860	HORVU4Hr1G006730
HORVU1Hr1G013870	HORVU3Hr1G074940	HORVU1Hr1G079170	HORVU4Hr1G072560	HORVU3Hr1G091230	HORVU5Hr1G076100
HORVU5Hr1G065370	HORVU7Hr1G099220	HORVU4Hr1G060970	HORVU4Hr1G066310	HORVU5Hr1G053480	HORVU4Hr1G026770
HORVU2Hr1G102790	HORVU3Hr1G075040	HORVU1Hr1G055340	HORVU6Hr1G028850	HORVU3Hr1G108300	HORVU5Hr1G065200
HORVU1Hr1G090250	HORVU5Hr1G124520	HORVU3Hr1G011850	HORVU6Hr1G005020	HORVU3Hr1G078840	HORVU2Hr1G023180
HORVU6Hr1G001060	HORVU5Hr1G125550	HORVU4Hr1G078450	HORVU1Hr1G080000	HORVU1Hr1G064750	HORVU5Hr1G022600
HORVU5Hr1G104670	HORVU5Hr1G006360	HORVU5Hr1G115870	HORVU1Hr1G075670	HORVU2Hr1G004640	HORVU3Hr1G034040
HORVU6Hr1G086830	HORVU7Hr1G073860	HORVU5Hr1G059910	HORVU2Hr1G108150	HORVU5Hr1G098170	HORVU2Hr1G105240
HORVU5Hr1G093500	HORVU5Hr1G091820	HORVU6Hr1G066950	HORVU7Hr1G012850	HORVU5Hr1G106550	HORVU1Hr1G008130
HORVU4Hr1G002570	HORVU2Hr1G005140	HORVU2Hr1G037540	HORVU3Hr1G113750	HORVU7Hr1G007580	HORVU5Hr1G070290
HORVU3Hr1G092940	HORVU4Hr1G034500	HORVU4Hr1G084590	HORVU4Hr1G016600	HORVU4Hr1G090300	HORVU3Hr1G010830
HORVU3Hr1G068430	HORVU2Hr1G124860	HORVU5Hr1G104800	HORVU1Hr1G063740	HORVU3Hr1G083650	HORVU7Hr1G114660
HORVU5Hr1G107330	HORVU2Hr1G033510	HORVU1Hr1G055800	HORVU2Hr1G121210	HORVU4Hr1G068530	HORVU1Hr1G015910
HORVU1Hr1G024100	HORVU6Hr1G035300	HORVU6Hr1G018830	HORVU6Hr1G014420	HORVU3Hr1G001540	HORVU7Hr1G052070
HORVU1Hr1G051330	HORVU5Hr1G077390	HORVU5Hr1G007670	HORVU6Hr1G004980	HORVU3Hr1G117390	HORVU3Hr1G089490
HORVU5Hr1G098770	HORVU4Hr1G085150	HORVU7Hr1G098330	HORVU5Hr1G095020	HORVU7Hr1G026570	HORVU1Hr1G069990

HORVU7Hr1G114170	HORVU3Hr1G027080	HORVU3Hr1G070270	HORVU5Hr1G054690	HORVU7Hr1G082930	HORVU3Hr1G068700
HORVU7Hr1G091560	HORVU3Hr1G035650	HORVU4Hr1G009520	HORVU7Hr1G002290	HORVU2Hr1G104270	HORVU1Hr1G090050
HORVU2Hr1G026820	HORVU7Hr1G088750	HORVU7Hr1G029600	HORVU3Hr1G111040	HORVU7Hr1G046640	HORVU3Hr1G092090
HORVU7Hr1G087810	HORVU1Hr1G024540	HORVU3Hr1G050590	HORVU5Hr1G006880	HORVU3Hr1G028840	HORVU2Hr1G118080
HORVU1Hr1G043380	HORVU5Hr1G005990	HORVU5Hr1G062050	HORVU5Hr1G017220	HORVU1Hr1G070840	HORVU2Hr1G019900
HORVU3Hr1G052560	HORVU6Hr1G078110	HORVU7Hr1G115250	HORVU7Hr1G018780	HORVU4Hr1G023570	HORVU2Hr1G010970
HORVU1Hr1G070460	HORVU5Hr1G095080	HORVU4Hr1G078510	HORVU1Hr1G049070	HORVU3Hr1G029670	HORVU5Hr1G065630
HORVU2Hr1G080480	HORVU7Hr1G076440	HORVU4Hr1G071300	HORVU4Hr1G059170	HORVU7Hr1G120070	HORVU5Hr1G048690
HORVU6Hr1G042090	HORVU1Hr1G089760	HORVU0Hr1G016430	HORVU7Hr1G001010	HORVU3Hr1G026330	HORVU7Hr1G080020
HORVU0Hr1G013290	HORVU3Hr1G081480	HORVU1Hr1G052030	HORVU7Hr1G102910	HORVU2Hr1G043330	HORVU5Hr1G092240
HORVU6Hr1G012400	HORVU1Hr1G079040	HORVU1Hr1G069800	HORVU1Hr1G089860	HORVU4Hr1G089620	HORVU1Hr1G018360
HORVU1Hr1G014580	HORVU5Hr1G123530	HORVU3Hr1G114240	HORVU0Hr1G018380	HORVU2Hr1G011790	HORVU3Hr1G061000
HORVU4Hr1G004270	HORVU6Hr1G078660	HORVU2Hr1G027640	HORVU0Hr1G020420	HORVU6Hr1G032720	HORVU3Hr1G102340
HORVU3Hr1G116470	HORVU2Hr1G001600	HORVU1Hr1G015560	HORVU5Hr1G106730	HORVU7Hr1G030000	HORVU5Hr1G114700
HORVU1Hr1G092670	HORVU5Hr1G089160	HORVU2Hr1G119220	HORVU1Hr1G001990	HORVU2Hr1G090730	HORVU3Hr1G028620
HORVU2Hr1G063510	HORVU7Hr1G043620	HORVU4Hr1G077360	HORVU5Hr1G097270	HORVU2Hr1G041110	HORVU3Hr1G023400
HORVU1Hr1G072780	HORVU1Hr1G089370	HORVU4Hr1G089030	HORVU3Hr1G052510	HORVU5Hr1G089110	HORVU5Hr1G071280
HORVU7Hr1G085270	HORVU1Hr1G045090	HORVU3Hr1G088140	HORVU3Hr1G084340	HORVU1Hr1G081840	HORVU4Hr1G003290
HORVU6Hr1G078910	HORVU4Hr1G015250	HORVU2Hr1G094630	HORVU1Hr1G011390	HORVU5Hr1G108750	HORVU5Hr1G095130
HORVU5Hr1G085800	HORVU5Hr1G108640	HORVU0Hr1G014720	HORVU5Hr1G117670	HORVU1Hr1G042250	HORVU3Hr1G089170
HORVU5Hr1G024410	HORVU5Hr1G088130	HORVU5Hr1G094570	HORVU6Hr1G026610	HORVU3Hr1G095780	HORVU5Hr1G096680
HORVU3Hr1G062490	HORVU5Hr1G068770	HORVU4Hr1G013460	HORVU4Hr1G002330	HORVU5Hr1G110890	HORVU5Hr1G070050
HORVU1Hr1G005110	HORVU5Hr1G080340	HORVU2Hr1G103150	HORVU5Hr1G017260	HORVU5Hr1G112670	HORVU1Hr1G047930
HORVU3Hr1G006930	HORVU5Hr1G080830	HORVU6Hr1G028590	HORVU2Hr1G024600	HORVU4Hr1G066900	HORVU3Hr1G089690
HORVU5Hr1G123200	HORVU0Hr1G003230	HORVU0Hr1G017160	HORVU5Hr1G067010	HORVU5Hr1G084700	HORVU5Hr1G094460
HORVU2Hr1G014150	HORVU4Hr1G071390	HORVU4Hr1G078950	HORVU5Hr1G104600	HORVU7Hr1G035850	HORVU1Hr1G092150
HORVU1Hr1G090110	HORVU1Hr1G073460	HORVU6Hr1G070830	HORVU7Hr1G041230	HORVU3Hr1G106070	HORVU4Hr1G046810
HORVU7Hr1G033490	HORVU0Hr1G006830	HORVU3Hr1G076550	HORVU3Hr1G006680	HORVU1Hr1G089840	HORVU5Hr1G111000
HORVU0Hr1G002870	HORVU2Hr1G017910	HORVU3Hr1G018630	HORVU4Hr1G015310	HORVU2Hr1G120010	HORVU7Hr1G113290
HORVU7Hr1G102070	HORVU1Hr1G055930	HORVU7Hr1G033430	HORVU1Hr1G070730	HORVU3Hr1G097900	HORVU4Hr1G018360
HORVU0Hr1G020320	HORVU5Hr1G080350	HORVU7Hr1G036410	HORVU1Hr1G047000	HORVU7Hr1G016870	HORVU7Hr1G088920
HORVU3Hr1G023780	HORVU6Hr1G085990	HORVU7Hr1G046830	HORVU2Hr1G105100	HORVU6Hr1G029750	HORVU5Hr1G041500

HORVU3Hr1G068710	HORVU6Hr1G020840	HORVU7Hr1G120930	HORVU4Hr1G053860	HORVU7Hr1G027080	HORVU3Hr1G053060
HORVU2Hr1G037620	HORVU2Hr1G107750	HORVU4Hr1G076820	HORVU3Hr1G001390	HORVU5Hr1G084230	HORVU0Hr1G012930
HORVU6Hr1G011450	HORVU5Hr1G051310	HORVU1Hr1G029090	HORVU3Hr1G092460	HORVU2Hr1G094020	HORVU3Hr1G018810
HORVU3Hr1G085930	HORVU3Hr1G073050	HORVU4Hr1G057290	HORVU7Hr1G040590	HORVU7Hr1G073390	HORVU3Hr1G069590
HORVU4Hr1G083070	HORVU2Hr1G102620	HORVU1Hr1G072290	HORVU7Hr1G070140	HORVU3Hr1G059720	HORVU3Hr1G116630
HORVU2Hr1G094240	HORVU6Hr1G074210	HORVU7Hr1G116160	HORVU0Hr1G002930	HORVU4Hr1G083940	HORVU7Hr1G040030
HORVU5Hr1G080110	HORVU3Hr1G097270	HORVU1Hr1G029280	HORVU4Hr1G060370	HORVU4Hr1G084320	HORVU3Hr1G019320
HORVU7Hr1G097460	HORVU2Hr1G079840	HORVU1Hr1G003540	HORVU6Hr1G079030	HORVU2Hr1G089130	HORVU6Hr1G078180
HORVU0Hr1G003010	HORVU6Hr1G021160	HORVU7Hr1G112710	HORVU5Hr1G006330	HORVU7Hr1G002690	HORVU4Hr1G076840
HORVU5Hr1G103730	HORVU0Hr1G002580	HORVU7Hr1G030780	HORVU7Hr1G090280	HORVU3Hr1G069890	HORVU7Hr1G031800
HORVU4Hr1G070470	HORVU7Hr1G115260	HORVU2Hr1G085740	HORVU0Hr1G006790	HORVU1Hr1G063380	HORVU0Hr1G039910
HORVU7Hr1G087420	HORVU3Hr1G067760	HORVU6Hr1G076450	HORVU4Hr1G082740	HORVU6Hr1G061280	HORVU2Hr1G030810
HORVU7Hr1G007540	HORVU7Hr1G046380	HORVU3Hr1G071410	HORVU5Hr1G063330	HORVU1Hr1G084720	HORVU2Hr1G045200
HORVU7Hr1G108190	HORVU3Hr1G007420	HORVU5Hr1G080840	HORVU4Hr1G060260	HORVU3Hr1G095240	HORVU4Hr1G075990
HORVU2Hr1G065330	HORVU3Hr1G099530	HORVU7Hr1G017790	HORVU7Hr1G089240	HORVU1Hr1G001200	HORVU3Hr1G086700
HORVU0Hr1G004470	HORVU7Hr1G021660	HORVU4Hr1G054850	HORVU4Hr1G060720	HORVU1Hr1G047010	HORVU7Hr1G100790
HORVU3Hr1G068760	HORVU2Hr1G084600	HORVU3Hr1G105870	HORVU3Hr1G062690	HORVU5Hr1G049030	HORVU1Hr1G029850
HORVU2Hr1G096700	HORVU5Hr1G080580	HORVU1Hr1G090820	HORVU6Hr1G030350	HORVU2Hr1G104980	HORVU1Hr1G046400
HORVU5Hr1G104580	HORVU4Hr1G068960	HORVU2Hr1G082370	HORVU5Hr1G060620	HORVU7Hr1G106600	HORVU0Hr1G005320
HORVU4Hr1G056500	HORVU7Hr1G036380	HORVU6Hr1G076020	HORVU4Hr1G016880	HORVU3Hr1G011460	HORVU7Hr1G013170
HORVU6Hr1G066050	HORVU4Hr1G063590	HORVU2Hr1G102960	HORVU6Hr1G070290	HORVU3Hr1G087320	HORVU3Hr1G052980
HORVU1Hr1G020450	HORVU3Hr1G019070	HORVU4Hr1G049920	HORVU1Hr1G045690	HORVU2Hr1G120340	HORVU1Hr1G052060
HORVU1Hr1G074840	HORVU3Hr1G081300	HORVU3Hr1G078420	HORVU3Hr1G068380	HORVU6Hr1G070250	HORVU6Hr1G071830

Table A6.1 PANTHER Gene Ontology Annotation of Upregulated Cold Acclimation Sequences in Barley Induced by Photoperiod Alone, Low Night Temperatures Alone, and a Combination of Both Factors

Sequences with a greater than 2-fold increase are shown along with some annotation from the UniProt online resource. Sequence presented with a bold face Sequence ID were also identified in an independent parallel experiment described in **Section 5.2**. The average and standard error is given for the fold change in expression level for: |P| sequences, derived from a single Complement; |I| sequences were derived from two Complements; |T| sequences, derived from 3 Complements. Key: PANTHER CC, Cellular Component; PANTHER MF, Molecular Function; PANTHER BP, Biological Process; PANTHER PC, Protein Class. IDs in bold type face were identified in two independent experiments (see **Section 5.2.2**).

Mapped ID	Gene Name	PANTHER Family/Subfamily	PANTHER MF	PANTHER CC	Pathway	PANTHER BP	PANTHER PC
P							
HORVU6Hr1G014270	Predicted protein;unassigned; ortholog	L-GULONOLACTONE OXIDASE 5-RELATED (PTHR13878:SF67)					
HORVU3Hr1G029770	Uncharacterized protein;unassigned; ortholog	GLYCEROL-3-PHOSPHATE ACYLTRANSFERASE 2-RELATED (PTHR15486:SF62)	phosphatase activity(GO:0016791);transferase activity, transferring acyl groups other than amino-acyl groups(GO:0016747)			macromolecule biosynthetic process(GO:0009059)	acyltransferase(PC00042)
HORVU2Hr1G100720	Uncharacterized protein;unassigned; ortholog	SUBFAMILY NOT NAMED (PTHR16223:SF156)	transcriptional activator activity, RNA polymerase II transcription regulatory region sequence-specific DNA binding(GO:0001228)	nuclear chromatin(GO:0000790)			
HORVU3Hr1G073280	Uncharacterized protein;unassigned; ortholog	SUBFAMILY NOT NAMED					

Mapped ID	Gene Name	PANTHER Family/ Subfamily	PANTHER MF	PANTHER CC	Pathway	PANTHER BP	PANTHER PC
		(PTHR34268:SF10)					
HORVU3Hr1G086940	Predicted protein;unassigned;ortholog	SUBFAMILY NOT NAMED (PTHR33477:SF7)					
HORVU1Hr1G065070	Uncharacterized protein;unassigned;ortholog	SUBFAMILY NOT NAMED (PTHR47100:SF3)		cytoplasm(GO:0005737)			
HORVU2Hr1G043830	Formin-like protein;unassigned;ortholog	SUBFAMILY NOT NAMED (PTHR23213:SF37)					
HORVU7Hr1G035050	Uncharacterized protein;unassigned;ortholog	PROTEIN TRICHOME BIREFRINGENCE (PTHR32285:SF22)	acetyltransferase activity(GO:0016407)	Golgi apparatus(GO:0005794);plasma membrane(GO:0005886);vacuole(GO:0005773)			
T							
HORVU3Hr1G058990	CTP synthase;unassigned;ortholog	SUBFAMILY NOT NAMED (PTHR11550:SF13)	identical protein binding(GO:0042802);ligase activity(GO:0016874)		De novo pyrimidine ribonucleotides biosynthesis->CTP synthase;;	nucleobase-containing small molecule biosynthetic process(GO:0034404);organonitrogen compound biosynthetic process(GO:1901566);pyrimidine nucleobase metabolic process(GO:0006206);pyrimidine nucleotide metabolic process(GO:0006220);ribonucleoside triphosphate biosynthetic process(GO:0009201);ribonucleotide biosynthetic process(GO:0009260)	cysteine protease(PC00081);ligase(PC00142)
HORVU5Hr1G098920	Pectin acetyltransferase;unassigned;ortholog	SUBFAMILY NOT NAMED	carboxylic ester hydrolase activity(GO:0052689)	plant-type cell wall(GO:0009505)		cell wall organization(GO:0071555)	

Mapped ID	Gene Name	PANTHER Family/ Subfamily	PANTHER MF	PANTHER CC	Pathway	PANTHER BP	PANTHER PC
		(PTHR21562:SF71)					
HORVU2Hr1G028920	Uncharacterized protein;unassigned;ortholog	SUBFAMILY NOT NAMED (PTHR22930:SF178)					
HORVU4Hr1G057000	Uncharacterized protein;unassigned;ortholog	UPF0057 MEMBRANE PROTEIN ZK632.10 (PTHR21659:SF79)					
HORVU2Hr1G099830	Uncharacterized protein;unassigned;ortholog						
HORVU3Hr1G006940	Uncharacterized protein;unassigned;ortholog	SUBFAMILY NOT NAMED (PTHR11527:SF141)	unfolded protein binding(GO:0051082)			protein complex oligomerization(GO:0051259);protein folding(GO:0006457);response to antibiotic(GO:0046677);response to drug(GO:0042493);response to heat(GO:0009408);response to inorganic substance(GO:0010035);response to reactive oxygen species(GO:0000302);response to salt stress(GO:0009651);response to toxic substance(GO:0009636)	chaperone(PC00072)
HORVU7Hr1G007800	Uncharacterized protein;unassigned;ortholog	SUBFAMILY NOT NAMED (PTHR33493:SF12)					
HORVU2Hr1G043980	Uncharacterized protein;unassigned;ortholog	SUBFAMILY NOT NAMED					

Mapped ID	Gene Name	PANTHER Family/ Subfamily	PANTHER MF	PANTHER CC	Pathway	PANTHER BP	PANTHER PC
		(PTHR31769:SF54)					
HORVU7Hr1G012310	Uncharacterized protein;unassigned;ortholog	SUBFAMILY NOT NAMED (PTHR33493:SF14)					
HORVU1Hr1G058310	Uncharacterized protein;unassigned;ortholog	NON-SPECIFIC SERINE/THREONINE PROTEIN KINASE (PTHR24346:SF30)	protein serine/threonine kinase activity(GO:0004674)	cytoplasm(GO:0005737)		intracellular signal transduction(GO:0035556)	non-receptor serine/threonine protein kinase(PC00167)
HORVU3Hr1G112020	Uncharacterized protein;unassigned;ortholog	SUBFAMILY NOT NAMED (PTHR33801:SF14)					
HORVU4Hr1G083250	Uncharacterized protein;unassigned;ortholog	SUBFAMILY NOT NAMED (PTHR12176:SF61)					
HORVU6Hr1G086820	Uncharacterized protein;unassigned;ortholog						
HORVU2Hr1G099820	Uncharacterized protein;unassigned;ortholog						
HORVU6Hr1G060540	Uncharacterized protein;unassigned;ortholog	SUBFAMILY NOT NAMED (PTHR27007:SF213)	transmembrane receptor protein serine/threonine kinase activity(GO:0004675)	plasma membrane(GO:0005886)		defense response to bacterium(GO:0042742)	
HORVU5Hr1G098190	Uncharacterized protein;unassigned;ortholog	SUBFAMILY NOT NAMED (PTHR33596:SF16)					
HORVU5Hr1G001750	Uncharacterized protein;unassigned;ortholog	SUBFAMILY NOT NAMED (PTHR31769:SF61)					

Mapped ID	Gene Name	PANTHER Family/Subfamily	PANTHER MF	PANTHER CC	Pathway	PANTHER BP	PANTHER PC
HORVU0Hr1G003190	Uncharacterized protein;unassigned; ortholog	SUBFAMILY NOT NAMED (PTHR31769:SF54)					
I							
HORVU2Hr1G073210	Uncharacterized protein;unassigned; ortholog						
HORVU3Hr1G112520	Uncharacterized protein;unassigned; ortholog	SUBFAMILY NOT NAMED (PTHR46101:SF8)					
HORVU2Hr1G103550	Uncharacterized protein;unassigned; ortholog						
HORVU7Hr1G009800	Uncharacterized protein;unassigned; ortholog	SUBFAMILY NOT NAMED (PTHR22601:SF68)	oligopeptide transmembrane transporter activity(GO:0035673)	integral component of plasma membrane(GO:0005887)			
HORVU1Hr1G055000	Uncharacterized protein;unassigned; ortholog	PLECKSTRIN HOMOLOGY (PH) DOMAIN-CONTAINING PROTEIN (PTHR16166:SF131)		extrinsic component of membrane(GO:0019898);intracellular(GO:0005622)		cellular process(GO:0009987);maintenance of location(GO:0051235);protein localization to Golgi apparatus(GO:0034067);protein targeting to vacuole(GO:0006623)	
HORVU1Hr1G005120	Uncharacterized protein;unassigned; ortholog	OUTER ENVELOPE PORE PROTEIN 16-1, CHLOROPLAST IC	amino acid transmembrane transporter activity(GO:0015171);protein transmembrane transporter activity(GO:0008320)	chloroplast membrane(GO:0031969);integral component of mitochondrial inner membrane(GO:0031305);mitochondrial inner membrane presequence translocase		protein import into mitochondrial matrix(GO:0030150);protein targeting to chloroplast(GO:0045036)	amino acid transporter(PC00046)

Mapped ID	Gene Name	PANTHER Family/ Subfamily	PANTHER MF	PANTHER CC	Pathway	PANTHER BP	PANTHER PC
		(PTHR15371:SF2)		complex(GO:0005744);organ elle outer membrane(GO:0031968)			

Table A6.2 PANTHER Gene Ontology Annotation of Down Regulated Cold Acclimation Sequences in Barley Induced by Photoperiod Alone, Low Night Temperatures Alone, and a Combination of Both Factors

Sequences with a greater than 2-fold increase are shown along with some annotation from the UniProt online resource. Sequence presented with a bold face Sequence ID were also identified in an independent parallel experiment described in **Section 5.2**. The average and standard error is given for the fold change in expression level for: |P| sequences, derived from a single Complement; |I| sequences were derived from two Complements; |T| sequences, derived from 3 Complements. Key: PANTHER CC, Cellular Component; PANTHER MF, Molecular Function; PANTHER BP, Biological Process; PANTHER PC, Protein Class. IDs in bold type face were identified in two independent experiments (see **Section 5.2.2**).

Mapped ID	Gene Name	PANTHER Family/Sub-family	PANTHER MF	PANTHER CC	Pathway	PANTHER BP	PANTHER PC
P							
HORVU5Hr1G125460	Uncharacterized protein;unassigned;ortholog	AWPM-19-LIKE FAMILY PROTEIN (PTHR33294:SF5)					
HORVU5Hr1G052730	Predicted protein;unassigned;ortholog	SUBFAMILY NOT NAMED (PTHR46371:SF19)					
HORVU5Hr1G091840	Predicted protein;unassigned;ortholog						
HORVU2Hr1G071450	Uncharacterized protein;unassigned;ortholog	NUDIX HYDROLASE 13, MITOCHONDRIAL (PTHR12629:SF1)	cytoplasm(GO:0005737);nucleus(GO:0005634)			phosphatase(PC00181)	
HORVU0Hr1G020630	Uncharacterized protein;unassigned;ortholog	SUBFAMILY NOT NAMED (PTHR31009:SF85)					

Mapped ID	Gene Name	PANTHER Family/Sub-family	PANTHER MF	PANTHER CC	Pathway	PANTHER BP	PANTHER PC
HORVU4Hr1G060670	Uncharacterized protein;unassigned;ortholog	SUBFAMILY NOT NAMED (PTHR43991:SF20)					
HORVU3Hr1G026920	Predicted protein;unassigned;ortholog						
HORVU3Hr1G070440	Uncharacterized protein;unassigned;ortholog	GLUCAN ENDO-1,3-BETA-GLUCOSIDASE 13 (PTHR32227:SF88)	anchored component of plasma membrane(GO:0046658)				
HORVU6Hr1G006840	Predicted protein;unassigned;ortholog						
HORVU2Hr1G108340	Uncharacterized protein;unassigned;ortholog						
HORVU2Hr1G012280	Uncharacterized protein;unassigned;ortholog						
HORVU7Hr1G027540	Uncharacterized protein;unassigned;ortholog	SUBFAMILY NOT NAMED (PTHR11260:SF552)	cytoplasm(GO:0005737)		glutathione metabolic process(GO:0006749)		
HORVU2Hr1G019900	Predicted protein;unassigned;ortholog	SUBFAMILY NOT NAMED (PTHR33433:SF2)					
HORVU7Hr1G025700	Uncharacterized protein;unassigned;ortholog	SUBFAMILY NOT NAMED (PTHR11945:SF382)	nucleus(GO:0005634)		plant ovule development(GO:0048481)	MADS box transcription factor(PC00250)	
HORVU3Hr1G066410	Uncharacterized protein;unassigned;ortholog	RNA POLYMERASE II TRANSCRIPTIONAL COACTIVATOR	nucleus(GO:0005634);transcription factor complex(GO:0005667)		positive regulation of transcription initiation from RNA polymerase II promoter(GO:0060261); protein-containing complex		

Mapped ID	Gene Name	PANTHER Family/Sub-family	PANTHER MF	PANTHER CC	Pathway	PANTHER BP	PANTHER PC
		KELP (PTHR13215:SF6)			assembly(GO:0065003); transcription initiation from RNA polymerase II promoter(GO:0006367)		
HORVU6Hr1G012400	Uncharacterized protein;unassigned;ortholog						
T							
HORVU1Hr1G093560	Uncharacterized protein;unassigned;ortholog	SUBFAMILY NOT NAMED (PTHR11240:SF47)			RNA catabolic process(GO:0006401)		
HORVU0Hr1G000340	Uncharacterized protein;unassigned;ortholog	CYSTATHIONINE BETA LYASE (PTHR11808:SF72)	cytoplasm(GO:0005737)	Methionine biosynthesis->O-Succinyl homoserine lyase;;	cellular amino acid metabolic process(GO:0006520);sulfur compound metabolic process(GO:0006790)	lyase(PC00144)	
HORVU2Hr1G024120	Uncharacterized protein;unassigned;ortholog	SUBFAMILY NOT NAMED (PTHR31225:SF92)					
HORVU1Hr1G090890	Predicted protein;unassigned;ortholog	SUBFAMILY NOT NAMED (PTHR33265:SF24)					
HORVU2Hr1G097980	Uncharacterized protein;unassigned;ortholog	SUBFAMILY NOT NAMED (PTHR34059:SF2)					
HORVU3Hr1G070880	Uncharacterized protein;unassigned;ortholog	SUBFAMILY NOT NAMED (PTHR28242:SF28)	cytoplasm(GO:0005737);nucleus(GO:0005634)		hormone-mediated signaling pathway(GO:0009755);phosphorelay signal transduction system(GO:0000160);response to cytokinin(GO:0009735)		

Mapped ID	Gene Name	PANTHER Family/Sub-family	PANTHER MF	PANTHER CC	Pathway	PANTHER BP	PANTHER PC
HORVU5Hr1G007890	Predicted protein;unassigned;ortholog	SUBFAMILY NOT NAMED (PTHR12632:SF17)			regulation of transcription by RNA polymerase II(GO:0006357);response to stress(GO:0006950);transcription by RNA polymerase II(GO:0006366)	nucleic acid binding(PC00171);transcription factor(PC00218)	
HORVU3Hr1G002000	Uncharacterized protein;unassigned;ortholog	GERMIN-LIKE PROTEIN SUBFAMILY 1 MEMBER 12-RELATED (PTHR31238:SF42)	cell wall(GO:0005618)				
HORVU3Hr1G013840	Uncharacterized protein;unassigned;ortholog	METALLOTHIONEIN-LIKE PROTEIN 2B (PTHR33543:SF1)					
HORVU3Hr1G024920	Uncharacterized protein;unassigned;ortholog						
HORVU5Hr1G085550	Uncharacterized protein;unassigned;ortholog	SUBFAMILY NOT NAMED (PTHR33207:SF34)					
HORVU5Hr1G092700	Uncharacterized protein;unassigned;ortholog	NUCLEAR TRANSCRIPTION FACTOR Y SUBUNIT A-10 (PTHR12632:SF39)			regulation of transcription by RNA polymerase II(GO:0006357);response to stress(GO:0006950);transcription by RNA polymerase II(GO:0006366)	nucleic acid binding(PC00171);transcription factor(PC00218)	
HORVU0Hr1G027640	Uncharacterized protein;unassigned;ortholog	SUBFAMILY NOT NAMED					

Mapped ID	Gene Name	PANTHER Family/Sub-family	PANTHER MF	PANTHER CC	Pathway	PANTHER BP	PANTHER PC
		(PTHR33779:SF11)					
I							
HORVU2Hr1G003480	Uncharacterized protein;unassigned;ortholog	SUBFAMILY NOT NAMED (PTHR24298:SF717)				oxygenase(PC00177)	
HORVU2Hr1G015930	Uncharacterized protein;unassigned;ortholog	SERINE/THREONINE-PROTEIN KINASE 36 (PTHR22983:SF6)			Hedgehog signaling pathway->Fused;;EGF receptor signaling pathway->Mitogen-activated protein kinase kinase 1 and 2;;FGF signaling pathway->Mitogen-activated protein kinase kinase 1 and 2;;PDGF signaling pathway->Mitogen-activated protein kinase 2;,,,,;		
HORVU2Hr1G030600	Predicted protein;unassigned;ortholog						

Table A6.3 GO Analyses Statistics Table for Set of Intersections Between Time Series and Foliar ABA Treatment Up Regulated Genes
Time Series $Up \cap ABA$ Up; see **Section 5.4.3**

GO biological process complete	<i>Hordeum vulgare</i> subsp. <i>vulgare</i> - REFLIST (35505)	Time\capABA (291)	Time\capABA (expected)	Time\capABA (over/under)	Time\capABA (fold Enrichment)	Time\capABA (raw P-value)	Time\capABA FRD
protein phosphorylation (GO:0006468)	1556	36	12.75	+	2.82	3.41E-08	2.63E-05
phosphorylation (GO:0016310)	1844	39	15.11	+	2.58	8.82E-08	5.68E-05
phosphate-containing compound metabolic process (GO:0006796)	2407	49	19.73	+	2.48	6.04E-09	2.33E-05
phosphorus metabolic process (GO:0006793)	2418	49	19.82	+	2.47	6.74E-09	1.30E-05
transmembrane transport (GO:0055085)	1310	25	10.74	+	2.33	1.21E-04	4.25E-02
cellular protein modification process (GO:0006464)	2525	44	20.69	+	2.13	3.05E-06	1.47E-03
protein modification process (GO:0036211)	2525	44	20.69	+	2.13	3.05E-06	1.31E-03
macromolecule modification (GO:0043412)	2679	46	21.96	+	2.09	2.15E-06	1.18E-03
cellular macromolecule metabolic process (GO:0044260)	4182	57	34.28	+	1.66	1.18E-04	4.58E-02
primary metabolic process (GO:0044238)	6971	84	57.13	+	1.47	1.53E-04	4.92E-02
biological_process (GO:0008150)	14733	168	120.75	+	1.39	3.13E-08	4.03E-05
Unclassified (UNCLASSIFIED)	20772	123	170.25	-	0.72	3.13E-08	3.02E-05

Table A6.4 GO Annotations for Set of Intersections Between Time Series and Foliar ABA Treatment Up Regulated Genes
Time Series Up \cap ABA Up; see **Section 5.4.3**

Mapped ID	Gene Name	PANTHER Family/ subfamily	PANTHER MF	PANTHER CC	Pathway	PANTHER BP	PANTHER PC
HORVU0Hr1G019950	ATP synthase subunit alpha; unassigned; ortholog	ATP SYNTHASE SUBUNIT ALPHA, MITOCHONDRIAL (PTHR43089:SF8)	ATP binding(GO:0005524); proton-transporting ATP synthase activity, rotational mechanism(GO:0046933)	plasma membrane(GO:0005886);proton-transporting ATP synthase complex(GO:0045259)	ATP synthesis->F1 alpha;;	ATP synthesis coupled proton transport(GO:0015986)	ATP synthase(PC00002);DNA binding protein(PC00009);anion channel(PC00049);hydrolase(PC00121);ligand-gated ion channel(PC00141)
HORVU3Hr1G082930	Uncharacterized protein; unassigned; ortholog	DNA POLYMERASE ALPHA CATALYTIC SUBUNIT (PTHR45861:SF1)	DNA replication origin binding(GO:0003688); protein heterodimerization activity(GO:0046982);purine nucleotide binding(GO:0017076)	CMG complex(GO:0071162); DNA helicase complex(GO:0033202); DNA polymerase complex(GO:0042575); GINS complex(GO:0000811); MCM complex(GO:0042555); MCM core complex(GO:0097373); nuclear DNA-directed RNA polymerase complex(GO:0055029); nuclear pre-replicative complex(GO:0005656); nuclear	DNA replication->Pol alpha;;	DNA biosynthetic process(GO:0071897); DNA replication initiation(GO:0006270);DNA strand elongation involved in DNA replication(GO:0006271);RNA biosynthetic process(GO:0032774); RNA catabolic process(GO:0006401); double-strand break repair(GO:0006302);mitotic nuclear division(GO:0140014); nuclear DNA replication(GO:0033260)	

Mapped ID	Gene Name	PANTHER Family/subfamily	PANTHER MF	PANTHER CC	Pathway	PANTHER BP	PANTHER PC
				replisome(GO:0043601);origin recognition complex(GO:0000808)			
HORVU5Hr1G120550	Serine/threonine protein phosphatase 2A regulatory subunit; unassigned; ortholog	SUBFAMILY NOT NAMED (PTHR10257:SF49)	enzyme activator activity(GO:0008047);phosphoprotein phosphatase activity(GO:0004721);protein kinase activity(GO:0004672);protein phosphatase binding(GO:0019903);protein phosphatase regulator activity(GO:0019888)	catalytic complex(GO:1902494);cytosol(GO:0005829);nucleus(GO:0005634)	EGF receptor signaling pathway->protein phosphatase 2A;;	protein autophosphorylation(GO:0046777);regulation of protein kinase activity(GO:0045859)	protein phosphatase(PC00195)
HORVU3Hr1G059230	Uncharacterized protein; unassigned; ortholog	ROOTLETIN, ISOFORM D (PTHR23159:SF31)			Nicotinic acetylcholine receptor signaling pathway->Myosin;;		
HORVU1Hr1G019290	Uncharacterized protein; unassigned; ortholog	ATP-DEPENDENT HELICASE BRM (PTHR10799:SF854)			Wnt signaling pathway->Switched/Sucrose Non Fermentation;;		DNA helicase(PC00011)

Table A6.5 GO Analyses Statistics Table for Set of Intersections Between Time Series and Foliar ABA Treatment Doenwnm Regulated Genes
Time Series Down \cap ABA Down; see Sections 5.4.3 and 6.10

GO biological process complete	<i>Hordeum vulgare</i> subsp. <i>vulgare</i> - REFLIST (35505)	Time \cap ABA (291)	Time \cap ABA (expected)	Time \cap ABA (over/under)	Time \cap ABA (fold Enrichment)	Time \cap ABA (raw P-value)	Time \cap ABA FRD
hemicellulose metabolic process (GO:0010410)	43	9	1.69	+	5.32	1.32E-04	2.44E-02
cell wall polysaccharide metabolic process (GO:0010383)	45	9	1.77	+	5.08	1.79E-04	3.01E-02
cell wall macromolecule metabolic process (GO:0044036)	66	13	2.6	+	5	8.07E-06	4.45E-03
hydrogen peroxide catabolic process (GO:0042744)	167	19	6.58	+	2.89	9.08E-05	2.19E-02
hydrogen peroxide metabolic process (GO:0042743)	167	19	6.58	+	2.89	9.08E-05	2.06E-02
antibiotic catabolic process (GO:0017001)	168	19	6.61	+	2.87	9.75E-05	2.09E-02
cofactor catabolic process (GO:0051187)	177	20	6.97	+	2.87	6.54E-05	1.81E-02
antibiotic metabolic process (GO:0016999)	172	19	6.77	+	2.81	1.29E-04	2.49E-02
reactive oxygen species metabolic process (GO:0072593)	182	19	7.17	+	2.65	2.50E-04	4.03E-02
drug catabolic process (GO:0042737)	242	25	9.53	+	2.62	3.38E-05	1.45E-02
carbohydrate metabolic process (GO:0005975)	838	58	33	+	1.76	8.50E-05	2.19E-02
oxidation-reduction process (GO:0055114)	2310	141	90.96	+	1.55	7.35E-07	1.42E-03
nitrogen compound metabolic process (GO:0006807)	5872	175	231.21	-	0.76	4.27E-05	1.50E-02
protein metabolic process (GO:0019538)	3955	109	155.73	-	0.7	4.97E-05	1.60E-02
macromolecule metabolic process (GO:0043170)	5394	146	212.39	-	0.69	4.39E-07	1.70E-03
cellular protein metabolic process (GO:0044267)	3327	90	131	-	0.69	1.34E-04	2.35E-02
cellular macromolecule metabolic process (GO:0044260)	4182	112	164.67	-	0.68	7.66E-06	4.93E-03

GO biological process complete	<i>Hordeum vulgare</i> subsp. <i>vulgare</i> - REFLIST (35505)	Time\capABA (291)	Time\capABA (expected)	Time\capABA (over/under)	Time\capABA (fold Enrichment)	Time\capABA (raw P-value)	Time\capABA FRD
cellular nitrogen compound metabolic process (GO:0034641)	2365	53	93.12	-	0.57	7.37E-06	5.69E-03
heterocycle metabolic process (GO:0046483)	1760	39	69.3	-	0.56	1.05E-04	2.13E-02
cellular nitrogen compound biosynthetic process (GO:0044271)	1268	26	49.93	-	0.52	2.69E-04	4.16E-02
cellular macromolecule biosynthetic process (GO:0034645)	1275	24	50.2	-	0.48	5.93E-05	1.76E-02
macromolecule biosynthetic process (GO:0009059)	1302	24	51.27	-	0.47	3.65E-05	1.41E-02
nucleobase-containing compound metabolic process (GO:0006139)	1560	28	61.42	-	0.46	3.03E-06	2.93E-03
nucleic acid metabolic process (GO:0090304)	1270	22	50.01	-	0.44	1.47E-05	7.12E-03
gene expression (GO:0010467)	1354	21	53.31	-	0.39	8.00E-07	1.03E-03
nucleobase-containing compound biosynthetic process (GO:0034654)	452	4	17.8	-	0.22	2.73E-04	4.05E-02

Table A6.6 GO Annotations for Set of Intersections Between Time Series and Foliar ABA Treatment Down Regulated Genes
Time Series Up \cap ABA Up; see **Section 5.4.3**

Mapped ID	Gene Name	PANTHER Family/ subfamily	PANTHER MF	PANTHER CC	Pathway	PANTHER BP	PANTHER PC
HORVU5Hr1G048100	Uncharacterized protein; unassigned; ortholog	ASPARAGINE SYNTHETASE (PTHR11772:SF40)	ligase activity (GO:0016874); protein homodimerization activity (GO:0042803)	Cytosol (GO:0005829)	Asparagine and aspartate biosynthesis->Asparagine synthetase;;	amide biosynthetic process(GO:0043604);cellular amino acid biosynthetic process(GO:0008652);monocarboxylic acid metabolic process(GO:0032787)	cysteine protease(PC00081);ligase(PC00142)
HORVU7Hr1G087810	Uncharacterized protein; unassigned; ortholog	SUBFAMILY NOT NAMED (PTHR10314:SF180)	anion binding(GO:0043168);cofactor binding(GO:0048037);drug binding(GO:0008144);heterocyclic compound binding(GO:1901363);organic cyclic compound binding(GO:0097159);small molecule binding(GO:0036094);transferase activity,	cytoplasm(GO:0005737)	Cysteine biosynthesis->O-Acetylserine-lyase;;	cellular amino acid biosynthetic process(GO:0008652);sulfur compound metabolic process(GO:0006790)	deaminase(PC00088);dehydratase(PC00091);epimerase/racemase(PC00096)

Mapped ID	Gene Name	PANTHER Family/subfamily	PANTHER MF	PANTHER CC	Pathway	PANTHER BP	PANTHER PC
			transferring alkyl or aryl (other than methyl) groups(GO:0016765)				
HORVU3Hr1G075040	Predicted protein; unassigned; ortholog	SUBFAMILY NOT NAMED (PTHR11999:SF96)			Dopamine receptor mediated signaling pathway->Aromatic L-amino acid decarboxylase;;5-Hydroxytryptamine biosynthesis->Aromatic L-amino acid decarboxylase;;Adrenaline and noradrenaline biosynthesis->Aromatic L-amino acid decarboxylase;;;		
HORVU7Hr1G038980	Uncharacterized protein; unassigned; ortholog	SUBFAMILY NOT NAMED (PTHR24072:SF315)	GTP binding(GO:0005525);GTPase activity(GO:0003924);protein kinase binding(GO:0019901)	cell cortex(GO:0005938); cell projection(GO:0042995);nucleus(GO:0005634);plasma membrane(GO:0005886)	FGF signaling pathway->Ras-related C3 botulinum toxin substrate;;Huntington disease->Ras-related C3 botulinum toxin substrate;;;	Rho protein signal transduction(GO:0007266);actin filament organization(GO:0007015);cell morphogenesis(GO:000902);establishment or maintenance of cell	small GTPase(PC00208)